University of Southampton

THE ROLE OF COLLOIDAL MATERIAL IN THE FATE AND CYCLING OF TRACE METALS IN ESTUARINE AND COASTAL WATERS.

By Eleanor Ruth Parker

Thesis submitted in partial fulfilment of the requirements for Ph.D.

Department of Ocean and Earth Science

May 1999

UNIVERSITY OF SOUTHAMPTON

ABSTRACT

FACULTY OF SCIENCE
OCEAN AND EARTH SCIENCE

Doctor of Philosophy

THE ROLE OF COLLOIDAL MATERIAL IN THE FATE AND CYCLING OF TRACE METALS IN ESTUARINE AND COASTAL WATERS.

By Eleanor Ruth Parker

Trace metals in natural colloidal material (1-400nm) were investigated in the River Beaulieu, the Trent-Humber system and the Celtic Sea. Colloidal and truly dissolved (<10,000molecular weight) fractions were separated by cross-flow filtration (CFF). Filtration artefacts (conventional and CFF) involving filter blockage and colloid aggregation/disaggregation transformations were minimised through appropriate protocols.

^{65}Zn equilibration experiments were carried out with Beaulieu River colloids (<0.4μm). The initial uptake of ^{65}Zn onto colloidal material (10 to 15 %) was very rapid (seconds to minutes) but a large fraction of the tracer remained in the truly dissolved phase. Preliminary modelling to estimate the fraction of colloidal zinc under variable SPM concentrations and Kc sensitivities was completed using different partition coefficients (Kc and Kf) derived during the equilibration experiments. Initial ^{65}Zn-colloid partitioning was related to the mass concentrations (and theoretical surface area) of colloids and colloidal aggregates. The ^{65}Zn radiotracer/colloid association was exchangeable but overall equilibrium partitioning of colloidal/truly dissolved ^{65}Zn did not change with increased total zinc concentration. Loose hydrophobic colloidal aggregates (filaments) with Mn hydroxide coatings formed during sample storage and were capable of removing ~60% of the ^{65}Zn. Field flow fractionation (FFF) of colloidal Beaulieu River water highlighted the significance of the smaller colloidal fractions (<0.08μm and 0.08 to 0.134μm) which contained the highest concentration of Fe, Mn and Zn when normalised to an assumed geometric surface area.

A spatial and seasonal investigation of colloidal trace metals in the Trent/Humber system identified groups of metals with varying colloidal associations in the order (high to low); Fe> Pb, Mn > Cu, Zn, Ni > Cd. Colloidal Fe, Pb and Mn all illustrated removal in the low salinity region of the estuary. Ni (mainly truly dissolved) showed somewhat conservative behaviour. Total dissolved Cd (and Zn) consistently showed a mid-estuarine maximum (truly dissolved), which was attributed to chloro-complex formation or ionic exchange with major seawater ions. For most metals, the positioning and intensity of the turbidity maximum zone (TMZ) appeared to have greatest control on their removal. Cu is controlled seasonally by input of organic ligands (truly dissolved/microcolloidal). The existence of separate organic and inorganic colloidal pools was proposed, which may have seasonally variable signatures. The presence of lower molecular weight (<10,000Da) colloids is significant for Pb and Cu.

Investigations of colloidal Al in the Celtic Sea highlighted problems with colloid disruption within the cross-flow system, and detection of Al colloids using a surface active fluorometric technique. Water column profiles of reactive and dissolved (<0.4μm) Al gave insights into processes controlling Al distribution and concentration. Resuspension of Celtic Sea sediment led to an instantaneous release of truly dissolved Al derived from authigenic mineral dissolution. FFF analysis of samples from the resuspension experiments showed that colloidal Al was not a significant fraction (<20% of total dissolved Al). On the basis of these experiments it was possible to estimate that, in the absence of scavenging, the input of truly dissolved Al from typical resuspension events could be sufficient to account for the 5-8nM increase in dissolved Al concentrations observed close to the bed.

This research has contributed towards a new approach to interpretation of trace metal speciation and processes in a variety of natural waters. Assessment of the role of colloidal and truly dissolved phases within the 'dissolved' fraction has enabled better understanding of particle/water/metal interactions. The description of trace metal/colloid partitioning and associations within these multicomponent systems has the potential to enhance their modelling in the future.

CONTENTS: **PAGE**

Chapter 1: General Introduction:

Chapter 2: Colloid separation and analytical methods:

Chapter 5: Colloidal partitioning of aluminium in the Celtic Sea.

LIST OF FIGURES: PAGE

Chapter 1: General Introduction:

Chapter 2: Colloidal separation and analytical methods

Chapter 3: Investigation of the influence of particle size spectra on the partitioning of trace metals in estuarine environments.

Chapter 4: Spatial and temporal distribution of colloidal trace metals in the Trent/Humber system.

Chapter 5:Colloidal partitioning of Al in the Celtic Sea.

LIST OF TABLES: PAGE

Chapter 1: General introduction.

Chapter 2: Colloid separation and analytical methods.

Chapter 3: Investigation of the influence of particle size spectra on the partitioning of trace metals in estuarine environments.

Chapter 4: Spatial and temporal distribution of colloidal trace metals in the Trent/Humber system.

PHOTOGRAPHS/PLATES: **PAGE**

PROCEDURE FLOW DIAGRAMS:

Chapter 2: Colloid separation and analytical methods.

Chapter 5: Colloidal partitioning of aluminium in the Celtic Sea.

ACKNOWLEDGEMENTS:

I would very much like to thank my supervisor Peter Statham for all his advice and discussions over the course of this project. I would also like to thank Alan Tappin, Dennis Burton, Paul Gooddy and Brian Dickie for their endless help and encouragement when things were going really pear shaped. Alan..I make it 57 pints in all!!!!

I would like to thank many others in the department but especially Kate Davis for her work on the figures when there was tonnes of other things to be done. Really, there are too many to mention.

Of course where would I be without those Cambridge Road girls and honorary member Jon..and many others too of course. I don't think I would have survived until Friday afternoon without you all.

I would like to acknowledge NERC for funding this research.

Last of all (but by no means least) I would like to thank my parents and Duncan for supporting me (in various ways) throughout this time.
I hope you enjoy reading the end product.

LIST OF ABBREVIATIONS:

APDC	Ammonium pyrrollidine dithiocarbamate.
BSEI	Back scatter electron microscopy.
BOD	Biological oxygen demand.
CASS-2	Coastal seawater reference material (National Research Council of Canada).
CF	Concentration factor (Initial volume/final volume).
CFF	Cross-flow filtration.
Coll. calc.	Colloidal trace metal concentration calculated from retentate fraction concentration (R-F/CF).
Coll. diff.	Colloidal trace metal concentration calculated by difference of total dissolved and truly dissolved concentrations (0.4f-F).
CRM	Certified reference material.
CTD	Instrument measuring conductivity, temperature and depth.
DDDC	Diethylammonium diethyldithiocarbamate.
DO	Dissolved Oxygen.
DOC	Dissolved organic carbon.
DR	Double reagent addition (reagent blank in lumogallion procedure).
D216	Research vessel Discovery cruise number 216.
EA	Environment Agency.
EDS	Energy dispersive x-ray microanalysis.
F	Cross flow filtration filtrate.
f (Ch.5)	Fluorescence.
FAAS	Flame atomic absorption spectrophotometer.
FEP	Fluorinated ethylene-propylene
FFF	Field-flow fractionation.
GFAAS	Graphite furnace atomic absorption spectrophotometer.
ICP-MS	Inductively coupled plasma-mass spectrophotometer
ITD	Isothermally distilled.
Kc	Partition coefficient (colloid/truly dissolved).
Kd/Kf	Partition coefficient (particulate/dissolved).
KDa	Kilo-Daltons (molecular weight filter cut-off).
LDPE	Low density polyethylene.

LFB	Laminar flow block.
LMSW	Low metal seawater.
LOIS	Land Ocean Interaction Study.
Milli-Q	Very high purity water, low in dissolved species (RO water that has been processed though a millipore filtration sytem, resistance~ 18ohms).
MOW	Mediterranean Outflow Water.
MW	Molecular weight.
NADW	North Atlantic Deep Water.
OM	Organic matter.
OMEX	Ocean-Margin Exchange.
PSPM	Permanently suspended particulate material.
PTFE	Polytetrafluoroethylene.
PVP	Polyvinylpyrrolidine (wetting agent used on polycarbonate track-etched filter membranes).
R	Cross flow filtration retentate fraction.
RACS	Rivers and Coastal study (part of LOIS).
RO	Reverse osmosis.
SBD	Sub-boiling distilled.
SEM	Scanning electron microscope.
SLEW	Estuarine water reference material (National Research Council of Canada).
SHMP	Sodium hexametaphosphate.
SPM	Suspended particulate matter.
SSA	Specific surface area.
TEM	Transmission electron microscope.
TMZ	Turbidity maximum zone.
TSPM	Temporarily suspended particulate material.
UV	Ultra-violet.
1643D	Trace metals in seawater standard reference (for river water). Supplied by NIST, standard reference materials program, Maryland.
0.4_f	0.4μm filtered (i.e. total dissolved).

CHAPTER 1 : General Introduction

1.1 What are colloids?

Natural colloidal material is an operationally defined particulate fraction lying in the size range of 1-400nm diameter (assuming spherical structure). However, this size definition is not necessarily uniformly accepted. For example, a definition of the colloidal fraction of 1-1000nm has also been used (Wells and Goldberg, 1994; Buffle and Leppard, 1995a, b). For the purpose of this investigation colloids will be defined as microparticles that will pass through a 0.4μm filter but are retained by 10,000 molecular weight (10KDaltons) or 0.01μm filter cut-offs. This is a purely filtration fractionation definition and therefore colloids are included operationally in the "dissolved" fraction (<0.4μm) of water column constituents. Trace metal species passing through 10,000 molecular weight or 0.01μm filters are classed as "truly dissolved".

Such generally accepted definitions in trace metal and filtration protocols do not specify colloidal composition. Colloidal material can vary widely in its composition, including particles comprised entirely of aluminosilicate lattice fragments, manganese and iron oxyhydroxides and organic matter (precipitated humic/fulvic acids and detritus) or an amalgamation of all or some of these components. Living entities such as bacteria, viruses and algae can also be considered colloidal (Figure 1.1). Colloidal particles do not settle by gravity and are kept in suspension by Brownian Motion effects.

Despite the compositional variation, colloidal material as a whole has the geochemically significant property of large surface area to volume ratio. The potential for adsorption to, and transport of dissolved species by these colloidal and aggregate phases has only recently been realised. Previously, the operational cut-off point for "particulate" and "dissolved" phases discounted the effect of the role of colloids as particles in aggregation/ disaggregation transformations and the consequent implications of these processes for transport and fate of species in natural waters.

Figure 1.1: The nature and size fractions of common particles in aquatic systems (from Buffle et al., 1992).

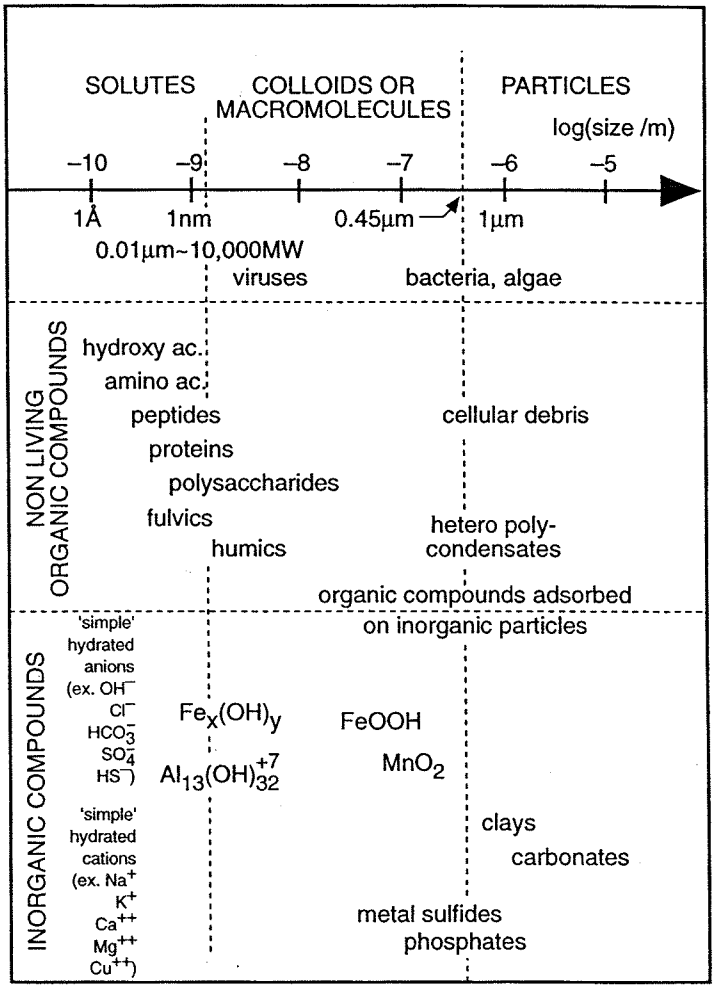

In estuarine and coastal waters, trace metals and surface active species or pollutants in particular are subjected to interactions with colloidal material. These areas are at present in the front line of natural and anthropogenic inputs of trace metals into the marine environment. As a result, if the role of colloidal material in dictating the fate of trace metals in these environments is to be understood, so must the geochemical transformation processes, recycling and other reactions that involve colloid/metal associations.

1.2 Colloidal Surface Properties:

The composition of colloidal material can be extremely variable. In such a particle pool the diversity of sites available for adsorption of metal ions and high concentration of such ligands is geochemically significant. Despite this heterogeneity in the composition of colloids, in natural waters the universal nature of dissolved organic matter can lead to the surfaces of colloidal material becoming remarkably chemically uniform due to an amorphous coating of natural organics (Hunter and Liss, 1982). The small variation in the coagulation probability constant and consistently negative charges for colloidal material determined under natural conditions indicates that solid surfaces are made more homogenous by their coating of organic material than would be expected from their variable mineral composition (Filella and Buffle, 1993). It has been observed that both natural and synthetic surfaces rapidly acquire organic coatings when in contact with seawater (Neihof and Loeb, 1972; Newton and Liss, 1989). This can lead to surprisingly characteristic geochemical and trace metal interaction processes and rheological behaviour associated with colloids in estuarine and coastal environments. To improve knowledge of the role of colloidal material in the marine environment the characteristics, surface chemistry and interactions of such a particle population must first be better understood.

All surfaces when immersed in a polar liquid such as water acquire a surface charge due to ionising surface groups, organic matter coatings, selective ion adsorption/desorption or ion exchange (Moir, 1981). Most materials acquire a negative charge in waters of natural pH. Ions that participate in the surface charging are known as potential

determining ions. These adsorb beyond the inner Helmholtz plane (Figure 1.2) and become part of the surface structure. Trace metal species may be included in this group. Via these mechanisms a colloidal dispersion/particle surface may have a net surface electrical charge due to the imbalance of its component positive and negative charges. This surface charge may result in the orientation or a distribution of polar molecules in proximity to the particle surface. Ions of opposite charge (counter-ions) are attracted to the colloidal surface, whilst, to a lesser extent, ions of a like surface charge (co-ions) are repelled. Figure 1.2 illustrates the resulting electrical double layer that forms around a negatively charged colloid and leads to its stabilisation.

The electrical double layer is often regarded as a two layer model. An inner region including the Helmholtz and Stern planes an outer and diffuse region in which the ions are not adsorbed but distributed according to the influence of electrostatic forces and thermal motion. The resulting model is based on the studies of Gouy (1910), Chapman (1913), Stern (1924) and Grahame (1947).

The inner Helmholtz plane represents the centres of specifically adsorbed ions held by chemical bonding. The outer Helmholtz or Stern plane represents the closest approach of hydrated counter-ions in solution. In both these layers the counter-ions are strongly associated with the particle and maintain their integrity as the particle moves through the fluid medium. Most of the surface charge is neutralised by the tightly bound counter-ions in the Stern layer. The remaining charge is balanced by the diffuse or Gouy layer of counter ions extending out into the dispersion medium. Somewhere between these two layers lies an interface known as the shear boundary, see Figure 1.2. Using micro-electrophoresis the potential at this boundary can be calculated and is called the zeta (ζ) potential. The magnitude of the zeta potential is a function of the surface charge, concentration, and valency of the counter -ions present in the system. It also gives an indication of the thickness of the diffuse double layer and as will be explained later, a measure of the stability of a colloidal dispersion (Shaw, 1992) .

Figure 1.2: The structure of the electrical double-layer according to the Gouy-Chapman-Stern-Grahame model (from Moir, 1981).

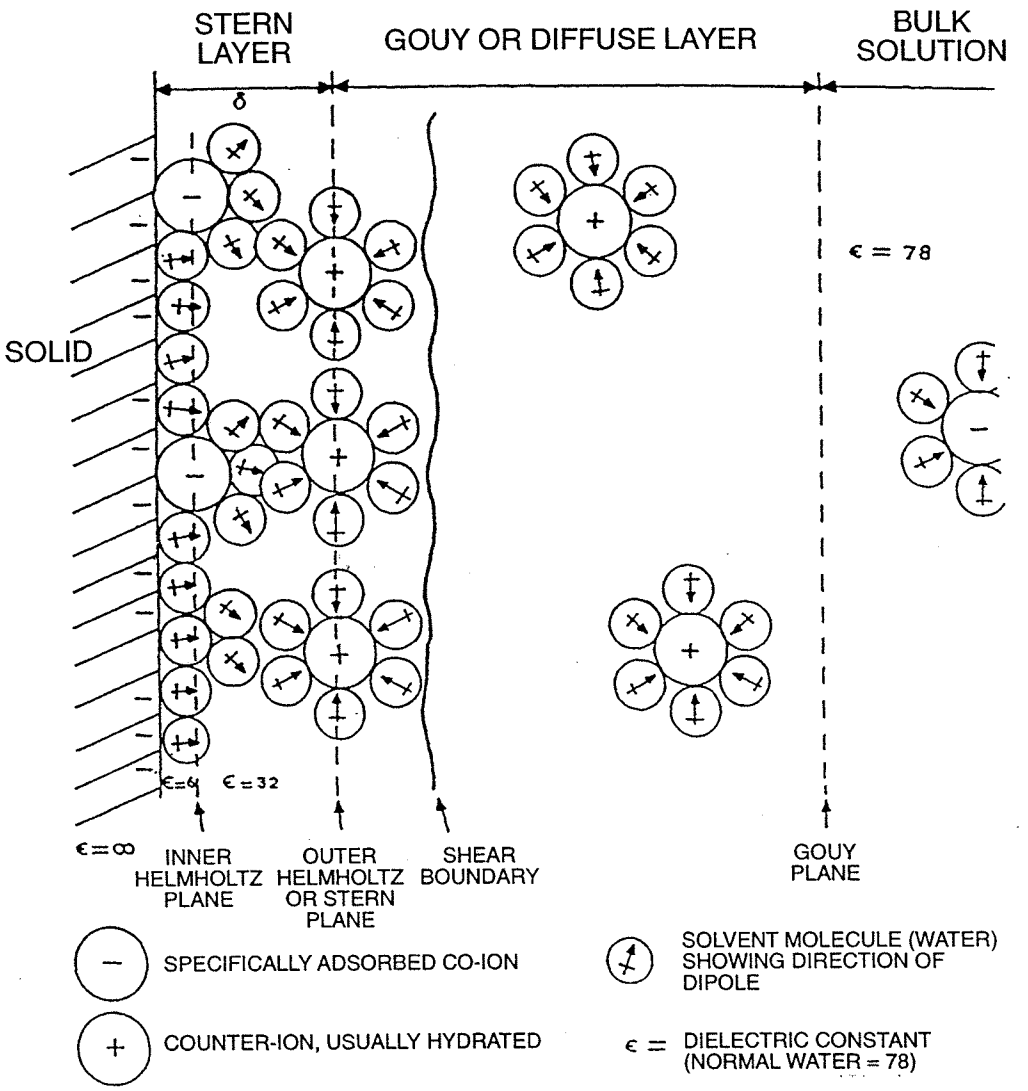

1.3 Colloid stability:

Stability of a colloidal dispersion is the net effect of opposing particulate forces;

- Van der Waal attractive forces (Va) which act to promote instability and aggregation.
- Inter particle electrostatic repulsion (Vr) of like charged particles act to maintain stability.

The balance of these forces and resulting stability/instability of a colloidal dispersion has been described by Deryagin and Landau (1941) and Verwey and Overbeek (1948). This theory (DLVO theory) of colloidal suspension stability looks at the energy changes that occur when two particles approach each other in a suspension. According to the DLVO model the stability of a system is represented by a potential energy versus particle distance approach diagrams. As can be seen in Figure 1.3, Va, the Van der Waal attraction force increases very rapidly with reducing inter-particle distance, whilst the double layer repulsion force, Vr, increases more slowly. The combination of these opposing forces is shown in curve Vt. At short range the Van der waal forces predominate, and there is net attraction between particles. At intermediate distances there is a maximum in repulsive force (Vmax). This maximum in repulsive potential energy forms a barrier to aggregation.

Aggregation can occur to two degrees;

- Coagulation: This is strong aggregation since the particles are strongly held together by attractive forces inside the primary minimum. High shear conditions are required to break up these aggregates.
- Flocculation: This occurs into the secondary minimum and the energies involved are much smaller. Here, the separation between particles is greater so bonding is weaker and aggregates are looser and larger. Flocs can be dispersed by light stirring forces, turbulence and resuspension shear (Shaw, 1992).

Figure 1.3: Potential energies between particles; showing energy barrier, primary minimum and secondary minimum (from Moir, 1981).

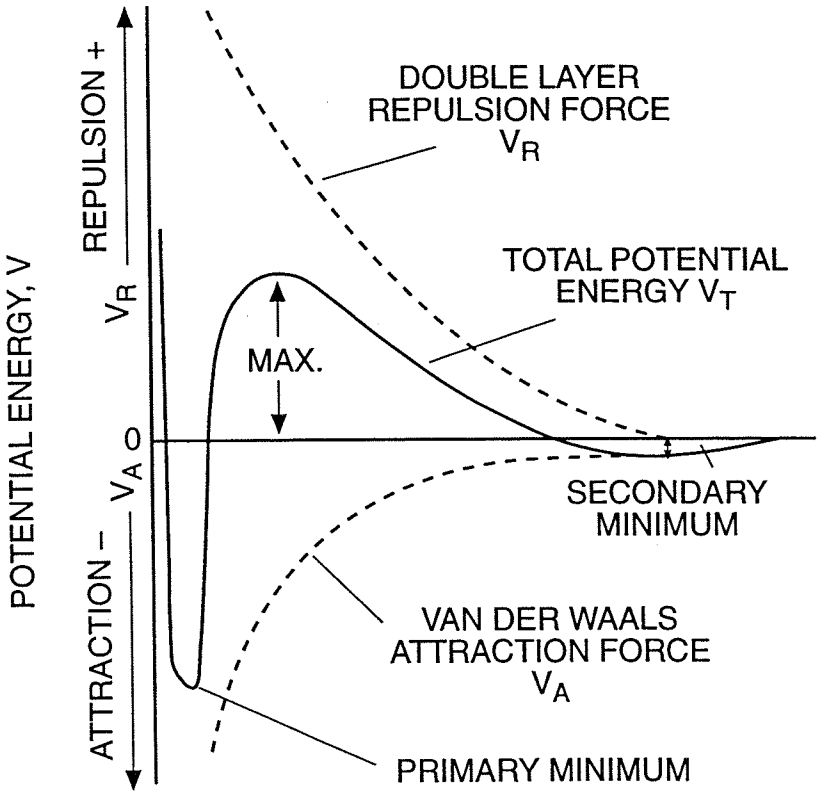

1.4 Colloid aggregation and disaggregation in natural waters:

In natural waters the stability of colloidal systems can be disrupted by a number of mechanisms that effectively lower the repulsive energy maximum or enable interacting particles to overcome it. Aggregation results. Coagulation (aggregation into the primary minimum) has been described by Edzwald (1972) as a two step process:

- destabilisation.
- particle transport.

The destabilisation step is concerned with eliminating or nullifying the repulsive energy barrier that exists between two colloidal particles in an aqueous system. Particle transport is concerned with inducing interparticle contact once a suspension has been destabilised via processes such as;

- Brownian Motion
- fluid motion/shear
- differential settling

1.4.1 Destabilisation:

Suspension destabilisation can be accomplished by four distinct mechanisms:

(i) adsorption to produce charge neutralisation .

Hydrolysed metal species, organic polyelectrolytes and/or surface active materials may be absorbed onto colloidal surfaces causing charge neutralisation. Specific chemical interaction between the adsorbing species and the surface active site on the colloid may overshadow the coulombic effect in bringing about particle destabilisation. A coagulant species having a positive charge can chemically adsorb onto the surface of a negatively charged colloid. At a certain concentration sufficient adsorption occurs to reduce the repulsive energy barrier that exists between the particles and destabilisation of the suspension results. It should be noted that higher concentrations of the same coagulant species can lead to sufficient surface adsorption as to reverse the colloid charge and cause restabilisation of the suspension.

(ii) adsorption to permit inter-particle bridging (Lamer and Healy, 1963) .

Anionic or non-ionic organic polymers attach to one or more adsorption sites on a particle. Parts of the polymer chains that extend into the bulk solution can make contact with other colloidal material, forming bridges. Under these circumstances the effects of the energy barrier are nullified via polymeric particle bridging. This process also effectively increases the target area (cross- sectional area) of a colloidal particle which will in turn enhance the frequency of particle collisions and therefore aggregation processes. The extent of aggregation by this method depends on the number of sites occupied by the organic polymer. If too few sites are occupied then the inter-particle bridging may be disrupted by shear from fluid motion. Conversely, if more sites are bridged, the free sites available for polymer adsorption become limited and so does aggregation. Hence, at polymer concentrations higher than the optimum, colloidal restabilisation may occur.

(iii) enmeshment in a precipitate of a metal hydroxide.

If chemical conditions are such that favour rapid precipitation of metal hydroxides, there may be a linked removal of colloidal material in such a precipitate.

(iv) double layer compression.

Suspension destabilisation by compression of the electrical double layer is postulated to be the primary mechanism for destabilisation of colloidal particles in estuarine systems. The repulsive energy barrier that exists between colloidal material in freshwater (low ionic strength) is reduced as the particles are transported into waters of increasing ionic strength (increasing salinity). The increase in electrolyte concentration and species such as Ca^{2+} or Mg^{2+} acts to compress the electrical double layer. As the diffuse layer shrinks closer to the particle surface, the barrier to closer particulate encounters is diminished and aggregation can occur as Van der Waal attractive forces become dominant. It has been shown that an increase in salinity to 3 is enough to cause complete destabilisation of a colloidal dispersion due to the reduction in double layer thickness to approximately 1nm (Hunter and Leonard, 1988).

The specific ability of an electrolyte to cause destabilisation of a colloidal dispersion (indicated by its critical coagulation concentration) is connected to the electrophoretic mobility of particles involved and the charge number (valency) of the electrolyte co-ions, concentration of the dispersion or specific character of the ions involved. This is the basis for the Schulze-Hardy rule.

1.4.2 Particle transport:

Once destabilised, aggregation of a colloidal suspension can occur by a number of mechanisms that bring unstable particles into contact. Primarily they are;

- Perikinetic conditions: Brownian motion.
- Orthokinetic conditions: fluid shear, differential settling.

For particles in the colloidal size fraction, perikinetic conditions are primarily important as these particles are too small to "see" larger scale turbulence/shear effects.

Under both conditions however, the rate of colloidal aggregation is a function of:

- rate of particle/particle interactions and therefore particle concentration.
- collision efficiency (the probability that a collision will have sufficient energy to overcome the repulsive potential energy barrier into the primary minimum or enable sufficient Van der Waal attraction to occur).
- colloidal target area (increases rate and efficiency of collisions).

Current coagulation theory has its origins in the work of Smolukowski (1917) who described aggregate growth as the irreversible adhesion of colliding particles in monodisperse systems. Many of the parameters influencing aggregation under such a system are applicable to natural polydisperse systems. However, the particle size spectra of natural colloidal systems and the multidirectional processes (aggregation/ disaggregation) limit the applicability of models derived from monodisperse abiotic systems. Steric stabilisation is one such complication of natural systems that limits colloidal aggregation theory.

1.4.3 Steric stabilisation :

As was discussed earlier, in natural waters the presence of suspended species in the water column can lead to stabilisation of colloidal dispersions even under high ionic strength conditions. There are several possible mechanisms for this steric stabilisation effect (Shaw, 1992):

- encounters between particles may involve desorption of stabilising agent at the point of contact. The positive free energy of desorption corresponds to particle/particle repulsion and enhanced stability.
- upon collision the adsorbed layers of particles may be compressed without penetration. This "denting" mechanism reduces the configurations available to the adsorbed molecules. Stability is enhanced by an elastic effect as a result of a decrease in entropy and increase in free energy. This mechanism however, may not be significant in reality.
- local increases of the concentration of polymer segments may result from interpretation of adsorbed layers between particles. This may lead to either an attraction or repulsion depending on the polymer-polymer/polymer-dispersion medium interactions. Elastic repulsion will also operate if significant interpenetration occurs.

Additional processes may act upon organically coated particles to inhibit their inter-particle approach and promote stabilisation. Close approach of colloids can be opposed either by osmotic effects (increase in concentration of adsorbed molecules) or a volume effect (free energy increase due to restriction of the potential configurations of adsorbed molecules). The size, chemical structure and adsorption density of the molecules involved will dictate the magnitude and range of these effects. Only if there is sufficient density of adsorbed molecules can particle separation beyond the range of Van der Waal force be maintained (Ottewill, 1977).

1.4.4 Sensitisation:

In contrast with steric stabilisation natural colloidal dispersions can be sensitised to aggregation by the presence of small concentrations of materials which, if present in larger amounts, would act as stabilising agents. For example: if colloidal particles and coagulant species in the bulk solution are oppositely charged, sensitisation results when the concentration (and adsorption) of the species is such that the charge on the colloids is neutralised. Stabilisation would result at higher concentration because of a reversal of the charge on the particles and increasing steric effects.

Similarly, at low concentrations, surface active chemical species may at first form an adsorbed layer on colloidal particles with any lyophobic (liquid hating) part orientated outwards, thus sensitising the dispersion. At higher concentrations a second, oppositely orientated layer would then give protection and therefore stabilisation.

Long chain species such as organic polymers can bring about sensitisation in the form of loose flocculation by a bridging mechanism in which the polymers are adsorbed with part of their length on two or more particles (Healy and Lamer, 1964; Gregory, 1975). Such flocculation normally occurs over a narrow range of polymer concentration because at higher concentrations, protective action is obtained, since bridging can only occur through particle collisions under conditions where further adsorption of such a polymer chain species is possible.

1.5 Implications of colloidal processes for trace metal transport and cycling:

The fate of trace metal species in natural waters is, to a large extent controlled by sorption processes and the dynamics of particles (including colloids). As metal species become associated with colloidal material through adsorption, surface precipitation or diffusion into particle interiors, the fate of the sorbed species become inextricably linked with the cycling and destiny of the particles.

1.5.1 Colloid / trace metal interaction models:

i) Schindler "Zero order" model (1975):

The relative rate of removal of trace metals from seawater is related to the intensity of interaction between trace elements and particle surface sites, given a constant particle flux. This model connects solution phase reactions, adsorption and trace metal scavenging. It introduces the concept that marine particles (colloids) may compete as chemical species against dissolved ligands for complexation of trace metals. As such, the colloidal fraction which has significantly larger reactive surface area per unit mass, and abundance as observed by Moran and Moore (1989) must have a significant role in trace metal scavenging.

Balistrieri et al (1981) illustrated that the critical parameters controlling the distribution of trace elements between solution and particulate or colloidal phases were;

- type of surface site
- site density
- site/metal interaction intensity.

It has been shown by many investigators that trace metals are closely associated with colloidal fractions in seawater. Niven and Moore (1987) examined the partitioning of ^{234}Th added to seawater among dissolved, colloidal and particulate fractions. They found that up to 64% of the total ^{234} Th was colloidally (1nm-0.2μm) associated. Similarly, according to Baskaran et al. (1992) up to 80% of natural ^{234}Th in Gulf of Mexico water

is found in the colloidal form. Such findings have illustrated the significance of the scavenging role that colloidal material can play in oceanic and coastal waters.

ii) "Brownian/colloidal Pumping" model - Honeyman and Santschi (1989):

Honeyman and Santschi maintained that the distribution of particle sizes in natural systems is the result of a number of processes which bring particles together (aggregation mechanisms) or break aggregates apart. As particles are transferred through the particle spectrum trace elements and radionuclides associated with those particles (sorbed or components of the particle matrix) are also moved through the particle fractions. Rate of trace metal transfer depends on the rate of particle progression through the spectrum and levels of trace metals associated with those particles. Figure 1.4 a, b, and c depict the component processes involved in colloidal pumping.

a) Trace elements sorb onto colloidal particles:

The sorption of trace metal species (Me) onto macroparticles and colloids is rapid. Characteristic complex formation times are in the order of milliseconds to minutes (Honeyman and Santschi, 1989). The particle / solution trace element distribution, and therefore the metal/particle association constants for macroparticles (Kf) and colloids (Kc) respectively, are dependant on the general solution conditions (pH, ionic strength, temperature), the concentration of metal binding sites available and the intensity of the Me / particle surface interactions.

b) Aggregation:

Colloidal particles are transferred up the particle size spectrum to larger aggregates by some coagulation mechanism (Brownian Motion, shear, differential settling, polymer bridging). Here, colloidal particles may aggregate with each other or, more likely, attach to large pre-existing aggregates (larger target area).

Metal sorption can also occur directly to sites on colloids or aggregates.

Figure 1.4: Component processes of colloidal pumping (from Honeyman and Santschi, 1989). Refer to text for explanation of stages a to c.

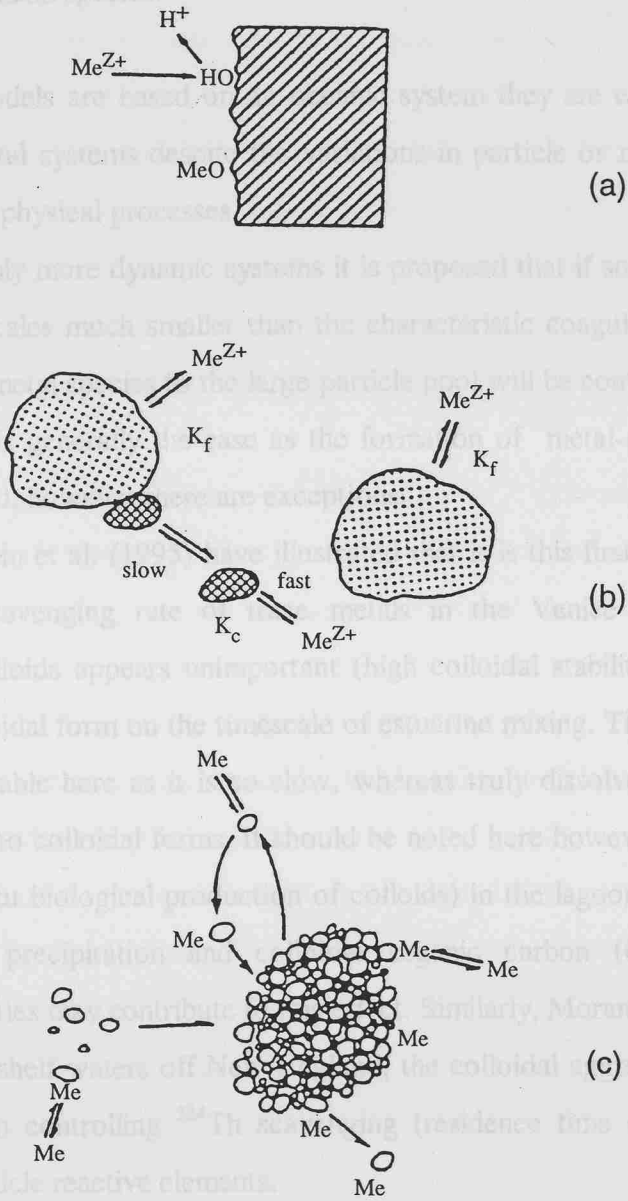

c) Appearance of Me species in macroparticulate pool;

The rate of appearance of a metal species as macroparticulates depends on:

- amount of sorbate associated with the colloidal fraction.
- rate of transfer of colloids to the macroparticle pool via aggregation.

Subsequent sedimentation of large macroparticles may govern the fate of the originally colloid associated metal species.

Although these models are based on an oceanic system they are equally applicable to estuarine and coastal systems despite the variations in particle or metal concentrations and more transient physical processes.

In these considerably more dynamic systems it is proposed that if sorptive equilibrium is achieved on timescales much smaller than the characteristic coagulation time, then the rate of transfer of metal species to the large particle pool will be controlled by the rate of aggregation. This is generally the case as the formation of metal-colloid complexes is comparatively rapid, however there are exceptions.

For example; Martin et al. (1995) have illustrated that it is this first step that ultimately determines the scavenging rate of trace metals in the Venice Lagoon. Here, the coagulation of colloids appears unimportant (high colloidal stability) and trace metals remain in the colloidal form on the timescale of estuarine mixing. The colloidal pumping step is not observable here as it is so slow, whereas truly dissolved metal species are rapidly converted to colloidal forms. It should be noted here however that high primary productivity (in-situ biological production of colloids) in the lagoon, formation of fresh colloids by Mn precipitation and colloidal organic carbon (COC) maximum at intermediate salinities may contribute to this effect. Similarly, Moran and Buessler (1993) suggested that in shelf waters off New England, the colloidal aggregation step may not be rate limiting in controlling ^{234}Th scavenging (residence time of 0.5 days) and by analogy other particle reactive elements.

It is clear that the characteristics of colloidal pumping and its effect on metal species transformation and transport is largely determined by the physiochemical features of the waters in which the colloids are dispersed (Martin et al., 1995).

1.6 Use of natural radiotracers to investigate colloidal scavenging of metals:

Due to their strong chemical reactivity and in-situ radiogenic sources naturally occurring thorium isotopes (^{234}Th, ^{228}Th, ^{230} Th) are useful tracers for studying trace metal scavenging and particle dynamics. Rates of scavenging can be quantified by measuring the disequilibrium between the parent and daughter nuclides that results from the removal of thorium from the water column on suspended and sinking particulate matter. ^{234}Th especially, with a half life of 24.1 days is an excellent tracer for quantifying rates of dissolved metal/ particle interactions on diurnal time scales (Moran and Buessler, 1993). Many investigations have used thorium and other tracers in conjunction with sequential extraction and ultrafiltration techniques to determine trace metal scavenging rates and illustrate that particle reactive elements are involved in the dynamic cycles of aggregation/disaggregation of particles in the water column of coastal marine systems.

Using ^{238}U /^{234}Th disequilibria Moran and Buessler (1992) determined a mean residence time of colloidal ^{234}Th with respect to aggregation into small particles, of 10 days. This is a factor of 6 less than for the dissolved (<0.4μm) pool. It is suggested that macromolecular colloidal matter has a short residence time and rapid turnover in the marine environment. In conjunction, the investigation of partitioning of radiotracers into colloidal fractions (Baskaran and Santschi, 1993; Moran and Buessler, 1993; Benoit et al., 1994) has clarified why colloidally associated trace metals will behave differently from species which are truly dissolved or associated with large settleable particles (Honeyman and Santschi, 1992). The processes of adsorption of trace metals onto colloidal material and coagulation of that material into macroparticulates helps explain these findings to date. In more recent studies, a direct approach to understanding the exact kinetics of aggregation processes has been adopted. For example, Stordal et al. (1996) used ^{203}Hg, a highly particle reactive radiotracer, to label colloidal material and monitor its progression within a particle population.

1.7 The Partition Coefficient and "Particle Concentration Effect":

The distribution of metals between dissolved and particulate phases is described using the partition coefficient (Kd)(Olsen et al., 1982);

$$Kd = \frac{C_p}{C_d} \qquad \text{Equation 1.1}$$

where C_p is the concentration of adsorbed metal per unit mass of suspended matter and C_d is the concentration of dissolved metal per unit mass of seawater.

Before the significance of the colloidal size fraction in trace metal geochemistry was realised, the operationally defined dissolved/particulate cut-off of 0.4μm included colloids in the dissolved phase. As result when looking at Kd, a significant fraction of trace metals appear in the "dissolved" phase despite being associated with colloidal particulate fractions. These metals would therefore be subject to processes controlling colloidal geochemistry. This colloidal inclusion can affect experimental determinations of sorption binding constants or conditional parameters such as Kd.

A possible consequence of this is the "Particle concentration effect" which is the observed decrease in the value of apparent partitioning constants with increasing particle concentration. Although this may be an artefact of experimental systems it also reflects real changes in the distribution of sorbed species in natural systems with differing particle concentrations (Honeyman et al., 1988).

There are two approaches adopted to explain this effect;

- Particle-particle interactions produce an inter-particle environment that is unfavourable to the formation of surface complexes. The greater the particle concentration, the greater the frequency of particle interactions and equilibrium is shifted progressively towards the solution phase species i.e. reduction of the number of surface sites as effective surface area decreases with coagulation (Honeyman and Santschi, 1992).

- The dissolved phase contains truly dissolved and also colloidal trace metals, and therefore trace metal labelled colloidal material contained in the "dissolved" phase reduces the partitioning constant from its "true" value. The extent of Kd reduction is determined by the intensity of trace metal binding (loading) on the colloidal material and the amount of colloidal material present.

Improvement in sequential filtration and cross flow filtration techniques has allowed the definition of metal species as filter retained, colloidal and truly dissolved fractions. The differentiation of these fractions has allowed the definition of conditional partitioning constants for colloidal (Kc) and filter retained (0.4μm) fractions (Kf). Kc and Kf also describe the relative affinity of any metal species (Me) for these two particle pools.

$$Kc = \frac{[Me_c]}{[Me_d] \cdot C_c} \qquad Kf = \frac{[Me_f]}{[Me_d] \cdot C_f}$$

Where:

C_c and C_f are the mass concentrations of filter passing (colloids) and filter retained particles respectively (kg L^{-1}).

Me_c is the sum of all colloidally associated metal species (M).

Me_d is the sum of all truly dissolved metal species (M).

Me_f is the sum of all metal species associated with filter retained particles.

1.8 Applications to estuarine and coastal environments:

The original models and research examining the dynamics and significance of colloidal material have been predominantly concentrated in oceanic waters (Moran and Moore, 1988a and b; Moran and Moore, 1989; Moran, 1991; Wells and Goldberg, 1991; Moran and Buessler, 1993; Wells and Goldberg, 1994). Wells and Goldberg (1994) estimated that the total available surface area attributable to small colloids (5-200nm) from the upper water column of the North Atlantic and Southern oceans is greater than $18m^2$ per m^3 of seawater. Colloidal particles observed at concentrations of 10^6-10^7 particles ml^{-1} in the North Pacific and off Nova Scotia (Wells and Goldberg, 1991) would have a calculated surface area of 90-$226m^2$ assuming spherical morphology. Additionally, the size spectra of small colloids in the open ocean shows increases in colloid numbers with decreasing size (often logarithmic). This finding and the fact that sub micron colloids that have largest surface area / mass ratios are most abundant in natural systems [possibly half or more of the total particle mass; (Moran and Moore, 1989)] identifies colloidal material as a significant reservoir of surface sites potentially available for complexing particle reactive metals.

In contrast to the oceanic environment, coastal and estuarine regions with characteristic high energy dissipation rates and relatively high particle concentrations and fluxes have not been investigated until more recently. This has mainly been driven by a natural progression of investigation from oceanic to coastal waters but also by improvement in techniques of ultrafiltration and heightened awareness of the increased importance of colloidal material under estuarine and coastal conditions.

1.8.1:Colloidal/ particle behaviour in estuarine systems:

Estuaries in particular are areas where particulate phases play complex but fundamental roles in trace metal cycling. Although there is sparse quantitative data on colloidal composition and loadings in estuaries (Baskaran and Santschi, 1993; Benoit et al., 1994) they are recognised as a significant part of the particle spectrum.

Particulate composition in estuaries can be a heterogeneous mix of mineral phases (clays, quartz, feldspar, carbonates) derived from coastal or catchment erosion. In addition, distinct and biogenic phases can be produced in-situ by biological production and flocculation mechanisms. The particle population is greatly affected by the presence of sometimes high concentrations of terrestrial and marine derived organic matter (OM). The exact nature and effect of OM on particle and colloidal behaviour in estuarine systems is not yet known. Organic matter can coat mineral particles and colloids along with Fe and Mn oxyhydroxides. The nature and charge (usually negative) of this particle/colloid and water interface will affect the nature of trace metal association.

Transport of particulate or colloidal material within estuaries is non-conservative due to the destabilisation, aggregation and sedimentation effects enhanced by ionic exchange and salinity changes. The effects of flocculation on particles, colloids (especially Fe) and organic material have been observed in many papers by Sholkovitz (Sholkovitz, 1976; Sholkovitz, 1978; Sholkovitz et al., 1978; Sholkovitz, 1979; Sholkovitz and Copland, 1981). Particles/colloids and particle reactive trace metals may be subject to many resuspension and flocculation/sedimentation cycles which may lead to their retention within the estuary for longer than the water body itself. For example: the residence time of suspended particles in the Humber is estimated at 18 years (Turner, 1990) whereas the freshwater flushing time is estimated at 40 days.

Many estuaries contain a turbidity maximum zone (TMZ) which is a region of elevated suspended particulate mater and is thought to be generated by estuarine gravitational circulation (Allen et al., 1980). In many estuaries the TMZ is maintained by tidally induced periodic resuspension of local sediment (spring/neap tidal effects) and up estuary transport of resuspendable material by tidal asymmetry (Millward and Turner, 1995). Induction of flocculation by ionic strength effects may also play a significant role. Particles in the TMZ have significantly elevated residence times (~1.4 years in the Tamar-Bale et al., 1985) compared to estuarine flushing times.

The TMZ has been identified as a region of effective particle size selection and coincidentally particle specific surface areas (SSA) as determined by gas adsorption techniques have been shown to be at a maximum in this region (Martin et al., 1986).

Variation in particle specific surface areas between estuaries has been linked to the reactive proportions of carbon to iron and manganese in TMZ particles (Millward et al., 1990). The increase of particle specific surface area within this zone perhaps indicates the presence of significant populations of colloidal material but this has not been confirmed by particle size spectrum analysis. The causes of the SSA maximum coincident with the TMZ has been suggested as size selection or disaggregation of particles, precipitation of fresh Fe-Mn phases or depletion of particulate organic carbon. Inevitably the TMZ is a highly localised region with a very significant scavenging potential whether colloidal species are important or not. Recently, particle microporosity investigation of estuarine particles has indicated that most of the internal volume of the pores in particles is contained within the size range <5nm illustrating that SSA and particle size alone are not responsible for the extent of metal ion adsorption.

Particle dynamics and turbulent mixing could significantly affect trace metal scavenging rates by colloidal pumping mechanisms. Kinetic energy in coastal environments is mostly dissipated near to the sediment water interface thereby causing impaction, coagulation and resuspension of particles. Energy dissipation and therefore shear coagulation is consequently higher near the sediment/water interface than in the water column. This source of particulate and colloidal material, linked to resuspension mechanisms may be more important for redox sensitive and particle reactive trace metals. In coastal and estuarine areas of varying energy dissipation, particle coagulation rates and therefore trace metal transfer may be dominated by turbulent shear above the sediment water interface (Honeyman and Santschi, 1992), or by Brownian mechanisms in the water column where energy dissipation is lower.

Compared to the ocean environment, the sources and processes of transformation of colloidal material in coastal and estuarine environments may vary more greatly on spatial and temporal (spring/neap, seasonal) scales. In many estuaries, the TMZ is generally shifted downstream during the winter or during low/neapier tides due to enhanced/predominant river flow. During river spates the TMZ may also be augmented by remobilization and downstream transport of sediments deposited during lower flows (Millward and Turner, 1995).

The exact processes controlling colloidal population size and dynamics have not yet been identified, mainly due to severe difficulties in colloidal characterisation and measurement. However, the assumption that processes controlling larger particles in the colloidal spectrum are also significant for temporal and spatial changes in colloidal populations is probably reliable until more detailed studies exist.

Eisma et al. (1991a) looked at the particle size of suspended matter in some West European estuaries and found no clear relation with particle concentration. However, Eisma and Li (1993) observed systematic alteration of floc sizes during the tidal cycle in the Dollard estuary. They suggested that this was a result of floc settling at slack tide, resuspension during early ebb and flood, flocculation of fine particles into larger ones at all stages of the tide and deflocculation of large flocs during settling. However, this work did not look at the colloidal fraction of the particle spectrum and there is a significant gap in present knowledge of the spatial and temporal distribution of colloidal material in estuarine systems and its association with trace metal species. It would follow that flocculation and deflocculation would also produce concurrent cycles of colloidal material over similar tidal periods but there is insufficient evidence to accept this hypothesis and it is likely that cycles of flocs would be different from colloidal particles as they are larger and far more weakly bound aggregates. It was observed (Eisma et al., 1991; Eisma and Li, 1993) that maximum floc size coincided with maximum suspended matter concentration (maximum collision frequency) and erosion of sediment from mud flats in several estuaries. Overall, it is clear that the dynamics and morphology of an individual estuary may, to a great extent affect the particle population in the water column (colloidal and macroparticulate) and therefore the transportation and fate of particle associated trace metals. The ultimate fate of trace metals resident in the particle pool will depend on the strength of flocculation mechanisms and whether the estuarine dynamics result in particle sedimentation or exportation to coastal waters.

Colloidal cycling theory developed for oceanic waters may be applied to coastal and estuarine environments in conjunction with prior knowledge of these systems. Under these circumstances many of the distributions of trace metals observed in such systems can be explained by incorporating colloidal influences into the regime. Benoit et al. (1994) observed a particle concentration effect in several Texan estuaries that indicated trace metal associations with a colloidal fraction as well as the other particulate and

dissolved phases. A 0.7 power dependence of colloid trace metal concentration on the SPM loading was established. Using colloidal theory and analysis of the colloidal fraction they concluded that filtrate trace metal levels in the system were mainly controlled by:

- resuspension of bottom sediments to yield colloidal and particulate metals.
- kinetically controlled partitioning of metals between solution and particles of all size fractions.

From research to date it can be seen that the role of colloidal material as a vector for trace metal species is very complex due to its dynamic nature within the estuarine environment. Figure 1.5 illustrates the dynamic processes controlling metal/ colloid interactions in estuarine and coastal waters. A greater understanding of these controlling processes is needed before the significance of colloidal material and associated trace metal geochemistry can be determined.

Figure 1.5: Component processes controlling trace metal and colloid interactions in estuarine and coastal waters (from Wells and Goldberg, 1994; Fang, 1995).

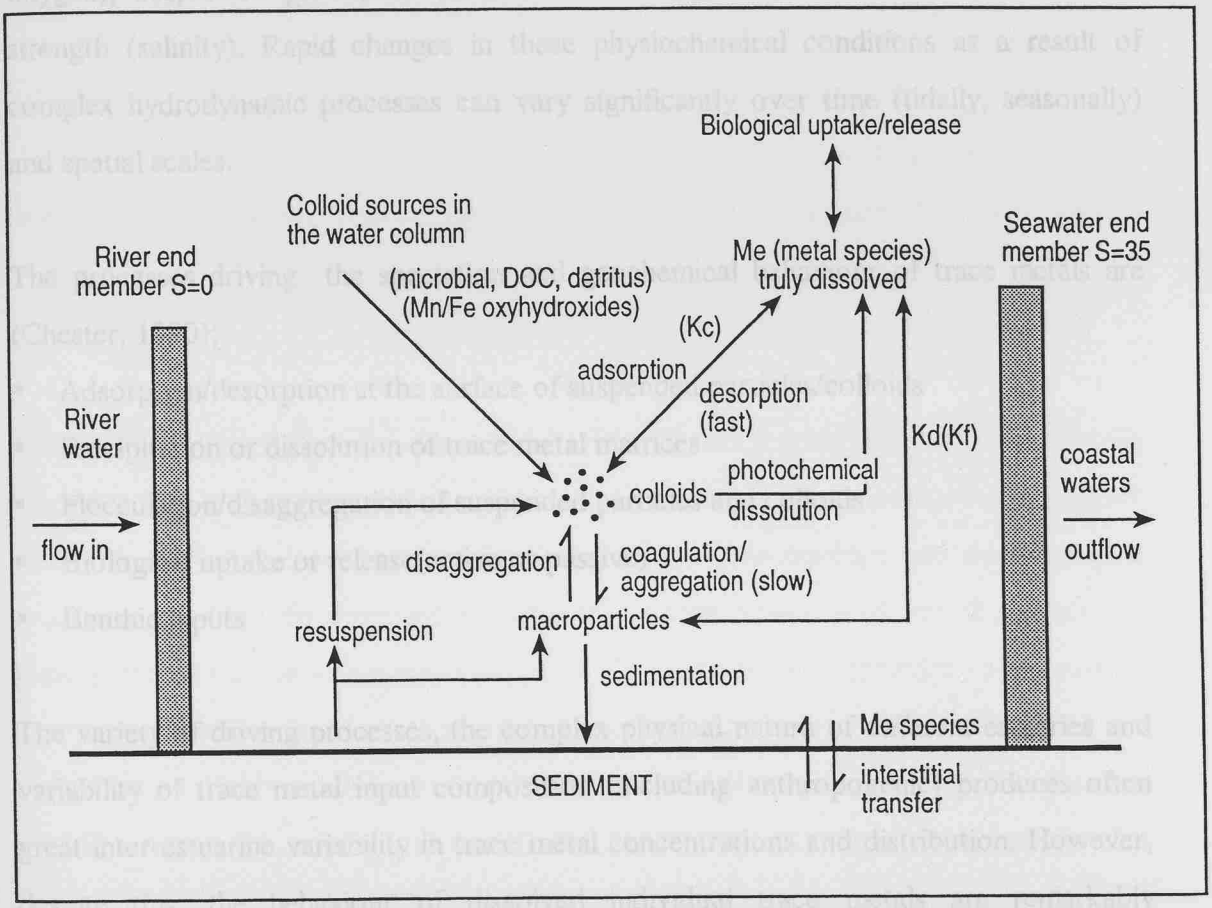

1.9: Trace metals in estuaries:

There is an extensive literature base and understanding of trace metal behaviour in estuaries. Trace metal behaviour in estuaries is dynamic and complex due to rapid changes in physical and biogeochemical parameters that can affect speciation. The master variables that can affect trace metal behaviour and speciation are pH, redox (dissolved oxygen), suspended particulate material concentration and characteristics and ionic strength (salinity). Rapid changes in these physiochemical conditions as a result of complex hydrodynamic processes can vary significantly over time (tidally, seasonally) and spatial scales.

The processes driving the speciation and geochemical behaviour of trace metals are (Chester, 1990);

- Adsorption/desorption at the surface of suspended particles/colloids
- Precipitation or dissolution of trace metal matrices
- Flocculation/disaggregation of suspended particles and colloids
- Biological uptake or release(active or passive)
- Benthic inputs

The variety of driving processes, the complex physical nature of different estuaries and variability of trace metal input composition (including anthropogenic) produces often great inter-estuarine variability in trace metal concentrations and distribution. However, despite this, the behaviour of dissolved individual trace metals are remarkably geochemically consistent.

Several past reviews have summarised the observed behaviour of major trace metals in estuarine systems and the processes affecting them (Fang, 1995; Millward, 1995 and the references there-in). For the purpose of this study the detailed behaviour of each metal in the total dissolved form is assimilated in the context of colloidal trace metal transformations and is discussed in detail in Chapter 4. Mainly, the trace metals measured in this study were chosen for their contrasting geochemical behaviours, especially with

respect to their particle reactivity. The main processes controlling the behaviour of total dissolved metals in the estuarine mixing zone are:

For Fe which is almost entirely colloidal, destabilisation and aggregation effects.

For Pb which is also highly particle reactive, adsorption and desorption at particle/colloid surfaces.

For Cd, mobilisation from particles in the low salinity region and chloro complex formation.

For Mn, scavenging or coprecipitation associated with Fe-oxyhydroxides. Redox behaviour and benthic inputs are also important.

For Cu, Zn and Ni, adsorption/desorption at particle surfaces, complexation with organic material (for Cu), input from resuspension events (porewaters) and changes in riverine signals.

Taking these transformation processes into account and their effect on trace metal speciation, in estuarine studies the reactivity of a dissolved constituent is conventionally interpreted by plotting their concentrations against a conservative index of mixing (Liss, 1976). Salinity is the variable widely used, although the concept and oceanographic principles of salinity becomes approximate at less than a salinity of one. A straight line joining the trace metal concentrations in the riverine and seawater end-members (theoretical dilution line-TDL) indicates conservative behaviour. This implies that the constituent is unaffected by in-situ removal or addition processes, its flux is therefore not modified within the estuary and import and export rates are equal. Relationships that deviate from the TDL indicate non-conservative behaviour and therefore net input or removal of trace metals (Figure 1.6). The main aim is then to identify the nature or process involved in the removal or input. Salinity/trace metal plots may be misleading if addition and removal processes are interacting in different areas of the estuary or if there is temporal variability in the riverine end-member. In these cases the property/salinity plot and assessment of input or removal should be carefully applied.

Figure 1.6: Representation of dissolved property / salinity plot.

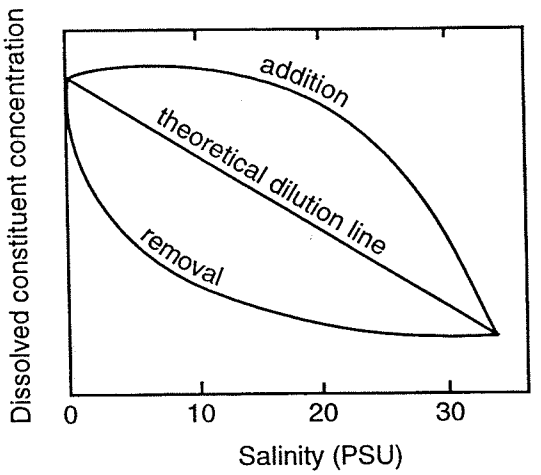

1.10 Colloidal Trace Metals in estuarine systems:

Using ultrafiltration techniques it was demonstrated over a decade ago that "dissolved" iron exists mainly in the colloidal form in marine environments (Boyle et al., 1977; Figueres et al., 1978; Moore et al., 1979). However, due to the problems with conventional ultrafiltration and contamination problems, until much recently, information concerning the distribution and behaviour of colloidal trace metals was still very sparse.

Over the last few years the understanding and amount of studies carried out on colloidal material has increased. This has mainly been a result of the utilisation of ultrafiltration cross-flow filtration systems which allow faster filtration and also reduce contamination. A fuller discussion of filtration effects is available in Section 1.10.1. The CFF ultrafiltration technique has been used to investigate the distribution and cycling of colloidal organic carbon, trace elements and radiotracers but mainly in oceanic environments (Moran and Moore, 1989; Wells and Goldberg, 1991; ; Baskaran et al., 1992; Moran and Buessler, 1992; Baskaran and Santschi, 1993; Guo et al. 1994). More recently, the literature on trace metal and colloidal organic carbon distributions and behaviour in estuaries has increased significantly. Table 1.1 illustrates the diversity of the

environments sampled and protocol implemented over a relatively short period of time. For a more comprehensive comparison of filtration approaches and resulting trace metal concentrations see Buessler et al. (1996).

One of the earliest papers on estuarine environments by Martin et al. (1995) described the colloidal trace metal distributions in the Venice Lagoon Italy. Their findings indicated that 87% of Fe, 58% of Pb, 54% of Mn, 46% of Cu, 34% of Cd and 18% of Ni of "dissolved" trace metal was actually associated with colloidal material. These findings were carried out in a very highly organic environment (18% of organic carbon was colloidal) and as a result when compared to other colloidal trace metal measurements there is often considerable variation (Sanudo-Wilhelmy et al., 1996; Wen et al., 1996; Kraepiel et al., 1997). As colloidal material is in a continuum with larger particle population and is controlled by the same variables that affect inter-estuarine variability it is not surprising that colloidal trace metal and organic carbon partitioning should be so varied over different estuarine conditions. However, this may also be a result of the inconsistent protocol of colloidal cut-off that is used in different studies i.e. 1-10KDa to 0.2 to 0.45μm. This variability in colloidal concentrations and also sample handling differences are discussed further in the next section (1.10.1) and in Section 1.10.3.

As reflected by the total dissolved observations in the past there are certain characteristics of colloidal trace metals that tie in with the observations of total dissolved fractions. The relative affinity of metals for humic substances and their reactivity with particle surfaces appear to determine the amounts of metal associated with colloids. The mixing behaviour of metals along an estuary appears to be determined by the relative contribution of the colloidal phase to the total dissolved pool (Sanudo-Wilhelmy et al., 1996). Despite this general behaviour there is little inter-estuarine consensus in colloidal trace metal partitioning, mainly due to variation in colloidal composition and significance, but also to the further division of colloidal pool into low molecular (~1 to 10KDa) and high molecular weight (10KDa to 0.2/0.4μm) fractions.

Table A1.1: Intercomparison of CFF protocol used by various groups for trace metal and organic carbon analysis in estuarine and coastal waters.

Study	System	CFF Cut-off	Prefiltration.	Cleaning/ preconditioning	water type	concentration factor	recovery	DOC levels
Moran and Moore 1989	Millipore Pellicon $0.464m^2$	10,000MW	0.45µm Gelman mini capsules	No preconditioing for prefiltration. CFF Millipore super-Q Some adorption of Al by CFF system Blanks; 2.5-4 to 1.8-3 nM	Scotian Shelf/Gulf Stream	70-100L to 1-1.5L CF= 18-86	Calc. 74-91% For same CF.	Not determined
Whitehouse 1990	Millipore/ Pelicon plate system	10,000MW (10KDa) 1-2nm $0.46m^2$	>1um large diameter	Milli Q <50% methanol 0.01M HCl recycled 2hrs SW blanks Flushed filtered SW between samples.	Halifax Harbour SW Scotian Shelf N.Atlantic Ocean River	CF=50-100 25-35l/hr permeate lower CF is more sensitive test of system performance Harbour~3.9 River OC higher, CF 5-7 more in colloidal phase and therefore lower recoveries	91-106% (100% within error) shelf and open ocean samples. Harbour <100% (71-86) 72 to 124% overall. River-lower recoveries	shelf 0.5-0.7 mg/l most in ultrafiltn. River 5.8-12 mg/l shelf F values >88% SW intermed.truly and coll. River mostly colloidal.
Benoit et al. 1994	Amicon hollow fibre $0.88m^2$ 13l/min filtrate	10,000MW (10KDa)	47mm nucleopore 0.4 µm P/C (cleaned) 0.5µm polypropylene cartridge	Between samples 1M HCl 10min.recirculated. Milli-Q rinsed.	Six Texas estuaries/ Galveston bay waters. High SPM 1.5-300mg/l	CF= 40 to 200	Colloid digestion Using preservation acid and 60minutes ultrasonics at 60°C. 22% ^{234}Th lost to ultrafiltration cartridge. No mass balance recovery.	6 to 0.5mg/l from fresh to seawater. Non-conservative COC 0.5 to 1.1mg/l (14 to 16% of DOC)

Study	System	CFF Cut-off	Prefiltration.	Cleaning/ Preconditioning	water type	concentration factor	recovery	DOC levels
Martin et al. 1995	Millipore Pellicon cassette system $0.462m^2$	10KDa (~3nm)	0.4µm 142mm diameter	Acid washes Milli-Q, 0.1N HNO_3, preconditioned with 1000ml of sample.	Salinity transect – surface samples Venice Lagoon	CF=10 to 12	Not available for trace metals as colloidal fraction (retentate not directly determined)- colloidal TM by difference. No indication of CFF artifacts. 85 to 98% for DOC.	149 to 425µM TOC
Swarzenski et al 1995	Millipore Pellicon $929cm^2$	10,000MW (x 4 plates)	0.4µm 142mm diameter	0.1M NaOH prerinse with filtered sample	Surface waters Amazon shelf Low discharge	5l to 50-100ml CF= 50 to 100 Very high	River mouth >95% salinity >30psu. Estuary ~87%	Not determined
Buessler et al. 1996 (intercomparison study)	Amicon/ Osmonic spiral wound	1000MW (1KDa)	0.2µm in line	NaOH /HCl /MQ wash	surface coastal and oceanic deep water	Mainly 2 but ranges 4-200 in open ocean Highest breakthrough with high CF and high OC waters	Integrated samples average of 2 as less filter interact. Fe sorption losses as decreases in permeate with time	surface coastal 100uM deep ocean 41uM

Study	System	CFF Cut-off	Prefiltration.	Cleaning/ Preconditioning	water type	concentration factor	recovery	DOC levels
Sanudo-Wilhelmy et al 1996	Filtron	10KDa	0.2µm	10% methanol 0.1N HCl (Whitehouse 1990)	South San Francisco Bay-surface waters Sacremento San Joaquin Rivers	CF=20 CF incresed 10 to 20 gives increase in permeate concentration (Fe, Cu, Ni)-break through, diffusion into permeate	>80% for most metals but Ag,Fe with high colloidal % (>80%) have low recoveries (16 to 89%) lowest where high DOC (~201µM). Cu sometimes low	68-201µM Higher DOC concentrations promote lower recoveries for highly colloidal metals (usually coincident with higher SPM)
Wen et al. 1996	Amicon spiral wound/ hollow fibre 0.88m^2	1-10KDa 20psi.. higher gel buildup.	0.45/0.2µm	Micro/ 0.1N NaOH/ 0.1N HCl/ 20-40l rinse Desalting probs. replacement of SW with RO trace metal changes (from Guo and Santschi 1996) Filtration time vs clean protocol	Trinity River Gulf of Mexico	CF=10 Also effects of progressive filtered volume and CF on permeate concentrations.	overall 88-109% estuarine samples Fe 60-66%(despite cleaning between samples). 1KDa recovery < 10KDa ie more filter interactions.. gel formation more likely.	50mg/l BCF=10 At lower DOC (15mg/l) lower BCF
This study (1996)	Millipore Minitan plate system 4 plates 240cm^2	10 KDa	0.4µm polycarbonate 47mm	Adapted from Martin et al. (1995) System and plates preconditioned with approx 100mls of sample.	Trent/ Humber surface water samples. Variable discharges	CF=1.5 to 2.5 Range of no CF effect (Wen 1996). No investigation of CF and metal concentrations in permeate done on this sytem.	Variable with metal and salinity. Mn, Zn, Ni, Cu usually >90%. Cd can be >100% Pb and Fe lower(~80% and 65%)respectively more colloidal and filter interaction	Tidal reaches: Trent 225 to 778 µM. Lower in higher salinity areas..Humber

1.10.1: Assessment of methods specific to colloidal trace metals and their handling:

Throughout the course of this study there has been increasing debate in the literature on the effects of sample fractionation by filtration on the natural colloidal size spectrum and the impacts that this may have on operationally defined "dissolved" trace metal concentrations. A brief discussion is given here of the pertinent artifacts that may result from sampling, prefiltration, cross flow filtration and analysis as a result of the inherently unstable nature of colloidal fractions and the trace metals associated with them. These issues were in the forefront of any sampling, prefiltration or ultrafiltration protocol developed or implemented during this study for trace metal/colloidal fractionation of natural or experimental samples.

1.10.1.a:Sampling protocol for colloidal material:

Once a water sample is taken from in-situ it becomes a closed system so any directional processes kept in steady state in the natural environment by dynamic exchange processes may act to alter the sample significantly from its original state. The main perturbations that can occur as a result of sampling are;

- Contamination by colloids and/or bacteria from sampling/sample storage equipment or the atmosphere, or loss of colloidal material by adsorption onto a vessel wall.
- Coagulation of the colloidal or macromolecular sample components which modifies the size distribution of the suspended particulate population and also the distribution of associated surface active species.
- Microbial changes which can act to enhance aggregation processes by increasing concentrations of metabolic products such as enzymes or polysaccharides or alter colloidal groups by degradation of non-living colloids.
- Processes such as flotation of colloidal material due to microbubble formation at higher than ambient temperatures can also result in alteration of the particle spectrum.

Total colloidal content of surface waters can be less than 0.1 to 1.0mg/L so contamination and losses can be serious problems. The major source of colloid contaminations in aquatic colloid studies are the filters and frits when filtration is used. Sample perturbations by contamination effects were minimised by careful handling of the original sample (sample bottle prerinsing/preconditioning) and thorough cleaning (phosphate free detergent and mineral acids) of all equipment that came into contact with the sample. Potential contamination from filters and frits was minimised greatly by trace metal cleaning protocols but also by using older frits that have been shown to release fewer particles. Rinsing with "pure water", in this case Milli-Q also reduces the likelihood of inter sample colloid contamination. All sample manipulation was carried out in a clean bench, particle free environment with handling time kept to a minimum. Loss of colloidal material from the sample via adsorption to vessel walls was minimised by pre-equilibration where possible.

A fundamental characteristic of a water sample containing colloidal material is its intrinsic instability due to coagulation and microbial processes (Buffle and Leppard, 1995 a and b). Coagulation mechanisms are the major transformation processes in experimental time scales. In a closed system, free macromolecules and colloidal aggregates will disappear from suspension comparatively quickly whereas larger aggregates are formed more slowly due to the small diffusion coefficient of their precursor aggregates. These aggregates in turn may either stabilise at a size too small for sedimentation or be transformed into large, rapidly sedimenting flocs. The exact nature of these changes will be dependent on sample characteristics i.e. the macromolecule conformation and composition, but also the colloid macromolecule concentration (Buffle and Leppard, 1995a and b). In a model closed system Filella and Buffle (1993) observed that the smallest colloids (<100nm) will disappear very quickly by coagulating into aggregates in the size range 0.1-1μm which are stable for up to several days. Chin et al. (1998) have observed the spontaneous assembly of marine dissolved (<0.2μm) organic matter (DOM) into polymer gels larger than colloidal diameter in 25 to 50 hours.
Anticoagulants such as sodium hexametaphosphate (SHMP) have been used by several authors to retard these sample changes. SHMP forms complexes with major cations in freshwaters such as Ca^{2+} and Mg^{2+} (Toy, 1973) thereby reducing the electrolyte

concentration and colloidal coagulation rates (Ali et al., 1984). Results of studies by Chen (1993) indicated that although SHMP does indeed prevent coagulation it also induces disaggregation of existing aggregates. Anticoagulants may also have wider reaching effects on bacterial activity and chemical speciation of trace metal cations or cause analytical interferences.

Additionally in natural samples the presence of micro-organisms (especially bacteria) may lead to the production of new macromolecular material, aggregation between micro-organisms and colloidal material and even the transformation of inorganic colloids (Buffle and Leppard, 1995 a and b). Mercuric chloride ($HgCl_2$) and Sodium azide (NaN_3) have been tested as antibiotic agents (Chen, 1993). Only $HgCl_2$ achieved an efficient bacteriostatic effect after a few hours but forms a colloidal precipitate of $Hg(OH)_2$ at natural pH. Clearly anticoagulants and antibiotics will produce chemical, biological or physical alteration of a colloidal sample and therefore, they were not used in this study.

To minimise effects of particle coagulation and microbial effects samples were handled according to protocol developed by Chen and Buffle (1996 a and b). This involved:

- Storage of all samples cool (4°C) and dark until fractionation. This acted to reduce coagulation and microbial growth and also to minimise colloidal flotation.
- Minimal agitation of samples during storage and handling.
- Fractionation by natural gravity sedimentation immediately after sampling. Decanted samples could be stored for up to 3 days without significant particle spectrum changes (Chen and Buffle, 1996 a and b) but here, the submicrometre colloidal fractions were processed within 24 hrs of decanting. Size fractionation by this method also reduced prefiltration artifacts as will be discussed later.

Although the sampling and handling protocol as described above was designed to minimise colloidal size spectrum alterations it was inevitable that some transformation processes would occur. To check the effect of these alterations on trace metal partitioning, storage checks on bulk samples were performed (see Chapter 4).

1.10.1.b: Colloid filtration techniques:

Just as "dissolved" and particulate fractions are defined operationally by a 0.4μm filter cut-off, colloidal material is presently defined by filtration (ultrafiltration) cut-off points. The advent of membrane filters and ultrafiltration techniques has allowed separation of particles down to molecular weight (MW) cut-offs and allowed the study of colloids to advance.

Three size fractions have been routinely determined in this study;
- <0.4μm- total "dissolved" material (colloidal and truly dissolved).
- 0.4μm to 10,000 MW(~1 to 400nm) (colloidal/macromolecular).
- <10,000 MW (Daltons) (<1-10nm) truly dissolved , species in true solution.

The macroparticulate (>0.4μm filter retained) fractions are usually determined in many studies but this fraction has not been measured in this study, as complementary data to the other fractions, for logistical reasons.

Some authors have used MW (molecular weight) filter cut-offs down to 1,000 Daltons to define the lower limit of the colloidal fraction. As will be discussed later, these operational cut-offs are characterised by the filter pore sizes or filter retention of artificial homogenous particle dispersions. There are numerous effects of natural sample filtration that may distort these effective cut-offs. Conventional filtration techniques retain particles of greater size than the cut-off on the filter surface. There are two main types of filters: depth and barrier (SEM images of these types of filters are shown in Figure 1.7).

Depth filters are usually formed of a random matrix of fibres or small particles for example; glass fibre, metal oxides and cellulose nitrate compositions. There is no well defined pore size and the cut-off point for such filter is defined by the size of filtrate particles. Depth filtration relies on interaction of the sample with the filter matrix either by physical trapping or surface contact (Howard and Statham, 1993). Use of filters of this type can be a problem due to adsorption of species directly onto the large available filter surfaces as the sample passes through.

Figure 1.7 : Scanning electron micrographs of commonly used filtration materials (Statham pers.comm.).

a) Plankton netting (45μm, x 185)

b) Filter paper (Whatman 42; 2.5μm, x 200)

c) Glass fibre filter (Whatman GF/F; 0.7μm, x 200)

d) Cellulose nitrate membrane (Sartorius; 0.45μm, x 10,000)

e) Polycarbonate membrane (Nuclepore; 0.4μm, x 10,000)

f) Aluminium oxide filter (Whatman Anopore; 0.1μm, x 10,000)

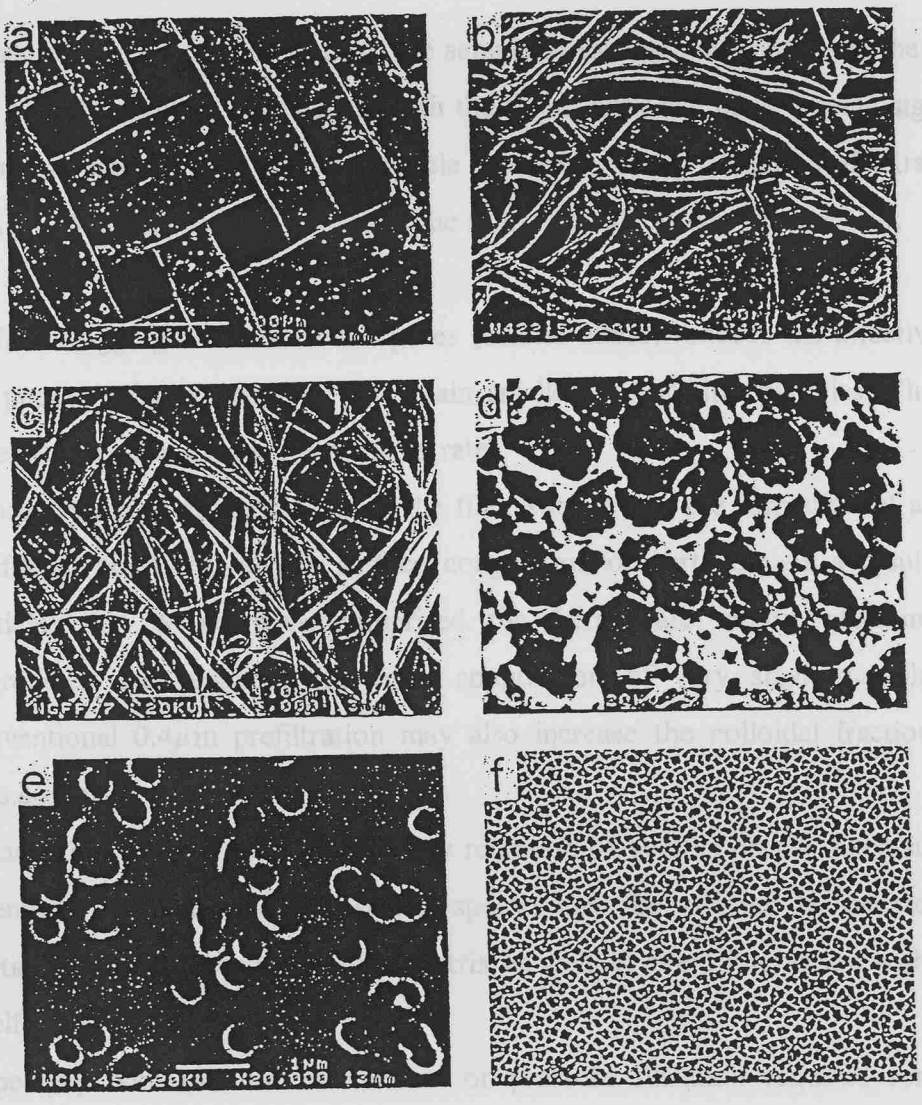

Barrier filters have much better defined pore sizes (some obtained by etching small holes of the appropriate size into the filter material). Filter materials include plastic films of cellulose ester or polycarbonate (as used in this study). Aluminium oxide filters that have a honeycomb structure of defined channels have high filtration capacities, but all barrier filters retain particles on the surface of the filter and so, the effective pore size will change as more particles are retained. These features of screen and depth filters create secondary filtration effects.

Secondary filtration effects:

Secondary effects are perturbations of the sample or filtrate that result from the filtration process or interaction of the sample with the filter. They can have varying significance depending on nature of the sample (particle spectrum), filter or method of filtration (see Figure 1.8). With conventional filtration the following effects can be observed;

- Surface clogging of track-etched pores (barrier filters) reduces the effective size of the pores so filters progressively retain smaller and smaller particles. This can be observed as a decrease in filtrate flow rate.
- Concentration of colloids close to the filter surface and the formation of a gel layer (Buffle et al., 1992) allows surface coagulation of particles. As a result, smaller particles that would have comprised the filtrate are incorporated into larger aggregates and retained. Increased coagulation of very small particles during conventional 0.4μm prefiltration may also increase the colloidal fraction (Tappin pers.comm.).
- Polarisation (charge accumulation) by retention of solutes on the filter surface can attenuate filter efficiency. Dissolved species can be affected by interaction with particles caught on or in the filter matrix as well as direct interaction with the filter itself.
- Especially with the use of vacuum or pressure filtration required for colloidal separation some material may alter in size or configuration to fit through filter pores (breakthrough). The particle spectrum may therefore be distorted especially if a lot of such material (e.g. organic) is present in a sample (Buffle et al., 1992).

Figure 1.8 : Schematic representation of size ranges where important filtration secondary effects are expected to play a significant role (Buffle et al., 1992).

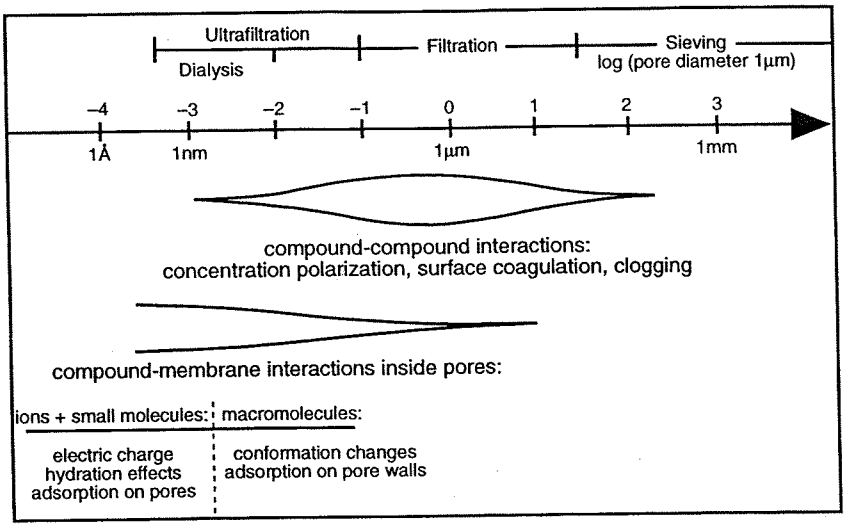

Because of these problems, the definition of the colloidal fraction by conventional filtration is by no means clear and may result in fractionation occurring in a different size range from the nominal pore size of the filter. The actual size range separated may alter over the course of sample filtration and is largely dependent on the filter type and manufacturer or surface area (Horowitz et al., 1996a and b). Many of the problems listed above can be reduced by the implementation of Cascade Filtration (prefiltration prior to ultrafiltration-0.4μm in this study) as well as appropriate choice of filters and filtration conditions (especially flow rates). Although Casacde filtration may largely reduce secondary filtration effects these benefits must be offset by the likely shift in particle spectrum induced by more handling steps. Employment of low flow rates and reduction of the diffusion layer above the filter by stirring or using tangential flow filtration will also greatly alleviate some of these problems.

Cross-flow filtration (CFF):

Cross-flow filtration differs from conventional filtration in that fluid flow is tangential as well as perpendicular to the surface of the filter membrane (see Figure 1.9). Size separation occurs with fluid containing solutes smaller than the nominal filter cut-off passing through the membrane (truly dissolved fraction in this study). The fraction that

does not pass through the membrane (colloids in this study) flows on tangentially across the filter and is recycled. CFF provides a technique for potentially contamination free and rapid fractionation of natural samples (Whitehouse et al., 1986; Moran and Moore, 1989; Whitehouse et al., 1990).

Figure 1.9: Schematic representation of colloidal fluxes in classical and tangential flow filtration (from Buffle and Leppard, 1995b).

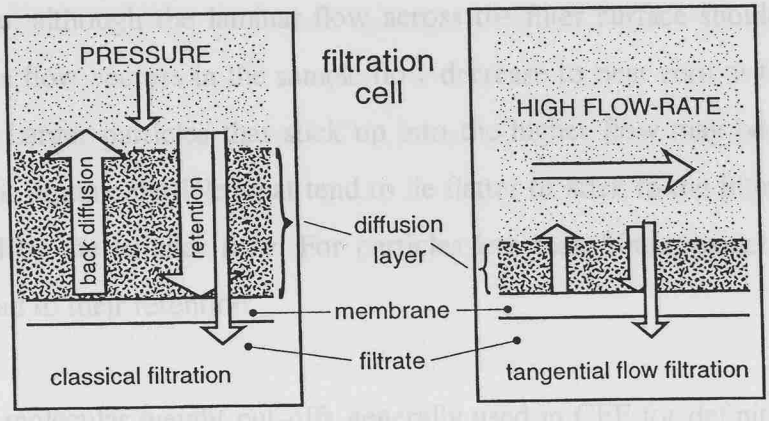

As with conventional filtration, the molecular weight cut-off filters used in CFF, may retain a variable spectrum of particle sizes. For example, the 10,000 MW filters used in this study effectively retain particles of greater than 10,000 Daltons but this may give a particle retention spectrum of 1-10nm by diameter. Although CFF plates can be characterised using monodisperse carbohydrate standards (Gustafsson et al., 1996) these test suspensions have limited applicability to natural waters where particle sizes, conformation and composition are far more diverse.

Many of the problems associated with conventional filtration are alleviated by CFF as colloidal/solute material is not greatly retained on the surface of the filter (concentration polarisation) due to laminar flow across the filter surface. However, as CFF of a sample retains particles of higher MW than the membrane size it progressively concentrates them as the filtrate is removed. For unstable systems such as colloidal suspensions this can be a problem as increased perturbation of the system via aggregation processes is possible as a sample is processed and concentrated. This concentration of the retentate fraction also has implications for analysis of this retentate fraction as will be discussed later.

Despite reducing concentration polarisation effects and potentially increasing filtrate flow rate (Whitehouse et al., 1990; Moran and Buessler, 1993) many of the secondary filtration effects that occur with conventional filtration still apply to CFF, especially in high SPM or DOC systems. Despite reduction of concentration polarisation and increased filtration rates, colloidal material can still be retained on the filter membrane if the flow gradient through the membrane is too high compared to the laminar flow across it (Buffle et al. 1992, Lead et al. 1997).

For example; although the laminar flow across the filter surface should keep it free of particles, the flow vectors in the sample flow decrease to near zero at the surface of the filter plate. Larger particles that stick up into the higher flow may be swept away but very small or organic particles that tend to lie flatter or stick to the filter surface will not be removed by the laminar flow. For particles less than 50nm diameter charge effects may also lead to their retention.

Due to the molecular weight cut-offs generally used in CFF for definition of a colloidal fraction it is difficult to minimise the filtration time of a sample (and therefore coagulation of sample particles) without increasing the likelihood of gel formation (and concentration polarisation) above the membrane surface. This is especially true in samples of high colloidal loading or organic material concentrations (i.e. estuarine or river samples). This in turn causes membrane-colloid interactions and increases the risk of breakthrough or errors in fractionation.

In this study, across filter flow rate and filtrate generation rate (sample processing time) were optimised to reduce the effects of gel formation or sample alteration by coagulation processes prior to and during fractionation. Filtration artifacts were also reduced as much as possible by fractionation of the sample naturally by gravity sedimentation prior to prefiltration and ultrafiltration. Although most of the filtration artifacts and associated sample perturbations discussed here are physical and related predominantly to size spectrum changes there are significant implications for alteration of the partitioning of colloidally associated trace metals.

1.10.2: Effects of filtration artifacts and protocol on determined 'total dissolved' trace metal concentration and partitioning.

In many studies of trace metals in natural systems, filtration by conventional or tangential approaches are the main techniques used for separating samples into partitions of "dissolved" and particulate species. Further to this, CFF has allowed investigation of colloidal material within the "dissolved" fraction down to molecular weight (1-10KDa) levels. As discussed previously, these size separation methods are by no means perfect and disruption of the original particle size spectrum and the distribution of associated trace metals seems inevitable. Recently, there has been increasing debate on the effect membrane filtration (conventional prefiltration and cross-flow filtration) has on the dissolved and colloidal trace metal concentrations observed in natural waters (mainly, Horowitz et al., 1992; Taylor and Shiller, 1995, Horowitz et al., 1996a and b).

1.10.2.a: Prefiltration:

Historically, the "dissolved" trace metal fraction has been operationally defined as those constituents that will pass through a 0.4-0.45μm prefilter. The use of this definition continues despite the fact that a "dissolved" trace metal concentration defined by a 0.4μm filtration may include substantial amounts of colloidally associated trace metal. Increasingly, there has been debate as to the applicability and appropriate nature of this procedure. Although it has long been appreciated that the 0.4μm boundary is a somewhat arbitrary cut-off in a continuum of particle species it has provided useful information and contrast in trace metal partitioning and transformations in natural systems.

Up to the mid 1970's there had been a history of elevated trace metal data for some metals due to contamination problems (namely Cu, Zn, Cd). With the implementation of clean/ultraclean sample handling and processing techniques there was a reduction in contamination and a concomitant decrease in reported levels of ambient dissolved trace metal concentrations in natural waters. This improvement in trace metal detection limits allowed generally lower and variable amounts of colloidally associated trace metals in samples to be detected. As a result, variability in dissolved trace metal concentrations of

similar water samples may be due to the filtration protocol implemented. A number of factors associated with filtration (aside from pore-size) such as filter diameter/surface area, manufacturer (i.e. filter structure), volume of sample processed, characteristics of the sample (amount of suspended sediment including colloids, colloidal trace metal loading, particle size distribution, colloidal composition and morphology) as well as filter type (screen or depth) were found to affect the filtrate metal concentration (Horowitz et al., 1992; Taylor and Shiller, 1995; Hall et al., 1996; Horowitz et al., 1996 a and b). This phenomenon was observed for most metals (Fe, Al, Cu, Zn, Pb, Co, Ni) and was mainly attributed to the inclusion/exclusion of colloidally associated trace metals from the filtrate by variation in secondary filtration effects (clogging, concentration polarisation, gel layer formation) as described previously. Dilution, sorption/desorption of trace metals from filters and filter retained particles or concentration breakthrough may also be factors. Thus, dissolved trace element concentrations derived by processing whole water samples through similar pore sized filters may not be comparable. In general, polycarbonate filters have been adopted for trace metal clean prefiltration due to lower blank values and better size fractionation (Laxen and Chandler, 1982). However, the problems with pore clogging and colloidal retention are worse for these screen filters and although these artifacts still occur with depth filters they are less pronounced (Hall et al., 1996).

From this debate two modes of thought have emerged to address this incomparability problem;

- To modify the sample as little as possible during filtration by using a very large surface area of filter membrane to reduce filter clogging, filter small volumes or use filters that are less prone to clogging (Horowitz et al., 1996a). This can be virtually impossible in systems of very high sediment or organic loading or with particle/colloidal size spectrums weighted towards a 0.4μm cut-off that can lead to rapid filter clogging.

- Filtration at the 0.4μm boundary is too fraught with sample specific variables to give an acceptable operational definition so it is better to look directly at the truly dissolved fraction (namely ionic trace metal species). This approach involves the method of "exhaustive filtration" (Taylor and Shiller, 1995) whereby a low surface

area polycarbonate screen filter is first clogged by the sample before the filtrate is collected. This technique is still subject to alteration of ionic trace metal concentrations by adsorption/desorption interactions with sediment retained on the filter surface and is dependant to a certain extent on the filtered volume.

Neither of these methods is artifact free, so it is more likely that a filtration protocol will be determined by the trace metal species under investigation and the requirements from the perspective of study of these species, e.g. whether they are bioavailable or transported under certain conditions.

The Trent/Humber system studied in this work is a very high SPM environment so it was vital to minimise any colloidal removal or generation via coagulation during prefiltration. A decanting method (Chen, 1993; Chen and Buffle, 1996 a and b) was implemented prior to 0.4μm prefiltration to reduce the loading of larger particles so only submicron particles (Chen, 1993) remained for prefiltration. Polycarbonate screen membranes (47mm diameter) were used for prefiltration as they are generally regarded as having a lower potential for trace metal contamination and the sample settling step would act to minimise clogging problems. Sodium acetate filters have been found to release particles and have greater unknowns in filter artifacts. Inevitably, some colloidal material was retained during prefiltration especially under high colloidal or organic loadings, therefore the colloidal trace metal concentrations are likely to be somewhat conservative. Breakthrough or creation of colloidal material may have also occurred (Tappin pers.comm) but the balance between this artifact and colloidal exclusion from the filtrate is unknown.

The exhaustive filtration approach was not applicable here as the colloidal fraction was mainly under investigation and therefore needed to be kept separate from the truly dissolved fraction. The fractionation of colloidal and truly dissolved trace metals was achieved using CFF.

1.10.2.b: Application of cross-flow filtration in trace metal studies:

Although there are clear benefits of CFF for trace metal work as indicated in its use in oceanographic studies (Moran and Moore, 1989; Whitehouse et al., 1990; Moran, 1991) this technique has increasingly encountered fractionation problems and other associated effects on trace metal concentrations in coastal and estuarine environments as discussed previously.

As with 0.4μm filters, filter plate cut-offs and morphology are manufacturer dependant. For example, filters may be flat plates with honeycomb structures or spiral wound and made of different materials (polysulphone as used in this study), all of which will interact differently with identical natural samples. Intercomparison exercises (Buessler at al., 1996; Greenamoyer and Moran, 1996) have illustrated that systems with plates of varying morphology and composition (i.e. polysulphone groups) with the same nominal cut-offs will fractionate colloidally associated trace metals in contrasting ways. Performance of an ultrafiltration membrane can vary with solute concentration and, performance at a given concentration can vary with the nature of the sample (Baker and Strathmann, 1970; Blatt et al., 1970; Whitehouse et al., 1990). Unfortunately, this situation is complicated by the lack of representative standards and reference material for colloidal/trace metal ultrafiltration. It is possible to characterise a system to a certain extent using ideal particle standards, usually carbohydrate suspensions (Gustafsson et al., 1996). It is unlikely though, that these standards truly represent how a CFF system will deal with heterogeneous natural samples of complex particle size distributions and compounds.

Several workers have investigated the effects of secondary filtration artifacts on the concentration of trace metals in the filtrate from CFF systems. As a sample is processed through a CFF system the retentate fraction is progressively concentrated as filtrate is removed from the sample. The ratio of filtrate volume to the initial volume is the concentration factor (**CF= initial volume/final volume**). Several authors (Sanudo-Wilhelmey et al., 1996; Wen et al., 1996) have shown the effect that this concentration factor (usually in the range 2 to 10) has on the trace metal concentration in the ultrafiltrate (truly dissolved fraction). At low concentration factors there are perhaps

minimal filtration effects but separation of the fractions is not complete and trace metal uptake onto the filter is more likely. In some studies the system is preconditioned with a small volume of sample and the first few mls of filtrate is discarded. Conversely, at high concentration factors breakthrough effects of colloidal material into the ultrafiltrate may occur, elevating the filtrate trace metal concentration. Generally the optimum concentration factor is sample, metal and system dependant. In this, and many studies an integrated filtrate sample at an intermediate concentration factor (~2) is taken to average any changes in ultrafiltrate trace metal concentration that occur during sample fractionation by CFF.

Similar to problems encountered with definition of the "dissolved" fraction by complete sample prefiltration there is still no generally accepted cross-flow filtration protocol (i.e. sample pretreatment, filter membrane colloidal cut-off, CFF system type and maunfacturer, concentration factor) so colloidal trace metals results derived using CFF remain relatively non-comparable (see Table 1.1). Several authors now are using 1KDa filter membranes when researching colloidal/truly dissolved species (Buessler et al., 1996; Wen et al., 1996). Although in some marine systems and for some metals, the 1-10Kda colloidal fraction is significant, it has been observed that the interactions of colloidal material and associated trace metals with filter membranes is exacerbated at these low MW levels as operating pressures must be increased to maintain reasonable sample processing times. For example, 1KDa recovery for Fe in Gulf of Mexico samples is significantly reduced compared to 10KDa Fe recoveries by mass balance (44% versus 50% respectively, Wen et al., 1996). A 1KDa colloidal/truly dissolved cut-off represents an extreme operational definition extreme, as it is impossible to tell when a low molecular weight macromolecule becomes a truly dissolved species and all the filtration artifacts seen at higher cut-offs are exacerbated. The low recovery with either cut-off indicates the extent of the interaction of colloidal Fe with the filter membrane and system.

CFF does have one advantage when considering the effects of filtration artifacts on trace metal concentration because, by analysis of the trace metal concentration in each of the three CFF components (total dissolved, retentate and filtrate) it is possible to calculate a mass balance recovery (%) for trace metal in the sample processed.

Trace metal concentrations in the colloidal fraction can be calculated in two ways;

a) by difference of total dissolved and truly dissolved fractions.

Colloidal concentration by difference (coll.diff.)= 0.4_f – F

Where;

0.4_f is the trace metal concentration in the total dissolved fraction.

F is the trace metal concentration in the truly dissolved fraction.

This method of calculation assumes that the CFF system is acting ideally and fractionation is occurring without size spectrum distortion which is not always the case.

b) the concentration of the retentate colloidal fraction is adjusted for its increase in concentration due to the removal of the truly dissolved fraction. Hence;

Colloidal concentration by calculation (coll.calc)= (R-F)/CF

Where;

R is the trace metal concentration in the concentrated colloidal retentate fraction.

F is as defined above.

CF is the concentration factor, the factor by which the concentration of the retained fraction is increased during CFF, i.e. initial sample volume/final sample volume after CFF.

Using concentrations determined from all three fractions (0.4_f, F and coll.calc) it is possible to determine a mass balance recovery (%) for each sample processed.

Recovery = 100 x [{F(CF-1) + R }/ (CF x 0.4_f)]

This recovery can highlight removal, addition or interactions of the sample with the filtration system or membrane. If the recovery is <100% there is an indication of interaction of colloidal metal with the filter plate or retention of material within the system, whilst recoveries greater than 100% indicate contamination by the CFF system.

Breakthrough of colloidal material into the filtrate can also be identified. It is possible to see from recovery comparisons which metals, or samples of different chemical (DOC) or physical (salinity, size spectrum) signatures are most affected by CFF processing artifacts.

Using recovery measurements it is possible to highlight element specific problems, sample volume effects or effects due to some other sample characteristic e.g. higher DOC that may lead to increased sample/system interactions. Comparisons of CFF system protocol and behaviour under various conditions (see Table A1.1) indicate that low recoveries are more frequent for samples with high DOC and for metals with high particle activity or high colloidal loadings e.g. Fe and Pb. Although recovery measurements give some indication of CFF system artifacts they only illustrate problems with the mass balance of total trace metal in the original sample compared to its component fractions and do not show whether the fractionation observed is true or distorted. They also give no indication of any analytical artifacts that may occur as a result of colloidal sample alteration during filtration.

1.10.2.c: Potential problems associated with determination of 'total' dissolved metals as a result of filtration artefacts.

During cross-flow filtration the colloidal fraction retained by the filter (retentate fraction) is progressively concentrated as the truly dissolved phase is removed. Not only may this distort particle separations but it also has implications for the effectiveness of conventional, surface active techniques used in trace metal extraction. The increased particle concentrations in the retentate fractions will promote colloidal aggregation/flocculation but this process may be exacerbated by acidification of samples for storage (actually designed to bring trace metals into solution) which will allows large aggregates to form in the concentrated samples and also induces precipitation of humic acids (Kramer et al., 1994). Large aggregate formation was observed in acidified Humber retentate samples

Mechanism of colloidal aggregation under low pH conditions

It has been previously determined that natural particles have organic coatings that will give a relatively homogenous adsorption surface (see Fiellia and Buffle, 1993) and that organically coated particles have like negative charges that will stabilise a colloidal sol (Neihof and Loeb, 1974; Hunter and Liss, 1979). Removal of particle organic coatings can increase the particle coagulation efficiency, α (fraction of collisions that result in aggregation) in natural waters (Gibbs, 1983). Changes in acidity, ionic strength and metal ion complexation can all affect stability of a colloidal dispersion and once destabilised (i.e. repulsion barrier has been attenuated) aggregation by Brownian motion of differential settling can occur where interparticle interactions are close enough for van der waal forces to predominate.

In natural waters (pH 7-8) but down to pH 3.5 (Buffle, 1990) organic coatings and macromolecules have like negative charges as a result of surface carboxylic acid functional groups that cause polymers and organic molecules to be expanded. Increased acidity, such as sample acidification (1ml/l SBD HNO_3) for storage could lead to protonation of these forms and molecule compression. The neutral state caused during increasing protonation may result in destabilisation of organic molecules or coatings and colloidal aggregation. Acidification can also result in precipitation of humic acids. Exposed inorganic species are also likely to be affected by pH decrease upon sample acidification. Most surfaces of metal oxides or clay edges have Si-OH and Al-OH groups. Under progressively acidic conditions these groups will accept a proton and become positively charged. The point where the net charge is zero is the isoelectric point and will vary between species. eg;

SiO_2 = pH 2

Fe_2O_2 (haematite) = pH 6-7

(see Drever, 1982)

Hence as pH decreases upon acidification some inorganic species will become neutral and then positive at varying pHs and this will invariably lead to destabilisation of the suspension and therefore aggregation.

Parks (1967) predicted that the isoelectric points of aluminosilicates could be assessed by the number of SiOH and AlOH groups at the surface. An aluminosilicate surface with mostly SiOH groups will have a lower isoelectric point compared to a surface with mostly AlOH groups. Therefore aluminosilicate composition of the colloidal species determines stability/instability at a given pH. But only if organic coating that gives colloid surfaces their homogeneity is removed.

It is possible at low pHs if all the particles remain organically coated that there may be some restabilisation (repeptization) as all the particles become positively charged. The organic coating of a colloidal species may not necessarily be monolayer so despite low pH and changes in polymer structure or removal of the outer layer, the reaction of the coated particles and charge behaviour may still be relatively uniform. It is likely that the organic coatings are quite homogenous in nature between samples as this material (more refractory fulvic acid from terrestrial and marine sources) will be ubiquitous thoughout the riverine and estuarine system. Biogenic/phytoplankton humics are shorter lived. Whether the organic coating will be removed from colloidal particle upon acidification will depend on the bonding between the organic material and the inorganic species (covalent/charge/ complexation etc.) Work in this area to further these ideas was outside the scope of this study.

As a result of colloidal flocculation/aggregate formation and humic acid precipitation in the concentrated and acidified retentate samples there may be several implications for the effectiveness of trace metal solvent extraction techniques.

It has been noted in several colloidal studies (Quentel et al., 1986; Ostapczuk, 1993; Benoit et al., 1994; Wen et al., 1996) that digestion of the colloidal retentate fraction and 0.4μm filtered fraction is necessary to release trace metals that may have been sequestered by colloidal aggregates in high colloidal concentration samples. Digestion of the samples (Wen et al., 1996-acidification, ultrasonification, UV exposure) is often required to ensure that the sample is well homogenised and trace metals associated with these aggregates are brought into solution. If the sample is not sufficiently disaggregated/homogenised the complexation and extraction of trace metals from within colloidal aggregate matrices during the extraction procedure may be inhibited. Mackey et

al. (1997) have reported interference effects and reduced extraction efficiencies for Cd, Co, Cu and Ni from unfiltered samples which was strongly correlated to the presence of high concentrations of suspended solids, dissolved organic matter and particulate iron in the original samples. Although retentate samples have been filtered, the concentrations of particulate and colloidal material can be artificially elevated as discussed previously. Indeed, removal of precipitated organic material from samples by UV irradiation is also advisable although there is some evidence that organic based colloids formed during UV irradiation may be capable of readsorption of metals. Also, at high iron concentrations iron-carbamate precipitates may form which can inhibit complete metal extraction (especially of highly particle reactive and Fe associated metals, e.g. Pb).

Although it is generally accepted (Tappin and Statham pers.comm) that the complexants used for trace metal solvent extractions (ADCP-DDDC) are strong enough to compete successfully for all trace metals in a concentrated and acidified sample it is clear that development of sample pretreatment to address some of the problems discussed above is required to give confidence in the extraction and determination of 'total' dissolved metals in colloidal samples. The approach taken for sampling and sample handling in this study is discussed in detail in section 4.3.3.

It can be seen that with cross-flow and prefiltration artifacts the absolute concentration of any trace metal fraction determined by filtration methods is dependant to a large extent on the pretreatment of that sample. In this study a combination of sample handling (cold, dark, decanted prior to prefiltration) and filtration (CFF, maximum laminar flow, minimum across filter pressure, optimal concentration factor) steps have been implemented to reduce any artefacts in colloidal trace metal determination. Unfortunately, unless universal filtration protocols are adopted, the trace metal concentrations of total dissolved, colloidal or truly dissolved fractions in many publications are relatively incomparable. With filtration artifacts relatively unquantified and with the lack of filtration standards perhaps spatial and temporal trends in systems are more meaningful that absolute concentrations. The effects of prefiltration and CFF fractionation artifacts on all trace metal data should be assessed critically during interpretation of total dissolved, truly dissolved and colloidal data.

1.10.3: Summary of present understanding of estuarine colloidal trace metal behaviour:

Dissolved iron is a highly colloidal (60 to 99%) as are the other particle reactive metals Pb and Mn. Their close association with particles facilitates their removal in the low salinity regions of estuaries. The loss of Fe and associated trace metals (colloid lead to iron correlation in Venice Lagoon R^2=0.98, Martin et al., 1995) in this region is due to coagulation of colloidal iron (Sholkovitz, 1976; Figueres, 1978). In several studies it has been observed that colloidal manganese is removed at lower salinities than Fe which may be partly linked to the association of Mn with high molecular weight colloids (Powell et al., 1996; Sanudo-Wilhelmy et al., 1996). Colloidal Mn may be involved in redox or photochemical processes that alters this highly non-conservative behaviour.

Colloidal Pb has shown wide variability in its colloidal significance but there are relatively few studies including its estuarine behaviour. Although highly particle reactive, colloidal lead tends to reside in the higher molecular weight fraction of colloidal organic carbon (Wells et al 1998), and can be removed in association with colloidal Fe (Martin et al., 1995). The percentage composition of colloidal Pb varies from 30 to 95% (Wen et al., 1996; Wells et al., 1998) but this is more a reflection perhaps of the variation in the composition of the complete particle spectrum.

Colloidal Cu is generally conservative, a behaviour which is perhaps linked to it's association with dissolved organic material which itself is highly conservative in behaviour. However, in some studies it has shown extensive removal in low salinity regions (to <10% colloidal) and transfer into low molecular weight colloids with increasing salinity (Sanudo-Wilhelmy et al., 1996).

There is no general consensus on the behaviour of colloidal Zn, Ni or Cd. In similar salinity regimes colloidal Zn has been observed as behaving conservatively (Sanudo-Wilhelmy et al., 1996) or has consistently low significance in the total dissolved fraction (<3 to ~30%)(Sanudo-Wilhelmy et al., 1996; Kraepiel et al., 1997; Wells et al., 1998).

Colloidal nickel and cadmium show non-conservative behaviour and both metals are progressively converted to lower molecular weight colloids as salinity increases (Powell et al., 1996). Colloidal fractions of both metals are highly variable (Ni, <2% to 40%; Cd, <10% to 34%) with higher fractions occurring in the riverine end-members.

In a recent study in the Gironde (Kraepiel et al., 1997) it has been indicated that colloidal populations of organic and Fe-Mn oxyhydroxides may be discrete (rather than colloidal material being a combination of mineral and organic matter) and which will directly affect behaviour of trace metals associated with them. These two distinct sub-fractions of the colloidal pool will behave differently; the finely dispersed iron oxides eventually coagulate and become part of the particulate load whilst the organic macromolecules, which bind most other metals are effectively dissolved constituents and therefore behave more or less conservatively. This hypothesis was used to explain contrasting behaviour of colloidal Cu and Ni from other trace metals. Such discrete pools have not yet been observed in other estuaries but clearly the existence of separate colloidal pools of differing composition and size fraction has wide reaching implications for future interpretation of trace metal behaviour.

Clearly there is strong evidence that colloidal trace metals are significant in many estuarine systems and even if the colloidal fraction of a given trace metal is low, the knowledge of trace metal partitioning will enable more accurate modelling of these multicomponent systems.

1.11 Research Objectives:

Colloidal material has been observed to be an important species in controlling the partitioning of trace metals in marine systems. However, there are still gaps in the knowledge of how colloidal material functions in the cycling and fate of trace metals under natural conditions.

This thesis was designed to address some of these issues and improve understanding of trace metal colloidal speciation and particle-water-metal interactions in multicomponent systems.

Three areas of investigation were identified;

1) To investigate the association of trace metals with colloidal material and the processes of adsorption/desorption, aggregation/disaggregation that would govern their role as vectors of these particle reactive species. Cycling of particle (originally colloidal) sorbed trace metal tracers through the "dissolved" and "particulate" phases in estuarine systems as part of the dynamic particle spectrum will be examined. [using the partition coefficient (Kd) approach.]

2) Investigation of the spatial and temporal distribution of colloidal trace metals in the Humber Estuary. The significance of colloidal trace metals in estuarine systems has been reported by a number of recent papers (Baskaran and Santschi, 1993; Benoit et al., 1994; Martin et al., 1995; Dai and Martin, 1995; Dai et al., 1995; Powell et al., 1996; Sanudo-Wilhelmy et al., 1996; Wen et al., 1996; Kraepiel et al., 1997; Wells et al., 1998). Through the LOIS (Land Ocean Interaction Study) there was an opportunity to look at colloidal trace metals in this system spatially and seasonally. The high particulate loading in this estuary contrast significantly from many previous studies. Despite investigation of dissolved metal partitioning using radionuclides and stable isotopes (Turner et al., 1993, Coffey, 1994), estimation of trace metal fluxes (Millward and Glegg, 1997) and investigation of particulate (defined by settling parameters) trace metals in the TMZ (Williams and Millward: in press) there has been no work to date on colloidal partitioning of trace metals in this system. Variation of trace metal partitioning into particulate and dissolved fractions will be investigated seasonally and tidally (diurnal/ spring-neap). It was intended that an insight into the

significance of the colloidal phase in such an estuary would be obtained from a process perspective.

Overall objectives of the Trent/Humber study would be to;

- determine the abundance and distribution of colloidal material within the Humber estuary.
- quantify the significance of colloidal material for trace metal transport within this system.
- investigate seasonal changes in the colloidal population and its implications for trace metal geochemistry.

Participation in an established sampling project would provide a good background data base of master variables (S, dissolved oxygen, pH) to enhance and clarify colloidal result.

3) Investigation of the role of colloidal material in the geochemical cycling of aluminium in the shelf region of the Celtic sea. Previous data (Hall pers. comm.) has indicated 90 % of Al to be present in the colloidal phase which is concurrent to a previous estimate of 15% (Moran and Moore, 1989). The distribution of Al throughout the water column will be examined with a particular regard to sources of Al associated with nepheloid layers, aeolian inputs and biological control. Comparisons of Al concentrations in identified water masses and throughout the water column from previous investigations would be possible.

This thesis is organised into six chapters.

Chapter 2 includes all the trace metal handling and analytical methodology used in the sampling, separation and determination of trace metal concentrations. It also includes development of a digestion method used for all trace metal samples to minimise problems in the determination of 'total' dissolved metals as a consequence of cross-flow filtration artefacts as is discussed in Section 1.10.2.c. Methodology for laboratory radiotracer and Aluminium resuspension work is also included along with a brief description of the Field-

Flow Fractionation technique utilised for direct separation and trace metal analysis of colloidal material

Chapters 3, 4 and 5 include the results and discussions of each of the research sections as listed above. Chapter 6 is contains a summary and discussion of the research findings with respect to colloidal trace metals but also wider issues raised during the course of this research. Chapter 6 also includes suggestions for future work that could be continued to further the research done here.

CHAPTER 2: Colloidal separation and analytical methods:

2.1: Methods for radiochemistry pilot experiments:

2.1.1: Sample collection:

10 litres of water were collected in clean carboys from two sites on the Beaulieu estuary, Hampshire. The riverine end member was taken from Hartford Bridge (GR:SU 380380: 0 psu) and the estuarine end-member from Bucklers Hard (GR:SU 410002: 28 psu). Samples were immediately filtered through ashless Whatman No.2 (~8μm) papers to remove large particulates that would clog filters of smaller cut-offs. Filtered samples were stored at 4 °C until utilised. For equilibration experiments the water samples were used directly for total samples or prefiltered through 0.4μm polycarbonate filters for colloidal particle spectrum experiments.

2.1.2: Gravimetric analysis of particulate fractions:

Gravimetric analysis was carried out on all samples to determine the particle population distribution prior to and during the equilibration experiments. Determination of mass of particulate material in each fraction enabled partitioning of radiotracer into each phase and hence Kd to be calculated. The particulate fractions identified were;

- paper (cellulose):Whatman ashless filters (No2) approx. 8μm; to remove large particulates (>8μm).
- 0.45μm cellulose nitrate Whatman filters. (8-0.45μm)
- 0.4μm polycarbonate Nuclepore filters (0.45-0.4μm)
- 0.02μm Whatman Anodisc (Aluminium oxide) filters (0.4-0.02μm: colloidal).
- <0.02μm: truly dissolved .

For filters made of highly hydrophobic material (e.g. polycarbonate) with very small pore sizes the surface tension of water can be a significant barrier to filtration. Agents are sometimes added to filters to reduce surface tension and help "wetting out" of the filter. Polycarbonate 0.01μm filters would have been used in preference for the lower colloidal cut-off, however due to problems of these filters "wetting out", aluminium oxide filters

were used and the colloidal size range was defined as 0.02 to 0.4μm by these filter cut-offs (see fraction defined above).

The cut-offs of prefilters and number of filters used in each fraction were altered during method development as the characteristics of the sample water and particle populations were better identified. For example; a 0.45μm prefilter was used prior to 0.4μm filters to reduce clogging effects and hence the removal of particulates smaller than the filter cut-off i.e. colloidal material (Cascade filtration, Buffle et al., 1992). To reduce this clogging, several filters (sometimes 4 to 5 per litre) were used at each fractionation stage.

Gravimetric procedure: riverine and estuarine samples

Sufficient filters for each experiment (2 duplicates) were prepared prior to filtration. This involved accurate weight determination prior to loading. All filters (except cellulose prefilters) were placed in a constant humidity tank for a minimum of 24hrs to equilibrate. The tank was held at a constant relative humidity of 63% by a saturated solution of ammonium nitrate. The filters were then weighed individually on a five figure balance (Sartorius R200D). After stabilisation the weight was recorded and the filter place in a plastic, numbered petri dish until utilised. All filters were handled with toothless polypropylene filter tweezers.

A litre of sample was removed from the sampling carboy. This was sequentially filtered using polycarbonate filtration equipment. After use each filter was removed from the filter holder and replaced in its petri dish. The filters were then removed from each dish and returned to the constant humidity tank for a minimum of 24 hrs before weight determination. In filtration of estuarine samples the filters were rinsed with Milli-Q to remove salts that may alter loading determination.

2.1.3: Pilot partitioning investigation using ^{65}Zn radiotracer:

Colloid equilibration experiments:

These experiments were designed to check the equilibration time required to allow the radionuclide to associate with colloidal phases in the water sample. It is essential that the radionuclide tracer is incorporated into the phases that are to be investigated (colloids). The equilibration time allowed should be sufficient to be representative of natural stable zinc particle/solution processes such as adsorption/ion exchange or complexation and transfer into colloidal matrix (clay lattice sites). The kinetic rates of such processes vary, and can affect uptake of radionuclides from the dissolved phase. In previous studies of unfiltered samples equilibration times of 24hrs to 5 days have been used (Turner et al., 1993, Turner and Millward, 1994).

Preparation of radionuclide working solution:

An initial stock solution of 1mCi (37mbq) ^{65}Zn (zinc chloride) in 0.1M HCl (USN 2601, Amersham ref. ZAS 1) was diluted to a 10ml volume by addition of 9.9ml of 0.1M HCl. The resulting working solution had a concentration of 0.1mCi/ml (100mCi/ml). The concentration of carrier zinc in the original undiluted isotope aliquot was 18g/l. This gave an increase of 0.36μg/l stable zinc concentration per litre of sample (given a 20μl addition).

Counter Optimisation:

The voltage supplied to the photomultiplier plates in the NaI (Tl) counter scaler (scaler-ratemeter SR3, Nuclear Enterprises Ltd.) was set to an optimum prior to experimental work. The optimal voltage for ^{65}Zn was determined by observing the maximum, background corrected counts recorded for a known activity over an increasing photomultiplier voltage. The maximum counts for ^{65}Zn was at 0.825 Kv (3.0 scaler), see Figure 2.1. The counter scaler was set to this throughout the experimental work. As can be seen from the optimal voltage plot the voltage was set just higher than the peak to compensate for any voltage variation.

Figure 2.1: Optimum voltage determination for ^{65}Zn detection (NaI-Tl counter).

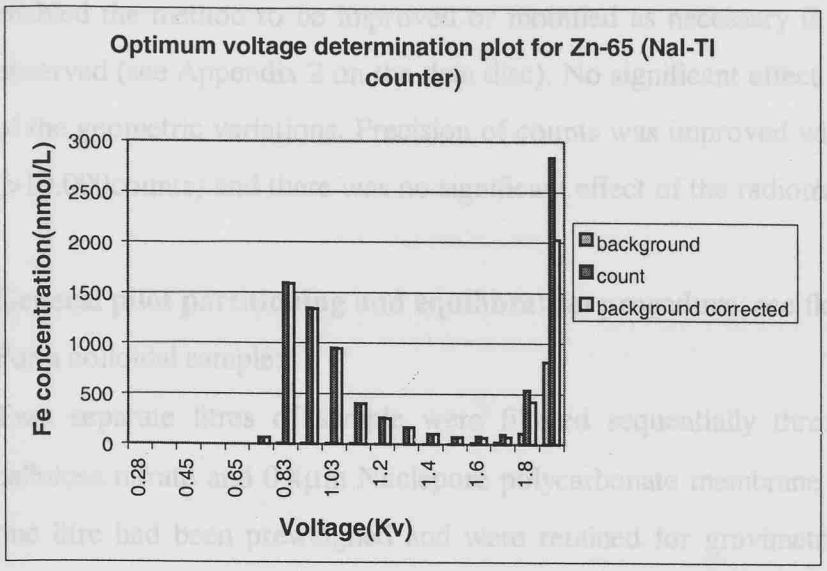

Counter efficiency:

The efficiency of the counter to gamma emissions from the ^{65}Zn source was calculated prior to all experiments. This was done using a source of known activity and comparing the expected count (100% efficiency) calculated from the source activity (1Bq= 1d.p.s.) and the actual count registered. This can be used to quantify the best activity and count duration required for the experiments. Unfortunately the NaI (Tl) counter proved inefficient (<1%). This presented a problem to achieve good count rates without using excessive activities of radionuclide. A compromise of activity and count duration was achieved.

Geometric checks:

Experiments for all aspects of the procedure were performed to ensure any changes in count rate were due to changes in activity distribution and not to procedure protocol. This was done by comparing count rates of a solution of known activity with and without geometric alteration. Checks were carried out for ;

-count volume

-filter handling effects (presence of elution plastic bag)

-count time and precision effects

-presence of the eluted filters (aluminium oxide/ polycarbonate)

-retention of radionuclide by filter matrix (non-particle associated)

The effect of the radionuclide spike on solution pH was also checked. These pilot checks enabled the method to be improved or modified as necessary if a significant effect was observed (see Appendix 2 on the data disc). No significant effect was determined for any of the geometric variations. Precision of counts was improved with increased count time (>10,000counts) and there was no significant effect of the radiotracer addition on pH.

General pilot partitioning and equilibration procedure: see flow diagram

For a colloidal sample:

Two separate litres of sample were filtered sequentially through 0.45μm Whatman cellulose nitrate and 0.4μm Nuclepore polycarbonate membrane filters. The filters from one litre had been preweighed and were retained for gravimetric analysis (see section 3.2.2). The other filtrate was transferred to an acid clean Nalgene LDPE bottle. A blank sample (5ml) was taken from this stock suspension. 20μl (20μCi) of the working radionuclide solution was added to the litre of sample behind shielding and the litre bottle was inverted several times to homogenise the suspension. The sample was also inverted prior to sampling but not shaken to prevent disruption of colloidal material/aggregates. It should be noted that the concentration of stable carrier Zn in each radionuclide addition and its subsequent dilution in the litre sample did not increase Zn concentrations so as to disrupt the natural particle/solution behaviour of the stable zinc present. The total dissolved Zn levels in Beaulieu River water have been measured as 37 to 100nM, 2.4 to 6.5μg/l (Fang pers.comm.). The stable Zn concentration after spike addition to a litre water sample is approximately 0.36μg/l. It was assumed that this would not constitute a consequential increase in stable Zn concentration within the water sample.

Complete water samples (Whatman prefiltration) and colloidal samples (0.4μm prefiltration) were both spiked with ^{65}Zn to compare the effects of particle size spectrum on adsorption/ desorption processes and subsequent dynamics of labelled particles. Control experiments of spiked Milli-Q (particle free) and unspiked samples were run in conjunction with the equilibration experiments. At t=0 a 20ml aliquot was removed from the spiked suspension. Aliquots were also removed at subsequent time intervals circa 0, 40, 85, 130, 180, 420, 1225 and 1435

F1: Flow diagram of radiochemistry pilot experiments (colloidal sample)

Starting with complete sample (8μm prefiltered).

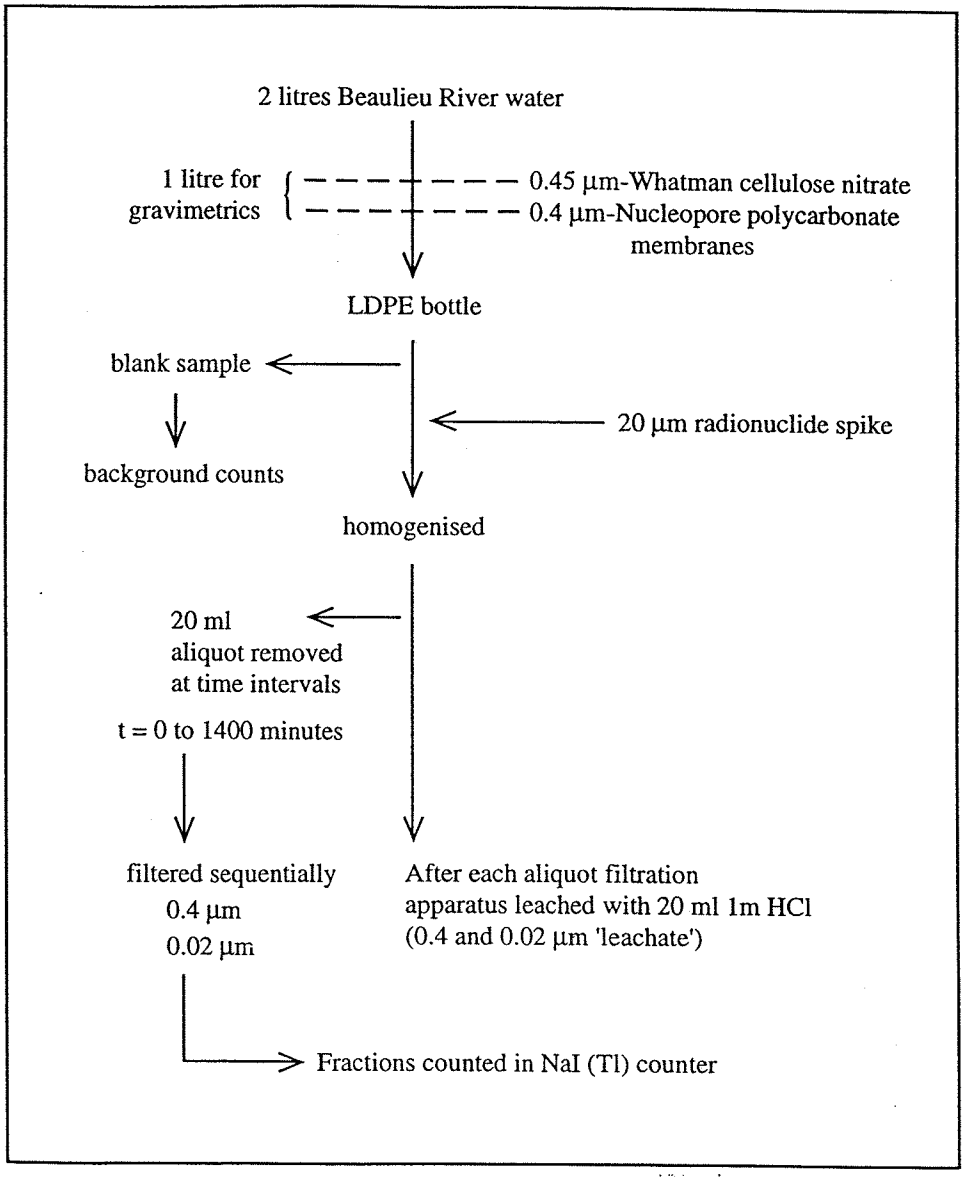

minutes. Each aliquot was filtered sequentially through 0.4μm polycarbonate and 0.02μm Anodisc aluminium oxide filters. The 0.4μm filter was designed to give an indication of any phase change in the ^{65}Zn partitioning or particle population. 5ml of the final filtrate was retained for counting. The ^{65}Zn retained on the filters was also counted after leaching with 5ml of 1M HCl for at least 15 minutes prior to activity determination. Elution maximised transfer of the radionuclide into the dissolved form to minimise geometric effects upon counting.

Activity was determined using a NaI(Tl) Scintillation counter. Each sample was counted for ten replicates of 10 seconds with corresponding background counts. Equipment rinses with 20 ml 1M HCl after each filtration stage (0.4 and 0.02 "leachate" counts respectively) enabled percentage recovery of total activity (i.e. a mass balance of total activity) to be determined. Milli-Q rinses between filtration steps reduced carry-over activities between samples to a minimum. Adsorption of the tracer to the filters used was also checked.
The fractions identified were;

Total: total activity of complete sample.
0.4: activity retained on a 0.4 filter (^{65}Zn associated with particles >0.4μm).
0.02: activity retained on a 0.02μm filter after 0.4μm prefiltration i.e. colloidal fraction.
Truly: truly dissolved ^{65}Zn, activity in sample that passes through a 0.02μm filter.
0.4 leachate: activity retained on equipment after 0.4μm filtration.
0.02 leachate: activity retained on equipment after 0.02μm filtration.

Although the total activity of the spike would decrease (decay) with time, this would have been insignificant over the duration of the experiment (<0.04 μCi / <0.2% of spike / < 1 count). Therefore there was no correction made for isotope decay.
The activity of spike used was estimated using counter efficiency to give a reasonable count total in the 10 seconds count interval. This count time and activity of spike was optimised with respect to achievable precision and sample numbers.
Temperature and pH were monitored throughout the experiment to ensure that any changes in partition of the Zn radiotracer could be accounted for if these parameters had

been the cause. This protocol was followed for complete samples and also the control experiments.

All glassware/plasticware in contact with the tracer was thoroughly cleaned between successive experiments (2% v/v Decon 90, triplicate rinses with Milli-Q). All other equipment was cleaned using procedures described in Section 2.2.1.

2.2: Clean protocol for trace metal work:

2.2.1: acid cleaning of equipment:

All equipment (especially Nalgene LDPE litre bottles) used for trace metal work was rigorously cleaned prior to use to minimise the risk of sample contamination. This involved consecutive cleaning steps in detergent and concentrated acids. All sample bottles used for sampling and storage of acidified fractions were cleaned using the following protocol;

-7 day soak in non-phosphate detergent (2% (v/v) Micro (rinsed with R.O. water).

-7 days soak in 50% (~6M) HCl (rinsed with Milli-Q).

-7 days soak in 8M HNO_3 (rinsed with Milli-Q water).

Final bottle rinses with Milli-Q water or SBD water were carried out in clean room suite/class 100 laminar flow bench. Each bottle was retained in a resealable plastic bag until and after use. All other equipment e.g. filter tweezers, filter holders were treated in a similar way although the length and concentration of acid used was varied for less resistant materials (e.g. polycarbonate filter holders were only soaked in 10% (v/v) HCl for a week after detergent cleaning. Polycarbonate filters were soaked in 10% SBD HNO_3 for 24hrs prior to rinsing well with Milli-Q and storage in fresh Milli-Q until use. The Minitan system and tubing was cleaned using a method adapted from Martin et al. (1995), see Appendix 1 for detailed protocol.

2.2.2: sampling:

Surface estuarine samples were taken manually with a clean polyethylene pole-sampler from small RIB or EA Seavigil. The sample was collected in a clean 1000ml Nalgene LDPE bottle that was attached to the end. Each bottle was prerinsed with the ambient water prior to the final fill. The bottle was then sealed in a plastic bag and stored cold and dark until fractionation. Plastic gloves were worn by sample handlers and exposure of the bottle and sample to the atmosphere was minimised throughout. Account was also

taken of positioning of the sampler in relation to the boat and water flow to avoid any trace metal contamination from the boat.

2.2.3: sample manipulation and storage:

Samples were immediately 0.4μm prefiltered and cross-flow filtered upon return to the lab using protocol described in Section 2.1.3 and Appendix 1. Samples were kept cool and dark as much as possible prior to fractionation. All sample manipulation was carried out in a Class 100 portable laminar flow bench and plastic gloves/non particle generating coats were also worn. Sample fractions were acidified with SBD HNO_3 (1ml/litre) under clean conditions and double bagged for storage. See Appendix 1 for detailed prefiltration and cross-flow filtration protocol.

2.2.4: sample analysis:

All acidified sample fractions were only opened in a clean room prior extraction. In the clean room all normal protocols were followed for maintenance of a clean environment (Howard and Statham, 1993).

All reagents used in the extraction procedure were cleaned by sub-boil distillation (HNO_3/NH_4) or cleaned using acid/chloroform/SBD water extracts (see Section 2.3.1). Manipulation and dilution of back extracts prior to graphite furnace atomic absorption spectrophotometry (GFAAS) analysis were carried out in a Class 100 laminar flow hood. Samples for GFAAS injection were held in acid cleaned polycarbonate cups. Exposure of the back extract to laboratory atmosphere prior to injection into the GFAAS was minimised. All apparatus used in extractions was acid cleaned as described in the previous section.

2.3: Determination of fractionated total dissolved trace metals:

Although the concentrations of trace metals in an estuarine environment are significantly higher than those encountered in the open ocean it is still necessary to use extraction techniques aid analysis of such samples for several reasons:

-Many metals of interest (especially Cd and Pb) occur in concentrations of 1nM or less.

-Seawater and its associated ions (e.g. chloride) at significant ionic strength will cause interference effects with many determination methods.

Because of this, a preliminary concentration and separation step is adopted in this study. Several preconcentration techniques have been used in the past to determine dissolved trace metals in seawater such as chelating ion-exchange (Chelex-100), co-precipitation and solvent-extraction.

Bruland et al. (1985) used Chelex 100 columns and solvent extraction methods (as well as an eletrochemical method-differential pulse anodic stripping voltametry) to investigate trace metal concentrations in the eastern Pacific Ocean. They found than Cu determinations by the Chelex-100 method were lower than those obtained by the other two methods. Westerlund and Ohman (1991) found similar effects of chelex on determined copper concentrations in the Weddell Sea, Antarctica. An additional problem for this study in particular is that trace metals in seawater bound with organic material or adsorbed onto colloidal species may not be sorbed by the Chelex-100 chelating resin (Abdullah et al., 1976; Fang, 1995). Mainly, for this reason a solvent-extraction approach for extraction of dissolved (including colloidal) trace metals was used in this study.

The solvent-extraction method is based on the formation of metal-carbamate complexes. Ammonium pyrrolidine dithiocarbamate (APDC) and diethylammonium diethyldithio-carbamate (DDDC) are used as chelating agents. The technique originally reported by Danielsson et al. (1978) used 1,1,2-trichloro-1,2,2-trifluoroethane (Freon-TF) as the solvent and was modified by Statham (1985) to include/improve extraction of Cd and Mn. The Freon solvent method has previously been used in this laboratory for analysis of

samples from a range of estuarine and marine environments (Morley et al., 1990; Althaus, 1992; Hall, 1993; Muller et al., 1994a and b; Fang, 1995). However due to regulation of Freon-TF use, a smaller volume APDC-DDDC/Freon TF method improved by Tappin (1988) has been modified here to use chloroform as the solvent.

2.3.1: APDC-DDDC/chloroform analytical procedure:

2.3.1.1: Reagent Preparation:

Ultra pure reagents were used in every step of the extraction procedure. These included sub-boiling distilled water (SBD-H_2O), SBD nitric acid (SBD HNO_3) and isothermally distilled ammonia solution (ITD-NH_4OH).SBD-H_2O was prepared by sub-boiling distillation of Milli-Q water. SBD HNO_3 was prepared by sub-boiling distillation of 16N AR grade nitric acid. ITD-NH_4OH was prepared by isothermal distillation of 0.880 S.G. AR grade ammonia solution under clean conditions. Two PTFE beakers were placed in a sealed container. One was filled with SBD-H_2O and the other was filled with the analytical grade ammonia solution. After several weeks the ammonia gas (NH_3) had equilibrated by redissolving in the SBD-H_2O. All these ultra pure reagents were stored double bagged in FEP bottles.

2.3.1.2: Chloroform:

Original acid stripping of chloroform proved to remove the stabiliser used in manufacture (amylene) so a washing approach with SBD water was adopted (A.D. Tappin pers.comm).

Every 100ml of chloroform required was washed 5 to 10 times with 1ml of SBD-H_2O. This was usually done in a 500ml LDPE separating funnel. The chloroform/water mix was shaken/rotated for 3-4 minutes per wash and the used water was discarded before the next wash with fresh SBD-H_2O. The washed chloroform was prepared fresh prior to each extraction batch as the effects of longer term storage on the washed chloroform was unknown.

2.3.1.3: Complexant:

The complexant used was 2% (w/v) analytical grade APDC and 2% (w/v) GPR grade DDDC in a 35% (w/v) NaCl solution. 35g of AR grade NaCl was dissolved in 1000ml of Milli-Q water. 20g of APDC and DDDC were added to the NaCl solution and after complete dissolution the complexant was filtered through a Whatman GF/F filter into a clean 1000ml LDPE bottle. Prior to use, the complexant was stripped using washed chloroform. Each 250mls of complexant was stripped by sequential extractions with 25mls of clean chloroform. Each strip involved the complexant and chloroform being shaken together for 5 minutes. The used chloroform was run off and cleaning strip was repeated three times. The cleaned complexant was prepared fresh prior to each batch of solvent extractions and as it only lasted for 3-4 days.

2.3.1.4: Seawater metal standards:

To assess the analytical quality of consecutive batches of solvent-extractions and also estimate extraction efficiency (recovery) of the APDC-DDDC/chloroform analytical method a series of standards in low metal sea water (LMSW) were made up that were analysed as samples within each extraction batch. This avoided the problem of adding highly concentrated standards (especially Fe) to LMSW inside the clean room and by using mixed spiking standards with appropriate ratios of metal concentrations, spikes added to the LMSW gave an environmentally realistic range of metal levels in the internal reference material.

To give a good approximation to the sample matrix in the standards a large bulk (10L) sample was collected from the River Itchen (salinity 13.5). This was prefiltered through Whatman GF/C and then polycarbonate 47mm, 0.4μm filters. The water was then UV irradiated for 8hrs in acid cleaned silica glass vials with 50μl of hydrogen peroxide per 250ml vial. All manipulations were performed inside a Class 100 laminar flow bench. This water was then passed through a Bio-rad 13ml column filled with approximately 15ml of ammonium form Chelex-100 resin (mesh size 50 to 100).

To prepare the Chelex-100, the resin was washed with 5 bed volumes of 2M SBD HNO_3, followed by 3 bed volumes of 2M ITD NH_4OH and then 5 bed volumes of SBD

H_2O (Althaus, 1992). Each litre of seawater was passed twice through the column to strip out trace metals. After each litre of seawater, the column was stripped of the adsorbed trace metals as described above in preparation of the Chelex-100, ready for a new seawater sample to be stripped.

The Chelex stripped seawater (LMSW) was then divided into ten, one litre volumes and each spiked with various masses of individual standard metal solutions to produce the concentration ranges listed in Table 2.1 below. These concentrations were designed to cover the ranges of trace metals encountered in the sample fractions to be extracted. The total acid added in conjunction with the metal standards was noted and the appropriate addition of SBD HNO_3 was made to give the LMSW standards the same acid content as the acidified natural samples i.e. 1ml/L (4% SBD HNO_3). The unspiked LMSW was also acidified and is the "blank" (standard 1).

Table 2.1 : Metal concentrations in LMSW standards:

Trace metal Standard	Cd **(nmol/L)** *(µg/l)*	Pb **(nmol/L)** *(µg/l)*	Cu **(nmol/L)** *(µg/l)*	Ni **(nmol/L)** *(µg/l)*	Zn **(nmol/L)** *(µg/l)*	Mn **(nmol/L)** *(µg/l)*	Fe **(nmol/L)** *(µg/l)*
1 (blank)	0	0	0	0	0	0	0
2	**0.449** *0.0504*	**0.243** *0.0504*	**16.0** *1.01*	**8.77** *0.515*	**15.6** *1.02*	**18.5** *1.02*	**18.1** *1.01*
3	**0.887** *0.0997*	**0.481** *0.0997*	**31.9** *2.03*	**17.4** *1.02*	**31.6** *2.07*	**185** *10.2*	**181** *10.1*
4	**1.75** *0.197*	**0.949** *0.197*	**78.7** *5.00*	**35.0** *2.05*	**77.5** *5.07*	**376** *20.7*	**456** *25.5*
5	**2.64** *0.297*	**1.43** *0.297*	**117** *7.45*	**87.2** *5.12*	**155** *10.2*	**927** *50.9*	**908** *50.7*
6	**3.54** *0.398*	**1.92** *0.398*	**157** *10.0*	**173** *10.1*	**232** *15.2*	**1370** *75.5*	**1820** *101*
7	**4.45** *0.500*	**2.41** *0.500*	**197** *12.5*	**260** *15.2*	**320** *20.9*	**1850** *102*	**5500** *307*
8	**5.32** *0.598*	**2.89** *0.598*	**239** *15.2*	**354** *20.8*	**474** *31.0*	**2300** *127*	**9200** *514*
9	**7.09** *0.797*	**3.85** *0.797*	**279** *17.7*	**441** *25.9*	**630** *41.2*	**3230** *177*	**18400** *1030*
10	**8.94** *1.01*	**4.85** *1.01*	**321** *20.4*	**526** *30.9*	**793** *51.9*	**3770** *207*	**27500** *1540*

2.3.1.5: Solvent extraction procedure:

The apparatus set-up for small volume extractions is described in Tappin (1988). Prior to the start of an extraction run the 125ml separating funnels used for each sample were cleaned internally using a rinse step. This involved 10ml of SBD-H_2O, 5ml of complexant and 3ml of chloroform followed by rotation for 5 minutes. The wash from this step was discarded, but was repeated between each sample to reduce sample carryover.

For each sample (see also Flow diagram F2): A 60ml aliquot of sample was poured into a 125ml funnel and neutralised with 300-320µl of ITD-NH_4OH. The funnel was agitated to ensure mixing. The exact amount of ammonia required for neutralisation varied between batches of ITD-ammonia. The amount of ammonia also varied for the LMSW standards and certified reference materials run at each extraction batch. The pH of samples and standards post extraction were checked to be between 6.5 and 8 to ensure complete extraction of metals such as Mn and Cd by the complexant (Statham, 1985).

8mls of 2% (v/v) APDC-DDDC complexant and 3mls of chloroform were added to the seawater sample. The funnels were then rotated for 5 minutes. After allowing the aqueous and chloroform phases to separate, the chloroform extract was run out into acid cleaned Teflon pots (Savillex 30ml). Care was taken not to transfer any of the aqueous phase. A second 3ml of chloroform was then added to the separating funnel and the rotation was repeated. The second chloroform extract was runoff into the first.

The number of chloroform extractions required for each sample varied due to the high Fe concentrations encountered in many of the estuarine samples, and especially the CFF retentate fractions. In many estuarine samples the high Fe concentrations resulted in brown/black Fe carbamate precipitates forming in the aqueous phase. From test extractions of the LMSW standards (see the data disc for extraction comparison plots) it was noted that Fe recovery at concentrations greater than 200µg/l decreased significantly from 100%. As a result of this, most Fe 0.4_f and R fraction samples were run directly on the flame AAS and calibrated with the LMSW standards.

F2: Flow diagram of the solvent extraction procedure for trace metals in aqueous samples (see text for full description).

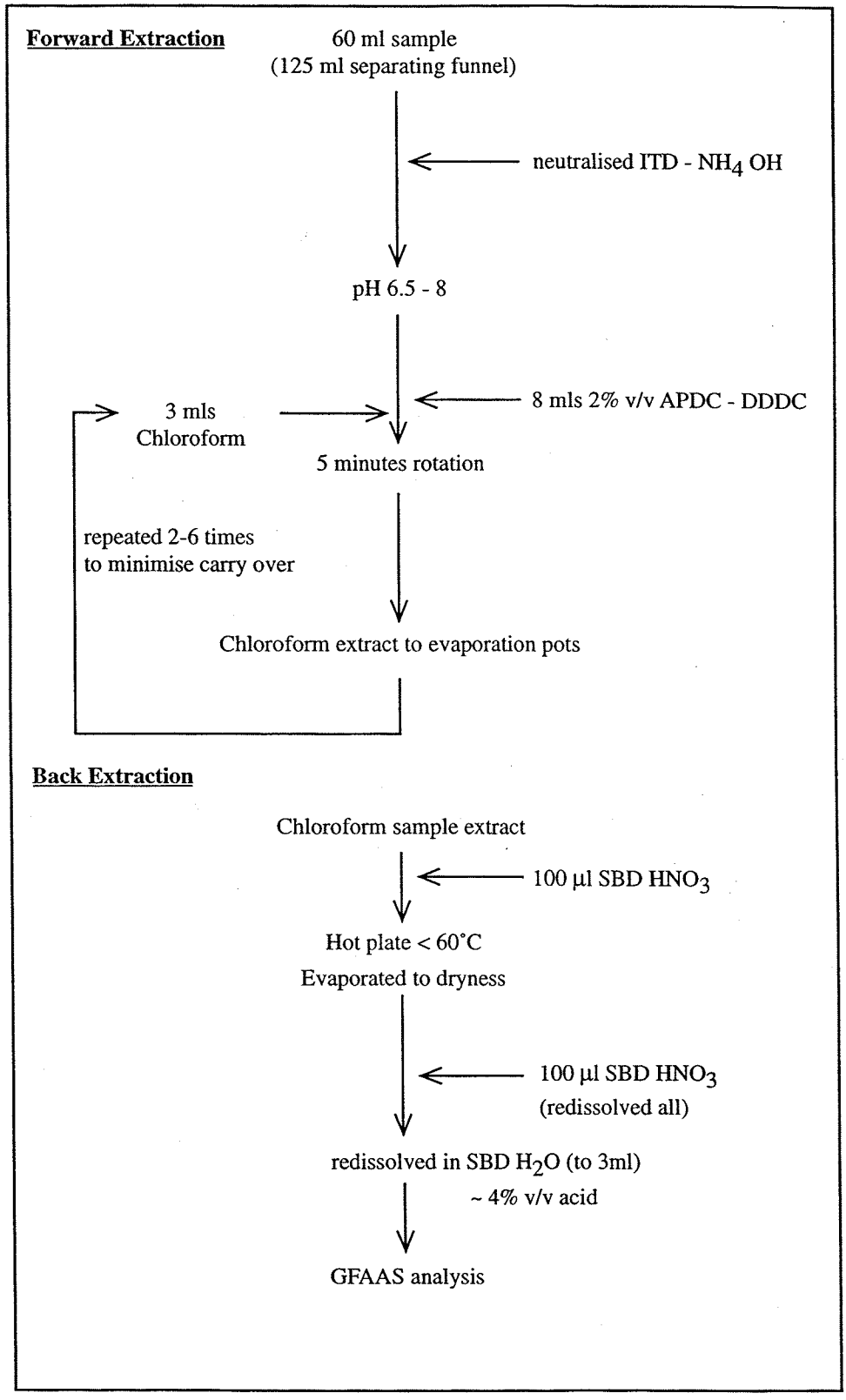

There was also reduced Pb extraction recovery (to 80-90%) above 0.4μg/l standard concentrations of Pb. It was suggested that the highly particle reactive Pb fraction may be associated with the Fe precipitates (Mackey pers.comm) formed in the aqueous phase, and increased stripping of the Fe precipitates would also improve Pb recovery. It was also noted that with only 2 x 3ml chloroform extracts there was significant carryover of Fe (2 to 6 μg/l; 35.8 to 107 nM) and Mn (0.4 to 1.2μg/l; 7.2 to 21.8 nM) from higher concentration standards to a subsequent blank. This carryover was removed by a third chloroform strip (see Mn and Fe plot 6 vs 9ml strip in Appendix 1 of the data disc). For the reasons discussed here, chloroform extracts were repeated a minimum of three times during each extraction but up to 7 times to remove all the Fe carbamate precipitates in high Fe concentration samples and prevent associated metal carryover or contamination.

After this forward extraction, 100µl of SBD HNO_3 was added to each of the combined sample chloroform extracts (this step was designed oxidise matrix components and also stopped fuming upon nitric acid addition which had been observed when no acid was present during the evaporation step). The sample pots were placed on a hot plate set at 50°C and evaporated to dryness. Care was taken not to boil the chloroform (b.p.chloroform~ 60°C) to prevent trace metal loss from the extracts.

For the back extraction, a second 100µl of SBD HNO_3 was added to each of the evaporated extracts. This was also evaporated to dryness. A further addition of 100µl of SBD HNO_3 was used to redissolved the residue. Each extract residue was then made up to 3 mls with SBD-H_2O (2.9ml addition of SBD H_20). This gives ~4% v/v acid in the final extract, ignoring any acid in the residue. Once completely redissolved the back extract for each sample was poured into an acid cleaned 6ml polypropylene tube. The concentration factor with this procedure was 20, 60ml of seawater being concentrated into 3mls.

Blanks (30ml SBD-H_2O, 4ml complexant, 3 x 3ml chloroform extracts), LMSW standards and certified reference seawaters (CASS-2 and SLEW) were also analysed in each extraction batch to assess the analytical quality of the technique and comparability of consecutive sample batches. Chloroform blanks (9ml chloroform evaporated down

and back extracted) and sample UV digestion blanks were also carried out for each extraction batch.

2.3.2: Determination of total dissolved trace metals by GFAAS:

The concentrations of total dissolved trace metals in the back extracts were measured by graphite furnace atomic absorption spectrophotometry (GFAAS) using a Perkin-Elmer 1100B AAS equipped with a HGA-700 graphite furnace and an AS-70 autosampler. A deuterium hollow cathode lamp (HCL) background correction system was used. All the elements were analysed using a pyrocoated tube with fixed L'vov platform except for Ni which was run without a platform. Furnace conditions were adapted from established programmes but modified where necessary (see Table 2.2). The two sets of conditions for lead was to allow for instrument sensitivity variation at different concentration ranges.

Back extracts were diluted with 4% SBD HNO_3 blank where the concentration was above the linear calibration for an element. An internal standard (1643D-Trace elements in waters standard reference-for river waters, supplied by The National Institute of Standards and Technology, Standard reference materials program, Gaithersburg, Maryland) was run with each set of metal analyse to check accuracy of the trace metal concentrations determined by standard calibration.

Fe concentrations in the total dissolved and retentate sample fractions in most of the extracted samples were too high to be run on the GFAAS so the unextracted, acidified samples were run directly by flame AAS with the LMSW standards and blank as calibration standards. The extracted truly dissolved (F) fractions were analysed for Fe on the GFAAS due to their much lower concentrations.

For the February survey which occurred at a time of very high river Trent flows, all samples were analysed without extraction on the GFAAS using a standard addition technique. This method of calibration normalises for matrix effects such as the presence of organic material or other ions in the samples that may cause chemical interference effects in the tube/furnace or other effects on the signal during the HGA cycle.

Table 2.2: GFAAS standard conditions for the analysis of total dissolved trace metals in sample extracts:

Element	Fe	Cu	Mn	Zn	Pb	Cd	Ni
Wavelength (nm)	248.3	324.7	279.5	213.8	217.0/ 283.2	228.8	231.9
Slit (nm)	0.2	0.7	0.2	0.7/0.2	0.7	0.7	0.2
Lamp (mA)	12	5	7	5	10/5	5	10
Integration time (secs)	3.0	3.0	3.2	3.0	2.0/3.0	2.0	3.0
Injection volume (μl)	10-20	10-20	20	10	20/30	10	20
Drying 1(°C)	120	150	150	120	150	150	130
Ramp (sec) Hold (sec)	5 10	5 10	5 10	5 10	12/5 20/10	5 10	5 15
Drying 2 & 3 (°C)	250	250	250		/300	250	600
Ramp (sec) Hold (sec)	5 10	5 10	5 10		/10 /10	10 10	10 10
Drying 4 (°C)					/850		
Ramp (sec) Hold (sec)					/10 /10		
Ashing (°C)	1250	1250	1100	700	400/850	500	1000
Ramp (sec) Hold (sec)	5 10	5 10	5 10	10 10	15/10 10/10	10 10	10 10
Atomisation (°C)	2500	2300	2200	1800	1800	1600	2300
Ramp (sec) Hold (sec)	0 3	0 5	0 3	03 3	0 2	0 4	0 3
Burnout (°C)	2800	2800	2800	2300	2400	2300	2550
Standard 1 Standard 2 Standard 3 (μg/l)	10.63 22.63 53.91	25.03 50.69 102.16	10.69 22.78 54.25	24.91 51.36 100.17	10.76 20.38 31.95	1.738 3.938 10.70	10.79 22.99 54.76

2.4: Digestion of Trent/Humber samples:

One year after sample collection preliminary analysis was carried out on the February survey samples by direct injection into the GFAAS with standard addition calibration.
It was noticed that there was white opaque material present in the 0.4μm filtered ("total dissolved") and retentate fractions but not in the ultrafiltrate. It was hypothesised that these could be bacterial or mould growths, inorganic precipitates or aggregates of colloidal material (Wen pers.comm.). Similar particulate matter has been observed by Muller (Pers.comm.) and Kramer et al. (1994) in stored samples and was attributed to precipitated humic acids at low pHs.

The whitish precipitates were isolated on a 0.4μm polycarbonate filter, air dried and carbon coated for SEM observation and analysis by EDS. The images illustrated the topographical (Secondary electron images; S.E.I.) and compositional (Backscatter electron images; B.E.I.) nature of the precipitates. Plates 1 and 2 show the precipitates to be polymeric organic structures that were originally identified as bacterial colonies but later were determined as fungi due to their size (>10μm wide) and micellular rather that discrete cellular structure (D.Purdie Pers. comm.). It was clear that these fungal growths were not derived from handling techniques as there were none present in the ultrafiltered fraction as fungal cells would have been removed from a sample by ultrafiltration. These growths had occurred despite the sample pH being less than 2. Similar growths have been noted in acidified North Sea samples (Tappin/Statham pers.comm.). It was also apparent that there were large colloidal aggregates associated with theses structures. Plates 3 and 4 show a variation in morphology of these organic structures (more mould like) and the high molecular weight element aggregates intimately associated with them.

By SEM probe analysis (EDS) the aggregates were identified as aluminosilicate clays (with K and Na lattice substitutions), silicate (quartz) and iron oxides. See Appendix 3 for description of the mechanism of colloidal aggregate formation under low pHs. It is obvious that these aggregates are much larger than the 0.4μm filter cut-off that they originally passed through. Although there must be some reservations in the interpretation of aggregate morphology using this technique it is clear that there are significant implications for sample analysis with respect to the homogeneity of the samples and precision of GFAAS injections.

Plate 1: Topographical images (S.E.I.) of fungal colonies on 0.4µm filters separated from samples collected in February 1996 and acidified to <pH2.

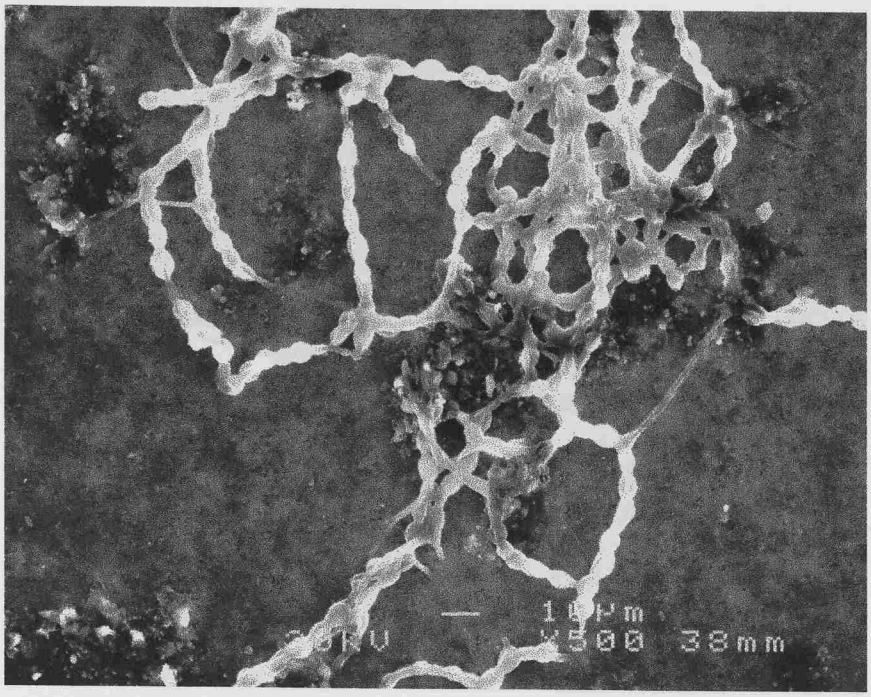

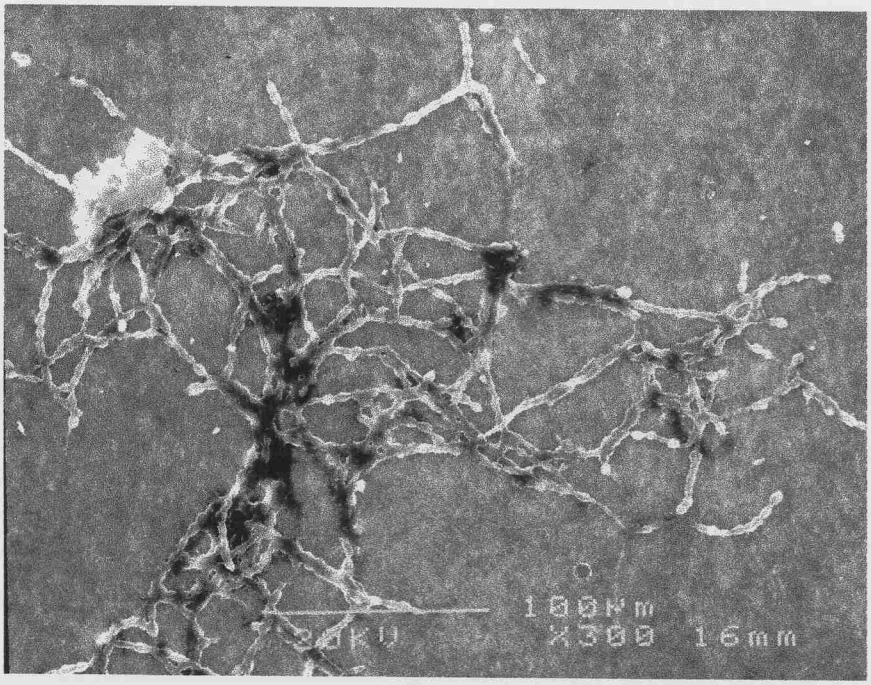

Plate 2: Topographical image (S.E.I.) of fungal colony strand (held on 0.4µm polycarbonate track-etched filter).

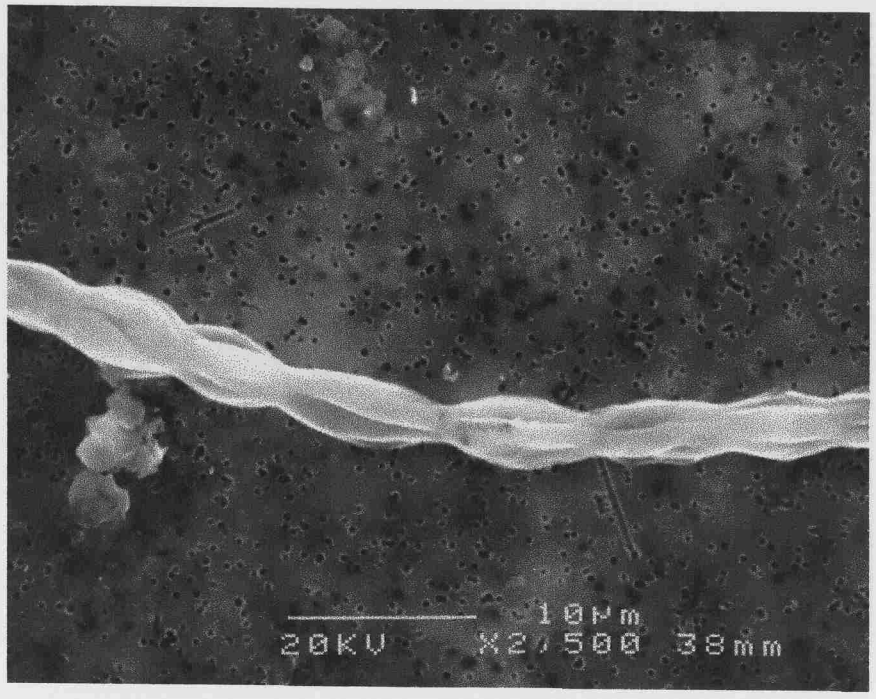

Plate 3: Topographical images of discrete aggregates formed from 0.4μm prefiltered Trent samples.

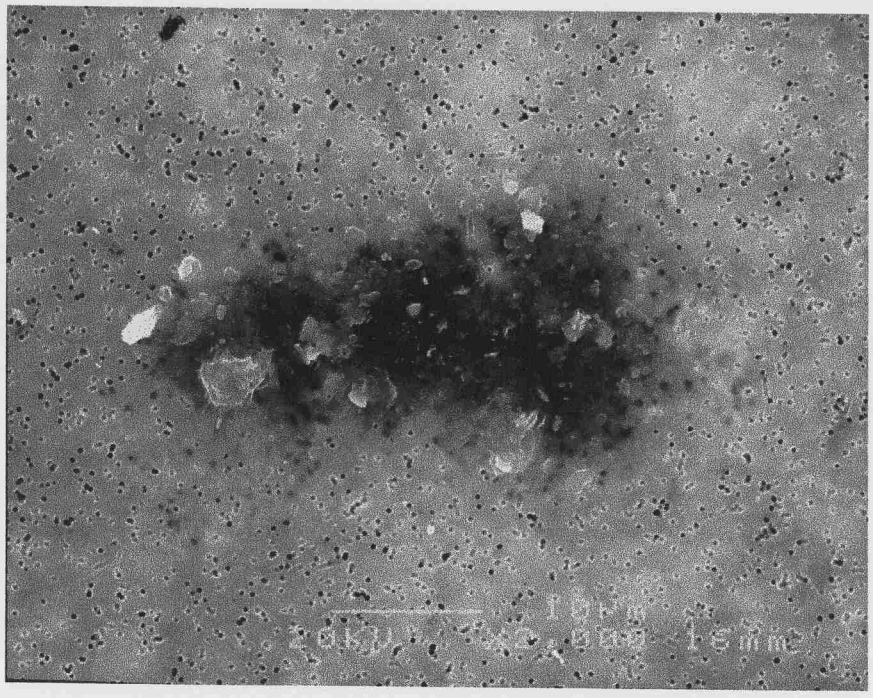

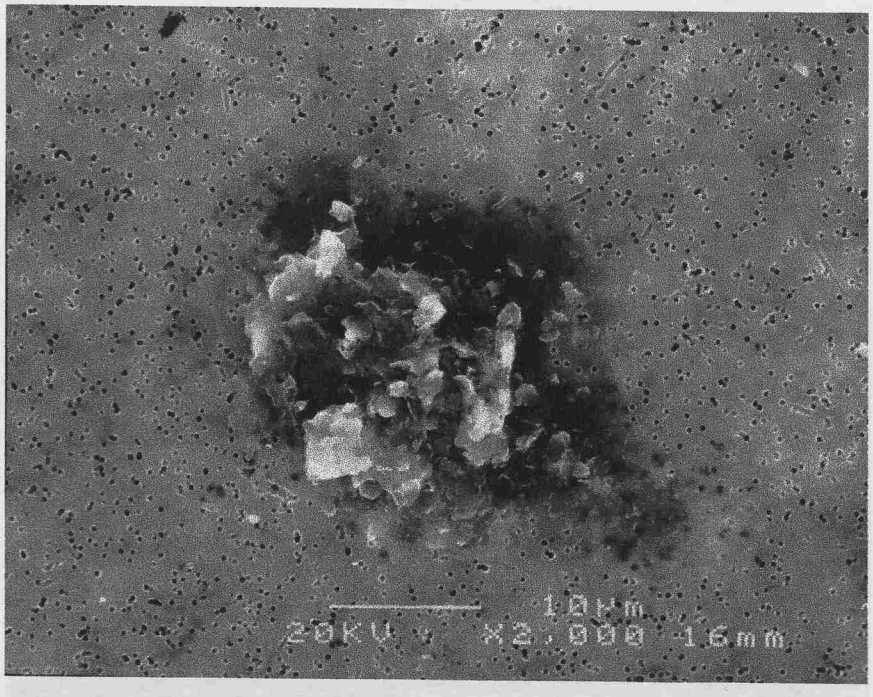

Plate 4: Organic structures and associated aggregates separated from acidified and stored Trent samples (0.4μm prefiltered).

A: Topographical (S.E.I.) image

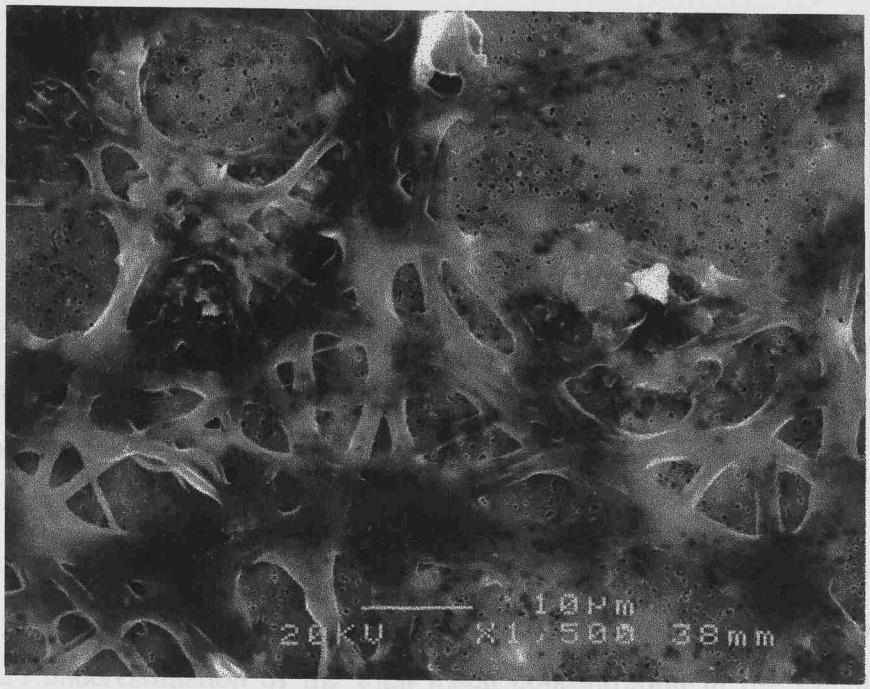

B: Compositional (B.E.I.) image: lighter particles are higher molecular weight elements (possibly metallic).

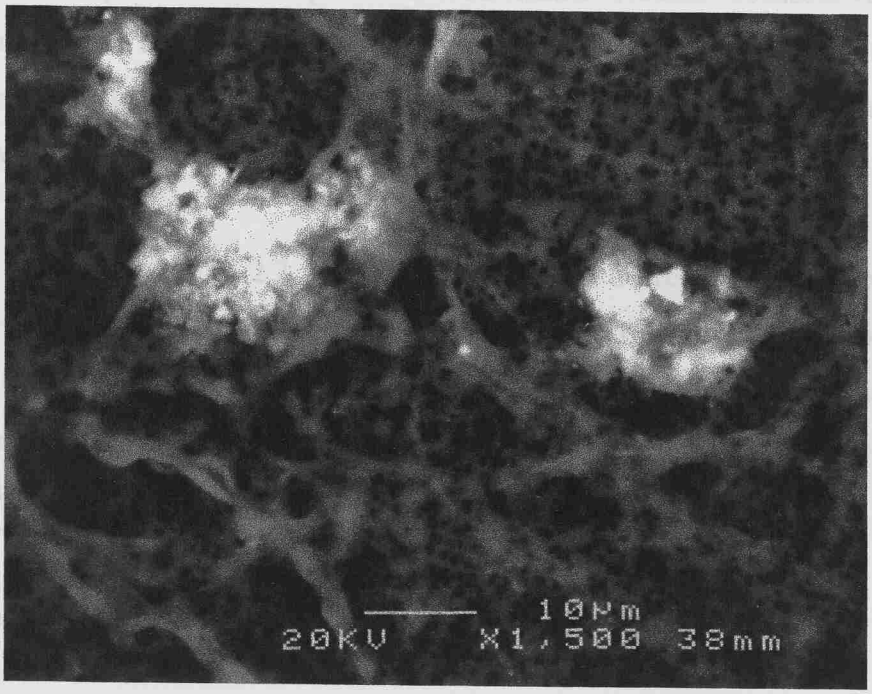

For example: from Stokes settling law;

$$U = \frac{2g(\rho_s - \rho)r^2}{9\eta}$$

Where:

ρ_s is the density of the mineral, ρ is the density of water, r is the particle radius and η is the viscosity of water, g is acceleration due to gravity (9.81 m/s^2)

Inorganic aggregates of 10μm diameter and density of ~2g/cm^3 would have a settling velocity of 6.11 μm/s. Therefore aggregates would theoretically settle out from the sample in a GFAAS cup within 1 hr. With standard addition calibration 3-4 samples per hour can be analysed.

Despite sample shaking prior to dispensing for the length of time the sample stays in the cup there would be effective removal of associated trace metals from solution and therefore an underestimation of the total metal concentration in the sample fraction. Analysis of a sample of such extreme heterogeneity in trace metal concentration (aggregates may sequester metals from the surrounding solution) would also compromise the precision of replicate measurements because consecutive replicate measurements could be artificially high or low. To determine whether this settling effect would be a significant problem a sample was analysed with and without mixing between analyses. Metals determined were Fe and Cu.

As can be seen from Figure 2.2 there was a significant decrease in the determined Fe concentration after 2 hours without sample mixing and decreased further up to 6-8 hours whilst the Cu concentration remained relatively constant under the same conditions. This may be due to the comparatively high iron oxide content of the aggregate whereas the Cu may be more organically associated with the less dense fungal colonies. Ultrasonic dispersion of the aggregates tended to lower trace metal concentration but improved replicate precision as did UV irradiation.

Figure 2.2: Changes in Fe and Cu concentration determined by GFAAS with and without mixing of sample during pipette replicates (1σ within markers).

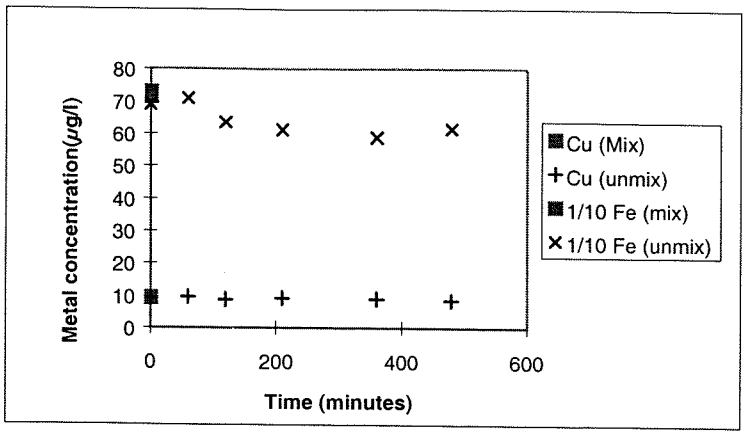

Due to the heterogeneity of colloidal and 0.4μm filtered samples there was a need to find a reproducible way of dispersing the aggregates and therefore homogenising the samples prior to analysis.

It has been noted in several colloidal studies (Quentel et al., 1986; Ostapczuk, 1993; Benoit et al., 1994; Wen et al., 1996) that digestion of the colloidal retentate fraction and 0.4µm filtered fraction is necessary to release trace metals that may have been sequestered by colloidal aggregates in high colloidal concentration samples. This digestion procedure is often deemed necessary to give good trace metal precision of sample subsampling in direct analysis and also good recoveries in solvent extraction techniques.

To test the significance of the precipitates/aggregates in affecting trace metal concentration determinations and precision in the non-extracted February samples a digestion procedure was performed on selected samples. The digestion involved;

Further acidification of samples with 1ml SBD HNO_3 per litre of sample,
Ultrasonification for 4hrs at 65°C (to disrupt inorganic aggregates),
UV irradiation for 8 hrs to digest organic species (Wen pers. comm.).

The precipitates were only observed to disappear after the UV treatment stage.
Milli-Q blanks for each stage were carried out and a reference standard (1643D) was run

in the before and after digestion sample analyses. The first metal to be monitored was iron, as a good contamination indicator species and also because there was significant iron signals in the aggregates analysed by EDS. Calculation of ultrafiltration mass balance recovery changes upon digestion for Zn and Cu were also done as well as procedural blanks for Pb and Cd. Digested F(truly dissolved) fractions acted as digest and analysis blanks (see Appendix 3 on data disc for raw data).

Procedural blanks were not significant for Cd, Pb, Zn and Cu and although the Fe blank was 1 to 2μg/l this was significant in comparison to sample concentrations. For all metals the digestion procedure increased the absolute concentration and improved the precision of trace metal concentration determined by approximately 1-2%, or more for some samples. The recovery for Zn and Cu was generally improved by digestion which indicates that a significant fraction of these metals lost in the mass balance was made available by the digestion technique. For Fe, the recoveries showed no consistent improvement, mainly because the increase seen in the 0.4μm fractions were proportionally larger than those in the retentate fraction, which affected the recovery calculation. The Fe recoveries were also still substantially less than 100% (56 to 65%) indicating that the majority of the iron lost in the mass balance is connected to interaction with the ultrafiltration system and not subsequent analysis protocol. Absolute concentrations of digested truly dissolved fractions were relatively unchanged within the error of the technique. SEM images of filtered digested samples indicated no fungal precipitates or aggregates remained.

Overall, the digestion procedure lead to an increase in the absolute concentration of Fe, Cu and Zn and an improvement in the analytical precision. These benefits of digestion in particular was not reflected in colloidal concentrations or a universal improvement in mass balance recoveries, mainly because the digestion procedure had a greater effect on the 0.4μm filtered, rather than the retentate fractions. This effect is probably linked to the very high concentrations of colloidal material in the retentate fractions. The changes in metal recovery and colloidal concentrations were mainly inconclusive. Although many of the changes in concentration and precision were not statistically significant (t-test), this digestion procedure was retained as standard for all sample treatment prior to extraction

and analysis. This served to improve homogeneity of samples, analytical precision and confidence in subsequent sampling and analysis protocol. It has also been suggested that digestions such as these also increase element availability to the solvent extraction procedure especially for colloidal Fe and other metals which need to be in a reactive phase i.e. hydrated ion or similar species (Danielsson et al. 1978; Danielsson et al., 1982) to be complexed.

2.4.1: Digestion comparison for the solvent extraction technique:

Large colloidal/organic aggregates were also observed in the samples from other surveys, but especially the concentrated colloidal (retentate) samples. To assess the effect of the same digestion procedure on the efficiency of the ADPC-DDDC/chloroform solvent extraction technique, three samples from low, intermediate and high salinity stations in the August and December (samples 225, 229, 220 and 1, 15, 11 respectively) transects were subdivided so that colloidal (R) and total dissolved (0.4_f) fractions could be analysed simultaneously with and without digestion. All survey samples were routinely digested before extraction and the undigested samples were extracted in the same batch as their corresponding digested samples to avoid any influence of inter batch variation. The results for the sample digests are discussed below (see Figures 2.3 a to g) and raw data is presented in Appendix 3 of the data disc.

2.4.2: Precision and absolute trace metal concentrations:

Precision was not significantly improved by sample digestion, however, as the standard deviation for all metal samples is less than 4%, a significant change would have been difficult to detect.

There was significant increases in concentrations of Fe, Pb and Zn in digested samples (once blank corrected). The largest increases occurred in the lower salinity samples (both 0.4μm filtered and retentate fractions) in the December survey. Cu and Mn showed an intermediate increase in concentration whilst digestion seemed to have no effect on Ni concentration in either fraction or survey. Cd response to sample digestion was mixed with increases in Cd concentration occurring in December samples (especially R fractions) but concentration decreases occurring with digestion in the August samples.

Figure 2.3 a to g: Comparisons of extracted trace metal concentrations from samples with or without digestion. a:Fe, b:Pb, c:Zn, d:Cu, e:Mn, f:Ni, g:Cd.(error bars are 1 standard deviation of triplicate measurements).

a:

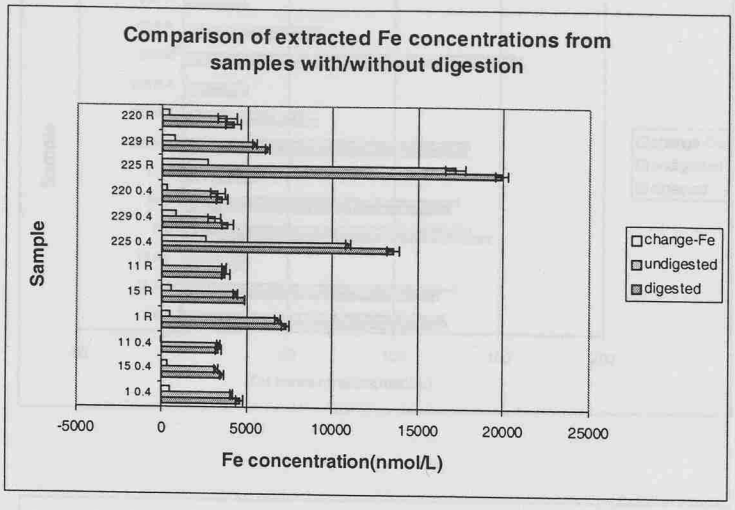

b:

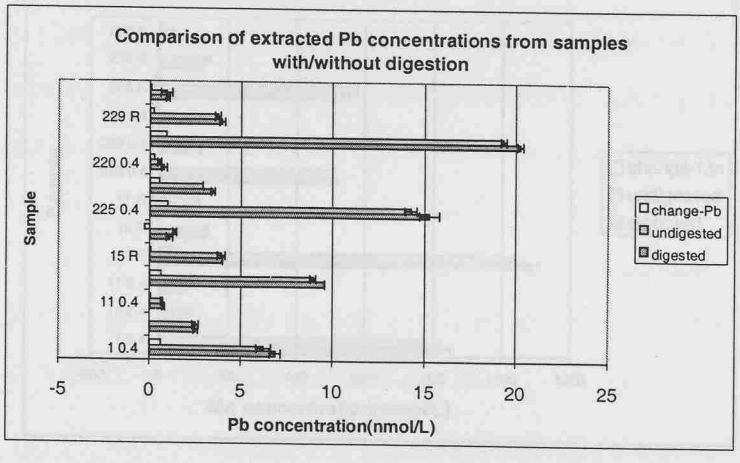

c:

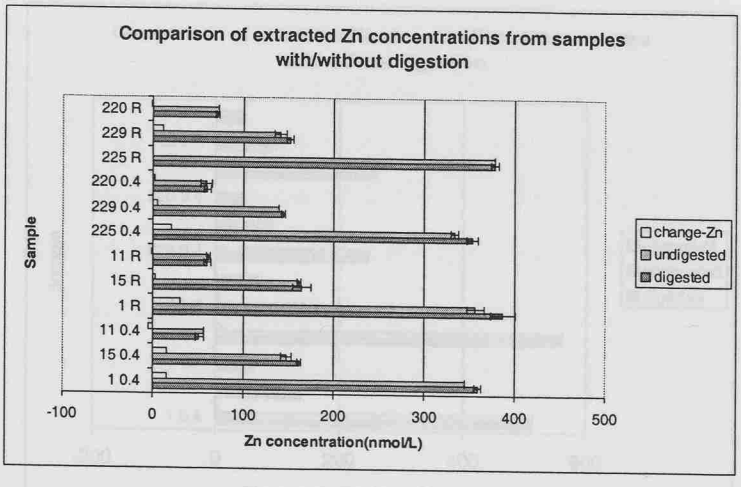

d:

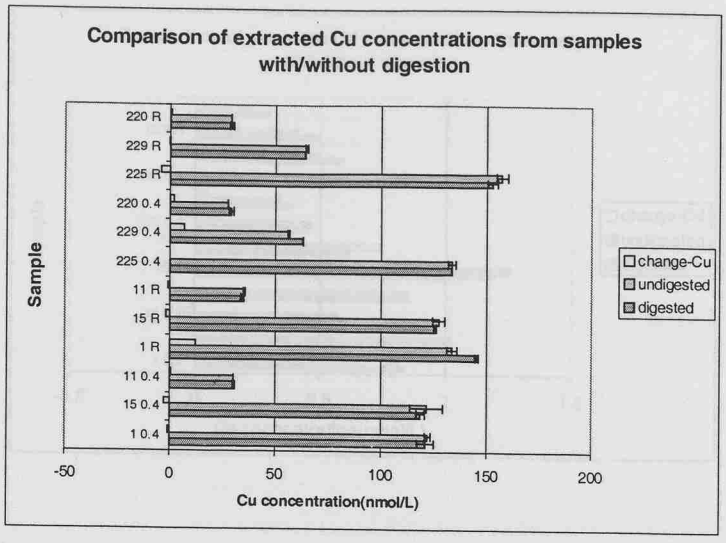
Comparison of extracted Cu concentrations from samples with/without digestion
Sample
220 R
229 R
225 R
220 0.4
229 0.4
225 0.4
11 R
15 R
1 R
11 0.4
15 0.4
1 0.4
-50
0
50
100
150
200
Cu concentration(nmol/L)
change-Cu
undigested
digested

e:

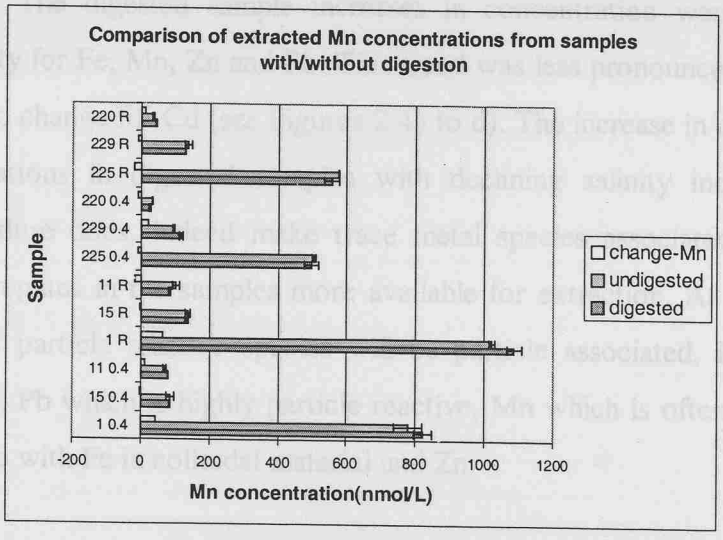
Comparison of extracted Mn concentrations from samples with/without digestion
Sample
220 R
229 R
225 R
220 0.4
229 0.4
225 0.4
11 R
15 R
1 R
11 0.4
15 0.4
1 0.4
-200
0
200
400
600
800
1000
1200
Mn concentration(nmol/L)
change-Mn
undigested
digested

f:

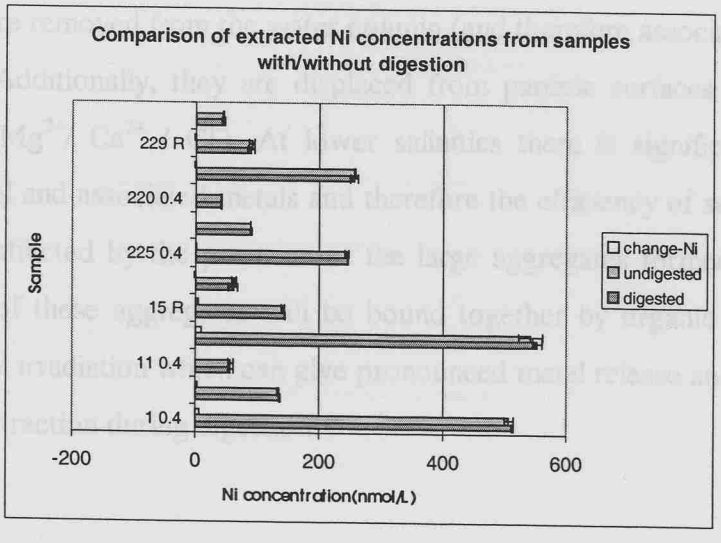
Comparison of extracted Ni concentrations from samples with/without digestion
Sample
229 R
220 0.4
225 0.4
15 R
11 0.4
1 0.4
-200
0
200
400
600
Ni concentration(nmol/L)
change-Ni
undigested
digested

g:

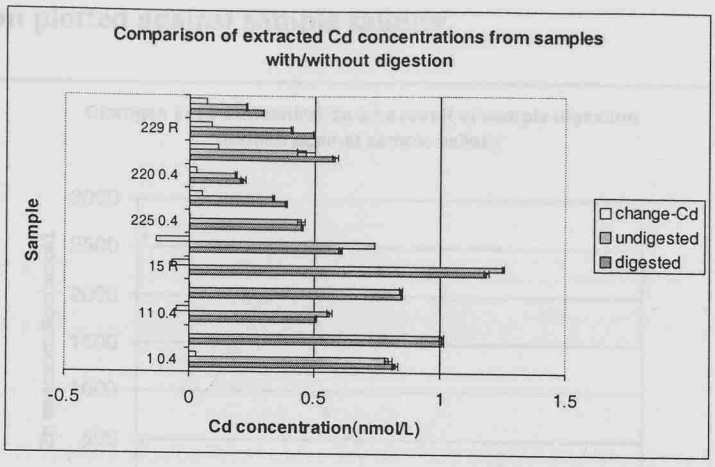

The trace metal concentration changes as a result of sample digestion were plotted against salinity. The digested sample increases in concentration were reduced with increasing salinity for Fe, Mn, Zn and Pb. This trend was less pronounced for Cu and Ni and there was no change for Cd (see Figures 2.4a to d). The increase in determined trace metal concentrations in digested samples with declining salinity indicates that the digestion procedure does, indeed make trace metal species associated with colloidal material or aggregates in the samples more available for extraction. At lower salinities, higher levels of particle reactive species will be particle associated, i.e. Fe which is largely colloidal, Pb which is highly particle reactive, Mn which is often coprecipitated/ highly associated with Fe in colloidal material and Zn.

With increasing salinity the colloidal species that contain these metals destabilise and aggregate and are removed from the water column (and therefore associated samples) by sedimentation. Additionally, they are displaced from particle surfaces by other major seawater ions (Mg^{2+}/ Ca^{2+} / Cl^-). At lower salinities there is significant amounts of colloidal material and associated metals and therefore the efficiency of sample extraction will be greatly affected by the presence of the large aggregates formed during sample storage. Many of these aggregates will be bound together by organic material that is destroyed by UV irradiation which can give pronounced metal release and improve metal availability to extraction during digestion.

Figure 2.4a to d: Changes in extracted trace metal concentration as a result of sample digestion plotted against sample salinity.

a:

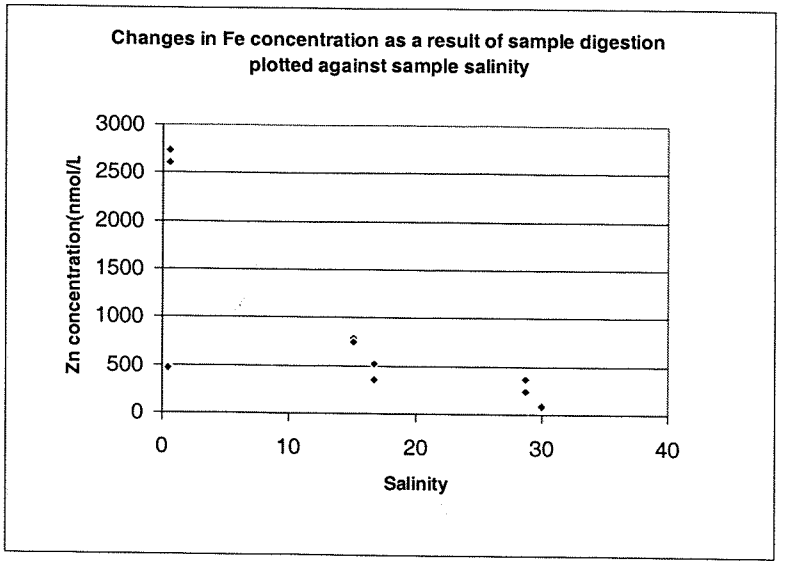

b:

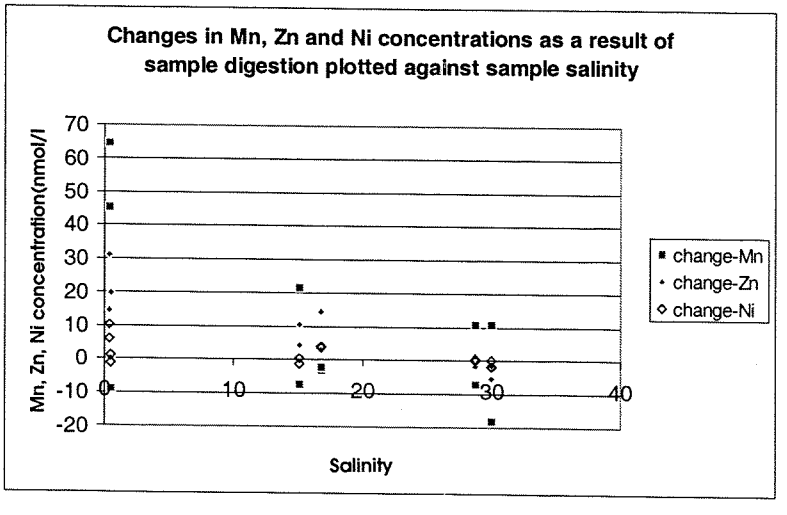

c:

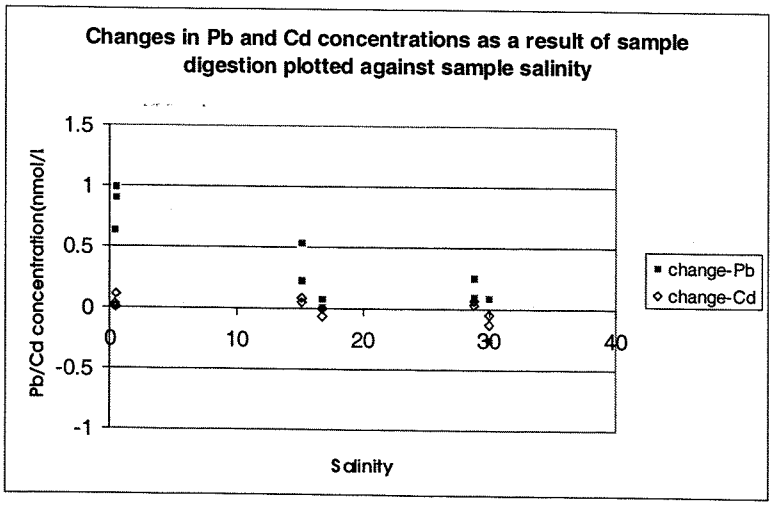

Figure 2.4d:

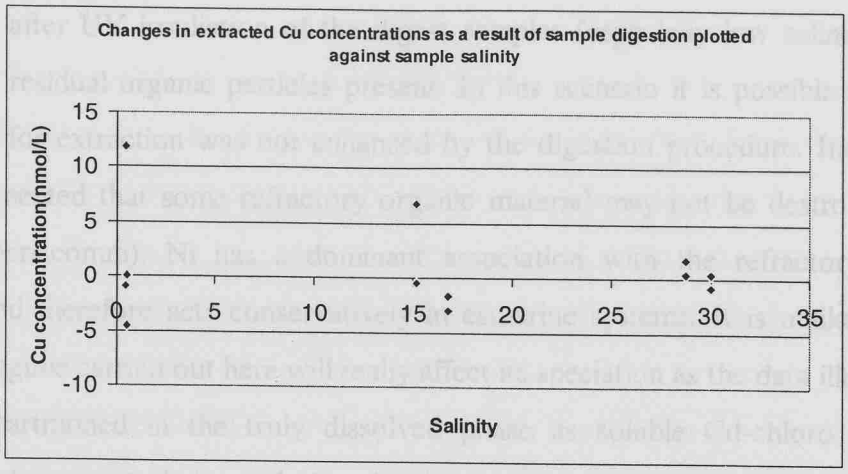

Figure 2.5: Comparison of average % change in trace metal concentration upon sample digestion.

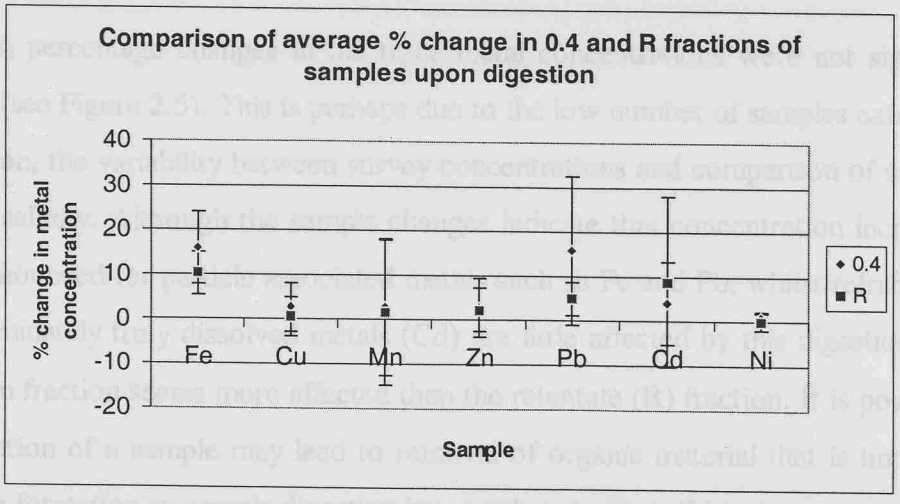

Figure 2.6: Comparison of trace metal recovery for digested and undigested samples.

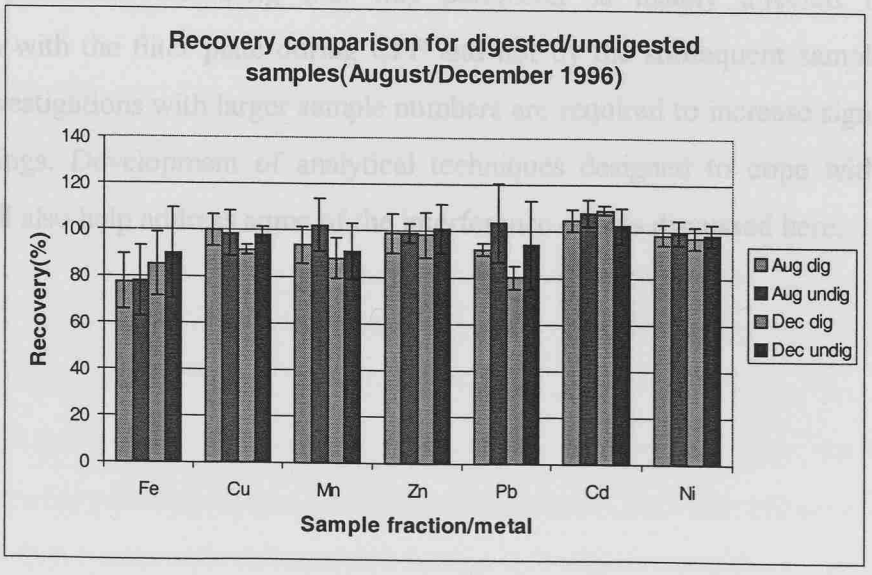

Cu often displays conservative behaviour in estuaries due to its complexation by DOM but, often, after UV irradiation of the digest samples (especially low salinity samples) there were residual organic particles present. In this scenario it is possible that the Cu availability for extraction was not enhanced by the digestion procedure. Indeed, it has been documented that some refractory organic material may not be destroyed by UV (Mackey pers.comm). Ni has a dominant association with the refractory phase of particles and therefore acts conservatively in estuarine systems. It is unlikely that the digestion regime carried out here will really affect its speciation as the data illustrates. Cd is highly partitioned in the truly dissolved phase as soluble Cd-chloro complexes. Therefore, digestion techniques designed to break up aggregates will have little effect on the extracted Cd concentration.

The mean percentage changes in the trace metal concentrations were not significantly different (see Figure 2.5). This is perhaps due to the low number of samples extracted for comparison, the variability between survey concentrations and comparison of samples of different salinity. Although the sample changes indicate that concentration increases are most pronounced for particle associated metals such as Fe and Pb, whilst refractory (Ni) or predominately truly dissolved metals (Cd) are little affected by this digestion method the 0.4μm fraction seems more affected than the retentate (R) fraction. It is possible that concentration of a sample may lead to removal of organic material that is important in aggregate formation so sample digestion has a reduced effect. Cd is the exception to this. Mass balance recoveries (Figure 2.6) of the samples are not significantly affected by the digestion procedure indicating that this parameter is mainly affected by sample interaction with the filter plate during CFF and not by the subsequent sample analysis. Further investigations with larger sample numbers are required to increase significance of these findings. Development of analytical techniques designed to cope with colloidal species will also help address some of the interference effects discussed here.

2.5: Field Flow Fractionation (FFF) procedure and protocol:

Field flow fractionation is a set of liquid chromatography-like elution methods (Beckett and Hart, 1993) that can be used to separate particles and colloids from a heterogeneous suspension. Field flow fractionation of colloids and macromolecules is carried out in a laminar fluid flow in a thin channel (See Figure 2.7a for channel orientation in centrifuge). The typical dimensions of a FFF channel are 30 to 100cm long, about 1 to 3 cm wide and 0.05 to 0.5cm thick. The particle suspension is performed in a laminar fluid flow (Lead et al., 1997) but the particle separation depends on a force that is applied perpendicular to the flow. This force may be gravitational (as used in this study) electrical, magnetic, a thermal gradient or a fluid cross flow (Buffle and Leppard, 1995a and b).

The sample solution or suspension is introduced into one end of the channel and the flow turned off. The field is applied at right angles to the flat face of the channel. The field drives the sample particles/molecules towards the accumulation wall (see Figure 2.7b). Each colloid type forms a cloud whose thickness and elevation above the wall depends on the strength of interaction of the particles with the field (partially size dependant) and rate of their back diffusion into the channel. The time during which the flow is turned off and the field applied to produce the colloid separation is the "relaxation period". The resulting separation of colloidal material depends on the physical properties of the colloidal particles such as density (and therefore composition), effective mass, particle dimensions etc.

Following the relaxation period, which must be long enough for particles situated at the top of the wall to be transported across the channel to the accumulation wall, the flow of carrier liquid down the channel is initiated. The velocity profile of carrier down the channel is parabolic with highest flow velocities at the centre of the channel and lower flows close to the accumulation wall (see Figure 2.7b). Hence, smaller colloids that form higher/larger clouds are carried away by the higher velocities and eluted first. As larger particles are pushed closer to the accumulation wall by the applied force, they are eluted after the smaller particles. Particle sizes can be calculated from first principles or elution curves but then checked via electron microscopy techniques.

Figure 2.7: **a) Schematic representation of the orientation of the field flow fractionation channel in a sedimentation centrifuge (from Beckett et al. 1988, 1993).**

b) Schematic representation of the hydrodynamic flow and perpendicular field applied to the separation channel in FFF (from Buffle and Leppard, 1995b).

(a)

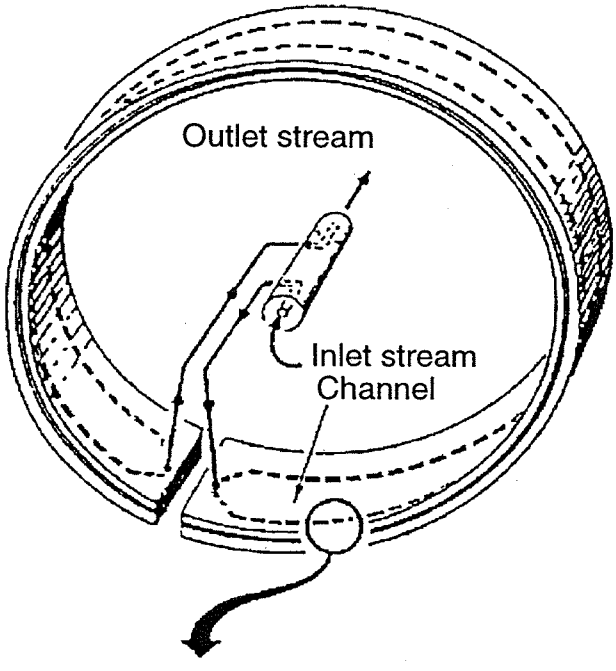

(b)

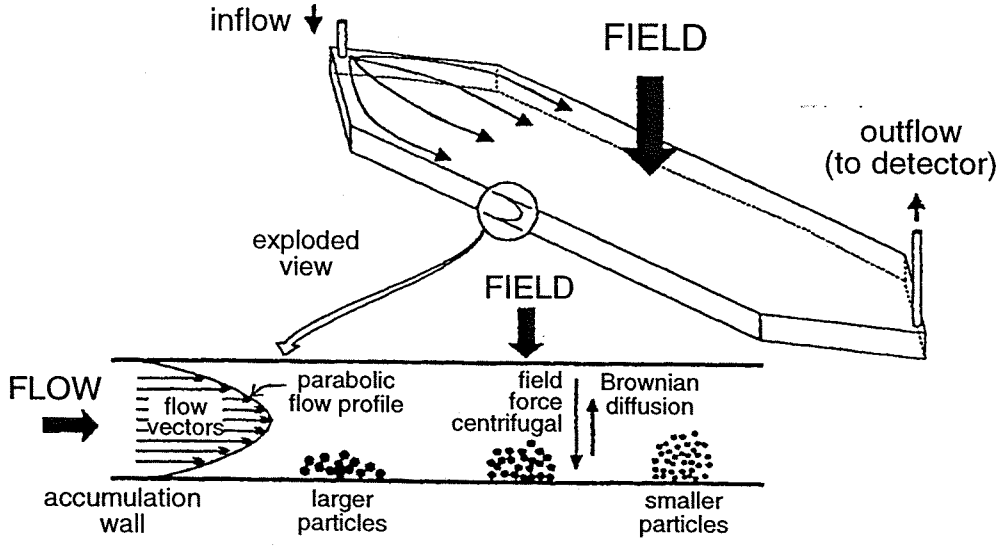

As with many techniques there are several advantages and disadvantages with FFF.

Advantages:

- There is much less opportunity for interaction of a sample with the stationary phase which may lead to anomalous retention behaviour and size calibration. This may reduce perturbations associated with filtration techniques such as CFF where colloidal interactions with the filter medium may occur.
- There is potential for separation of wide ranges of particle size (1nm to 100 m) when several elution regimes are combined.
- FFF is a separation technique based on the diffusion coefficients of colloids which is a key parameter governing their behaviour in natural systems.
- FFF provides a complete size distribution of colloidal material with the potential for chemical analysis of the fractions.

Disadvantages:

The structure of colloids and aggregates may alter during FFF for several reasons:

- Only small sample masses can be introduced into the FFF channel and the eluted fractions are significantly diluted (up to 200 fold) which may lead to disaggregation of colloidal material and makes any chemical analysis (i.e. extraction for trace metal analysis) much more difficult with respect to detection limits. Preconcentration techniques that would improve these problems may result in coagulation effects.
- Standards and FFF theory used to calibrate elution runs encounter problems when compared to natural colloids. For example; FFF standards and theory assume spherical particles of uniform density and natural colloids/particles are likely to be much more complex in morphology and composition.
- The "relaxation" step which allows formation of colloidal clouds proportional to their physical properties prior to elution also results in a substantial increase in particle concentration and therefore collision frequency within these clouds and also during particle migration. This potentially could lead to aggregation and colloid size spectrum changes.

2.5.1: Trace metal size spectrum determination for Celtic Sea sediment suspension and Beaulieu River water samples:

Field flow fractionation separation was carried out on stock sediment suspension from the Celtic Sea used in Al resuspension experiments and a colloidal sample from the Beaulieu Estuary that was used in ^{65}Zn radiotracer experiments. This work was carried out at Lancaster University with a particle/colloid fractionator model S-101 FFFractionation LLC (FFFractionation, Utah). The aim of this work was to identify the distribution of Al (Celtic Sea stock suspension) and Fe, Mn and Zn (Beaulieu water sample) with particle/colloid size as defined by FFF. This would identify the natural (initial) colloidal trace metal distribution with size for the resuspension and radiotracer time series experiments.

2.5.1.1: Sample preparation and FFF assumptions:

Celtic Sea sediment sample:

As a result of the high dilution factors during FFF the sediment stock used for the Al resuspension experiments was used for FFF to enable the lumogallion technique (Hydes and Liss, 1976-see Appendix 4 for method and protocol) to be used for fraction analysis. It was assumed that as the particle distribution in this stock when homogenised would be similar to the particle size spectrum produced upon injection of this stock into a filtered seawater sample as in the resuspension experiments. Hence, the distribution of particulate/ colloidal Al would also be similar. An initial measurement of total reactive and dissolved Al was made prior to the injection of the 0.4μm prefiltered stock suspension. Each combined fraction was collected in a bottle cleaned/preconditioned for Al work (see section 5.5.1 for preparation details) and kept cold and dark until Al analysis by the lumogallion technique. Two separate FFF runs were done on the Celtic Sea sediment suspension after differing lengths of storage (~2 days difference) to see if the size distribution of the Al changed significantly over this time.

Beaulieu Estuarine sample:

A bulk, large volume (~4 litres) Beaulieu river end-member sample was taken. This sample was prefiltered using a 47mm, 0.4μm polycarbonate membrane mounted in a laminar flow block (see Appendix 4 for protocol). This form of CFF is designed for small volume sample filtration whilst minimising the potential for sample perturbation and removal of colloidal material during prefiltration. Procedural filtration blanks were carried out for the metals that were analysed (Fe, Mn, Zn). The colloidal filtrate was retained for subsequent FFF.

Due to the low natural concentrations of trace metals several identical FFF fractions were combined to give sufficient sample volume for trace metal preconcentration (17 to 30 fold) by a APDC-DDDC chloroform solvent extraction technique (see section 2.3.1.5 for method). Total dissolved (0.4μm filtered) aliquots were removed from the original sample prior to its fractionation and extracted along with the FFF fractions and blanks. All samples and fractions stored for later trace metal analysis were acidified with SBD HNO_3 (1 ml/L) under clean conditions, immediately after fractionation.

Both the Celtic Sea and Beaulieu FFF samples were prepared the day prior to fractionation and kept cold and dark until used, to minimise potential size spectrum changes. Two fractionating runs were carried out on each of the samples. Each fractionating run had parameters designed to give better separation resolution over two particle size ranges (0-0.2 μm and 0.2 to 0.4 μm). Individual run specifications are given in Table 2.3. The carrier stream used was 0.001M sodium nitrate and blanks for each trace metal (Al, Fe, Mn, Zn) were collected prior, during and post a FFF cycle for equivalent sample/elutant volumes.

The particle density assumed for Celtic Sea and Beaulieu particles was 2g/cm^3. This was probably too low for Celtic Sea sediment that is usually composed of carbonates, quartz and aluminosilicate (clay) materials but perhaps too high for Beaulieu colloids that are highly organic with Fe and Mn oxyhydroxide associations. In previous studies (Beckett et al., 1993) particle densities for silica and most silicates or cell organic matter have

been assumed as 2.5 and 1.5 g/cm^3 respectively. However, without accurate % by weight composition of both these suspensions and considering the possibility of particles of heterogeneous composition, 2g/cm^3 provides a good working compromise. It must be remembered however that the assumed density will affect the calculated elutant times and therefore the colloidal clouds will elute sooner or later than calculated i.e. the more organic colloids will sit higher in the channel so may be eluted sooner than calculated for a higher assigned density. The reverse is true for more inorganic/mineral particles.

Table 2.3 : Run details for FFF of natural samples.

Run parameters	Run 1 (<0.2μm)	Run 2 (0.2μm to 0.4μm)
Injection time	0.8 seconds	0.8 seconds
Equilibration time	10 minutes	10 minutes
Injection delay	49.92 seconds	41.60 seconds
Injection rpm	2400	1400
Hold time	60.0 minutes	70 minutes
Hold rpm	500	150
End rpm	500	150
Delta rho	1	1
T1	5 minutes	5 minutes
T$\propto$	-40 minutes	-40 minutes
Run time	87.0 minutes	109.0 minutes
Flow rate	1.25 ml/min	1.5 ml/min

The injection volume for both samples was 0.5ml with an elutant dilution factor of approximately 189.8 and 180.3 for runs 1 and 2 respectively. To achieve sufficient sample volume for trace metal and Al analysis the elutant fractions were combined into seven larger fractions in addition to a truly dissolved fraction (see Table 2.4). Even with the high concentrations of the Celtic Sea stock suspension there was insufficient material to determine a particle mass for each of the FFF sample fractions. Hence, each combined fraction cannot be normalised for the amount of colloidal material it contains and the distribution is purely a total trace metal distribution over several particle size ranges.

Table 2.4: Theoretical size ranges and elutant times for FFF combined fractions.

Fraction	FFF elutant time (mins.)	Theoretical size range(μm)
Run 1		
F1	3.4 to 22.1	<0.08 (truly dissolved)
F2	22.1 to 38.1	0.08 to 0.134
F3	38.1 to 54.1	0.134 to 0.166
F4	54.1 to 70.1	0.166 to 0.190
F5	70.1 to 75.9	0.190 to 0.197
Run 2		
F6	2.8 to 29.2	0.0329 to 0.180
F7	29.2 to 39.2	0.180 to 0.273
F8	39.2 to 49.2	0.273 to 0.354
F9	49.2 to 60.1	0.354 to 0.418

For both sample runs separate samples were taken over similar elutant times, one for metal analysis and one for SEM/TEM (Scanning Electron Microscopy/Transmission Electron Microscopy) particle sizing to check comparison of calculated elutant sizes from the FFF and actual particle sizes in the elutant samples. Electron dispersive (EDS) microanalysis work was also performed on the dried samples to assess colloidal composition.

CHAPTER 3:

Investigation of the influence of particle size spectra on the partitioning of trace metals in estuarine environments.

3.1 Introduction:

As has been discussed previously, colloids have a great potential to alter behaviour of dissolved trace metals by their preferential adsorption onto colloidal surfaces or transport throughout a particle population via colloidal aggregation/disaggregation processes. The transport of trace metals on colloidal vectors and their subsequent partitioning into particulate or "dissolved" phases can be described using the partition coefficient (Kd) as discussed in section 1.7. The two phases involved have been operationally defined to date as particulate (retained by a 0.4μm filter cut-off) and dissolved (passes through a filter of 0.4μm cut-off). The Kd is in effect the distribution of the total metal species present between these two phases. The presence of colloids i.e. particles incorporated into the dissolved phase, may affect initial trace metal adsorption characteristics and also future transport and mobility between fractions. The "particle concentration effect" is one such way in that colloids have been implicated in affecting experimental determinations of sorption binding constants or conditional partition coefficients such as Kd. This can either be a result of affecting the processes governing trace metal fractionation or by changing the defined partitioning though ways of expressing the Kd.

For a uniform particle size population, an increase in Kd with increasing particle concentration (C_f) would be expected as the increased available reactive surface area/binding sites would act to remove species from solution. The "particle concentration effect", as discussed in section 1.7, in converse, is the observed decrease in apparent partitioning "constants" (Kd) with increasing particle concentration (C_f). There are, at present two explanations for this effect:

- Particle-particle interactions create an interfacial environment that is comparatively unfavourable to surface complex formation and so the greater the particle concentration, the more frequent and intense the interparticle interactions and the more equilibrium is shifted towards the dissolved phase (Honeyman and Santschi, 1992).

- Trace metals associated with colloids in the "dissolved" phase act to reduce the partitioning constant from its "true" value. The extent of the reduction will be proportional to the intensity of trace metal binding to colloids and also the mass and size distribution of colloidal material.

It should be noted that although this effect is to a certain extent an experimental artifact it also reflects real changes in the distribution of sorbed species in natural systems where Kds are by no means constant and subject to rapid and dynamic changes in parameters such as pH, ionic strength, temperature, dissolved oxygen, particle type and binding capacity, etc.

It is possible however, that the overall effect of colloidal trace metals on an absolute Kd may be variable. For example; a particulate mass increase seen as an increase in C_f (particle concentration >0.4μm) is disproportional (smaller) to adsorption area available if there is a higher proportion of colloidal material included in the dissolved phase. An increase in colloid interactions will inevitably increase aggregation processes and hence C_f. By these enhanced aggregation processes trace metals can be carried out of the dissolved phase, increasing Kd. This is converse to the particle concentration effect described earlier. The exact effect of colloidal material on partition constants has not been addressed specifically

In this and other studies there are three main pools in which trace metals may be retained:

-colloidal associated (~0.01μm to 0.4μm)

-particulate (>0.4μm).

-truly dissolved (<~1-10nm, <0.01μm).

Conditional partitioning constants can be written to express the relative affinity of a metal species for either of the particle phases. The partitioning constants Kf (particulate) and Kc (colloidal), see section 1.7 for definition and discussion, depend on solution conditions (pH, salinity, temperature, dissolved oxygen) and the presence of metal complexing ligands. They will therefore vary widely in natural systems.

The aim of the research reported here was to investigate how the size fractionation of particulate material (i.e. the presence of colloidal material) affects the partitioning (as described by Kd) of trace metals in natural waters. Whether the colloidal fraction is included in the defined particulate (colloidal particulate or coll.part.) or dissolved (colloidal dissolved or coll.diss.) phase will alter the resulting Kd. Kd is the ratio of the distribution of an element between a dissolved and particulate phase (see section 1.7). Therefore for its determination in any experiment, gravimetric as well as partitioning data must be acquired. The laboratory experiments were therefore two fold:

i) Gravimetric analysis of particulate fractions.
ii) Partition investigation using a ^{65}Zn radiotracer.

Pilot experiments were carried out to develop the best methods of ultrafiltration and filtration cut-off points and for optimisation of radionuclide procedures.

The overall strategy of these experiments was to investigate the adsorption of radiotracers (as an analogue for stable trace metals) onto colloidal material and monitor partitioning changes as a result of physical or chemical changes (adsorption/ desorption, aggregation/disaggregation) as described by partitioning constants (Kd, Kf and Kc).
In conjunction with these objectives other techniques were applied to further develop colloidal partitioning ideas. For example, the effects of sample storage temperature on the resulting colloid/aggregate size spectrum and radiotracer partitioning, and the nature of the association of the zinc radiotracer with colloidal material (by stable zinc additions to labelled colloidal population) were both investigated. The original colloidal material and older colloidal aggregates were investigated using scanning electron microscopy with energy dipersive x-ray microanalysis to give better insight into compositional and conformational changes over various timescales. Coulter counter work was also carried out to gain idea of the colloidal spectrum as part of the wider particle population. Some field-flow fractionation (FFF) work was also performed to identify the partitioning of stable trace metals, within a similar colloidal population as that used for the radiotracer investigations. The natural distribution of trace metals on colloidal material and the nature of the association of trace metals with colloids had not been looked at previously.

3.2: Results of pilot experiments:

3.2.1: Gravimetric analysis:

Measurable masses of colloidal material were collected from the river end-member samples (Beaulieu). The colloidal mass concentrations range from 1.3-4.2 mg/l (14 to 30% of SPM) as can be seen from the gravimetric data in Table 3.1. A large component of this mass is suspected to be organic given the nature of the estuary, the brown colour of the water prior to 0.02μm filtration and also the high clogging rate that was experienced in all the filtration procedures. Duplicate filtration of a bulk sample collected on the 12/06/95 illustrated the reduction in colloidal mass (~1 to 1.5mg/l) when the sample was prefiltered with 2, 0.4μm filters as opposed to 3 filters. This colloidal material appears to be retained on the 0.4μm filters, probably by clogging mechanisms.

It can be seen from the gravimetric data that the fraction of colloidal material is high in the riverine samples (14 -30%) relative to total SPM, whereas in the estuarine samples the colloidal SPM fraction is very small (<1%). Further measurements and improved protocol are required to substantiate these findings. There are still problems in obtaining significant masses of colloidal material from seawater samples due to the large volumes of seawater that needs to be filtered.

Due to the time constraints of the procedure, only one gravimetric determination could be achieved over the time scale of any experiment, this is also true for seawater samples. Changes in the sample particle spectrum that may affect the radionuclide partitioning and therefore Kd, could not be determined. Any Kd calculations must therefore be interpreted with caution. Unfortunately alternative procedures that would have minimised these logistical problems and reduced perturbation of the natural particle spectrum caused by conventional ultrafiltration and other separation processes were unavailable although cross-flow / tangential flow systems were implemented in subsequent experiments.

Table 3.1: Beaulieu gravimetric determinations (mg/l):

Fraction	Date					Run 1	Run 2	Run 1	Run 2	Run 1	Run 2
Hartford Bridge (River)	**26/04/95**	**04/05/95**	**11/05/95**	**16/05/95**	**Mean**	**12/06/95 (0.4 x 2)**	**12/06/95 (0.4 x 2)**	**12/06/95 (0.4 x 3)**	**12/06/95 (0.4 x 3)**	**19/06/95**	**19/06/95**
Paper(>8)	5.2 ± 0.9	3.8 ± 1.1	6.7 ± 0.3	14.1	7.5 ± 4.0	9.4	6.3	6.9	6.4	0.3	0.6
0.45	3.1	3.7	5.4	4.2	4.1 ± 0.9	3.8-4.8	5.8-6.9	6.8-7.9	6.9	6.4	3.5-8.5
0.4	0.1	0.1	0.4	0.1	0.2 ± 0.2	0.2	0.5	0.1	0.1	0.3	0.5
0.02	2.3	3.3	2.7	3.3	2.9 ± 0.4	n.d.	2.3	n.d.	2.6-4.2	n.d.	1.3
Total	10.7	10.8	15.2	21.7	14.6 ± 4.5	n.d.	14.9-15.9	n.d.	16.0-17.6	n.d.	5.8-10.9
Colloidal %	21.5	30.1	17.4	15.3	21.1 ± 5.7	n.d.	14.3-15.3	n.d.	16.3-23.9	n.d.	12.1-24.4
Bucklers Hard (Estuary)											
Paper	22.4 ± 10.3	16.5 ± 2.6	44.3 ± 6.2	35.5 ± 1.9	n.d.						
0.45	16.5	n.d.	2.5		n.d.						
0.4	0.4	n.d.	0.2		n.d.						
0.02	n.d.	n.d.	0.05		n.d.						
Total	39.2 ± 10.5	n.d.	47.0		n.d.						
Colloidal %	n.d.	n.d.	0.1		n.d.						

3.2.2: Pilot equilibration experiments:

Raw count data for these experiments are given in Appendix 2 of the data disc. The control samples indicated no changes in natural background counts or total ionic ^{65}Zn (i.e. tracer adsorption to vessel walls or decay) over the timescales of the equilibration experiments.

3.2.2.1: Complete particle spectrum:

Plots for equilibration partitioning, mass balance recovery and pH/temperature are given in Figure 3.1. An initial decrease in truly dissolved ^{65}Zn was observed immediately after addition of the spike. However the truly dissolved fraction recovered to a relatively constant 90% of total ^{65}Zn activity. The other identified fractions were small compared to the truly dissolved. Originally, there was some partitioning of zinc into the particulate and colloidal fractions (~10%) but generally the particulate fraction held more tracer (2-7%) than the colloidal fraction (0.5-4%). It would be unwise to read too much from the data from this single experiment.

Mass balance recovery is improved by the filtration equipment acid washes, indicating that significant activity of the tracer (~10%) can be retained in the system. This activity loss decreased during the experiment as sample handling and processing improved.

There was some change in pH over the course of the experiment but it is unlikely that it was sufficient to cause any change in tracer partitioning. Significant (>10%) desorption of Zn from iron oxides begins to occur at pHs less than 6.5 (Benjamin and Leckie, 1981) and the pH was only lower than this for a short period. This low pH condition did not correspond to the early ^{65}Zn loss from colloidal material. The very low pH point (t=~250 minutes) is assumed to be an error as there is no apparent reason for this rapid change in a closed system. Temperature increased from 15 to 25°C during the experiment. This may have been sufficient to effectively remove some colloidal material from the suspension by flotation mechanisms.

Figure 3.1: Plots of ^{65}Zn partitioning, recovery and pH/temperature for experiments using a complete sample (04/05/95).

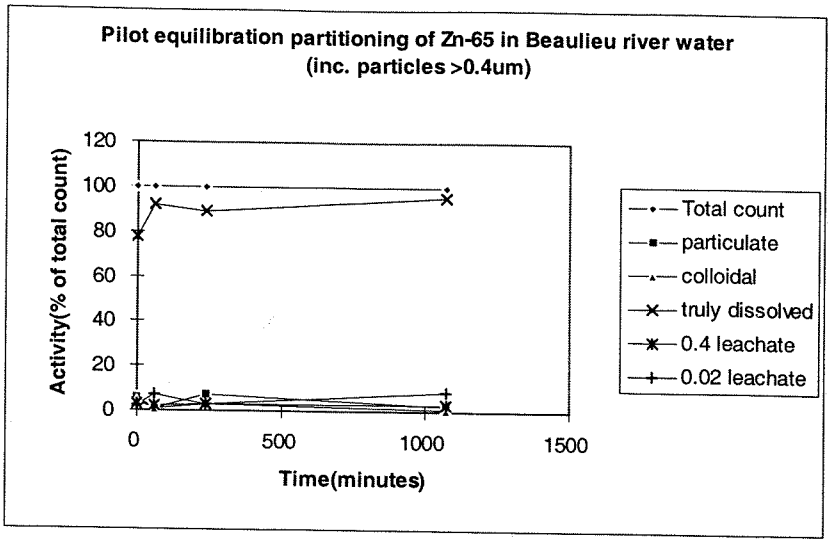

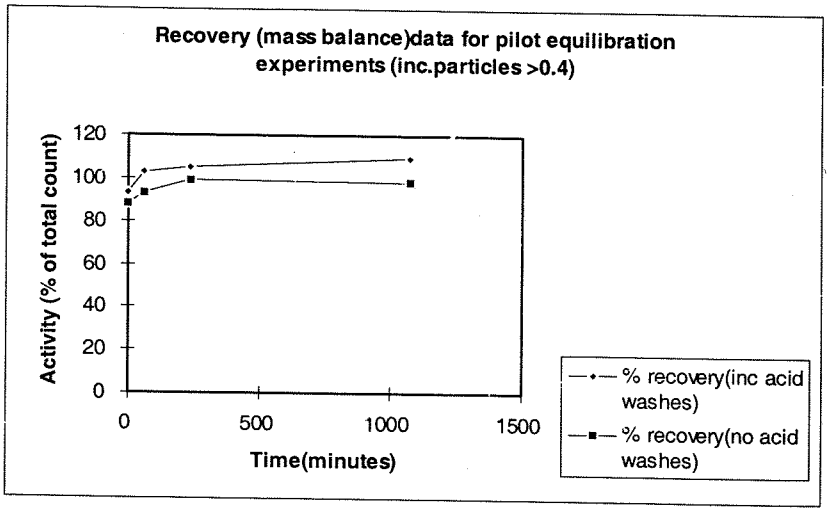

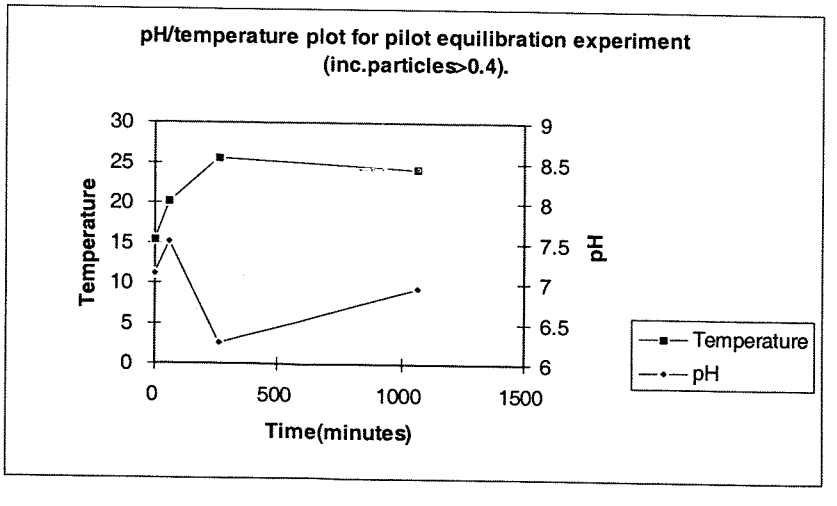

3.2.2.2: Colloidal Equilibration:

Equilibration, mass balance and pH/temperature plots for colloidal suspensions are displayed for duplicate experiments in Figures 3.2 and 3.3.

In experiments with only colloidal particles i.e. no competition with larger particles, an initial uptake of the tracer (14-17%), and corresponding decrease in truly dissolved Zn is observed. The colloidal sequestering of the Zn radiotracer is greater here than in the complete river samples. However, as in the experiment using the full particle size spectrum the partitioning of the zinc into the colloidal phase is relatively short lived and after less than 45 minutes the Zn-65 labelled colloidal fraction is relatively insignificant (<1%).

Temperature and pH plots show that temperature increased considerably over the duration of the experiments. The effect of this on the findings is as yet unknown and future experiments will be conducted at ambient temperature or in a constant temperature environment. In comparison pH was relatively constant and remained well above the level where Zn desorption may occur. Recovery (% of total spike) improved as handling experience progressed.

Figure 3.2: Plots of ^{65}Zn partitioning, recovery and pH/temperature for experiments using colloidal material (19/05/95).

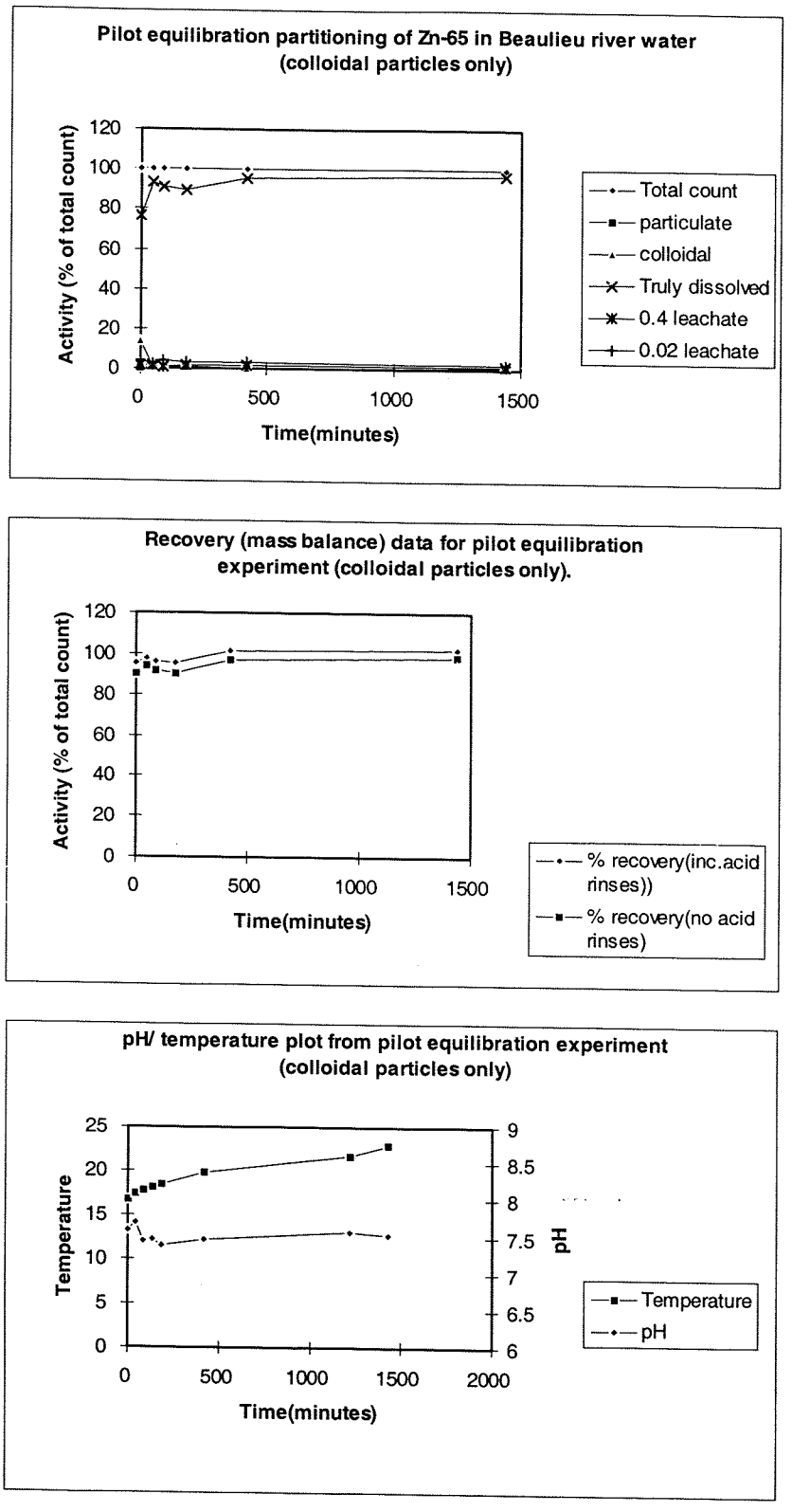

Figure 3.3: Plots of ^{65}Zn partitioning, recovery and pH/temperature for experiments using colloidal material (19/06/95).

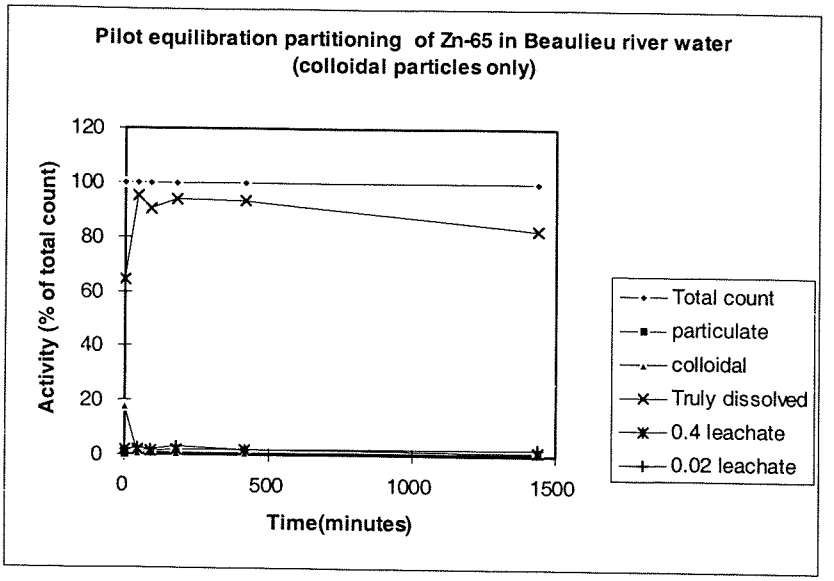

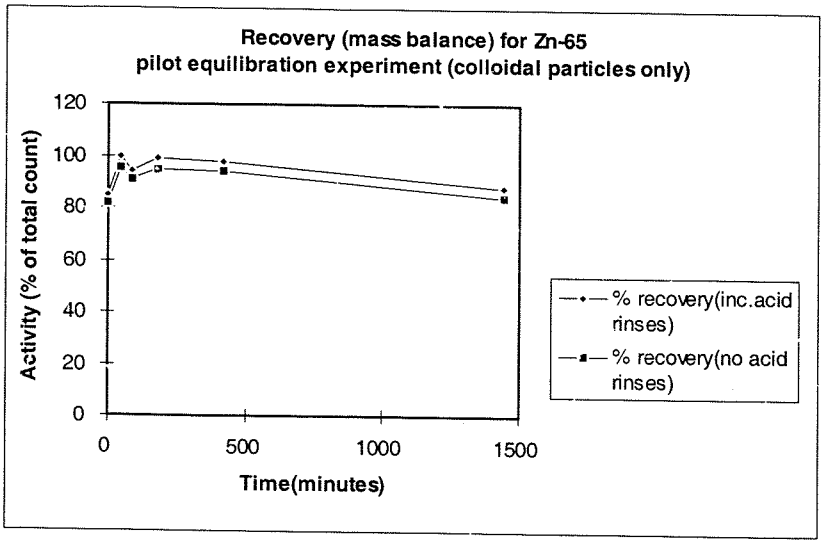

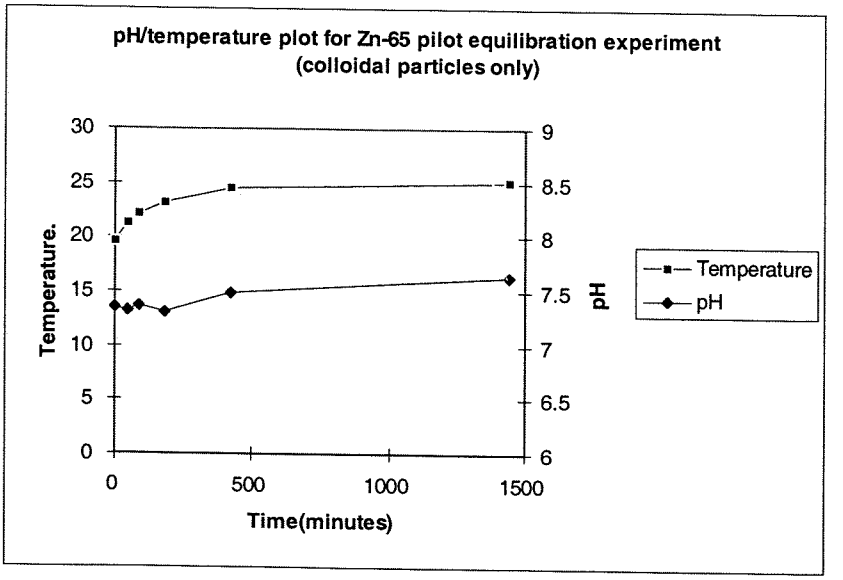

3.2.2.3: Partition coefficient (Kd, Kf, Kc) comparisons:

Although the application of Kd principles is limited due to the uncertainty of the existence of equilibrium conditions in the experiments and by the limited temporal resolution (i.e. single measurement) of gravimetric particle mass spectrum measurements, it is possible to observe some contrasts in Kd and Kc resulting from the varying sample conditions.

The partition coefficients for the complete sample (Figure 3.4) are erratic. The partition coefficient (Kd) has different magnitudes as a result of the incorporation of the colloidal material into the dissolved (Kd coll.diss.) or particulate (Kd coll.part.) phases. This is probably due to the relatively small partitioning of the radiotracer into the colloidal and particulate fraction but illustrates the effect that when significant, the inclusion of colloidal tracer into the dissolved fraction will act to reduce the observed Kd (see Figure 3.4). The overall fluctuations in the partition coefficients is mainly brought about by changes in the truly dissolved phase as the zinc tracer it is variably partitioned into the particulate and colloidal phases. Kc is relatively unaffected due to the consistently low partitioning of tracer into this fraction. The decrease in Kc indicates a shift in partitioning towards the truly dissolved phase which may be a result of disaggregation or desorption.

The Kds determined in this tracer experiment are in the same order of magnitude as those determined by other authors from estuarine radiotracer simulations for ^{65}Zn: Fang, 1994 (Beaulieu); Althaus, 1992; Turner et al., 1993; Williams and Millward -in press (Humber), see Table 3.6 in summary section. The partition coefficients for the complete sample in this study are slightly lower indicating more tracer residing in the truly dissolved phase. This may be an artifact of the procedure used here or the effect of comparatively low SPM.

Kd measurements are not appropriate for the colloidal equilibration experiments because of exclusion of particles >0.4μm, so only Kf and Kc were determined (see section 1.7 for definitions). Kf is very small here due to the absence of particles greater than 0.4μm and there is no indication of significant aggregation.

Figure 3.4: Partition coefficients for complete and colloidal sample equilibration experiments.

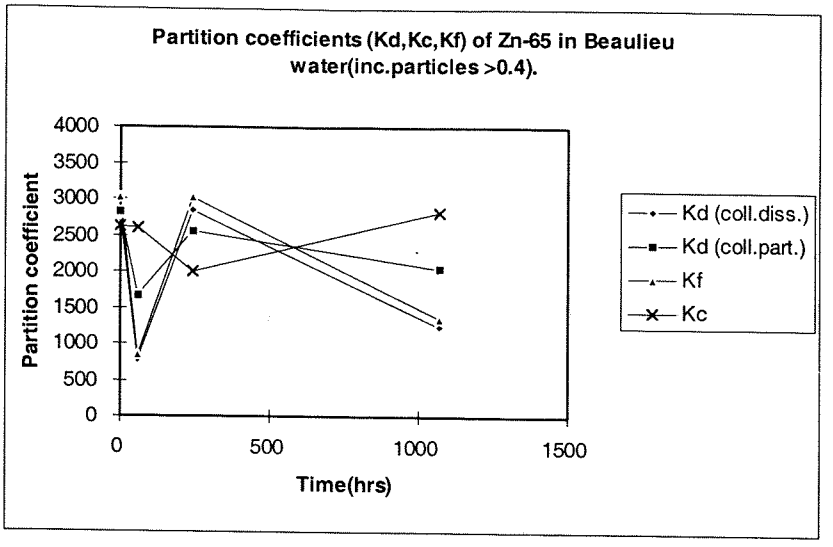

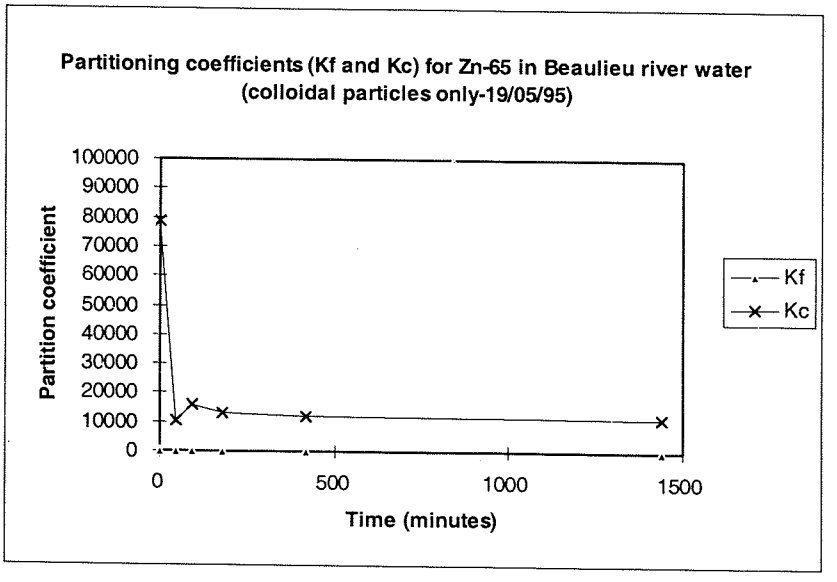

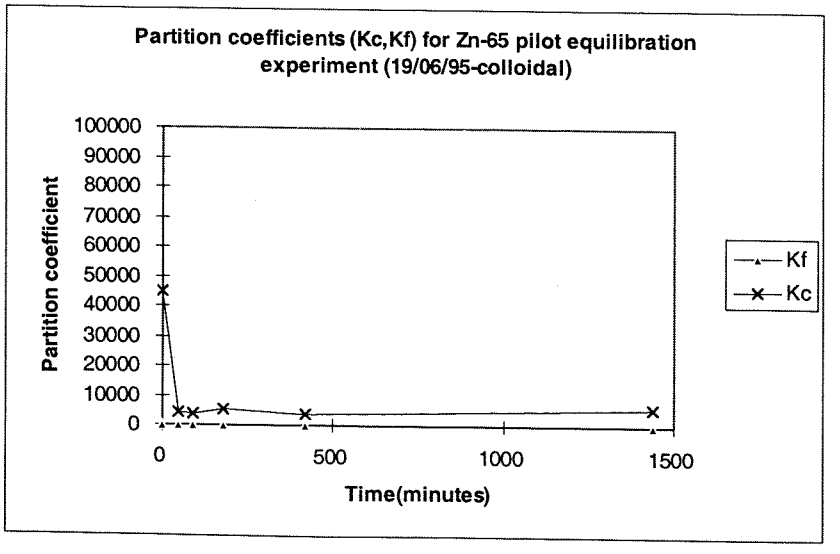

Initial Kc measurements in the colloidal samples were at least an order of magnitude higher than in the complete sample equilibration experiments. Kc decreases dramatically as the Zn tracer is lost from the colloidal phase (the only particles present). Kc is significantly higher for the first colloidal replicate and this is confirmed by greater colloidal partitioning of the ^{65}Zn tracer in this experiment. This is probably linked to the greater mass of colloidal material (3.3mg/l - 30% of SPM) available for tracer uptake compared to the second replicate experiment (1.3mg/l - 22% of SPM). It is possible that colloidal material composition or conformation and it's affinity for the Zn tracer will vary between colloidal samples.

In the complete particle spectrum colloidal material is available to take up trace metal species but is in competition with other particulate binding sites, hence the partition coefficients are lower. This may be a function of the characteristics of Beaulieu particles and requires further investigation.

With such low level and short lived partitioning of the tracer into particulate and colloidal fractions application of partition coefficients to such experiments has been difficult. The added ambiguity of unknown particle spectrum changes and lack of equilibrium conditions has limited their applicability and they have not been used in the next section of the radiotracer experiments.

3.3: Pilot experiment discussion and implications for further work:

The feature of rapid initial ^{65}Zn uptake by colloidal material observed instantaneously after the spike addition is probably due to adsorption onto sites in the colloidal surface or matrix. This is to a certain extent expected due to the large surface area that colloidal material presents for trace metal uptake. The initial uptake of the tracer is dependant on the compositional and conformation characteristics of an individual colloidal population and may be inhibited by the presence of other particles. However, the apparent subsequent release of the tracer on such a short time scale indicates that this binding/adsorption is either reversible or there is a shift of the colloidal phases into smaller particles (disaggregation) or into the dissolved phase.

Possible reasons for desorption of a tracer from colloidal particles would be a decrease in pH or displacement of radioactive Zn by stable metal present. However, the consistency of pH throughout the experiments makes the first explanation unlikely. Although the natural stable Zn concentrations were estimated to be essentially unperturbed by the carrier stable Zn in the tracer addition, it is possible that increased Zn concentration or contamination from external sources may have occurred during sample handling. Additionally, if the colloidal uptake of ^{65}Zn occurred at an elevated rate compared to other ionic species, the slower uptake of other ions may lead to Zn radioisotope displacement. Chloride ions added in the spike may have some indirect effect on the colloid/^{65}Zn interaction. It is also possible that gradual (i.e. timescale of minutes) organic complexation of Zn may occur in the dissolved phase. Over longer timescales it is possible that organically complexed Zn may not be removed from solution whilst the zinc initially associated with inorganic phases might be. In effect if they are rapidly formed, the zinc-organic complexes may in fact control the subsequent reactivity of the radiotracer zinc by competition between ionic and organically associated zinc tracer. All these ion exchange and complexation processes need to be quantified.

It is possible that the transfer of the Zn tracer into the dissolved phase was as a result of disaggregation of colloidal material (aggregates). However, it is difficult to see why this would occur without significant changes in the experimental system such as ionic strength, pH or sheer effects. As no significant aggregation and therefore transfer of the

tracer into particles retained by a 0.4μm filter was observed over the same time scales and subsequently during the experiment, it would seem likely that the particle spectrum is in fact reasonably stable. Unfortunately, due to the time limitations of the gravimetric procedure, any disaggregation of colloidal material could not be detected i.e. time interval for collection of colloidal particles was much greater than the timescales over which changes in colloidal forms might occur. Indeed, one of the main problems with experiments of this type is the evolution of the particle spectrum with time upon sample collection. Even in riverine waters aggregation/ disaggregation processes (see Introduction, section 1.4) continually occur to alter the particle distribution from the natural state (Buffle and Leppard, 1995a). Studies like these that monitor an experimental closed system will undoubtedly vary from the true system in the open water column. Colloidal behaviour may have been altered by separation from the natural particle population. There is also the possibility that alteration of colloidal material by sampling or handling techniques may affect its uptake of the tracer.

For example: it is possible that the apparent loss of zinc radiotracer from the colloidal material in the bulk solution may be due to a loss of labelled colloidal material by a flotation effect (Buffle and Leppard, 1995a) caused by the temperature increase after sampling. At increased temperatures microbubble formation may result in flotation of colloidal material. Once held at the water/air interface the buoyant colloidal material and any associated tracer would be effectively removed from the sample and therefore not accounted for in aliquot sampling. This process could not be studied as gravimetric determination was only done at t=0 due to time constraints of the procedure. Despite the significant temperature increase it seems unlikely that this process is the cause of colloidal activity loss as the total activity determined for the whole sample did not decrease and the tracer loss is probably too rapid to be explained by this physical mechanism. If this process is occurring it would be minimised by performing experiments at ambient or constant temperature. It is also unlikely that microbial action, which may transform organic matrices or increase particulate material by bacterial growth, and thus affect metal partitioning, is significant on such a short time scale.

As explanation for the "particle concentration effect" it is hypothesised that the presence of metal-carrying colloids in the dissolved phase will decrease the observed Kd from its

true value. The magnitude of this decrease is proportional to the fraction of colloidal material in the particle population and the affinity of the metal for this phase. However, due to the low level and short term labelling of the colloidal and particulate phases in the equilibration experiments here, these sorts of trends were difficult to detect.

From these few experiments it is not clear if an equilibrium state had been reached and as such the trends in the calculated Kd (true and conditional), Kf and Kc are erratic and difficult to explain. The natural Kd value has been somewhat compromised in an entirely colloidal system where the rapid uptake process are favoured and Kc values are artificially high. The Kd values determined here will need further comparison to those from water samples where the particle population is intact. However, although the partition coefficient concept has been difficult to apply and interpret in this case the concept of Kd as a description of partitioning of trace metal species between two phases is still useful, for example as an input into particle/solute system models and as a single integrated value to describe dissolved / "particle" interactions.

Preliminary modelling using Kc:

Despite the reservations of the longevity of the tracer partitioning it is possible to use the Kc derived in the ^{65}Zn partitioning experiments (complete sample) along with colloidal weight to describe the partitioning of the Zn tracer under different SPM concentrations and colloidal % of total SPM. The equation used to model this has been modified from Althaus (1992).

$$\% \text{ colloidal zinc} = 100 - (100)/ (1 + Kc \cdot X \cdot SPMt)$$

Where;

Kc is the colloidal partitioning constant (colloid and truly dissolved) derived from the partitioning of ^{65}Zn in a complete Beaulieu River sample (2.5×10^3).

X is SPMc/ SPMt i.e. the fraction of total SPM that is colloidal. For the original experiment X was approximately 30 percent.

Plot of percentage colloidal zinc with SPM concentration for several % colloid compositions can be seen in Figure 3.5a. The model here indicates that the most rapid increase in colloidal zinc partitioning would occur between SPM concentrations of 100mg/l and 10g/l. The results also indicate how a change in colloidal % of total SPM can alter colloidal zinc partitioning.

This method of modelling the colloidal partitioning of ^{65}Zn would enable predictive assessment of colloidal zinc in other systems where the colloidal percentage is unknown but total SPM has been measured. The Beaulieu system is somewhat unusual in that the particulate material is highly organic so application of this type of model could only be applied in similar systems. Kf and Kc values were very similar and so modelling for filter retained particles (>0.4μm) produced very similar curves.

Figure 3.5b illustrates how using this technique it is possible to assess the impact (Kc sensitivity) of variation in partitioning coefficients (i.e. change in binding affinity, particle composition, surface area effects etc) and how it could affect the percentage colloidal zinc fraction. The results of this type of modelling indicate that an increase in Kc from 2.5 to 3.5 (x 10^3) results in a 10% increase in colloidal zinc. In comparison, an order of magnitude increase or decrease in Kc results in a 45 or 35% increase or decrease in colloidal zinc percentage respectively.

Mainly, this exercise enables the colloid/truly dissolved/particulate system to be described for zinc in the Beaulieu River and is useful for modelling systems where colloidal SPM or partition coefficients are not as well defined.

Figure 3.5a: Plot of % colloidal zinc with SPM concentration for several % colloidal compositions.

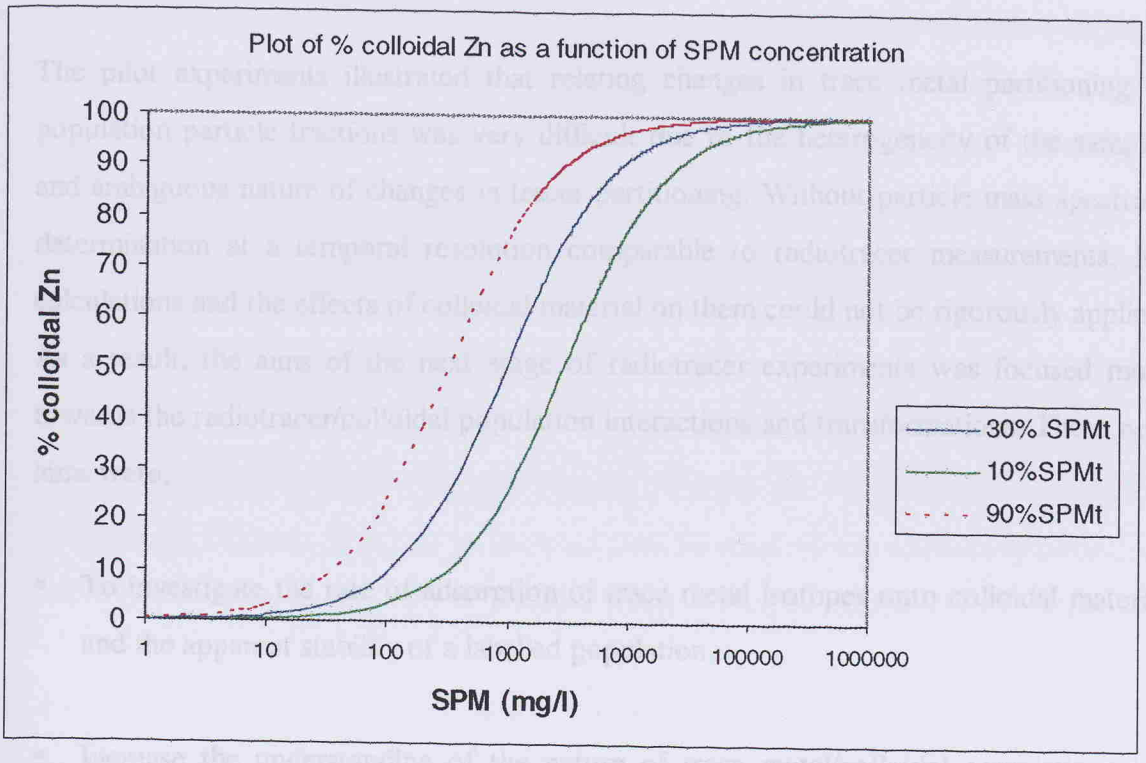

Figure 3.5b: Percentage colloidal zinc sensitivity to Kc.

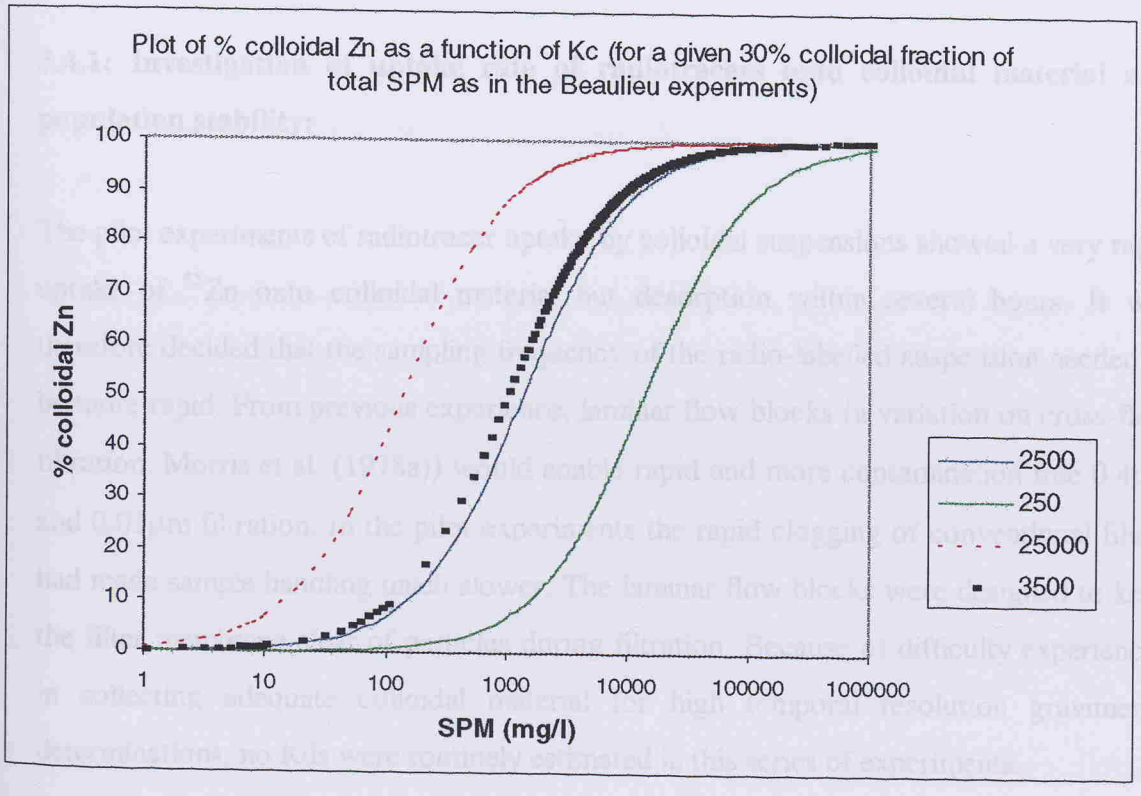

3.4: Radiotracer studies of the stability of metal tracer labelled colloids and metal tracer exchange with solution:

The pilot experiments illustrated that relating changes in trace metal partitioning to population particle fractions was very difficult due to the heterogeneity of the samples and ambiguous nature of changes in tracer partitioning. Without particle mass spectrum determination at a temporal resolution comparable to radiotracer measurements, Kd calculations and the effects of colloidal material on them could not be rigorously applied. As a result, the aims of the next stage of radiotracer experiments was focused more towards the radiotracer/colloidal population interactions and transformations. These new aims were;

- To investigate the rate of adsorption of trace metal isotopes onto colloidal material and the apparent stability of a labelled population.

- Increase the understanding of the nature of trace metal/colloidal associations i.e. complexed versus exchangeable.

3.4.1: Investigation of uptake rate of radiotracers onto colloidal material and population stability:

The pilot experiments of radiotracer uptake by colloidal suspensions showed a very rapid uptake of ^{65}Zn onto colloidal material but desorption within several hours. It was therefore decided that the sampling frequency of the radio-labelled suspension needed to be more rapid. From previous experience, laminar flow blocks (a variation on cross-flow filtration, Morris et al. (1978a)) would enable rapid and more contamination free 0.4μm and 0.01μm filtration. In the pilot experiments the rapid clogging of conventional filters had made sample handling much slower. The laminar flow blocks were designed to keep the filter membrane clear of particles during filtration. Because of difficulty experienced in collecting adequate colloidal material for high temporal resolution gravimetric determinations, no Kds were routinely estimated in this series of experiments.

All experiments were conducted with river water samples so theoretically the particle/colloid populations should be stable i.e. ionic strength constant. Bulk samples (4.5 litres) were used for all the experiments to reduce experimental artifacts associated with small scale closed systems as much as possible. The bulk samples were stirred but at a minimal rate consistent with homogenous mixing. This was designed to minimise aggregation or disaggregation processes whilst keeping the samples well mixed. All experiments were to be carried out at ambient laboratory temperature (15 to 20°C) to prevent colloidal flotation and in the dark (by covering) to minimise bacterial growth.

Due to practical constraints it was not possible to create all the ideal experimental conditions. For example; it was not possible to keep the water samples at ambient temperature (approx. 8° C). It is accepted that flotation of the smallest colloids may occur due to reduced solubility of included gases at a higher temperature which in turn may lead to an increase in aggregation, removal of colloidal material or affect trace metal equilibria. With available techniques it was not possible to quantify this effect and homogenisation of the river sample prior to filtration and colloidal separation ensured that any such material would still be incorporated into the bulk colloidal sample. It is assumed that once filtered at room temperature the colloidal particle population will be at equilibrium with the rest of the sample. The sample was not kept cold until use to prevent repetition of this problem. The sample was used within 12hrs of colloidal separation.

The original particle/colloidal mass concentration distribution was determined for each sample. Measurement of some colloid mass concentration storage changes over experimental timescales was also performed.

3.4.1.1: Development of conventional prefiltration techniques for river water samples prior to radiotracer experiments and gravimetric analysis.

Previous experience had shown that the organic polymer/colloidal loading in the Beaulieu River water can be so high that direct 0.4μm filtration can be very slow due to rapid clogging of barrier type filter pores. Therefore, to achieve accurate gravimetric analysis of the size spectrum a litre sample was filtered with as many filters as required to prevent significant decrease in flow rates (4-5 per litre) as described in Section **2.1.2**.

Initially, prefiltration with 5 and 2μm polycarbonate filters was tried after the 8μm filtration, but there was still significant subsequent clogging of the 0.4μm filters (only 50-70mls would pass). Following discussion with filter manufacturers, pre-filters of 0.8 and 0.65μm cellulose nitrate composition were implemented. Although they improved the filterable volume at 0.4μm cut-off to 100-120mls, for three replicate litres per sample for gravimetric analysis this would prove far too many filters. The 0.45μm prefilter was deemed unusable as the cut-off would be too close to that of the polycarbonate 0.4μm and may act to remove some colloidal fraction smaller than the 0.45μm cut-off. This may be a problem with the mixed cellulose filters as they retain particles on their surface as defined by the pore size of the cellulose matrix but this matrix also acts as a depth filter which may subsequently remove smaller particles by interaction (adsorption/charge held) with the filter matrix.

As a result of the possible effects of these types of filters on the particle spectrum the smaller pore size filters (i.e. 0.8, 0.65 and 0.45μm) whose effective cut-offs may overlap significantly with the 0.4um polycarbonate filter were rejected as prefilters. Instead a larger 0.4μm filter (142mm diameter) was implemented. The larger surface area enabled increased sample volume to be filtered before clogging occurred (approx. two filters per litre were used).

The final gravimetric protocol per litre of Beaulieu River sample was;
8μm x 1 ; 1μm x 5 ; 0.4μm x 2 (142mm) ; 0.02μm x 1.

Although this cascade filtration approach physically enables fractionation of the high organic content Beaulieu River samples with minimal removal of the colloidal size fraction, it is highly likely that there will be some distortion of the initial particle spectrum resulting from these manipulations. Similar optimisation of the filtration cascade would be needed for other freshwater/estuarine type samples.

3.4.1.2: Cross-flow filtration (0.4μm -laminar flow) of Beaulieu River samples:

Laminar-flow filtration apparatus blanks:

Laminar flow block (LFB) filtration was used in preparation of the colloidal samples prior to radiotracer addition but also for fractionation of the time-series samples. It was vital therefore to check that there was no significant stable Zn increase upon preparation of the colloidal phase or future aliquot filtrations that may alter the Zn tracer fractionation. Milli-Q blanks and 10% HCl leaches were done with the laminar flow block apparatus and the acid cleaned 0.4 / 0.01μm filters (Nucleopore). Filtrate and retentate samples were then analysed on the GFAAS for stable Zn concentrations.

The Milli-Q rinses of the system and frit were not significantly elevated for stable Zn. However, the Milli-Q filtrate samples for the 0.4 and 0.01μm filter blank concentrations were increased by 1.89 and 4.60 μg/l of stable Zn respectively. The 10% HCl leaches were higher, and increased by 9.01 and 10.4 μg/l of stable Zn above the blank HCl signal for 0.4 and 0.01μm filtrates respectively (see Appendix 2 in the data disc). Although the filters appear to be a significant source of stable Zn these leach conditions were effectively a worst case scenario as both the Milli-Q (lower ionic strength) and acid leach would be more likely to remove any available Zn than river water. The natural background stable Zn concentrations of Beaulieu water range from 6.5 to 50μg/l range (Holliday and Liss, 1976; Dolamore-Frank, 1983; Fang, 1995) so an input of stable Zn from filter leaching of this magnitude would be relatively low compared to the zinc concentration in the sample.

As a precaution, after trace metal cleaning of the flow blocks, during colloidal sample filtration from the initial river water the system was flushed well (preconditioned) with river water and the first 5-10mls of unspiked river water filtrate was discarded to minimise any stable Zn release. Before, and between fractionation of radio-labelled aliquots the system was flushed well with Milli-Q to prevent activity carryover or stable Zn contamination. To optimise sample process time and avoid activity carry-over between samples a strict protocol was developed for processing radio-labelled samples. This was incorporated into the experimental method for investigation of colloidal uptake of ^{65}Zn.

3.4.1.3: Experimental method for colloidal uptake of ^{65}Zn:

See flow diagram F3 for method outline described below. A colloidal sample (4 litres) obtained from 0.4μm laminar flow block filtration of Beaulieu River water was placed in a trace metal clean carboy on a magnetic stirrer. An original 125ml sample was removed by clean syringe and fractionated to give background activities for all the fractions. A 20μl spike of ^{65}Zn radiotracer was added to the suspension. It was previously checked that the addition of this amount of radiotracer would not cause pH alteration of the colloidal bulk sample or significant addition of stable Zn.

At time intervals ranging from minutes to hours, 125ml aliquots of the colloidal suspension was removed and cross-flow fractionated. The fractions measured for activity were;

Total (unfiltered colloidal sample),
0.4μm filtrate (colloidal and truly dissolved species),
0.4μm filter (^{65}Zn labelled colloidal aggregates or colloids retained on the filter),
0.01μm filtrate (truly dissolved species),
0.01μm filter (colloidal material retained on the filter).

Activity was counted in a NaI (Tl) counter as before. Due to the lower activity of the radiotracer, count time was elevated to achieve statistically significant count levels (not

F3: Flow diagram of procedures for final radiotracer experiements (sample preparation and long term lebelling).

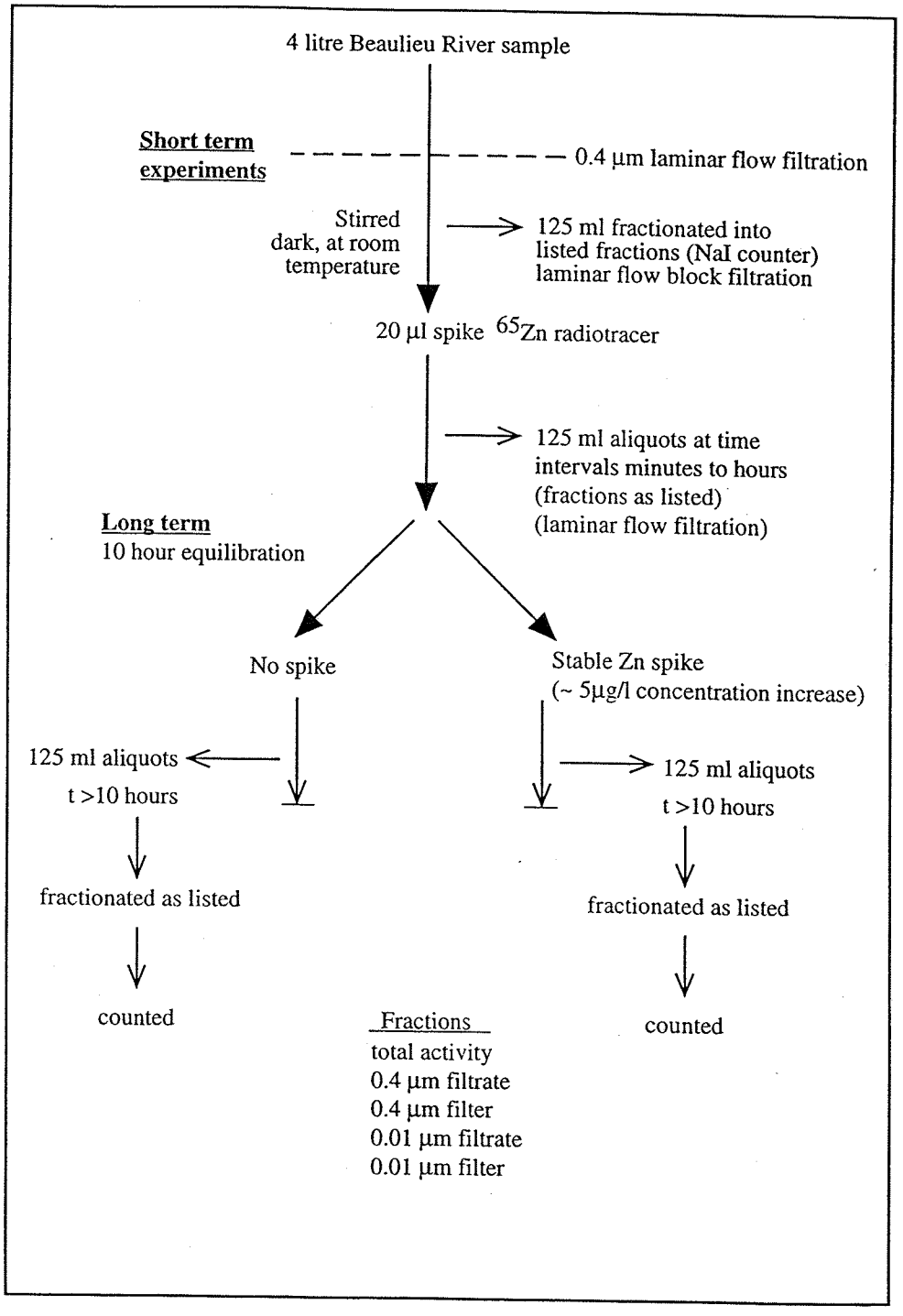

<10,000counts). Background counts were taken for each fraction. Checks were also done to estimate the activity retained on the polycarbonate filters of both cut-offs without particles present (i.e. any adsorption). Short term and longer term experiments were run to give an insight into the rates of tracer uptake and subsequent transformations as well as indication of any equilibrium state being achieved. The minimum filtration time for each labelled aliquot by laminar flow block was approximately 30 minutes. Higher temporal resolution sampling (minimum of 30 minutes) was carried out close to the original tracer addition where more dynamic changes were expected.

Duplicate litres of experimental sample were used for simultaneous initial and storage gravimetric determination of particle mass concentrations.

3.4.2: Tracer/colloid association investigation: stable Zn addition.

To investigate the nature of the association of ^{65}Zn with colloidal/aggregate material an experiment was designed to run after the spiked colloidal system had reached equilibrium/steady state. It was hypothesised that if the Zn tracer was associated with colloidal material in an exchangeable form as part of a dynamic equilibrium (i.e. stable and tracer zinc is continually exchanging on and off the particle surface) it would be displaced from the colloidal fraction if there was an increase in stable zinc in the system. There would be proportionally more stable zinc able to fill binding sites on colloidal material so the colloidal fraction of ^{65}Zn would decrease and conversely the truly dissolved ^{65}Zn fraction would increase. However, if the Zn tracer was stably complexed at the colloid surface, an increase in stable zinc concentration would have no effect on the partitioning of the radiotracer. A flow diagram of the method described below is included in diagram

To investigate this theory a two litre colloidal sample was spiked with ^{65}Zn and left to reach steady state over 10 hours. After this time, the suspension was respiked with additional stable zinc sufficient to increase the zinc concentration by 5µg/l (triple the original stable zinc concentration). The stable zinc spike was added in a nitrate form which negated the presence of ions (Cl^-, Mg^{2+}, or Ca^{2+}) that may cause competitive

complexation effects within the colloid/metal system and may alter the interaction of the colloidal material and associated radioactive tracer (Paalman et al., 1994). Paalman et al. (1994) observed a reduction in the sorption capacity of suspended matter for Cd in the presence of Cl^-, Ca^{2+} and Mg^{2+} ions which they attributed to competition for sorption sites. It is likely that Zn is subject to similar competitive complexation effects in the presence of these ions and colloidal material. After this spike addition, time series removal and fractionation of suspension aliquots would indicate any partitioning changes of the radiotracer.

A high resolution time series of radiotracer fractionation was conducted as previously but a control experiment was run in parallel with no stable Zn addition. This experiment also gave indications of longer term changes in the radiotracer equilibrium/steady state conditions and partitioning.

3.5: Radiotracer studies of the stability of metal tracer labelled colloids and metal tracer exchange with solution: results and discussion

3.5.1: High temporal resolution adsorption experiments:

Replicate short-term radiotracer experiments were run to examine the uptake of the ^{65}Zn tracer by natural colloidal suspensions. Colloidal suspensions were isolated from prefiltered bulk samples as described in Sections 3.4.1.1 and 3.4.1.2. For comparison of colloidal flotation/aggregation effects of storage upon tracer uptake, two experiments were run;

a) one set that had been stored overnight (12hrs) dark at **room temperature**

b) one stored **cold (~4°C)** and dark overnight.

Over several time intervals aliquots were removed from the bulk suspensions and filtered sequentially through 0.4μm and 0.01μm polycarbonate filters held in laminar flow blocks. Plots 3.6 and 3.7 show the background corrected activity and percentage plots for total, dissolved, colloidal and truly dissolved fractions over time. The total particle associated fraction (colloids plus colloidal aggregates) and aggregate fractions are also plotted to indicate transfer of tracer via aggregation into the particulate phase. PH and temperature plots are also displayed in Figures 3.6 and 3.7. All the raw activity/count data for samples and filters can be found in the Appendix 2 section of the data disc.

Control filtration of spiked, particle free water indicated that 2-4% of the residual activity unaccounted for by the counted fractions was due to adsorption of tracer onto polycarbonate filter matrices. Despite CFF methodology during sample filtration it was noticed that some of the filters (especially 0.4μm cut-off) had material (a brown, organic coating) on their surfaces and retained a significant activity. It is suggested that this was colloidal aggregate/colloidal material retained by matrix/charge effects. The 0.4μm and 0.01μm retained activity was incorporated into the particulate and colloidal fraction respectively. The significance of this material retention is discussed later.

Both spike experiments showed similar trends in partitioning of the radiotracer (see Figures 3.6 and 3.7 for background corrected and percentage plots of ^{65}Zn fractionation). There is rapid initial (within first sampling cycle, ~30minutes) adsorption (8 to 18%) of the zinc tracer into the colloidal phases. This is in agreement with the initial rapid adsorption step proposed by Honeyman and Santschi (1989) in their "colloidal pumping" model. Simultaneously, between 20-25% of the tracer is lost from the truly dissolved phase indicating that the tracer is also adsorbed directly onto larger particles (colloidal aggregates) as well as directly onto colloidal material.

It appears that the initial adsorption rate is a function of colloidal versus aggregate mass in the particle populations. The cold stored (~4°C) sample, Figure 3.7 (colloidal concentration 8.45mg/l, ~89% mass concentration) showed a more rapid and greater colloidal partitioning (18% versus delayed 12%) of the radiotracer than the sample previously stored at room temperature, Figure 3.6 (colloidal concentration 5.67mg/l, ~43% mass concentration). It was hypothesised that this was probably a factor of the larger surface area available for tracer uptake from colloidal material compared to colloidal aggregates. It was likely that the sample that had been stored overnight at room temperature had pronounced colloidal aggregation and associated decrease in particle surface area compared to the sample stored cold. Without checking the particle distribution of the samples in detail via light scattering or similar techniques it was not possible to completely prove this hypothesis. The colloidal mass information also indicates the inherent instability of riverine colloids. Within 12 hours of cold and dark storage 11% of the initial colloidal mass has been lost to particles >0.4μm diameter via aggregation (57% aggregation occurs when the same sample is stored at room temperature).

Subsequent transformations of the tracer partitioning indicated continuing/ simultaneous adsorption and desorption as well as particle-colloid and colloid-aggregate aggregation/disaggregation processes. This is in contrast with the predominantly unidirectional approach seen in work by Honeyman and Santschi (1989; 1992) and Wen et al. (1996) based on colloidal pumping theory. However, transfer of labelled colloidal material and zinc tracer into the particulate phase is an indication of this pumping process

Figure 3.6: Activity, percentage activity and pH/temperature plots for high resolution time-series (room temperature storage prior to experiment).

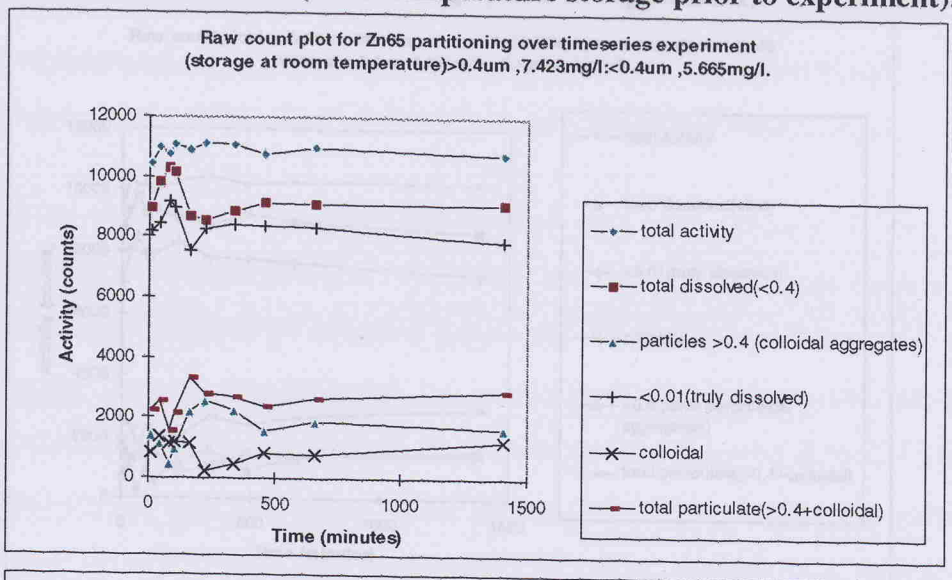

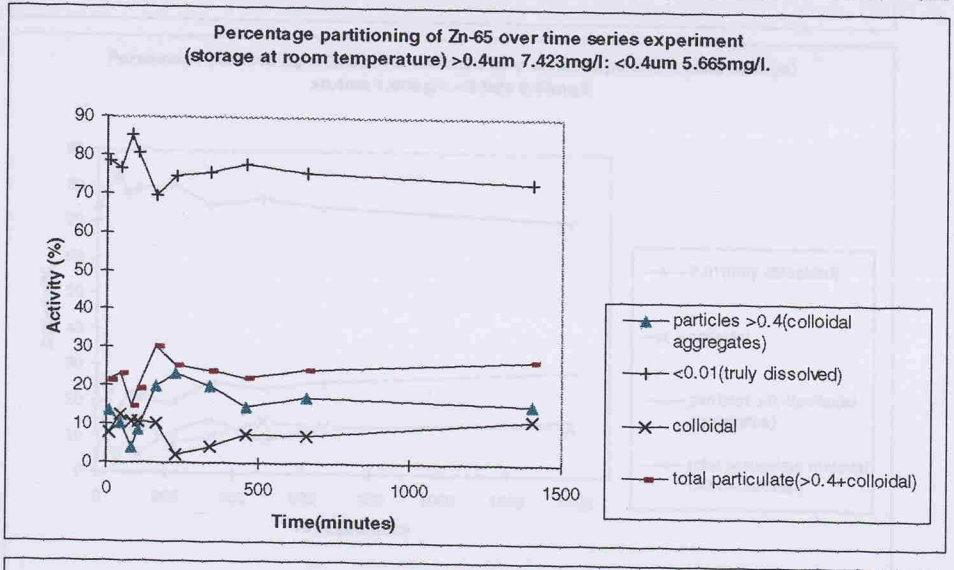

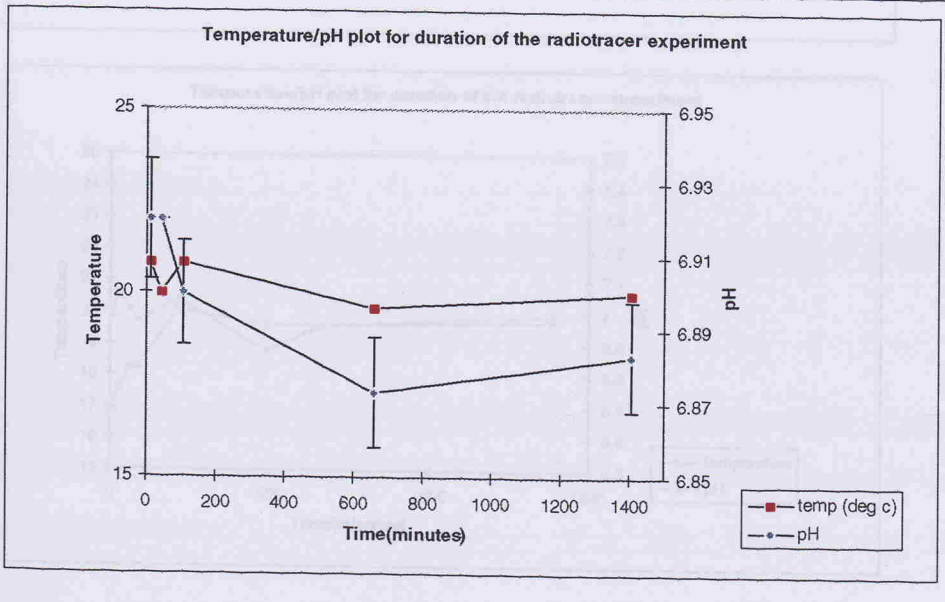

Figure 3.7: Activity, percentage activity and pH/temperature plots for high resolution time-series (cold storage prior to experiment).

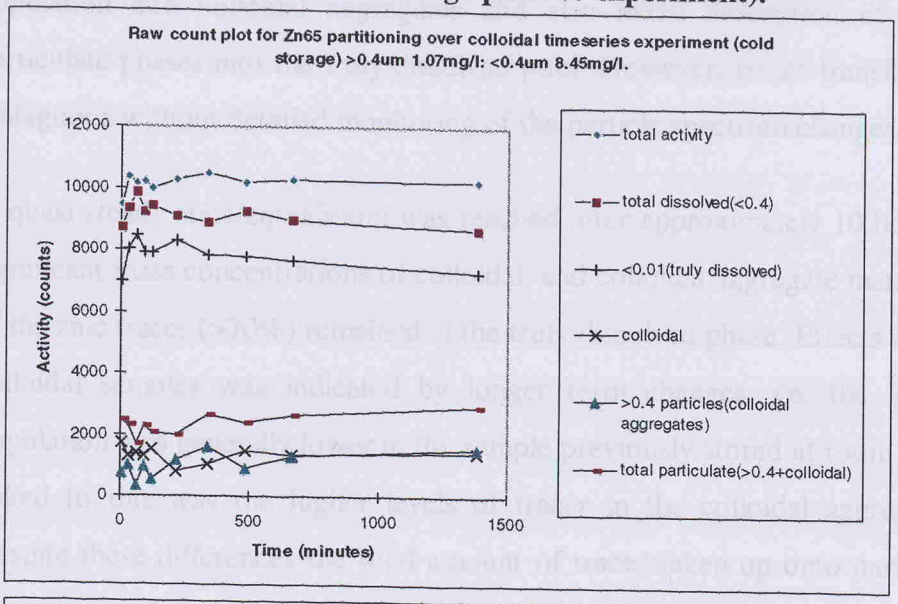

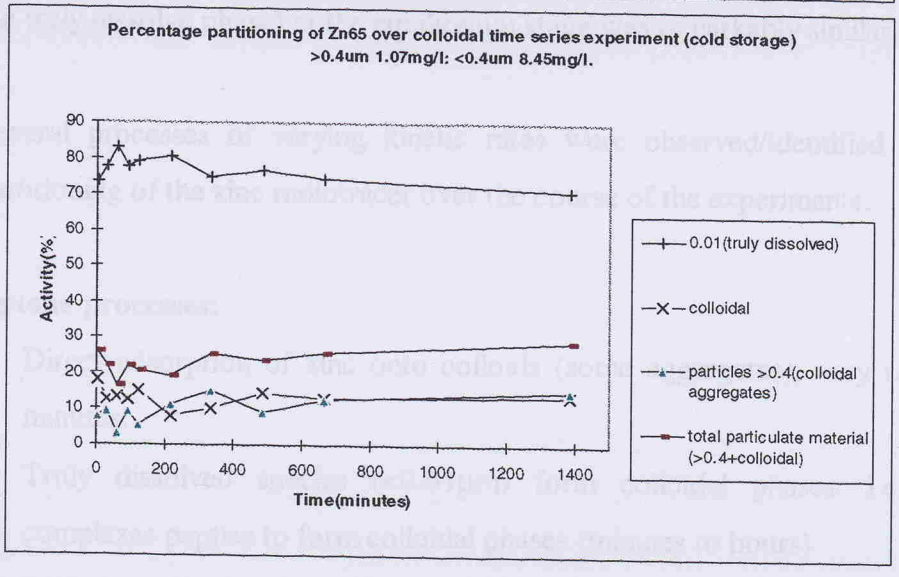

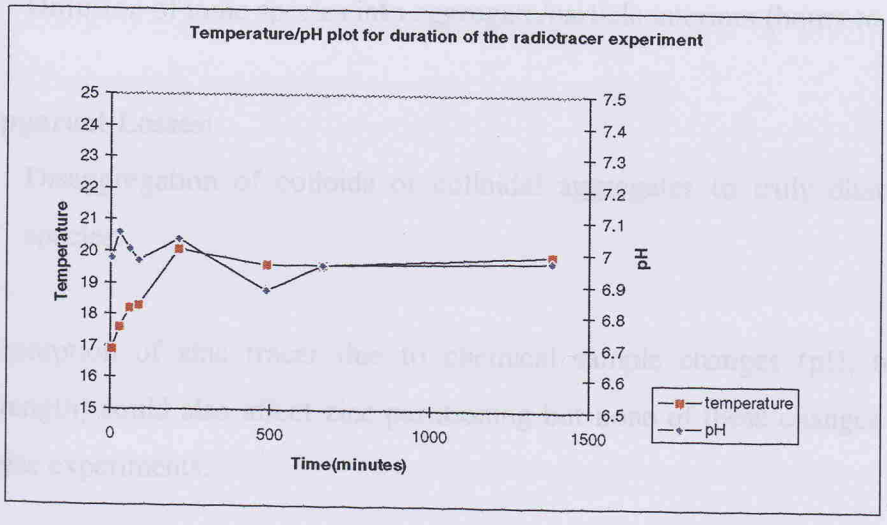

occurring to some extent. There is apparent transfer of tracer from the colloidal population into colloidal aggregates and also initial desorption of the tracer from particulate phases into the truly dissolved pool. However, tracer transformations can be ambiguous without detailed monitoring of the particle spectrum changes.

A quasi steady state/equilibrium was reached after approximately 10 hours. Despite the significant mass concentrations of colloidal, and colloidal aggregate material the majority of the zinc tracer (>70%) remained in the truly dissolved phase. Effects due to storage of colloidal samples was indicated by longer term changes. i.e. the labelled colloidal population was generally lower in the sample previously stored at room temperature and linked to this was the higher levels of tracer in the colloidal aggregate population. Despite these differences the total amount of tracer taken up onto particles (i.e. not in the truly dissolve phase) at the equilibrium stage was remarkably similar.

Several processes of varying kinetic rates were observed/identified as affecting the partitioning of the zinc radiotracer over the course of the experiments.

Uptake processes:

- Direct adsorption of zinc onto colloids (some aggregates), very rapid, seconds to minutes.
- Truly dissolved species (<0.01μm) form colloidal phases. i.e. organic/amino complexes peptise to form colloidal phases (minutes to hours).
- Diffusion of ionic species into aggregate/particle interiors (hours to days).

Apparent Losses:

- Disaggregation of colloids or colloidal aggregates to truly dissolved or colloidal species.

Desorption of zinc tracer due to chemical sample changes (pH, temperature, ionic strength) could also affect zinc partitioning but none of these changes were observed in these experiments.

Ionic exchange/replacement of tracer Zn with stable isotopes can also affect partitioning (D.Burton pers.comm.). This replacement of tracer Zn by stable forms results in a net change in the tracer partitioning but often a dynamic ionic exchange equilibrium can occur with no net change in tracer partitioning being apparent. It is difficult to identify if such changes occurred in this study. The balance of these processes all interact to produce the ^{65}Zn partitioning and changes observed in the first 300 minutes of the experiments.

0-30 minutes: very rapid adsorption of Zn-65 to colloids (and colloidal aggregates). The colder stored sample has a greater proportion of the original colloidal material still in the colloidal phase so it presents a greater surface area to volume ratio for tracer adsorption.

30-300 minutes: particle transformation processes (aggregation/disaggregation). Some adsorption and desorption too.

>700 minutes: particle size distribution/tracer partitioning closer to steady state. Truly dissolved phase slowly decreasing indicating a slow adsorption process, perhaps diffusion into colloids or colloidal aggregate matrices.

It is possible that at this quasi steady state there are still particle and zinc tracer transformations occurring but there is little net change as any processes are compensated in both directions of change. The closed system and apparent equilibrium state created here will probably rarely happen in the natural environment where conditions are constantly changing. The timescales of this experiment and the transformation rates will need comparison and extrapolation to natural processes.

These first experiments have shown that there is significant and rapid partitioning of the ^{65}Zn tracer into colloid and colloidal aggregate material. However, without particle spectrum data the associated tracer phase transformations are difficult to attribute to any particular particle or sorption process. The long-term changes (>24 hours) in tracer partitioning have not been observed here and would be of great importance when applying the results of these type of experiments to the natural environment. The nature of the association of the tracer with colloidal particles was addressed in the next series of experiments.

3.5.2: The nature of colloid-tracer association:

Figures **3.8** A to D show the background corrected data for the time-series tracer partitioning after stable zinc addition and the long-term experiment that acted as a control.

Figure 3.8 A to D: Raw data for partitioning changes after stable zinc addition and long-term storage (control).

A:

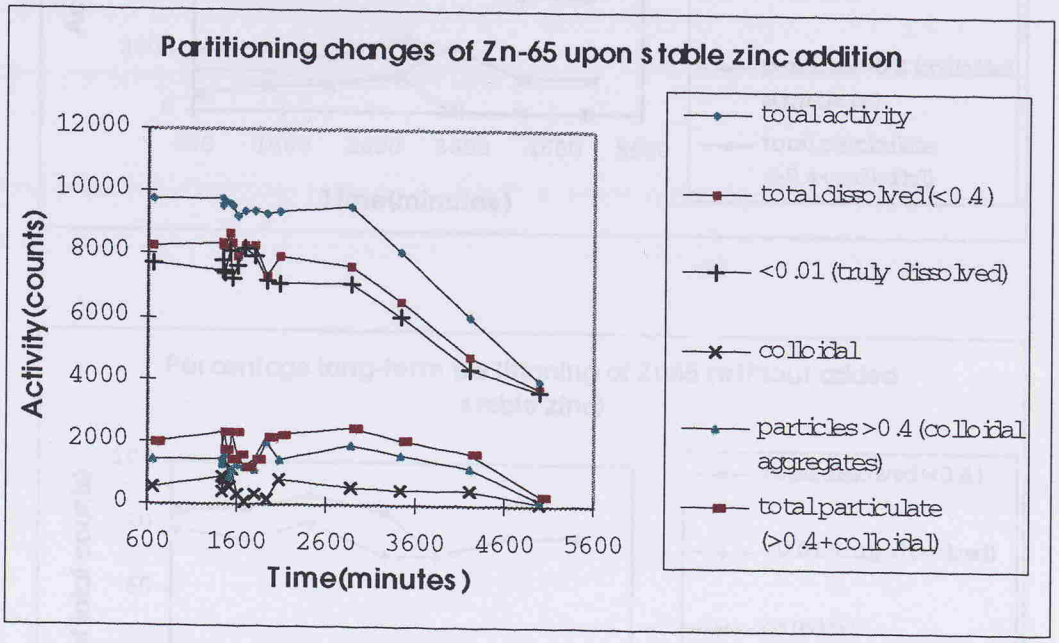

B:

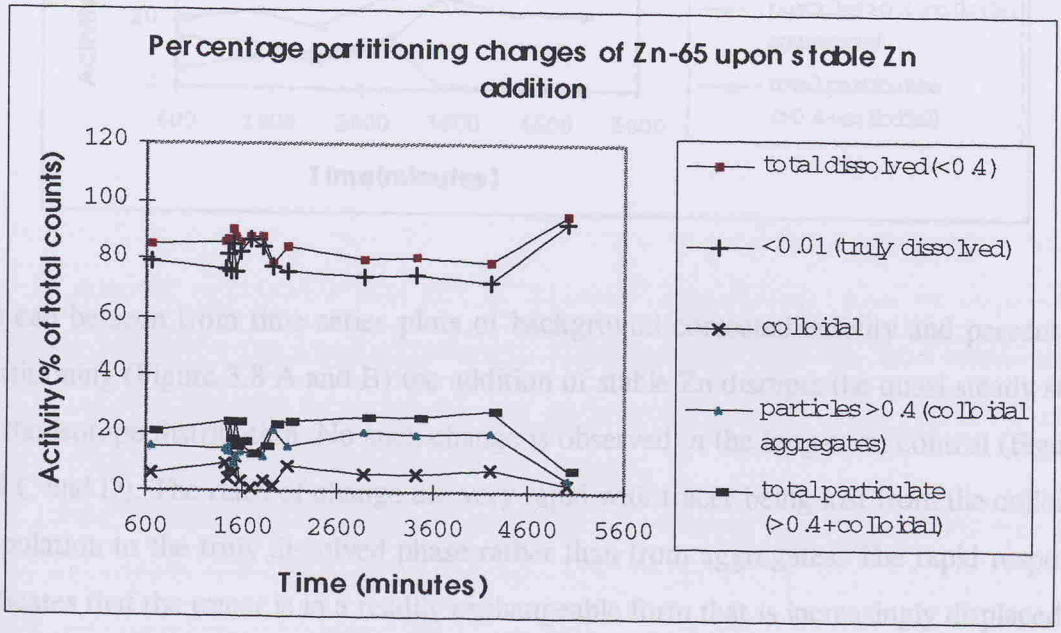

C:

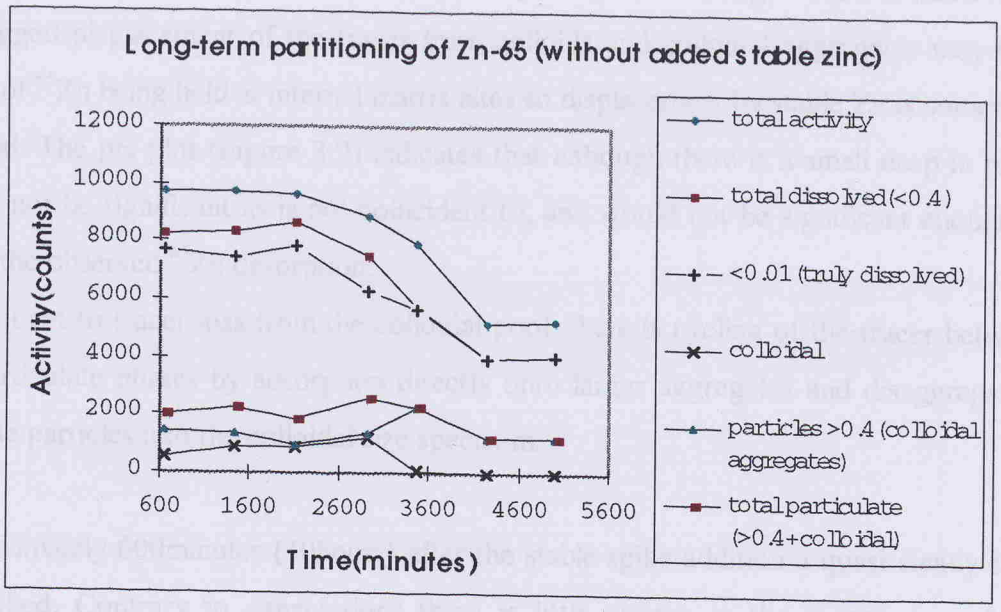

D:

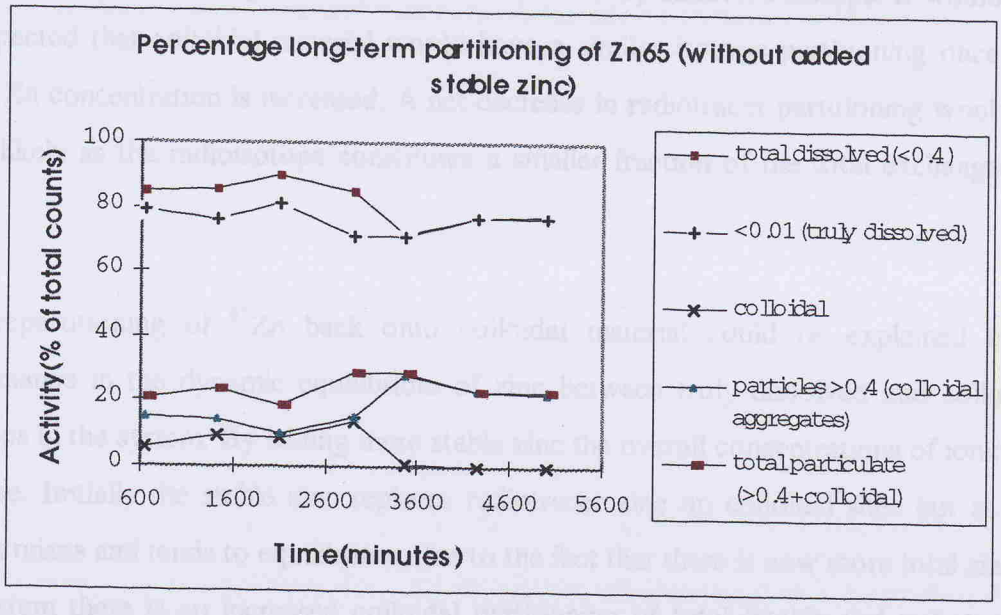

As can be seen from time series plots of background corrected activity and percentage partitioning (Figure 3.8 A and B) the addition of stable Zn disrupts the quasi steady state of the isotope distribution. No such change is observed in the long-term control (Figures 3.8 C and D). The rates of change are very rapid with tracer being lost from the colloidal population to the truly dissolved phase rather than from aggregates. The rapid response indicates that the tracer is in a readily exchangeable form that is increasingly displaced by the added stable Zn (even until there is virtually no radio zinc left on colloidal material and >90% of the tracer is in the truly dissolved phase). The loss of tracer from the

colloidal phase may result initially from desorption/ionic exchange which is more rapid but lagged displacement of the tracer from colloids and colloidal aggregates may be a result of ^{65}Zn being held at internal matrix sites so displacement by stable Zn is somewhat delayed. The pH plot (Figure 3.9) indicates that although there is a small drop in pH it would not be significant as is not coincident to, and would not be significant enough to cause the observed ^{65}Zn desorption.

Subsequent to tracer loss from the colloidal pool, there is cycling of the tracer between the particulate phases by adsorption directly onto larger aggregates and disaggregation of these particles into the colloidal size spectrum.

Approximately 600minutes (10hours) after the stable spike addition a quasi steady state is reached. Contrary to expectations there is little change in the partitioning of the isotope into the colloidal phase or an increase in the truly dissolved isotope. It would not be expected that colloidal material would have a similar isotope partitioning once the stable Zn concentration is increased. A net decrease in radiotracer partitioning would be more likely as the radioisotope constitutes a smaller fraction of the total exchangeable Zn.

This repartitioning of ^{65}Zn back onto colloidal material could be explained by a maintenance in the dynamic equilibrium of zinc between truly dissolved and colloidal fractions in the system. By adding more stable zinc the overall concentrations of ionic Zn increase. Initially the stable zinc replaces radiotracer zinc on colloidal sites but as the system mixes and tends to equilibrium, due to the fact that there is now more total zinc in the system there is an increased colloidal partitioning of total (stable and radiotracer) zinc. As a result, more radiotracer zinc is "pumped" into colloidal sites by displacing other ions with lower total concentrations or binding affinity. Overall, total (stable and radio.) colloidal zinc has increased but the partitioning between truly dissolved and colloidal phases (and hence Kd) has remained constant.

There seems to have been an increased partitioning into larger aggregates. This may be due to a change in colloidal or aggregate morphology and ligand sites available to zinc species and therefore the tracer. As in previous experiments without indications of changes in the particle size spectrum, only the net changes in isotope partitioning resulting from ionic exchange and particle dynamics can be detected.

Figure 3.9: pH time series plots for the long-term (control) and stable zinc experiments.

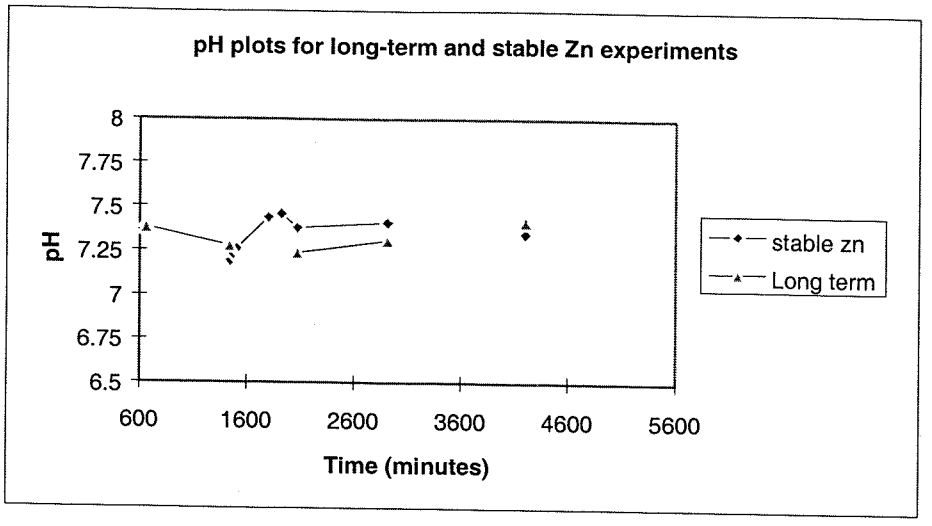

As both the stable zinc experiment and the long-term experiment indicate there is a significant loss of isotope activity by the end of the experiments. This is discussed below.

3.5.3: Radiotracer activity loss:

Both the long-term and the stable Zn addition experiments ran for up to 70hours. The long-term experiment indicated that the steady state in zinc tracer did not alter significantly until approximately 35hrs after the original ^{65}Zn spike was added (see Figure 3.8, C and D). After this time there was significant reduction in the total activity present in the sample. In successive measurements the total activity decreased until at ~4200 minutes (end of the experiment) only 60% of the original activity remained. It was apparent that although some of the ^{65}Zn was being partitioning into aggregates greater than 0.4μm (colloidal fractions had no significant tracer activity) the greatest proportion of the tracer was lost from the sample altogether. This trend was also observed in the stable zinc experiment over the same time-scale (Figures 3.8, A and B).

Upon examination of the suspension after this time there were loose, brown coloured aggregates visible in the samples. These were extremely hydrophobic and were held at the water/air interface or on the container sides. Any tracer associated with these aggregates was therefore effectively removed from the suspension.

To assess the radiotracer removal by these aggregates the suspension was rehomogenised by vigorous stirring to disperse the aggregate material evenly throughout the remaining sample. Before homogenising the "total" sample count was; 4173 counts (per 5 ml). Post-homogenisation the total sample count was; 9780 counts (per 5ml). The activity lost from the sample was therefore 5607 counts which compromised 57.3% of the total isotope activity present. Acid washes of the sample container indicated that a maximum of 4.5% of the lost activity could be attributed to removal to the container walls. Almost 95% of the activity lost was therefore removed onto the aggregated material. The time series data suggest that this removal occurred by initial direct adsorption of the remaining truly dissolved radiotracer onto these aggregates and delayed removal of labelled colloid and colloidal aggregate material (see Figures 3.8 C and D).

Some of the ^{65}Zn labelled aggregates were isolated on a 0.4μm filter for observation and elemental analysis by Scanning Electron Microscopy (SEM). The aim of this section of work was to identify the possible composition of the aggregates and where the radiotracer was held.

Back scattered electron microscope imagery (BSEI) and point source element detection by energy dispersive (EDS) x-ray microanalysis identified the aggregates as organic filaments coated predominantly with iron and manganese precipitates (see photographs 1a to d). The brighter filaments in the compositional images (a and b) are those with Fe/Mn coatings. The only zinc detected appeared predominantly associated with filamentous manganese (see Appendix 2 for the EDS traces). Most importantly, the colloidal material and associated Fe and Mn which had aggregated into the filamentous material, had a much greater affinity in this conformation for the zinc radiotracer which lead to its comprehensive removal from the sample (12 to 18% colloidal ^{65}Zn when tracer originally added, but ~60% of ^{65}Zn activity held in the loose aggregates). It was impossible to tell if the organic filament were natural polymer chains or perhaps bacterial chains. This information would have significant implications for the process of the aggregate formation and therefore the conditions and timescales that affect it.

Photograph 1a: Compositional image of filamentous aggregates (x100)

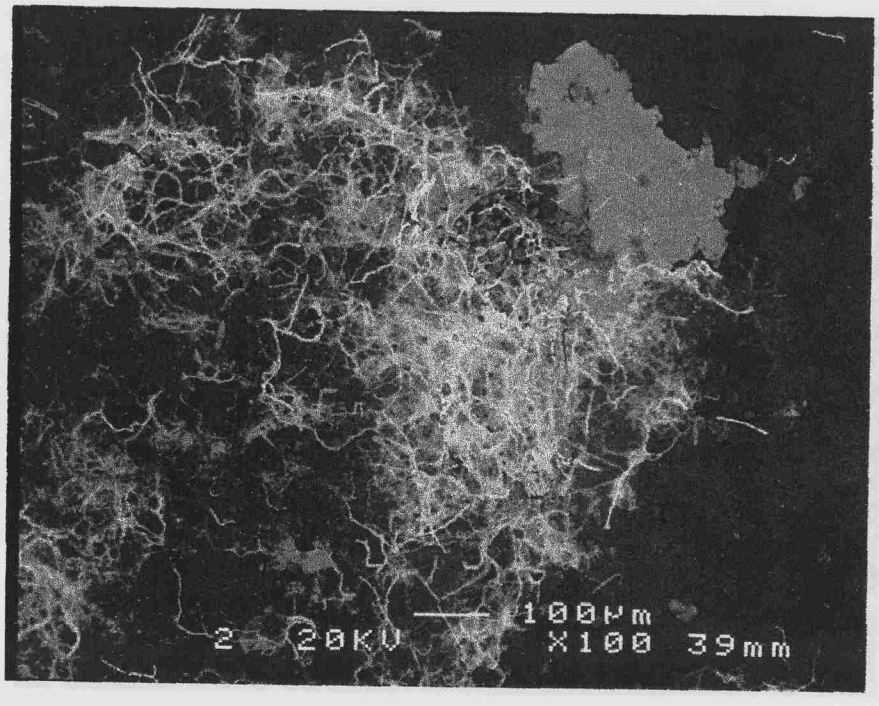

Photograph 1b: Compositional image of filamentous aggregate (x200). Brighter filaments have organic-Fe/Mn oxide composition. Amorphous, light grey material is completely organic.

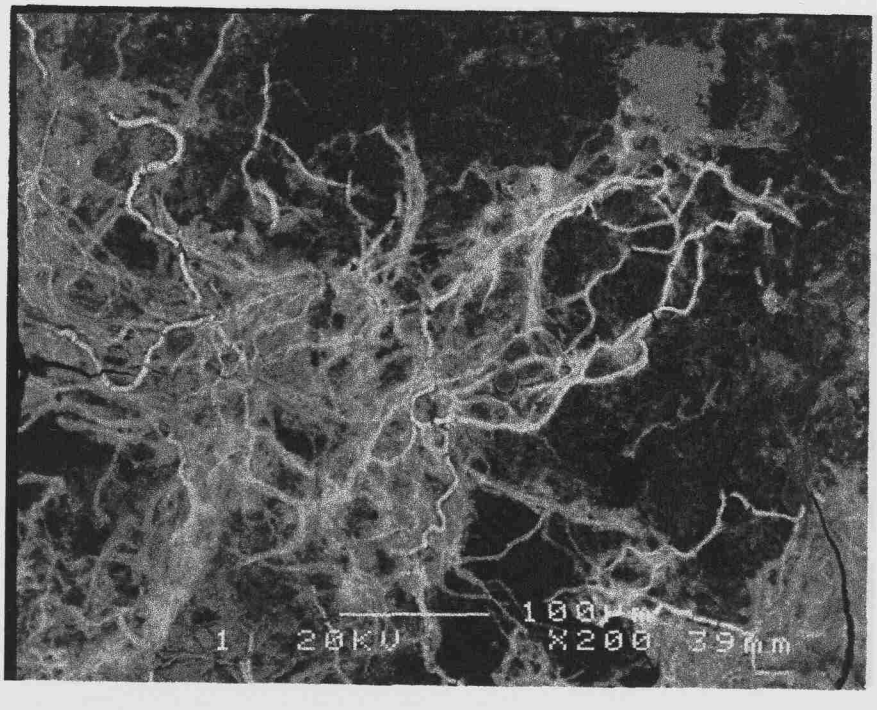

Photograph 1c: Topographical image of filamentous aggregate (x200)

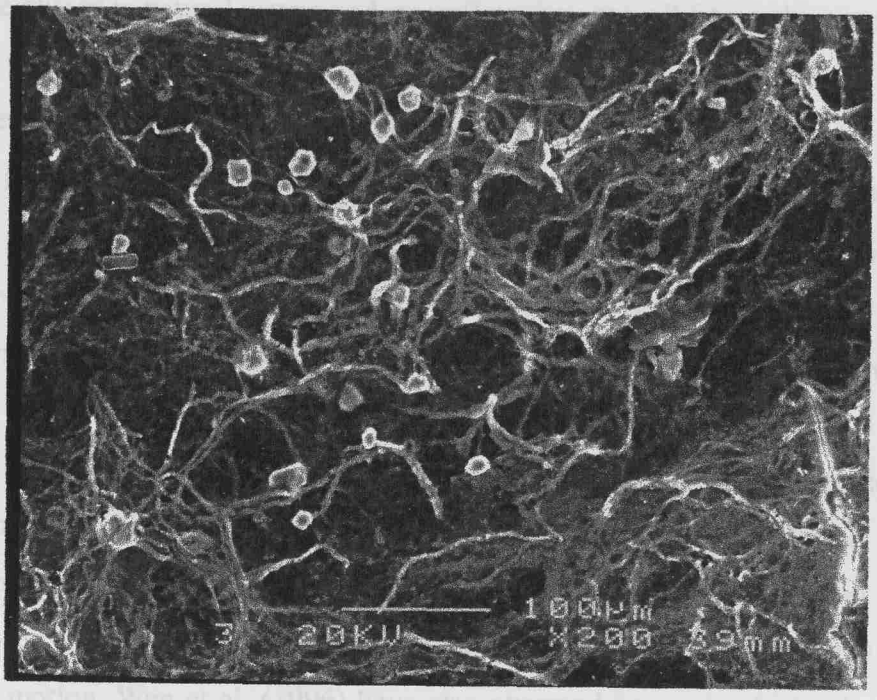

Photograph 1d: High magnification (x3000) of organic aggregate background and brighter metal oxide filament (top left)

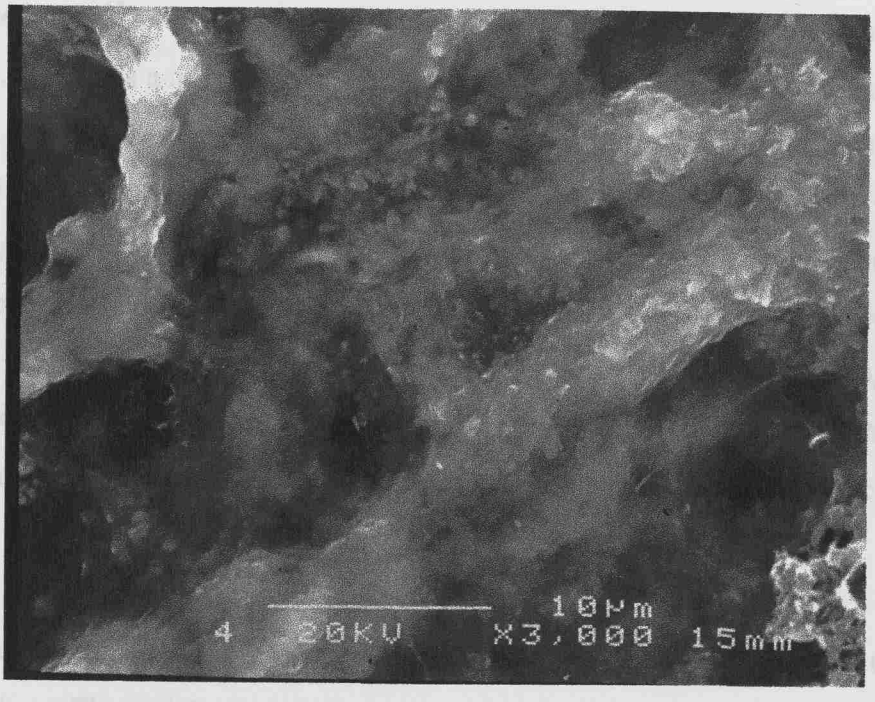

The scavenging of radiotracer Zn and also Mn and Fe onto highly hydrophobic organic based particles has important implications for repartitioning of trace metals into particulate phases in natural waters and may affect their overall fate in these systems.

This observed formation of polymer aggregates is not unique. Chin et al. (1998) observed formation of polymer gels of >1μm in 0.22μm prefiltered stored seawater in under 50 hours. The equilibrium size of these microgels was 5μm formed between 50 and 83 hours of storage. The main polymer assembly process suggested was a physical one (polymer bridging) as inhibition of microbial activity using sodium azide had no effect on the rate or size of gel formation. It is likely that the process of aggregate formation here is similar to that suggested by Chin as the organic concentrations are so much higher and although the ionic strength of these samples is much lower, significant aggregation processes have been show to occur relatively rapidly. Stordal et al. (1996) has proposed that this slow coagulation process over several days is mainly driven by Brownian motion. Wen et al. (1996) have also observed how microbial redox reactions can affect colloidal Fe molecular weight distributions over similar experimental timescales. Beaulieu colloids are known to have a high Fe content (see later FFF work).

3.5.4: Filtration artifacts and implications for tracer distributions:

During the initial ^{65}Zn partitioning experiments it was noticed that after 0.4μm filtration especially, there was a brown/organic film of material retained on the filter membrane. As discussed in previous sections, even with CFF there are filtration artifacts that can affect particle size fractionation and therefore metal/tracer partitioning. The filter may retain particles great than the filter cut-off by charge or sticking (organics) but also by coagulation effects/polarisation if the filtrate gradient is too strong. Once this has happened the material on the filter acts to clog the pores effectively reducing the pore size and retaining particles that normally would pass through. Dissolved metal or tracer species may also be affected as they pass through the material collected on the surface of the filter.

During the fractionation of each sample aliquot elution counts were taken for 0.4μm and 0.01μm filters. The activity detected on these filters was either that retained by the filter

matrix by adsorption (proved to be negligible) or the activity associated with the colloidal aggregates or colloids retained by the filters. The activity retained by 0.4μm and 0.01μm filters for the longer term experiments is plotted in Figures 3.10 A and B. Despite the implementation of cross-flow filtration, significant retention of labelled particulate material (including colloids) occurred to a variable extent during the partitioning experiments. For both filter types the peak in activity retention (particle retention) occurs just prior to the increased activity removal by the filament formation.

Figures 3.10 A and B: Activities of Zn-65 tracer retained on 0.4μm and 0.01μm filters during fractionation of long-term experiment aliquots.

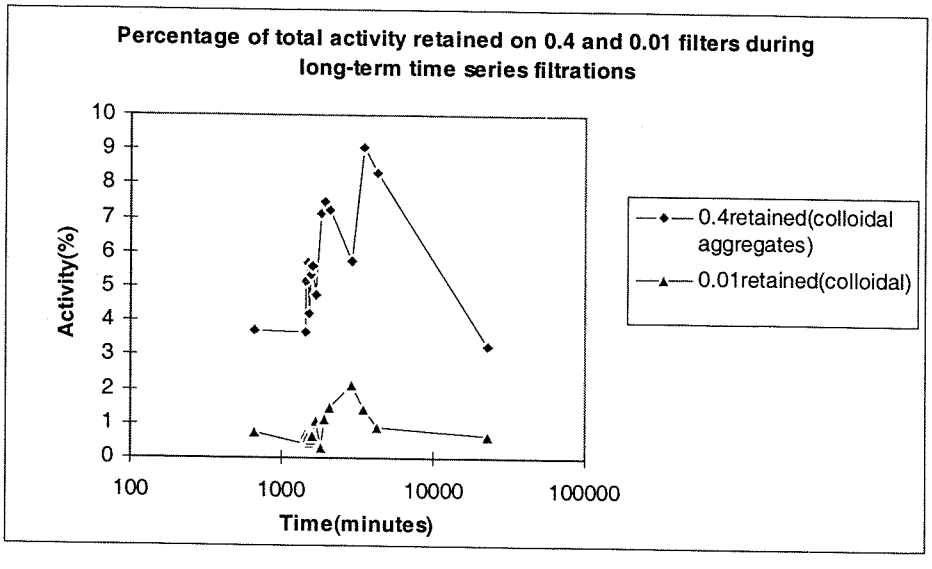

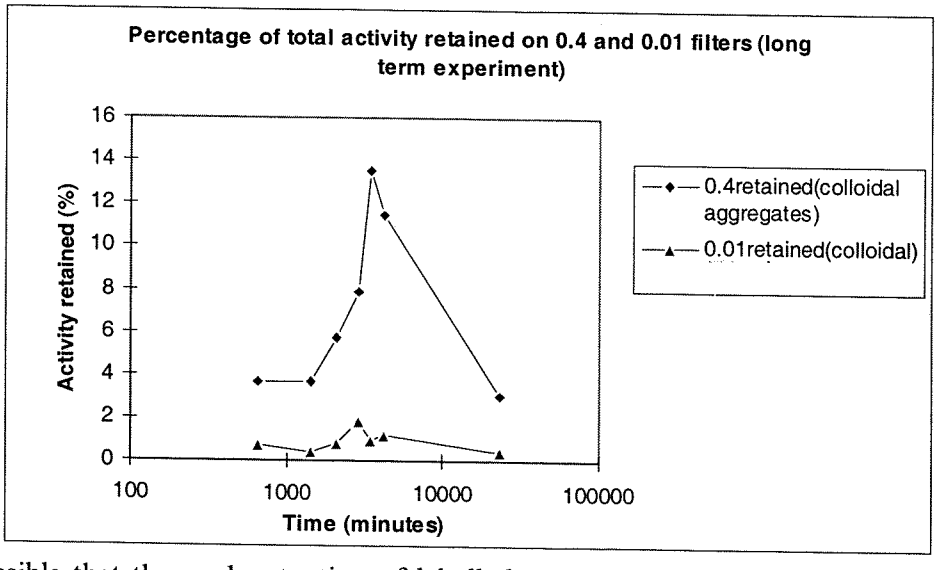

It is possible that the peak retention of labelled particles mirrors changes in the particle spectrum towards ~0.4μm which enhances colloid/colloidal aggregate retention before removal into much larger aggregates. The retention of zinc tracer was more pronounced

for the 0.4μm filters. Colloidal aggregate or colloidal retention may comprise from 4 to 12% of the total tracer activity whereas retention by 0.01μm filters was less significant (0.3 to 2.2 % of total activity). Inclusion of these measurements allowed a mass balance of ^{65}Zn tracer to be calculated for each aliquot fractionation (0.4μm or 0.01μm).

Recovery 0.4 (%)= (0.4filtrate + 0.4filter + >0.4)/total) x 100

Recovery 0.01 (%)= (0.01 filtrate + 0.01 filter + >0.01)/0.4 filtrate) x 100

For the test samples;

Recovery for 0.4 fractionation was 102.8 +/- 0.5%

Recovery for 0.01 fractionation was 100.4 +/- 0.5%

By independent calculation of 0.4μm fractionation using CFF protocol (total, 0.4 filtrate and retentate counts with concentration factor, see Section 1.10.2b for recovery equation) the complementary mass balance recovery was 90%. This indicated the clear interaction and retention of sample tracer (10%) on the 0.4μm filter membrane.

These findings illustrated the significant retention of labelled particles on 0.4μm and to a lesser extent, 0.01μm filters and the effect it had on the recovery calculations if these fractions were not included. Although inclusion of these fractions indicates the magnitude of the filter/tracer association it did not give any insight into balance of the tracer labelling i.e. whether the tracer retained is from the >0.4 colloidal aggregate, colloid or truly dissolved fractions or the effect on the estimated colloidal fraction. Additionally the magnitude of these interactions was variable for different aliquots which indicated filter volume dependant retention. Under these circumstances it was not possible to routinely adjust any of the fractions for the activity retained on the filters.

To investigate this problem further, activity of filtrate samples was compared with volume filtered. The 0.4μm filter was used as this was the fractionation where most artifacts appeared to occur. Activity counts were taken from two, 5ml aliquots of 0.4μm filtrate; one was taken from the first 10ml of filtrate (true fractionation) and the other from the last 10mls. An integrated sample (as was counted in all the experiments) was also counted. Table 3.2 illustrates the various filtrate counts and implications for colloidal fractions.

TABLE 3.2: Total and colloidal activity removal onto 0.4 μm filters.

a) Dissolved activity (counts/1000secs) removal onto 0.4μm filters:

Total activity	activity in first 10ml of 0.4 filtrate (true partitioning of activity)	activity in last 10mls of 0.4 filtrate	activity removal between first and last 10ml of filtrate	% of original filtrate activity	activity in integrated sample	activity removal in integrated sample from first 10mls	% of original filtrate activity	activity retained on 0.4 filter (potentially particulate and colloidal)	% of total activity
5115	5277	4809	468	**8.87**	5063	214	**4.05**	384.8	**7.5**
5958	5608	5171	437	**7.79**	5187	421	**7.51**	428.3	**7.2**

b) Colloidal activity removal onto 0.4μm filters:

Given 0.01μm (truly dissolved) activity of 4171counts

Total activity	Colloidal activity in first 10ml of 0.4 filtrate	Colloidal activity (% of total activity)	Colloidal activity in last 10mls of 0.4 filtrate	% of total activity	Colloidal activity removed between 120mls	% of total activity	Change in % of original colloidal activity	Colloidal activity in integrated sample	% of total activity	Colloidal activity removal in integrated sample	% of total activity	Change in % of original colloidal activity
5115	1106	**21.6**	638	**12.5**	468	**9.15**	**42.3**	892	**17.4**	214	**4.2**	**19.3**
5958	1437	**24.1**	1000	**16.8**	437	**7.33**	**30.4**	1016	**17.1**	421	**7.1**	**29.3**

Some retention of truly dissolved activity is possible too. Separation check was carried out mid experiment (maximum removal to filters)

There was a significant decrease in the second filtrate activity (7.8 to 8.9 % of total dissolved-Table 3.2a) compared to the activity in the first 10ml of filtrate. This loss was comparable to the activity retained on the 0.4μm filter. There was also significant reduction in the activity of the integrated sample comparable to a loss of 4 to 7.5 % of original filtrate (total dissolved) activity. The significant changes in 0.4μm filtrate activity with relatively small filtrate volume (120mls) indicates that the tracer retained on the filter membrane is most likely colloidal rather than colloidal aggregates >0.4μm. Table 3.2b illustrates the effect that this retention of labelled colloidal material has on the determined colloidal fraction as a percentage of the total activity present.

Clearly, the colloidal percentage determined is greatly affected by retention on the filter. The colloidal fraction as a percentage of the total activity present decreases from 21.6 to 24.1% to 12.5-16.8% over 120mls of filtrate (integrated sample activity loss is ~17%). Although the integrated sample is less altered than a sample collected after 120mls there is still significant underestimation of the colloidal fraction (decrease by 19.3 to 29.3% of the true colloidal fraction). The colloidal fractions cannot be adjusted for this effect as the magnitude of the colloidal retention has been shown to be variable for each aliquot filtered and this sort of detailed fractionation cannot be performed for each sample filtered.

This single fractionation indicates that the activity of colloidal partitioning of ^{65}Zn are potentially underestimated by ~15% in this study (this filter retained fraction has previously been incorporated into >0.4μm colloidal aggregate partition in the activity data plots). This should be noted when discussing zinc tracer partitioning.

3.5.5: Gravimetric analysis:

Gravimetric analysis of the initial samples was carried out following the filtration protocol detailed in section 3.4.1.1. The mass distribution of the colloidal population and larger particles was established at the beginning of the experiments (see Table 3.3) but clearly, it was expected due to the inherent instability of particulate/colloidal material that the particle spectrum and mass distribution would change over the timescale of the experiments.

Table 3.3: Beaulieu gravimetric determinations (mg/l) for continued radiotracer experiments:

	Original sample gravimetrics	**Cold (2-4°C) stored (12hrs)**	**Room temperature stored (12hrs)**
Whatman No2 (>8μm)	7.98 ± 0.58		
>8μm to 1μm	3.52 ± 0.79		
1μm to 0.4μm	1.17 ± 0.05	1.07 ± 0.15 (>0.4μm)	7.423 ± 1.2 (>0.4μm)
0.4μm to 0.02μm (colloidal)	9.45 ± 0.5	8.45 ± 0.5	5.665 ± 0.65
Total	22.12	9.52	13.09
Colloidal %	42.7	88.8	43.3

Because of the time constraints involved with particle spectrum mass determinations it was only possible to take a single measurement of the particle size/mass distribution for the original Beaulieu water sample. Without subsequent mass distribution measurements of macroparticles and colloids at the temporal resolution of experimental tracer activity measurements calculations of Kd values (Kc) were inhibited, especially as the time when the mass distribution of the particulate fractions was best represented was when the partitioning of the ^{65}Zn tracer was most rapidly changing i.e. at t=0. A storage experiment was carried out to look at colloidal mass over time. It was unknown whether colloidal inputs from the truly dissolved fraction (peptisation reactions) or removal by sedimentation, flotation or colloidal disaggregation would be detectable.

Figure 3.11 illustrates the initial decrease in colloidal mass observed from CFF of the original sample to 12hrs storage in the cold and dark and then relatively small changes over the experimental timescales under room temperature (~50hours is the exception).

It is unlikely that there would be flotation of colloidal material originally present at ambient cold temperatures during cold storage, but during equilibration with room temperature this may occur.

Figure 3.11: Colloidal mass changes of CFF stored Beaulieu River water (error bars are 1σ of triplicate gravimetric determinations).

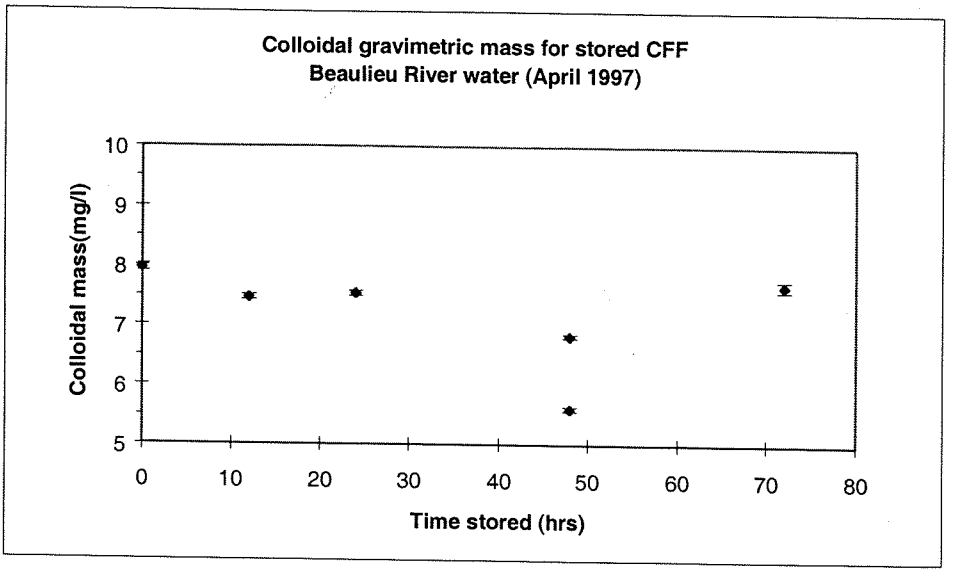

Aggregation over 12 hours under cold storage has previously been substantial enough to cause sedimentation, so it is likely that this process is also involved in removal of colloid material. Over the experimental period there were visible changes in the particle size distribution as observed by the formation of large aggregates. It is possible that flotation effects and gentle stirring exacerbated this aggregation. However, the removal of a large fraction of colloidal mass by this process is not seen in the gravimetric analysis. As there is no fractionation of the colloidal mass there would only be mass changes observed if there was material added from the truly dissolved phase or removed via sedimentation.

Clearly, for the highly organic colloids in this study the mass distribution is not really significant compared to the available surface area. It is the organic polymers that have aggregated and these will form a very small weight percentage in the particle spectrum. It is these low molecular weight polymers though that were observed to govern the zinc tracer distribution. As has been seen in this experiment, there may be no significant change in colloidal mass but a change in colloidal conformation, suggesting therefore that surface area has far more effect on tracer behaviour and partitioning.

3.5.6: Coulter Counter work:

Some Coulter Counter work was carried out in conjunction with the radiotracer experiments to gain some idea of the complete particle spectrum of the Beaulieu samples and also when various filtration approaches were applied. All sample were stored cold (2 to 4 °C) and dark from sampling or separation until counting.

3.5.6.1: Complete Beaulieu River water spectra:

Figure 3.12 illustrates a typical particle size spectrum for Beaulieu River water. It suggests that there is a large colloidal pool and most particles counted lie below 3μm diameter. This is to some extent expected as there is a wide spectrum of organic particles, fulvic and humic acids in this water that drains from the New Forest. The size distribution is heavily weighted towards the smaller fractions, which may help explain the easy clogging of 0.4μm filters encountered in this study. Figure 3.12 indicates the temporal changes in magnitude of colloidal and micro particle signals. The 28 February sample coincided with a high flow event and as a result there are 2-3 times as many particles as in later samples. The sub-micron particles and colloidal population decreases during lower flows.

Figure 3.12: Complete Coulter counter particle spectrums for Beaulieu River water collected on different dates.

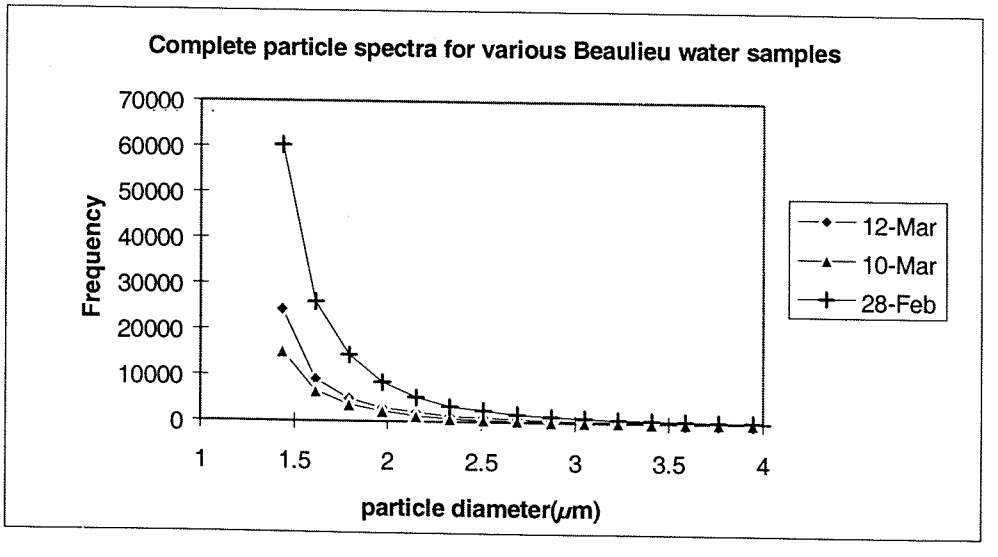

3.5.6.2: Effect of conventional versus laminar flow block cross flow filtration effects on the particle size spectra.

Figure 3.13 illustrates the difference in spectrum resulting from conventional vacuum filtration and CFF. After three days cold storage the CFF sample has a much higher colloidal fraction and other particles <3μm. The conventional filtered sample has very low counts in this size range and strongly indicates that clogging of the filter membrane during filtration led to removal of colloidal and other particulate material from the sample.

Figure 3.13: Comparison of conventionally and cross-flow filtered (0.4μm) Beaulieu River water particle size spectrums.

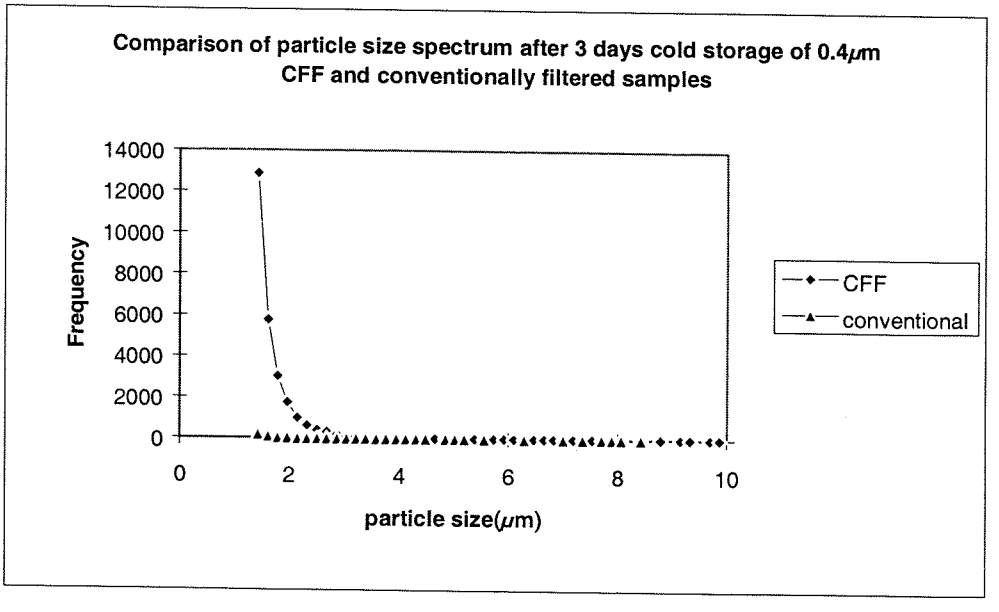

3.5.6.3: Effects of stirring:

Figure 3.14 indicates the effect of stirring on an 8μm prefiltered sample. Stirred sample which was kept at room temperature has larger size particles and frequency than the sample that was stored, unstirred in the cold. Increased temperature and stirring increases the energy and collision frequency of particles and colloids and enhances aggregation.

Figure 3.14: Particle size spectrum changes resulting from stirring.

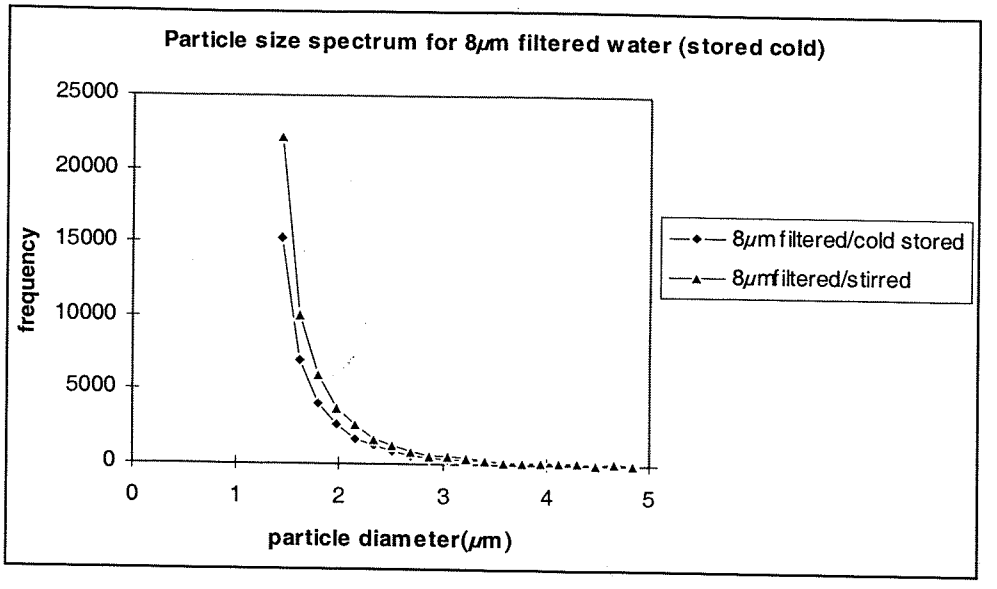

The main draw back with the Coulter counting technique is that the smallest particle size detectable is 1.4μm. Although there is no direct measurement of the colloidal spectrum it is still possible to gain some sort of insight into the spectrum immediately above it and infer a continuum into the colloidal spectrum. As with any technique there are some problems with Coulter counting, especially for Beaulieu River water the highly polymer/organic nature of most of the particles can cause overlap counting artefacts.

3.6: Trace metal size spectrum distribution for Beaulieu River samples using field-flow fractionation:

Field flow fractionation (FFF) studies of natural samples to date have generally been restricted to achieving high resolution separation and sizing of a wide range of particulate, colloidal and macromolecular material. Environmental samples that have been separated using this technique include humic substances (Beckett et al., 1987; 1988), clays (Murphy, 1995), bacteria (Sharma et al., 1993), suspended particulate material and soil colloids (Chittleborough et al., 1992). Additionally Beckett et al. (1988) used flow FFF to determine the molecular weight of humic and fulvic acids from natural samples. Sedimentation FFF has been used by Karaiskakis et al. (1982) and Beckett et al. (1988) to separate and size characterise colloidal particles in river water but the investigation of trace metal species associated with various FFF determined size spectrums has not been addressed. Due to the high dilution factors of FFF any investigations of trace metal size distribution has been confined to polluted sites where trace metal concentrations are many times greater than occur naturally (Lead pers. comm.).

Using trace preconcentration/solvent extraction techniques and combination of identical size fractions it has been possible in this study to determine a size spectrum distribution for Fe, Mn and Zn in colloidal material from the Beaulieu River. This has not been done previously for natural trace metal concentrations. Sample handling, preparation and FFF protocol are discussed in Section 2.5. The size partitioning of Zn especially, was designed to give the initial stable Zn distribution on natural material prior to radiotracer experiments of ^{65}Zn adsorption/transformation. FFF determination of size fraction partitioning of Fe and Mn that occur naturally in colloidal and humic material in this system, as determined from SEM EDS work, would also give an insight into the relative importance of various size fractions for these metals.

3.6.1: Extraction blanks and data quality:

The samples were analysed using the APDC-DDDC/chloroform method described in Section 2.3.1 and eluted in the size fractions listed in Table 2.4 (N.B. fractions 4 and 5 were combined to give sufficient sample volume for solvent extraction). Extraction and blank data are listed in Table 3.4. The extraction procedure blanks for Fe, Mn and Zn

were 1.47, 0.08 and 0.29 nmol/L respectively. The detection limit for the extraction procedure was 3.55, 0.07 and 0.89nmol/L for Fe, Mn and Zn. Extraction data quality checks using CRMs and LMSW standards are shown in Figure 3.15. Extraction for Mn and Zn were good for the range of concentrations encountered in the field-flow fractions. As encountered previously, the extraction efficiency for high Fe LMSW standard concentrations (>40nmol/L) was not as good. This was mainly due to extraction problems resulting from a chloroform/aqueous emulsion that formed in high DOC samples. However, the original FFF sample concentrations (diluted approximately 200 fold during fractionation) lay within the good recovery (LMSW standards and CRMs) section (>90%). Blanks for sample processing (laminar flow block CFF and 0.4μm prefiltration), Milli-Q used at Lancaster University and acidifying procedure inside a clean room are listed in Table 3.4. These were all acceptable when compared to the sample concentration, and sample fraction concentrations were adjusted for these blank values.

Table 3.4: Quality assessment of FFF procedure and fraction extraction (nmol/L).

Blanks:							
	Fe	σ	**Mn**	σ	**Zn**	σ	
Chloroform	**1.87**	0.66	**0.52**	0.15	**2.11**	0.36	
Blank	**1.47**	1.16	**0.08**	0.02	**0.29**	0.29	
Detection l.	**3.55**	0.00	**0.07**	0.00	**0.89**	0.00	
MQ LFB	**1.08**	0.03	**0.04**	0.00	**0.20**	0.03	
MQ 0.4F	**4.28**	0.05	**0.28**	0.01	**1.84**	0.00	
MQ Lanc.	**1.45**	0.01	**0.08**	0.01	**0.05**	0.00	
MQ unacid	**2.25**	0.02	**0.09**	0.01	**0.20**	0.07	
NaNO3	**13.69**	0.06	**1.27**	0.07	**23.13**	0.46	
NaNO3	**16.70**	4.32	**1.01**	0.09	**21.11**	1.18	
Std 1	**20.95**	0.50	**21.48**	0.23	**14.50**	0.32	
Std 3	**31.52**	0.63	**51.14**	1.57	**43.29**	0.32	
Std 8	**43.15**	0.09	**146.0**	1.29	**114.7**	0.64	
Std 15	**84.52**	0.57	**210.7**	6.76	**223.6**	4.04	
Standards		**CASS**		**SLEW**		**1643D**	
Fe	**Actual**	**22.56**	3.04	**42.44**	5.55	**1633.0**	69.83
	Obs.	**16.47**	1.43	**49.83**	0.13	**1649.3**	0.00
Mn	**Actual**	**45.69**	6.55	**311.3**	20.03	**685.5**	15.11
	Obs.	**44.78**	1.77	**267.0**	1.32	**642.7**	14.43
Zn	**Actual**	**18.97**	3.82	**16.83**	2.14	**1108.6**	9.94
	Obs.	**23.34**	1.87	**16.52**	0.61	**1055.7**	68.58

Figure 3.15: LMSW standard and CASS-2/SLEW extraction efficiency for Fe, Mn and Zn during FFF sample extractions.

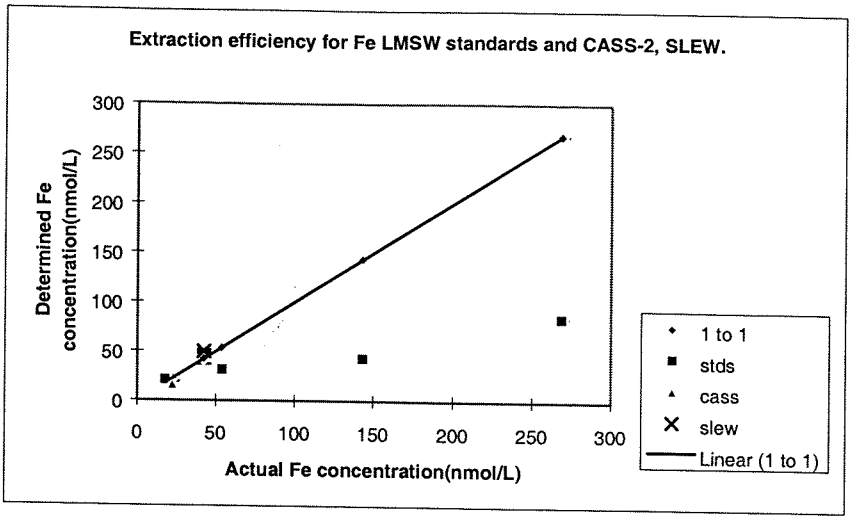

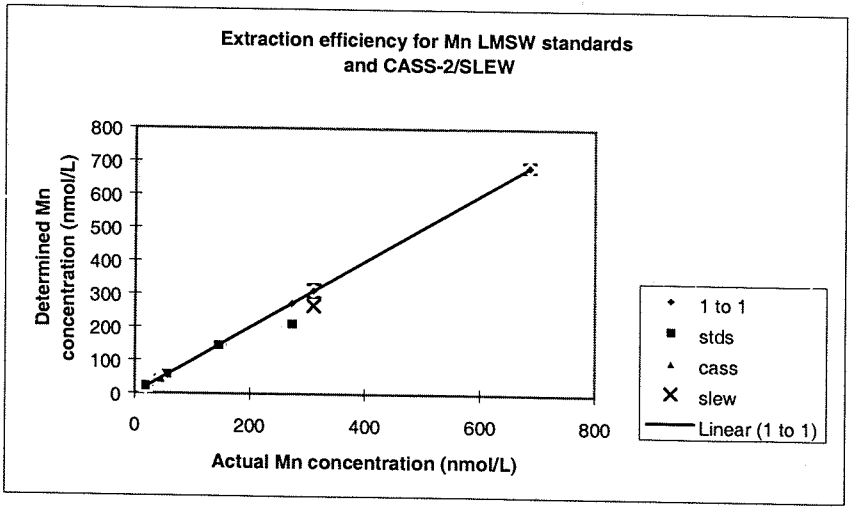

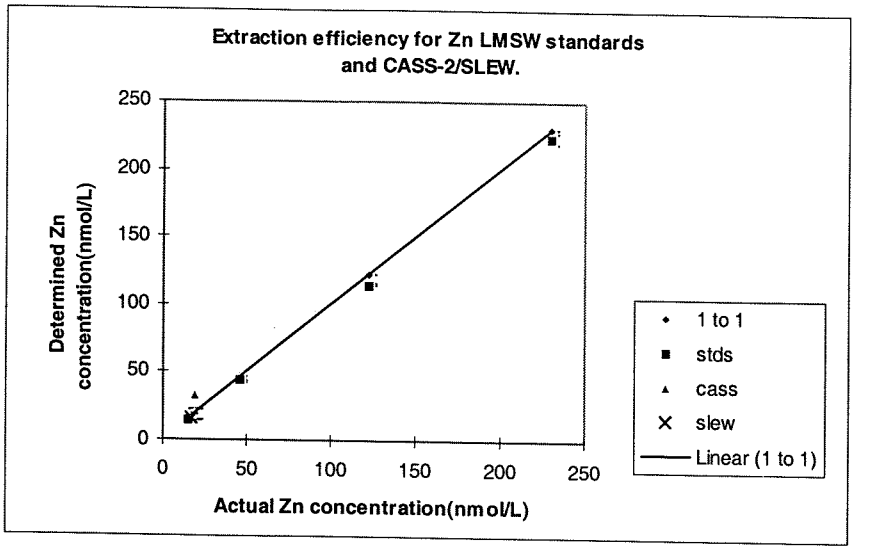

3.6.2: Assessment of FFF application to trace metal work:

The FFF equipment at Lancaster was not housed in a clean environment and although injection of the sample could be carried out using clean techniques it was not possible to acid clean the FFF stainless steel channel as would be the usual approach for trace metal work. Blanks of the carrier fluid (0.001M $NaNO_3$) allowed an estimate of the instrument and environment blank to be made (i.e. atmospheric exposure during elution times). Although these were higher than ideal (especially for Zn) they were not so high as to interfere with the determination of the sample metal concentration. Sample fraction concentrations were adjusted for these blank values.

3.6.3: Trace metal size distributions:

Figure 3.16a illustrates the comparative distributions and concentrations (nmol/L) of Fe, Mn and Zn in the total dissolved (<0.4μm) and colloidal FFF fractions. As expected the concentrations of Fe were very high compared to Mn and Zn in some fractions, so the <0.180μm and total dissolved fractions have been removed in Figure 3.16b to give a clearer indication of the metal distributions in the remaining size fractions.

There is a significant fraction of total iron (19.4%, see Table 3.5) in the truly dissolved phase and although the data suggests an increased partitioning of Fe into smaller colloidal fractions this may be an artifact of variable particle masses in each fraction. On average iron is evenly partitioned (40.9 vs. 41.0 %) between colloidal material greater than and less than 0.2μm respectively.

There is a higher proportion of manganese (34.7% of total dissolved) present in the truly dissolved phase (<0.08μm). 64% of Mn is found in the colloidal fractions but there is no significant trend with colloidal size and the percentage of Mn in each fraction is relatively consistent, 9 to 13% of total dissolved.

Zinc also shows a significant truly dissolved fraction, 23.0% versus 77.7% colloidal. Unlike Fe and Mn the mean fraction distribution for Zn indicates an increased partitioning into the smaller colloids. 47.5% of Zn is partitioned into colloidal material

less than 0.2μm in diameter versus 30.2% of Zn present in colloidal material larger than this fraction.

Figure 3.16: Trace metal size FFF distributions for Beaulieu River colloidal material (total metal is <0.4μm). Figure 3.16a includes all the FFF fractions separated from a sample whereas 3.16b has had the larger total and <0.18μm fractions removed to give better resolution for the other remaining fractions. The error bars are 1σ of triplicate metal analysis.

a:

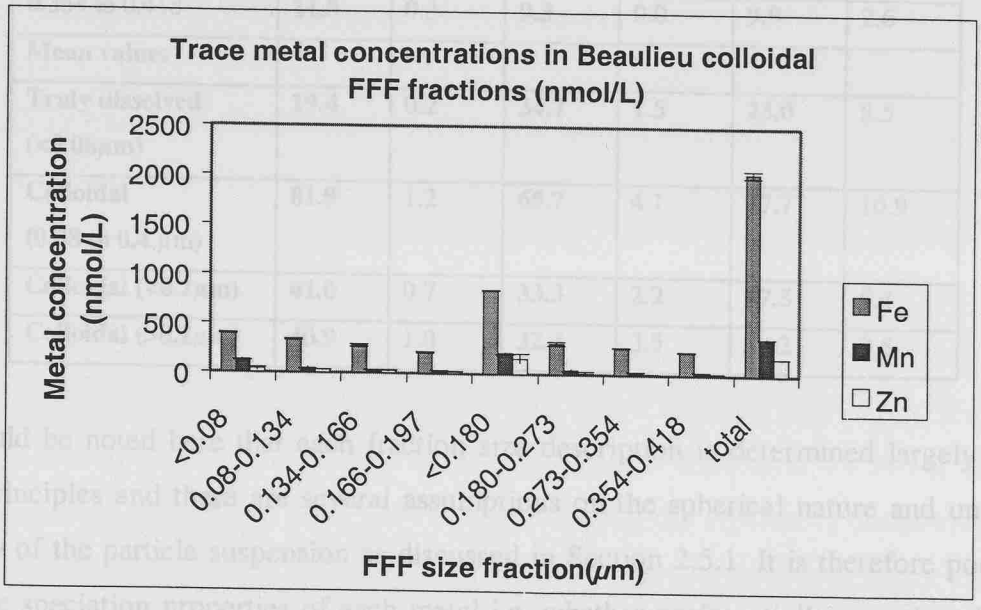

b:

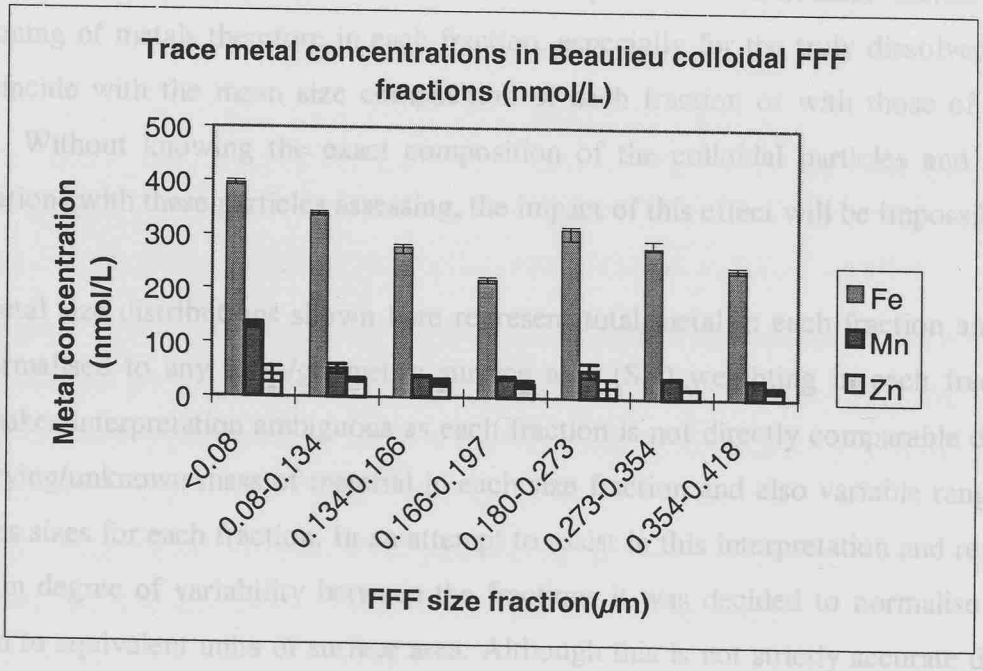

Table 3.5 : Trace metal FFF fractions as percentage of total dissolved metal

Fraction (μm)	Fe	σ	Mn	σ	Zn	σ
<0.08	**19.4**	0.2	**34.7**	1.5	**23.0**	8.5
0.08 to 0.134	**16.7**	0.2	**13.6**	2.1	**17.8**	1.9
0.134 to 0.166	**13.6**	0.6	**10.1**	0.3	**15.5**	3.7
0.166 to 0.197	**10.7**	0.2	**9.6**	0.7	**14.1**	3.3
<0.180	**41.7**	0.1	**56.1**	2.9	**91.1**	25.2
0.180 to 0.273	**15.4**	1.0	**13.3**	3.4	**10.5**	9.1
0.273 to 0.354	**13.7**	0.2	**9.9**	0.3	**9.9**	0.0
0.354 to 0.418	**11.8**	0.3	**9.3**	0.0	**9.9**	2.6
Mean values						
Truly dissolved (<0.08μm)	**19.4**	0.2	**34.7**	1.5	**23.0**	8.5
Colloidal (0.08 to 0.4 μm)	**81.9**	1.2	**65.7**	4.1	**77.7**	10.9
Colloidal (<0.2μm)	**41.0**	0.7	**33.3**	2.2	**47.5**	5.4
Colloidal (>0.2μm)	**40.9**	1.0	**32.4**	3.5	**30.2**	9.5

It should be noted here that each fraction size description is determined largely from first principles and there are several assumptions on the spherical nature and uniform density of the particle suspension as discussed in Section 2.5.1. It is therefore possible that the speciation properties of each metal i.e. whether preferentially complexed with hydroxides or organics may affect the elution profile of individual metals. The partitioning of metals therefore in each fraction, especially for the truly dissolved may not coincide with the mean size composition of each fraction or with those of other metals. Without knowing the exact composition of the colloidal particles and metal associations with these particles assessing, the impact of this effect will be impossible.

The metal size distributions shown here represent total metal in each fraction and are not normalised to any mass/geometric surface area (SA) weighting in each fraction. This makes interpretation ambiguous as each fraction is not directly comparable due to the varying/unknown mass of material in each size fraction and also variable ranges in particles sizes for each fraction. In an attempt to assist in this interpretation and remove a certain degree of variability between the fractions it was decided to normalise each fraction to equivalent units of surface area. Although this is not strictly accurate due to

lack of a particle size/mass spectrum and assumptions about particle shape (i.e. spherical) it was hoped that it would enable more meaningful interpretation of the data. It is assumed that the total concentration of metal present in a size fraction is dependant on the binding sites available and complexation capacity of those sites. To a large extent therefore it is the particle diameter and hence geometric surface area (assuming spherical morphology) available to each metal that will affect the weighting of metal partitioning for a given fraction. It is noted that internal surface area of aggregates that is not calculated here may add to effective colloidal adsorption surface area (specific surface area-SSA). Assuming a size spectrum continuum of particles the truly dissolved species (<0.08μm) were also included in this process.

Figure 3.17 illustrates the distribution of Fe, Mn and Zn after this normalisation by FFF fraction surface area. The complete fractions <0.18μm and <0.4μm are included for comparison.

Figure 3.17 indicates that once normalised the apparent distribution of trace metal species can change significantly. All three metals follow a similar distribution here with the smaller colloidal fractions (<0.197μm) having higher concentrations of Fe, Mn and Zn per fraction unit surface area. The <0.08μm fraction has significant concentration of all the metals but especially of Fe. The total dissolved and combined <0.18μm fractions reflect this metal/particle size relationship as the smaller diameter fraction, which incorporates not only smaller colloids but also those incorporated into the truly dissolved phase, has a higher trace metal concentration than the total dissolved. Increased partitioning of all the metals into smaller diameter colloidal fractions was expected due to the increased surface area to volume ratio associated with particles of smaller diameter.

The highest density of trace metal occurs on the smaller colloidal particles, or in the truly dissolved phase. The truly dissolved phase has the highest density of trace metal (especially for Fe) per unit area whilst at colloidal sizes greater than 0.18μm the density of metal concentrations is much reduced. Indeed, Mn and Zn concentrations are virtually insignificant compared to partitioning in other fractions. The combined <0.18μm and total dissolved densities reflect the contrasting average metal densities for small colloidal or complete colloid samples.

Figure 3.17: Trace metal FFF size distributions normalised per fraction unit area (μm^2).

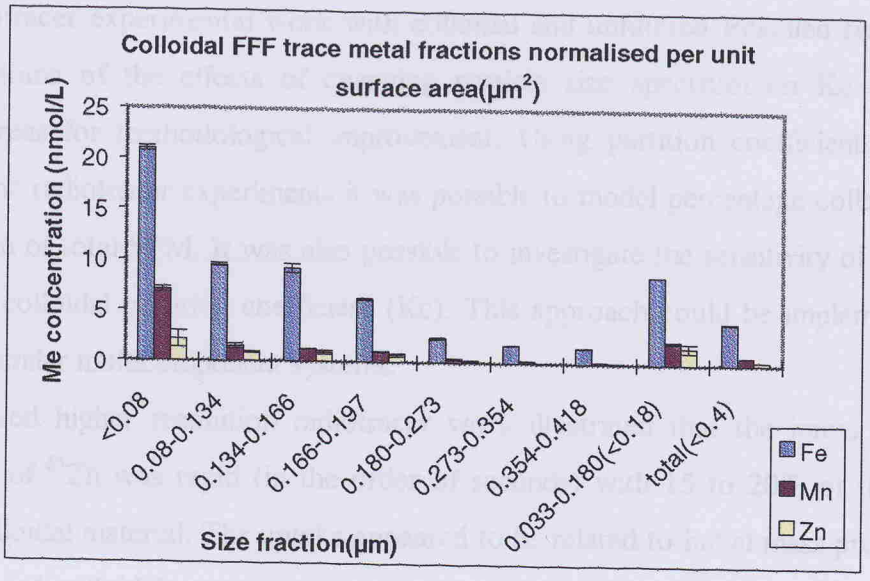

It is possible that smaller colloidal material may be compositionally different to larger colloids due to variation in origin and therefore have different binding site type, density and therefore complexation capacity for various trace metals. This would be likely to reinforce any size dependant metal partitioning and very difficult to study. It is suggested that the very high concentration density of all the metals in the <0.08μm fraction is attributable to the very small colloids inevitably present in this fraction, but this may also be an artifact normalising to surface area in this fraction that includes ionic metal species. Despite this high metal density, this truly dissolved fraction is not as significant as colloidal species in the overall total partitioning of total dissolved metal (only 19, 34 and 22% for Fe, Mn and Zn respectively). The comparatively lower total metal loadings in this fraction may be attributed to a low mass of colloidal species or removal of colloids <0.08μm to larger size fractions via aggregation. Although precautions were taken to minimise sample size spectrum changes prior to fractionation it is inevitable that some metal and particle transformations will have occurred

The particle size dependant trace metal distribution observed here has far reaching implications to the physical processes that will affect colloidal material and hence trace metal transport. Larger colloids are far more likely to aggregate and settle out whereas smaller colloids of high trace metal content are more likely to be permanently suspended in the river/estuarine system and travel further. Size distribution of a trace metal will also affect it's bioavailability (Buffle, 1990).

3.7: Colloidal radiotracer summary and future work

Initial radiotracer experimental work with colloidal and unfiltered Beaulieu river water illustrated some of the effects of changing particle size spectrum on Kd and also indicated areas for methodological improvement. Using partition coefficients derived from the zinc radiotracer experiments it was possible to model percentage colloidal zinc as a function of total SPM. It was also possible to investigate the sensitivity of colloidal zinc to the colloidal partition coefficient (Kc). This approach could be implemented to modelling similar multicomponent systems.

The continued higher resolution radiotracer work illustrated that the initial colloidal partitioning of ^{65}Zn was rapid (in the order of seconds) with 15 to 20% of the tracer labelling colloidal material. The uptake appeared to be related to initial mass proportions of colloids and colloidal aggregates, and subsequent changes in particle size spectrum. This uptake was proportional to any storage changes in the colloidal spectrum and hence the mass proportion of colloidal to colloidal aggregates in the original sample. Tracer uptake was preferential onto colloidal material that had not aggregated and therefore had a higher surface area to volume ratio. Colloidal particle and tracer transformations were apparent very rapidly. However, due to the dynamic equilibrium nature of the tracer/colloid association, changes in the tracer partitioning were somewhat ambiguous. The tracer/colloid association was proved to be an exchangeable rather than a complexation interaction, as colloid partitioning was affected by addition of stable zinc. An increase in stable zinc actually increased the overall partitioning of total zinc (stable and radiotracer) into the colloidal phase as the partition coefficient between colloidal and truly dissolved phases effectively remained constant.

Long-term storage experiments revealed significant coagulation of colloidal particles into loose organic polymer aggregates which had coatings of Mn hydroxides. The radiotracer had a higher affinity for these aggregates which removed ~60% of the tracer from the truly dissolved phase. The hydrophobic nature of the aggregates combined with their potential to strip metals from the truly dissolved phase has significant implications for trace metal removal onto particles in natural systems. Rapid polymer bridging aggregation in highly organic waters (as in the Beaulieu) and its effect on trace metal removal over colloid residence timescales and varying salinity conditions needs further investigation. Mass balance calculations for the 0.4μm and 0.01μm filtration indicated

that even with laminar flow filtration up to 15% of labelled colloidal material could be retained on the filter surfaces via charge or hydrophobic effects.
Detailed colloidal/trace metal size separation by field-flow fractionation indicated that the highest total concentration of "dissolved" (<0.4μm) metals (Fe, Mn and Zn) was in the truly dissolved <0.08μm and 0.08 to 0.134μm fractions. When data was normalised to surface area per fraction, the highest densities of trace metals (Fe, Mn and Zn) were found in the smallest colloidal fraction, indicating that this fraction is probably the best scavenger of trace metals.

The original aim of this range of work was to investigate the effect of particle size spectrum and colloidal material on the partition coefficients (Kd, Kf, Kc). However, from initial and higher resolution experiments it was very clear that the accurate measurement of parameters (mainly particle mass distributions) on the timescales required to give good determinations of these coefficients was not possible. This problem was exacerbated by rapid alteration of the sample particle size distribution and lack of equilibrium of tracer partitioning conditions which are essential for representative partition coefficient determination.

As a result of this, the application of Kd to this type of system must be done with a degree of caution. It should be appreciated that the Kd determined at a point in time from experimental investigation has limited application to the real system from which the sample was originally taken. Aside from sample alteration discussed previously, the Kd is determined on a long timescale compared to the variability of the system the sample was taken from. In such dynamic estuarine systems the equilibrium/ steady state between particle and solution phases that the Kd describes (Turner et al., 1993) is rarely reached so a Kd determination is for that particular moment that the sample was collected. As such the conditional constant derived from this also depends solely on the water conditions (SPM, ionic strength, pH) at the same moment. Although some indication of the effect of particle size fractionation on Kd was demonstrated in the initial experiments, the partition coefficient was not routinely determined for the higher resolution experiments for the reasons discussed above. Purely for comparison purposes, colloidal/truly dissolved partition coefficients (Kc) have been determined for the initial tracer partitioning stage in the high resolution radiotracer experiments. These partition

coefficients and Kd, Kf and Kc values from the pilot experiments and other studies are listed in Table 3.6

The partition coefficients for the complete (Kd) filter retained, Kf (>0.4μm) and colloidal (Kc) fractions are remarkably similar in the Beaulieu River sample. This indicates that the complete particle population (particles and colloids) has similar composition (i.e. all particles have a predominantly organic and Fe/Mn oxyhydroxide composition, confirmed by SEM analysis) and the unusually high particle size distribution weighting towards the colloidal pool (>30% of mass in colloidal size fraction).

The Kcs derived for the colloidal samples in the pilot and higher resolution experiments were all at least an order of magnitude higher than in the complete sample. This must be a result of the mass distributions or competition within the complete sample for zinc activity that reduced colloidal partitioning (there is no filtration effect). The ^{65}Zn Kcs for colloidal samples stored cold, or at room temperature were 29.2 x 10^3 and 17.4 x 10^3 respectively (these increased to 37.2 x 10^3 and 20.9 x 10^3 when colloidal aggregates formed during storage were included). The Kc measurements reinforce the increased partitioning of the ^{65}Zn tracer into the more abundant colloidal material in the cold stored samples observed in the earlier experiments. This change in the Kc calculation would equate to a 5-10% increase in colloidal zinc percentage (from modelling using Kc values). Fang (1995) measured Kd values for zinc in the Beaulieu Estuary ranging from 25.1x 10^3 to 158.5 x 10^3. The colloidal Kcs measured in this work lie at the lower end of this range. In some ways this is not surprising as the Coulter counter work indicates that complete (unfiltered) Beaulieu samples are highly dominated by particles in the colloidal size range (up to ~2μm). The Kd derived in this study for a complete freshwater end-member samples was an order of magnitude less than the Kd derived by Fang. As has been shown through the gravimetric analysis protocol developed in this study it is very easy to remove colloidal species during 0.4μm filtration by clogging of filter pores. The removal of colloidal zinc (which is incorporated into the dissolved phase in a conventional Kd) will lead to artificially high Kd's and may help explain this order of magnitude difference.

Study	Study type	Water type	SPM	Kd	Kf	Kc
This study	Pilot expts. radiotracer	Complete	>0.4μm = 7.57mg/l colloidal 3.26mg/l	1.9 x 10^3 (coll diss) 2.3 x 10^3 (coll part)	2.1 x 10^3 (mean)	2.5 x 10^3 (mean)
This study	Pilot expts. radiotracer	Colloidal	Colloidal 3.32mg/l	N/A	~0.02	78.5 x 10^3 (t=1) 23.5 x 10^3 (mean)
This study	Pilot expts. radiotracer	Colloidal	Colloidal 1.32mg/l	N/A	~0.02	44.7 x 10^3 (t=1) 11.3 x 10^3 (mean)
This study	High Res. expts	Colloidal - stored cold (inc.colloid aggregates)	>0.4μm 1.07mg/l colloidal 8.45mg/l	N/A	N/A	29.2 x 10^3 (37.2 x 10^3)
This study	High Res. expts	Colloidal-room temp. storage (inc.colloid aggs)	>0.4μm 7.42mg/l colloidal 5.67mg/l	N/A	N/A	17.4 x 10^3 (20.9 x 10^3)
Fang 1994 Beaulieu	Stable metal fractions	Complete sample	N/A	25.1-158.5 x 10^3	N/A	N/A
Althaus 1992 Humber	Stable metal fractions	Complete	N/A	25.1 x 10^3	N/A	N/A
Turner et al. 1993 Humber	Stable/ radiotracer	Complete	N/A	7.3 x 10^3	N/A	N/A
Williams and Millward (in press) Humber	Radiotracer	Complete	N/A	5.3 x 10^3	N/A	N/A

Table 3.6: Partition coefficients (Kd, Kf and Kc) of zinc or ^{65}Zn derived from natural waters.

Comparative low salinity Kd's calculated for the Humber ranged from 7.3 x 10^3 (Turner et al, 1993) to 25.1 x 10^3 (Althaus, 1992). Radiochemical experiments (Williams and Millward, in press) involving the adsorption of radioactive ^{65}Zn onto Humber Estuary SPM gave a zero salinity Kd of 5.3 x 10^3. These elevated Kd values compared to Kd values in the Beaulieu may be a result of significant colloidal Zn incorporated into the "dissolved" phase in the Beaulieu or to the increased inorganic nature of the Humber particulate material. A comparison of partition coefficients for PSPM and colloidal material with conventional Kd's for differing estuarine systems would perhaps give an insight into this change in Kd/Kc.

Radiochemistry future work:

Although charge considerations would infer organic riverine colloids to be stable, Beaulieu River water colloidal material is clearly not, with aggregation and disaggregation transformations occurring. In this study it cannot be determined whether the uniform partitioning observed after approximately 10 hours is really an equilibrium or steady state situation. It is likely that such closed system conditions will rarely be attained in the natural environment. Simultaneous analysis of the colloidal size, mass and perhaps more importantly, surface area spectrum and use of a more particle active tracer may remove an element of the ambiguity of some of the observed tracer transformations (adsorption vs. aggregation). Stordal et al. (1996) has produced evidence for colloidal pumping via coagulation by monitoring natural colloids tagged with ^{203}Hg. Mercury is a very particle reactive element so adsorption/desorption transformations are minimal and changes in the particle population can be isolated. This work indicates that colloidal pumping and transfer of tagged colloids into the particle pool occurs in a two stage process; a fast (<1hour) initial process and a slower process that is driven by Brownian coagulation that occurs over several days. These two processes are indicated in the experiments reported here, but without the clarity given by use of a highly surface active isotope, and therefore the transformations observed here are somewhat ambiguous.

The nature and formation mechanism of the Fe/Mn filaments (i.e. bacterial or natural precipitates) requires further investigation, especially as they seem to have a sorptive affinity for the truly dissolved radiotracer greater than the original colloidal population.

This may be a surface area effect due to conformation changes in the colloidal aggregates or may be due to a change in the nature/composition of the binding sites. The time scales and rates of trace metal adsorption initially and the long-term particle transformations need to be put in context of the natural environment and associated processes. The temperature of the experiments is somewhat higher than ambient so, despite dark storage, microbial processes are likely to be more pronounced than under natural conditions.

Once the ambiguity of the trace metal transformations has been resolved it would be easy to extend this sort of experiment to other colloidal samples of different conformation /composition. For example: comparison of uptake of different isotopes by colloidal populations from the Trent/Humber system (more inorganic) and Beaulieu riverine colloids (highly organic. Fe/Mn oxyhydroxide dominated). Also, colloidal material from various sources over temporal scales (i.e. elevated river flow colloidal population compared to low flow population) may have varying sorption/ transformation characteristics. Using FFF approaches it may be possible to look at individual colloidal fractions/particle sizes to assess isotope uptake with respect to colloidal composition and conformation. A hypothesis has been suggested in the present literature that due to their larger surface area to volume ratio, colloidal material will adsorb truly dissolved metal species preferentially to larger particles. This can be reflected in Kd determinations (with colloidal material included in the dissolved or particulate phases) but high resolution mass/surface area distributions are required to give credibility to Kd estimations. All these changes could be investigated over contrasting stability (salinity/estuarine) conditions and also temporally and spatially (axially and within the water column) in the Beaulieu Estuary.

The greatest tidal erosion and resuspension, which is a source of colloidal material, is observed to occur on the ebb tide (Springs) in many estuaries. The partition effects of colloidal material and hence role in trace metal transport will depend greatly on zones of highest loading and type (metal affinity) of material available. Resuspension is highest near bed in the water column but so is release of metals, often in dissolved form. Colloidal loadings may be significant here or higher up in the water column due to floc break-up. Quantification of the net effect of colloid/metal sources and aggregation/

disaggregation processes within the water column is needed. Biological action and organic loadings will also affect the colloidal metal loadings observed and should be taken into account.

Characterisation of colloidal material collected in the Beaulieu by SEM/TEM is often lacking in colloidal studies. Investigation of compositional and conformational variation of colloidal material in conjunction with other studies (water column, spatial variability) is possible using these techniques.

Field Flow Fractionation (FFF) Future Work:

The main problem with the interpretation of the trace metal size distribution here is the lack of particle size frequency or mass spectrum giving a total colloidal mass or surface area in each fraction. Usually with FFF techniques a fractogram (absorption curve) is produced that will record the particle size/mass spectrum during the elution run. With the very high dilution of the Beaulieu samples this was not possible. To improve the accuracy of the size distribution particle size spectrums derived from light scattering techniques would be invaluable. Although equally useful, fraction mass spectrums would prove very difficult to achieve given the large volumes of colloidal samples that would need to be processed to give significant colloidal mass in each of the elutant fractions.

Although the data discussed here has given some sound insights into colloidal trace metal (Fe, Mn, Zn) size distribution, the fraction resolution was limited by the sample volume required for preconcentration and solvent extraction. Application of high resolution analytical and detection techniques (i.e. ICP-MS C.Shand pers.comm.) would improve this problem. Additionally, although sedimentation FFF has given good colloidal separation in this study to increase resolution of the size fractions flow FFF would be more appropriate, especially for the smaller colloidal material.

Characterisation of the colloidal size fractions would greatly complement metal size partitioning information. As discussed previously, association of a given trace metal with a particular ligand, for example in this case Fe with humic material or Mn and inorganic oxyhydroxides, will greatly affect the elution time of such particles and the resulting

colloidal size fraction classification. Resulting metal size distribution data may therefore be biased by the speciation of a metal in the natural sample. Clearly, a colloid's composition is rarely homogenous but some idea of colloidal compositional size distribution and hence the speciation of various metals in each size fraction will help resolve some of this ambiguity.

Chapter 4: Spatial and temporal distribution of colloidal trace metals in the Humber Estuary:

4.1: The Trent/Humber system

The catchment area of the Humber system (circa 25,000Km^2) is the largest in the United Kingdom. From its mouth at Spurn Head the estuary extends 62Km to Trent Falls where it divides into two river systems; The Ouse (tidal length 62Km) and the Trent (85Km). See Figure 4.1 for tidal limits of the main tributaries and Humber location. For the purpose of this study the terminology of Grant and Middleton (1990) is adopted such that the section of the estuary from Trent Falls (the Trent/Ouse confluence) to Spurn Point is referred to as the Humber Estuary. All the sampling transects in this study continued from Gainsborough (limit of tidal (saline) intrusion in the Trent-river end member) on the Trent, down past Trent Falls towards Spurn. The River Ouse was not sampled.

Average flow for 1964 to 1973 (Gameson, 1976) indicated that the River Ouse contributed over half of the flow at Trent Falls. Combined mean annual freshwater flows for 1982 to 1989 (Humber Estuary Committee, 1990) were 169 to 299m^3/s. However this type of data discounts the flow extremes (as seen in the February survey, 1996) and flows ranging from 60 to 1500m^3/s have been recorded (Morris, 1988). The fresh water residence time of the Humber Estuary has been estimated at ~80 days (Coffey, 1994). However, freshwater flushing is very important in the estuary and the flushing time has been estimated at ~40days (Turner, 1990; Tappin pers.comm.) although this will vary considerably with respect to freshwater flows and hence season.

The Humber estuary may be described as macrotidal with tidal ranges of 3.5 to 6.0 metres. Penetration of saline influence into the estuary varies with tidal state and river discharges and at Trent falls salinities may vary from zero at low tide and high flow events to 6 or 7 at high water. When high river flow events occur, freshwater may extend some 20Km downstream of Trent Falls. There is increasing tidal asymmetry in the Humber Estuary from Spurn Head (near sinusoidal flood-ebb cycle) to a 2 hour flood, 10 hour ebb cycle at Gainsborough in the Trent. The average net transport after one tidal cycle (i.e. the tidal excursion) has been reported as 5 to 14 Km (Gameson, 1976; Shell U.K., 1987;).

Figure 4.1: Location and site of the River Trent and Humber Estuary (From: Millward and Glegg, 1997; Sanders et al., 1997;).

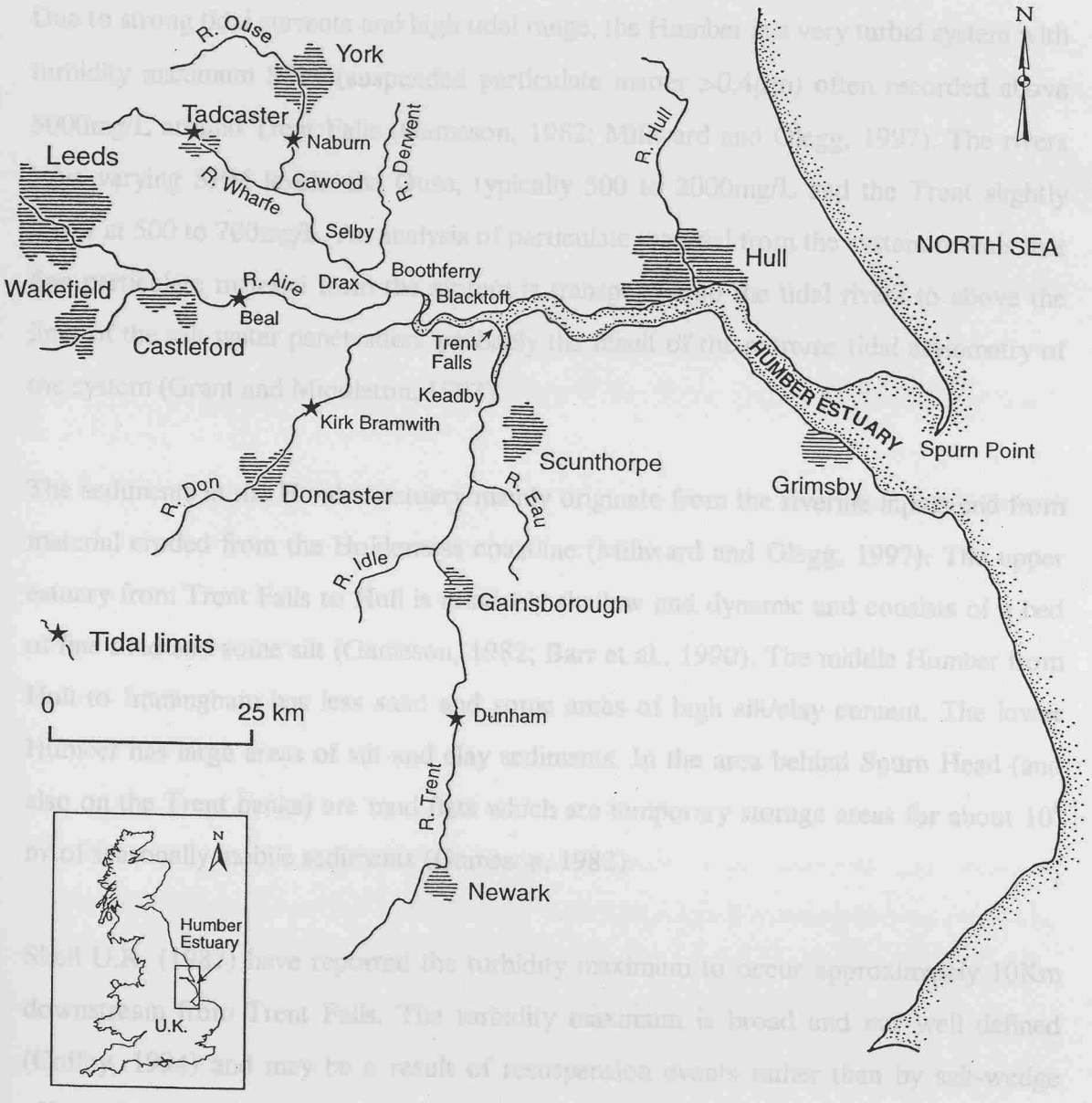

The water circulation is generally well-mixed due to the strong tidal forcing (2m/s near Hessle). Vertical salinity differences of 5psu close to Spurn Head decrease to zero further up the estuary (Coffey, 1994) and salinity gradients across the estuary are small (1 to 2 psu) depending on the tidal state.

Due to strong tidal currents and high tidal range, the Humber is a very turbid system with turbidity maximum SPM (suspended particulate matter >0.4μm) often recorded above 5000mg/L around Trent Falls (Gameson, 1982; Millward and Glegg, 1997). The rivers have varying SPM levels; the Ouse, typically 500 to 2000mg/L and the Trent slightly lower at 500 to 700mg/L. An analysis of particulate material from the system reveals that fine particulate material from the system is transported up the tidal rivers to above the limit of the salt water penetration, probably the result of the extreme tidal asymmetry of the system (Grant and Middleton, 1993).

The sediments in the Humber estuary mainly originate from the riverine inputs and from material eroded from the Holderness coastline (Millward and Glegg, 1997). The upper estuary from Trent Falls to Hull is relatively shallow and dynamic and consists of a bed of fine sand and some silt (Gameson, 1982; Barr et al., 1990). The middle Humber from Hull to Immingham has less sand and some areas of high silt/clay content. The lower Humber has large areas of silt and clay sediments. In the area behind Spurn Head (and also on the Trent banks) are mud flats which are temporary storage areas for about 10^6 m^3 of seasonally mobile sediments (Gameson, 1982).

Shell U.K. (1987) have reported the turbidity maximum to occur approximately 10Km downstream from Trent Falls. The turbidity maximum is broad and not well defined (Coffey, 1994) and may be a result of resuspension events rather than by salt-wedge effects. The specific surface area characteristics of particles within the turbidity maximum are generally higher ($40m^2/g$) than those from the Humber Estuary as a whole (10 to 30 m^2/g) (Millward et al., 1990). This has been attributed to precipitation of Fe and Mn on particles in the turbidity maximum. When investigated further these particles showed a potential for irreversible adsorption of trace metals by incorporation into interior pore sites within the particles.

A severe oxygen sag in the vicinity of Trent Falls (probably linked to the turbidity maximum zone) was identified by Gameson in 1982. Oxygen levels are influenced mostly by sediment concentrations, mixing and seasonal biological activity. The large human population in the Humber system catchment has had a large effect on the DO concentrations in the rivers and estuary (Urquart, 1979). Inputs of high biological oxygen demand (BOD) i.e. sewage discharges (Strickland and Parsons, 1972) and discharge of power station cooling water have effects on DO respectively by biological consumption or temperature changes.

Fluxes of nutrients to the system are highly seasonal. The mean daily riverine fluxes of nutrients to the Humber system (1990 to 1993) were 380, 8400 and 740 kmol/day for phosphate, nitrate and ammonium respectively (Sanders et al., 1997). Fluxes of nitrate and phosphate are dominated by winter flows in the River Trent. The tidal Trent has a large internal source of ammonium, removes about 80% of its dissolved phosphate load and functions as a sink for nitrate (Sanders et al., 1997). The tidal Ouse is an overall source of nitrate to the main Humber system. Nitrate behaves conservatively within the main estuary but seasonality in the nitrate flux to the system is preserved. Seasonality in phosphate flux is almost eliminated in the lower part of the tidal rivers. Overall, the Humber system removes 85% of its dissolved phosphate load and 4% of its dissolved inorganic nitrogen load.

The Humber estuary receives large pollutant loads from industrial and domestic discharges. The banks of the Humber have undergone much industrialisation especially around the Immingham and Grimsby areas. The input of anthropogenic Fe, discharged in dilute sulphuric acid (TiO_2 works at Grimsby), can give rise to fluxes of Fe an order of magnitude higher than the riverine input. However, due to their high specific areas iron oxide precipitates can promote efficient scavenging of dissolved trace metals from solution (Millward et al., 1996). Although the intertidal mud flats along the most industrialised areas of the Humber have high metal concentrations compared to other estuaries (Jaffe and Walters, 1977) the Humber has been reported as not badly polluted when compared to other major European estuaries (Grant and Middleton, 1990).

Particulate and dissolved trace metal concentrations (Coffey, 1994; Althaus, 1992), trace metal partitioning (Turner et al., 1993), sediment sources/sinks (Barnett et al., 1989; Grant and Middleton, 1990; 1993,) and trace metal estuarine fluxes (Millward et al., 1996; Millward and Glegg, 1997) in the Humber have been investigated in many studies. However, to date, aside from work by Williams and Millward (in press) on trace metals associated with permanently suspended particulate material (PSPM) there has been very little direct investigation into the role of colloidal material in this estuarine system and the implications that colloids may have for trace metal residence times, scavenging or transport.

The significance of colloidal trace metals in estuarine systems has been reported by a number of recent papers (Baskaran and Santschi, 1993; Benoit et al., 1994; Dai and Martin., 1995; Martin et al., 1995; Sanudo-Wilhelmey et al., 1996; Wen et al., 1996). Through the LOIS project there was an opportunity to look at colloidal trace metals in the Humber. The high particulate loadings and associated changes in redox conditions in this estuary contrast significantly from those previous studies. There has been no work to date on colloidal partitioning of trace metals in this system.

Variation of trace metal partitioning into dissolved and colloidal fractions was investigated seasonally, over an axial transect salinity range. This was designed to give an insight into the significance of the colloidal phase in the Trent /Humber system from a process perspective.

Objectives of the study were to;

- Determine the abundance and distribution of colloidal material within the Humber estuary, using CFF techniques.
- Quantify the significance of colloidal material for trace metal transport within this system. Trace metals Mn, Zn, Fe, Cu, Cd, Ni, Pb were investigated.
- Investigate seasonal changes in the colloidal population and its implications for trace metal geochemistry.

4.2: Sampling, handling and analysis methods:

4.2.1: Sampling regime:

Surface water samples were collected during six surveys under the LOIS RACS project in the Trent/Humber system in 1996.

The surveys were designed to cover main seasonal changes in the estuary system. Although most of the surveys included a complete axial transect and salinity gradient from Gainsborough (river end-member in the Trent) to Spurn Head at the mouth of the Humber, several surveys included the tidal reaches, anomalous conditions or tidal cycle sampling approaches to give better insight into processes occurring under differing physical conditions. Where possible the same LOIS stations were sampled in consecutive surveys to give better inter survey comparability (see Trent/Humber stations Figures 4.2a and b).

The sampling surveys undertaken in 1996 were:

February 28 - Trent sampling-anomalous high flow conditions, entirely freshwater samples.

April 17 - Trent/Humber transect: salinity 0-14

July 29-30 - R.Trent tidal cycle at Derrythorpe Jetty: salinity 0 to 8

August 12-13 - Trent Humber transect: salinity 0 to 31

October 1-2 - Trent Humber transect: salinity 0 to 10, 20 to 30 (boat ran aground mid-transect).

December 16-17 - Trent Humber transect: salinity 0 to 32.

The location description and sampling dates for each site on the Trent and Humber are listed in Table 4.1.

Figure 4.2a: LOIS RACS Core programme Humber/Ouse station grid (Uncles pers.comm). Only transects covering stations 10 to 37 were sampled in this study.

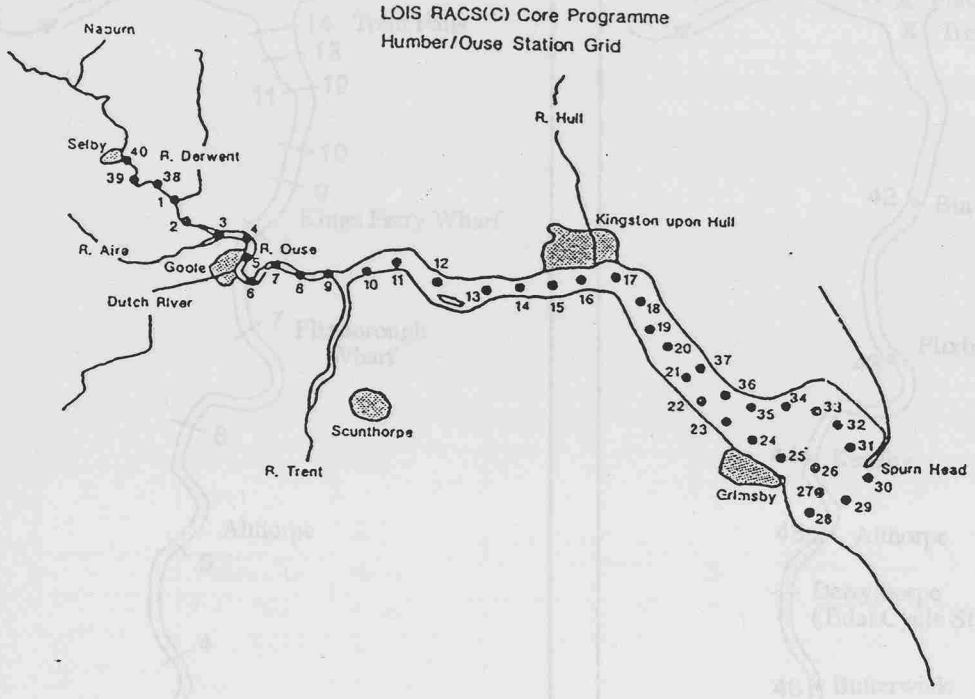

Figure 4.2b: LOIS RACS Core programme and February sampling sites on the Trent.

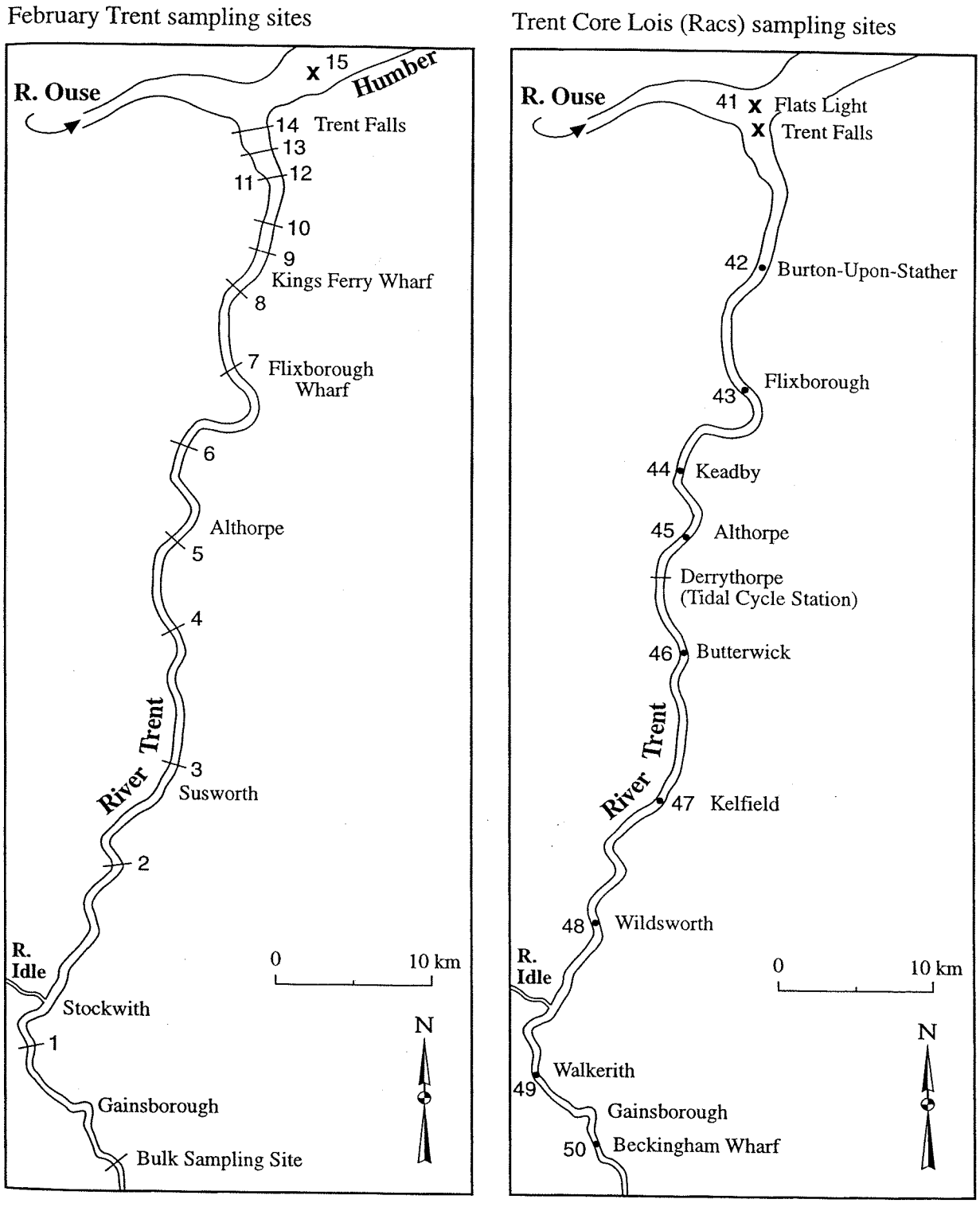

Table 4.1. Locations of Trent/Humber LOIS sampling stations sampled:

Station No.	Station name	River	February	April	August	October	December
50	Gainsborough	Trent		✓	✓	✓	
49	Walkerith	Trent	S. of E.Stockwith	✓			
48	Wildsworth	Trent	S. of E. Ferry	✓	✓	✓	
47	Kelfield	Trent	Susworth	✓			
46	Butterwick	Trent	S. of M180 Bridge	✓	✓	✓	
45	Althorpe	Trent	Althorpe Tower	✓			
44	Keadby	Trent	S.of Amcotts Hook	✓	✓	✓	✓
43	Flixborough	Trent	Flixborough Wharf	✓			✓
42	Burton Stather	Trent	S.of Waterton N. of Kings Ferry Wharf (EB) S. of Cliff End (EB) Cliff End (EB/MC) N.tip, Island Sand (EB)	✓	✓	✓	✓
41	Flats Light	Trent	Trent Falls	✓	✓	✓	✓
40	Cochranes, Selby	Ouse		✓			
10	Walker dyke	Humber	East Walker Dyke		✓		✓
11	Whitton Ness	Humber		✓			
12	Oyster Ness	Humber		✓	✓		✓
13	North Ferriby	Humber		✓			
14	Hessle	Humber		✓	✓		✓
15	Barton & Barrow	Humber		✓			
16	No.26A light	Humber-Hull			✓		✓
17	No. 24 light	Humber-Hull			✓	✓	✓
19	Paull Sands	Humber			✓	✓	✓
21	No.11 A S	Humber-SB			✓	✓	✓
22	No 10A	Humber-SB			✓	✓	✓
23	Diffuser-Burcom	Humber-SB			✓	✓	✓
24	Grinsby Rd.	Humber-SB			✓	✓	✓
25	No.4B S.shoal	Humber-SB			✓	✓	✓
27	Haile Chnl.	Humber-SB			✓	✓	✓
28	Haile Sand Fort	Humber-HM			✓	✓	✓
29	Bull Sand	Humber-HM			✓	✓	✓
30	Binks	Humber-HM			✓	✓	✓

NB: February samples taken from RIB , approximate positions in table and figure. July tidal cycle all taken at Derrythorpe Jetty.

4.2.2: Sampling and analysis protocol:

Litre samples were collected using a polyethylene pole-sampler directly into sample prerinsed, acid cleaned (see section 2.2.1 for protocol) low density polyethylene (LDPE) bottles using clean handling techniques (see Sections 2.2.2 and 2.2.3). Samples were stored cold and dark to minimise any colloidal or trace metal concentration changes (see artifacts discussion section 2.1). Due to the high suspended load often encountered in the Humber estuarine system samples were quick decanted (after Chen and Buffle, 1996a and b) prior to prefiltration through (1 to 4) acid cleaned 47mm, 0.4μm polycarbonate filter membranes (see section 2.2.1 and Appendix 1 for cleaning protocol). This would help minimise secondary filtration effects such as pore clogging that would lead to removal of the colloidal material that existed in the original sample. The colloidal samples were processed immediately through a Millipore Minitan system with 10,000MW cut-off polysulphone plates (see Appendix 1 for cleaning and protocol for sample filtration).

All sample processing was completed within 24hrs of sample collection. Samples were acidified immediately with SBD HNO3 (1ml/L) and stored until extraction by a APDC-DDDC/chloroform solvent extraction technique (see Section 2.3). Concentrations of total dissolved trace metals (Fe, Cu, Mn, Zn, Pb, Cd and Ni) in each fraction were measured by graphite furnace atomic adsorption spectrophotometry (GFAAS) or flame AAS-see Section 2.3.2. These trace metals were chosen for their contrasting geochemistry which would give a good insight into the physicochemical processes affecting their partitioning in the Trent and Humber. Milli-Q and natural sample blanks (cross-flow refiltration of truly dissolved fractions as described in section 5.3.1 for the Minitan system and Appendix 4 for the laminar flow block) were taken at each survey for all filtration steps and sample manipulation processes.

The size fractions determined for each trace metal were;

Total dissolved (<0.4μm including colloidal and truly dissolved species),
Colloidal (10,000MW to 0.4μm),
Truly dissolved (< 10,000MW).

The colloidal fractions were determined in two ways;

- Colloidal concentration (nmol/L) was determined by the difference between total dissolved and truly dissolved fractions (**Coll.diff**).
- Colloidal concentration was determined by analysis of the retentate fraction (colloidal fraction that does not pass through the 10,000MW filter plate) after cross flow filtration of the complete prefiltered sample (**Coll.calc**).

Sample and filter membrane interaction (especially for coll.calc.) was monitored using a mass balance recovery technique as described in section 1.10.2.b.

In conjunction with these survey samples, bulk (unfiltered) samples were taken at Gainsborough, Hessle (mid-salinity site under the Humber bridge) and Spurn Head to assess changes in bulk and colloidal trace metal concentrations over the timescales samples were stored prior to prefiltration (0.4μm) and CFF. Effects of prefiltration protocol was also assessed with respect to filtration artefacts affecting trace metal concentrations.

Background physical (salinity, SPM/turbidity, DO, temperature, water depth) and chemical (pH, nutrients, chlorophyll/fluorescence) data was also collected in conjunction with the main samples. This data was either provided by samples taken adjacent to, and using a similar method to the pole sampler or by the Environment Agency Qubit underway data which was logged continuously during the survey. Due to the heterogeneity of the estuarine system it is unlikely that either method provided an exact replicate of the conditions in the trace metal sample taken (except April survey where samples were split) but due to the time and sample volume constraints of colloidal ultrafiltration it was not possible to take duplicate samples/or split samples for master variable analysis. Both sources of background data were assumed to be as close to the trace metal sample for purposes of inter estuarine trend and seasonal data analysis.

4.2.3: Bulk/colloidal storage and prefiltration artifact investigations:

4.2.2.1: Bulk and colloidal storage:

As discussed in previous sections is has been well documented that natural colloidal samples are inherently unstable once removed form the open estuarine system and almost immediately changes in particle size distributions (Filella and Buffle, 1993) and associated trace metals (Chen and Buffle, 1996a and b) will occur. In the six surveys carried out in the Trent/Humber system, although all sample manipulations were carried out within 24hrs of collection it is possible that for some metals and colloidal material, significant changes did occur. To check the magnitude and rate of these changes, large volume samples were collected at stations representative of the complete sample spectrum encountered in the surveys (Gainsborough, Hessle and Spurn Head) and stored. Samples were stored in two ways; as bulk samples that were stored as complete samples and were not prefiltered until removed from the main sample (just as the survey samples) or as colloidal samples that were stored in a large volume after 0.4μm prefiltration. The bulk sample was stored unfiltered to monitor prefiltration changes whilst the sample stored after 0.4μm prefiltration was designed to monitor the stability of the colloidal population and trace metal partitioning in samples once prefiltration had been completed. Litre aliquots were removed from the large volume bulk or colloidal samples at intervals 0 to 30 hours after collection. The samples were fractionated, acidified and analysed using the same protocol as for the survey samples.

4.2.2.2: Investigation of prefiltration artifacts:

As discussed in the Chapter 1 there is great debate on the effect that prefiltration treatment of a sample has on the eventual trace metal concentration (total dissolved, colloidal or truly dissolved) that is determined (Horowitz et al., 1992; Taylor and Shiller, 1995; Horowitz et al., 1996a and b). Despite decanting all samples it is likely there is some modification of the litre sample required for CFF during 0.4μm prefiltration. To investigate this, several litre aliquots from the same decanted bulk sample were prefiltered using 1, 3 or 4, 0.4μm filters prior to immediate CFF. The same three trace metal fractions were collected, acidified and analysed as for the other survey samples.

4.3: Trace metal extraction results

4.3.1: Extraction efficiency of the chelation-solvent extraction technique.

Prior to any sample extraction the complete LMSW standards and two CRM's (Certified Reference Materials), CASS-2; coastal seawater reference material and SLEW; estuarine water, both supplied by the National Research Council of Canada, NRCC, were extracted to check that the chloroform solvent would give as good recoveries as the freon method. There was good extraction efficiency for most metals (see Appendix 1 of data disc for plots) apart from Fe and Pb. Above 200μg/l standard concentration the Fe recovery was less than 80% and decreased further with increasing concentrations. Although further repeat chloroform extractions would improve the Fe recovery, due to the excessive volume of chloroform required to stip out all Fe, it was decided to analyse the high Fe concentration samples directly on the flame AAS without extraction, using the LMSW standards for calibration. Only the truly dissolved (F) Fe fractions were extracted and run on the GFAAS. The concentrations of these fractions were low enough to lie in the >90% recovery range.

Pb extraction efficiency was also reduced at higher standard concentrations (>0.4μg/l) as discussed in the extraction section (2.3.1.5) this was attributed to association of the Pb complex with the Fe precipitates at high Fe concentrations. Extra solvent extraction steps to remove the Fe precipitates into the extract also improved the Pb recovery to above 90%. In previous works trace metal concentrations have been adjusted to allow for incomplete recoveries of trace metal standards or CRM's. This has not been done in this study due to the non-linear nature of the extracted LMSW standard calibrations with high and increasing metal concentrations, this seems to be a feature of the chloroform solvent. It has also been suggested (Mackey et al. 1997) that there may be interference effects that cause low extraction efficiencies in natural samples that contain colloidal material (even CRM's). Factors such as high concentrations of colloidal SPM, dissolved organic matter and particulate iron were indicated as causing the low extraction efficiencies seen by Mackey et al. (1997) although they had no direct evidence. These species are prominent in the samples collected from the Trent/Humber system (especially in the concentrated retentate fractions) so the same interferences are likely to apply to varying degrees in axial transect samples. As

it is not possible to quantify their effect in each sample and these interferences are not directly represented in the LMSW samples which were comparatively colloid and DOM free and spiked with truly dissolved metal standards, the adjustment of the sample concentrations using the LMSW recoveries does not seem comparable. Although the CRM's used here (CASS-2 and SLEW) are an improved representation of the extracted survey samples they will not cover the full extreme of the potential interference effects up towards the river end-member. As the extracted sample concentrations will not be adjusted and due to extraction interferences, the concentrations determined are likely to be a minimum representation of the actual concentration. The LMSW standards and CRM's in conjunction will provide the best estimate of the actual sample recovery as well as the assessment of the precision and accuracy of the technique.

4.3.2: Assessment of solvent extraction and analysis data:

GFAAS and flame AAS absorption peak plots were used to calculate the total dissolved trace metal in each sample. Each sample was analysed in duplicate or triplicate and the mean concentration (nmol/L) and standard deviation of the sample was calculated using GFAAS/flame AAS response to calibration standards. The final concentration of the sample was normalised for blanks (procedural (including chloroform) and UV digestion).

The combined mean blanks (procedural, chloroform and UV digest), precision and detection limit were determined for each of the trace metals for the technique as a whole and in each batch of solvent extraction (see Table 4.2 and Appendix 3 of data disc). Precision was estimated by replicate analysis of CRM's (CASS-2 and SLEW) in triplicate for each extraction batch and also by interbatch analysis of LMSW standards that were analysed as samples. The detection limit of the technique for each metal was calculated as three times the standard deviation (3σ) of the mean blank value. Extraction of the LMSW standards also indicated the extraction efficiency (recovery) of the technique and each batch (see Appendix 3 of data disc). A comparison of the extracted CRM concentrations to their certified values gave a good indication of the accuracy of the extraction technique as a whole and also of each batch.

Table 4.2: Data quality assessment Blank (procedural, chloroform, digestion), detection limit, recoveries, accuracy and precision from CRM's and GFAAS internal standard (1643d).

	Procedure blank (nmol/L)	Chloroform blank (nmol/L)	UV digest blank (nmol/L)	Detection limit (nmol/L)	Average Recovery (%)	CASS-2 certified value (nmol/L)	Extracted CASS-2 value (nmol/L)	SLEW certified value (nmol/L)	Extracted SLEW value (nmol/L)	1643-d certified value (nmol/L)	GFAAS 1643-d value (nmol/L)
Metal											
Fe	1.9	0.35 ± 0.059	21.1 ± 11.1	2.5	100.6 ± 10.0	22.56 ± 3.04	24.8 ± 2.5	42.44 ± 6.63	39.4 ± 2.2	1629.5 ± 69.8	1623. 9 ± 56.5
Cu	0.64	0.39 ± 0.69	4.2 ± 2.8	0.58	101.2 ± 5.9	8.14 ± 0.98	9.5 ± 0.68	25.49 ± 1.73	23.7 ± 0.68	322.6 ± 59.8	349.6 ± 11.0
Mn	0.13	0.043 ± 0.06	1.7 ± 1.4	0.33	96.1 ± 8.4	45.69 ± 6.55	45.2 ± 12.6	311.3 ± 20.0	267.8 ± 48.9	686.2 ± 14.6	738.1 ± 91.5
Zn	0.24	0.13 ± 0.069	3.3 ± 1.9	0.46	96.2 ± 7.8	18.96 ± 3.82	20.9 ± 1.7	16.82 ± 2.14	16.3 ± 1.7	1108.4 ± 9.9	1107.0 ± 49.3
Pb	0.033	0.0075 ± 0.008	0.34 ± 0.60	0.16	117.0 ± 30.8	0.058 ± 0.019	0.067 ± 0.024	0.130 ± 0.024	0.12 ± 0.031	87.6 ± 3.1	91.1 ± 8.0
Cd	0.0056	0.0052 ± 0.0023	0.075 ± 0.073	0.013	78.8 ± 15.2	0.267 ± 0.044	0.27 ± 0.086	0.169 ± 0.018	0.14 ± 0.063	57.6 ± 3.3	62.9 ± 9.2
Ni	0.69	0.32 ± 0.17	5.5 ± 7.0	1.1	99.8 ± 6.5	6.58 ± 1.06	7.2 ± 0.74	12.10 ± 0.852	11.8 ± 0.6	989.9 ± 46.0	1046.0 ± 6.5

As can be seen from the data quality assessment table the mean recoveries of extracted LMSW standards indicate a good extraction efficiency for Fe, Cu, Mn, Zn, and Ni (>95%)although there may be a tendency for recovery and precision to decrease at higher standard concentrations. However, there seems elevated and low extracted values for Pb (117.0 ± 30.8 %) and Cd (78.8 ± 15.2 %) samples respectively. Low recoveries for Cd (~73%) with chloroform have also been reported by Tappin (Pers. comm.). As the more detailed individual extraction batch information illustrates (Appendix 3 of the data disc) the Pb recovery is good for some batches but high for lower LMSW standard concentrations and particularly extraction 1 (April storage samples). Cd recovery appears consistently low however and increases with trace metal concentration. Low Cd recovery could be caused by pH less than 6 (Statham, 1985) but post extraction pH checks did not show any problem here. It is possible that colloidal Cd may have not been complexed easily by the dithiocarbamate complexant which is also colloidal (N.Morley pers. comm.).

This apparent poor recovery for Pb and Cd is offset by the acceptable accuracy and precision of the CRM extractions for the same metals. This may be purely a limit of the chloroform technique towards higher concentrations but clearly the matrix of the sample is important here. Milli-Q test standards previously extracted gave good recoveries for Pb and Cd, whilst LMSW standards and CRM's can give inconsistent extraction qualities. For the other metals, extraction of the CRM's gave precision and accuracy that were consistent with certified values. The main exception was Mn where mean extracted SLEW values were significantly lower than the certified, and the precision was also compromised. The detailed batch plots (Appendix 3 of the data disc) indicate that this is largely due to lower concentrations extracted in batches 1 to 4. They also indicate that generally the inter and intra batch precision is good for all the metals.

When compared to results from this laboratory using the Freon-TF extraction method (Althaus, 1992; Fang, 1995) the analytical blanks and detection limits fall into similar ranges for all metals apart from Pb and Ni where the Ni blank, and Pb and Ni detection limits are approximately an order of magnitude higher. When compared to studies using chloroform as a solvent (Bruland et al., 1979; Bruland and Franks, 1983) is

seems that the detection limit for Ni is also significantly higher. However, neither the blanks or detection limits for all metals proved a problem when compared to the trace metal concentrations encountered in the estuarine samples.

It is vital that data quality is assessed at this level of detail (i.e. per extraction batch) which average quality assessments will disguise. Clearly some extraction runs are not as good, for methodological (problems with extraction i.e. interference effects, low pH) or analytical (poor GFAAS detection, calibration) reasons. These problems may also be metal specific within an extraction run. For example: Cd concentrations in extractions 6 and 7 look low and elevated respectively for extraction and analytical reasons. Samples affected in this way must be identified and assessed accordingly during data interpretation. It is assumed that data quality and matrices of extracted standards are analogous to samples. However, given the discrepancy between CRM and LMSW standard recovery/ accuracy/ precision for the same metal clearly more complicated matrix or interference effects (Mackey et al., 1997) can affect the effectiveness of the chloroform solvent extraction.

However, despite the reservations with the extraction technique discussed above, the overall recovery of CRM's and LMSW standards for all the metals is >95% (apart from poorer recoveries for Cd and Pb) and other indicators of extraction and analytical data quality are very good. Because of this, confidence in sample extraction and analysis is high.

4.4: Trace metal Trent/Humber results

4.4.1: Background data:

Background data (temperature, pH, dissolved oxygen (DO), turbidity, chlorophyll-a/ fluorescence, nutrients) axial plots for the six surveys in 1996 taken from underway sampling on the Seavigil or discrete samples are displayed in Figures 4.3a to c. Plots for the same variables with time for the July tidal cycle and February survey are found in Appendix 3 of the data disc.

Temperature (Figure 4.3a) varies substantially with season and also within the estuary during the summer months. The temperature transect is largely produced by mixing of the freshwater and saline end-members and this varies with seasonal changes in the temperatures of the River Trent and seawater end-members.

The pH (Figure 4.3a) transect characteristics are less changeable. The seawater pH of ~8.0 remains unchanged throughout the six surveys whereas the Trent river water input pH ranges from 7.6 to 8.2. There is a pH minimum of 7.3 to 7.4 at salinity 5 to 10 which appears in all the transects. This may be some effect of the turbidity maximum. In several transects pH, temperature and DO separate into two discrete plots indicating measurement of two separate surface water masses.

The transmission (Figure 4.3b) transects indicate that the turbidity maximum lies mainly between 3 and 15 psu in the estuary and is closely linked to other variables, mainly DO, pH and chlorophyll-a. Turbidity is reduced at low and high salinities due to low SPM in the Trent compared to estuarine samples and due to destabilisation, flocculation and sedimentation of particulate material within the turbidity maximum zone which removes SPM from the water column at high salinities. The saturation of transmission does not always allow comparison of transmission minima but the comparative changes in transmission between seasonal transects can indicate associated changes in turbidity, i.e. the August survey displays lower transmission (higher turbidity) and the saturation of transmission covers a larger salinity range. The December survey has overall higher transmissions indicating lower turbidity, even within the turbidity maximum region.

Figure 4.3a: Seasonal axial transects of temperature (black) and pH (red) in the Trent/Humber

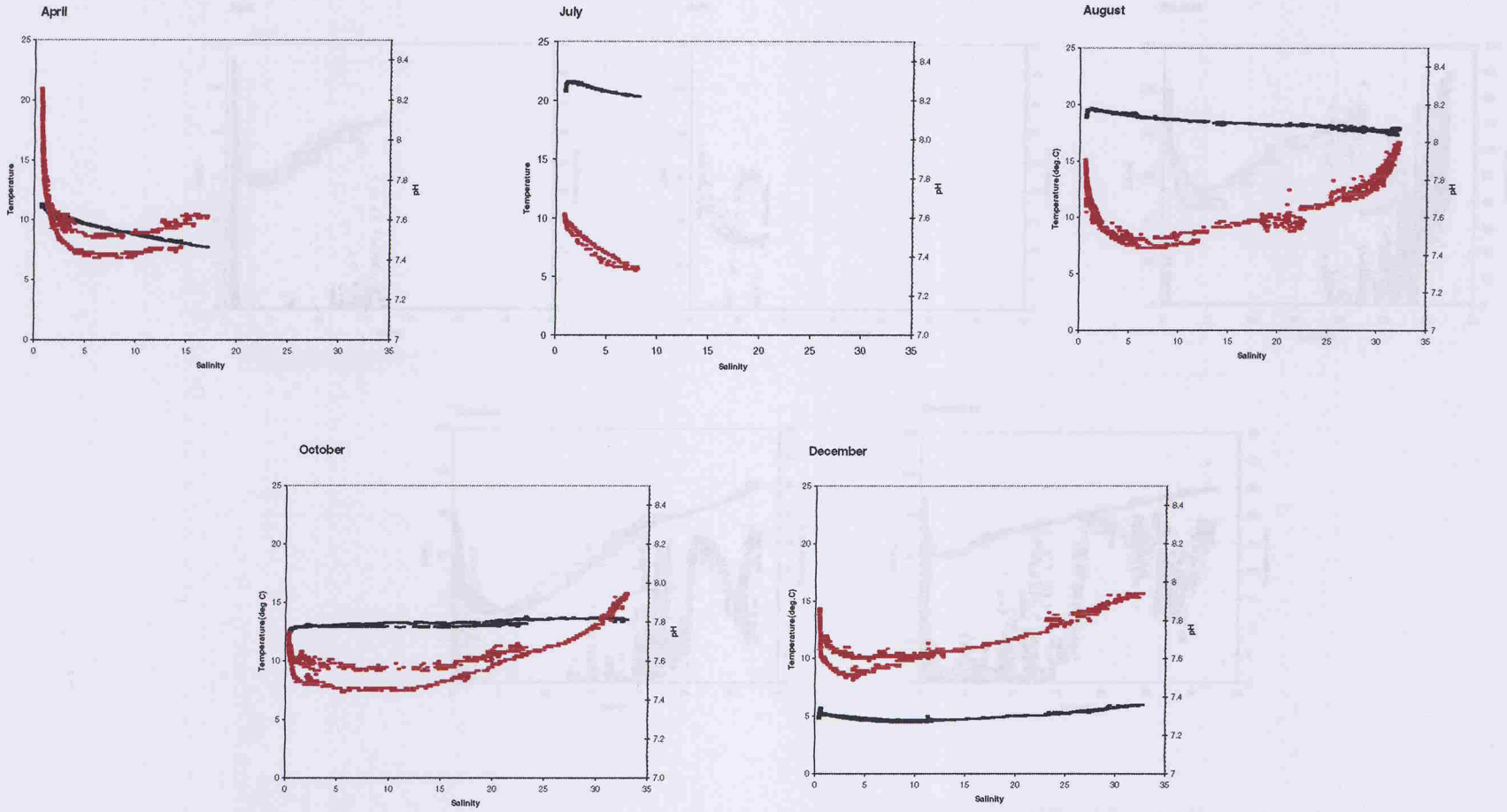

Figure 4.3b: Dissolved oxygen (%) -red , and turbidity (transmission) -brown, for seasonal axial transects of the Trent/Humber

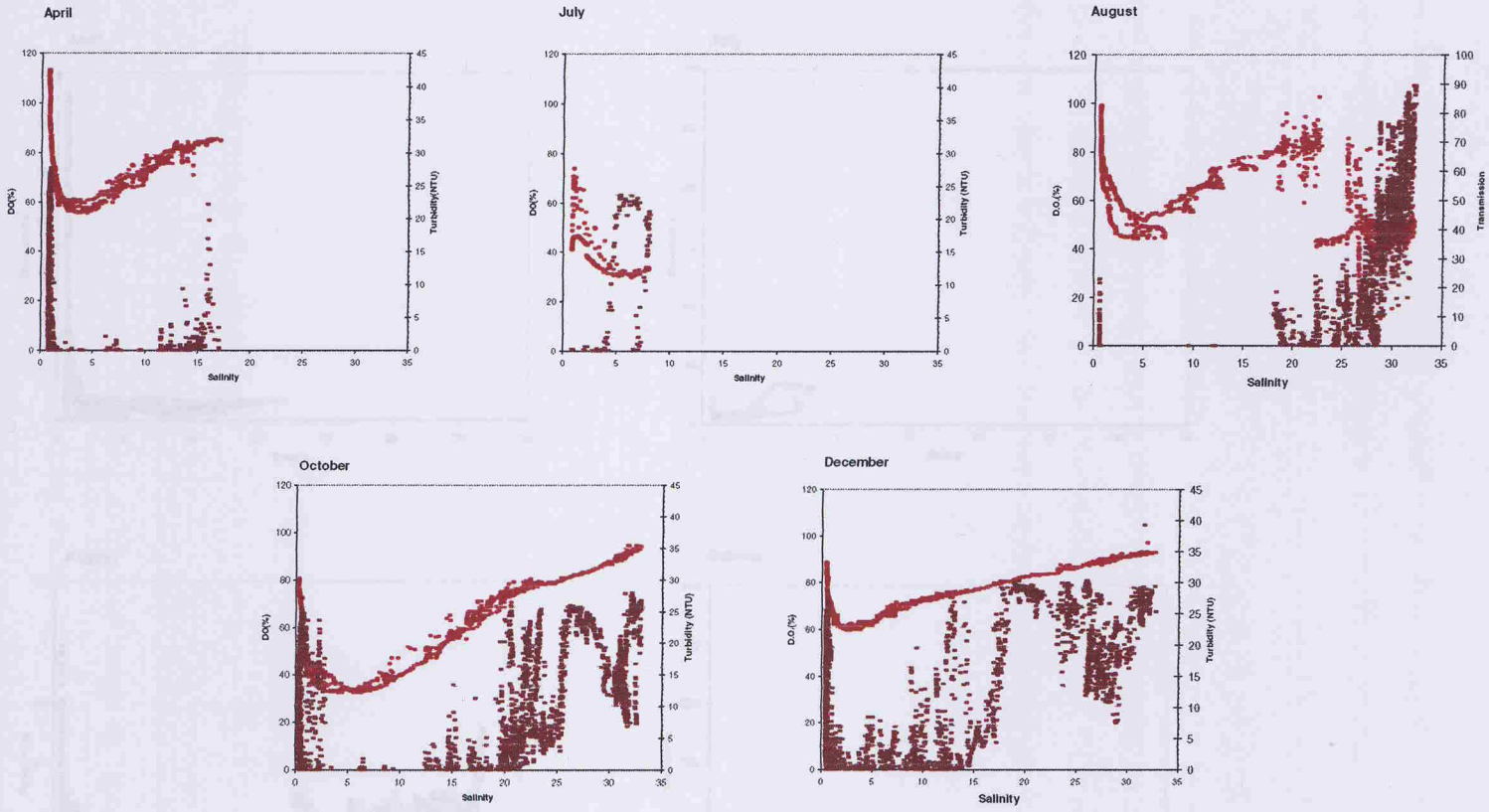

Figure 4.3c: Chlorophyll concentrations in seasonal axial transects of the Trent/Humber

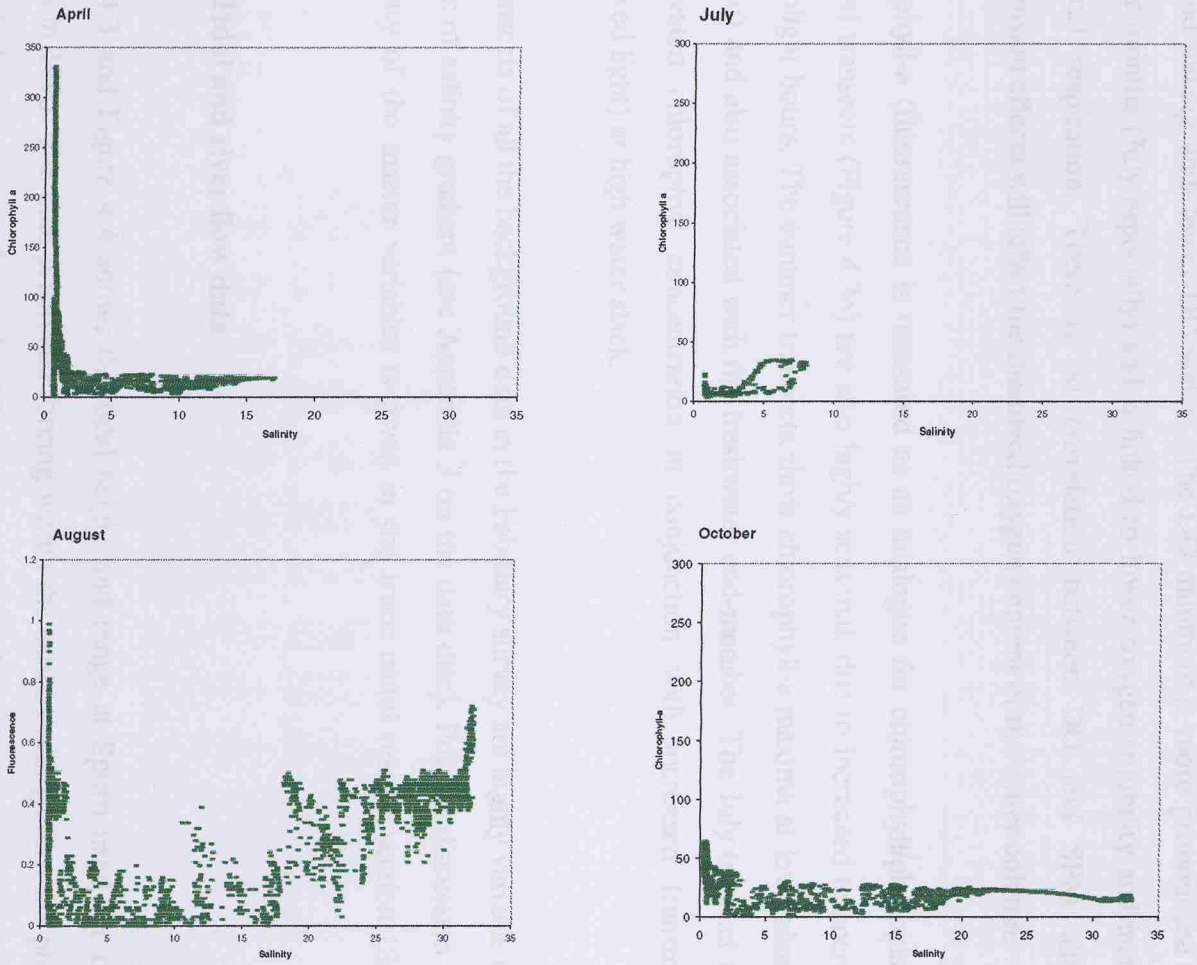

The peak in transmission in the July transect results from a period of slack water at high tide which allows settling of suspended particulate material.

All the dissolved oxygen transects (Figure 4.3b) show a rapid decrease at low salinities to a minimum (40 to 60%) at 3 to 10 psu. This profile is produced by more oxygenated river water being altered once it enters the main estuary. This could be via consumption within the water column/turbidity maximum (biological or chemical oxygen demand) or input and mixing with lower DO water. The DO minimum is more pronounced in the summer months (July especially) and is linked to lower oxygen solubility and increased biological respiration. There is no correlation between DO and SPM although resuspension effects will affect the dissolved oxygen content of the water column.

Chlorophyll-a (fluorescence is measured as an analogue for chlorophyll/phytoplankton biomass) transects (Figure 4.3c) are also highly seasonal, due to increased temperatures and sunlight hours. The summer transects show chlorophyll-a maxima at low salinites (3 to 8 psu) and also associated with the freshwater end-member. The July transect shows an elevated chlorophyll concentration in conjunction with increased transmission (improved light) at high water slack.

The transects of all the background data in the February survey are highly variable due to the lack of salinity gradient (see Appendix 3 on the data disc). Further discussion of the sesonality of the master variables is given in the trace metal results section (Section 4.4.8).

4.4.2: Tidal and river flow data

Table 4.3 and Figure 4.4 shows the tidal height and range at Spurn head for the six surveys in 1996. The tidal prism and forcing within the estuary will govern the physico-chemical characteristics of the Humber estuary and tidal reaches as it will affect the position of the turbidity maximum zone, resuspension events and mixing regime of water masses within the estuary. This will all determine the distribution and partitioning of trace metals.

Table 4.3: Tidal ranges at Spurn Head for Trent/Humber survey dates (high and low tidal heights and ranges are quoted over the relevant timescale (24 to 48hrs) of the surveys).

Date	High water heights (m)	High water times (GMT/BST)	Low water heights (m)	Low water times (GMT/BST)	Tidal range (m)	Tidal cycle stage
28 February	5.3/5.4	00:33/13:01	3.0/2.9	06:18/19:08	2.3/2.5	Neap
17 April	6.8/7.0	05:05/17:04	1.1/0.8	11:04/23:30	5.7/6.2	Spring
29 July	6.6/6.8	04:04/16:41	1.4/1.3	10:29/22:51	5.2/5.5	Neap to spring
30 July	7.0/7.1	04:52/17:31	0.9/1.0	11:22/23:39	6.1/6.1	Neap to spring
12 August	6.2/6.1	04:08/16:41	1.9/2.0	10:36/22:44	4.3/4.1	Neap to spring
13 August	6.4/6.3	04:46/17:15	1.6/1.8	11:15/23:21	4.8/4.5	Neap to spring
1 October	7.5/7.0	07:29/20:04	0.9/0.7	01:30/14:01	6.6/6.3	Spring
2 October	7.2/6.7	08:13/20:47	1.1/1.1	02:11/14:41	6.1/5.6	Spring
16 December	6.4/6.6	09:42/21:43	1.5/2.0	03:25/15:40	4.9/4.6	Spring to neap
17 December	6.2/6.4	10:45/22:48	1.7/2.3	04:25/16:41	4.5/4.1	Spring to neap

Figure 4.4: Plot of tidal range for each Trent/Humber survey in 1996.

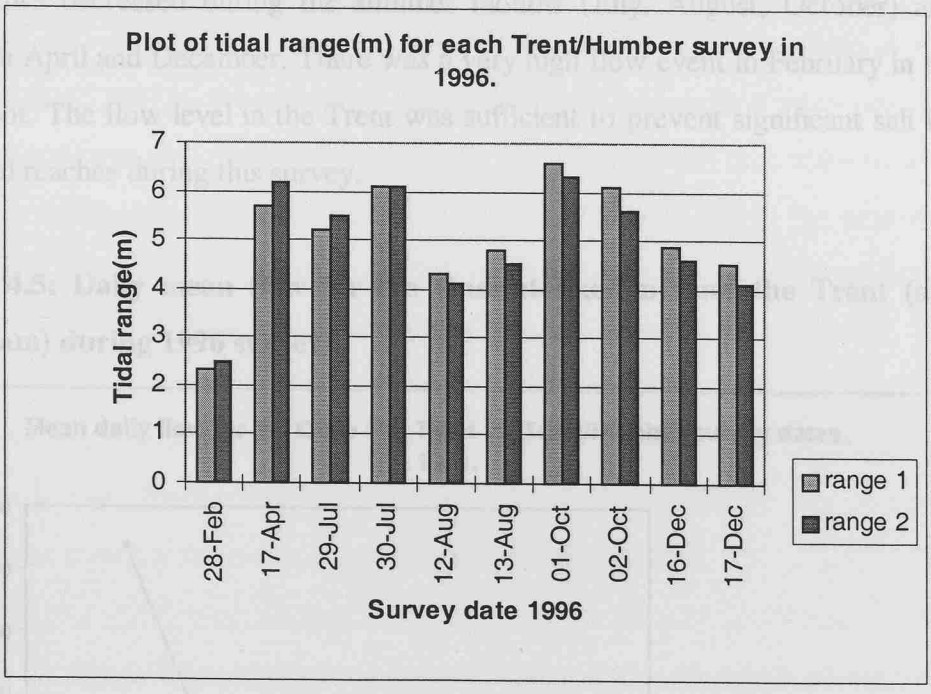

Table 4.4 and Figure 4.5 illustrate the daily mean flows for the Trent at North Muskham and the Ouse at Skelton. The inputs and mixing ratios of these two end-members will greatly affect the distribution of trace metals below Trent Falls, the extent of saline influence and therefore the position of the turbidity maximum zone.

Table 4.4: Daily mean flow data for the Trent (North Muskham) and Ouse (Skelton) during Trent/Humber surveys in 1996.

Survey date(1996)	Ouse (Skelton) Mean daily flow(m^3/s)	Trent (North Muskham) Mean daily flow(m^3/s)
28 February	50.42	107.4
17 April	14.88	43.34
29 July	6.648	35.32
30 July	11.01	35.47
12 August	12.9	43.44
13 August	9.586	33.0
1 October	32.0	30.88
2 October	18.31	27.42
16 December	27.14	41.66
17 December	28.11	40.95

It is possible to see that the Trent is the major input of freshwater into the Humber system. The daily mean flow for the Trent is usually 50% higher than that of the Ouse (except the October survey where the Ouse flow was anomalously high). Overall the river flows decreased during the summer months (July, August, October) and were higher in April and December. There was a very high flow event in February in the Ouse and Trent. The flow level in the Trent was sufficient to prevent significant salt intrusion into tidal reaches during this survey.

Figure 4.5: Daily mean flow for the Ouse(at Skelton) and the Trent (at North Muskham) during 1996 surveys.

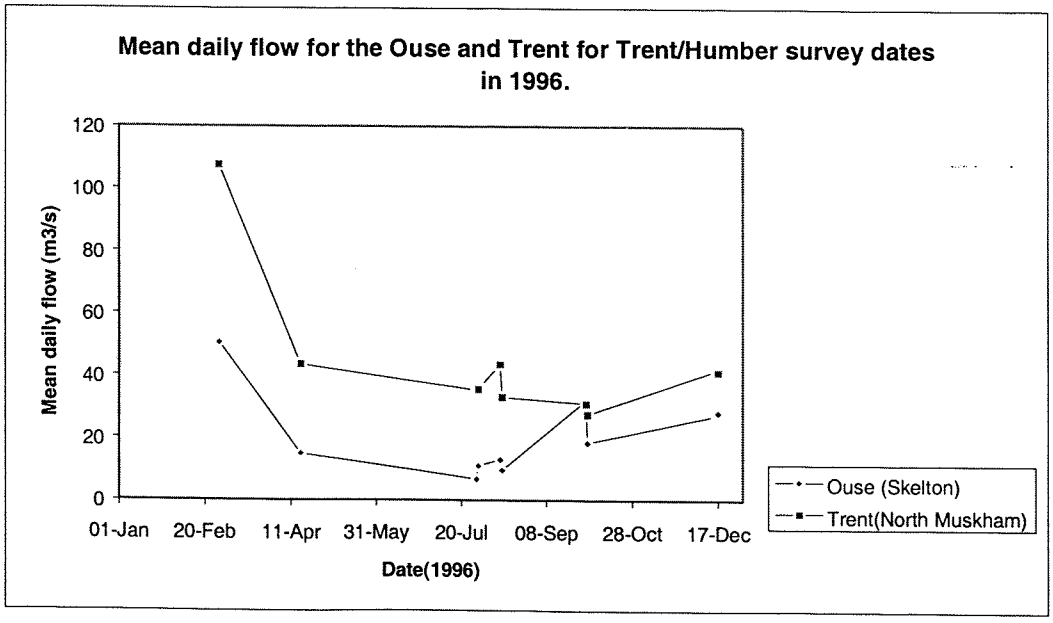

4.4.3: Minitan filtrate blanks

Filtrate (<10,000MW, truly dissolved) samples from Hessle and Gainsborough were refiltered using the Minitan system to assess metal contamination from the system under natural ionic strengths and pH. Table 4.5 and Appendix 3 of the data disc contain data for the effect of refiltration on the trace metal concentrations.

For Fe, Cu, Mn, Zn and Pb there is an apparent decrease (removal) of trace metal from the filtrate upon blank filtration (mainly for the Hessle samples). This would indicate a removal of trace metal onto the cross-flow system (plates, tubing etc.). However, in conjunction with this removal there is an increase in the retentate concentration and calculated colloidal fraction.

This would not occur if the metal removed from the filtrate sample was retained in the system because the sample theoretically only contains truly dissolved trace metal species. In reality, it is possible that colloidal material of less than 10 KDa (Wen et al., 1996; Buessler et al., 1996) is present in the filtrate sample so aggregation processes that occur during sample manipulation and concentration can allow further separation to occur. The decrease observed in the refiltrate concentration is therefore due to the removal of this aggregated material. The extent of the metal removal will be dependant on the partitioning of each trace metal into this lower molecular weight fraction. This may explain why the metals with high colloidal fractions as seen in this study are not necessarily the metals most affected by refiltration (Cu and Zn here although Fe is most consistent). The Hessle samples are more consistently affected by this process as the higher ionic strength will enhance aggregation of small colloids.

Cd and Ni which have lower colloidal signatures show no effect or an increase in concentration in the refiltrate. This is attributed to lower molecular weight aggregate break-up rather than some sort of contamination effect. There is an increase in the retentate fraction for Ni (and Cd at Gainsborough where the colloidal fraction is significant) indicating some sort of separation and retention of colloidal material despite the filtrate being unaffected.

Table 4.5: Refiltrate blank trace metal concentrations (nmol/L).

	SAMPLE	Fe nmol/L	Fe 1σ	Cu nmol/L	Cu 1σ	Mn nmol/L	Mn 1σ	Zn nmol/L	Zn 1σ	Pb nmol/L	Pb 1σ	Cd nmol/L	Cd 1σ	Ni nmol/L	Ni 1σ
FILTRATE	Hessle a	28.7	0.2	143.4	1.6	66.3	0	245.1	2.3	5.39	0	1.26	0.017	129.1	6.15
	Hessle b	20.9	1.7	121.3	0.7	61.0	2.0	247.0	2.5	4.74	0.04	1.15	0.022	146.5	6.15
	Gainsbor' a	13.6	1.4	108.6	0.9	60.3	1.2	290.2	0.8	3.14	0	1.07	0.017	373.0	3.38
	Gainsbor' b	9.50	0	107.5	0.7	59.9	0.1	271.6	5.1	3.23	0.04	1.14	0.017	374.6	1.13
RETENTATE															
	Hessle a	101.8	5.5	114.7	1.5	84.2	1.1	265.6	5.1	7.24	0.48	1.28	0.004	156.5	2.25
	Hessle b	309.3	0.2	132.0	6.0	64.2	0	275.6	0	19.1	0.32	1.16	0.021	169.3	2.25
	Gainsbor' a	116.1	4.3	118.8	1.5	74.6	1.1	326.8	4.5	4.27	0.32	1.18	0.017	404.6	6.15
	Gainsbor' b	278.1	3.4	153.9	0.4	123.5	2.3	379.6	2.3	6.96	1.59	1.42	0	466.9	0
COLLOIDAL CALC.															
	Hessle a	44.9		-17.6		11.0		12.6		1.14		0.009		16.87	
	Hessle b	216.4		8.01		2.4		21.4		10.8		0.009		17.15	
	Gainsbor' a	71.8		7.14		10.0		25.6		0.79		0.078		22.11	
	Gainsbor' b	134.3		23.2		31.8		54.0		1.87		0.139		46.17	

4.4.4 Results of storage change experiments:

The storage plots for various samples [bulk (unfiltered) or colloidal (<0.4μm) collected at Gainsborough, Hessle and Spurn] and sample fractions are contained in Appendix 3 of the data disc.

Iron:

Significant changes in the dissolved and colloidal Fe concentration occur after a relatively short period after sample collection. The decrease in measured colloidal and total dissolved fractions indicates some sort of sedimentation effect. More rapid changes are seen in Gainsborough and Hessle samples than in those from Spurn. This is probably a result of the higher colloidal loading in the upper estuary and river so there is still a significant colloidal population present for aggregation and sedimentation.

There is no change in the truly dissolved Fe which indicates the loss in colloidal Fe is by sedimentation and not disaggregation or desorption. There is no obvious difference in the rates of change between the bulk and colloidal samples. This is probably linked to nearly 100% of dissolved Fe being colloidal.

The rate of Fe removal by colloidal aggregation is greatest for the Gainsborough sample. The decrease in total dissolved/colloidal Fe concentration at Gainsborough is 3000 to 4000nM over 20hrs storage. This removal rate is 1500nM and 500nM per 20 hours at Hessle and Spurn respectively. The slower changes at Spurn can be linked to the reduced levels of colloidal material. However, it would be expected that with increased salinity and colloidal loading at Hessle, aggregation and colloidal removal processes would be greater than at Gainsborough. It is possible that a different mechanism (perhaps organic polymer bridging) is acting at Gainsborough to enhance aggregation and sedimentation despite lower colloidal destabilisation. Discrepancies between bulk and colloidal Fe concentrations may be due to sample handling problems i.e. generation of colloidal material during prefiltration (Tappin pers. comm.).

Copper:

Overall, there is very little change in Cu concentration or partitioning during sample storage. The exception is the bulk sample at Gainsborough where there is a rapid

decrease in total and colloidal Cu within the first few hours. There is no detectable repartitioning into the truly dissolved phase so this looks like some aggregation and sedimentation effect. There are no changes observed in the colloidal sample which indicates a scavenging effect of colloids by larger particles only present in the bulk sample (perhaps organic polymers). This scavenging acts to remove colloidal Cu from the bulk sample. There is some indication of an initial repartitioning of truly dissolved Cu into the colloidal phase in the Spurn samples. From these samples it is possible to see the seasonal and inter-estuarine changes in Cu fraction percentages.

Manganese:

In the Gainsborough samples Mn is often >90% colloidal (except for the February survey). This decreases further down the estuary. The Gainsborough samples undergo changes in Mn concentration by sedimentation effects. There is no repartitioning into the truly dissolved phase. The removal of colloidal Mn is increased in the bulk samples probably due to scavenging by larger particles. In the February samples (Gainsborough) there is lower colloidal Mn (~40%) and there is transformation of colloidal Mn to the truly dissolved phase during sample storage.

In the Spurn samples there is a repartitioning of truly dissolved Mn into colloidal material, by precipitation or adsorption effects.

Zinc:

In the bulk stored samples at Gainsborough and Hessle colloidal Zn is removed by sedimentation effects (probably by scavenging by larger particles). This process is more rapid in the Gainsborough samples due to higher colloid and particle loadings. In the stored colloidal and Spurn samples there is no colloidal removal and significant repartitioning of truly dissolved Zn into the colloidal phase (adsorption).

Lead:

Like Fe, Pb is highly colloidal. Gainsborough and Hessle bulk and colloidal samples all show total dissolved Pb concentration decreases by colloidal removal. There is little repartitioning into the truly dissolved phase so colloidal removal by aggregation and sedimentation is indicated. The rate of colloid removal is enhanced in the bulk samples

(especially the October Gainsborough sample) where larger particles may act to scavenge colloidal Pb.

In the Spurn samples the Pb concentrations are much lower. Colloidal removal is seen in the colloidal sample and increased colloidal concentrations occur with storage in the bulk sample. There is no simultaneous decrease in truly dissolved Pb which indicates colloidal Pb generation from disaggregation of larger particulate flocs.

Cadmium:

Cd concentrations were least affected by storage changes. In the Hessle and Spurn samples Cd is highly partitioned (>90%) into the truly dissolved fraction. In these colloidal and bulk samples the changes in concentration and partitioning were largely undetectable. Storage changes in Cd occurred in the bulk Gainsborough samples where there was significant colloidal Cd (20-40%) and these particles were scavenged out by larger particles present. Cd concentration changes in stored colloidal samples were not detectable.

Nickel:

There is very little change in Ni partitioning in any of the stored samples. Total dissolved Ni (colloidal and truly dissolved fractions) is removed in bulk Gainsborough samples, probably by scavenging of colloidal and truly dissolved Ni by large particles (the colloidal samples shows little storage changes). The Spurn samples are in opposition, illustrating both Ni desorption and adsorption from/to colloidal material. Only in the colloidal Spurn sample are the changes comprehensive with colloidal Ni being reduced to below detection and truly dissolved Ni increasing.

Summary:

Almost all the metals are affected to some degree by storage but this is small in comparison to the overall fractional trace metal concentrations and partitioning changes within the estuary. Most of the concentration changes involve particulate processes such as aggregation, sedimentation and scavenging. As a result it is the particle reactive and highly colloidal elements (Fe, Pb) that are most affected. The bulk (unfiltered) samples also show greater and more rapid changes due to the presence of additional particulate

material. Mn, Cu and Zn are less affected by storage changes. There is little detectable change in Cd concentrations or partitioning during storage and Ni illustrates inconsistent changes.

Any changes that do occur are more pronounced in the Gainsborough and Hessle samples, probably because of the higher colloidal (including organic polymers) and particulate loadings in these samples that can promote aggregation. Changes that occur in the Spurn samples were more a function of adsorption/desorption effects rather than particle dynamic changes. There were no significant seasonal differences in sample storage change trends.

4.4.5: Sample prefiltration effect on trace metal concentrations and partitioning

The potential effect of conventional filtration artefacts on total 'dissolved', colloidal or truly dissolved trace metal concentrations is discussed in Section 1.10.2. This next section was designed to assess whether these effects may be significant in altering trace metal concentrations. Figures 4.6 (absolute concentration) and 4.7 (percentage partitioning) illustrate the effects of 0.4μm prefiltration using 1, 3 or 4 filters per litre on the trace metal concentrations and partitioning of Fe, Cu, Mn, Zn, Pb, Cd and Ni for a bulk Gainsborough sample.

For Fe, Cu, Mn, Zn and Pb there is a detectable increase in total dissolved (0.4μm) concentration with an increase in the number of prefilters used. i.e. as the filter volume per filter decreases. The increase in total dissolved metal concentration is attributed to an increase in the colloidal metal. The effect of more filters used in prefiltration, the increase in total dissolved and therefore colloidal metal is greatest for trace metals that have significant colloidal fractions (Fe, Mn and Pb~100% colloidal). Metals that have lower colloidal fractions (Cu and Zn~60% of total dissolved) are less affected. This change in the apparent total dissolved metal concentration with prefiltration treatment has been previously attributed to the clogging of 0.4μm filters (Taylor and Shiller, 1995; Horowitz, 1996a and b) and removal of colloidal material by the clogged filter (progressively reduced pore size).

Figure 4.6: Effect of 0.4μm prefiltration (1 to 4 filters per litre) on trace metal partitioning.

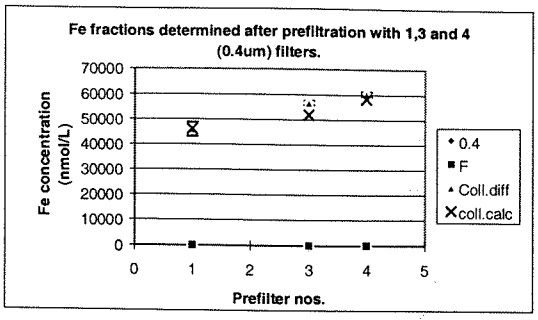

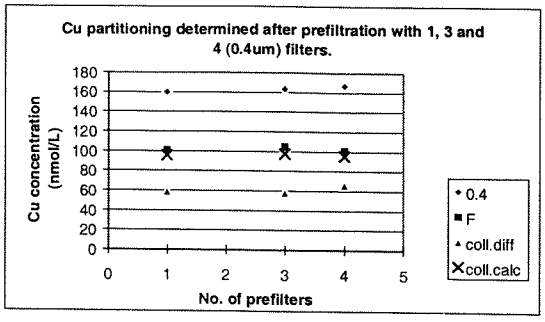

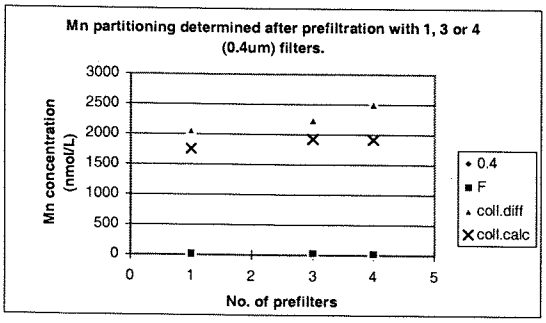

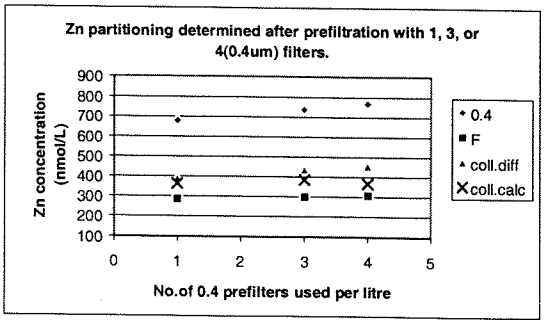

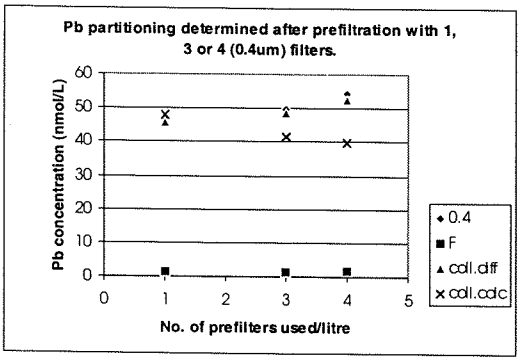

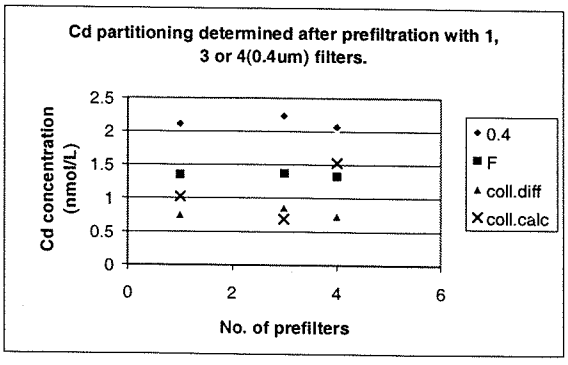

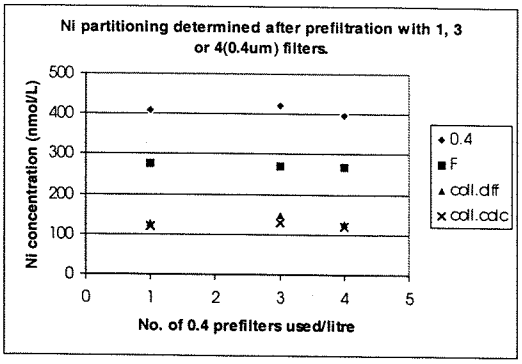

Figure 4.7: Effect of 0.4μm prefiltration (1 to 4 filters per litre) on percentage trace metal partitioning.

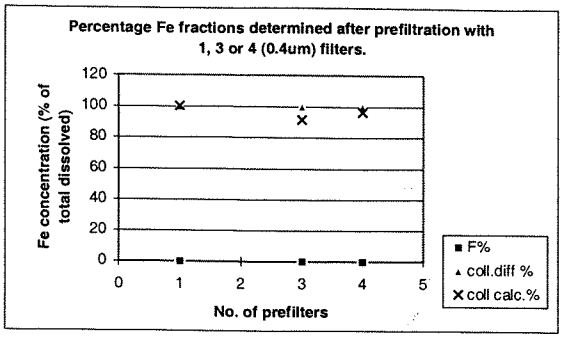

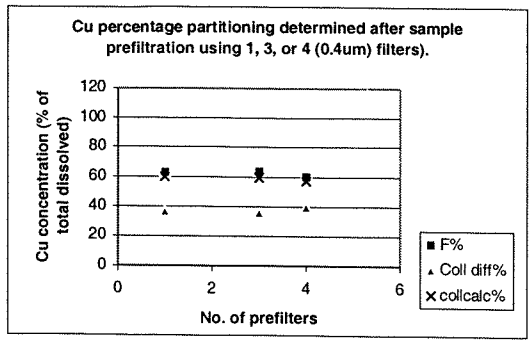

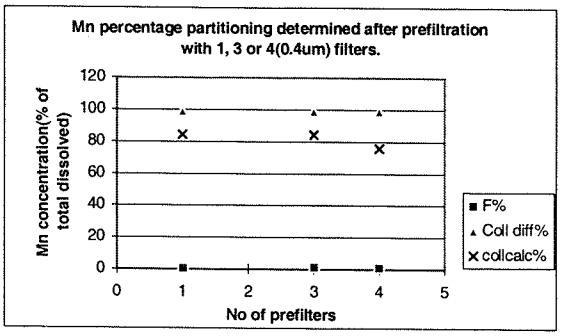

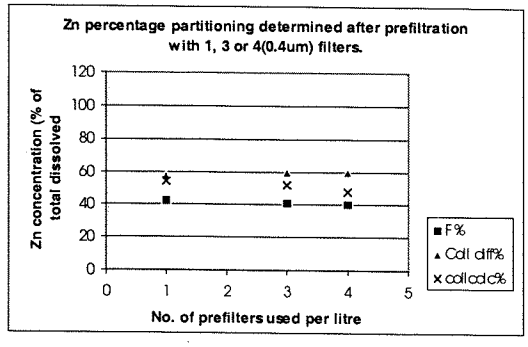

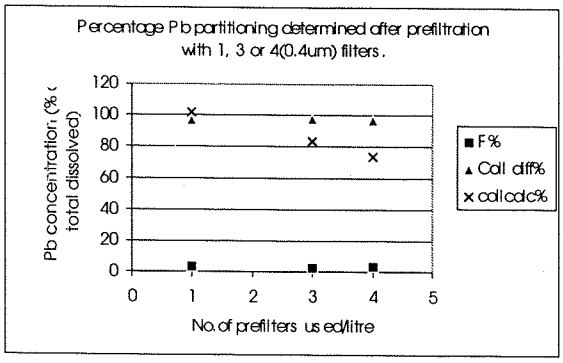

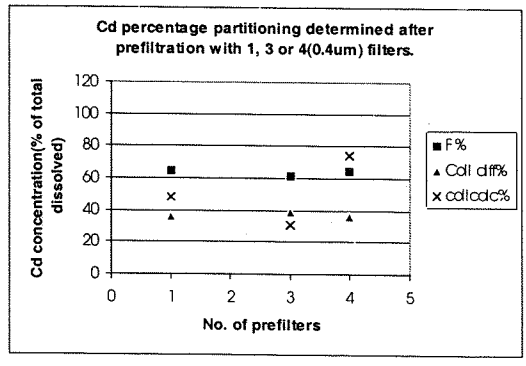

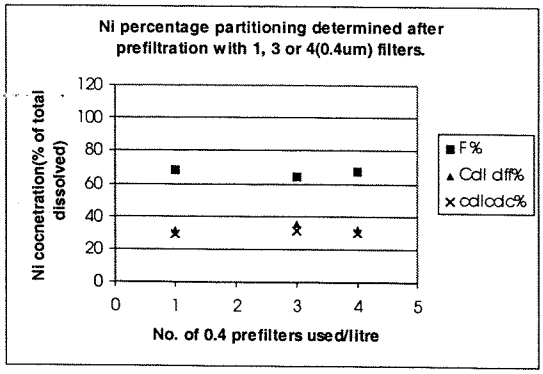

This hypothesis is confirmed by this study because the increase in the total dissolved metal concentrations (with smaller filtrate volume per filter) can be accounted for by the simultaneous increase in colloidal metals. There is no change in the truly dissolved fractions.

The effect of retention of colloidal material on prefilters can have a significant effect on the total dissolved metal concentration determined. For example; the Fe, Mn and Pb total dissolved concentrations increase by approximately 38, 25 and 22% respectively when the filtrate volume is reduced from 1000 to 250ml per prefilter. Total dissolved Cu and Zn concentrations, which have lower colloidal fractions, are less affected by prefiltration artifacts (6 and 14% increase in total dissolved concentrations respectively).

Cd and Ni total dissolved, truly dissolved and colloidal concentrations are relatively unaffected by the number of prefilters used per litre of sample filtered. Their colloidal fractions are much lower in the Gainsborough samples (40 and 30% respectively) so even a large retention of colloidal material will have a smaller effect on the overall metal concentration in the filtrate.

This interpretation of the data assumes that there is one colloidal particle population that partitions trace metals to varying degrees and not several populations that partition certain trace metals preferentially and may interact and be retained by the filters to varying degrees. That is, the prefiltration effect is a result of the varying colloidal partitioning of the different trace metals and not a physical separation effect of different types of colloidal material that may be more or less selective for certain metals.

4.4.6: Sample fractionation comparison with filtration protocol

During the April survey, trace metal samples were split in half and separated using different filtration approaches. This provides a good intercomparison using an identical initial sample for the effects of filtration protocol and technique on the determined total dissolved trace metal concentrations. A critical discussion of potential filtration artefacts derived from fltration protocols and filtration techniques is given in Chapter 1. Once

filtered, the storage, extraction and analysis procedures implemented for both sets of samples was identical and carried out in the same laboratory.

The first set of samples (filtration protocol of Tappin) was 0.4μm prefiltered under pressure using 47mm polycarbonate, acid cleaned filter membranes. The bulk samples were shaken well before filtration and the complete sample was filtered (approx. 100mls) allowing a filtration cake to build up on the surface of the filter membrane. For the second set of samples (filtration protocol of Parker) the complete sample was decanted to remove large particles that might clog filter membranes prior to 0.4μm filtration. The 0.4μm filtrate (total dissolved) was then processed through a Minitan CFF system to separate the colloidal and truly dissolved fractions. Total dissolved (for both sample sets), colloidal and truly dissolved samples (Parker only) were acidified and analysed according to the protocol described in sections 2.2 and 2.3. Figures 4.8 a to g illustrate the trace metal fraction plots against sample salinity for both sets of samples. The truly dissolved (TD Parker) fraction is included on the plots for comparison.

The results of the intercomparison show that filtration protocol greatly affects the total dissolved concentration of trace metals. There is no direct agreement of total dissolved concentration between the two filtration protocols for any of the metals. The discrepancies in the concentrations can be attributed to the colloidal fractions of the trace metals and the effect the two filtration protocols may have on them.

For Ni, Zn and Cu (Figures 4.8 A,B and E) the total dissolved concentrations from decanted samples (Parker) are higher than those which were filtered whole (Tappin) although the trends observed with salinity are very similar.

For Ni and Zn the total dissolved concentrations determined by Tappin are very similar to the truly dissolved fraction determined by Parker (R^2 = 0.81 and 0.92 for a 1:1 plot respectively). This suggests that due to significant clogging of the 0.4μm prefilter during complete sample filtration (Tappin), colloidal species will be retained and the total dissolved trace metal concentration determined by this method is closer to a truly dissolved trace metal measurement (<10,000MW by cross flow filtration).

Figure 4.8 A to G: Filtration protocol comparison plots of April trace metal samples.

A: Ni

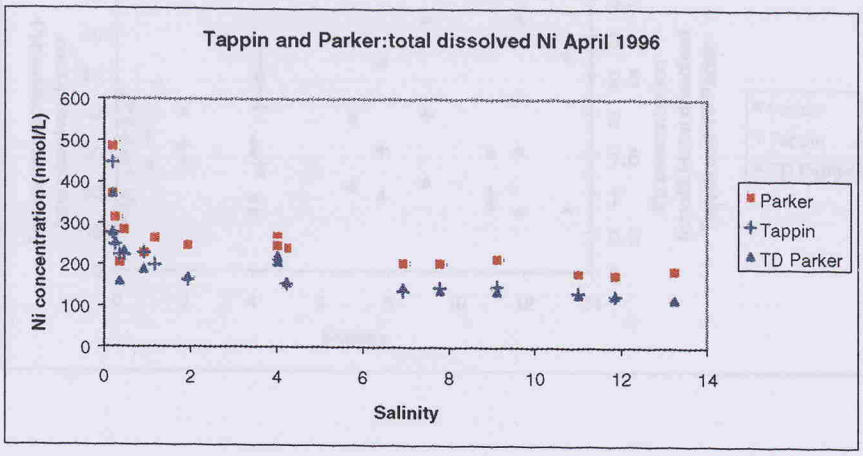

B: Zn

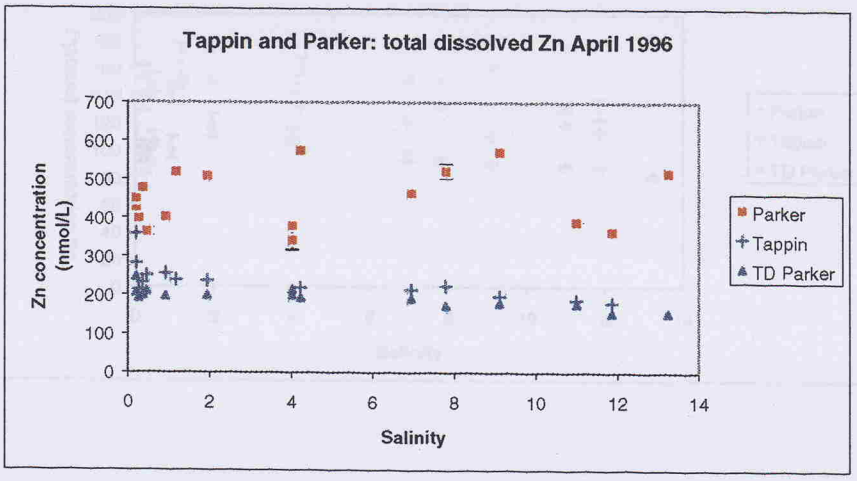

C: Fe

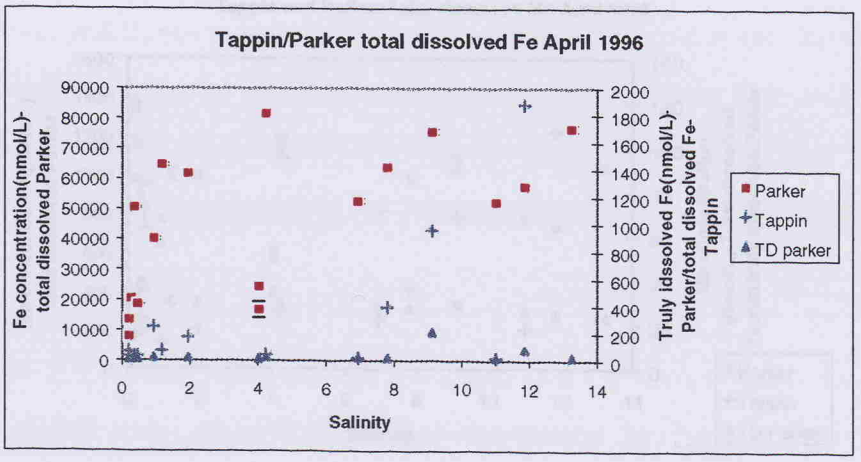

D: Pb

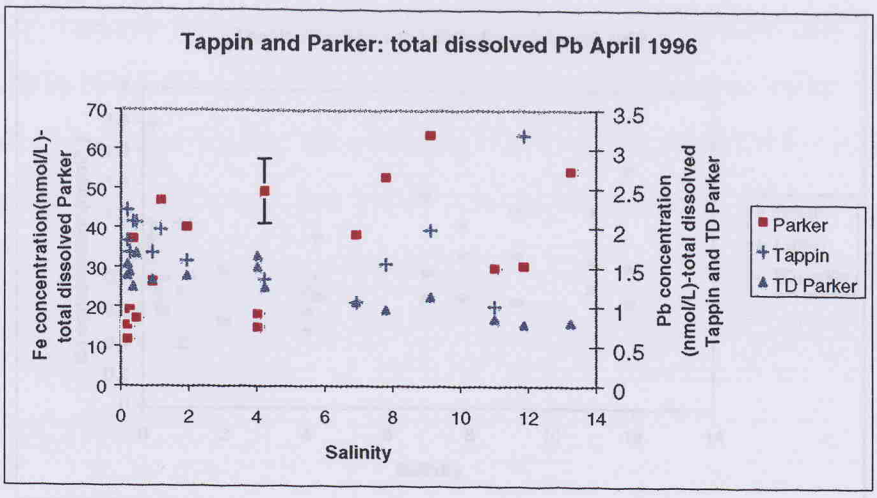
Tappin and Parker: total dissolved Pb April 1996
Fe concentration(nmol/L)-total dissolved Parker
Pb concentration (nmol/L)-total dissolved Tappin and TD Parker
Salinity
Parker
Tappin
TD Parker

E: Cu

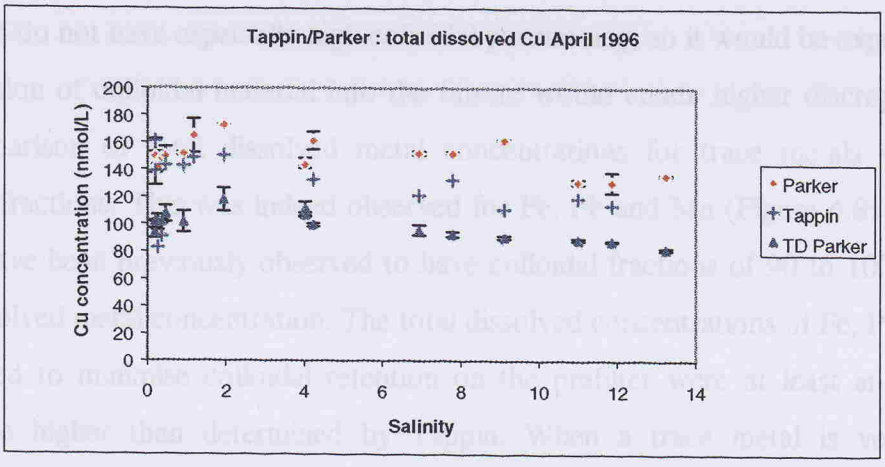
Tappin/Parker : total dissolved Cu April 1996
Cu concentration (nmol/L)
Salinity
Parker
Tappin
TD Parker

F: Mn

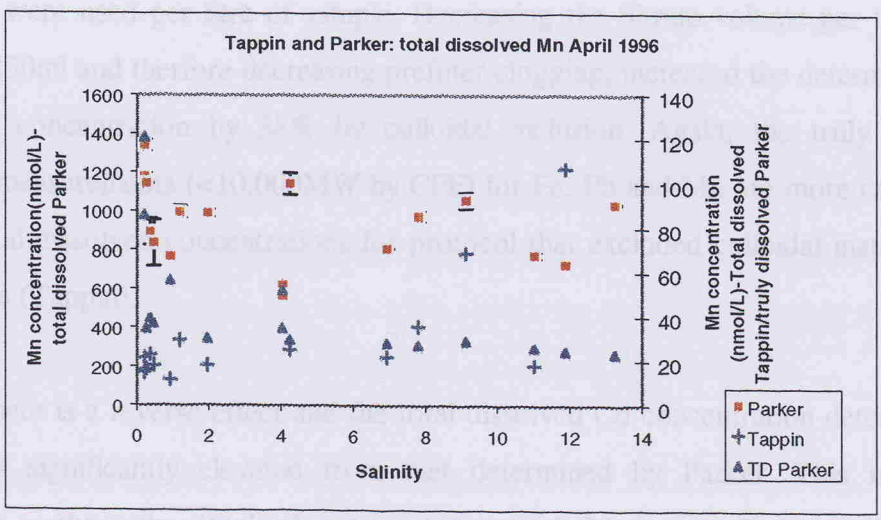
Tappin and Parker: total dissolved Mn April 1996
Mn concentration(nmol/L)-total dissolved Parker
Mn concentration (nmol/L)-Total dissolved Tappin/truly dissolved Parker
Salinity
Parker
Tappin
TD Parker

G: Cd

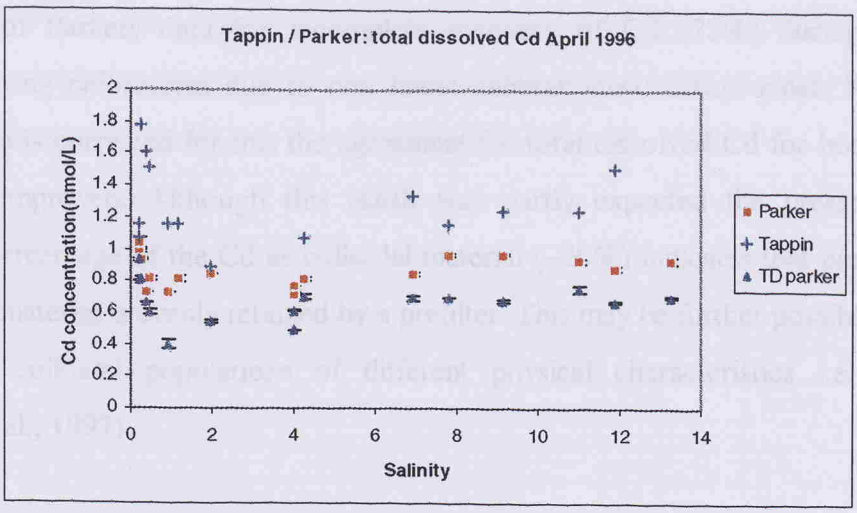

Ni and Zn do not have especially high colloidal partitioning, so it would be expected that the inclusion of colloidal material into the filtrate would create higher discrepancies in the comparison of total dissolved metal concentrations for trace metals with high colloidal fractions. This was indeed observed for Fe, Pb and Mn (Figure 4.8; C, D and F) that have been previously observed to have colloidal fractions of 90 to 100% of the total dissolved metal concentration. The total dissolved concentrations of Fe, Pb and Mn determined to minimise colloidal retention on the prefilter were at least an order of magnitude higher than determined by Tappin. When a trace metal is very highly colloidally partitioned (>90%) even a small retention of colloidal material during filtration will have a significant effect on the total dissolved concentration. This has already been observed (especially for Fe) in this study where various numbers of prefilters were used per litre of sample. Decreasing the filtrate volume per filter from 1000 to 250ml and therfore decreasing prefilter clogging, increased the determined total dissolved concentration by 38% by colloidal inclusion. Again, the truly dissolved (Parker) measurements (<10,000MW by CFF) for Fe, Pb and Mn are more comparable to the total dissolved concentrations for protocol that excluded colloidal material from the filtrate (Tappin).

For Cd there is a reverse effect and the total dissolved Cd concentration determined by Tappin is significantly elevated from that determined by Parker. This is perhaps surprising as the truly dissolved and total dissolved Cd data by Parker indicates that

there is still a significant colloidal Cd fraction. This is perhaps offset by the lack of adjustment of Parkers data for incomplete recovery of Cd (73%) during solvent extraction using chloroform due to non linear calibration/extraction plots. When the total Cd data is corrected for this the agreement for total dissolved Cd for both sets of samples is improved. Although this result was partly expected the presence of a significant percentage of the Cd as colloidal material (~20%) indicates that perhaps not all colloidal material is evenly retained by a prefilter. This may be further possible if there are several colloidal populations of different physical characteristics i.e. organic (Kraepiel et al., 1997).

This limited intercomparison has demonstrated the importance of filtration protocol and artifacts on the determination of total dissolved trace metal concentrations. Consequently, when comparing trace metal data, the prefiltration methodology may be just as important for some trace metals as the type of filters or cut-off used. Changes in total dissolved trace metal concentrations by inclusion/exclusion of colloidal species will be greatest for metals (Fe, Pb, Mn) and samples (riverine, turbidity maximum zone) where colloidal fractions are significant.

4.4.7: Mass balance recovery overview for Trent/Humber sampling

For every sample fractionated and analysed as part of the Trent/Humber study a trace metal mass balance (recovery) was calculated as discussed in section 1.10.2 and Whitehouse et al. (1990). This parameter indicates the performance of the cross-flow filtration system in comparison to different metals and other sample characteristics.

The mean metal mass balance recoveries for the February Trent survey (entirely freshwater) and the Trent/Humber in 1996 transects are displayed in Table 4.6. The mass balance for most metals is very good (>90%). However, there are some exceptions where recovery is substantially less than 100%, indicating some interaction of the sample with the filter system and retention of colloidal material on the filter plate.

The recovery is consistently low for Fe (sometimes as low as 66% in the Trent survey). This is partially linked to its predominance in the colloidal fraction which increases the

significance of the effect of colloidal interactions with the filter membrane. Other highly colloidal metals (Mn and Pb) show reduced recoveries. The Mn recovery is improved in the February survey as manganese was anomalously partitioned into the truly dissolved phase in this survey. The reverse is true for Ni for the February survey.

Table 4.6: Mean trace metal CFF recoveries (%) for Trent samples (February 1996) and combined Trent/Humber surveys (April to December 1996).

	Fe	Cu	Mn	Zn	Pb	Cd	Ni
Trent (February)	**66.5**	**99.9**	**98.4**	**89.4**	**85.9**	**100.9**	**78.6**
1 σ	*16.7*	*14.2*	*8.8*	*17.7*	*16.0*	*16.1*	*17.6*
Trent/Humber	**84.3**	**96.7**	**88.7**	**93.9**	**84.8**	**98.9**	**98.0**
1 σ	*12.1*	*8.4*	*11.6*	*8.4*	*12.3*	*12.0*	*6.1*

Generally, several factors can combine to increase or decrease recovery by affecting the interaction of the sample with the filter plate/system. As has already been discussed, a major factor is the colloidal significance (colloidal percentage of total dissolved trace metal) for a given metal. Clearly, if a metal has low partitioning into a colloidal phase it will be minimally affected by colloidal retention within the CFF system. This effect is illustrated in Figure 4.9 which indicates the relationship of metal recovery with the colloidal trace metal percentage. As colloidal trace metal % decreases, the recovery and comparability of colloidal concentrations determined by difference or from the retentate fraction improves. It is clear that the colloidal concentrations calculated from the retentate fraction can be significantly underestimated for Fe which has poor recovery compared to Cd which has good recovery. Colloidal material retained on the filter plate/membrane is not included in the retentate fraction and is therefore underestimated during analysis.

Recovery can be seen to decrease as colloidal percentage increases ($R^2 = 0.77$) i.e. there is more effect on a metal by colloidal interaction with the filter plate if it has a significant colloidal partitioning.All the samples in the Trent February survey were freshwater so this relationship is established without salinity effects affecting sample composition. It has been observed in the Trent/Humber transects that recovery for certain metals is also affected by factors such as DOC and SPM (colloidal SPM) and salinity which will indirectly affect both these parameters. Characteristics of a sample that will increase

particle aggregation (colloidal concentration, ionic strength, DOC) or interaction with the filter (DOC concentration via sticking/charge effects) are likely to reduce trace metal recovery.

Figure 4.9: Correlation of recovery for trace metals with percentage colloidal fraction.

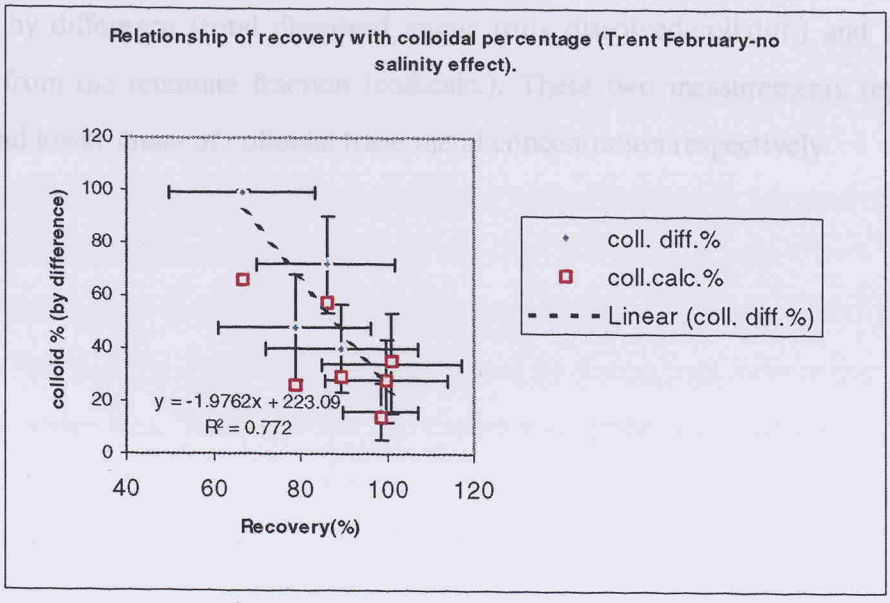

Samples of low colloidal loading and low DOC concentrations (usually high salinity samples) generally have better recoveries than samples with higher colloidal populations or DOC (usually riverine samples). It is possible that individual sample characteristics will affect the recovery observed. For example; SPM and colloidal loading is often high in the turbidity maximum zone despite increasing salinity and although riverine samples are generally high in DOC it is possible for localised primary production in the estuary to create anomalous recovery conditions. Generally, although recovery and ideal separation of samples by CFF improves towards coastal waters the diversity of natural conditions that govern a samples salinity, DOC, colloidal loading and particle spectrum will combine to determine the interaction of a sample with a filter membrane during separation.

Mass balance (% recovery) measurements will identify problems with sample separation and therefore indicate whether the colloidal concentration calculated using the retentate fraction (colloidal calc.) is reliable. However, although the recovery will indicate an

overall interaction of sample material with the CFF system (colloidal retention on the filter membrane) without conducting detailed filtration series experiments for each sample the effect on the filtrate (via breakthrough, ionic exchange or enhanced aggregation of low molecular weight colloids) cannot be assessed. For this reason, in the following Trent/Humber transects colloidal trace metal concentrations have been determined by difference (total dissolved minus truly dissolved-coll.diff.) and also by calculation from the retentate fraction (coll.calc.). These two measurements represent the upper and lower limits of colloidal trace metal concentration respectively.

4.4.8: Trent / Humber trace metal seasonal axial transects 1996; results and discussion

4.4.8a: Master variable seasonal changes:

See Figures 4.3 a,b and c (Section 4.4.1) for the seasonal plots of master variable data.

River and estuarine water temperatures varied from 8 to 10 °C in April to around 20 °C in July and August (upper reaches) and decreased in the winter months to a minimum of 5-6°C in December. In the winter months there was an increase in temperature seawards and the reverse in the summer months.

The pH changes in the estuary were little affected by season with a consistent sag around mid to low salinities. The minimum pH altered perceptibly and was lowest in the July survey (7.35) and highest in the winter surveys (7.5 to 7.6). The pH changes in the Trent were relatively small (7.6 to 8.2) with lower pH's occurring during the summer months. This change and also the pH minimum may be linked to gas solubility but also to respiration/primary production in surface waters. The pH of the seawater end-member was invariable (7.9 to 8.0).

When looking at the DO concentrations with season it seems that the pH and DO are closely linked with season and biological activity. In all the surveys the DO pattern was similar with a rapid oxygen sag in the low salinity region. This was largely governed by the position of the turbidity maximum in this area which lowers DO and pH (resuspension of sediment with a chemical oxygen demand, anoxic porewater (lower pH) and bacterial sediment respiration). It is clear that there is a seasonal aspect to the extent of the oxygen demand of the TMZ. During the summer months the DO sag was lower (30 to 50%-April to October) as opposed to 60% in the winter months. Although this could be linked to changes in sediment loads produced by neap-spring tidal effects and DO solubility effects, it is clear that during the summer there was increased biological action that could act to accentuate changes. For example, in the July tidal cycle there was a clear chlorophyll maximum that coincided with the TMZ and lowest DO and pH levels. Increased respiration (degradation of organic matter, bacterial respiration on sediment

surfaces within the TMZ) and primary production promoted by higher insolation and water temperatures during the summer months will lead to higher CO_2 production (creates lower pH in solution) and DO consumption.
During summer months, sediments will be driven increasingly anoxic by elevated bacterial activities and organic carbon loadings which will create a larger oxygen demand once resuspended within the TMZ.
The DO levels in the river and seawater were consistently high (90 to 100%) throughout the year.

The turbidity readings had a similar distribution throughout the year with the main TMZ lying in the same salinity region (low to mid salinity). Although the position and strength of the TMZ was largely governed by the neap-spring cycle there was some seasonal influence on overall sediment concentration and composition. From the data available here, during the summer there was a more extensive and higher concentration TMZ. This was probably due to lower river flows so the sediment in the TMZ would be less diluted in the water column (there will be a higher sediment to water ratio which will exacerbate sediment/water interactions) there is also a biological component in the turbidity signal. The reverse was seen in the winter where there was more dilution of the TMZ (Uncles et al., In press) (the minimum in transmission/NTU was more isolated) and there was elevated sediment input from the Trent.

The comparative inputs of the Trent and the Ouse are also important seasonally (see Table 4.4 and Figure 4.5). The Trent generally had a greater flow than the Ouse (apart from October 1) but the Ouse was far more seasonally influenced with substantially lower flows during the summer months (April, July, August) than the Trent. The metal concentrations of the two inflows will govern metal concentration downstream from the confluence.

4.4.8b:Trace metal data:

The axial transects for each trace metal fraction have been plotted for February, April, July, August, October and December 1996 surveys in Figures 4.10a to g. The plots for the percentage composition of each trace metal fraction in the same axial transects are situated in Appendix 3. The transects will be used for trace metal partitioning and behaviour discussions as well as seasonal comparisons. Full percentage composition and mass balance recovery data is included in the data disc.

The February survey is discussed separately due to the anomalous conditions (very high flow) encountered during this survey. The freshwater input from the River Trent at this time was so high as too virtually prevent salt intrusion up the tidal reaches. Because of this lack of salinity gradient the trace metal plots have been plotted with distance from Gainsborough (usual limit of salt influence). The July tidal cycle introduces a temporal perspective to physical/chemical changes and associated trace metal alterations during flood conditions. This temporal approach to the system is discussed separately from the axial transect plots for this survey.

For all the trace metal vs. salinity/distance plots the associated riverine (Trent and Ouse: from Institute of Hydrology and LOIS data base) and seawater end-member (Althaus, 1992) trace metal concentrations have been plotted, to indicate the likely conservative mixing line and to facilitate the identification of metal inputs or removal.

The symbols used for trace metal fractions and end-members on the transect plots are;

Total dissolved trace metal (<0.4µm)	black diamond (◆)
Truly dissolved metal (<10,000MW-CFF)	red square (■)
Colloidal metal (by difference) (10,000MW-0.4µm)	black triangle (▲)
Colloidal metal (from retentate) (10,000MW-0.4µm)	black cross (x)
Trent (Institute of Hydrology and LOIS data-base):	green circle (●)
Ouse -LOIS data-base:	
(plotted at Trent/Ouse confluence on transects):	purple triangle (▲)
Seawater (Althaus, 1992):	blue diamond (◆)

As a result of combination of seasonal transects into one figure, some of the resolution and detail on individual transects i.e. metal concentration changes N.B. iron August, end-member positioning has been obscured. The complete data set plotted for the individual transects is contained in Appendix 3 of the data disc.

4.4.8c: February trace metal partitioning in the Trent:

The February survey was concentrated in the tidal reaches area of the Trent from Gainsborough (limit of salt intrusion) downstream to Trent Falls (see Figure 4.2 for sampling sites). There was very high river flow (~107m^3/s) during this time which prevented significant saline intrusion up into the Trent. As the background data shows (Appendix 3 of the data disc) the chloride concentration varied from 4.7mmol/l at East Stockwith (station 1) to 6.3mmol/l at East Walker Dyke in the main Humber (station 15). There was also little gradient in SPM and nutrients (PO_4, NO_3 and Si) showed a gradual decrease in concentration towards Trent Falls.

The February transects for trace metals (see Figures 4.10a tog) show far more variability in concentration and partitioning in the tidal reaches due to lack of significant salinity gradient. However, significant metal and spatial features can be identified.

Iron and lead (4.10a and b):

Both Fe and Pb are highly surface active elements. Total dissolved Fe occurs almost entirely in the colloidal phase (95 to 100%). Dissolved lead is usually about 80% colloidal in the Trent for this survey. Iron and lead show progressively increasing concentrations over the Trent transect, with most significant increases occurring in the stations at Trent Falls and into the Humber. The most likely causes of this increase in Fe and Pb concentrations are cumulative effects down the Trent such as sediment erosion. The substantial increase in colloidal Fe material around Trent Falls and into the main Humber may be associated with low molecular weight colloid coagulation, disaggregation of larger particles, resuspension processes or advection of high SPM Humber/Ouse water. Colloidal Pb also increases towards the Ouse/Trent confluence, probably for the same reasons as Fe, although the last sample in the main Humber has very high truly dissolved Pb compared to the colloidal material. This implies some source of truly dissolved Pb via disaggregation of colloidal aggregates or desorption of Pb from colloidal material. Resuspension release of porewaters may also be important.

Figure 4.10a: Seasonal axial transects of iron in the Trent/Humber

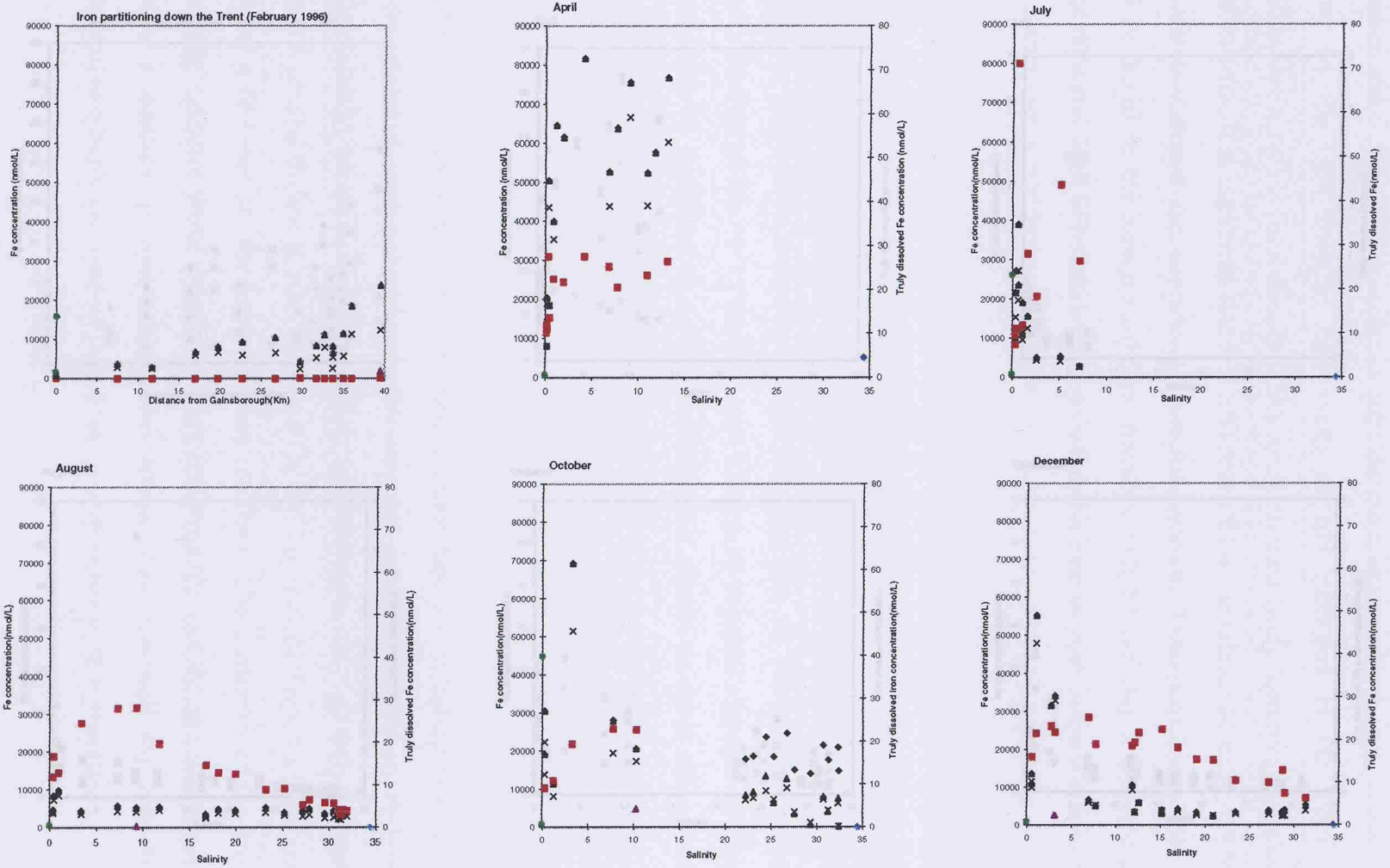

Figure 4.10b: Seasonal axial transects of lead in the Trent/Humber (1996)

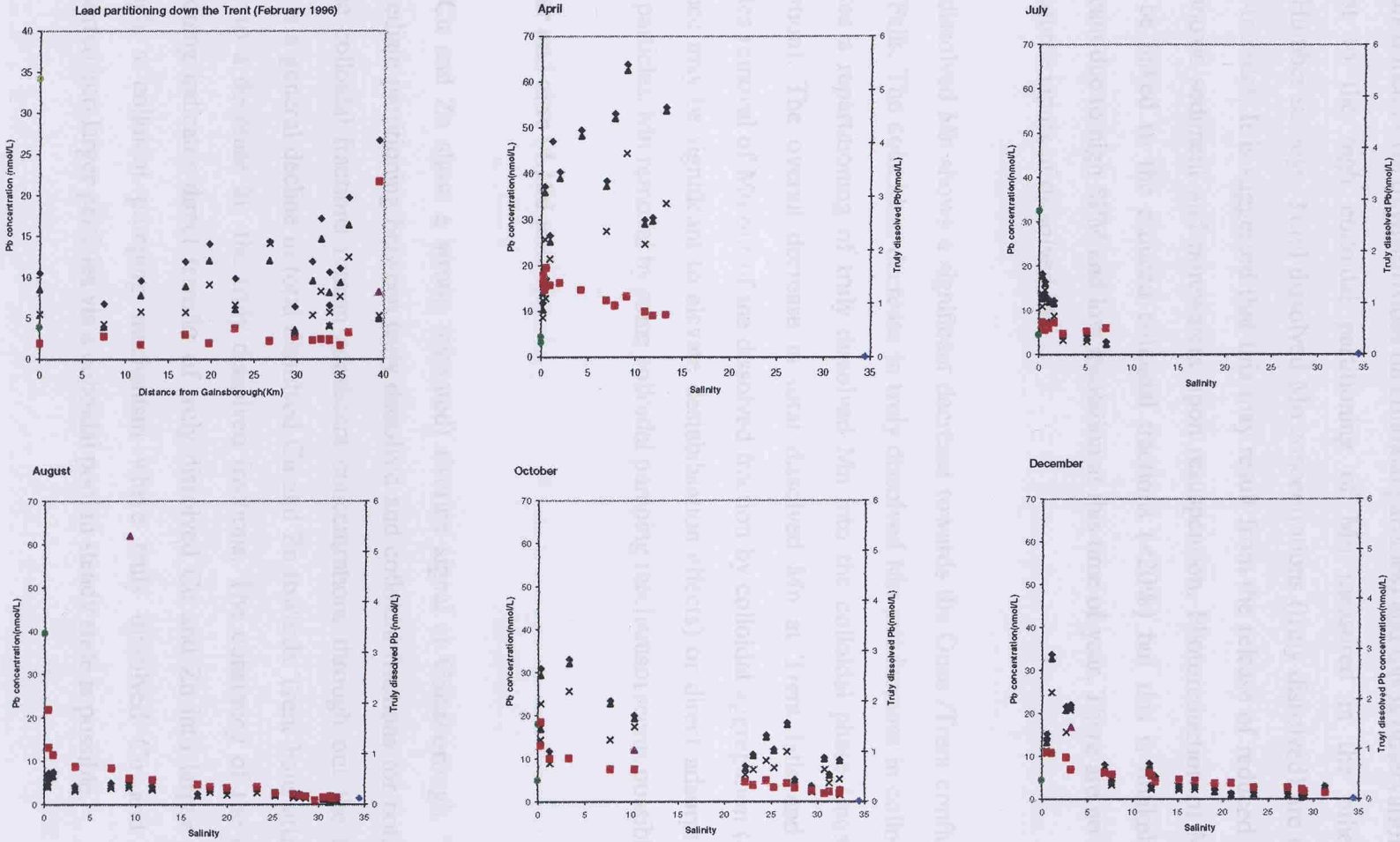

Manganese (4.10c):

Under the February survey conditions manganese was found predominantly in the truly dissolved phase (55 to 98% of total dissolved). Manganese is usually a highly colloid partitioned metal (Mn oxyhydroxides on colloidal particles) and this is observation was in contrast to the high colloidal partitioning of Mn measured in the other main Trent/Humber surveys. Total dissolved Mn concentrations (truly dissolved) are elevated in mid-transect. It is suggested that this may result from the release of reduced Mn (II) from anoxic sediment and porewaters upon resuspension. Photoreduction of Mn (IV) could be linked to the reduced colloidal fractions (<20%) but this is unlikely to be significant due to high SPM and low insolation at this time of year. There are no obvious point source inputs of dissolved Mn.

Total dissolved Mn shows a significant decrease towards the Ouse /Trent confluence at Trent Falls. The coincident decrease in truly dissolved Mn and increase in colloidal Mn indicates a repartitioning of truly dissolved Mn into the colloidal phase (reoxidation/ adsorption). The overall decrease in total dissolved Mn at Trent falls and beyond indicates removal of Mn out of the dissolved fraction by colloidal aggregation (chloride influence may be significant to elevate destabilisation effects) or direct adsorption into larger particles. Mn removal by some colloidal pumping mechanism seems possible.

Copper and zinc (4.10d and e):

Both Cu and Zn show a strong (elevated) riverine signal at Gainsborough. There is intermediate partitioning between truly dissolved and colloidal fractions for both metals but the colloidal fractions remain consistent concentrations through out the transect. There is a general decline in total dissolved Cu and Zn towards Trent Falls attributable mainly to a decrease in the truly dissolved fractions. The constancy of the colloidal partitioning indicates direct transfer of truly dissolved Cu and Zn into larger particles although a colloidal pumping mechanism where truly dissolved Cu and Zn are transported into larger particles via a colloidal pool in steady state is possible.

Figure 4.10c: Seasonal axial transects of manganese in the Trent/Humber (1996)

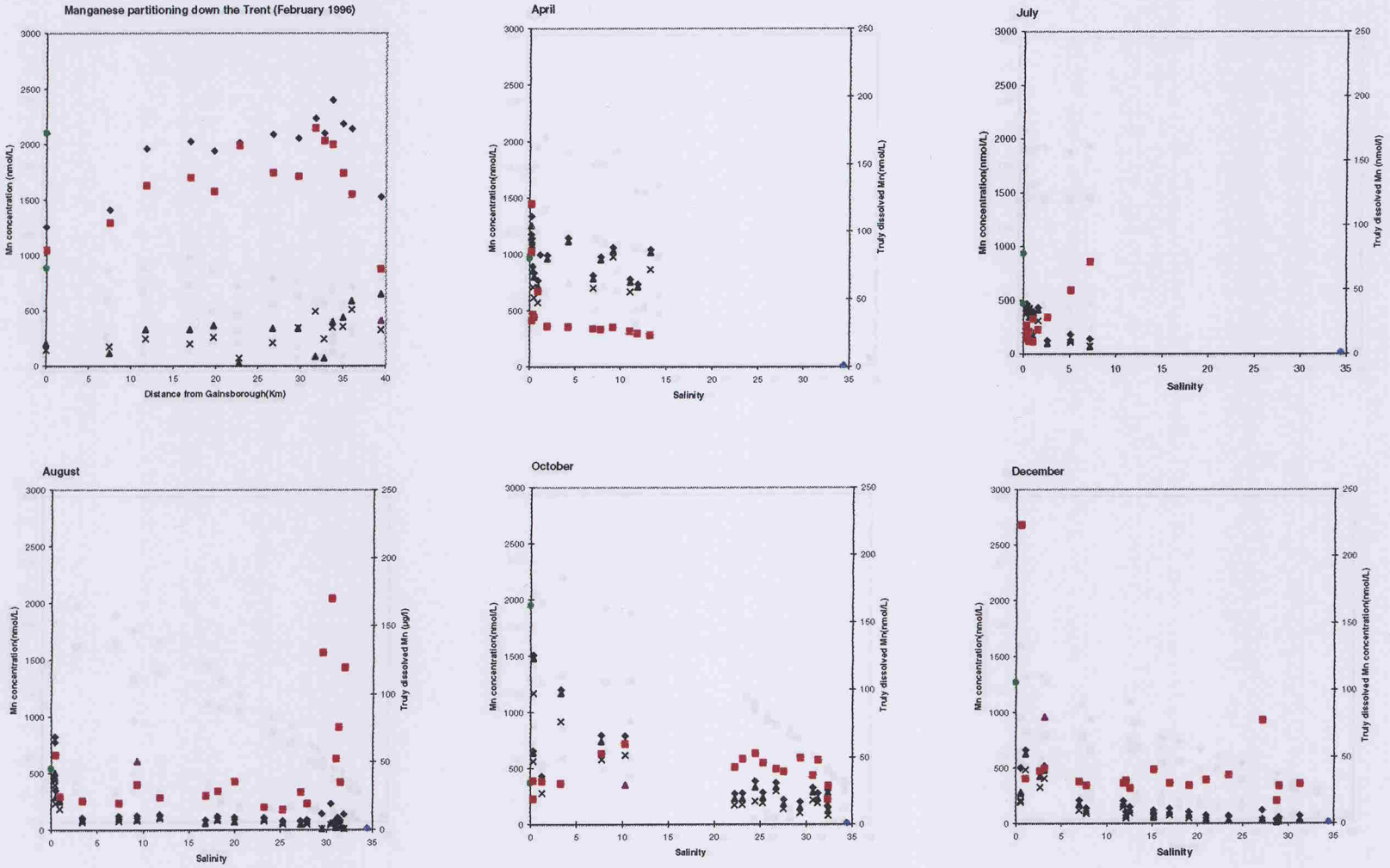

Figure 4.10d: Seasonal axial transects of copper in the Trent/Humber (1996)

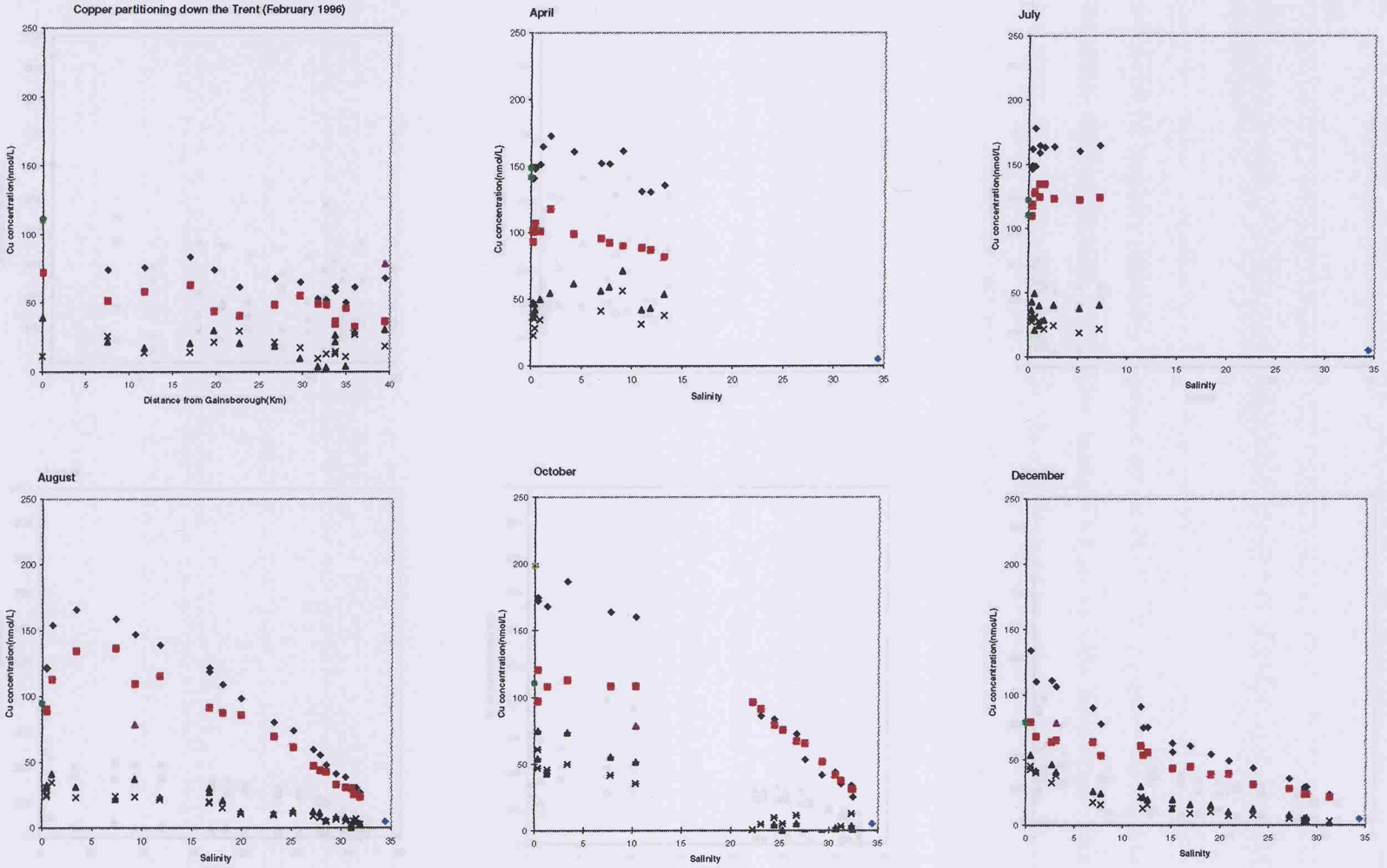

Figure 4.10e: Seasonal axial transects of zinc in the Trent/Humber (1996)

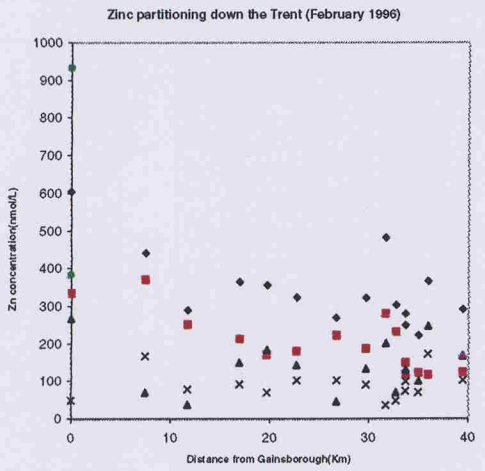

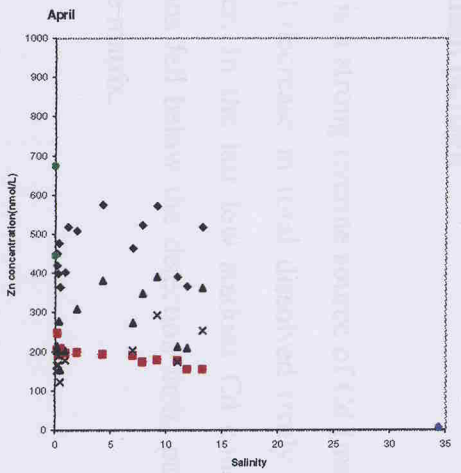

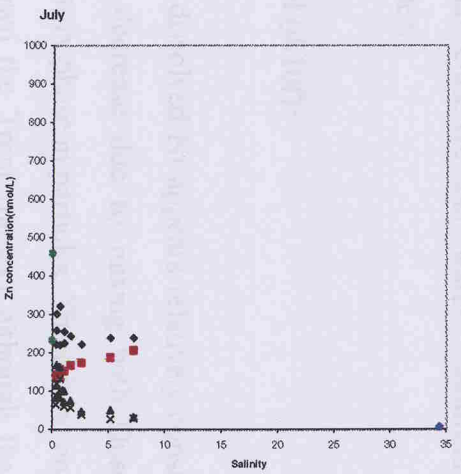

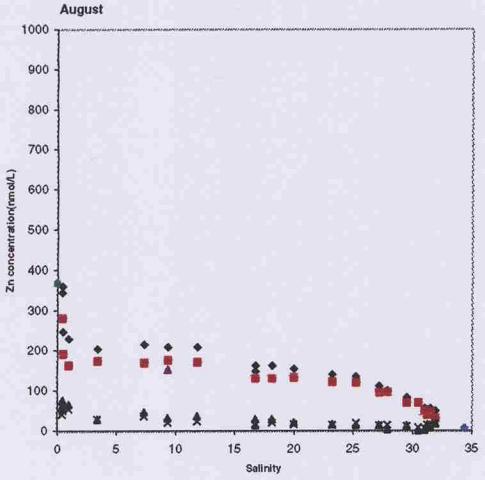

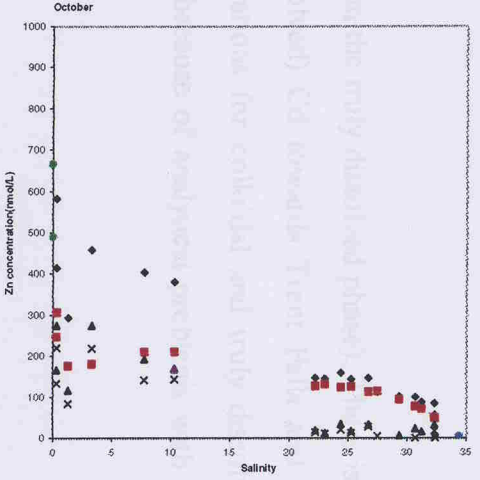

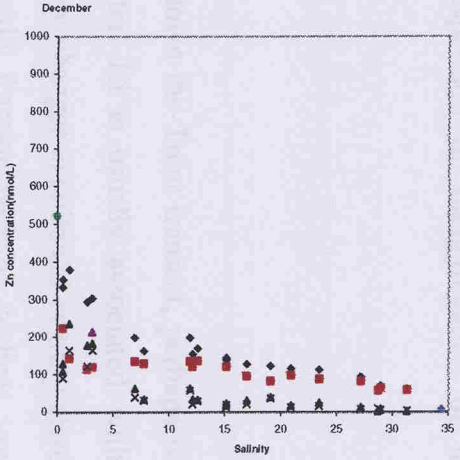

The increase in colloidal Fe over this area of truly dissolved Cu and Zn removal indicates that colloidal Fe-oxyhydroxide scavenging is possible. Further investigation of riverine colloidal material would be required to elucidate this. A significant increase in colloidal partitioning at stations 11 to 15 indicates a significant advective input of colloidal material Ouse/Humber waters, sediment resuspension or disaggregation of larger particles.

Nickel (4.10f):

Total dissolved Ni appears relatively constant down the Trent transect, perhaps with a small decrease due to mixing with Ouse water. Ni is usually associated with the refractory phase in particles. There is no consistent changes in colloidal or truly dissolved Ni down the Trent transect although the colloidal fraction perhaps declines towards Trent Falls and the Ouse confluence.

Cadmium (4.10g):

There is a strong riverine source of Cd (mainly in the truly dissolved phase). There is an overall decrease in total dissolved (truly dissolved) Cd towards Trent Falls and the Humber. In the last few stations Cd concentrations for colloidal and truly dissolved fractions fell below the detection limit, partly because of analytical problems with the sample matrix.

Figure 4.10f: Seasonal axial transects of nickel in the Trent/Humber (1996)

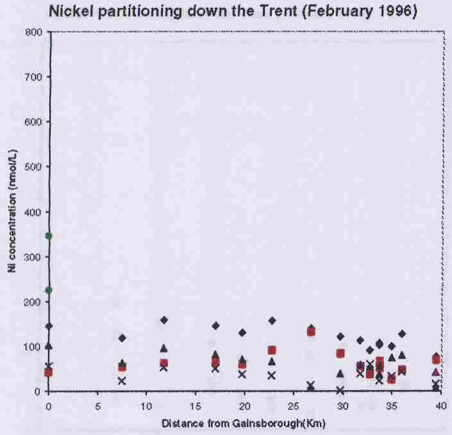

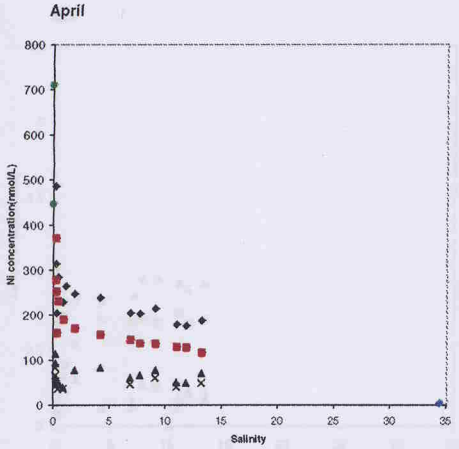

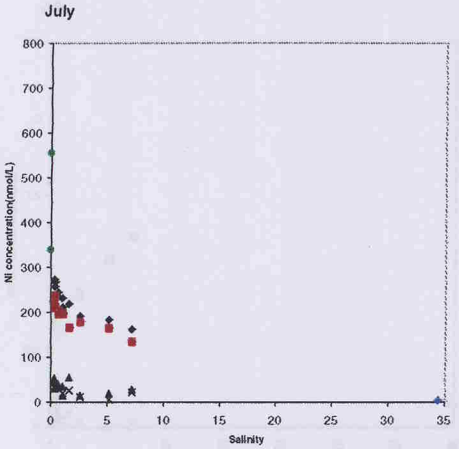

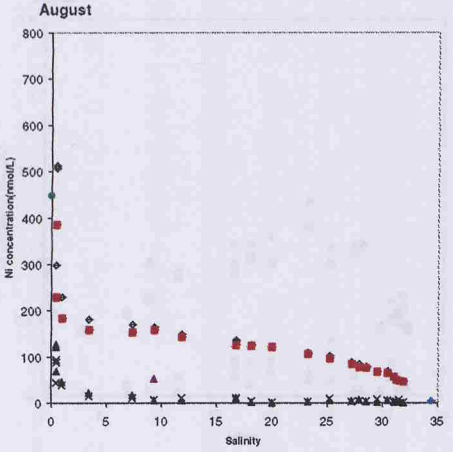

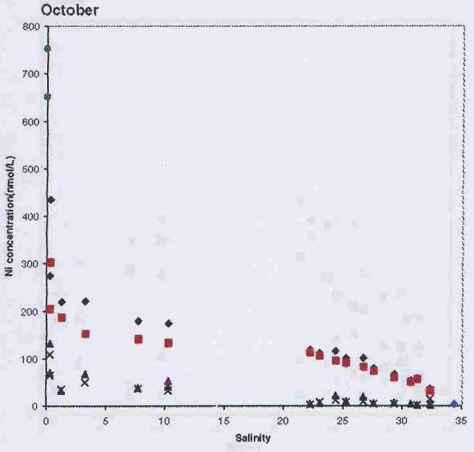

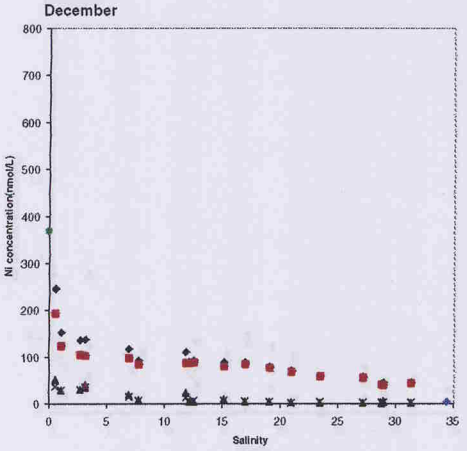

Figure 4.10g: Seasonal axial transects of cadmium in the Trent/Humber system (1996)

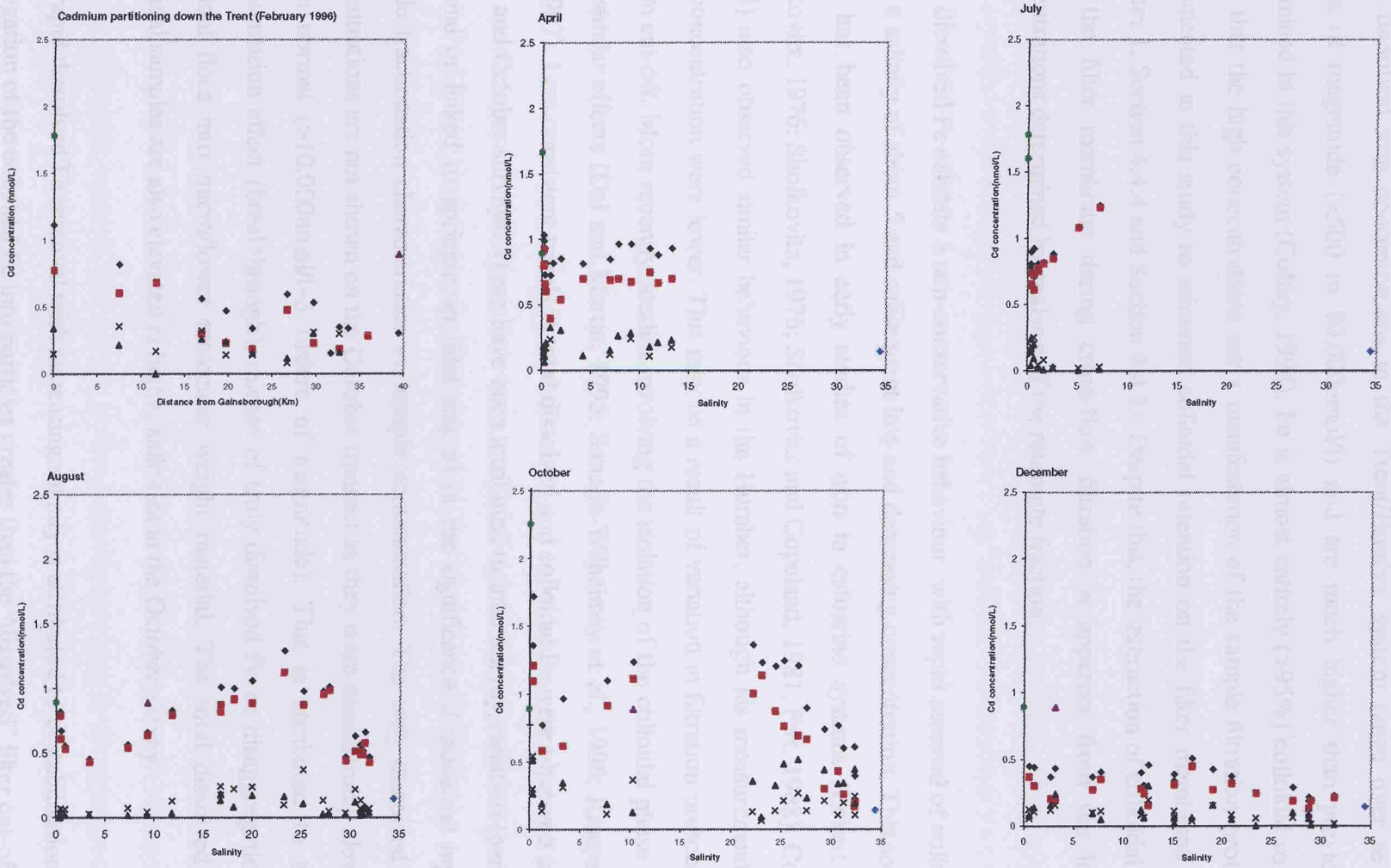

4.4.8d: Seasonal axial transects of the Trent/Humber:

Iron: Figure 4.10a

Overall behaviour

Total dissolved iron concentrations in the Trent/Humber system range over several orders of magnitude (<500 to 80,000nmol/l) and are much higher than previously determined in this system (Coffey, 1994). Fe is almost entirely (>95%) colloidal so it is likely that the high concentrations are a manifestation of the sample filtration protocol implemented in this study to minimise colloidal retention on the filter membrane (see Chapter 1, Section 4.4.4 and Section 4.4.5). Despite this, the interaction of colloidal iron with the filter membrane during cross-flow filtration is apparent from the lower concentrations determined by analysis of the retentate fraction.

Total dissolved Fe exhibits a non-conservative behaviour with rapid removal of colloidal Fe to a salinity of about 5 and subsequent low and decreasing concentration. This sort of trend has been observed in early studies of iron in estuarine systems (Eckert and Sholkovitz, 1976; Sholkovitz, 1976; Sholkovitz and Copeland, 1981; Fox, 1988). Coffey (1994) also observed similar behaviour in the Humber, although his measurements of iron concentration were lower. This may be a result of variation in filtration protocol at 0.4μm cut-off. More recently, studies involving the isolation of the colloidal phase have seen similar effects (Dai and Martin, 1995; Sanudo-Wilhelmey et al., 1996; Kraepiel et al., 1997). Less consistent trends in total dissolved and colloidal Fe were observed in the April and October surveys. These have been attributed to inter survey variation (perhaps seasonal or linked to spring/neap tidal stages) in the significance if industrial inputs, sample fractionation characteristics or sample contamination. The truly dissolved iron concentrations are not shown on the October transect as they were considerably elevated above normal (>10,000nmol/l~3 orders of magnitude). This is attributed to some contamination effect (breakthrough), release of truly dissolved Fe or disaggregation of colloidal flocs into micro/lower molecular weight material. The total dissolved and colloidal samples are also elevated at higher salinities in the October survey.

The rapid dissolved Fe removal with increasing salinity is attributed to destabilisation and aggregation of the colloidal Fe into particles greater than the "dissolved" filter cut-off.

Although low molecular weight organics or silicate and phosphate can be effective in stabilising colloidal iron in river waters (Moore et al., 1979; Cameron and Liss, 1984) several studies have shown in mixing experiments that over 95% of dissolved (colloidal) iron can be removed from solution by salt addition (Sholkovitz, 1976; Boyle et al., 1977; Sholkovitz, 1978). Although sedimentation of iron colloidal aggregates seems likely, the removal of colloidal aggregates from the water column once aggregated is not certain (Mayer, 1982). It has been previously illustrated that organic matter (DOC) is frequently associated with colloidal iron (Moore et al., 1979). Removal of DOC during estuarine mixing, 10% of which is removed in iron-rich aggregations, has been demonstrated in mixing experiments by Sholkovitz (1976), Sholkovitz et al. (1978) and Sholkovitz and Copland (1981). The high mass composition and loose flocculated nature of colloidal Fe aggregates may inhibit floc sedimentation. Mayer (1982) observed that neither gravity nor suspended sediment may be effective in removing/scavenging flocculated iron from suspension. Without corresponding particulate Fe data is in not possible to identify if flocculated colloidal Fe has been removed from the water column by sedimentation or removed into particles that are retained by the 0.4μm "dissolved" prefilters.

The truly dissolved Fe fraction (<10KDa) is insignificant (<1% or < 50nmol/l) compared to the higher molecular weight colloidal fraction. This has also been observed in the Ob and Yenisey Rivers in Russia by Dai and Martin (1995) who found that virtually all the Fe in these systems was included in a high molecular weight fraction (>10KDa). In some colloidal studies low molecular weight Fe has been more significant but still illustrates rapid removal with increasing salinity. This has been explained as aggregation of micro colloidal material (<10KDa) by the same processes as larger colloids. In this study the truly dissolved/low molecular weight colloidal Fe exhibits a peak concentration (20 to 40nM) at salinities of 5 to 10 before dropping to much lower levels. This trend is observed in all the surveys and is therefore seasonally independent. This increase in truly dissolved/low molecular weight Fe could be linked to an increase in, Fe desorption from colloidal surfaces, the microcolloidal population within the turbidity maximum or by disaggregation of microcolloidal flocs due to increased shear. Additionally, conformation changes in organic material that occurs at low salinities can lead to disaggregation of

microflocs (Eisma, 1986) and release of truly dissolved Fe-humic species. Overall though this is a minor effect and source of truly dissolved Fe within the estuary.

Seasonal trends:

The behaviour of Fe in the Trent/Humber system is relatively similar throughout the year. Total dissolved iron is consistently almost entirely partitioned into the colloidal fraction (95-100 %) and the truly dissolved fraction is very low but may show a maximum around 5-10 psu. Throughout the year there is removal of colloidal iron in the low salinity region but the overall function of the TMZ as a sink or source for colloidal Fe varies with spring/Neap cycles. The Trent input of colloidal Fe varies over an order of magnitude with season. The Fe concentration varies from 10000 to 80000nmol/L but can be much lower, for example, in February where Fe concentration at Gainsborough was less than 2000nmol/L. Clearly, the inputs are affected by river flow. In winter months there is higher flow and although there may be more net input the concentration is low because of the dilution effects. The reverse is true in the summer months.

Once inside the estuary, the tidal state and the role of the turbidity maximum will govern iron behaviour. April and October transects fell at spring tides and also at higher combined river flows. The removal of colloidal Fe is much reduced and a significant iron signal is carried down towards Spurn. In surveys that fall at neap tides the colloidal Fe removal by the TMZ is very effective and the lower estuary Fe concentrations are much reduced.

The flow and Fe concentration signal of the Ouse will also greatly affect the iron concentration further down the estuary. Although the flow in the Ouse is often substantially lower than the Trent (apart from October) the iron concentration of the Ouse may greatly affect the overall transect.

The major form of colloidal Fe in many rivers (including the Trent/Ouse) is Fe-oxyhydroxides (Boyle et al., 1977; Mayer, 1982; Fox and Wofsy, 1983; Fox, 1988; Hunter and Leonard, 1988). These Fe-oxyhydroxides are very efficient scavengers of other trace metals (Millward and Moore, 1982) so colloidal Fe-oxyhydroxide dynamics may control the partitioning and behaviour of other trace metals.

Lead: Figure 4.10b

Overall behaviour:

Lead is a highly particle reactive element and shows a high particle affinity in seawater (Balls, 1985; Burton et al., 1993). Total dissolved concentrations are comparatively low to other elements as Pb is effectively scavenged from the water column by particulate material. Colloidal Pb comprises 80 to 95% of the total dissolved lead fraction. Colloidal and truly dissolved Pd transects show varying behaviours in the Trent/Humber transects. Both truly dissolved or colloidal Pb fractions show removal at low salinity areas or more conservative behaviour lower down the estuarine system in different surveys. In several surveys, truly dissolved Pb may scavenged out of the water column whilst colloidal lead behaves more conservatively. Similar conservative behaviour of dissolved Pb has been observed by Kraepiel et al., (1997) in the Gironde estuary. The truly dissolved Pb has very low concentrations (<2nmol/l) and comprises <20% of the total dissolved Pb concentration.

In contrast to these findings, previous studies have indicated a mid salinity (15 to 20) dissolved Pb minimum (this is only observed here in the October survey) or little concentration variation over the salinity range 5 to 34 as a function of the high particle affinity of Pb (Fang, 1995; Danielsson et al., 1983; Chiffoleau et al., 1994). In contrast to work by Kraepiel et al. (1997) in the Gironde estuary, Elbaz-Poulichet et al. (1984) concluded in the same estuary that dissolved Pb is adsorbed onto particles at lower salinities due to an increase in turbidity and specific area of particles in the turbidity maximum but underwent some mobilisation in the lower estuary. This mobilisation was associated with exchangeable and organic fractions. In this study there seems consistent removal of colloidal and truly dissolved (microcolloidal) Pb at lower salinities onto particulate material (perhaps coincident with the turbidity maximum), but there is no observed remobilization of Pb lower in the estuary and after initial removal total dissolved Pb (colloidal and truly dissolved) displays conservative behaviour. Truly dissolved (microcolloidal) lead exhibits seasonally consisted behaviour but colloidal lead behaviour in the Trent/Humber system appears less seasonally consistent. Colloidal lead in the April and October surveys (Spring tides) is not scavenged to the same degree which indicates more complicated controls on its behaviour in the estuary. The similarity

and interchangeable behaviour of colloidal and truly dissolved lead at the other times of the year suggests lead is associated with a continum of microcolloidal/colloidal particles. The total dissolved Pb concentrations are much higher than those encountered in other estuarine systems (0.24nmol/L-Gironde, Elbaz-Poulichet et al., 1984; 1.3nmol/L Itchen-Fang, 1995) but his may be due to significant anthropogenic sources in the river catchment and estuary itself or reduced removal of colloidal Pb as a result of prefiltration (0.4μm) artefacts.

Seasonal trends:

There is no clear seasonal change in Pb concentrations or partitioning. Lead is highly colloidal in all of the surveys but perhaps less so in August. Although there is some indication of higher truly dissolved inputs in the summer (especially April and August) this is not consistent.

As with iron, the main influence on Pb concentration within the estuary is the effect of the TMZ as governed by the tidal range (sediment resuspension) or river flow (positioning and dilution). Both April and October surveys fell on spring tides with higher combined flows and the removal of lead (especially of colloidal material) down the estuary was noticeably attenuated and truly dissolved lead was more conservative.

Although the input concentrations of colloidal and truly dissolved lead were reasonably variable, 7 to 30nmol/L and 0.6 to 2.0nmol/L respectively, the overall lead concentrations and partitioning characteristics within the estuary were relatively constant with season. The main variation in lead behaviour seems to governed by the turbidity maximum regime, the tidal range and associated particle characteristics.

Manganese: Figure 4.10c

Overall, the most striking feature of the Mn transects is the high total dissolved (colloidal and truly dissolved) concentrations at the low salinity end of the estuarine transects. There is rapid removal of total dissolved Mn (mainly colloidal) in salinities less than 3 and concentrations remain low down the length of the estuary. The total dissolved Mn concentration is dominated by the colloidal phase (80 to 90% at low salinities) but the truly dissolved fraction is more significant (~40%) in the high total dissolved samples.

Similar rapid removal of total dissolved Mn have been observed in the Humber estuary by Coffey (1994) and for the Gironde (Kraepiel et al., 1997) and Tamar (Morris and

Bale, 1979; Knox et al., 1981; Ackroyd et al., 1986). Other colloidal studies have observed the dependence of total dissolved Mn concentrations on the low molecular weight fractions (Powell et al., 1996-Ochlockonee Estuary) or conservative dissolved Mn behaviour (Holliday and Liss, 1976; Moore et al., 1979). Truly dissolved (low molecular weight) manganese has variable behaviour sometimes showing removal at low salinities (April, August, December), release at higher salinities (August, July) or relative;ly constant concentration mid-estuary (April, October, December).

The high Mn concentrations at the head of the estuary could result from either high river inputs (the Trent end-member concentration is very similar) or to dissolved Mn release from reducing sediments (indicated by higher truly dissolved fraction here). The Mn removal most likely occurs in the turbidity maximum which has been found to be a zone of Mn scavenging (Morris and Bale, 1979; Knox et al., 1981). The removal mechanism and high removal rate of Mn onto particles in the low salinity zone may be dependant on the surface properties of the particles in the turbidity maximum (Coffey, 1994). Mn auto-oxidation to freshly precipitated Mn phases is potentially a significant control on Mn removal from the dissolved pool via oxidation (Pankow and Morgan, 1981; Yeats and Strain, 1990). The lack of dissolved Mn removal observed in the Trent may be due to the lack of sufficient Mn oxyhydroxide coatings on riverine particles.

Initial contact with saline water may induce hydrolysis of previously complexed or free dissolved Mn which enables auto-oxidative sorption/precipitation onto existing Mn oxyhydroxide surfaces (Morris and Bale, 1979; Morris et al., 1982; Morris, 1986; Coffey, 1994). A combination of sorption/precipitation and colloidal destabilisation and aggregation within the high SPM turbidity maximum induced by initial saline increases are dominant processes for dissolved Mn removal, sufficient to overcome any other physical controls (i.e. DO concentration) on Mn chemistry.

Morris et al. (1982) identified that in the Tamar estuary over a neap to spring tidal cycle there was a change in the effect of this zone from Mn removal to addition, reflecting the change from net deposition to resuspension of bottom sediments (colloidal and truly dissolved metal in pore water release from anoxic sediments). This is clearly demonstrated in the April and October surveys that occurred during spring tides where

there is elevated colloidal (April) and truly dissolved/low molecular weight (October) manganese concentrations contrasting to the other surveys that occurred at neap or neap to spring tidal phases.

In several transects (August, October and December) there is significant elevations in the truly dissolved Mn concentrations in the lower estuary. Althaus (1992) observed similar tidally related dissolved Mn increases in the outer Humber. This is most significant and defined for the August survey. This remobilization of low molecular weight Mn (from colloidal phases) could be linked to disaggregation effects or photochemical transformations (Mn IV reduction) occurring at the higher salinity, low SPM surface waters which receive higher insolation. Anthropogenic inputs or sediment remobilization effects from intertidal muds around Spurn Bight may have some role.

Manganese is a redox sensitive element and transitions occur between the soluble Mn(II) and insoluble Mn(III) and Mn(IV). In all the transects there is a significant dissolved oxygen sag in association with the turbidity maximum. But the rapid removal of dissolved Mn indicates that estuarine processes are dominant enough to extensively remove Mn at low salinities despite low dissolved oxygen conditions. The effect of DO is more pronounced in the freshwaters of the Ouse compared to the Trent (Coffey, 1994). In surveys where Mn release is observed this is linked to additional sediment remobilization as a function of spring-neap stage or high flow event rather than a significant change in dissolved oxygen content.

Seasonal trends:

It has proved very difficult to determine any seasonal trends in Mn concentrations or partitioning. In most transects the Mn is highly colloidal and is removed in the low salinity regions apart from in the spring tide and higher combined riverine flow surveys (April and October) where the scavenging effect of the TMZ is reduced or it acts as a source of colloidal Mn. This is reflected in the April (and October) surveys where colloidal Mn is still observed at significant concentrations at Spurn. The rates of colloidal removal varies significantly between surveys. This is linked to the river flow (i.e. TMZ dilution) and the net effect of the TMZ at the time (neap/spring range). The lower DO conditions found in the summer months and ideal conditions for photoreduction do not

necessarily seem to have a significant effect on Mn concentration and partitioning (increase in truly dissolved manganese). In most cases any effects that are occurring are probably masked by the strong particle/Mn interactions in the low salinity region. In the July survey the release in truly dissolved Mn does not compensate for the decrease in concentration in the colloidal fraction. Here, the truly dissolved Mn release is more likely to be a desorption effect. However, it is possible that the truly dissolved Mn mid salinity maximum in the October survey may de due to photoreduction as colloidal Mn is still elevated in this area of the transect but SPM concentrations will be low.

The main seasonal contrast in Mn concentrations and partitioning was observed between the high flow February survey and the later, lower flow surveys. In the February survey the truly dissolved Mn concentrations were an order of magnitude higher (~80% of total dissolved) than those in the later surveys where Mn was highly colloidal. This has been attributed to increased erosion of anoxic sediments and truly dissolved Mn release due to the anomalously high flow. Unfortunately the impact of this truly dissolved Mn injection into the Humber estuary and its mediation by the TMZ was not observed.

Zinc: Figure 4.10d

Zinc is a comparatively less surface active element. However, the behaviour of Zn in the Trent/Humber transects exhibited no consistent input or removal over the five axial surveys. One consistent feature is that Zn resides mainly in the truly dissolved (low molecular weight) fraction and the conventional colloidal fraction is less significant. All the surveys (except July) illustrate removal of truly dissolved Zn in the low salinity region. Colloidal Zn can be removed in the low salinity, high turbidity region (July, December and to some extent October), but it can also act conservatively (August).

Removal of total dissolved Zn in the low salinity region has been observed periodically in the Humber by Coffey (1994) and routinely by Ackroyd et al., (1986) in the Tamar estuary. Although this type of decrease in dissolved Zn could be produced by a mixing of Trent and Ouse waters (dissolved Zn concentrations in the Ouse being significantly lower than in the Trent) this profile still exhibits removal on a mixing diagram. The potentially rapid uptake of Zn onto particles surfaces has been illustrated by Millward et al. (1992)

using Tamar estuary particles from the turbidity maximum zone. In the other Humber surveys this removal role of the turbidity maximum was minimal. The function of the TMZ (turbidity maximum zone) may fluctuate due to changes in active particle sites and flushing time (proportional to river flow) which dictates the extent of Zn sorption (Millward et al., 1992). Mainly, the characteristics of the TMZ and its overall effect on trace metal concentrations is governed by the changes in net sediment disturbance responding to spring-neap tidal energy variations and tidal pumping of a particular estuary.

Mid-estuarine, truly dissolved Zn maxima can be observed in most of the surveys over a salinity range from 3 to 15. This type of Zn behaviour has been observed in several studies in the Gironde (Kraepiel et al. 1997- 0 to 15‰) and Tamar (Ackroyd et al., 1986; Morris et al. 1978-3 to 20‰). Direct pore water infusions, desorption/dissolution from tidally resuspended sediment or seaward fluxing riverine particles or organic matter degradation have been proposed to explain the addition of truly dissolved Zn to the estuarine water column.

Dissolved Zn concentration is far more conservative over the lower section of the Humber and in the October survey. Zn conservation in the lower Humber estuary has been observed by Coffey (1994) and in the lower Beaulieu by Fang (1995). Conservative Zn behaviour over a complete transect has been observed in the October survey and for colloidal Zn in this study and by Elderfield et al. (1979) in the Conwy.

Seasonal trends:

All of the zinc transects are characterised by advective mixing of Trent and Ouse water or by removal of truly dissolved/colloidal Zn in the low salinity region. There is no consistent seasonal effect of river input concentrations so the main influences on the partitioning and concentration of Zn in the estuary appears to be the position and role of the TMZ. In April and partly in October the TMZ has a role of colloidal input in contrast to in the other surveys. In some surveys there is truly dissolved Zn release at mid and lower salinities via desorption processes.

Copper: Figure 4.10e

The dissolved Cu distribution for all surveys is far more consistent than for other metals. In general, dissolved Cu resides in the truly dissolved (lower molecular weight) fraction which can comprise 70 to 80% of total dissolved Cu (more in the lower estuarine reaches). In many estuaries the dissolved Cu tends to show conservative behaviour (mainly governed by the truly dissolved fraction) which has often been attributed to its strong complexation with organic ligands/DOM (Coale and Bruland, 1990) which also behaves conservatively under estuarine conditions (Van den Berg et al., 1987; Apte et al., 1990). Conservative behaviour of dissolved Cu has also been observed by Coffey (1994) for the Humber estuary and many authors for other estuaries (Eaton, 1979; Boyle et al., 1982; Danielsson et al. 1983; Edmond et al. 1985; Shiller and Boyle, 1987).
However, in the Trent/Humber in 1996 total dissolved Cu is rarely conservative, or occurs in the lower estuary. Although colloidal Cu behaves conservatively in the August survey its behaviour is inconsitent in the rest of the surveys. In all the surveys (except December) there is an input of truly dissolved (low molecular weight) Cu observed in the low salinity region (0 to 5‰) of the estuary (perhaps due to release from larger particles or an external source). This upper estuarine maximum is most pronounced in August. After the input of truly dissolved (low molecular weight) Cu there is generally conservative behaviour down the estuary. This <10KDa Cu input and subsequent conservative behaviour is converse to Cu removal observed by Ackroyd et al. (1986) in the Tamar and for the Rhine and Elbe (Duinker, 1980; Duinker et al., 1982).

This does not mean that Cu removal by adsorption onto particles in the TMZ is not occurring (zero salinity Cu concentrations for April survey especially are below the Trent river end-member concentration) it is more likely that this process is masked by other coincident effects. For example: Laxen (1985) illustrated that Cu adsorption onto hydrous ferric oxide is largely masked by a strong competitive complexation of Cu with soluble humics. Although Cu has a slower adsorption rate onto TMZ particles than Zn (Millward et al., 1992), 40% of dissolved Cu in some river waters may be removed during estuarine mixing due to apparent aggregation with colloidal Fe and humic substances (Sholkovitz and Copland, 1981). Even if these processes are occurring they are offset by more dominant sources of dissolved Cu. These processes could include;

transformation of Cu associated with organic polymers into lower molecular weight fractions, copper exchange from resuspended sediment, exchange from colloids during periods of higher river discharge (Windom et al., 1983), an increase in Cu solubility as a result of decreased pH. Millward and Moore (1982) also showed that the adsorption isotherm for Cu onto iron hydroxide increased with increasing pH. The zone of truly dissolved Cu input occurs in conjunction with a falling and lower pH which may inhibit Cu adsorption or encourage increased solubility. The salt marshes near Trent Falls have also been identified as a significant source for dissolved Cu, especially during the ebb tide (Coffey, 1994). This may be a contributory factor to Cu input in the low salinity zone but is perhaps too localised.

In the lower estuary there is some indication of progressive transfer of Cu from colloidal into a truly dissolved (low molecular weight) fraction. This may be linked to pH changes and Cu solubility. A similar conversion of Cu from high MW species in riverine waters to low molecular weight (<1KDa) species with increasing salinity has been observed by Powell et al. (1996) in the Ochlockonee Estuary. This has been attributed to progressive desorption of Cu from Fe-oxyhydroxides or dissociation from organics by major seawater ions (this process could also provide a truly dissolved maxima in the low salinity region).

Seasonal trends:

The seasonal copper transects are more consistent than had been observed for the more particle reactive elements. The Trent colloidal and truly dissolved Cu concentrations are relatively constant over the five seasonal transects but there is a suggestion of lower dissolved Cu concentrations (truly dissolved and colloidal) in the winter surveys (including the February survey) and an increase in truly dissolved Cu partitioning during the summer surveys. The lower winter Cu concentrations may be due to increased dilution but it is interesting to note that the truly dissolved concentrations in the estuary seem unaffected by the initial river inputs. The increase in truly dissolved Cu during the summer surveys is likely to be associated with the higher DOC levels in these months due to increased biological activity.

In addition, the truly dissolved releases/maximums in the low salinity region are most significant in the summer months (August). It is likely that during the summer more Cu

in the Trent is associated with organic particles/low molecular weight colloids. In the low salinity region organic matter can disaggregate (Eisma, 1986) forming low molecular organic colloids. This may account for the increase in apparent truly dissolved Cu. The increased association of Cu with organic low molecular weight colloids means that they are not removed quickly from the water column by aggregation processes and are carried further down the estuary. This may help explain why there is a significant truly dissolved Cu concentration even at high salinities whilst colloidal Cu has been removed.

Nickel: Figure 4.10f

Due to its dominant association with the refectory phase of particles (Campbell et al. 1988) dissolved Ni has often illustrated conservative behaviour in estuarine systems (Windom et al., 1988; Shiller and Boyle, 1991; Althaus, 1992). Dissolved Ni shows consistent conservative behaviour in the Trent/Humber transects but only in the lower estuary (>3‰). In the low salinity zone there is rapid decrease in total dissolved Ni (mainly truly dissolved/microcolloidal). This may be due to mixing with lower Ni concentration Ouse waters or some scavenging of low molecular weight / truly dissolved Ni onto larger particles in the turbidity maximum zone. Ni may be sorbed onto Fe-oxyhydroxide surfaces (Lion et al., 1982; Millward and Moore, 1982) or complexed with organic matter. Scavenging of truly dissolved Ni onto Fe colloidal material and removal from the dissolved pool by destabilisation and aggregation processes in the low salinity region is most likely. There is apparent removal of colloidal Ni (~20% of total dissolved Ni) via Fe colloid association by the same mechanism. Colloidal Ni is entirely removed in the lower estuary so truly dissolved (<10KDa) Ni is completely dominant(~100% of total dissolved).

Seasonal trends:

The Ni transects are little affected seasonally or by the tidal range at time of the survey (April and October surveys show no obvious differences from the other three more neap tide surveys although the colloidal concentrations are slightly elevated and removal is not as complete in the upper estuary). All the transects show the decrease in dissolved Ni (truly dissolved) in the low salinity region (most likely by mixing with Ouse water or removal within the TMZ) and then more conservative behaviour. Although the Ni

concentrations in the Trent and Ouse end-members may vary seasonally, (the total dissolved Ni input from the Trent freshwater end-member varies quite considerably, 250 to 500nmol/L), the predominance of Ni in the truly dissolved fraction and it's low particle affinity diminishes the seasonal impact of TMZ variability.

Cadmium: Figure 4.10g

Total dissolved cadmium is often found predominantly (>90%) in the truly dissolved phase in the Trent/Humber system, although, it is clear that particulate matter plays a crucial role in controlling the behaviour of Cd. In the low salinity region of the transects there is rapid decrease in total dissolved (predominantly truly dissolved) Cd. This may be a dilution effect or a removal of low molecular weight/truly dissolved Cd by coagulation/adsorption with colloidal Fe which is rapidly removed in this TMZ. This is mirrored to some extent in findings by Powell et al. (1996) where medium molecular weight (1 to 10 KDa) Cd was removed in the low salinity region in the Ochlockonee Estuary. In several surveys (April, July and October) an increased colloidal Cd percentage (20 to 40%) can be observed in the low salinity regions which is also rapidly depleted/diluted conservatively.

In many of the transects there is a mid-salinity total dissolved (truly dissolved) maximum. The actual range of the input (0 to 25‰) and position of the maximum is seasonally variable. The mobilisation of Cd from particulate material (no source from colloidal material) by substitution with major seawater ions (Mg^{2+} and Ca^{2+}) and subsequent formation of highly stable and soluble Cd-chloro complexes (Elbaz-Poulichet et al., 1987) is the most likely process for this increase. Although there is no comparative data for the Humber estuary, similar mid estuarine maxima in truly dissolved Cd have been observed in recent colloidal studies on the Gironde (Kraepiel et al., 1997) and San-Francisco Bay (Sanudo-Wilhelmey et al., 1996). Williams and Millward (in press) have proposed that desorption of Cd (and Zn) from permanently suspended particulate material (PSPM) in the low salinity tidal reaches will occur. This is perhaps demonstrated by the release of truly dissolved Cd from colloidal material in this region of the Trent/Humber system although this process seems to occur from particulate material in the mid estuary (this may include PSPM that is advected downstream). The broad shape

of the Cd maximum is produced by tidal advection of the higher Cd concentration water up the estuary or conservative Cd behaviour down stream. Confirmation of the desorption of Cd from particulate material and better resolution of the salinity range of this process would be given by particulate Cd data.

Seasonal trends:

Despite its usual partitioning into the truly dissolved phase Cd is greatly affected by particles in its estuarine behaviour. In many ways Cd behaves similarly to Zn although the mid transect maximum of truly dissolved Cd is far more evident. Although the Trent inputs of Cd are quite variable the overall behaviour of Cd is reproduced in each survey transect; low salinity removal/dilution of truly dissolved Cd, Cd desorption over a large salinity range and conservative mixing at high salinities. The April survey is in contrast to the other transects but this is probably linked to the increased tidal range and changing role of the TMZ.

4.4.9: Tidal cycle trace metal changes

A tidal cycle of observations was carried out at Derrythorpe Jetty on 29/30th July 1996. Samples were taken at regular intervals during the flood and ebb tides. The background parameters are plotted in Figure 4.11. The trace metal absolute concentration and percentage partitioning plots are found in Figures 4.12 a to g.

The salinity range encountered was 0 to 7 ‰. A small tidal bore was observed on the flood tide. This rapid influx of saline water (increase in water depth) was coincident with a spike in elevated DO (increase of ~ 25-30% saturation and 2mg/l). Concurrent with these changes was a sharp decrease in pH (from 7.6 to 7.3) and an increase in salinity to a maximum 2 hours later. Over slack water at high tide, the DO levels fall to lower than measured previously (30%/2.5mg/l) and there is a coincident decrease in turbidity (increased transmission) and increase chlorophyll-a. The decreased turbidity and concomitant chlorophyll-a maxima (are removed downstream) as the tide turns after high tide. At the beginning of the tidal cycle the Trent river water is the predominant signal but this is progressively influenced by the tidal prism towards high tide. As the tide drops the river water again becomes more dominant.

Iron: Figure 4.12a

Total dissolved Fe is entirely colloidal (>95%). The tidal bore injects a significant amount of colloidal Fe into the surface waters (this may be due to shear disaggregation of larger aggregates or associated resuspension) illustrated by the elevated Fe levels after the DO spike and increased salinity. After the bore there is pronounced removal of this colloidal material. This is probably due to destabilisation and aggregation effects within the turbidity maximum or aggregation and settling of colloidal flocs during slack water.

Lead: Figure 4.12b

Lead is also a highly colloidal element and is affected by the tidal cycle in a similar way to Fe. Total dissolved/colloidal Pb levels are initially increased after the bore but Pb is quickly removed from the water column, either by aggregation effects concomitant with Fe colloids or by scavenging onto particles in the turbidity maximum.

Figure 4.11: Background data over a tidal cycle (July 1996)

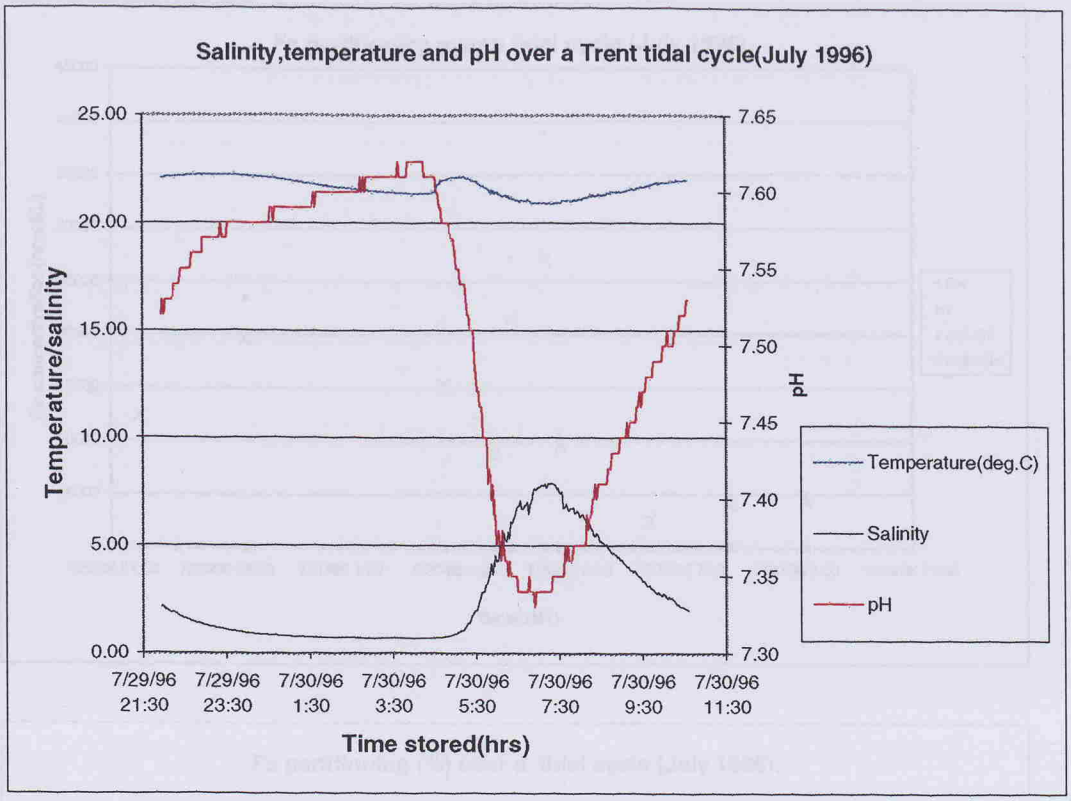

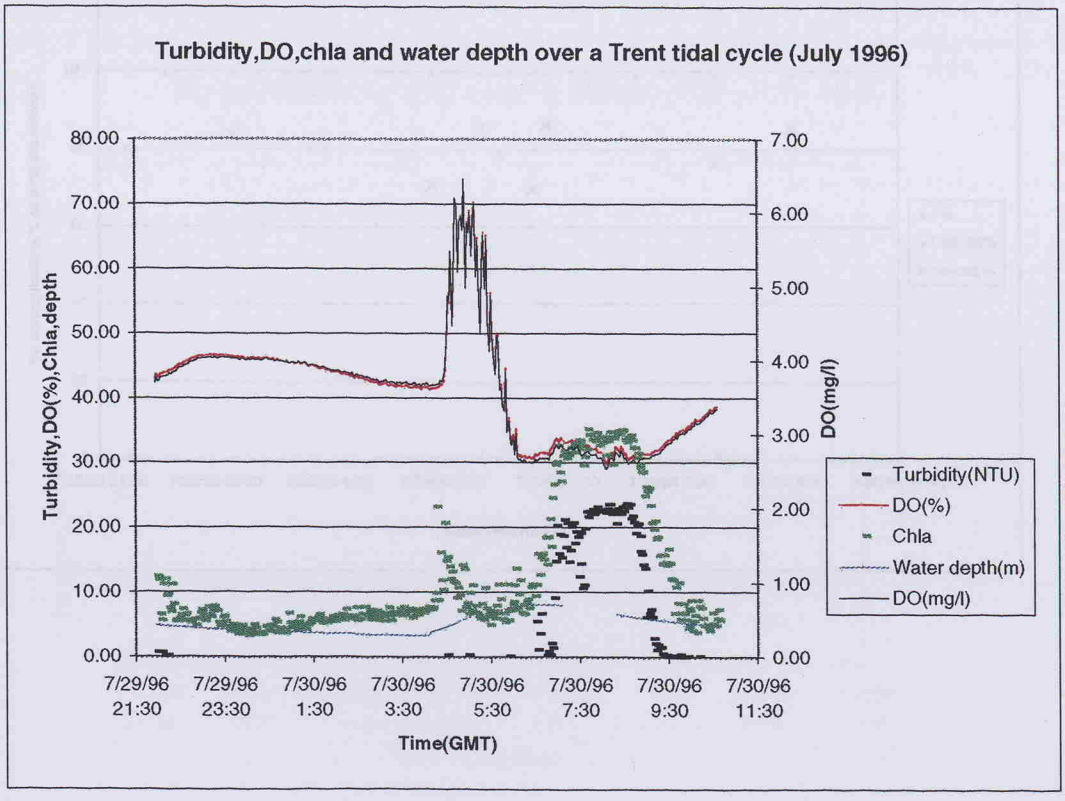

Figure 4.12a

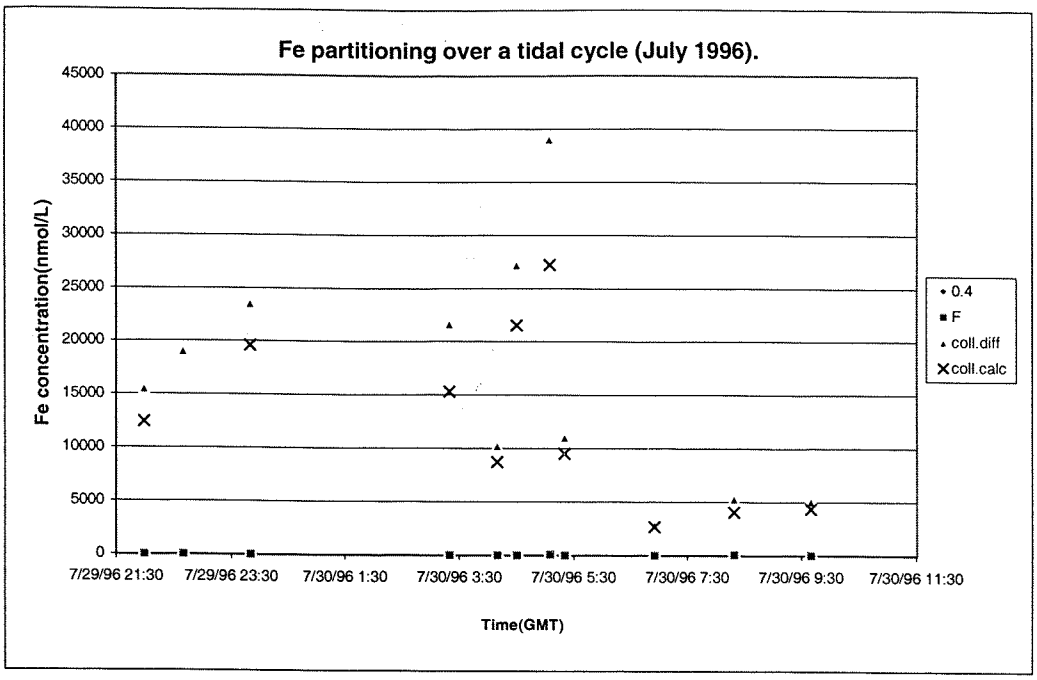
Fe partitioning over a tidal cycle (July 1996).
Fe concentration(nmol/L)
45000
40000
35000
30000
25000
20000
15000
10000
5000
0
7/29/96 21:30
7/29/96 23:30
7/30/96 1:30
7/30/96 3:30
7/30/96 5:30
7/30/96 7:30
7/30/96 9:30
7/30/96 11:30
Time(GMT)
0.4
F
coll.diff
coll.calc

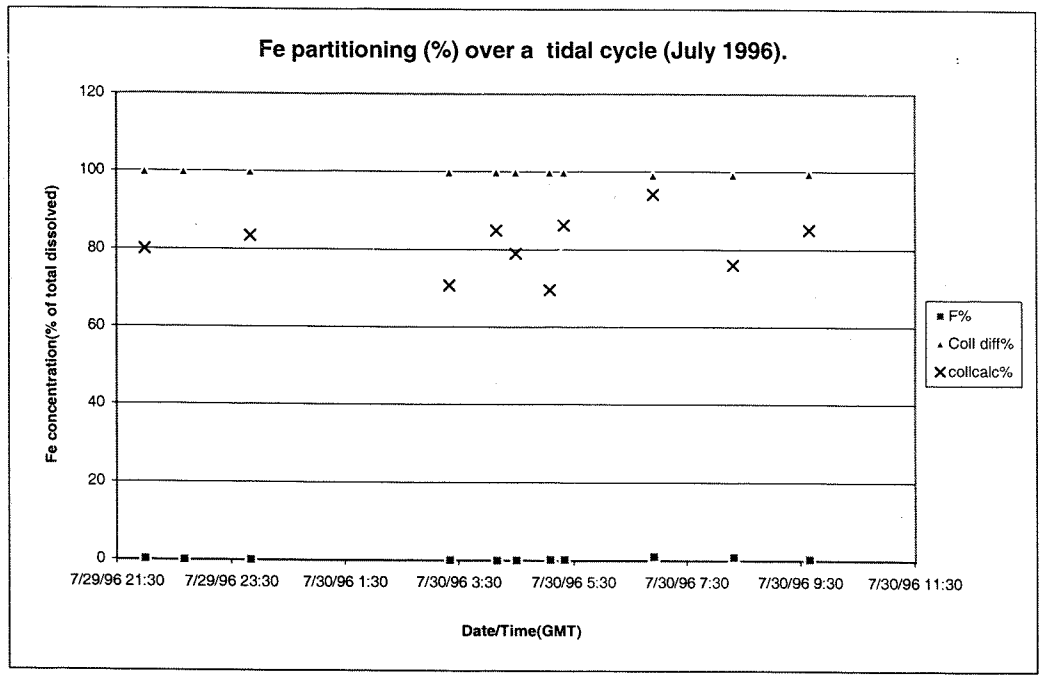
Fe partitioning (%) over a tidal cycle (July 1996).
Fe concentration(% of total dissolved)
120
100
80
60
40
20
0
7/29/96 21:30
7/29/96 23:30
7/30/96 1:30
7/30/96 3:30
7/30/96 5:30
7/30/96 7:30
7/30/96 9:30
7/30/96 11:30
Date/Time(GMT)
F%
Coll diff%
collcalc%

Figure 4.12b:

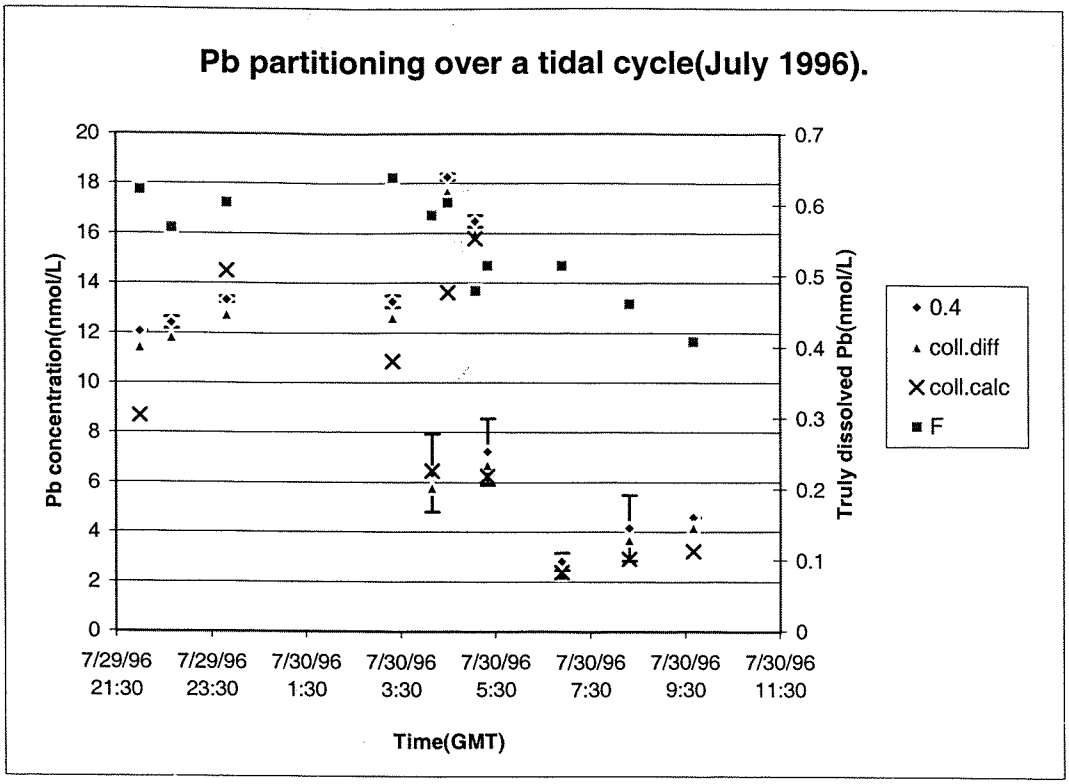
Pb partitioning over a tidal cycle(July 1996).
Pb concentration(nmol/L)
Truly dissolved Pb(nmol/L)
0.4
coll.diff
coll.calc
F
7/29/96 21:30
7/29/96 23:30
7/30/96 1:30
7/30/96 3:30
7/30/96 5:30
7/30/96 7:30
7/30/96 9:30
7/30/96 11:30
Time(GMT)

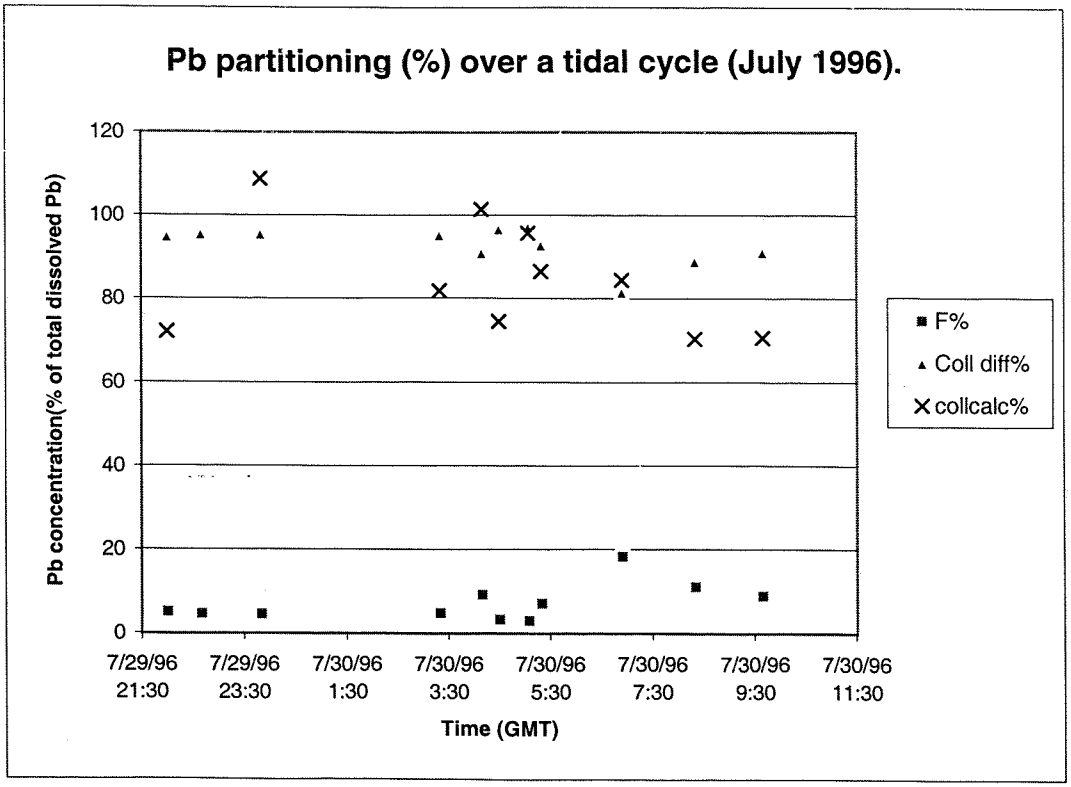
Pb partitioning (%) over a tidal cycle (July 1996).
Pb concentration(% of total dissolved Pb)
F%
Coll diff%
collcalc%
7/29/96 21:30
7/29/96 23:30
7/30/96 1:30
7/30/96 3:30
7/30/96 5:30
7/30/96 7:30
7/30/96 9:30
7/30/96 11:30
Time (GMT)

There is a progressive removal of truly dissolved (low molecular weight) Pb with increased salinity and SPM. This indicates that this form of Pb is more likely a low molecular weight colloidal Pb form that is being removed by similar processes to those affecting larger colloids.

Manganese: Figure 4.12c

Manganese is also predominantly colloidal but does not exhibit as significant an increase in colloidal/total dissolved concentrations associated with the bore. Concurrent with Fe and Pb there is colloidal Mn removal in the higher salinity and turbidity region. There is some increase in truly dissolved Mn in the lower DO region after the bore. This truly dissolved Mn release is most likely to be linked to redox effects (Mn^{2+} release from Mn oxyhydroxides (Mn IV)) or photoreduction processes in the surface waters (although the SPM may be too high to allow this to occur). Desorption or pH effects may also be significant.

Zinc: Figure 4.12d

Zinc is a comparatively less surface active element than Fe, Pb or Mn and therefore has reduced partitioning into the colloidal fraction. Prior to the bore the total dissolved, truly dissolved and colloidal Zn fractions are relatively stable. There is a more discrete input of dissolved Zn (in the colloidal form) by the bore (perhaps from shear disaggregation of larger aggregates) but overall after this there is no net change in total dissolved Zn in the higher salinity regime. With the salinity increase there is an increase in truly dissolved (low molecular weight) Zn and a decrease in colloidal Zn from the bore associated maximum. These changes indicate a repartitioning of Zn from the colloidal to lower molecular weight species. This may be due to disaggregation effects in the increased shear of the tidal bore or desorption effects as pH decreases and salinity rises. It is probable that some scavenging of colloidal Zn within the turbidity maximum is also occurring.

Figure 4.12c:

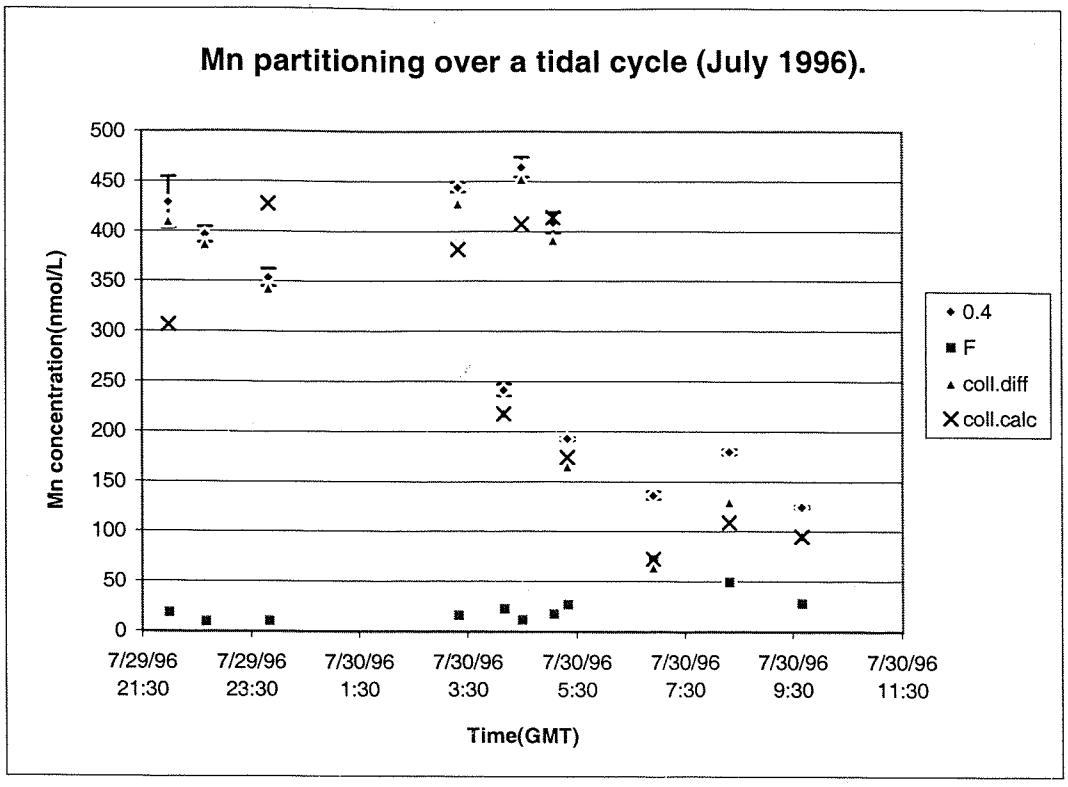
Mn partitioning over a tidal cycle (July 1996).
Mn concentration(nmol/L)
500
450
400
350
300
250
200
150
100
50
0
7/29/96 21:30
7/29/96 23:30
7/30/96 1:30
7/30/96 3:30
7/30/96 5:30
7/30/96 7:30
7/30/96 9:30
7/30/96 11:30
Time(GMT)
0.4
F
coll.diff
coll.calc

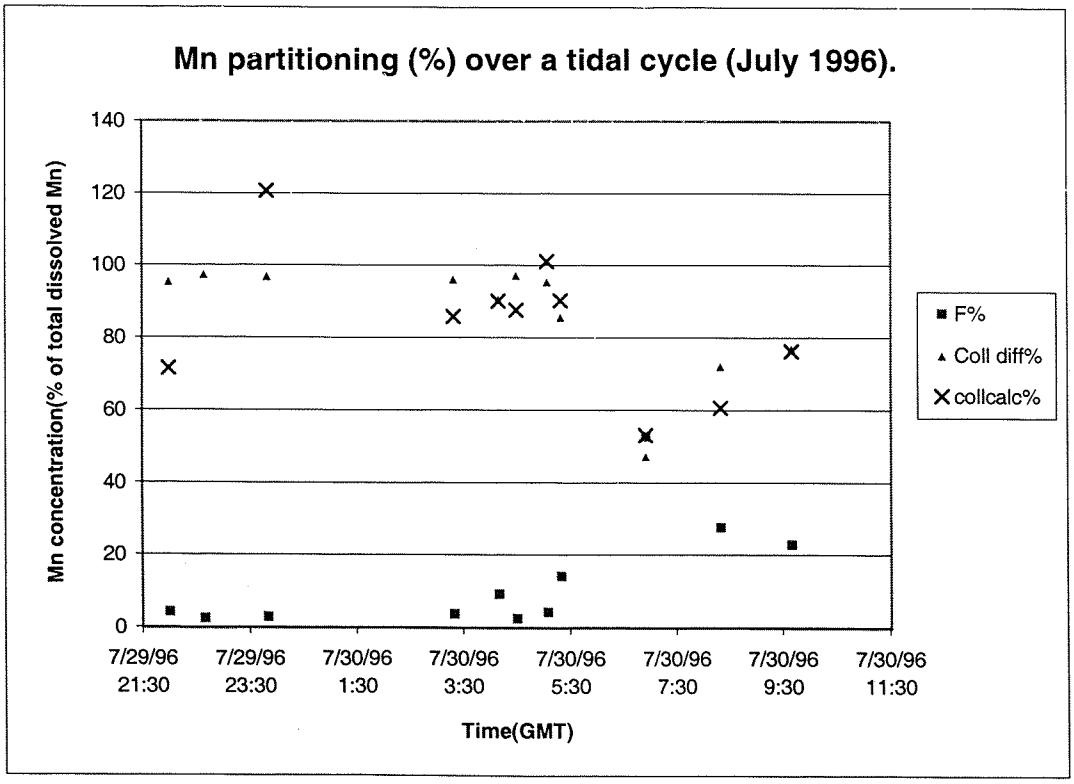
Mn partitioning (%) over a tidal cycle (July 1996).
Mn concentration(% of total dissolved Mn)
140
120
100
80
60
40
20
0
7/29/96 21:30
7/29/96 23:30
7/30/96 1:30
7/30/96 3:30
7/30/96 5:30
7/30/96 7:30
7/30/96 9:30
7/30/96 11:30
Time(GMT)
F%
Coll diff%
collcalc%

Figure 4.12d:

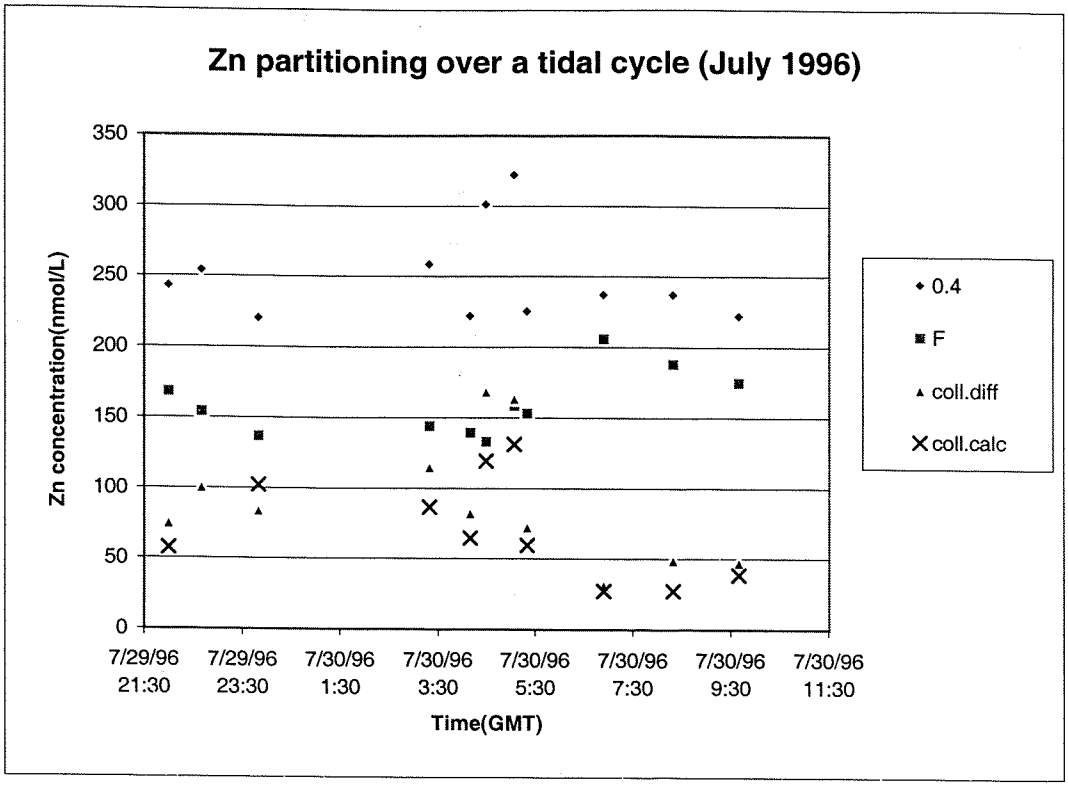
Zn partitioning over a tidal cycle (July 1996)
Zn concentration(nmol/L)
350
300
250
200
150
100
50
0
7/29/96 21:30
7/29/96 23:30
7/30/96 1:30
7/30/96 3:30
7/30/96 5:30
7/30/96 7:30
7/30/96 9:30
7/30/96 11:30
Time(GMT)
0.4
F
coll.diff
coll.calc

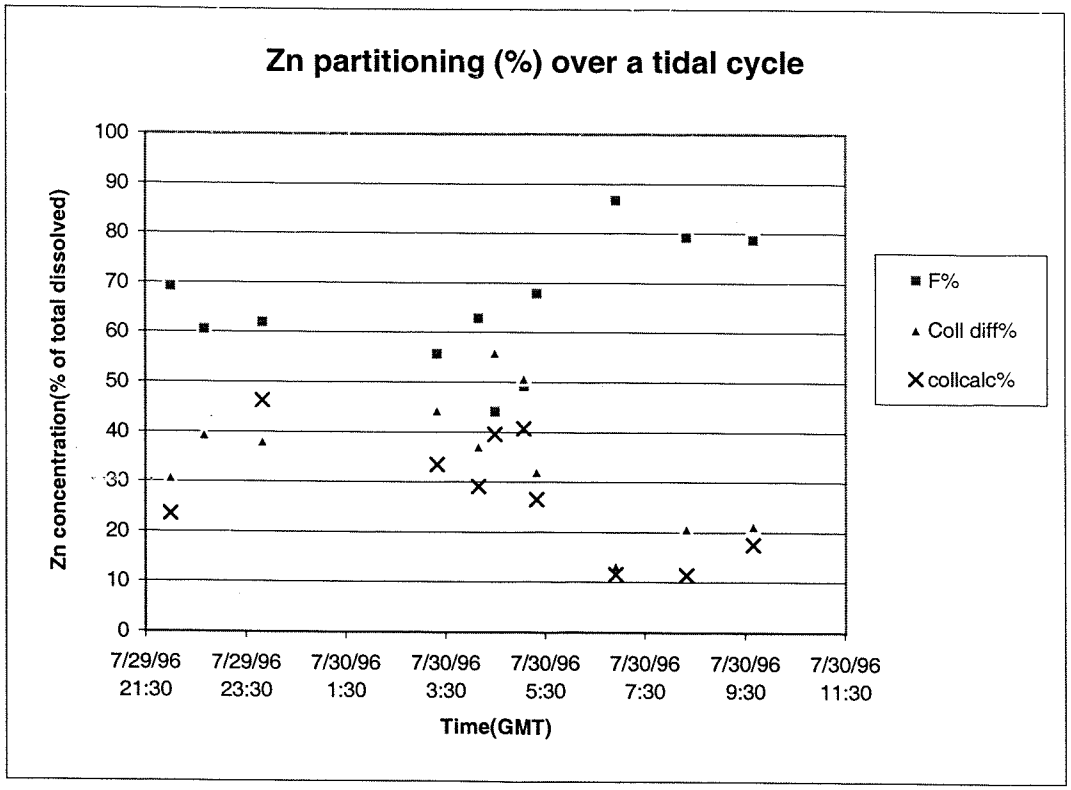
Zn partitioning (%) over a tidal cycle
Zn concentration(% of total dissolved)
100
90
80
70
60
50
40
30
20
10
0
7/29/96 21:30
7/29/96 23:30
7/30/96 1:30
7/30/96 3:30
7/30/96 5:30
7/30/96 7:30
7/30/96 9:30
7/30/96 11:30
Time(GMT)
F%
Coll diff%
collcalc%

Copper: Figure 4.12e

All copper fractions (total dissolved, colloidal and truly dissolved) exhibit a brief elevation in concentration with the passing of the tidal bore (perhaps due to disaggregation, resuspension, desorption or increased solubility effects. Total dissolved and truly dissolved Cu concentrations are not significantly altered by the increasing tidal (seawater) influence. The colloidal Cu fraction remains elevated up to and after high tide. This change in the colloidal fraction could be linked to its complexation with DOM which may mask any removal effects in the turbidity maximum. The enhanced biological activity in this zone (higher chlorophyll a) may also attribute to higher colloidal Cu.

Nickel: Figure 4.12f

There is no striking effect of the tidal bore on Ni concentration (probably due to its predominant association with the refractory phase of particles) but there is significant removal of total dissolved (mainly truly dissolved) Ni as salinity begins to rise. Removal of Ni in this low salinity zone is often linked to scavenging onto larger particles (sorption onto Fe-oxyhydroxide surfaces or complexation with organic matter). Within the turbidity maximum there is progressive release of truly dissolved Ni, probably via desorption from particles.

This decrease in truly dissolved Ni with increasing salinity/decreasing pH and then apparent release of truly dissolved Ni from particles upon salinity decrease seems geochemically inverse. It is likely that Ni is displaying conservative behaviour here (it is predominantly associated with refractory phases of particles) and the increase and decreases are products of the mixing and comparative dominance of the River Trent or seawater Ni signals.

Cadmium: Figure 4.12g

Although Cd is found predominantly in the truly dissolved phase, particulate material has a significant role in controlling its behaviour. During the passage of the bore there is a pulse in colloidal Cd. This is associated with the pulse in SPM. As salinity increases there is an increase in truly dissolved Cd until it comprises 100% of the total dissolved Cd. There is also rapid decrease in colloidal Cd concentrations.

Figure 4.12e:

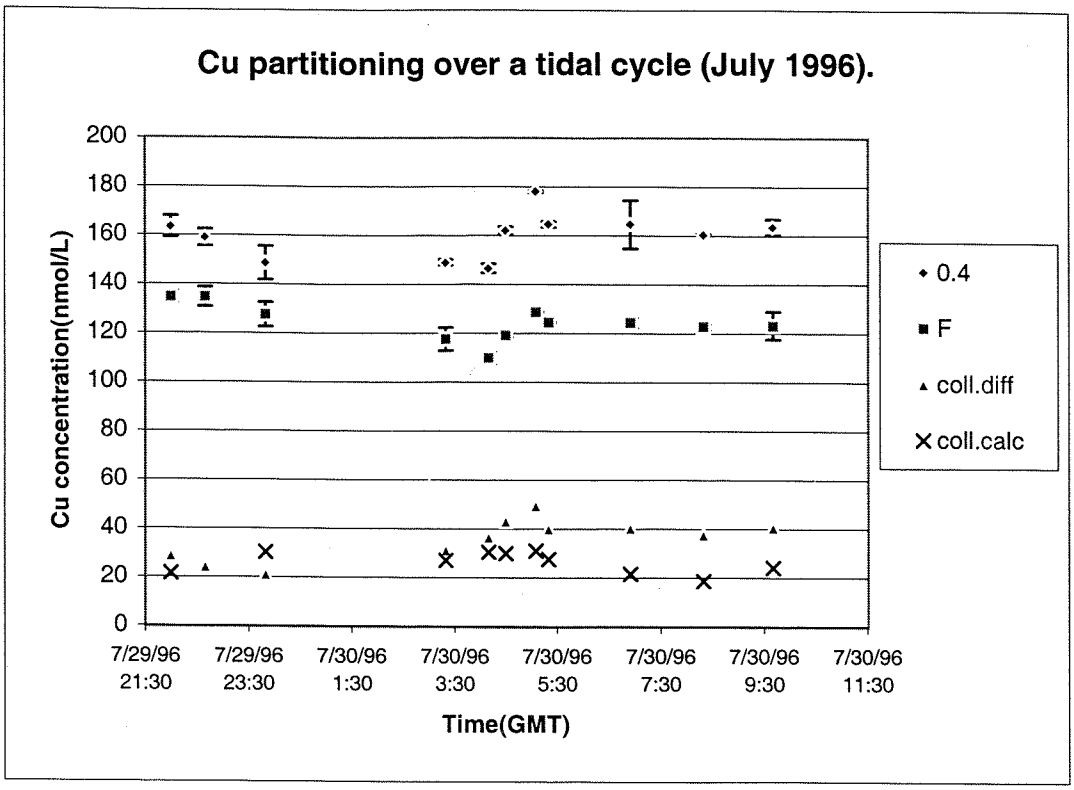
Cu partitioning over a tidal cycle (July 1996).
Cu concentration(nmol/L)
200
180
160
140
120
100
80
60
40
20
0
7/29/96 21:30
7/29/96 23:30
7/30/96 1:30
7/30/96 3:30
7/30/96 5:30
7/30/96 7:30
7/30/96 9:30
7/30/96 11:30
Time(GMT)
0.4
F
coll.diff
coll.calc

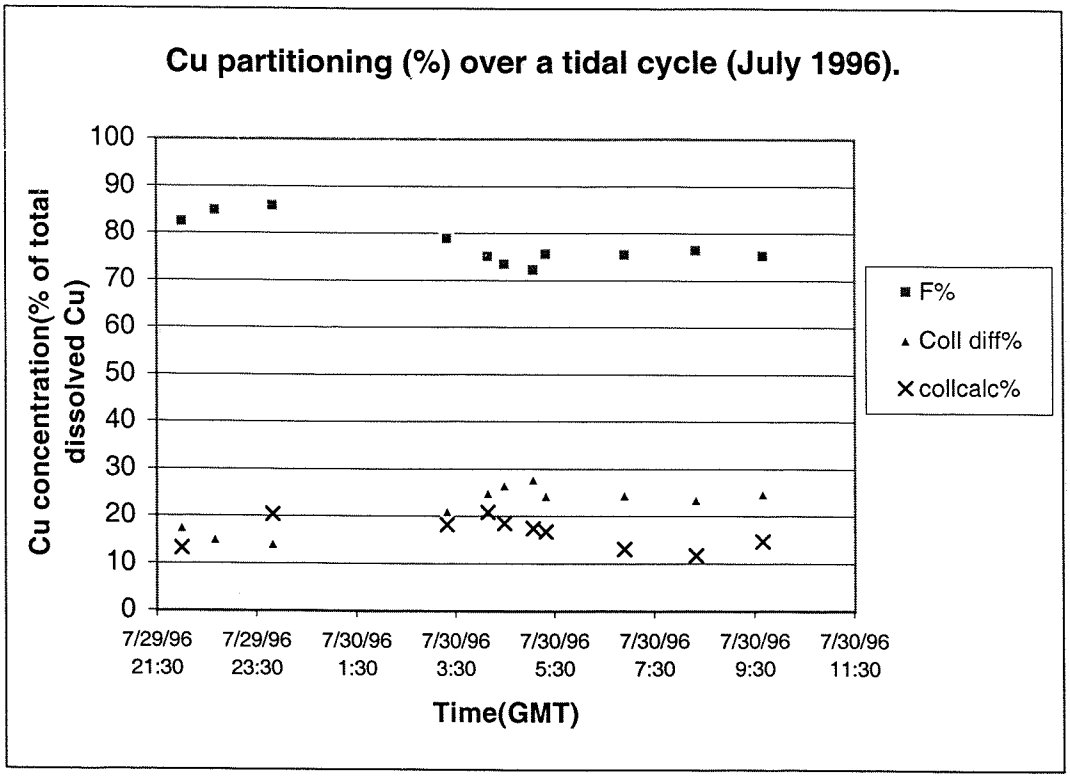
Cu partitioning (%) over a tidal cycle (July 1996).
Cu concentration(% of total dissolved Cu)
100
90
80
70
60
50
40
30
20
10
0
7/29/96 21:30
7/29/96 23:30
7/30/96 1:30
7/30/96 3:30
7/30/96 5:30
7/30/96 7:30
7/30/96 9:30
7/30/96 11:30
Time(GMT)
F%
Coll diff%
collcalc%

Figure 4.12f:

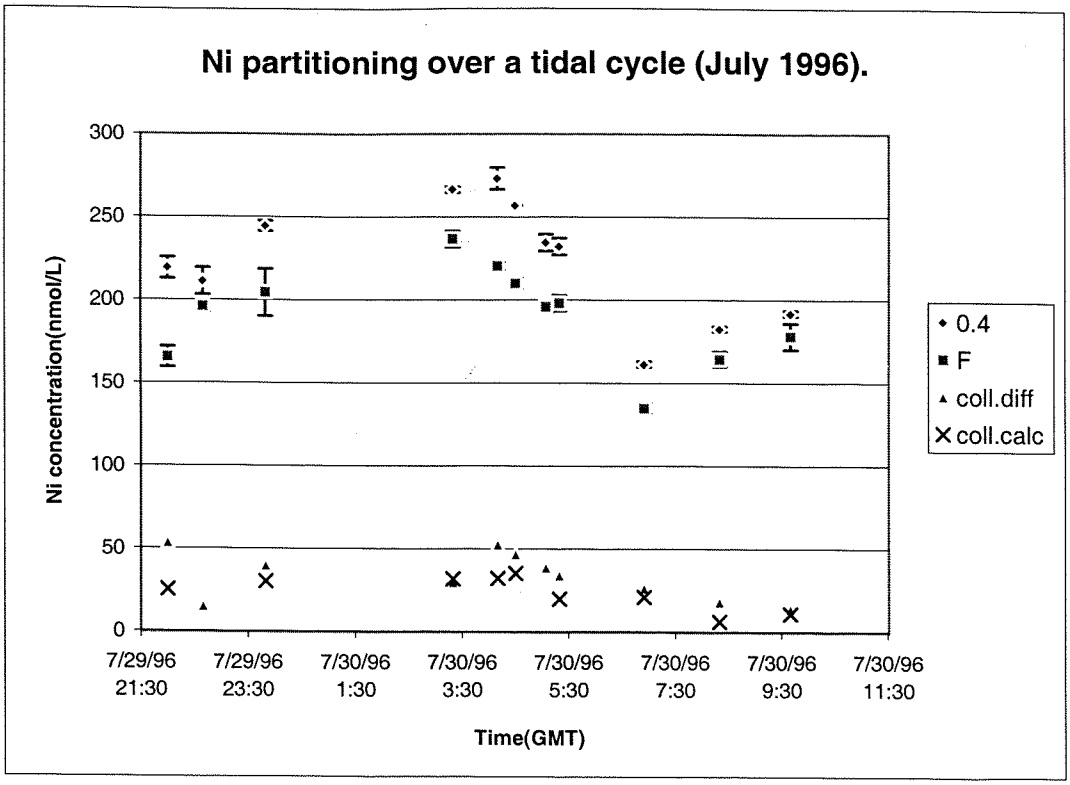
Ni partitioning over a tidal cycle (July 1996).
Ni concentration(nmol/L)
300
250
200
150
100
50
0
7/29/96 21:30
7/29/96 23:30
7/30/96 1:30
7/30/96 3:30
7/30/96 5:30
7/30/96 7:30
7/30/96 9:30
7/30/96 11:30
Time(GMT)
0.4
F
coll.diff
coll.calc

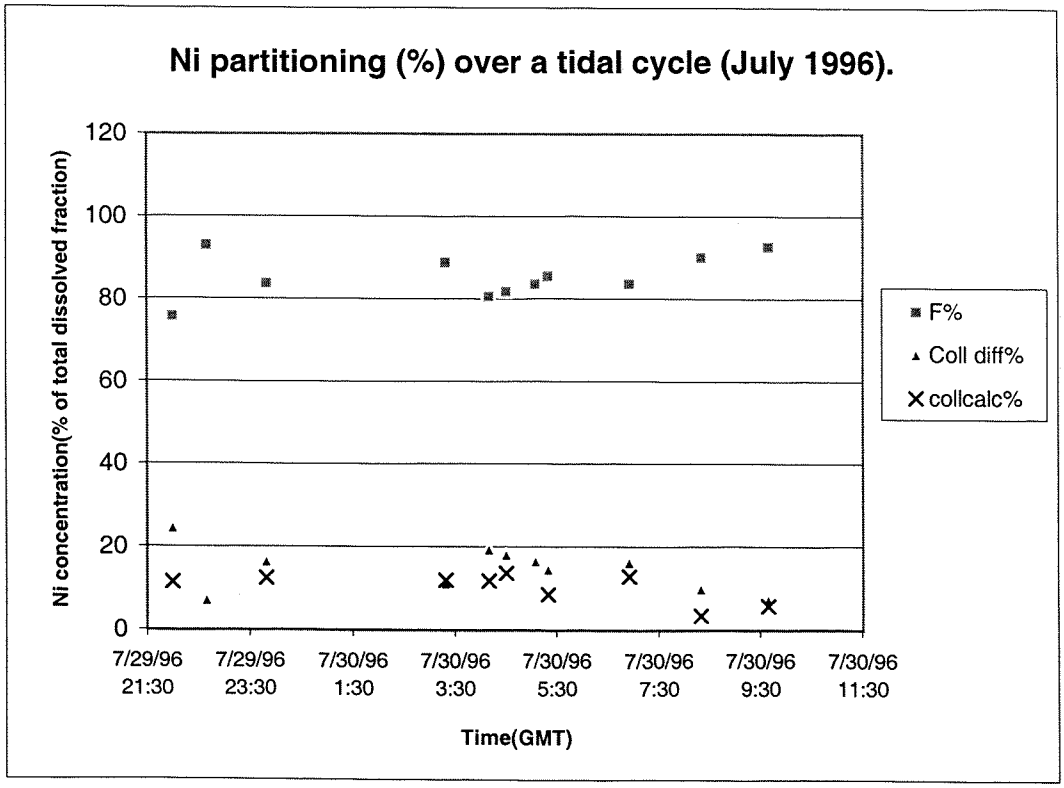
Ni partitioning (%) over a tidal cycle (July 1996).
Ni concentration(% of total dissolved fraction)
120
100
80
60
40
20
0
7/29/96 21:30
7/29/96 23:30
7/30/96 1:30
7/30/96 3:30
7/30/96 5:30
7/30/96 7:30
7/30/96 9:30
7/30/96 11:30
Time(GMT)
F%
Coll diff%
collcalc%

Figure 4.12g:

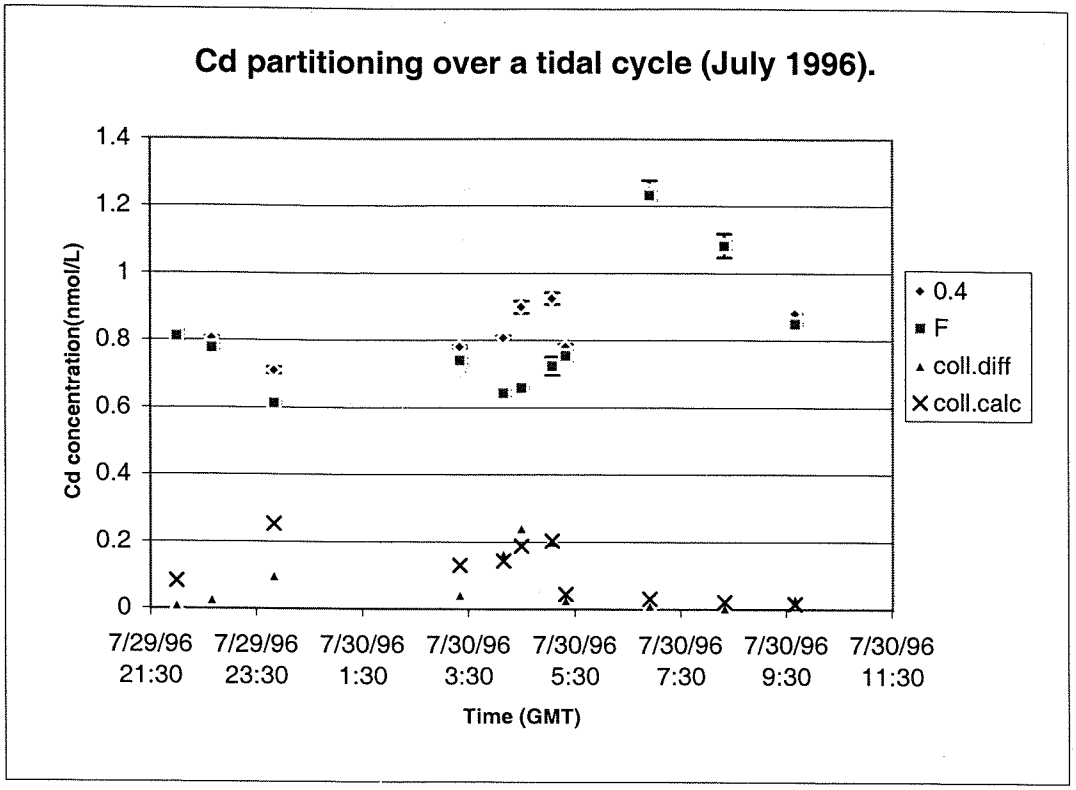
Cd partitioning over a tidal cycle (July 1996).
Cd concentration(nmol/L)
1.4
1.2
1
0.8
0.6
0.4
0.2
0
7/29/96 21:30
7/29/96 23:30
7/30/96 1:30
7/30/96 3:30
7/30/96 5:30
7/30/96 7:30
7/30/96 9:30
7/30/96 11:30
Time (GMT)
0.4
F
coll.diff
coll.calc

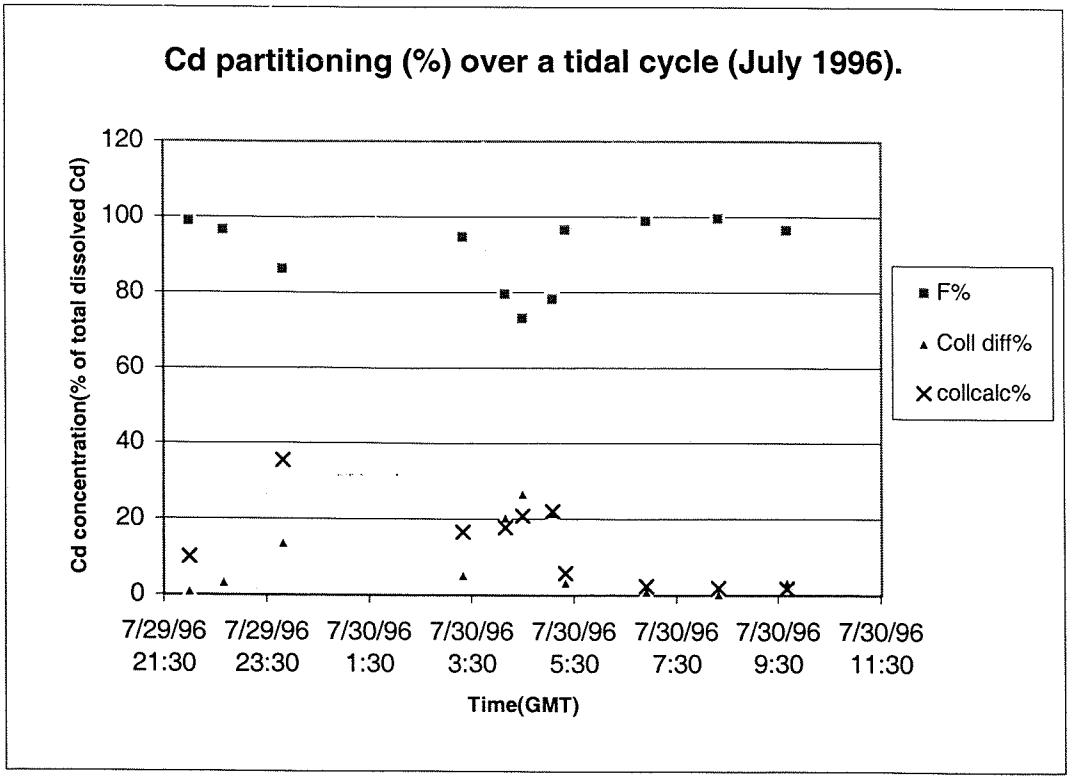
Cd partitioning (%) over a tidal cycle (July 1996).
Cd concentration(% of total dissolved Cd)
120
100
80
60
40
20
0
7/29/96 21:30
7/29/96 23:30
7/30/96 1:30
7/30/96 3:30
7/30/96 5:30
7/30/96 7:30
7/30/96 9:30
7/30/96 11:30
Time(GMT)
F%
Coll diff%
collcalc%

These changes in Cd partitioning are representative of the association of Cd with colloidal Fe at low salinities which can be removed by coagulation process in the turbidity maximum zone. The increase in truly dissolved Cd with increasing salinity is indicative of the mobilisation of Cd from particulate material by substitution with seawater ions (Mg^{2+} and Ca^{2+}) and formation of stable, soluble Cd-Chloro complexes. The decrease in truly dissolved Cd once salinity begins to decrease and pH increases indicates the reversibility of the association of Cd with SPM and the effect of pH on sorption/desorption processes.

4.5: Trace metals in the Trent/Humber system: summary, conclusions and future work.

Storage experiments of bulk (unfiltered) and colloidal (0.4μm filtered) samples from a range of salinities indicated detectable decreases in the colloidal fraction due to the inherent unstable nature of colloidal material and aggregation during storage to particles >0.4μm or large enough to sediment. Metals with significant colloidal fractions (Fe, Pb, Mn) were most affected. Metal concentration changes in the bulk samples were faster than those in the colloidal samples, probably due to increased SPM (>0.4μm) which catalysed aggregation and sedimentation changes. Adsorption/desorption changes were smaller in comparison.

Prefiltration experiments and comparisons indicated that filtration protocol could greatly affect the total dissolved concentration of a given metal. As had been suggested by previous authors (Buffle and Leppard, 1992; Taylor and Shiller, 1996; Horowitz et al., 1996 a and b) the retention of colloidal material by clogged filters was identified as causing the apparent decrease in dissolved metal with increasing filtrate volume. Colloidal concentrations were increased when the sample volume per filter was reduced.

The application of different prefiltration protocols has significant implications for dissolved metal determinations. This was best illustrated in a direct comparison of dissolved metal concentrations determined for identical original samples but using complete (Tappin) or decanted (Parker) samples prior to filtration. Considerable differences in the total dissolved fractions were observed for metals with significant colloidal fractions i.e. Fe, Pb, Mn and Cu. Whereas there was little/reduced effect for metals that where not highly colloidal Ni, Zn, Cd. The significance of retention of colloidal material using conventional filtration protocol (Tappin) indicates that in high SPM environments, or samples with significant particle distributions close to the 0.4μm prefiltration cut-off it is likely that dissolved metal measurements have effectively removed a large percentage of colloidal material from the filtrate and therefore dissolved concentrations have been increasingly underestimated. Indeed, for highly colloidal elements the measurements made by conventional filtration protocol (Tappin) are closer to a truly dissolved (<10,000MW) measurement in this study. Standardisation of

filtration protocol and therefore of the nature of the "dissolved" fraction is required before trace metal concentrations can be truly comparable.

Although CFF is heralded as the solution to most problems that occur with conventional filtration in estuarine environments with high colloidal loadings and organic material concentrations the separation of dissolved fractions is by no means ideal. Although the mass balance recoveries for most metals were good (>90%), some highly colloidal metals showed poorer recoveries (60-80%) due to interaction of the colloidal material with the filter membrane. Although the colloidal measurements by difference depends less on a given sample characteristics (SPM, colloidal composition and morphology, DOC, salinity) and is therefore more reliable , it gives no indication of the samples interaction with the CFF system and therefore potential changes to the truly dissolved fraction via breakthrough effects. Both colloidal measurements (difference and direct measurement) are required to give a more informed colloidal measurement.

Concentrations of Fe, Pb, Mn, Cu, Zn, Ni and Cd in total dissolved, colloidal and truly dissolved fractions were determined for Trent/Humber transects throughout 1996. Seasonal and tidal aspects of trace metal behaviour were investigated. Analytical (extraction and metal analysis) quality of the data was checked using certified reference materials and digestion checks on the extraction protocol. Upper (colloidal difference) and lower (colloidal calculated from retentate) estimates of the colloidal trace metal concentration were assessed for each sample to allow data interpretation in the context of filtration artefacts.

Table 4.7 summarises the controlling factors on the partitioning and seasonal/inter-survey variability of trace metal behaviour in the Trent/Humber system.
Iron, lead and manganese were all observed to be highly colloidal metals in the Trent and Humber. The colloidal fractions of these metals were removed efficiently from the dissolved pool in the low salinity region that routinely coincided with the turbidity maximum (TMZ) and low dissolved oxygen zone. Flocculation/coagulation mechanisms here transported colloidal metals into larger particles and to the sediments. Any inter-survey variability of the metals distribution was closely linked to the characteristics of the TMZ (seasonal or tidally driven).

Table 4.7: Axial trace metal behaviour and controlling factors of inter-survey variability in the Trent/Humber.

Metal	Predominant total dissolved metal fraction	*Total dissolved* behaviour	*Colloidal* trace behaviour	*Truly dissolved* (microcolloidal) behaviour	Seasonal/inter survey variability
Fe	Colloidal	Removal in low salinity region.	Removal in low salinity region	Upper estuarine maximum (5-10ppt)	TMZ function (tidal vs. river flow)
Pb	Colloidal	Removal in low salinity region.	Removal in low salinity region	Removal in low salinity region (microcolloids)	TMZ function (tidal vs. river flow)
Mn	Colloidal Truly dissolved (Feb)	Very rapid removal at low salinity (<Fe)	Very rapid removal at low salinity	Removal, mid estuarine max, photochemistry	TMZ function (tidal vs. river flow)
Zn	Truly dissolved. Colloidal in April/Oct-high tide range/R.flow	Low salinity removal, small mid estuarine addition	Low salinity removal, complete removal by mid-lower estuary.	Low salinity removal, small mid estuary addition.	TMZ function (tidal vs. river flow)
Cu	Truly dissolved (microcolloids) Incr. colloid in springs TMZ	Upper estuarine maximum, conservative higher salinities.	Conservative, elevated April/Oct. Slight removal Dec.	Upper estuarine max., conservative Dec and higher salinities (S>20)	Seasonal influx of organic microcolloids, TMZ for colloids.
Ni	Truly dissolved	conservative mixing/low salinity removal. Conservative high salinities	Removed very rapidly at low salinities. More significant spring tides.	Rapid removal at low salinity/conservative mixing, conservative at high salinities	Little seasonal or TMZ (tidal) effects. Apr/Oct-spring dominated increased colloids.
Cd	Truly dissolved although colloidal significant in	Sorption/removal of microcolloids low	Very low/variable behaviour, low salinity	Low S removal, mid est. max (Cl complex / SW	Seasonal position of mid est. maximum (river

Uncles et al. (in press) observed that in the winter and spring months the Humber TMZ is more dilute and occurs further down the estuary whereas in the summer the TMZ is most concentrated and occurs further up in the estuary. Additionally, the TMZ may occur above or below the fresh/saltwater interface depending on river flows and season. Aside from this seasonal effect, in this study the neap/spring state of the tide was observed to have a larger effect on the net role of the TMZ in metal partitioning/removal. For example, during higher tidal ranges in the spring tides there is often increased sediment erosion (Morris et al., 1982) and the TMZ can act as a source of dissolved (colloidal and truly dissolved) metals (April and October surveys). This in turn affects the axial transport of metals towards the Humber mouth. During lower tidal ranges the TMZ has a more pronounced role of trace metal removal.

Truly dissolved manganese shows several anomalies to this general removal behaviour as concentrations can be elevated by photoreduction effects when SPM declines (higher salinities) or release of anoxic porewater from resuspended sediments (February resuspension of winter accumulated sediments during a spate event-Uncles in press).

Nickel has a minimal colloidal association and is not really affected by the TMZ, although in some estuaries it may be scavenged by colloidal iron. In the Trent/Humber system it has a transect comprising of two conservative mixing lines between; Trent and Ouse water and riverine and seawater (below the confluence). Because of this minimal effect of the TMZ there is little seasonal effect on Ni behaviour and the profiles are very uniform and reproducible throughout the year.

Zinc and cadmium are geochemically very similar in their behaviour in the Humber. Both elements undergo adsorptive removal /mixing or dilution at high salinities. This removal effect is more pronounced for Zn than Cd. As particles are advected downstream Cd and to a lesser extent Zn desorb to create mid salinity truly dissolved maxima (a benthic source of truly dissolved Cd and Zn is also possible but there is minimal evidence for this). Desorption of Cd is caused by ion competition exchange effects with Ca^{2+} and Mg^{2+} or complexation with chloride ions (Elbaz-Poulichet et al., 1987; Comans and van Djik, 1988; Kraepiel et al., 1997). Similar mechanisms may account for the Zn release but occur to a lesser extent (Kraepiel et al., 1997). Williams and Millward (in press) have indicated that sufficient Cd and Zn desorption from permanently suspended particulate material (PSPM) may be sufficient to account for these maxima. The PSPM is defined by

three hours settling and is less than 15μm, combining colloidal and also larger particulate material so significant down estuary transport is possible. Again the behaviour of these metals is mediated by the TMZ and seasonal and tidal effects on its position and SPM concentrations.

Copper is usually linked with Zn in its estuarine behaviour and normally displays removal in the low salinity region. However, although Cu shows a lower truly dissolved concentration at low salinities and a truly dissolved Cu maximum at low salinities in the TMZ, colloidal Cu is removed further down the estuary or behaves conservatively. This Cu behaviour contrasting to all the other metals suggests (as in Kraepiel et al., 1997) that there may be two pools of colloidal (low molecular weight and particulate) material present in the Trent/Humber system; Fe oxides which coagulate in the low salinity zone (associated with the TMZ) and can scavenge other trace metals (Pb, Mn some Zn and Cd) from the water column, but also organic macromolecules which are effectively dissolved constituents so they behave more or less conservatively. This is seen for truly dissolved (and to some extent colloidal) fractions after the initial truly dissolved increase. This increase is partially explained by conformation changes in humic acids and mobilisation of carbohydrates that occurs at low salinities and can lead to disaggregation of microflocs (Eisma, 1986) into low molecular weight colloids (seen here as truly dissolved). Cu behaviour is far less seasonally dependant as there is little effect of the TMZ size or position on Cu concentrations and partitioning. Although the observed Cu changes are small, undoubtedly the concentration and type of organic macromolecules/polymers will alter seasonally.

Conclusions:

The main factor in controlling the inter-survey variability of trace metal behaviour throughout the estuary has been the processing of metals within the turbidity maximum. Although DO and pH changes in the TMZ may have significant impact on the behaviour of trace metals in this region (lower pH promotes desorption, indicates resuspension, lower DO in the summer months due to increased particle bacteria respiration (Uncles in press) may affect redox sensitive elements –Mn) it is the overall intensity and positioning

of the TMZ that seems to be the predominant control on particle/colloid associated species.

In this low salinity region (TMZ) colloidally associated metals can be rapidly removed (Mn, Fe, Pb) although metals with significant microcolloidal populations (Pb, Fe) may be transferred further down the estuary before removal. The positioning and intensity of the TMZ can vary with tidal state and season (Uncles et al. in press). During higher river flow the SPM concentrations within the TMZ are diluted and the TMZ is pushed further downstream. Also during spring tides the tidal forcing and resuspension of colloidal material is elevated. Both these conditions occurred in the April and October surveys which lead to increased colloidal metal concentrations (Fe, Pb, Mn, Zn, Cu, Ni), attenuated removal of colloidal metals to further down the estuary (especially Pb, Fe, Zn) and delayed desorption maxima of colloid associated metals (Zn, Cd). Only Copper shows minimal inter-survey in its estuarine behaviour. It is suggested that total dissolved copper behaviour is controlled to a greater extent by a separate organic colloid/ligand pool (which is controlled by seasonal riverine input) whereas other metals are closely linked to the Fe/Mn oxyhydroxide particle pool. The exception to this is perhaps nickel which shows conservative behaviour throughout the estuary with only minimal effects of the TMZ on the colloidal fraction.

This study has clearly indicated the significance of colloidal fractions for some trace metals in the Trent/Humber system. Previous trace metal studies in the Humber have not addressed the partitioning of trace metals within the total dissolved fraction. Figure 4.17 compares the total dissolved trace metal concentrations found in the Humber system by various authors (This study, 1999; Lasslett, 1995; Coffey, 1994; Althaus, 1992) under similar tidal and river flow (seasonal) conditions. Of the data that overlaps there is good agreement in the seawater end-members (Althaus, 1992; Lasslett, 1995) and behavioural trends in the estuary itself (Coffey, 1994). The trace metal behavioural trends for Mn (very rapid low salinity removal) and Zn (low salinity removal, mid-estuarine maximum) are especially close. However, although the overall trends for Fe and Cu appear similar, the Fe concentrations in this study are much higher compared to those determined by Coffey (1992) and the upper estuarine maxima in total dissolved copper concentrations

Figure 4.13: Dissolved trace metal concentration comparisons in the Humber:

Althaus (1992) - Humber plume / tidal stations (---)
Coffey (1994) - estuary transects (September 1991) (•)
Laslett (1995) - nearshore data (↕)
This study (1996) - August transect (x)

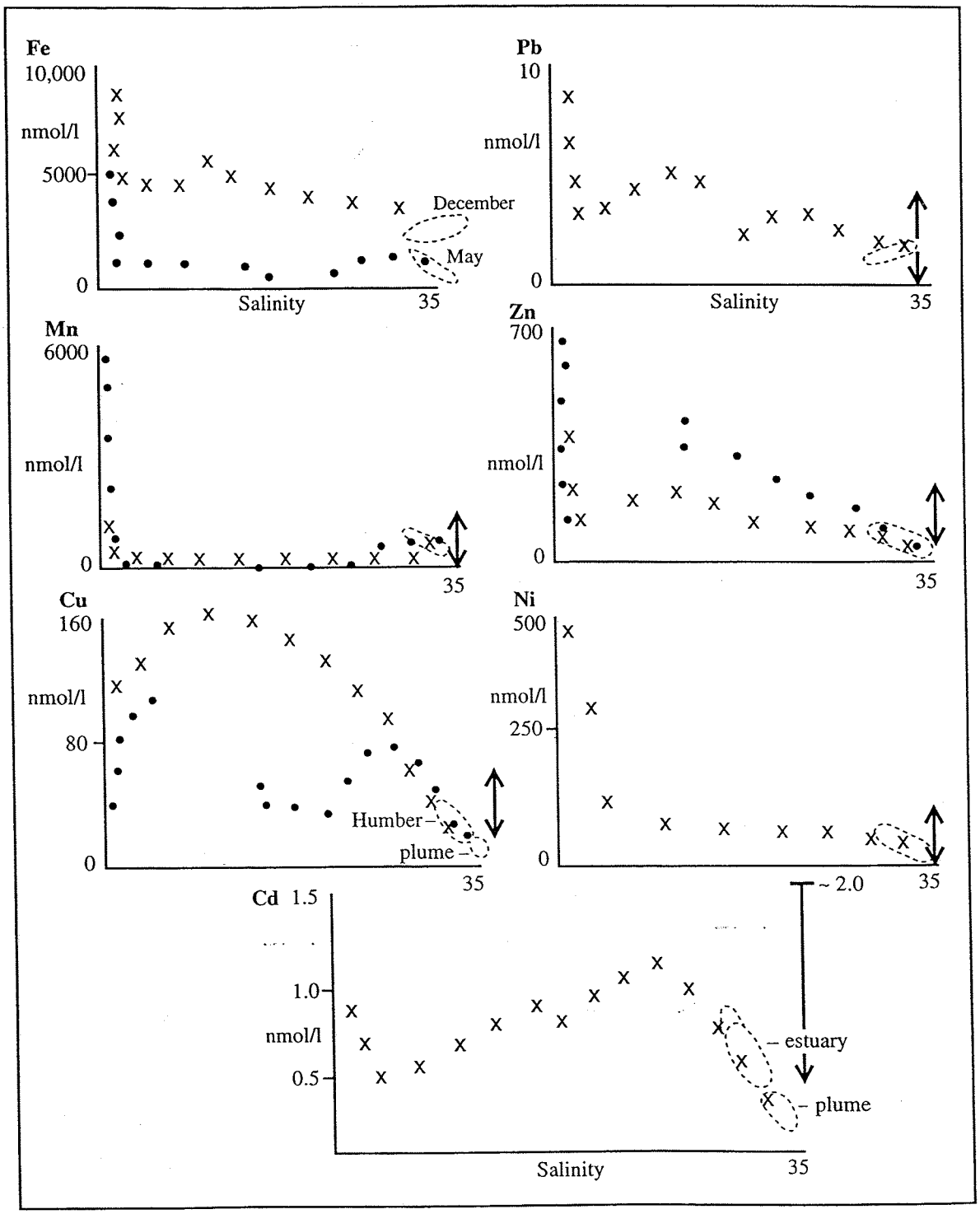

(microcolloidal/truly dissolved) is reduced. These changes may be due to inter survey variability or artefacts of filtration protocol. These discrepancies between studies illustrate the added value of having partitioning data within the total dissolved fraction to assess colloidal or truly dissolved (low molecular weight colloids) significance within the estuary. Not only does this add to the understanding of the processes occurring spatially and temporally within the estuary it can help reassess the partitioning data used for modelling particle-water-trace metals interactions in this system.

From the data presented in this study it is possible to identify metals for which present-day models may be working well. For example: total dissolved Ni here was observed to behave more or less conservatively with the predominant fraction existing in the truly dissolved fraction (except for the upper estuary in April and October). This data confirms that conventional partition coefficients for Ni therefore accurately describe it's behaviour within the estuary (there will be more uncertainty in the upper estuary until conditions found in the April/October surveys i.e. higher river flow pushing TMZ further down the estuary, spring tides producing elevated resuspension). A similar situation exists for total dissolved Cd and Zn which both are mainly truly dissolved. The results of this study have confirmed that the mid-estuarine total dissolved Cd maxima previously observed in several estuaries (Elbaz-Poulichet et al., 1987) is most likely a desorption of Cd from particles (>0.4μm) into the truly dissolved phase. The mid-estuarine maximum for Cd in the Humber has been reproduced in a model by Ng et al. (1996) by applying SPM distributions and partition coefficients (particle/dissolved) to a conservative mixing regime. Although the modelled maximum occurs in the same salinity range (peak~20ppt) the modelled concentrations are lower and the peak is broader and shallower. The data in this study indicates a amplitude of Cd release of ~0.5nmol/l compared to the models 0.2nmol/l. It is suggested that there are other inputs in the Humber which may account for this discrepancy. Similar modelling of Zn should also be possible.

Unfortunately, it is clear from this data, that the partitioning of trace metals within the total dissolved fraction becomes far more complex for trace metals where colloidal species (organic or inorganic) are significant (Fe, Pb, Mn) or microcolloidal species in the truly dissolved phase (Pb, Cu) complicate behaviour within the estuary. If the trace metal colloidal fraction is dominant it may be possible to model the dissolved phase as a

particle pool but there will still be the complications where data on the intensity and positioning of the TMZ is not good. Problems may also arise when colloidal populations are highly organic in comparison to the Fe/Mn dominant conditions normally assumed. Clearly, a greater understanding of particle-water interactions in the multi-component systems that exist within the conventional total dissolved fraction, as provided in this study, is required to accurately model trace trace metals in the Humber system.

Future work:

Due to problems with gravimetric determinations of colloidal masses and delayed particulate trace metal analysis it has not been possible to calculate partition coefficients (Kd's and Kc's) for the Trent/Humber transects. It would also have been useful to compare dissolved, colloidal and truly dissolved trace metal concentrations in regression calculations which may give an indication of associations not be directly apparent from property/salinity transects.

Previous trace metal work carried out on the Humber has largely concentrated on the operational definition (<0.4μm) of dissolved species. Further fractionation of the "dissolved" component of natural samples into colloidal and truly dissolved phases has given a better understanding of filtration and storage effects. Although most of the trends in total dissolved trace metals have been previously observed in the Trent/Humber system the identification of the colloidal and truly dissolved fractions as significant trace metal components has given a further insight into metal behaviour and understanding of partitioning changes throughout the estuarine transects. The effect of filtration protocol on highly colloidal metals also indicates that up to now the total dissolved fraction of metals such as Fe and Pb may have been severely underestimated (but also Mn, Cu and Zn to a lesser degree). Standardisation of filtration protocols to enable intercomparison of trace metal dissolved data is required.

Although there is significant seasonal changes in the SPM distributions and turbidity maximum magnitudes in this system (Uncles et al., in press), the major control on trace metal behaviour and concentration appears to be the tidal range oscillations and amount

and type of sediment comprising the TMZ. Although this zone has been characterised to some degree by particle concentration, particle surface area and characteristics, flocculation characteristics and SPM stratification (Millward et al., 1990; Morris et al., 1982; Uncles et al., in press and references therein) there is little blending of the rationale used for such physical and trace metal investigations. Specifically there is a paucity of data on the characteristics of colloidal material as operationally defined in trace metal studies. As a result the information available is difficult to equate to trends in trace metals observed. This deficiency could be addressed in the future by direct sampling of colloidal material within the TMZ . Similar work has been done by Williams and Millward (in press) but the PSPM defined there by three hours sedimentation is considerably larger (~15 μm) than colloidal material defined in this study.

Even with a comprehensive seasonal study of trace metal fractions in the Humber system there is still a problem with trace metal transformations having some sort of ambiguity with several processes occurring simultaneously. It is very difficult to differentiate between steady state colloidal metal partitioning and a dynamic exchange state (uni or multi directional) that has no net effect. In this scenario, it is impossible to tell if the colloidal phase is acting as an important intermediary between truly dissolved (low molecular weight) metal species and the particulate phase, despite its low partition (e.g. for Cu, Zn). Perhaps further investigation using tracer methods for colloidal metals would be possible to observe colloidal aggregation/disaggregation transformations in natural conditions.

As has been discussed in the previous section the data presented here has given a better understanding of particle/water/metal interactions within the conventionally derived 'dissolved' fraction. This insight into the colloidal partitioning of trace metals in these systems will enable re-evaluation of existing models and implementation of this knowledge to model these systems in future.

Chapter 5: Colloidal Partitioning of Aluminium in the Celtic Sea:

5.1: Introduction:

The continental shelf area of the Celtic sea and the adjacent Atlantic ocean have previously been studied with respect to dissolved forms of Al by Hydes (1983), Kremling (1985) and during several OMEX cruises. There is a gap in our knowledge as to whether the dissolved Al in the water column is truly dissolved or resides to some extent in a particle associated, colloidal phase.

Aluminium in the Celtic sea area has been observed to show a characteristic water column distribution that is influenced by particle/solution and biological interactions. Data from the North west Atlantic (Hydes, 1979; 1983) has placed Al in a group of elements whose distributions are not biologically affected to a great extent below surface waters. Its concentration profile shows a minimum in mid waters due to adsorption onto particles, and maxima at surface and bottom waters created by significant aeolian deposition and infusion from bottom sediments respectively. These features of the Al profile have been identified in the Pacific Ocean by Orians and Bruland (1985; 1986). Although the vertical distribution features are the same, the dissolved Al concentrations in the Pacific Ocean (especially the deep waters) are 8 to 40 times lower than in the North / East Atlantic due to geographical and inter-ocean variation in the processes that control Al distributions and absolute concentrations (atmospheric sources, particle scavenging throughout the water column, regeneration in bottom waters).

A significant feature of the aluminium profile in the Eastern Atlantic is the appearance of the Mediterranean Outflow Water (MOW) which is seen as a high Al signal (about 25nM) corresponding to the elevated salinity signal of the MOW. Mean surface concentrations are around 25.4 ± 7.3 nmol/kg Al and vary substantially with the influence of the Saharan aerosol input (Kremling, 1985). These surface concentrations are consistent with a predominately aeolian source from dissolving dust particles (Hydes, 1979; Moore and Millward, 1984; Maring and Duce, 1987). Hydes (1983) also showed high surface values in the upper waters (16-33nM) but observed no increase in deep waters that would suggest a sediment source. Previously where significant sediment sources of Al have been reported (Pacific Ocean) there is often a concurrent low water column concentration (Orians and Bruland 1985; 1986).

Any sediment source of Al will impact less against the higher Atlantic concentrations, but it may also be a weaker source due to the calcareous sediments in the Celtic Sea area than red clays characteristic o the Pacific (D. Burton, pers.comm.). Al levels in the Eastern Atlantic appear uniform below the thermocline. It has been suggested that scavenging of the charged and uncharged hydroxy-aluminum species present in solution is apparently rapid and close to irreversible with only minor release at the sea floor (Measures et al., 1986). Dissolved Al may also show localised maxima due to fluvial or shelf advective inputs although they may be relatively minor compared to the fairly high water column concentrations.

Despite the fact that dissolved Al does not display a typical nutrient water column profile there is strong evidence that dissolved Al is involved in biological uptake processes by phytoplankton (mainly diatoms) in surface waters, either by active incorporation into organic tissue as an associated nutrient, or adsorption into siliceous/opaline tests (Moran and Moore, 1988 a and b). More recent experimental evidence shows that Al is equally reactive toward living and non-living plankton cells which indicates that the majority of uptake of Al from solution reflects a surface reaction rather than a physiological requirement (Mackin and Aller, 1989). However, field studies to date have shown disparate results. Mackenzie et al. (1978) showed a covariance of dissolved Al with Si in the Eastern Mediterranean that was evident within a seasonal thermocline, nitrate minimum and oxygen maximum zones and throughout the water column. Caschetto and Wollast (1979) observed a similar covariance, but this Al/Si relationship does not often hold throughout the water column and has not been observed in open ocean regions.

More recently, seasonal variations of dissolved Al in coincidence with phytoplankton blooms observed in coastal and deep-water sites have confirmed biological removal of Al from surface waters (Moran and Moore, 1988a and b; Hydes, 1989). This process can be so significant that at bloom times surface waters may be lower in Al than deeper waters, despite significant aeolian inputs (Olafsson, 1983; Hydes et al., 1988; Hydes, 1989), and may take Al concentrations below detection limits (Hydes, 1995 pers.comm.). Aeolian inputs are potentially capable of regenerating an Al surface maximum once biological action is depleted.

The incorporation of Al into siliceous frustules and their subsequent dissolution may, in part, account for direct correlations between dissolved Al and Si in some deep-sea water-column profiles (Mackenzie et al., 1978; Caschetto and Wollast, 1979; Hydes et al., 1988). However, dissolved Al does not usually show a positive correlation with Si in the deep sea (Hydes, 1979; Stoffyn and Mackenzie, 1982; Hydes, 1983; Measures et al., 1986) and it is possible that increasing dissolved Al with depth in the water column reflects processes unrelated to biogenic opal dissolution (Moore and Millward, 1984; Mackin and Aller, 1989). Additionally, Al incorporation into diatom frustules has been observed to decrease dissolution rate and solubility (Van Bennekom et al.,1991). The effect of Al on silica dissolution is attributed to inhibition of OH^- ions that catalyse dissolution (Iler, 1973; 1979).

In the Celtic Sea area there is generally no significant increase of dissolved Al below the thermocline and therefore little apparent recycling of scavenged Al or silica dissolution. Hydes (1983) observed no deep increase in dissolved Al at depth that would suggest Al regeneration from frustules or sediments. However, interstitial water investigations in the Mediterranean have shown that dissolution of biogenic silica takes place during early burial, releasing Al and Si into solution in upper layers of sediment (Chou and Wollast, 1991). There is therefore a significant recycling potential for Al within the sediments. Al release could occur as in other sedimentary environments via diffusion or resuspension processes. Moore and Millward (1984) also suggest that at deep sea sites the increased pressure would favour dissolution of Al from matrices such as clays, and that, aluminosilicate rich deep sea sediments would form a significant source of dissolved Al. Rapid dissolved Al production has also been associated with Fe reduction in sediments (Mackin and Aller, 1989).

Moran and Moore (1991) have suggested that the resuspension of sediments is a significant source of dissolved Al to the deep North West Atlantic Ocean. Elevated levels of dissolved Al observed in near bottom waters have been associated with nepheloid layers induced by strong western boundary currents. Continued resuspension and deposition of sediments within a nepheloid layer promotes the release of Al from the sediments to the overlying water. Under these conditions, it is likely that colloidal forms of dissolved metals would predominate. Due to the rapid scavenging onto colloidal

material upon release from the sediment a large proportion of metal released would be held in this phase but as colloidal material will only sediment via aggregation processes, the colloidal forms of these metals are free to be transported further up into the water column. The residence times of such metal species would be increased substantially by their association with colloidal material. Hence, the sediments and associated nepheloid layers may be a source for colloidal Al. The near linear increase in dissolved (perhaps colloidal) Al with depth observed in the deep north west Atlantic (Moran and Moore, 1991) is attributed to release of Al from resuspended sediment associated with nepheloid layers, but characterisation of the "dissolved", sediment derived Al is required.

At present the work on colloidal Al is restricted. Moran and Moore (1989) found that colloidal Al was consistently between 5 and 10 % of the "dissolved" fraction in coastal and open ocean waters off Nova Scotia. Colloidally associated Al was high in the Gulf Stream surface waters but they did not find "dissolved" Al to be colloidally associated in deep waters. However, they did not observe any nepheloid layers or resuspension events. In contrast, several measurements of Al in the NE Atlantic showed 90% of "dissolved" Al to be colloidally associated (Hall pers.comm). These conflicting reports illustrate the need for clarification of the role of colloidal material in these continental shelf / open ocean environments and their association with nepheloid layer events. If colloids prove a significant fraction of dissolved Al there are several implications for the geochemistry of this element in the oceans:

- Colloidal material may act as a source/ sink for "dissolved" Al in the water column and will affect residence times.
- Different processes such as aggregation/disaggregation in addition to adsorption and scavenging processes will become involved in controlling the distribution of Al.
- The role of nepheloid layers as colloidal sources will have significant implications for the release / uptake of oceanic Al .

To investigate the significance and role of colloidal material to the geochemistry of Al in the Celtic Sea, two approaches were required;

- Vertical profiling of the water column and identification of Al phases at different depths with special attention being given to the sediment/water interface, and any observed nepheloid layers.

- Resuspension experiments to quantify Al release and colloidal forms associated with nepheloid layers or resuspension events.

It should be noted that the Al concentration profiles observed through water column sampling are often the net result of several, often conflicting processes, that may affect Al geochemistry and water column concentrations. For example: sediments may act as sources as well as sinks for dissolved metals. Dissolved metals may be released from deep sea sediments due to diagenetic processes, diffusion or resuspension events (nepheloid layer formation). However, sediments are also a source of scavenging particles (colloids, clays, metal hydroxide precipitates) which will remove dissolved metals from the water column to the sediments. The net result of this may be that the highest concentration of a dissolved metal may not occur right at the sediment water interface where it is released but at a point further up in the water column where the scavenging effect of the sediment associated particle population is reduced. Under these circumstances it is particles such as colloids that will be transported further up in the water column that are significant as scavenging agents and may be the major form of "dissolved" metals.

The approaches discussed above to investigate the significance and role of colloidal material to the geochemistry of Al in the Celtic Sea were carried out on OMEX cruise D216 (in the Celtic Sea) and in laboratory experiments at the Southampton Oceanography Centre.

5.2: Methods and protocol for Al determination:

5.2.1: Discovery cruise 216 (Celtic Sea):

5.2.1.1 Sampling and sample handling:

All the samples for this investigation were collected on RRS Discovery Cruise 216 between August 26 and September 12, 1995. The cruise track is shown in Figure 5.1. Vertical profiles were collected at the labeled sites using trace-metal clean, Teflon lined lever Niskin bottles mounted on a CTD rosette. Samples were prefiltered through acid cleaned 0.4μm Nucleopore polycarbonate filters directly from the Niskin bottles in a clean container on board. Sample bottles were rinsed with the target sample water prior to sample collection. The samples were stored at 4°C in clean Nalgene bottles until analysis was commenced no more than one hour after collection. Cleaning procedures for Al work is slightly different than for other trace metals. Only 10% HCl is used as there is evidence (Hydes pers. comm. 1995; this study, section 5.5.1.2) that strong acid cleaning can lead to adsorption of sample Al onto container walls. Al analysis was carried out using the lumogallion fluorescence method (Hydes and Liss, 1976), see appendix 4 for method. Filtration using a Millipore cross-flow Minitan system with 10,000 MW cutoff polysulphone filter plate allowed analysis of the retentate (colloidal) and filtrate (truly dissolved) fractions for Al by the same method. The Al fractions analysed were;

- **Total/reactive** (unfiltered sample); this represents all reactive Al naturally present in the sample that will complex with the lumogallion reagent (dissolved and also weakly bound to SPM).
- 0.4μm filtered fraction (**dissolved**)
- 10,000MW retentate (**colloidal**)
- 10,000MW filtrate (**truly dissolved species**)

Surface samples were also collected at intervals in the cruise from the ships non-toxic seawater supply. These samples were handled and analysed in the same way as the vertical profile samples.

Supporting data (bottle salinity, CTD temperature, dissolved oxygen, nutrients and chlorophyll α) was collected during the cruise for each water column profile.

Sediment samples were also collected by box core or multicorer for resuspension experiments. These samples were stored at 4°C in dark conditions until needed.

Figure 5.1: The principal stations in the OMEX research area, Discovery Cruise 216.

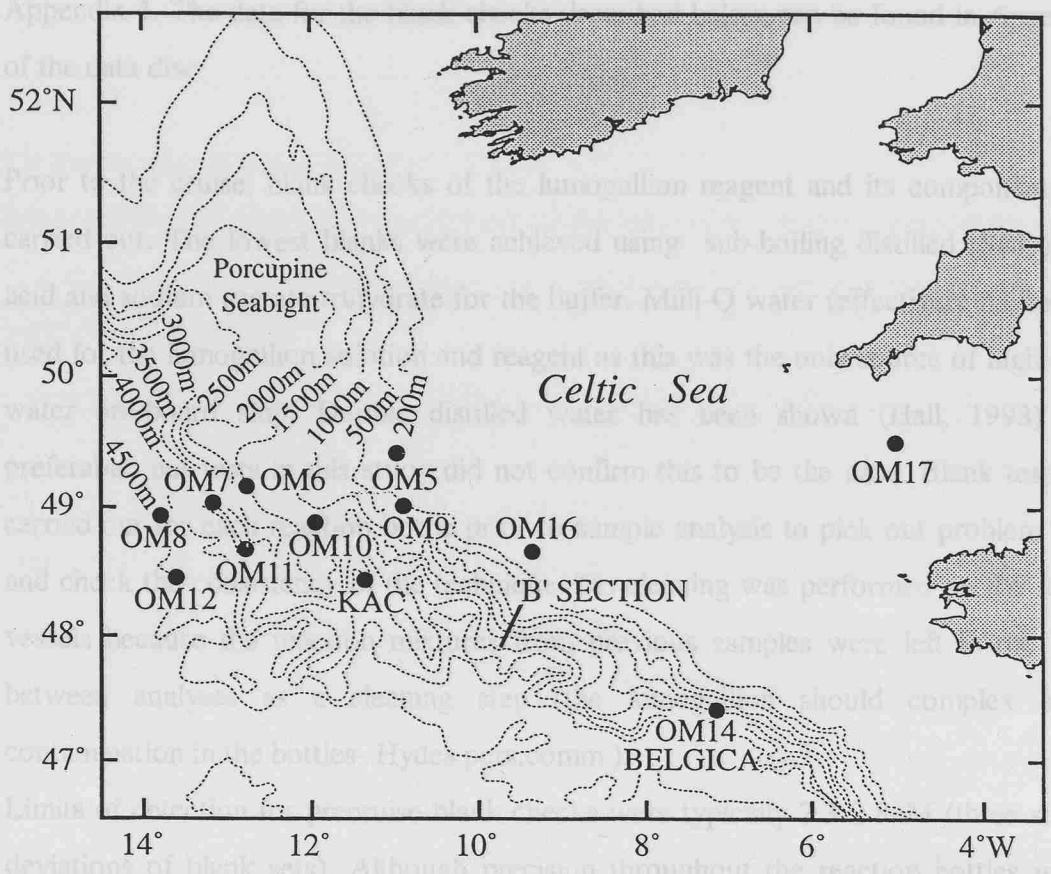

5.2.1.2: Analytical procedures and their performance:

A full description of the lumogallion method (Hydes and Liss, 1976) is given in Appendix 4. The data for the blank checks described below can be found in Appendix 4 of the data disc.

Prior to the cruise, blank checks of the lumogallion reagent and its components were carried out. The lowest blanks were achieved using sub-boiling distilled (SBD) acetic acid and sodium acetate trihydrate for the buffer. Milli-Q water (effectively Al free) was used for the lumogallion solution and reagent as this was the only source of high quality water on board ship. Double distilled water has been shown (Hall, 1993) to be preferable, but tests in this study did not confirm this to be the case. Blank tests were carried out for each reaction bottle prior to sample analysis to pick out problem bottles and check the consistency of the technique. No cleaning was performed on the reaction vessels because the reaction mixtures from previous samples were left in the vessels between analyses as a cleaning step (the lumogallion should complex any Al contamination in the bottles- Hydes pers.comm.).
Limits of detection for precruise blank checks were typically 2.3-2.8nM (three standard deviations of blank sets). Although precision throughout the reaction bottles was not good (10-40%) which may partly have been a consequence of such a low blank, the inter-batch precision of replicate samples was good to within 2-3% and the blank levels improved with each batch as the bottles were progressively cleaned by the lumogallion reagents.

Fluorescence measurements were corrected for natural fluorescence, although this proved negligible in these oceanic waters, and for reagent blanks (determined from a double reagent addition). Calibration using standard additions to the samples at regular intervals during analysis allowed for any competitive complexation of the reagent (Hall, 1993) and also compensated for drift in instrument response.

The equation for calculating aluminium concentration from the florescence measurements is;

$$\text{Al concentration (nM)} = (f - DR) \times \frac{37.06}{f'}$$

where:

f is the fluorescence of a sample.

DR is the fluorescence value determined for the lumogallion reagent (reagent blank).

f' is the fluorescence difference between unspiked and Al spiked sample (i.e. standard addition calibration).

Constant (37.06) is the concentration of Al (nM) in the standard.

For colloidal Al determination the concentration factor of the colloidal Al in a sample was calculated from the decrease in sample volume upon recirculation through the Minitan system (CF= initial volume/final volume). In the colloidal retentate fraction the Al has been artificially concentrated due to filtrate removal. Therefore;

Colloidal Al = (R-F) / CF

Where;

R is the Al concentration in the retentate fraction,

F is the Al concentration in the filtrate.

This approach assumes that; 1) there is minimal loss of sample volume in the Minitan system other than filtrate removal, 2) the concentration of the colloidal material does not affect the detection technique (lumogallion complexation), 3) there is minimal loss of dissolved or colloidal Al to the membrane surface or system by adsorption processes

The Minitan system was cleaned using the protocol described in Appendix 1. Milli-Q blanks for the system were completed. The retentate and filtrate fractions were both analysed for Al to detect any contamination that may have been attributed to the filtration system used (tubing, filters, silicon separators etc). There was no significant

system derived contamination of the filtrate or retentate. The system was transported to sea assembled, with Milli-Q water inside.

Filters plates with a 10,000MW cutoff were used new on the cruise and were rinsed thoroughly in a Milli-Q bath for 24hrs to remove preservative and any other associated contaminants prior to insertion into the system. Blank checks were repeated with Milli-Q prior to oceanic sample analysis. Large volume preconditioning of the system and soaking of the filter in seawater (Moran, 1991) was not carried out as the Al concentrations in the samples were expected to be low, so subsequent leaching of Al out of a preconditioned system was to be avoided (water available for conditioning was relatively high in Al and Al uptake onto the tubing, separators or filters was a problem to avoid.). The system and filters were preconditioned with a small volume, approximately 100-200ml, of each sample prior to filtrate or retentate sampling.

5.3: Results of Celtic Sea studies:

5.3.1: Sample handling artifacts

5.3.1.1: Minitan blanks and sample contamination

The Minitan system was set up on board after rinsing with Milli-Q. The filters and silicon separators were also Milli-Q rinsed prior to installation in the system. Several blanks (Milli-Q recirculation and flushing) were done to check that the system had not picked up any Al contamination during transport (all blank and sample contamination data is listed in Appendix 4 on the data disc). No significant difference (<1nM) between original Milli-Q, filtrate and retentate (colloidal) Al concentrations was observed.

On the basis of these results the Minitan system was used to separate colloidal fractions from water column profile samples.

Profile colloidal sample contamination:

For many samples there was a problem of colloidal sample Al contamination. The Al concentrations determined for filtrate and retentate (colloidal) fractions were in sum, higher than the total dissolved Al determined by the lumogallion method. The filtrate fraction was especially high (10 to 50 times the dissolved fraction alone). The much higher Al contamination apparent in the filtrate indicated that the filter plates or this part of the Minitan system was the source of the contamination problem. This was observed despite rinsing of the system prior to each sample with 1 litre of Milli-Q and also flushing of the system with the sample (preconditioning) prior to filtrate/retentate collection.

Blank checks after apparent sample contamination:

The Minitan system, especially the filter plates, was seen as a source of contamination. However, the concentrations of Al contamination seen in the Milli-Q blanks (maximum 4nM) after sample contamination problems were not comparable to the contamination observed in the profile samples (maximum 400nM). Despite uncontaminated Milli-Q blanks, cross-flow filtered water column samples continued to exhibit Al contamination (the sum of the colloidal and truly dissolved fractions was higher than the original

dissolved (0.4μm filtered) sample. The nature of the contamination was linked to the high ionic strength of the seawater samples and despite low Milli-Q blanks and conditioning of the system, unknown Al species present were being progressively leached out of the system by the seawater samples.

To address some of the questions raised by these results and help achieve useful data from the remaining samples several tests were carried out;

1) A filtrate and retentate refiltrate blank was performed for each sample to determine the magnitude of the contamination associated with each fraction. This was done by passing the filtrate or retentate samples back through the system to note any additional contamination. By removing this blank concentration from the measured Al, an estimate of the true Al concentration for each sample could be determined.

i.e.: Blank due to contamination (filter, separators etc.) = $[Al]_2 - [Al]_1$

Where:

Al_1 is the original sample Al concentration, Al_2 is the Al concentration of the sample which had been passed through the system a second time.

This assumed that there was no change in the particle population or level of contamination in either the retentate or filtrate fractions during the refiltration time.

The seawater filtrate blanks from OM7 illustrated that the Minitan system was not a significant source of Al contamination to the filtrate fraction. The maximum increase seen in the filtrate blank concentration was 4nM, but this was insufficient to explain the levels of contamination seen previously in the filtrate samples. The retentate blanks indicated an Al uptake by the system. The removal of one filter plate (total of four used routinely) did not alter the contamination seen in the blanks indicating that the filter plates were probably not a direct source of Al.

2) A check was undertaken to detect any contamination from the system tubing.

It is possible that metal species may be adsorbed /desorbed from the silicon tubing of the pump and Minitan system. In this case, a leaching or desorption effect is suggested. To

test if the silicon tubing was a significant source of Al contamination, a length of the silicon tubing was filled with 0.4μm filtered seawater and circulated by pump for 24hrs. The Al concentration determined before and after this treatment was compared.
There was a very small increase in Al concentration of the sample due to exposure to the tubing (approx. 1nM). However, this increase was too small to explain the magnitude of the contamination observed in the seawater samples and occurred over 24hrs, whereas filtration of a given sample was very rapid and any one sample was in contact with the silicon tubing for a maximum of 30 minutes.

Conclusions drawn from Al contamination problems:

The lack of contamination seen in the Minitan refiltrate blanks indicated that there was an additional source of contamination, possibly particle associated, generated from within the sample itself.

It is possible that particle/aggregate break up during filtration releases dissolved Al phases into the sample or increases the availability of reactive surface Al to lumogallion complexation. This would help explain the increase in filtrate Al whilst there is minimal contamination of the refiltrate blank. This would also explain increased levels of Al in retentate too as this fraction would also contain as yet unfiltered truly dissolved Al released from particles. The wash out effect of the Al contamination maybe due to decreasing particle breakup/loading or increased conditioning effect which acts to reduce release of Al. It seems that the Al increases are linked to particle break up in the initial sample, or some kind of CFF system conditioning effect.

Due to these problems the colloidal data collected cannot be used. However, the fractionation of the Al that did occur indicated that the colloidal fraction was relatively significant although this cannot be quantified due to the undefined contamination levels and the lack of understanding of the processes occurring to incite Al release. It is possible that uptake and release mechanisms are acting simultaneously within the Minitan system so the conditions governing the final observed Al concentrations (net effect) are unknown and difficult to quantify.

Overall, this series of contamination experiments has illustrated that CFF separation of colloidal Al and its detection using a surface active method (lumogallion technique) is not as straightforward as once thought. It is most likely that disruption of loose aggregates within the colloidal size range is occurring during cross flow filtration which increases the Al available for lumogallion complexation and therefore the "dissolved" Al detected (ionic or colloidal forms). This disruption of the colloidal particle population has significant effects on determined trace metal partitioning at low particle concentrations but has equally large implications for CFF as a means of particle separation in environments where the particle populations are increasingly significant.

An attempt was made to collect additional water profile samples from a cruise to the Western Atlantic in 1996. It was hoped that the presence of western boundary currents in the sampling area would give a clearer indication of the significance of colloidal Al in resuspension events. However, this sampling regime was abandoned due to a fire that stopped the required samples being taken.

5.3.1.2: Influence of sample storage and conventional filtration on Al concentrations:

Several profiles of water samples were stored on D216 for later analysis for colloidal material by conventional filtration.
Due to unforeseen circumstances these water samples had to be stored for 1 month at 4°C in the dark before analysis. Figure 5.2: a to c shows the Al fractions determined for the deep section of OM8 (precision of the data points lies within the markers).

The sample fractions determined were:
Dissolved (D216): Al concentration determined for this 0.4μm filtered sample on D216.
Stored dissolved: remeasured Al concentration for D216 0.4μm filtered sample after storage.
0.4 filtered: Al concentration in stored 0.4μm filtered sample after 0.4μm refiltration.
0.01 filtered : Al concentration in 0.01μm filtered, 0.4μm refiltered stored sample.

Figure 5.2 **a: Deep dissolved Al profile for OMEX station 8 (stored samples).**
b: Deep dissolved Al profile, OMEX station 8 (expanded).
c: Changes in dissolved Al concentrations for stored/refiltered samples.

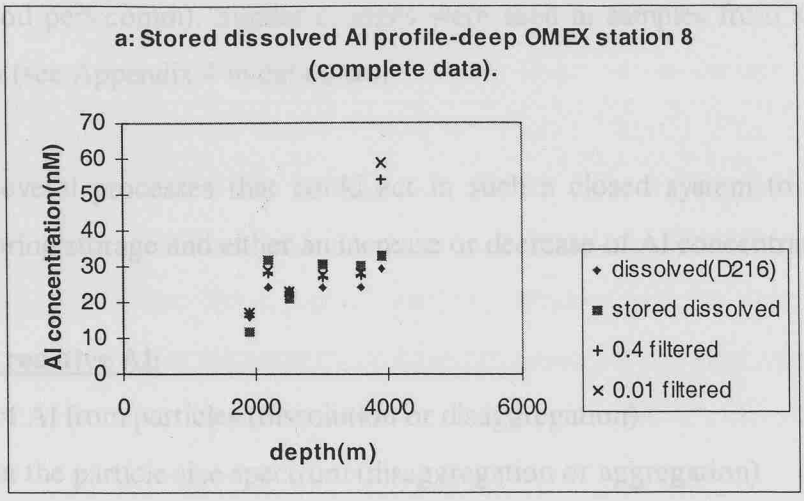

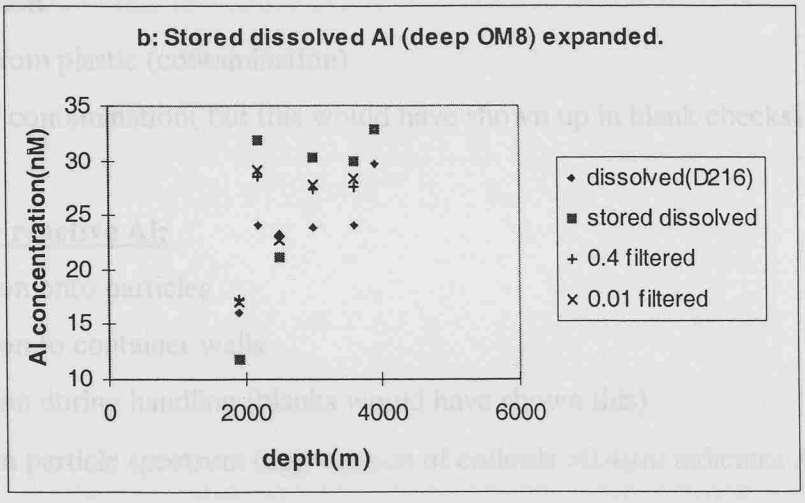

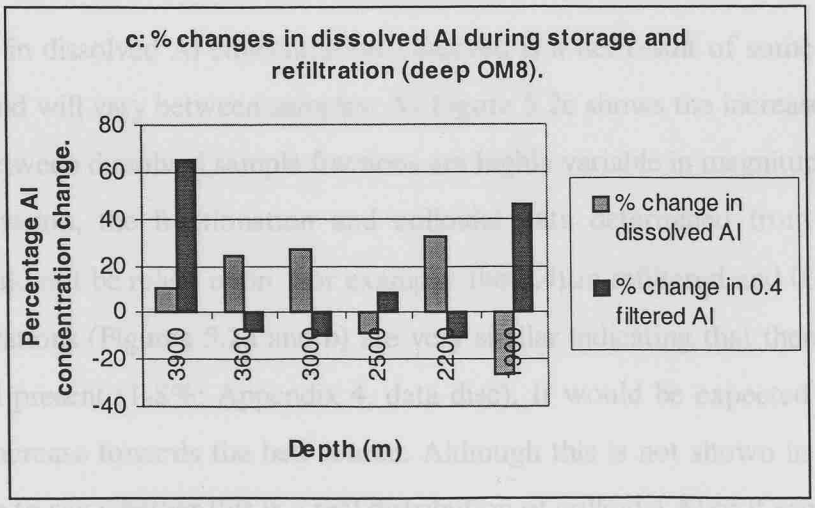

The samples had significantly altered during the month storage. In all cases the dissolved Al concentration had increased or decreased significantly from that measured originally on board (dissolved D216). Similar alterations in reactive and dissolved Al concentrations have also been observed for stored or frozen estuarine samples (Tappin and Sherwood pers.comm). Similar changes were seen in samples from station OM10, deep section (see Appendix 4 in data disc).

There are several processes that could act in such a closed system to cause sample alteration during storage and either an increase or decrease of Al concentration;

Increase in reactive Al:

- release of Al from particles (dissolution or disaggregation)
- change in the particle size spectrum (disaggregation or aggregation)
- evaporation
- release from plastic (contamination)
- handling contamination(but this would have shown up in blank checks)

Decrease in reactive Al:

- adsorption onto particles
- adsorption to container walls
- adsorption during handling (blanks would have shown this)
- change in particle spectrum (aggregation of colloids >0.4μm indicates Al removal)

The change in dissolved Al concentration observed is a net result of some / all of these processes and will vary between samples. As Figure 5.2c shows the increases / decreases observed between dissolved sample fractions are highly variable in magnitude. As a result of this alteration, the fractionation and colloidal data determined from these stored samples could not be relied upon. For example: the 0.4μm refiltered and 0.01μm filtered Al concentrations (Figures 5.2a and b) are very similar indicating that there is very little colloidal Al present (1-8%; Appendix 4, data disc). It would be expected that colloidal Al would increase towards the bed source. Although this is not shown in the data, it is not possible to say whether this is a real distribution of colloidal Al or if sample alteration

has affected the colloidal fraction significantly. Microbial degradation of organic colloids or aggregation processes would also have a pronounced effect on colloidal levels. Because of these alteration problems it is not possible to estimate the fraction and therefore significance of the colloidal Al .

Additionally, these samples also showed increased levels of conventionally filtered Al compared to the original Al concentration determined shortly after collection, see Appendix 4 in data disc. The Milli-Q and filtrate filter blanks here showed no contamination so the unloaded polycarbonate filters were not the source of Al. It was concluded that again the break up of particles retained on the filter surface and subsequent leaching during filtration could have produced the elevated Al concentrations observed in both the 0.4 refiltered (colloidal) and 0.01 filtered (truly dissolved) fractions. Blanks determined for each filtration allowed the Al contamination to be quantified and the Al fractionation to be more accurately determined as discussed above.

5.3.2: Water Column Profiles:

Appendix 4 (data disc) contains all the raw data for total reactive (unfiltered) and dissolved (reactive Al passing through a 0.4μm filter) Al and Si data for the vertical profiles at each site. The total fraction is the reactive Al either dissolved or on particle surfaces but available to complex with the lumogallion reagent. As such, there can be marked differences between total and dissolved concentrations especially if there is significant Al in/on suspended particulate material present in a sample that is not included in the dissolved phase or is unavailable for complexing on particle surfaces.

Figures 5.3 and 5.4 illustrate the combined profiles for the master variables (CTD temperature, bottle salinity and dissolved oxygen), silicate, nitrate, phosphate and chloropyll-a for all the OMEX sites. The vertical profiles for total reactive and dissolved (<0.4μm) Al for each site are plotted in off slope transects (OM 5 to 8, OM 9 to11) and a composition of OM16, Belgica, KAC, B6 and OM17 in Figures 5.5 to 5.8. Figures 5.9 to 5.10 are the combined (total and dissolved) vertical profiles for pre and post storm "Iris" sites. Iris was a tropical storm that passed over the Celtic Sea area just before sampling of stations B6, Belgica and OM17. The precision for all the data of these plots lies within the point marker (+/-1%). Detection limits had a range of 1.8 to 3.4 nM (2.4 nM +/- 1.2).

5.3.2.1: Al Profile characteristics:

The shape of the Al profiles have several features common to many of the sites. They are;

surface maximum (20-40m): - the magnitude of this peak is quite variable (20-35nM) between total and dissolved Al fractions and also between sites. The Al maximum appears to coincide with a chlorophyll-a maxima which lies around 20 to 50 metres. OM5 and OM6 don't have surface maxima and the profiles are more uniform.

Al minimum: - the deeper sites show a pronounced Al minimum (10-17nM) in total and dissolved fractions immediately below the maximum and >1500m.

Figure 5.3 : Combined profiles of CTD temperature, dissolved oxygen, bottle salinity and chlorophyll-a for all stations on Discovery 216.

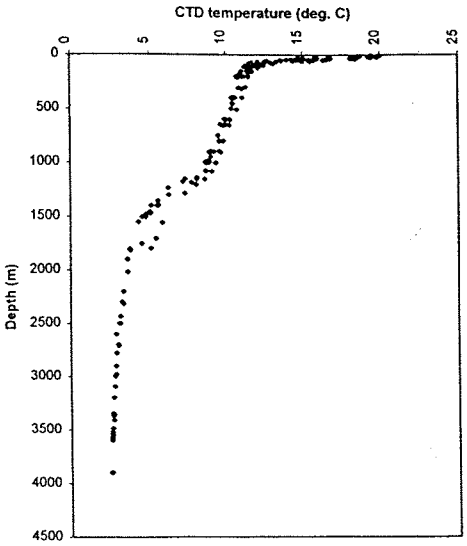

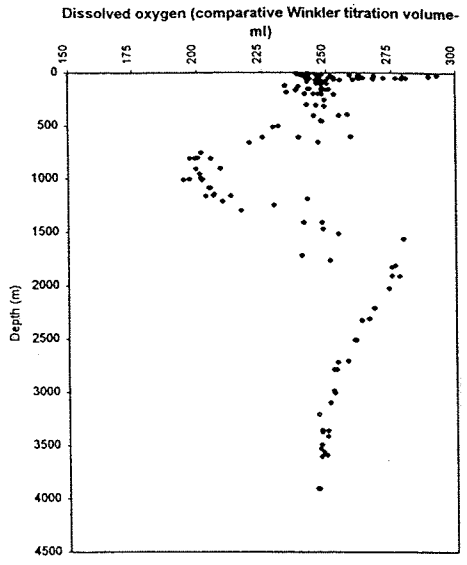

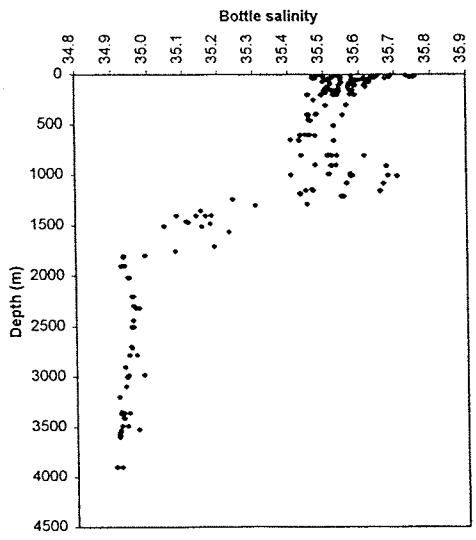

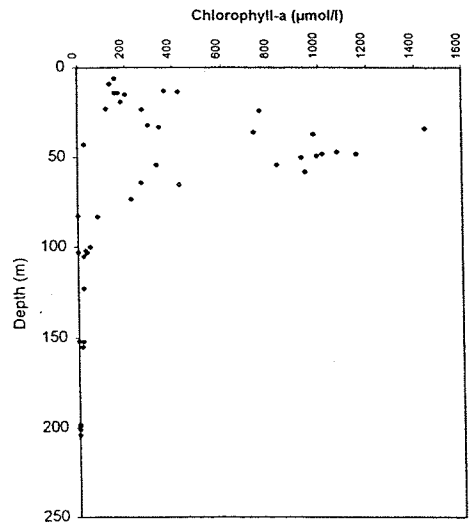

Figure 5.4: Combined profiles of silicate, nitrate, phosphate and nitrate/phosphate plot for all stations on Discovery 216.

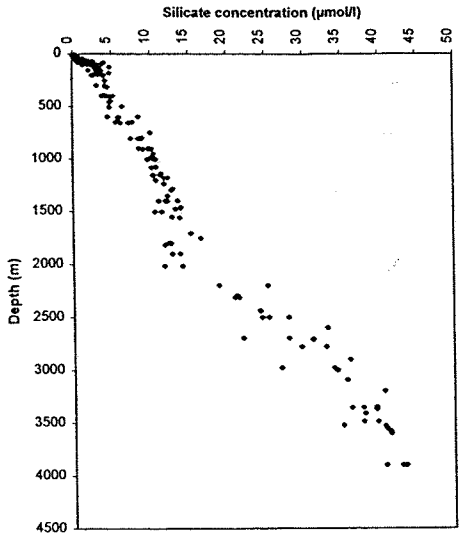

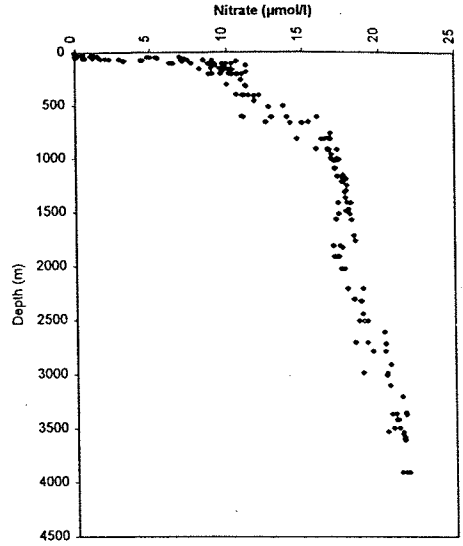

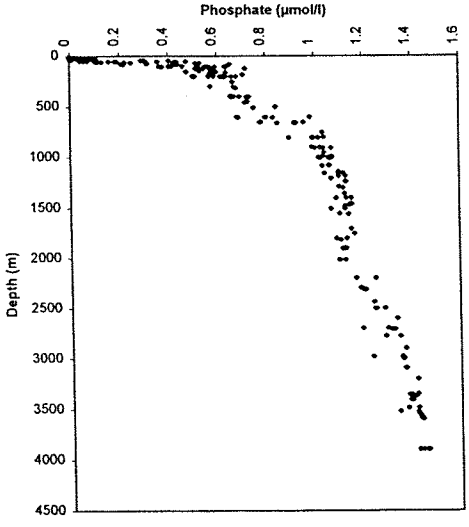

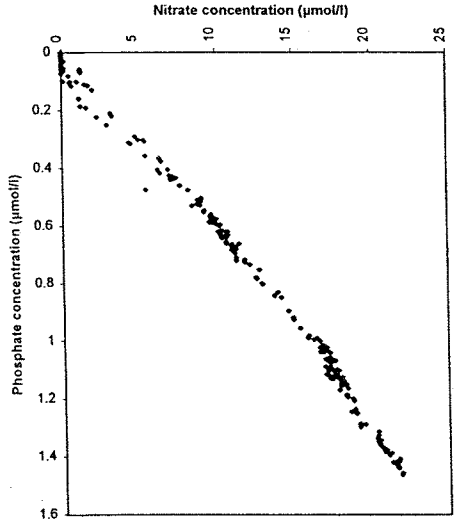

Figure 5.5: Total reactive (o) and dissolved (o) aluminium profiles (OMEX station 5 to 8-D216)

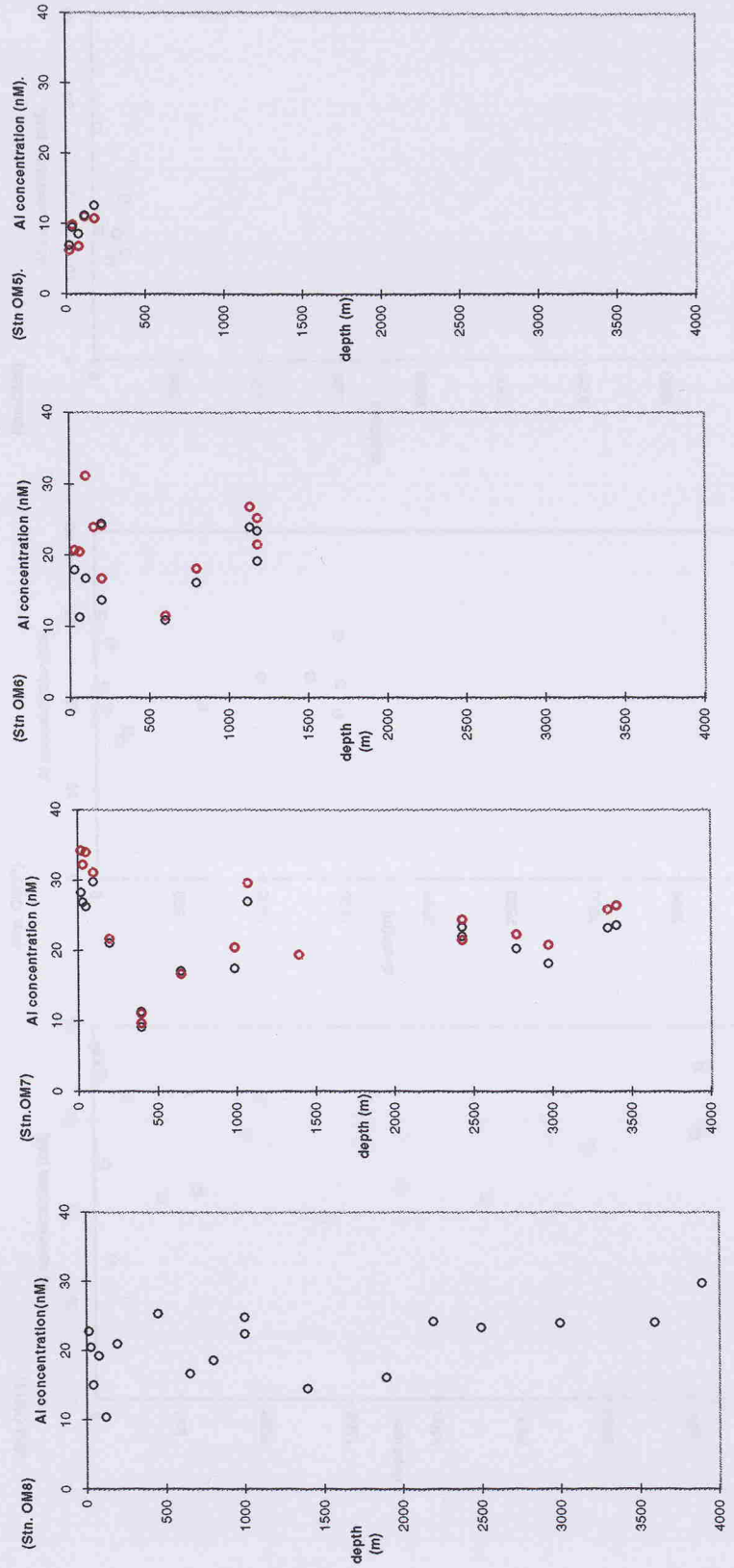

Figure 5.6: Dissolved aluminium profiles, shelf transect OMEX stations OM9 to OM11.

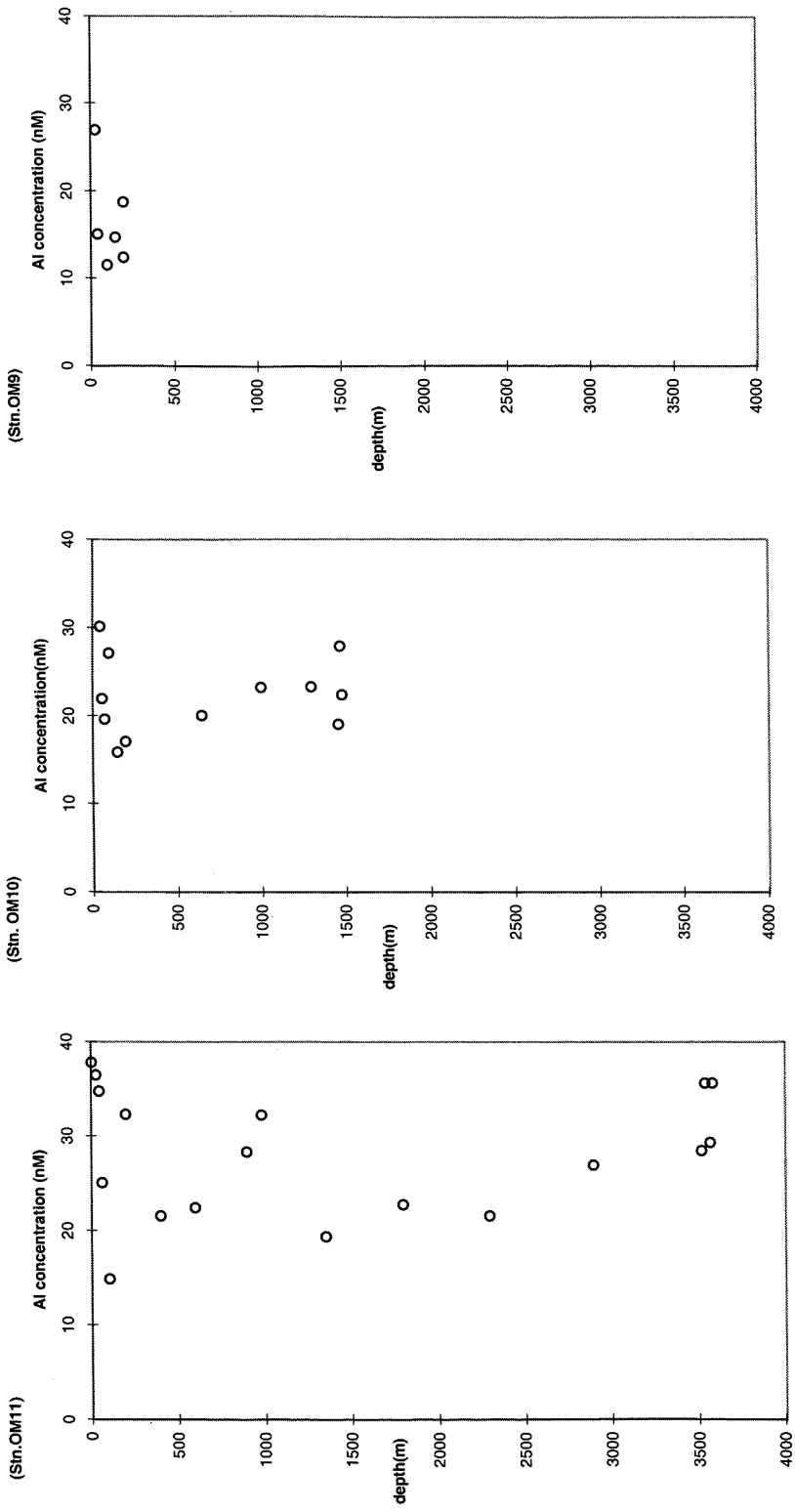

Figure 5.7: Total reactive (o) and dissolved (o) aluminium profiles for OMEX stations; OM16, Belgica, KAC (King Arthurs Canyon) and B6.

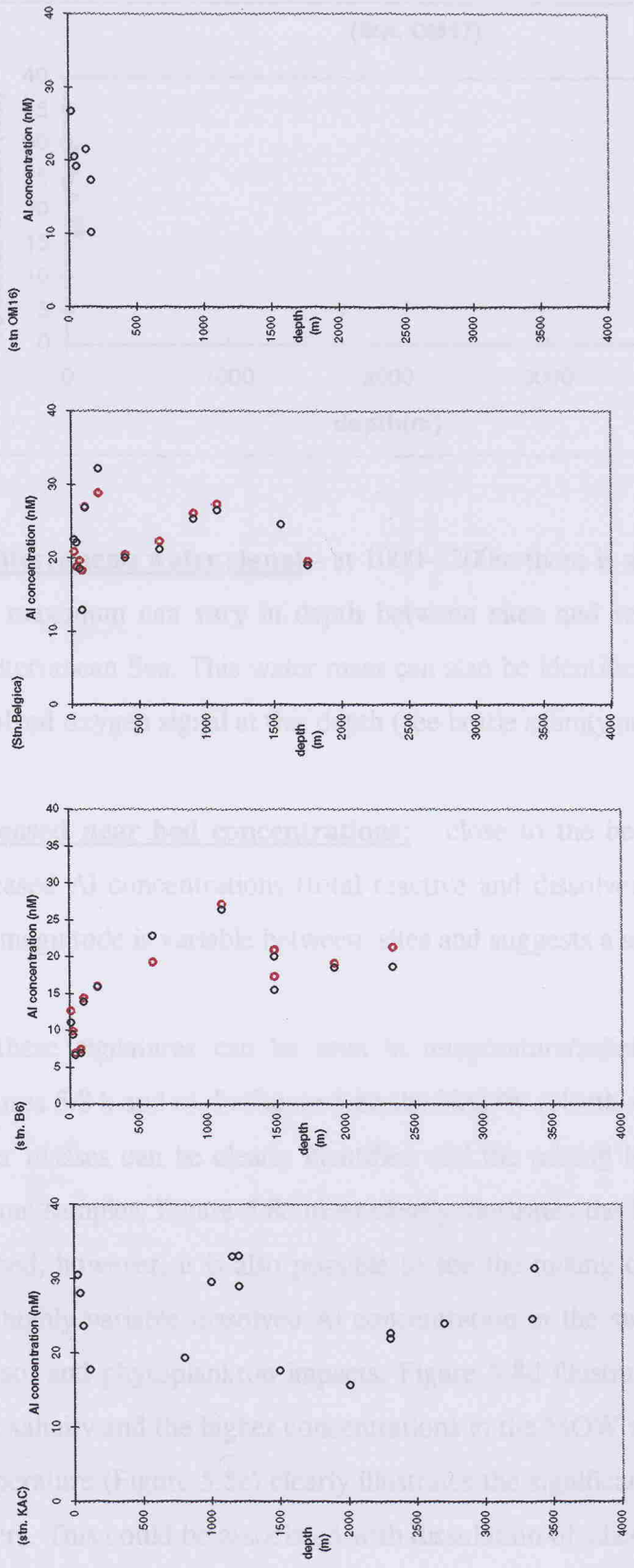

Figure 5.8a: Total and dissolved Al profile for station OM17 (well on-shelf).

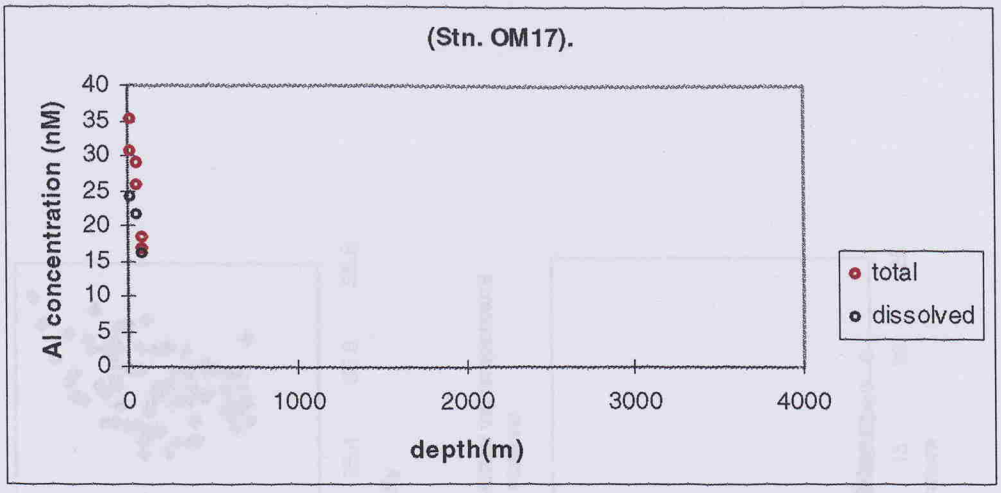

Mediterranean water signal:- at 1000-1200m there is a clear Al maximum (25-30nM). This maximum can vary in depth between sites and represents the outflow from the Mediterranean Sea. This water mass can also be identified by a higher salinity and lower dissolved oxygen signal at this depth (see bottle salinity and DO plots, Figure 5.3).

Increased near bed concentrations: - close to the bed (bottom 5 to 50m) there are increased Al concentrations (total reactive and dissolved) on many of the site profiles. The magnitude is variable between sites and suggests a sediment source.

All these signatures can be seen in temperature/salinity and Al concentration plots (Figures 5.8 b and c). In Figure 5.8b the NADW (North Atlantic Deep Water) and MOW water masses can be clearly identified and the mixing between them in the mid-water-column samples. Figure 5.8c most clearly illustrates the increase in dissolved Al close to the bed, however, it is also possible to see the mixing of the MOW and surface water, and highly variable dissolved Al concentration in the surface waters due to changeable aerosol and phytoplankton impacts. Figure 5.8d illustrates the changes in dissolved Al with salinity and the higher concentrations in the MOW and near bed. The Si plot versus temperature (Figure 5.8e) clearly illustrates the significant input of Si in the deeper, cold waters. This could be associated with dissolution of siliceous tests (release occurs over a wider temperature range/depth) at depth or release from sediment (porewater diffusion or resuspension).

Figure 5.8b: Temperature/salinity plot for all Celtic Sea stations

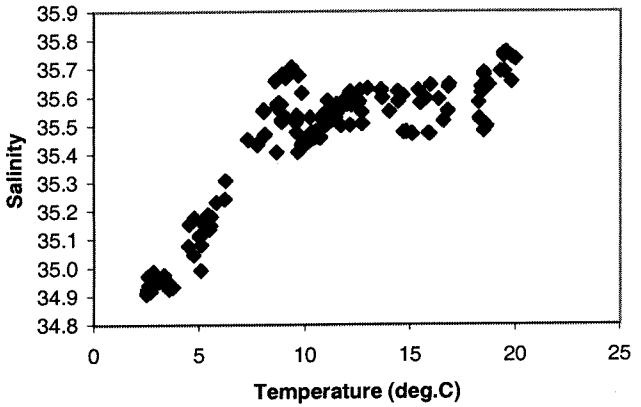

Figure 5.8c:Dissolved Al plotted vs. temperature for all Celtic Sea stations.

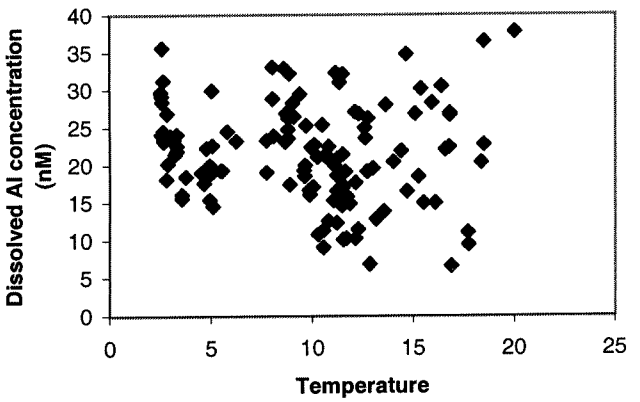

Figure 5.8d: Dissolved Al concentration plotted vs. salinity for all Celtic Sea stations.

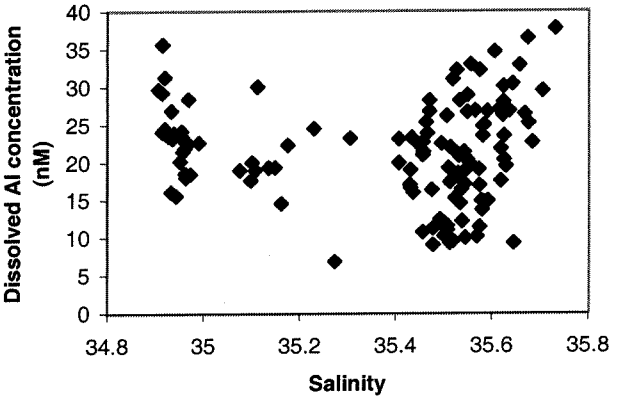

Figure 5.8e: Si concentration plotted vs. temperature for all Celtic Sea stations

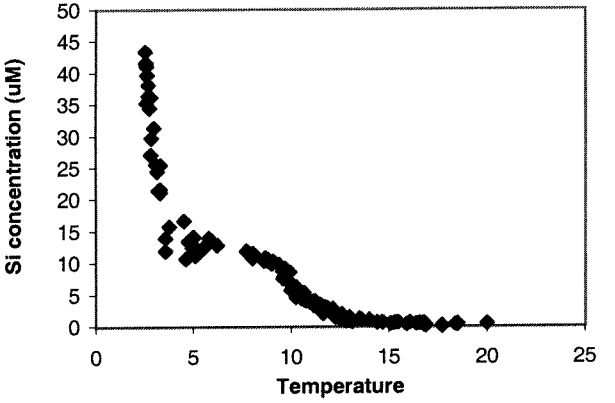

5.3.2.2: Comparison of total reactive and dissolved profiles:

Both total and dissolved Al fractions have the same profile characteristics discussed previously. In several surface profiles around the chlorophyll maximum there is large discrepancy between the total and dissolved Al. In other profiles such as Belgica and B6 (situated at the deep end of the "B" section), total and dissolved Al in surface waters show little difference. A significant difference in these two measures of Al is also seen closer to the bed where higher particle levels occur (e.g. OM6 and OM7). There is generally good agreement between total reactive and dissolved Al concentrations when there are low particle loadings in the water column.

Despite good procedural blanks the noise observed in the data has been subsequently attributed to a possible contamination problem originating from the lever Niskin sampling bottles (D.Hydes pers. comm.). However, a contamination blank for the Niskin bottles was not performed. The contamination observed in the samples does not appear to be reproducible so the Al concentration profile data has not been adjusted for this.

5.3.2.3: Offshelf profiles:

There are several features that change as a result of shelf influence;

- Increasing uniformity of Al concentration in the deep water masses. Al concentrations are uniform or gradually increasing towards the bed. This is compatible with the theory of "oceanographic consistency" where significant deep water masses have similar and characteristic signals. Horizontal advection of these water masses ensures along-shelf continuity in the profiles.

- Increasing influence of sediment signals in the shelf area. This is seen particularly as increased Al concentrations close to the bed. Al can be released here by diffusion across the sediment water interface or resuspension events that can lead to nepheloid layer formation. Advection of shelf water with higher Al signals off-shelf may also be observed.

There is some indication of shallowing of the MOW signal off-shelf at some sites. The MOW Al signal also seems to become less diffuse and strengthen (increase in Al concentration). This may indicate the core of the MOW that is less affected by advection or sediment signals in deeper water away from the influences of the shelf break.

5.3.2.4: Effects of Iris storm mixing:

As mentioned previously, Iris was a tropical storm that passed over the Celtic Sea area just before the sampling of B6, Belgica and OM17. The storm had a number of effects on the Al concentration profiles (see Appendix 4 on the data disc for combined station profiles pre and post Iris). The Al surface maxima were mixed down into the water column, thus reducing the Al concentration and also deepening the maxima. The removal of Al from the water column seems attenuated by the mixing effects of the storm.

No site was visited prior to and after the storm so there is no direct information on temporal variability of the Al profiles. Total reactive and dissolved Al concentrations for surface waters from sites profiled before (OM6 and OM7 or OM11, 16 and KAC) and after the storm (B6 and Belgica) are displayed in Figures 5.9 and 5.10 respectively.

Figures 5.9: Total reactive aluminium profiles for stations a;pre and b;post Iris.

A:

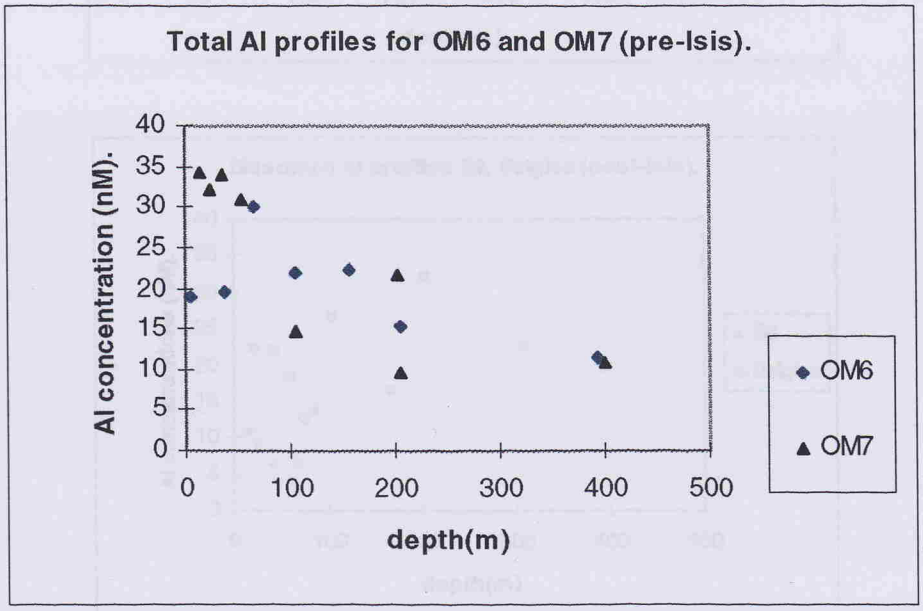

B:

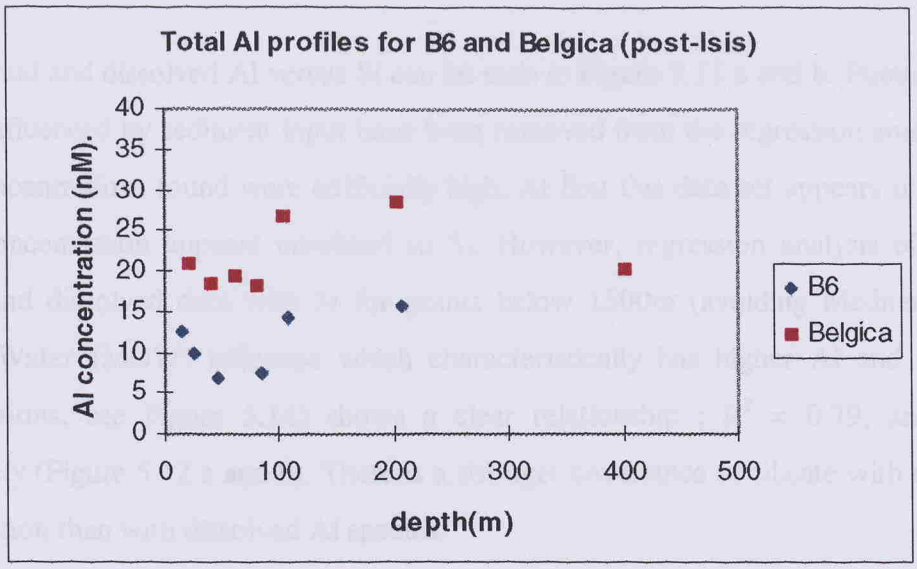

Figure 5.10: Dissolved aluminium profiles of OMEX stations A:pre and B:post Iris.

A:

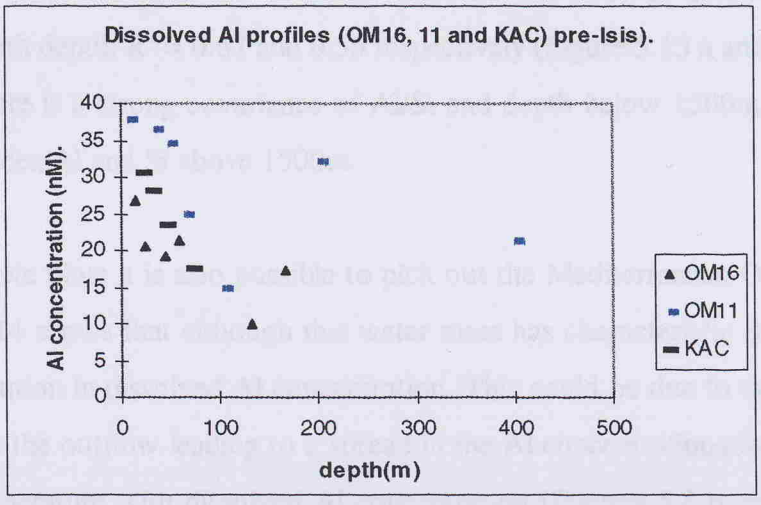

B:

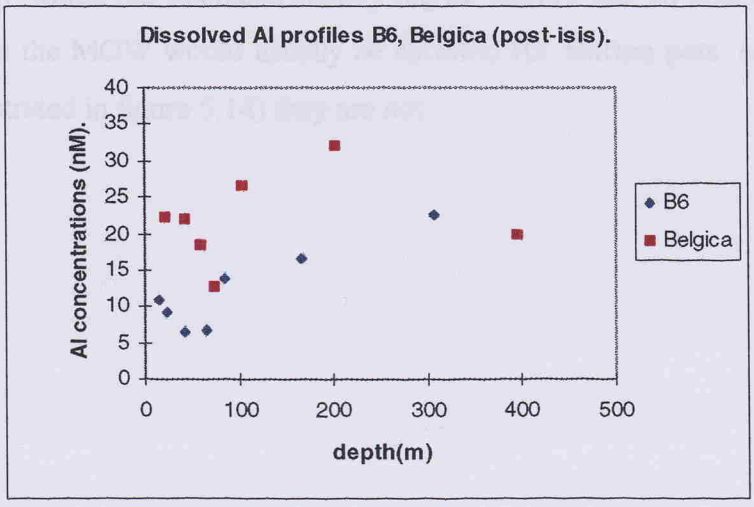

5.3.2.5: Al/Si/depth covariance:

Plots of total and dissolved Al versus Si can be seen in Figure 5.11 a and b. Points in the data set influenced by sediment input have been removed from the regression analysis as the Al concentrations found were artificially high. At first this data set appears scattered and Al concentration appears unrelated to Si. However, regression analysis of total reactive and dissolved data with Si for points below 1500m (avoiding Mediterranean Outflow Water (MOW) influence which characteristically has higher Al and low Si concentrations, see Figure 5.14) shows a clear relationship ; R^2 = 0.79, and 0.63 respectively (Figure 5.12 a and b). There is a stronger covariance of silicate with total Al concentration than with dissolved Al species.

The same is true for regression analysis of Al and depth (Si increases almost linearly with depth in Figure 5.4). For total reactive and dissolved Al there is a clear increase in concentration with depth; R^2 = 0.67 and 0.56 respectively (Figure 5.13 a and b).
Undoubtedly there is a strong covariance of Al/Si and depth below 1500m. There is no covariance between Al and Si above 1500m.

From the complete plots it is also possible to pick out the Mediterranean Outflow water mass. Figure 5.14 shows that although this water mass has characteristic Si signal there is a wide distribution in dissolved Al concentration. This could be due to entrainment of other water into the outflow leading to a spread in the Al concentrations found. Plots of salinity and temperature with dissolved Al concentration (Figures 5.8 b and c) indicate clearly the MOW which has characteristically higher salinity and Al concentrations. Si concentrations in the MOW would usually be elevated (D. Burton pers. comm.) but in this case (as illustrated in figure 5.14) they are not.

Figure 5.11 a and b: Plots of total reactive and dissolved Al concentration versus silicate concentration for all water depths.

a:

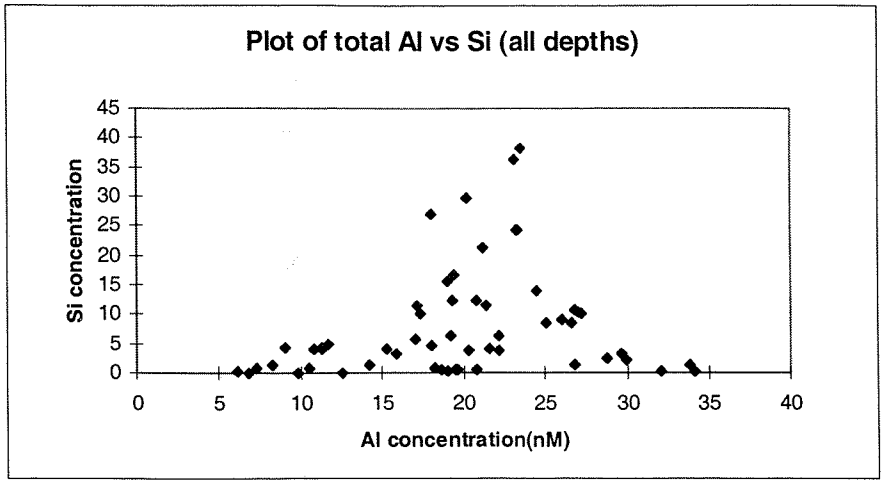

b:

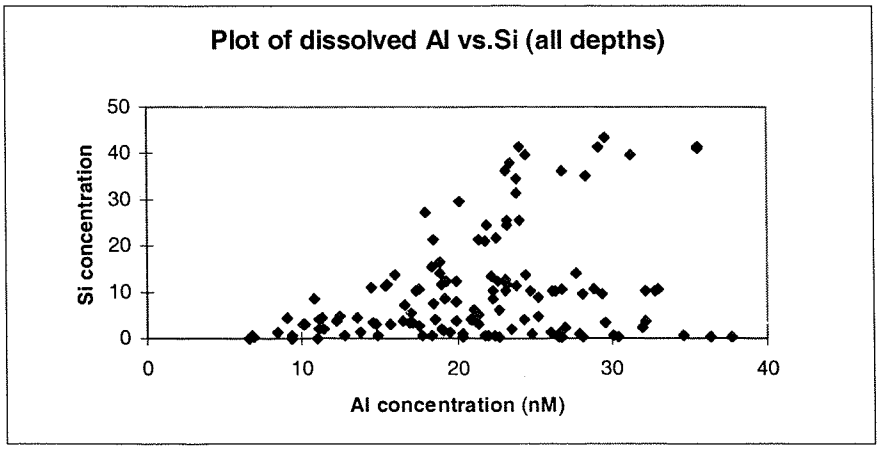

Figure 5.12 a and b: Regression plots for total reactive and dissolved Al/Si (depths greater than 1500m).

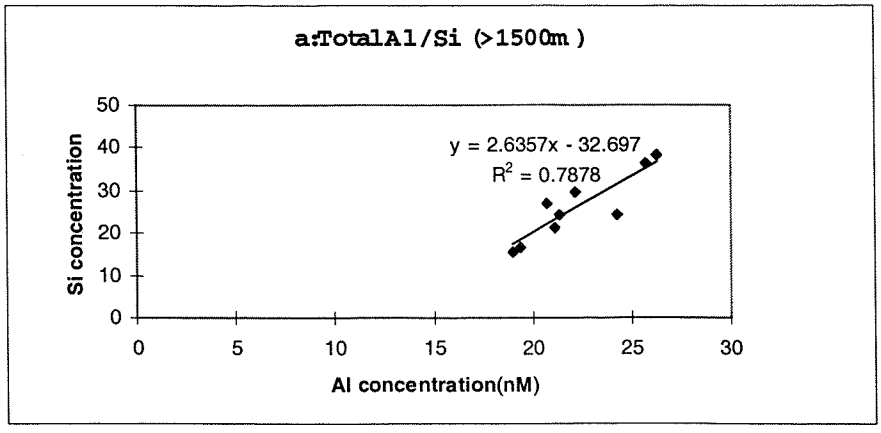

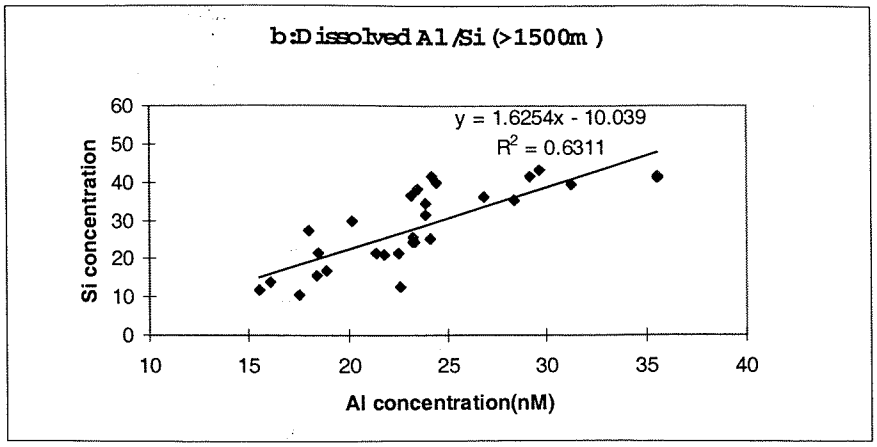

Figure 5.13 a and b: Total and dissolved Al concentrations vs. depth (>1500m)

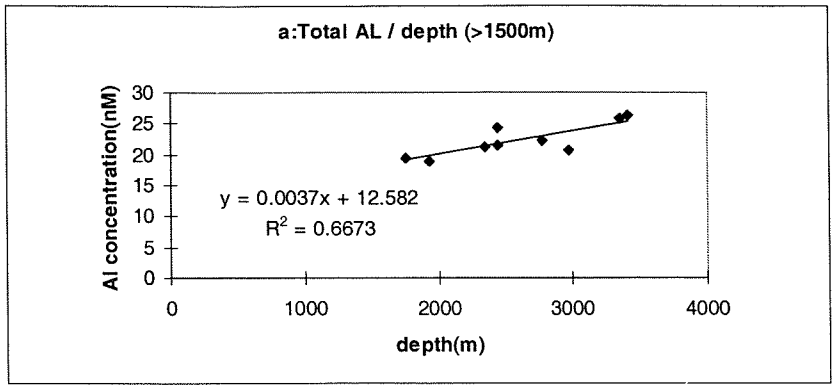

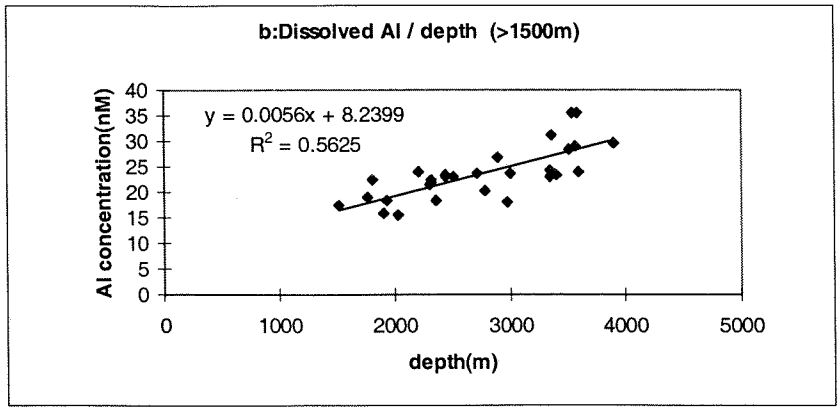

Figure 5.14: Dissolved Al/Si concentration plot for Mediterranean Outflow Water.

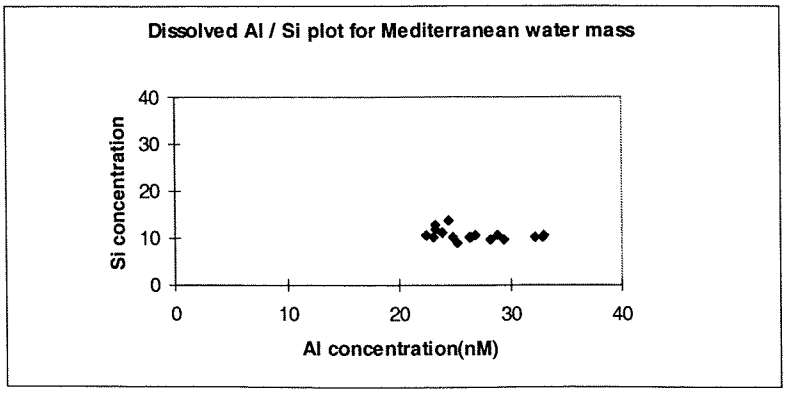

5.3.2.6: Underway Al:

The underway dissolved and total Al concentrations are plotted against bottle number in Figure 5.15 (detection limits for both types of analysis were 3.6-3.9 nM (3.7 +/- 0.212). Precision of data lies within the markers). There are several interesting features;

- The surface total and dissolved Al concentrations here are much lower than those determined in the surface rosette profiles (2-8nM compared to 6-35nM at 20-40m).

- The dissolved Al concentrations appear to be increased but this may be due to real variations, contamination from the non-toxic supply or filtration artifacts (Appendix 4, data disc). Any such contamination however, must be small as Al concentration values are still less than those in samples from Niskins.

- Concentrations of both total and dissolved Al increase markedly towards coastal / shelf areas where shelf sediment influence may act as a source of Al.

Figure 5.15: Total reactive and dissolved Al underway data, D216.

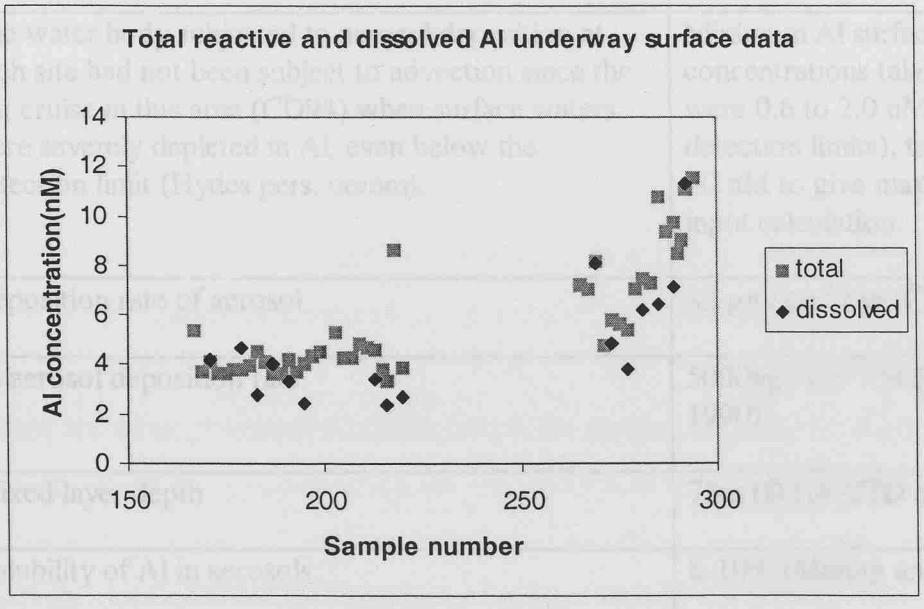

5.4: Discussion of Celtic Sea aluminium water profiles:

5.4.1: Surface maxima:

The observed Al maxima in the surface waters could be explained by several processes;

-direct aeolian input

-advection of water from areas with sediment input or high aeolian input.

Dust or aerosol particles can be deposited from overlying air masses onto the sea surface via wet or dry deposition. In the Celtic sea area the main source of aeolian Al inputs are related to the Saharan aerosol and also anthropogenic inputs from adjacent land masses (Jickells, 1995). To estimate whether the Al concentrations in the surface waters were consistent with an aeolian source, a calculation using several assumptions was made. Assumptions and data are given in Table 5.1

Table 5.1: Assumptions and data used for assessment of aeolian inputs to Celtic Sea surface waters.

Assumption	Value used in calculation
The water body subjected to aerosol deposition at each site had not been subject to advection since the last cruise in this area (CD94) when surface waters were severely depleted in Al, even below the detection limit (Hydes pers. comm).	Minimum Al surface concentrations taken on CD94 were 0.6 to 2.0 nM (below detection limits), taken here as ~0 nM to give maximum aeolian input calculation.
Deposition rate of aerosol	82 μg / cm^2 / yr (Chester, 1990)
Al aerosol deposition rate	5000ng / cm^2 / yr (Chester, 1990)
Mixed layer depth	75m (D216 CTD data)
Solubility of Al in aerosols	8-10% (Maring and Duce, 1987)
Added aerosol Al remains in the mixed layer	No scavenging term

Including the assumptions and information listed above it is calculated that the potential increase in Al surface concentration resulting from Al aeolian inputs would be 0.43nM (minimum) to 1.9nM (maximum) over the 3 months between the adjacent Charles Darwin (CD94) and Discovery (D216) cruises in the Celtic Sea. The maximum surface concentrations of Al were calculated using aerosol deposition rates recorded by C.Hunt over OMEX D216 (max. Al deposition rate 21.9μg/cm^2/yr, Al aerosol concentration is 697ng/m^3, over 71 days between cruises).

This calculation does not allow for potentially significant wet deposition (Saharan aerosol Al is ~17% soluble in rain water - Chester et al., 1997) but even so, aeolian input could not explain the observed surface maxima of 20-35nM. This significant increase in surface Al concentration over such a small timescale also calls into question the assumption made by Measures and Brown (1997) that dissolved Al in the surface waters of the Atlantic is a steady state feature in which Al supply from the partial dissolution of incoming mineral dust balances its scavenging removal by biological processes. Clearly in the short term this is not the case.

From the Al profiles and underway sampling it is apparent that the Al maximum lies approximately 20-40 m down in the water column. The actual surface waters that would be directly affected by aeolian inputs have lower Al concentrations (4-10 nM). Even these lower concentrations could not be caused by estimated aerosol inputs. Advection of surface waters from an area of high aerosol loading, or shelf sediment influence or storm mixing is a more likely explanation for the elevated Al surface concentrations.

There are other processes that may create the shallow Al maxima observed. The apparent surface depletion in comparison to the maximum at 20-40m suggests some sort of scavenging process and perhaps release or recycling deeper in the mixed layer. This is partially consistent with findings in surface coastal waters of biological removal by phytoplankton (Hydes, 1989). The biological effect here is small compared to removal observed in June where Al concentrations were extremely low (<1nM in some cases -Hydes

pers.comm.). At this time of year primary production might still have an effect, although reduced. It is possible that scavenging of dissolved Al could occur passively by other particles (inorganic aerosols, dead bacteria/phytoplankton) with associated regeneration lower down in the water column. There is a strong indication that some form of removal coupled to biology (productivity) is occurring because of a Si/ Al covariance determined in the lower water column (>1500m) although this may be remnant from the spring/summer bloom.

Overall, it is possible that biological scavenging and recycling of Al within the mixed layer (hence lower surface concentrations and coincident chlorophyll-a and Al maxima) or advection of shelf water which has a high Al sediment signal into the area has caused this subsurface maximum. The patchiness in Al surface concentrations observed here has also been observed in several other studies (Hydes, 1989; Hydes and Kremling, 1993). Often these have been related to differing water origins or biological action. The patchiness observed in Al in surface waters is not surprising given the patchy nature of phytoplankton populations and scavenging particle concentrations occurring in an area of low lateral mixing such as the Celtic sea.

5.4.2: Profile variation:

Al concentrations were seen to vary between sites especially with respect to the Mediterranean outflow signal. The variations in Al concentration in the upper profiles are not seen in the deep water masses, and therefore the variations appear real.

The Mediterranean Outflow Water (MOW) is continually diluted as it moves away from the Strait of Gibraltar. There are several mechanisms by which dissolved Al could be altered;

- entrainment of other water masses that could increase or decrease Al concentrations,
- scavenging by particles (organic or inorganic).

Both of these processes can have different spatial effects as the MOW flows further from its source. It would be expected that more Al would be removed by scavenging and the MOW would be increasingly altered as it moves from its source. Figure 5.10 shows this effect to

some extent. For sites in sucession along the shelf (KAC to OM8) there is a progressive reduction in the dissolved Al concentration peak (>30 to ~ 20nM) and the elevated Al signal becomes more diffuse.

5.4.3: Al/Si covariance:

In this study as in previous works, a relationship between Al/Si and depth has been observed. In deep waters (>1500m) total and dissolved Al and Si concentrations increase with depth. It is proposed that this trend is due to the scavenging of dissolved Al species by phytoplankton (primarily diatoms) or siliceous particles in the surface, and release via dissolution or degradation of diatomaceous organic matter deeper in the water column (it is likely however that the second process is far more rapid and may occur in the upper water column). Such biological uptake has been observed by Moran and Moore (1988a and b), and Hydes (1989). However, the exact mechanism of biological removal, either by passive or active uptake (incorporation into organic tissue or siliceous tests) is still uncertain. Martin and Knauer (1973) found significant amounts of Al incorporated into diatom siliceous frustules after organic matter digestion. Further investigation is also needed to determine the details of the release process.

As discussed previously, points in the data set influenced by sediment input have been removed from the Al/Si regression analysis as the Al concentrations found were artificially high. Although, sediments may have a biologically derived Al component, associated with Si frustules (Chou and Wollast, 1991) this does not appear to be the only source of Al here as the Si levels were much lower in comparison to the observed Al release at these stations. Al release from non-biogenic sources such as dissolution of clay matrices (Moore and Millward, 1984) or regeneration from inorganic particles is possible. The influence of these biogenic and inorganic processes on Al speciation may contribute to the discrepancy between the significance (r^2) of the Si and dissolved or total reactive Al correlations i.e. The Si/total Al correlation is stronger illustrating that less of the dissolved Al may have biogenic

origins (e.g. dissolution of clay particles) but more biogenic Al (Si associated) falls into the particulate total reactive Al fraction (>0.4μm) .

5.4.4: Sediment as an Al source:

A clear input of dissolved Al (increase of 3-6nM compared to overlying water) has been observed at the deepest profile sampling points, 8 to 20 metres from the bed (a similar signal was observed 500m away from the bed at OM8). This Al release could occur by several diffusion or resuspension mechanisms (Moran and Moore, 1991). Unfortunately, it was not possible to identify the form (colloidal or truly dissolved) of these inputs. Studies sediment porewaters in the Mediterranean Sea (Chou and Wollast, 1991) indicated that the dissolution of biogenic silica takes place during early burial, releasing dissolved Al and Si into solution in the upper sediment layers. However, sediment associated points in the vertical profiles give a comparably high Al concentration compared to Si (see section 5.3.2.5). It follows that although there may be some Al release associated with regeneration of biological material there is an additional source of Al from the sediments that is non-biogenic. This additional release may be due to dissolution of Al from clay matrices (Moore and Millward, 1984) or regeneration from inorganic scavenged particles.

Al release from the sediments can occur via diffusion mechanisms or by resuspension effects. Advection of water with higher dissolved Al concentrations is also possible, for example in station OM8 where an increased Al concentration is observed 500m from the bed. Although no nepheloid layers were identified from the transmissometer trace, they are often short lived phenomenon so the increase in dissolved Al could still be attributed to a residual solution imprint of such processes. Sediment characterisation and resuspension experiments should provide some indication as to whether the observed Al increase could be attributed to resuspension events (pore water release, desorption, increased complexation of surface exchangeable aluminium-by lumogallion) or whether diffusion of metals from the sediments is more important.

5.5: Investigation of Celtic Sea sediment resuspension as a source of dissolved Al:

From the D216/OMEX Al profiles it was observed that there were clear inputs of dissolved Al close to the bed. Such a sediment source of Al could be attributable to diffusion, or resuspension mechanisms such as nepheloid layer formation (Moran and Moore, 1991).

A set of sediment resuspension and porewater investigations were designed to identify the form (truly dissolved or colloidal) of the dissolved Al input seen in the water column profiles and whether the observed Al increase could be attributed to resuspension events (pore water release, dissolution of aluminosilicates, desorption, increased complexation of surface exchangeable metals by lumogallion) or diffusion of metals from the sediments.

This study is divided into the following sections:

Resuspension experiments to investigate Al release upon resuspension of surface sediment from box cores taken on OMEX D216. This should indicate the phase of any Al release and also the lifetime in solution of Al during and after original resuspension. Using laminar flow blocks (CFF) the dissolved Al can be identified as colloidal or truly dissolved forms.

Photo-oxidation experiments to check that porewater released into solution does not contain organic matter or other species that can interfere with the lumogallion technique.

Leachate experiments to identify the available Al in the sediment upon resuspension. Two extraction methods were compared ($MgCl_2$ and acetic acid) to see if they could throw light on differences in the association of Al with sediment particles. Essentially, the $MgCl_2$ displaces Al by ionic exchange processes whilst the acetic acid is capable of dissolving sediment material including $CaCO_3$. The acetic acid method is the main method used in the literature to assess leachable Al in water column particles.

Porewater Al concentration determination to assess the potential source of Al to the overlying water column from sediment porewater via diffusion or resuspension. Interstitial investigations in the NW Mediterranean (Chou and Wollast, 1991) have indicated that the dissolution of biogenic silica takes place during early burial, releasing dissolved Al and Si into solution in the upper sediment layers. These authors found dissolved Al concentrations of 100-750nM in the surface sediment layers. These values can be compared with the concentrations determined here for Celtic Sea sediment porewater.

Field-flow fractionation (FFF) investigations of the size spectrum distribution of total reactive and dissolved Al from sediment stock suspension used in the resuspension experiments.

Coulter Counter investigations of the particle spectrum (>1μm) during resuspension and after sedimentation. This technique should give an insight into the particle dynamics during and post resuspension.

5.5.1: Celtic Sea sediment study: methods

5.5.1.1: Cleaning of new Nalgene bottles as reaction bottles for the lumogallion technique:

After several months of storage several lumogallion reaction bottles showed signs of growth on their interiors. To replace these bottles, new Nalgene bottles were aged with lumogallion solution. The lumogallion reagent was left in the sample bottles for a week. Lumogallion solution was discarded prior to sample analysis and bottle blanks were carried out to check bottles were clean before use (See Appendix 4 for details).

5.5.1.2: Clean techniques:

All sample manipulations, dilutions and the lumogallion analyses were carried out using clean techniques in a laminar flow hood (class 100).

Bottles for resuspension Al samples were cleaned as detailed in Appendix 4.

5.5.1.3: Aluminium resuspension experiment: see flow diagram

Celtic Sea sediment samples (box core surface scrapes) were taken from stations OM6 and OM5 during D216. Forty litres of deep water (low Al concentration) for resuspension of this sediment was also collected during the cruise and stored in an acid rinsed polycarbonate carboy. The sediment and bulk seawater were stored in a constant temperature laboratory at ambient seawater temperature (2-4°C) and in the dark.

The low Al concentration seawater was prefiltered (0.4μm) prior to use in the first resuspension experiments. For subsequent experiments using large volumes, the seawater was not prefiltered as filtration of the 15 litres required incurred too much chance of contamination from external sources during sample handling and unfiltered seawater was much more representative of natural resuspension conditions. For each of the resuspension experiments there was a control with no sediment addition. The resuspension plots were normalised for any Al concentration and partition changes observed in the control, although changes were not large (<1nM) in comparison to changes in the resuspensions.

For each suspension experiment (see flow diagram), 4 litres of low Al seawater was left stirring overnight in clean LDPE bottles to equilibrate (any Al removal to bottle walls will have occurred during this time-D.Hydes pers. comm.). For the pilot experiment (90µg/l SPM) three FEP bottles (10% HCl cleaned) containing 1 litre of filtered low Al seawater were used (2x1 litre resuspension, 1x1 litre control). All the resuspension and control experiments were kept in the dark at 2-4°C (i.e. as close to ambient conditions as possible). Total reactive, dissolved and truly dissolved Al concentration measurements were taken prior to resuspension (t=0) for each of the sediment resuspensions and controls.

5.5.1.4: Stock sediment suspension:

A stock suspension was made from the Celtic Sea sediment as described in Moran and Moore (1991). An aliquot (0.511g) of sediment was weighed into a 250ml LDPE bottle

F4: Celtic Sea sediment resuspension flow diagram.

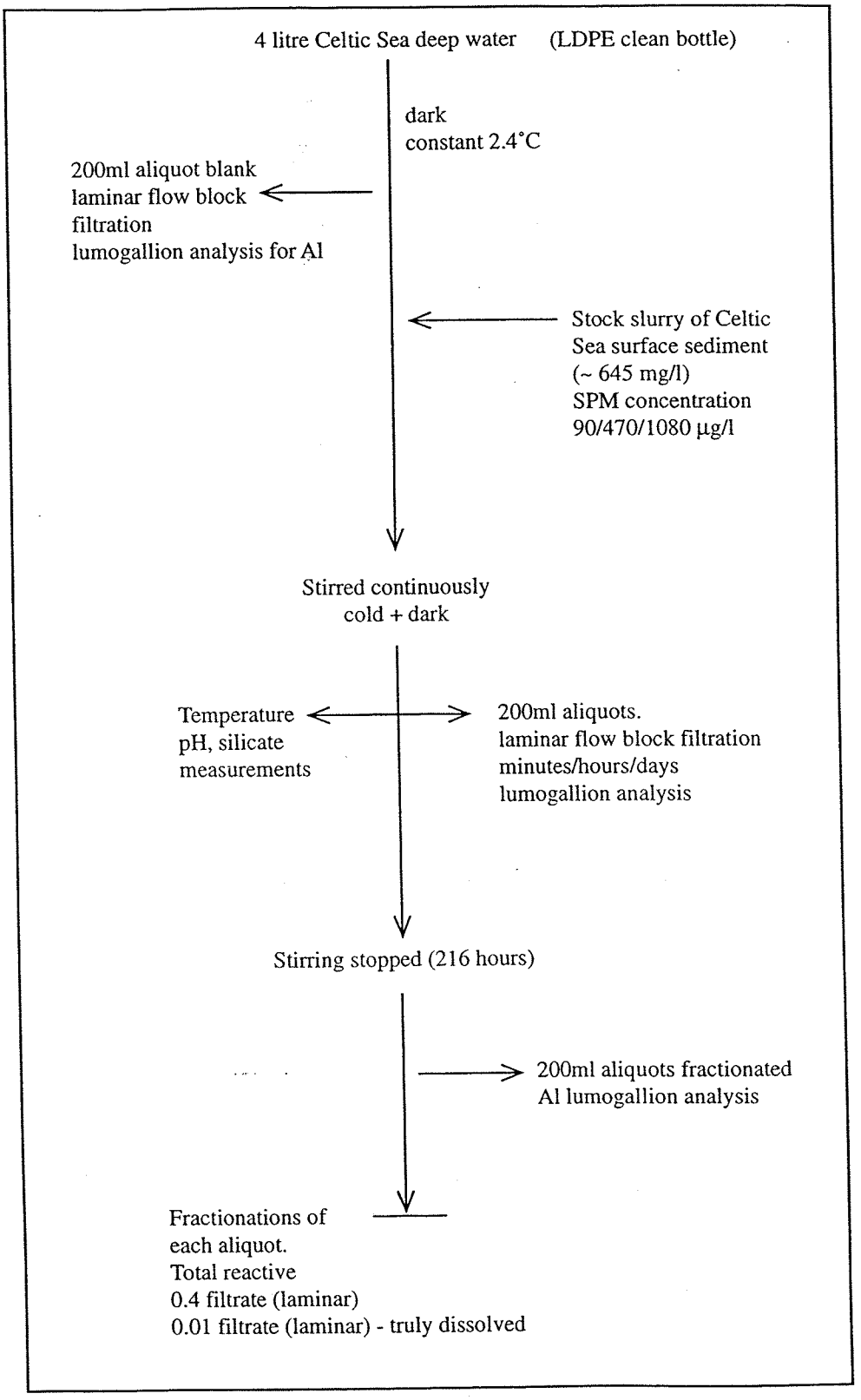

and the volume was made up to 250mls with 0.4μm filtered low Al seawater. The resulting stock suspension was shaken well to ensure complete homogenisation.

Gravimetric analysis of this initial stock was completed (50ml filtered onto 0.4μm filter, in triplicate), to give accurate estimations of the sediment concentrations in the resuspension experiments. Resuspension experiments of various SPM concentrations were set up by injection of differing volumes of stock suspension into the low Al seawater (duplicates of each sediment concentration were run simultaneously). Although SPM concentrations in each resuspension could be calculated from the stock sediment suspension concentration, several litres were also used to attempt accurate gravimetric determination of the particulate (0.4μm) and colloidal (0.01μm) fractions directly.

5.5.1.5: Time series resuspension experiments:

Upon injection of the sediment slurry (volume varied to give different sediment concentrations) and throughout the course of the experiments the samples (resuspensions and control) were stirred continuously to maintain homogeneity.

200ml aliquots of suspension or control were removed at several time intervals ranging from minutes to hours/days. The samples were taken from middle of the suspension via a clean syringe and tubing. It was assumed that the resuspension remained homogenous throughout the experiments. Temperature, pH and Si were also measured or sampled at the time of sampling. Samples for Si analysis were kept cold until determination by a procedure modified from Strickland and Parsons (1972).

For some of the resuspensions (R1 a and b and R2 a and b) the sampling was continued for up to 1 week, and continued after stirring was stopped to look at the longer term effects of sediment resuspension (e.g. possible readsorption with time) and also at the longevity of resuspension events once the resuspending force has disappeared.

Each sample removed was fractionated into (see Appendix 4 for detailed procedure);

Total reactive (unfiltered),

dissolved (<0.4μm),

truly dissolved (<0.01μm).

The colloidal Al was calculated from the difference between total dissolved and truly dissolved Al concentrations. The Al concentration of each of the fractions was determined using the lumogallion method (Hydes and Liss, 1976) which was calibrated by standard additions. This method was scaled down to analyse 5mls of sample to minimise filtration time and therefore optimise sampling resolution. As Table 5.2 illustrates, there was no significant difference in the Al concentration determined by the 20ml or 5ml methods.

Table 5.2: Accuracy/precision check for scaling down of the lumogallion technique to 5mls.

	Lower Al conc. (rep.1)	**Lower Al conc. (rep.2)**	**Higher Al conc. (rep.1)**	**Higher Al conc. (rep.2)**
Volume	20ml (eppendorf)	5ml (micropipette)	20ml (eppendorf)	5ml (micropipette)
Total Al (nM) (n=5)	6.2	6.6	18.7	18.6
Standard dev.	0.22	0.19	0.09	0.05

5.5.1.6: Use of laminar flow block filtration:

Originally, there were some problems with conventional filtration with 25mm 0.01μm polycarbonate filters. It was not possible to generate the pressure required for filtration by hand. There was a problem with the PVP wetting agent effectively clogging the filter pores, but even upon acid cleaning (10% HCl) the problem was not solved.

To enable filtration at the 0.01μm cut-off it was decided to use laminar flow blocks. Although this approach would enable a 0.01μm filtration, the time taken to change filters and the increased sample volume required would be a disadvantage to high resolution measurement. It also meant that large volume resuspensions had to be carried out to compensate for the increased sample volume that was required.

Laminar flow block cleaning and filtration blank procedures are described in Appendix 4.

Blank results:

Table 5.3 illustrates the laminar flow block and equipment blanks.

There was no significant increase or decrease in total Al concentrations relative to Milli-Q (0.68 ± 0.12) when sampling with the syringe. Tubing and frit blanks showed a measure of Al removal (0.5-1nM (1-5 % of total Al) but the 0.4 / 0.01μm Milli-Q filter and seawater filtrate blanks showed no detectable change in Al concentration so there was no grounds for concern over the use of the laminar flow block for fractionation of the resuspension samples. It was assumed that there was very low adsorption of Al onto the polycarbonate filters used in the laminar flow blocks. Polycarbonate filters have been used in many trace metal and Al studies for this reason (Moran and Moore, 1991; A. Tappin pers.comm.). Also, the refiltrate seawater blanks (fb) illustrate that Al removal by the system/ filters is not occurring significantly.

Table 5.3 Milli-Q and seawater blanks (nM) for laminar flow blocks: filters, tubing, frits and syringe sampler.

Filter or equipment blank	**Milli-Q**	**Std.dev.**	**Seawater lower Al conc.**	**Std.dev.**	**Seawater higher Al conc.**	**Std.dev.**
Total	0.68	0.12	7.17	0.1		
0.4	0.92	0.19	5.78	0.1		
0.4fb			5.60	0.1		
0.01	0.92	0.19	4.76	0.01		
0.01fb			4.53	0.10		
Total	0.68	0.12	12.04	0	24.27	0.38
Tubing	0.84	0.06	11.74	0.18	22.48	0.19
Frit/ filtrate	0.64	0.06	10.37	0.98	21.81	0.05
Total					24.27	0.38
syringe					25.0	0.12

5.5.2: Results of Celtic Sea sediment resuspension experiments:

5.5.2.1: Stock suspension and experimental resuspension SPM measurements:

Stock suspension concentration was ~ 645.84 ± 81.25 mg/l
(This very concentrated slurry was injected in very small volumes (reproducible) to give low concentrations comparable to in-situ measurements in the deep water of the Celtic Sea area).

The resuspension experiment SPM concentrations (including colloidal mass by exhaustive filtration) were;

Pilot	90μg/l
R1a and b	470 ± 10μg/l
R2a and b	1080 ± 120μg/l

5.5.2.2: Magnitude of Al release and Al partitioning changes:

Figures 5.16 to 5.19 show the concentrations of Al in the control and resuspension experiments (for all figures error bars are 1σ of triplicate analytical measurements. If not show the standard deviation lies within the marker. On log timescale (x-axis) for longer experiments 0.1 is time 0 before addition of sediment). Si concentration remained between 28-29μmol/l for the duration of the resuspension and control experiments. Stirring of the suspensions was stopped at 216 hours.

Figure 5.16 shows that there was change in the form of Al in the unfiltered control sample even though the Al concentration changes in the filtered control are minimal. This probably due to the presence of some particulate or colloidal material in the unfiltered seawater control. All resuspension plots were normalised to account for differences in Al concentrations observed in the controls.

Significant total reactive Al releases (1.5-12nM) were observed at all particle concentrations, 90 to 1080μg/l (see Figures 5.17 and 5.18). Higher time resolution sampling of a 470μg/l resuspension (Figure 5.19) showed that the peak of the total reactive Al release occurred within the first 30 minutes of resuspension, 60% of this

release occurs almost instantaneously, within the first 5 minutes of resuspension (the reaction does not fit a simple first order rate law but there is an initial release rate of ~8.5nM/min/mg of sediment). This is consistent with the observations of Moran and Moore (1991) who suggested that the increase in dissolved Al was primarily due to rapid dissolution of authigenic mineral phases. This hypothesis is supported here as a large percentage of the increase in dissolved Al upon resuspension (1.8-7.1nM) is accounted for by an increase in the truly dissolved phase Al (1.7-6nM) in the resuspension Figures for R1a and b and R2 a and b. The absolute and percentage partitoning plots of Al (Figures 5.17, 5.18 and 5.21) also indicate that a significant fraction of the total reactive Al increase is attributable to the presence of Al species on particles greater than 0.4μm (~40%). The colloidal signature only increases measurably (~1nM) at higher SPM resuspensions (1080μg/l).

Figure 5.16: Low SPM (90µg/l) resuspension (in filtered seawater) and control (unfiltered) for Al partitioning (higher SPM resuspensions). Errors (1σ of three replicate measurements) are quoted in Appendix 4 of the data disc.

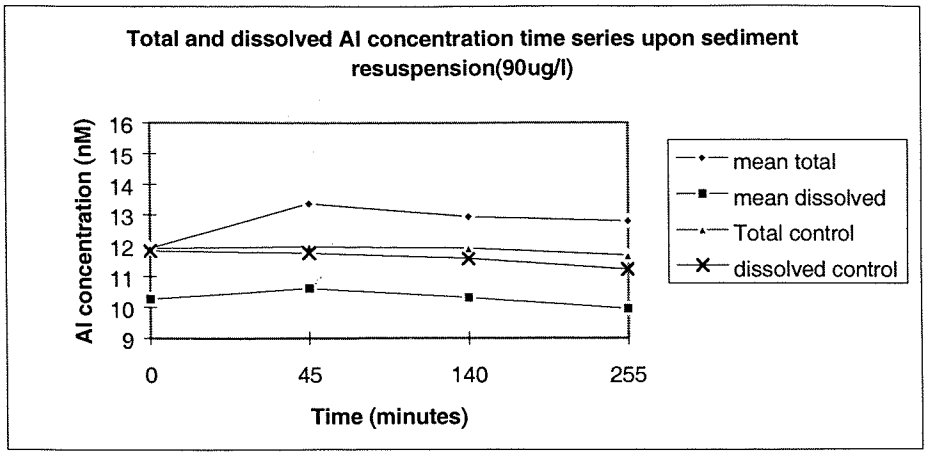

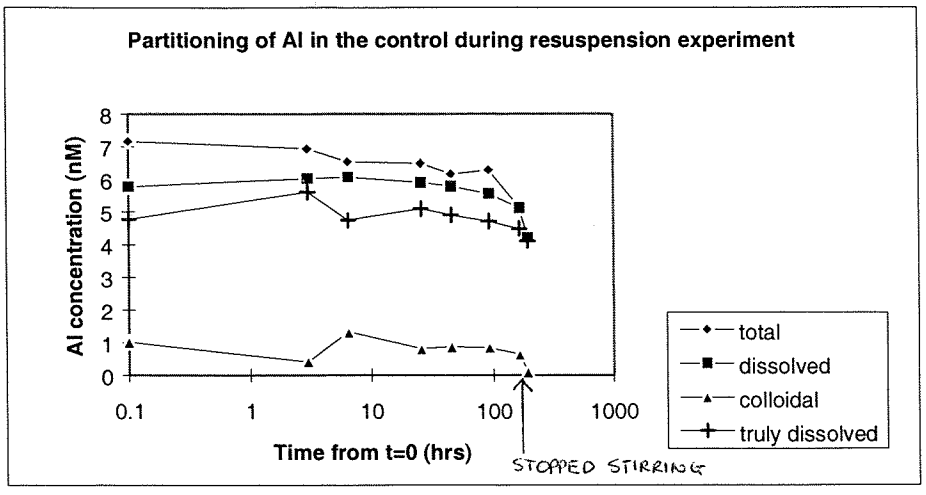

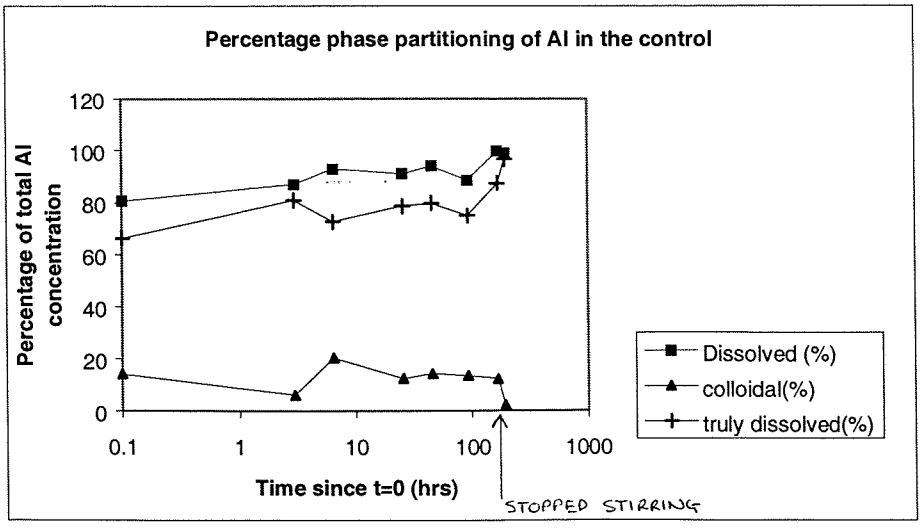

Figure 5.17 A and B: Partitioning of Al during duplicate (A and B) sediment resuspension experiments (SPM 470µg/l).

A:

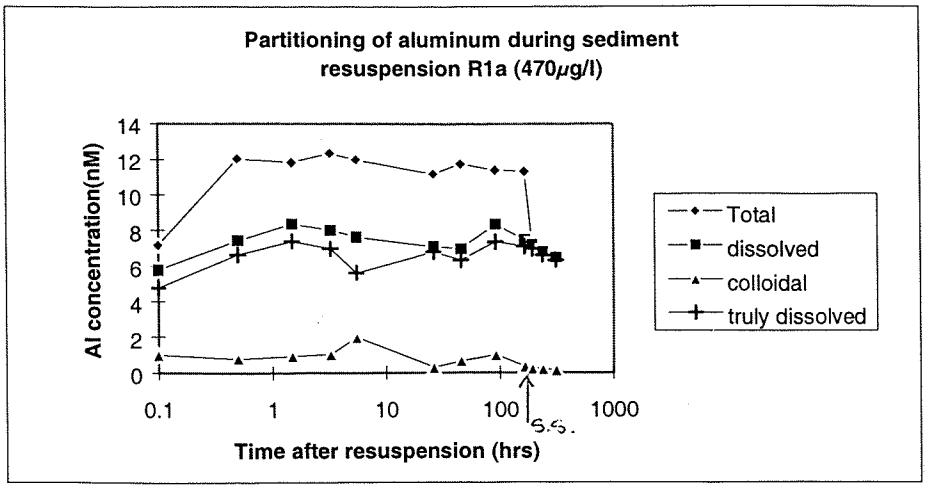

B:

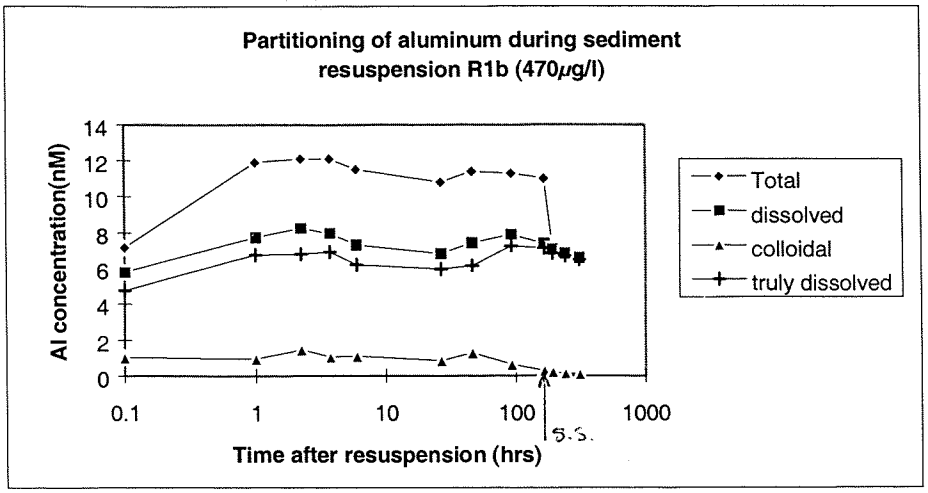

Figure 5.18: Partitioning of Al in duplicate resuspension experiments (1080µg/l).

A:

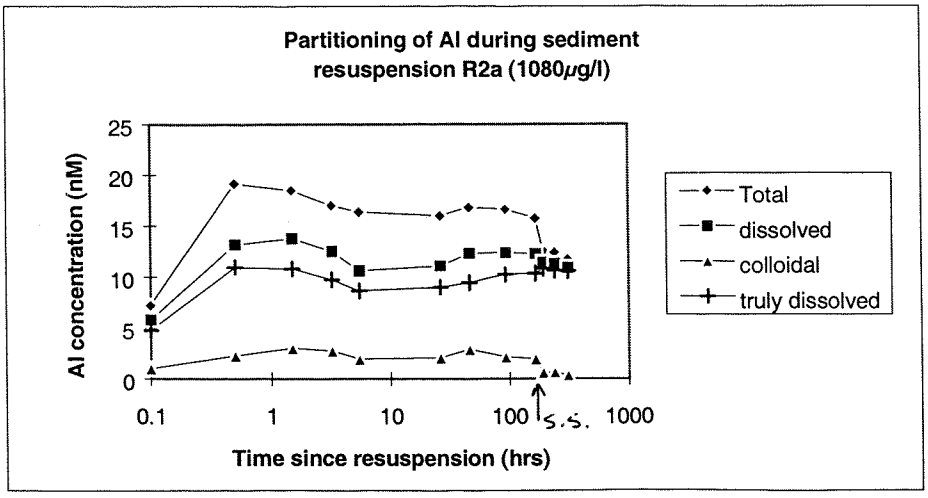

B:

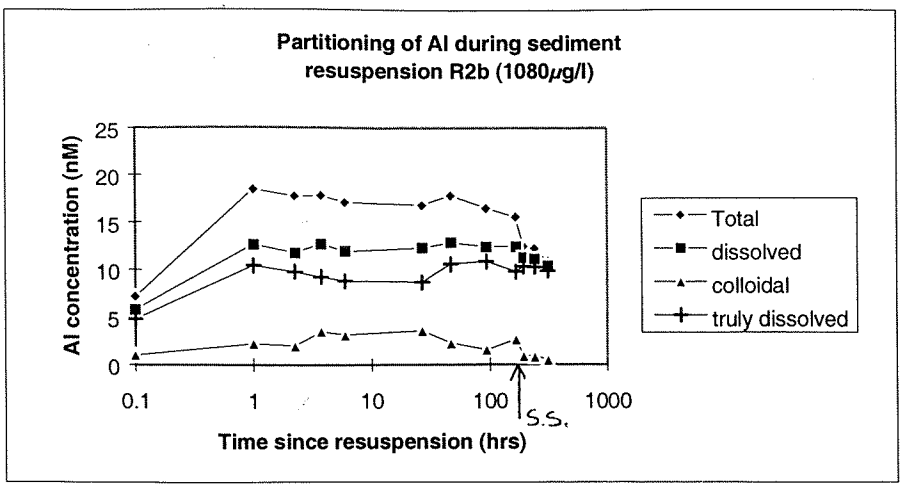

Figure 5.19: High resolution resuspension of total reactive Al (SPM 470μg/l).

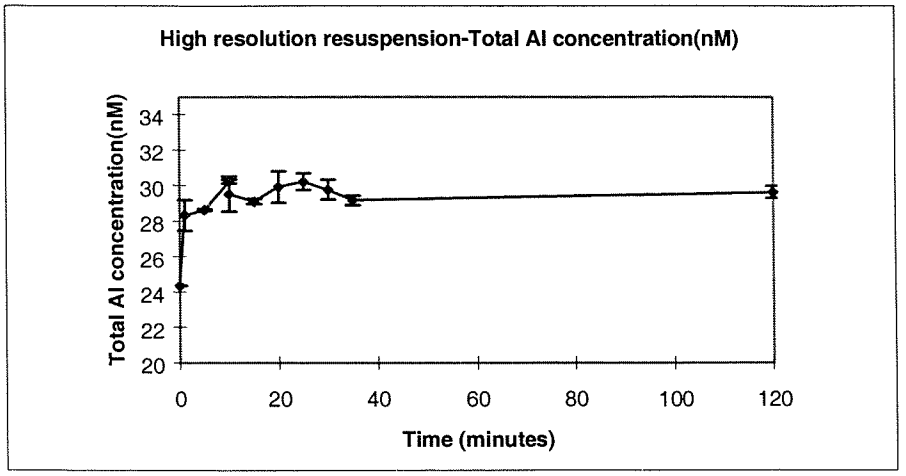

5.5.2.3: Al release compared to SPM addition:

The initial total reactive, dissolved and truly dissolved increases in Al concentration appear directly proportional to resuspended sediment concentration. R^2 =0.9953, 0.9322 and 0.971 respectively (see Figures 5.20 a, b and c).

The gradients of the regression lines give an estimate of the Al release per unit SPM. The releases are 10.7, 6.2 and 5.3 nM/mg sediment for total reactive, dissolved and truly dissolved Al respectively. By inference, the initial release due to particles (>0.4μm) and colloids is 4.5 and 0.9 nM/mg of sediment respectively. The particle, colloidal and truly dissolved fractions comprise 42, 8.4 and 49.6 % of the initial total reactive Al release respectively. Given the linear nature of total reactive Al release with SPM concentration it is possible to assess the initial rate of total reactive Al release as ~8.5 nM/min/mg.

Figure 5.20: Initial increase in a) total reactive, b) dissolved, c) truly dissolved Al concentrations with SPM concentration.

a)

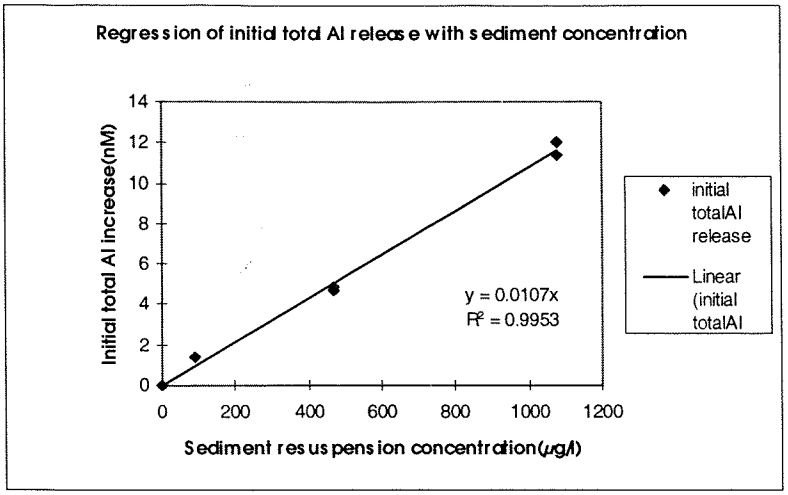

b)

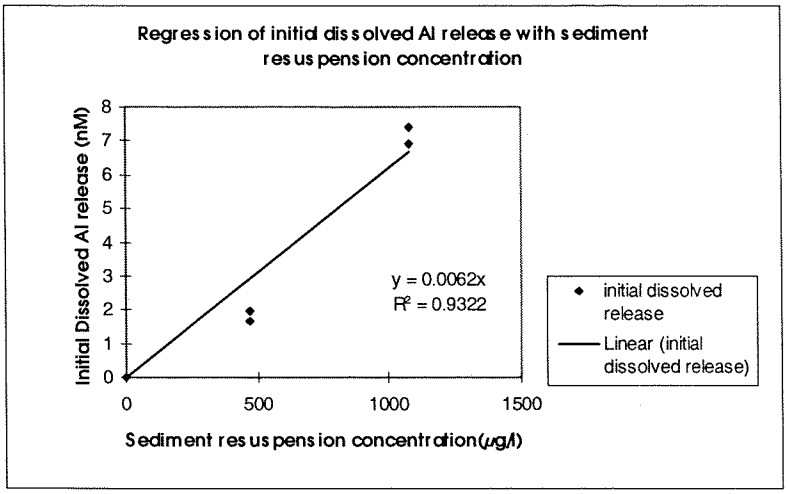

c)

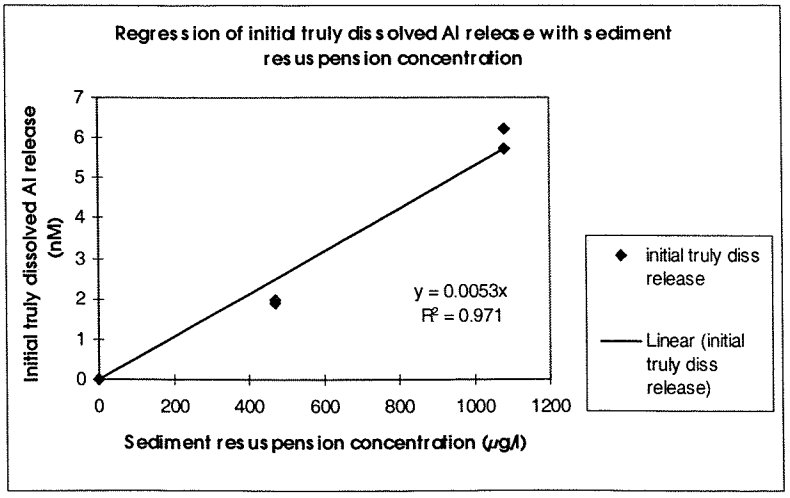

Figure 5.21: Percentage (of total reactive) partitioning for Al during duplicate resuspensions(470/1080μg/l).

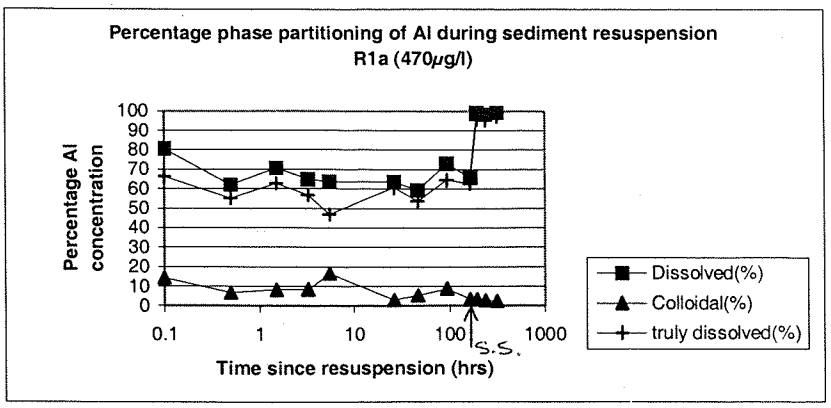

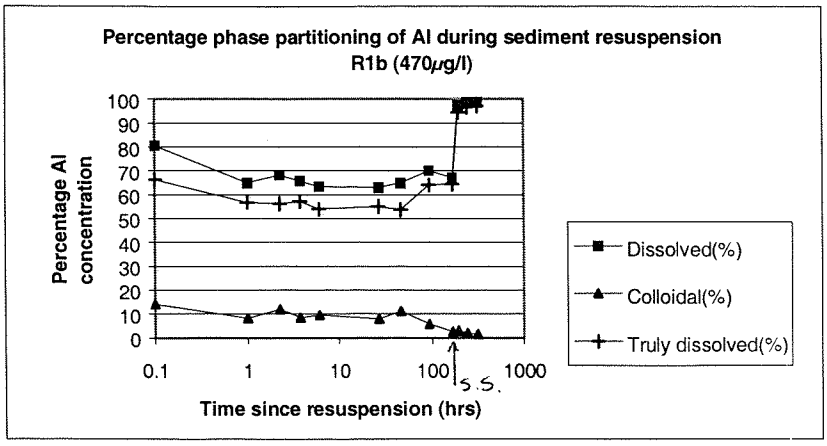

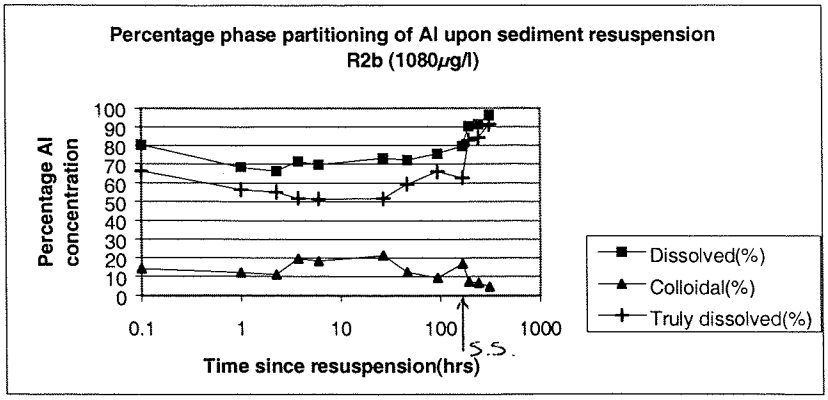

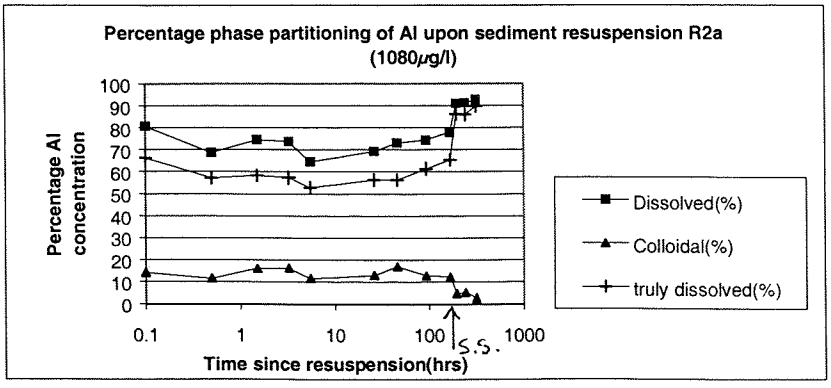

Figure 5.22: Al release (above concentration at t=0 (0.1) ,SPM comparisons)

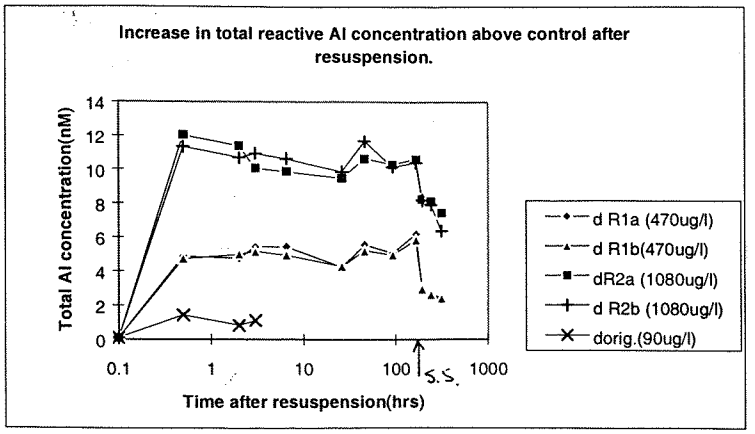

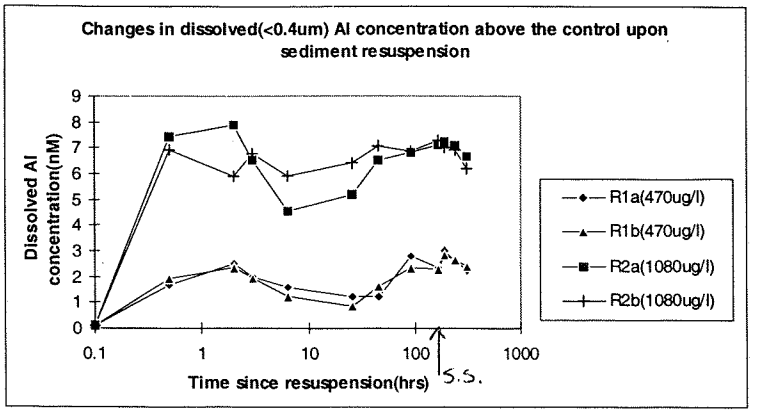

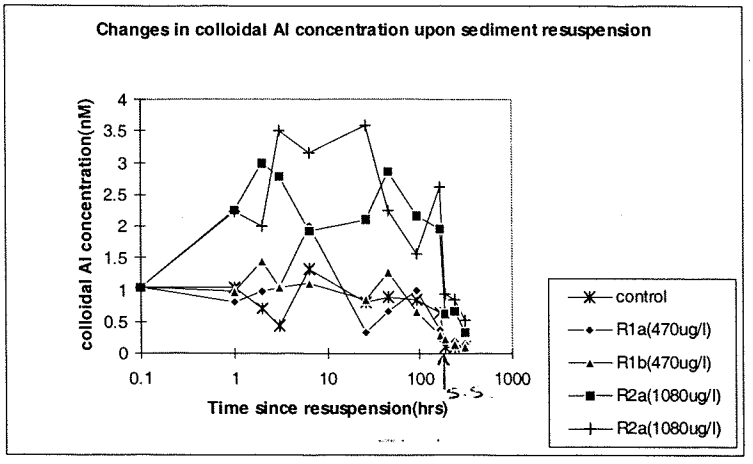

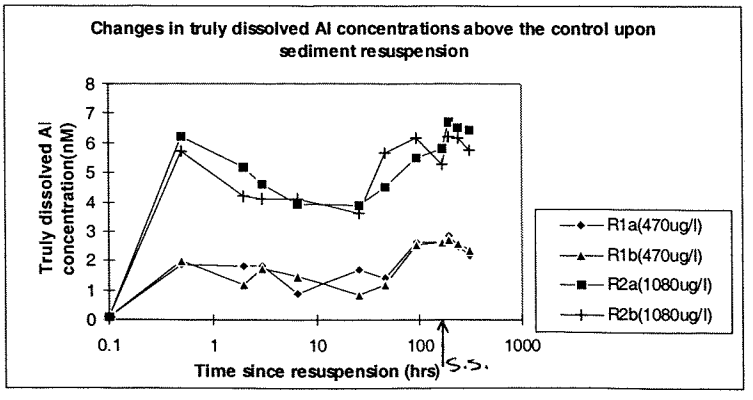

5.5.2.4: Partitioning changes with time:

Figures 5.21 and 5.22 show the Al partitioning changes above the control concentrations and percentage Al partition changes during the resuspension experiments.
Increases in the initial Al concentration appear attributable to release of truly dissolved and particulate (>0.4μm) Al phases. The colloidal phase increases initially in the highest SPM resuspension only. The colloidal traces have not been normalised to the control changes.
After an initial increase all phases remain relatively constant with minor fluctuations and slight decreases over time. There appears to be some cycling between the truly dissolved and colloidal phases as total and "dissolved" Al concentrations remain relatively constant. The truly dissolved is the major phase in both resuspension concentrations comprising 50-65% of the total reactive Al. Al associated with particulate material (>0.4μm) increases from 20% to 40% of total reactive Al and remains significant until resuspension ceases indicating minimal aggregation removal or scavenging. The colloidal Al fluctuates between 3-15% but is higher where the sediment concentration is higher (20% here).

5.5.2.5: Effect of stopping stirring (see Figures 5.17, 5.18, 5.21, 5.22):

When stirring is ceased (after ~216 hours) i.e. after a simulated resuspension event, there is rapid decrease in the total reactive Al which is accounted for by aggregation and sedimentation of particles >0.4μm i.e. not included in the dissolved phase.

"Dissolved" Al shows a minimal decrease, mainly as a result of colloidal aggregation and sedimentation. Truly dissolved Al decreases very slightly and may be scavenged by aggregating and sedimenting particulate or colloidal material. Eventually, truly dissolved Al is the main phase remaining (90 to 100% of total reactive Al).

5.5.2.6: Net changes in Al during and after resuspension:

A considerable time after the resuspension event (up to 1 week), "dissolved" (mainly truly dissolved levels) are increased from the initial background Al levels prior to resuspension (~0.75 to 5.5nM for 470 and 1080ug/l respectively). Colloidal Al levels are

decreased from original levels in resuspended samples. This may be due to effective removal of colloidal Al by aggregation and combination with larger resuspended and sedimenting particles.

5.5.2.7: Comparison of resuspension data with the current published literature:

Relatively little work has been done on the release of Al or colloidal Al upon sediment resuspension (Mackin, 1986; Moran and Moore, 1991).

In this study there is a pronounced dissolved Al release upon resuspension (1.8-7.1nM) despite high Si levels (28μmol/l). It seems that Si concentration of the ambient water and its affect on release of truly dissolved Al from dissolution of authigenic mineral phases is closely linked to the magnitude of Al release upon sediment resuspension (Hydes Pers.comm.). Mackin (1986) illustrated that a doubling of Si concentration (325 to 600μM) would lead to a significant decrease in dissolved Al release upon sediment resuspension (Al release was decreased from 80 to 50nM respectively for the two Si concentrations). The formation and dissolution of authigenic aluminosilicates is highly reversible and Si concentrations can control not only the dissolution of authigenic minerals but also their reformation (Mackin, 1986; Moran and Moore, 1991). The release observed in this study is significantly lower than seen by Moran and Moore (1991) who measured a 60-70nM dissolved Al increase at Si concentrations of 4μM and at similar SPM. This contrast may be due to the varying initial Si concentrations (Mackin, 1986) or different sediment properties i.e. authigenic mineral content. The resuspension releases in this study are significant enough to account for elevated dissolved Al close to the sea floor in the Celtic Sea, however, further sediment characterisation experiments i.e. dissolution experiments, leachable Al $[Al]_{HAc}$ vs. $MgCl_2$ and porewater analysis will give further insight into the role of these sediments as an Al source and contrast OMEX sediment to that used by Moran and Moore (1991).
Background Al concentrations in the suspending seawater are slightly lower than encountered by Moran and Moore in their study, 5.8nM vs. 11nM respectively. However Moran and Moore (1991) illustrated that the original Al concentration has a minimal effect on Al resuspension release (4nM suppression of Al release for a 10 fold increase in

original Al concentration). Differences in dissolved seawater Al concentration would therefore not have a detectable effect on Al release here.

Moran and Moore (1991) observed a decrease in dissolved Al within 30 minutes to 1 hour of the initial peak Al release that they attributed to authigenic mineral reformation. They also observed that the dissolved Al concentration plateaued out at approximately 30nM (30-40nM less than the peak dissolved Al concentration) where it was stable for several days to a week. Authigenic mineral reformation perhaps should have been favoured in this due to higher Si levels (28 vs. 4 μmol) but this was not observed and dissolved Al levels (especially truly dissolved) remained elevated for a week or more until the end of resuspension and for several days afterwards. There seems to be more Al cycling within the resuspension in this study rather than a direct removal of dissolved Al which has been encountered in previous studies.

Despite the possible controls of Si concentration on the reversible formation/dissolution of authigenic mineral phases which can affect dissolved Al concentrations, in this study there is a significant fraction of the total reactive Al concentration increase that is associated with the particulate (>0.4μm) phase which is determined more by the magnitude of resuspension than the Si concentration. In this case the increase in total reactive Al is as much governed by the type and concentration of sediment resuspended and whether the Al available on the particle surfaces is available for complexation and detection by the lumogallion reagent.

5.5.3: Photo-oxidation experiment:

There is some evidence in the literature that there is a problem with the determination of Al concentration in porewaters using the lumogallion technique. Mackin and Aller (1984a) suggested that a competitive complexation of aluminium with any Fe, F^-, organics or phosphate in the sediment porewater would decrease the lumogallion fluorescence signal, by approximately 10% (Hydes and Liss, 1976) and lead to an underestimation of Al in the porewater. Mackin and Aller (1984a) used $CaCl_2$ additions to reduce the activities of the interfering ions. This set of experiments was designed to investigate if organic species/matrix changes upon sediment resuspension would affect the total reactive (unfiltered so maximum potential effect) Al concentration measured by the lumogallion technique as in the resuspension experiments

To do this, two aliquots of the same resuspension sample were taken. One aliquot was analysed immediately after resuspension. The second sample was given UV treatment to photo-oxidise any organic species that may have been released upon sediment resuspension. Both samples were then analysed by the lumogallion technique. The total Al concentration in all samples was determined using several standard additions to see if the same Al spike gave the same lumogallion response irrespective of prior treatment.

There may be some Al loss during photo-oxidation due to Al species binding onto the sides of the silica sample vials (200ml). Some heating of the sample will also occur. The absolute difference in total Al concentration of the two samples is not as important as the difference in the gradients of the standard addition calibration curves, which will indicate if there is any competitive complexation of the Al/lumogallion by organic or other matrix species present from resuspension (quenching). If there is competitive complexation the fluorescence increase for a given Al spike will probably be reduced in the untreated sample where organic/complexing species are present. Photo-oxidation should destroy all the organic species present, although other complexing matrix species may not be ruled out. Analysis of a typical seawater sample (seawater blank) should quantify some effects of matrix species.

5.5.3.1: Experimental procedure:

Silica UV cells (200mls) were initially cleaned in 50% HCl, and then given a 10% HCl wash with triplicate Milli-Q rinses immediately before use. The internal supports in the UV exposure cupboard were made of Al so the parts in contact with the Si cells were coated with a marine paint. The silica vials had lids that fit over the lip of an extended cone so that no fraction of a sample came in contact with the lip of the vial that had been exposed to the outside of the UV cabinet. The entire outside of each cell was rinsed with Milli-Q before they were opened in a clean environment. Blank seawater Al measurements were done in triplicate prior to resuspension to assess the original total reactive Al concentration, and thus by difference, effects of photo-oxidation on Al concentration.

The experimental procedure consisted of injection of 800µl of sediment stock suspension into 1litre of seawater and stirred over 4 hours to homogenise and allow porewater and matrix species release. Three samples were removed using a clean syringe for determination of the total reactive Al concentration after resuspension.
Three, 200ml samples were also removed at the same time and photo-oxidised for approximately 4 hours. Al concentrations in seawater blank, photo-oxidised and unphoto-oxidised resuspension samples were determined by the lumogallion technique and compared. All sample manipulations and lumogallion analysis was carried out under clean conditions in a laminar flow hood (class 100).

5.5.3.2: Results:

The standard addition calibration curves for seawater blank, resuspension and photo-oxidised resuspension samples are all linear (R^2 = 0.9988, 0.9979 and 0.9953 respectively-Figure 5.23) indicating that any complexation effects do not vary with increasing Al additions and therefore the calibration curves are appropriate and reliable.

The photo-oxidised samples show a marked decrease in determined Al. This has also been observed by Hydes and Liss (1976) where erratic results and incomplete recovery of added Al after photo-oxidation was observed. It is possible that this Al removal is

partially due to removal of Al onto the sides of the silica photo-oxidation cell. Aluminium-silica associations has previously been identified in diatomic incorporation of Al into tissue and Si frustules (Hydes, 1979; Moran and Moore, 1988a and b).

Figure 5.23: Standard addition calibrations for seawater blank and (un) photo-oxidised samples from sediment resuspensions.

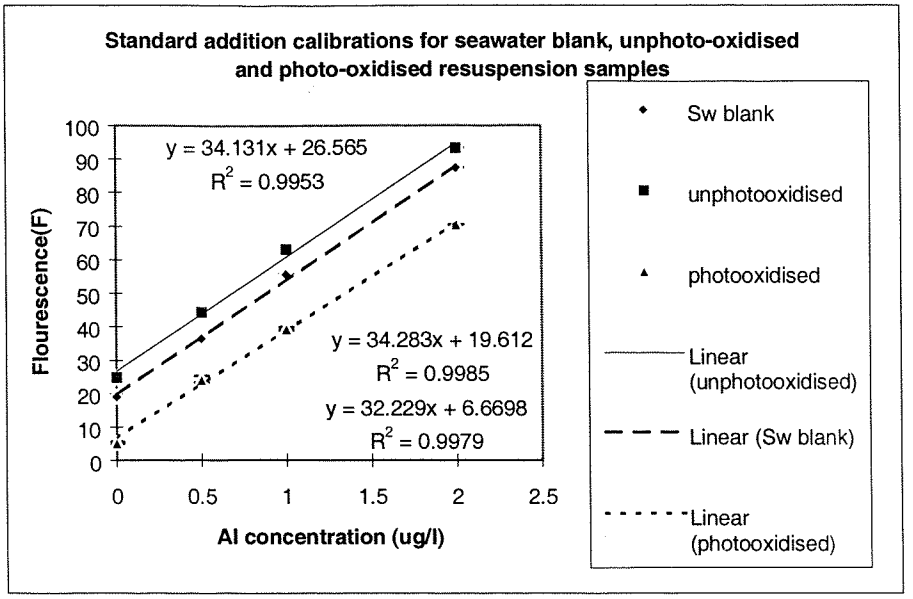

The gradients of the unphoto-oxidised and photo-oxidised resuspension samples are not very different from the seawater blank or each other (34.283 (SW) versus 34.131 and 32.295 respectively). Hence, for both samples the increase in fluorescence is not significantly different for a given Al concentration increase. This indicates that there are insufficient organic species in the resuspended samples to cause significant competitive complexation of the lumogallion reagent which may alter the Al concentration determined.

When the standard addition calibrations are overlaid (see Figure 5.24), at lower Al concentrations the means of samples from the two treatments are not significantly different (T-test, t= 2.918, $p>0.05$). At the highest Al concentration the means are significantly different at the 95% confidence level (t=15.95 $p>0.05$). This should not be a problem though as all the resuspension sample concentrations are well below this 95%, 1µg/l significance limit. Overall, therefore the Al determinations for resuspension

samples using the lumogallion reagent addition technique are reliable and not subject to significant interference effects.

Figure 5.24: Overlaid calibrations for interference effect samples.

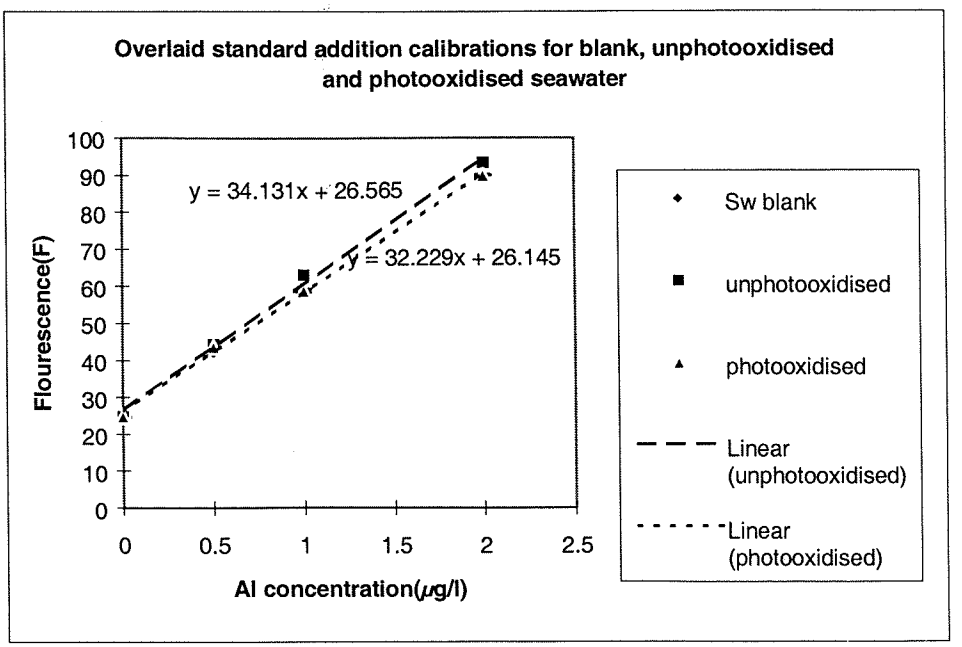

The background fluorescence of seawater and resuspension samples were both 0.1 which negates any increase in fluorescence due to organic or other fluorescent species released upon resuspension.

5.5.4: Determination of leachable particulate Al.

Moran and Moore (1991) and Orians and Bruland (1986) used an acetic acid leach method to estimate surface-bound exchangeable Al on suspended particles.
Tessier et al. (1979) also refers to this method, but alleges that it may incorporate some carbonate bound fraction. The $MgCl_2$ method used by Tessier to estimate exchangeable metal species is based on ionic exchange/competition i.e. adsorbed species, and involves reactions at pH 7 rather than direct leaching.

To characterise the sediment used in the resuspension experiments both methods were compared as well as the effect of drying sediment prior to exchangeable Al determination. This would ascertain whether the hydration of a sediment could affect the detection of leachable Al which has implications for resuspension experiments where dried sediments may be used.

5.5.4.1: Leaching methods:

Tessier ($MgCl_2$):

An aliquot of the Celtic Sea sediment (OMEX) used in the resuspension experiments was well homogenised. Three, 1g and five, 0.5g measures of this sediment was weighed into foil boats and dried overnight or until constant weight at 100°C. From the masses of sediment before and after drying, the pore water content (%), and hence dry weight of the sediment was determined.

Three, 0.1g aliquots of the sediment were weighed into clean (10% (v/v) HCl cleaned), 30ml centrifuge tubes. 8ml of 1M $MgCl_2$ was added and the mixture agitated on a rotation table at room temperature (~20°C) for 1hr. After this time the sample was centrifuged for 30mins at 2500rpm or until there was clear phase separation. At such rpm it is possible that colloidal material may still be present in the supernatant.
2.5ml of the supernatant was pipetted off and then 22.5mls of Milli-Q was added to the sample. The sample was then diluted further by 1000 fold (100µl in 100ml) and then

analysed for Al using the lumogallion technique. The technique used standard addition calibration to determine the Al concentration which would allow for any competitive complexation effects.

Three blanks were also completed:

8mls of $MgCl_2$ (no sediment) was agitated simultaneously with the other leachate samples and then centrifuged. 2.5mls of this $MgCl_2$ supernatant was made up to 25mls with Milli-Q and the Al concentration measured as for the other samples.

Any leached Al derived from the sediment pore water can be discounted by using the sediment % pore water concentration (by weight) and estimated Al pore water concentration (Chou and Wollast or centrifugation of the OMEX sediment). This was done in a later experiment.

Acetic acid method:

Three, 0.1g aliquots of Celtic Sea sediment were put into 30ml centrifuge tubes. 8mls of 25% (4.5M) ultrex acetic acid was added and the tubes were agitated for 2hrs at room temperature (~20°C). The tubes were centrifuged for 30minutes at 2500rpm and 2.5mls of the supernatant pipetted into a clean tube. The supernatant was neutralised with 0.9mls of ammonium hydroxide (35% v/v AR grade). The resulting sample was diluted to 25mls, and then a further 1000 times with Milli-Q. Total reactive Al was measured using the lumogallion technique (Hydes and Liss, 1976) but using a standard addition technique to compensate for any competitive complexation or matrix effects with the lumogallion.

Triplicate blanks were completed with 8mls of acetic acid (no sediment) rotated with the other leachate samples. After centrifugation, 2.5mls of this acetic acid supernatant were made up to 25mls with Milli-Q water. They were also diluted by 1000 prior to lumogallion analysis.
Natural fluorescence (without lumogallion) of leachate extracts was also checked.

Leaching of both wet and freeze dried sediment samples was carried out using the above methods to ascertain whether the hydration of a sediment could affect the detection of leachable Al. All sample manipulations, dilutions and final lumogallion analysis was carried out under clean conditions.

5.5.4.2: Determination of porewater Al:

This procedure was designed to determine what fraction of the observed $MgCl_2$ and acetic acid sediment leachates was due to Al in the pore water present in the wet sediment. The same Al would also be available upon freeze drying of the sediment but may be in a precipitated and therefore less available form.

20g of the homogenised sediment was put into clean 30ml centrifuge tubes. The sediment was centrifuged for 30minutes at 2500rpm to separate the porewater from the sediment (this rpm is consistent with the leaching experiments and will remove particles >0.4μm, but may not remove all colloidal species). 2.5ml of the supernatant was pipetted into a clean tube and diluted to 25mls with Milli-Q. 100µl of this sample was then further diluted in 100mls of Milli-Q. This would give a comparable Al dilution to that of the sediment leachate samples. Triplicate blanks of 20ml of Milli-Q were run through the centrifuge and dilution processes.

5.5.4.3: Results:

Sediment porewater content:

The gravimetric analysis of the sediment showed a 64.1 ± 0.1 % porewater content.

Al leachate concentrations:

The standard addition calibrations for the $MgCl_2$ and acetic acid leachates are linear (R^2 = 0.9993 - 0.9999 see Figure 5.25). This and the comparability of the standard addition calibration gradients indicates that there is no significant quenching of the lumogallion reagent that may have been due to any species present in the leachate matrix. The gradients of the standard addition calibrations are similar apart from the wet acetic acid

leach which has a lower gradient but this is only significant at higher Al concentrations, substantially greater than those encountered in the diluted leachate or porewater samples. This indicates that there are no interferences such as Fe complexation (Mackin and Aller, 1984a) that may displace/depress the lumogallion determination of Al concentration. The background fluorescence of the samples was undetectable, less than 0.1 f unit.

Figure 5.25: Lumogallion standard addition calibrations for $MgCl_2$ and Acetic acid leaches.

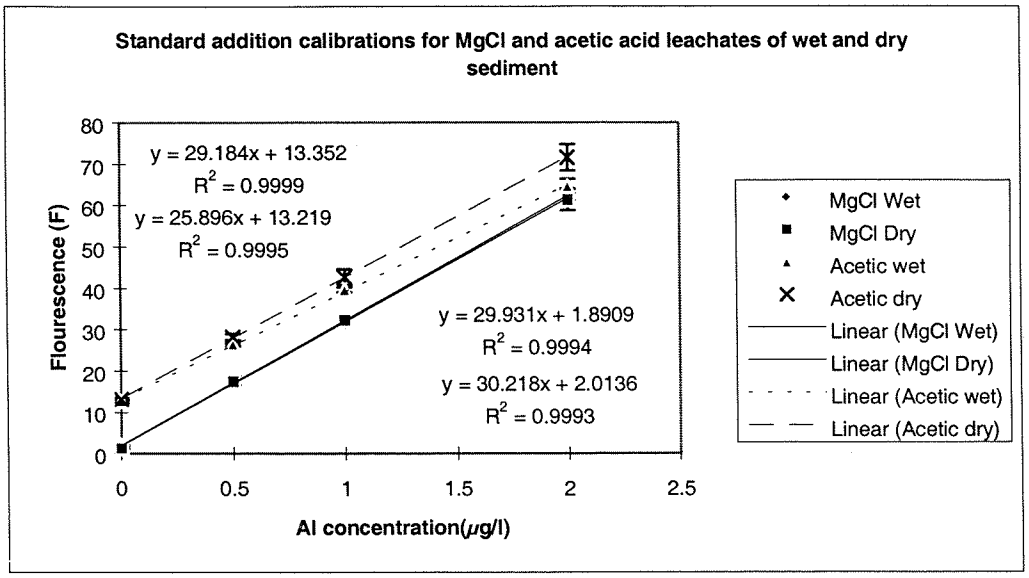

The Al concentrations of the various leachates were normalised to 100mg of dry sediment. The lumogallion reagent blank and blank value for the procedure were removed from the leachate fluorescence values prior to Al concentration calculation.

The Al concentration (nM) was then back calculated to give µg Al / 100mg dry sediment.

For example:

$MgCl_2$ leachate concentration of 2.46489 ± 0.22727 nM.

diluted x 1000

Therefore actual concentration = 2464.89 ± 227.27 nM

diluted x 10

Al concentration = 24648.9 ± 2272.7 nM

= 24.6489 ± 2.2727 µmol/l

= 665.0643 ± 61.321 µg/l

= 0.6651 ± 0.0613 µg/ml

= 5.320 ± 0.491 µg/8ml

Total Al in leach from 0.1g of wet sediment is 5.320 ± 0.491µg Al.

The sediment is 64.06 ± 0.087 % porewater.

Therefore 35.94 ± 0.086 % is sediment.

100mg / 35.94mg = 2.78

Therefore for 100mg of dry sediment the leachable Al by this method is 2.78 x 5.320 ± 0.491µg = 14.791 ± 1.364 µg Al / 100mg sediment.

This equates to 147.9 ± 13.6 µg Al / g sediment.

These calculations were done for all the leachate concentrations for both extraction methods. For the freeze dried sediment variable factors were used to normalise to 100mg as the percentage porewater content of the sediment was not identical to a bulk dried sample.

$MgCl_2$ method:

Wet sediment 147.9 ± 13.6 (9.22%) µg Al /g sediment.

Dry sediment 90.5 ± 16.8 (18.58%) µg Al /g sediment.

Acetic acid method:

Wet sediment 1083.2 ± 29.3 (2.71%) µg Al /g sediment.

Dry sediment 1012.0 ± 59.9 (5.917%) µg Al /g sediment.

The Al available to the $MgCl_2$ leach is 7 and 11 times less than to the acetic acid leach for the wet and dry sediment respectively.

This would perhaps be expected as the $MgCl_2$ leach occurs at a neutral pH (pH 7) and occurs primarily by ion exchange of Al from the sediment matrix/surface. The acetic acid is a more aggressive leach (~pH 2-5) and it has been suggested that this leaching technique may also remove carbonate associated Al (Tessier et al., 1979). It seems therefore that the $MgCl_2$ leach is more an estimate of the exchangeable Al whereas the acetic acid leach may incorporate some carbonate associated Al. The sediment analysed here is carbonate rich (20 to 80%-Heathershaw and Codd, 1986).

Freeze drying the sediment has no significant (t-test, $t = 1.85 > 0.05$) effect on the Al extracted by the acetic acid leach whereas there is a significant decrease (t-test, $t = 4.59 < 0.05$) observed in the dried sediment $MgCl_2$ leach .

This may be due to some alteration in the exchangeability of the Al ions that occurs upon drying which makes them less available to ion exchange. Therefore, Al resuspension work should only be done with wet sediment. The acetic acid leach is far more aggressive so the speciation of the available Al is not as important.

Porewater Al concentration determination:

Porewater concentrations at the dilution factors of the sediment leachate proved undetectable.

Mean porewater concentration is 1.08nM ± 0.132
Mean procedural blank Al concentration is 1.38nM ± 0.235
Mean Milli-Q Al concentration is 0.67nM ± 0.118

The procedure blank corrected porewater is ~ 0.375nM +/- 0.365 and the wet sediment porewater has a negligible signal relative to the total Al leachate concentrations.

Analysis of the first porewater extraction (x 10 dilution):

Porewater concentration diluted 10 fold is 46.51nM ± 3.87

Therefore concentration in sediment porewater is 465.1 nM ± 38.7

This value is comparable to Al porewater concentrations found by Chou and Wollast (1991) in the NW Mediterranean of 100-750nM in the top 10cm. This Al concentration in the porewater may be sufficient to allow diffusional input of Al into the water column, but the magnitude of this signal is difficult to predict due to the complex Al sediment geochemistry (Mackin and Aller, 1984a and b).

It is possible to calculate (using stock suspension concentration and injection volumes) that this porewater would not provide a significant Al signal (~ 6.079×10^{-4} nM) upon resuspension at the concentrations of the resuspension experiments here. It is therefore unlikely that at natural resuspension SPM concentrations the sediment porewater has a significant effect on Al input into the water column. It is possible to conclude that the increase in total reactive Al concentration due to increase in truly dissolved Al observed in resuspension experiments is not produced by porewater release and must be entirely due to desorption of Al from resuspended particles or dissolution of authigenic mineral phases.

Standard addition calibration plots for lumogallion analysis of porewater at two dilution factors (x 100 and x 10) indicates that there is no significant competitive complexation of aluminium or the lumogallion reagent by species present in the porewater matrix. Additionally, the linearity (R^2 ~ 0.9997) of the standard addition calibration curve over several Al concentrations indicates there is no evidence of quenching reactions that may affect Al detection by this method (see Figure 5.26 A and B, below).

Figure 5.26: Standard addition calibration for OMEX sediment porewater at different dilutions:A; x100, B; x10.

A:

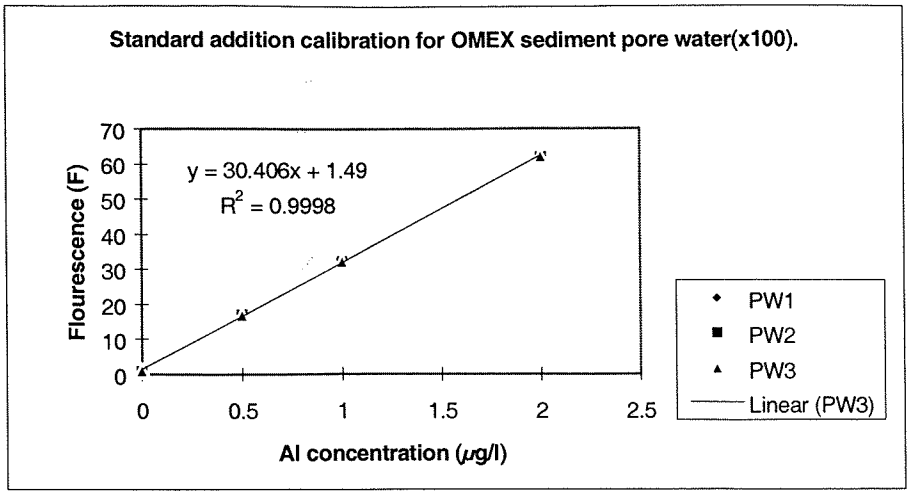

B:

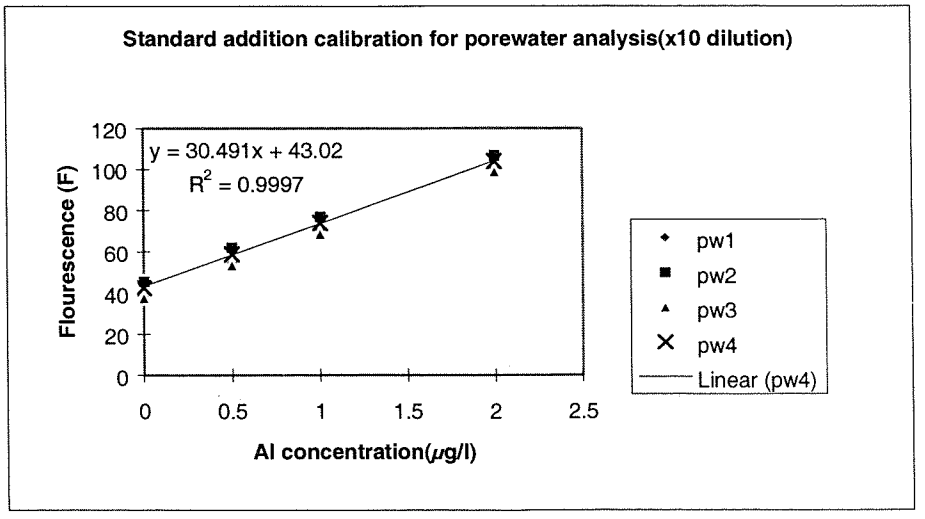

Because of problems with the coulter counter cut-off (lower limit of 1.4µm) and high concentration of the particles in the stock and diluted suspensions a metal speciation approach was taken to look at the Al distribution with particle size using a field-flow fractionation (FFF) technique.

5.5.5: FFF of Al in resuspended Celtic Sea sediment :

From previous investigations and OMEX Al profile results, it has been determined that a small fraction (< 15%) of dissolved Al is colloidal. It was decided that FFF separation of the Celtic sea sediment stock used in the resuspension experiments would give some indication of Al distribution within the colloidal population and assist interpretation of the resuspension experiment and Celtic Sea profile data. Although the natural and resuspension Al and sediment concentrations were much lower than in the stock suspension it was assumed that the size distribution partitioning of Al would be similar. There has been no work of this kind done to date.

Samples were run as described in section 2.4. As can be seen from Figure 5.27 the total reactive Al in the Celtic Sea stock is predominantly in the particulate and truly dissolved phases. Approximately 65 to 70% of the "total" (unfiltered) reactive Al is operationally defined as dissolved (<0.4μm) and nearly all of dissolved Al is actually included in the truly dissolved FFF fraction (<0.08μm). The colloidal fractions of Al are often very small and close to the detection limit of the technique. The small increase in dissolved Al between runs is probably due to Al release from particles, dissolution of minerals in the stock or increased availability/detection of Al species already present.

Figure 5.27: Al content of field flow fractions of Celtic Sea stock sediment suspension.

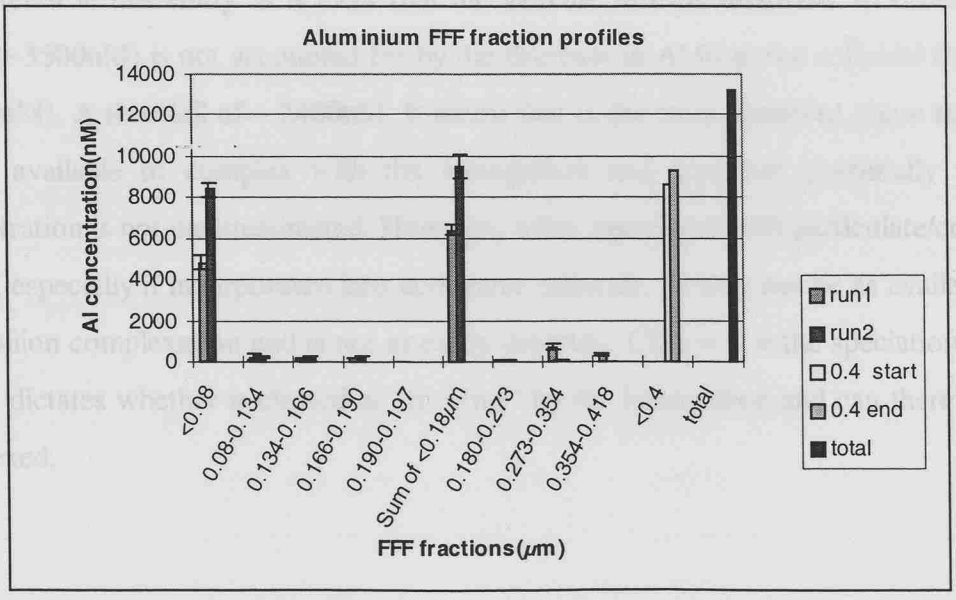

The sample was originally fractionated (FFF) in Run 1 and then 2 days later in Run 2. From Figure 5.28 it is possible to see that there has been a transfer of Al into the truly dissolved phase mainly from the larger colloidal fractions (0.273-0.354μm and 0.354-0.418μm). There is little change in the Al partitioning in the smaller colloidal fraction so it is likely that this is a dissolution effect (probably of authigenic mineral phases) as seen in the resuspension experiments and not a disaggregation process.

Figure 5.28: Al size fraction distribution (colloidal FFF fractions only).

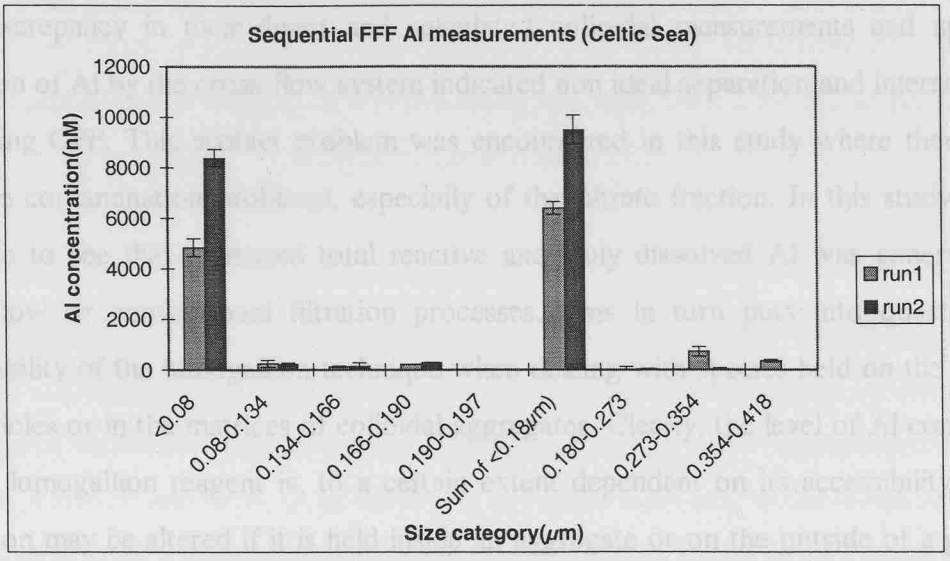

However, this repartitioning of Al also illustrates a problem with the applicability of the lumogallion technique when dealing with colloidal systems that has been repeatedly encountered in this study. It is clear that the increase in truly dissolved Al observed in Run 2 (~3500nM) is not accounted for by the decrease in Al from the colloidal fractions (~1050nM). A shortfall of ~ 2400nM. It seems that in the truly dissolved phase the Al is readily available to complex with the lumogallion and therefore potentially the Al concentration is not underestimated. However, when associated with particulate/colloidal phases, especially if incorporated into authigenic minerals, Al may not be as available for lumogallion complexation and is not as easily detected. Clearly it is the speciation of the Al that dictates whether is classed as "reactive" by the lumogallion and can therefore be complexed.

5.6: Aluminium in the Celtic Sea: Discussion/summary

Although the colloidal data from the D216 profiles was not available, it is clear from the resuspension experiments and FFF study that colloidal Al is not a very significant fraction (~0 to 20% in resuspension) in the N.E. Atlantic, Celtic Sea area. This is comparable to the findings of Moran and Moore (1989) who found that colloidal Al comprised less than 5% (by direct measurement) to 15% (by difference) of the "dissolved" Al in coastal and open ocean waters off Nova Scotia.

The discrepancy in their direct and calculated colloidal measurements and apparent retention of Al by the cross-flow system indicated non ideal separation and interaction of Al during CFF. This artifact problem was encountered in this study where there were variable contamination problems, especially of the filtrate fraction. In this study it was possible to see that increased total reactive and truly dissolved Al was generated by cross-flow or conventional filtration processes. This in turn puts into question the applicability of the lumogallion technique when dealing with species held on the surface of particles or in the matrices of colloidal aggregates. Clearly, the level of Al complexed by the lumogallion reagent is, to a certain extent dependant on its accessibility i.e. Al detection may be altered if it is held inside an aggregate or on the outside of a particle. This is perhaps where the main apparent contamination problems arise when dealing with colloidal aggregates that do not always remain coagulated during sample handling and fractionation by CFF.

The Al profile seen typically in this study [see Figures 5.6 (OM11) and 5.7 (KAC)] shows a subsurface maximum, a deeper (>1500m) water column minimum (due to scavenging processes), Mediterranean Outflow water (MOW) signals (characterised by higher Al concentrations and salinity), and increasing Al with depth/near bed. These features have all been documented before in various environments.

Unlike previous studies, the subsurface maximum here cannot be attributed to dissolution of Al species from aerosol input (see Section 5.4). The originally very high background Al concentrations indicate that this signal originates from advection of a water mass from an area of significantly higher aerosol input or sediment influence. Additionally as the

maximum actually occurs several 10's of metres below the surface, coincident with the chlorophyll-a maximum it is likely that this Al maximum may be biologically mediated by some uptake and recycling processes within the mixed layer. The Al minimums observed directly below the subsurface maximum and in the mid water column are produced by removal of the Al by scavenging onto inorganic detritus or other particles. Both the surface extremes in Al profile concentrations are attenuated to some degree by increased water column mixing due to storm conditions.

The Mediterranean Outflow Water (MOW) signal is observed in all the deeper profiles. The high Al signal in this water mass is attenuated by water entrainment or mixing and biological/particle scavenging as it flows along the shelf. It is possible to pick out the core of the dissolved MOW Al signal where it is less diffuse.

The total reactive and dissolved Al/Si/depth covariance in waters below the MOW influence (>1500m) suggests regeneration of Al from detritus (biogenic) opal rather than pressure dissolution effects (Moore and Millward, 1984) or other water column processes (Mackin and Aller, 1989), but there is no direct evidence for this. Dissolved Al and Si correlations have been observed in other deep-sea water column profiles (Mackenzie et al., 1978; Caschetto and Wollast, 1979; Hydes et al., 1988) but this increase in Al with depth was not previously seen in the Celtic Sea area (Hydes, 1983). It has been observed that Al incorporation into diatom frustules acts to decrease dissolution rate and solubility (Van Bennekom et al., 1991). The stronger correlation of Si with total reactive Al indicates to a certain extent that more of the biogenically associated Al is held on particles >0.4μm (rather than colloidal or truly dissolved phases).

Through investigation of sediment porewater characteristics and resuspension experiments it has been determined that the near sediment maximum observed in several profiles was not attributable to porewater diffusion from the Celtic Sea sediments or porewater release during resuspension events as the measured Al porewater concentrations were too low. However, it has been observed in this study, as in others (Mackin and Aller, 1984 a and b; Mackin, 1986; Mackin and Aller, 1989; Moran and Moore, 1991) that resuspended sediments can act as a source of dissolved Al. In this

study it was additionally observed that the Al release seen upon resuspension was largely in the truly dissolved phase but a significant fraction was also associated with particles >0.4μm (as indicated by the increase in total reactive Al). The colloidal fraction was not integral in Al release from the sediments. The effect of pressure on the equilibrium between dissolved Al and pelagic clays as investigated by Moore and Millward (1984) has not been accounted for here.

A table of comparison of Celtic Sea sediment Al release upon resuspension is compared with data from Moran and Moore (1991) and Mackin (1986), see Table 5.4. The experiments conducted by Mackin (1986) indicate the inhibiting effect of increasing Si concentration on Al release upon sediment resuspension. The generally lower Al release observed in this study when compared to resuspension releases described by Moran and Moore (1991) is largely attributed to the higher Si concentration in the resuspending water (28nM) that can inhibit dissolution of authigenic mineral phases upon resuspension. This is in contrast to the much higher levels of available Al measured by acetic acid leaches of the Celtic Sea sediment. However, the sediment used by Moran and Moore had been collected from intermediate and deep waters which may explain the much lower leachate values (nM concentrations in the water column). Variation in sediment content of soluble mineral phases will also produce a difference.

In previous resuspension experiments [Mackin (1986), Moran and Moore (1991)] it has been suggested that post resuspension, dissolved Al levels are regulated by dissolved Si through the rapid formation of authigenic minerals (Mackin and Swider, 1987). In the current study, despite the rapid initial increase in Al concentration there is no decline in dissolved Al caused by later removal of Al through this mineral formation. Compared to other investigations, the net increase in dissolved Al (90 to 100% truly dissolved) in this study after sediment resuspension is of increased significance because it is a more stable feature and constitutes a higher proportion of the initial Al release.

Table 5.4 Comparison of leachable Al and Al release upon sediment resuspension.

Mean dissolved Al releases:

	Initial dissolved Al release	net dissolved Al release
Minas basin (1mg/l)	60-70nM	19nM
Total (SPM-µg/l)		
OMEX (1080)	11.68nM	4.1nM
OMEX (470)	4.8nM	none
OMEX (90)	1.45nM	-
Dissolved		
OMEX (1080)	7.165nM	5.50nM
OMEX (470)	1.945nM	0.75nM
Truly Dissolved		
OMEX (1080)	5.95nM	4.86nM
OMEX (470)	1.808nM	1.65nM
Particle leaches		
intermediate waters		2nM
deep waters		0.5-1nM
OMEX sediment		40.0nM/g sed.

Al/Si releases: SPM (0.15-8.7mg/l)

	Initial Al conc.	Si conc.	Al increase
Moran and Moore (1991)			
Minas Basin	11nM	4µM	9-14nM
	109nM	4µM	5-11nM
Sohm Plain	11nM	4µM	4-10nM
OMEX (SPM 0.47-1.08mg/l)	5.8nM	28µM	0.75-5.5nM
Mackin(1986)	10nM	0µM	~125nM
	15nM	325µM~85nM	
	25nM	600µM~50nM	

Many studies have estimated the input of Al available from authigenic minerals and sediments by using leaches to quantify the Al available for release upon resuspension. In this study the acetic acid leach is used as the maximum estimate of Al available to deep waters from Celtic Sea sediment. In general, the $MgCl_2$ leach used here is probably more representative of the actual Al likely to be released under natural resuspension conditions (~pH7). However, the acetic acid leachate concentrations are used in sediment release comparisons as this conforms to the procedure used by most authors.

Calculation to assess potential input of Al to deep waters by Celtic Sea sediments:

The following assumptions were made for this calculation;

Near bed SPM concentrations were reported (I. Hall pers. comm.) as;

OM5 SPM (taken at 182m, 4m from the bed) 126µg/l,

OM7 SPM (taken at 3359m, 52m from the bed) 24µg/l.

From these measurements it is evident that SPM concentrations near-bed may be depth dependant and the SPM profile may be dependant of the separation/settling of sediment from the water column. Here, the best approximation of resuspension sediment concentrations is assumed to be best represented by the sample taken closest to the bed, but is likely to be an upper limit of sediment concentrations as elevation above ambient water column SPM concentrations has not been accounted for.

From leachate experiments in this study;

Acetic acid leachable Al = 1.083mg Al / g sed.

Therefore, the potentially available Al is 1.36458×10^{-4} mg Al (/126µg sed.)

= 0.136 µg Al / 126 µg sed.

= 5.057 nM / 126µg sed.

(for OM7 SPM concentrations this would be 0.96nM Al / 24 µg sed.)

For a sediment concentration of 126µg/l the increase in dissolved Al seen in the resuspension experiments would have been; 0.52-0.836nM.

For an increase in Al of this concentration a 8.6-15.89 % dissolution of available/ leachable Al would be necessary. A similar release (~10%) of leachable particulate Al was observed by Moran and Moore (1991) for Minas Bay sediments (Bay of Fundy).

In the near bed OMEX water column samples an increase of 3-6nM was observed. This would require 59-100% dissolution of the leachable Al in one suspension event which is unlikely (although water column recycling of Al cannot be ruled out).

The particle dissolution required to generate the observed Al input is governed by the resuspension SPM concentration. There is need for more accurate data on nepheloid layer SPM concentrations, extent of sediment resuspension and their frequency and longevity. However, because the Celtic Sea sediment sample does not produce the elevation in Al concentration observed during a single resuspension does not mean that sediment resuspension cannot account for the elevated Al signals observed in the Celtic Sea profiles close to the bed. In the resuspension experiments in this study, after stirring was stopped to indicate the cessation of a resuspension event, although as expected the particle (>0.4μm) and colloidal reactive Al sedimented out quickly, there was comparatively very little scavenging of the truly dissolved Al that had been released originally. In fact, the truly dissolved Al that remained accounted for 90 to 100% of the net dissolved Al increase. The maximum net elevation in dissolved Al concentration was to 0.75 to 5.50nM and 1.645 to 4.855nM for dissolved and truly dissolved respectively (for 470 and 1080μg/l SPM concentrations).

For a SPM concentration of 126μg/l (recorded at station OM5 4m from bed) this would create an approximate net input of 0.20 to 0.64nM of dissolved Al and 0.441 to 0.567nM of truly dissolved Al. It is clear that the input of truly dissolved Al is disproportionally high in resuspension events and at lower resuspension concentrations especially. It is possible to see that if there is minimal scavenging of dissolved forms of Al (mainly truly dissolved) between resuspension events then it is possible for a near bed elevation in dissolved Al concentration to build-up. As it was not possible to identify the speciation of the of the Al in the near bed samples from D216 it was not possible to identify the phase or source of the Al release (truly dissolved, larger particle etc.) which

would confirm the processes responsible for the elevated Al concentrations. This periodic resuspension mechanism for Al injection into bottom waters has been previously investigated by Moran and Moore (1991) in the deep western boundary of the North Atlantic which is a high energy region characterised by nepheloid layers of resuspended sediments (McCave, 1986).

There is no direct evidence in the literature for nepheloid layers in the Celtic Sea area, although the SPM concentration measured near bed at OM5 (126μg/l) is high compared to those seen (44-57μg/L) in the vicinity of the deep western boundary current of the Atlantic Ocean (McCave, 1986; Moran and Moore, 1991). It is not possible to say whether the SPM levels recorded at OM5 and used for Al release calculations is representative of the average near bed conditions. The elevated Al concentrations observed in the Celtic Sea area may be produced from an accumulated effect of continuous small scale resuspensions produced by shelf currents, or a result of much larger and infrequent resuspension events. Because of these unknowns, to assess accurately the likely role of sediment resupension in Al release to the water column there is increasing need for higher resolution SPM data near bed and also information on nepheloid layer existence, SPM concentrations, extent of sediment resuspension, frequency and longevity in the Celtic Sea and shelf area.

5.7: Future Work:

It was not possible to carry out any of these resuspension experiments under the pressure conditions found at the sea floor. The effect of pressure on the dissolution of authigenic minerals and Al release from clay matrices has had some investigation (Moore and Millward, 1984) but the implications and effects on transformation processes are not as yet resolved.

Due to the problems encountered with the cross-flow system used in this study the significance of colloidal forms of Al in the Celtic Sea has still not been absolutely quantified. Research needs to be concentrated on areas where colloidal material is expected to have a pronounced effect. The biologically active surface waters and near bed deep waters fall into this category. The generation of colloidal material, its cycling

in the water column and association with Al and other trace metals in nepheloid layer processes needs further investigation.

This study has indicated some potential problems with the lumogallion technique when it is used for looking specifically at particulate/colloidal species. The increased detection of Al by the lumogallion technique as a result of CFF fractionation of a sample despite no indication of contamination produces uncertainties about colloidal Al detection using this technique. It is possible that availability of an Al species may be determined by its availability for complexation by the lumogallion reagent and will therefore be affected by its original site on a particle/or aggregate matrix and subsequent changes in particle morphology or aggregate break-up. Comparison is required for Al determination in particulate fractions between the lumogallion technique which is very much a surface species detection method and other methods which are less affected by the speciation of Al for detection. The disruption of colloidal aggregates during CFF has wider reaching implications for high shear colloidal separation techniques if the colloidal particle size spectrum is altered during sample fractionation.

Chapter 6: Summary and conclusions of colloidal work:

Chapter 6: Summary and conclusions of colloidal work:

Previous to the start of this study on colloidal and trace metal interactions, colloidal material had been identified as a significant particle species potentially important in the fate and cycling of trace metals in the ocean (Wells and Goldberg, 1991; Moran and Buessler, 1992; Baskaran and Santschi, 1993; Moran and Buessler, 1993; Wells and Goldberg, 1994). Over the course of this research further studies have been published on the significance of colloidal trace metals in coastal and estuarine systems (Benoit et al., 1994; Buffle and Leppard, 1995a and b; Fang, 1995; Martin et al., 1995; Chen and Buffle, 1996a and b; Muller, 1996; Sanudo-Wilhelmy et al., 1996; Wen et al., 1996; Kraepiel et al., 1997; Lead et al., 1997; Wells et al. 1998, and references there-in). At the time of its design this piece of research looked at several aspects of colloidal behaviour that examined largely new areas. Now the data from this study can join the wealth of research that more recently has been published and contributes to the general understanding of colloidal material and its role in transporting trace metals in estuarine systems.

This colloidal study has identified areas where there is inconsistency within the accepted colloidal separation and handling protocols and therefore limited comparability of published literature. Table A1.1 illustrates the diversity of waters sampled and cut-offs and protocol used by different groups in "colloidal" separation. Whether the lower colloidal limit is set at 1 or 10 KDa in some cases can be very significant in the assessment of colloidal material and trace metal partitioning For example; low and high molecular weight Pb (Wells et al., 1998). In this study with the lower limit set at 10KDa it is clear that trace metal species defined as colloidal by some studies are included in the truly dissolved phase. The same effect is true for the upper colloidal cut-off (0.4 vs. 0.2μm). As Chapter 1 discusses, sample filtration protocol will also greatly affect effective cut-offs. This entire problem of defining colloidal material by an effective cut-off and the lack of universal sample handling and filtration protocol will mean that a large part of the colloidal data in the literature is generally incomparable.

A similar problem is encountered as a result of filtration artifacts. Throughout this study the debate on the effects of filtration artifacts on particle separation and trace metal

concentrations during conventional and cross flow filtration has been developing. It has been observed here that inconsistent filtration protocols (conventional and cross-flow) can lead to alteration of the observed trace metal partitioning. For example; lack of sample decantation prior to 0.4μm prefiltration of Humber samples led to cake build-up on the filter membrane, retention of colloidal material on the prefilter and therefore reduction in the measured total dissolved concentrations for trace metals with significant colloidal fractions i.e. Fe and Pb (see Section 4.4.6). A full discussion of filtration artifacts occurs in Chapter 1, but it has become very apparent during this investigation that although CFF of samples has alleviated many of the problems suffered by conventional filtration it is by no means ideal in colloidal separation, especially in estuarine or highly organic environments. Cross flow systems are designed to prevent build-up on the surface of the filter membranes by laminar flow across the membrane surface. However, the actual flow velocity close to the membrane surface is effectively zero (parabolic flow velocity profile). If a particle held on the membrane does not extend above this viscous sub-layer, it will not be removed. Generally, inorganic particles may be removed as they are more spherical in morphology but organic polymers or other colloidal material that may be retained by charge effects will accumulate. It is therefore still possible for concentration polarisation to occur in CFF systems and alteration in colloidal separation to occur by effective clogging of the membrane and cake build-up (Cooney, 1992; Jiao and Sharma, 1993; Kawakatsu et al., 1993; Foley, 1994; Bowen and Jenner, 1995). Aside from surface coagulation due to concentration polarisation, chromatographic effects (variable rates of solute and colloid adsorption to the membrane surface) and macromolecule fractionation (interactions due to different electrostatic and hydration properties of small molecules and membrane pores) can alter the anticipated trace metal concentrations in the permeate and retentate fractions (Buffle et al., 1992). It is likely that at lower molecular weight cut-offs or higher filtration pressures/concentration factors these types of artifacts will be exacerbated (Leonard pers. comm.).

The net effect of increasing filtration pressure or concentration factor (in CFF) is not always to remove colloidal material/trace metals from a sample by retention on the filter membrane. Sanudo-Wilhelmy et al. (1996), Wen et al. (1996) and Tappin (pers. comm.) have observed a converse effect where trace metal concentrations in the filtrate can increase with larger filtrate volumes. High concentration factors in CFF can lead to this

metal/colloid "breakthrough" into the filtrate due to 3-D steric effects and concentration polarisation (Buffle, 1990; Kilduff and Weber, 1992). This effect was not observed here, probably because samples were decanted prior to 0.4μm prefiltration to minimise conventional filtration artifacts and the concentration factor during cross flow filtration was kept to an optimal level (CF=2).

In this and many other studies a mass balance approach for trace metal fractionation was adopted to estimate the interaction of a colloidal sample with the CFF system. For some elements (especially Fe) and in highly organic and high colloidal loading environments this recovery may be low (minimum of 60%) see Table A1.1 (Chapter 1) and section 4.4.7. Although this indicates a retention of colloidal material it is not possible to determine the exact effect or extent of the effect on the trace metal partitioning. It only indicates if trace metal material has been lost from the samples. For this reason colloidal concentrations determined by difference but also by analysis on the colloidal retentate fraction should be quoted. Although CFF system checks to determine trace metal concentration changes with concentration factor (Sanudo-Wilhelmy et al., 1996; Wen et al., 1996) can help with this problem, additionally, detailed characterisation and separation performance analysis of a CFF system should be completed before sample processing (Gustaffson et al., 1996). There is still a problem however because the only reference standards available to classify CFF separation are carbohydrate monodispersed solutions of given molecular weight and these are by no means comparable to natural waters of variable organic content, colloidal size spectrums and trace metal partitioning. Inter-comparison studies (Buessler et al., 1996) often carried out in oceanic waters will hide the real magnitude of any of these observed effects. For example: as a worst case scenario, during CFF of a radiotracer labelled highly organic Beaulieu colloidal suspension with 0.4μm cut-off there was up to 15% retention of colloidal material on the filter membrane. In this case it was clear that CFF artifacts led to colloidal retention and inclusion in the particulate fraction but it is not possible to obtain this information for every sample with stable trace metal isotopes. CFF as well as prefiltration artifacts must be accounted for during colloidal trace metal data analysis and interpretation.

Despite these problems, CFF is still a powerful technique to separate particulate size fractions if the potential effects of sample alteration by this method are investigated and minimised accordingly. Taking these problems into account this research has aimed to improve understanding of trace metal/colloid associations and knowledge of their distribution and significance in the natural marine environment. Throughout this research the role of organic matter in colloid and trace metal behaviour remains relatively unknown and is a difficult area requiring further investigation. The size definition of colloidal material by filtration has enabled an improved separation and spatial/temporal description of macromolecules/microparticles included within the "dissolved" phase. However, the problems with filtration as a method for investigation of trace metal partitioning and the use of size as a separation criterion may be limited in the future. It seems that it would be more geochemically appropriate in natural system to categorise trace metal species not just by size but by parameters more transferable to the natural system. For example: definition by complexation with a given ligand (Muller, 1996), indirect sizing by gravitational effects i.e. by field flow fractionation which doesn't involve any interaction with a membrane (although there are other artifact problems) and settling velocity over timescales relevant to estuarine conditions (PSPM from the TMZ defined by settling , Williams and Millward, in press).

Clearly, the utilisation of CFF ultrafiltration systems has enabled the identification of colloidal material as an important particulate fraction in explaining the behaviour of trace metals in estuarine and coastal systems. Perhaps in combination with new techniques and approaches that compensate for the shortfalls of filtration, and allow the assessment of micro-particle dynamics, the role of colloidal material in a wider and applied sense will be better understood and advanced.

The first section of this research studied the uptake of trace metals (^{65}Zn) onto natural (Beaulieu River) colloidal particles. Using partition coefficients (Kc and Kf) derived from the pilot radiotracer experiments it was possible to model percentage colloidal zinc as a function of total SPM. It was also possible to investigate the sensitivity of colloidal zinc to the colloidal partition coefficient (Kc). This approach could be implemented to modelling similar multicomponent systems.

The colloidal partitioning of ^{65}Zn was rapid (in the order of seconds) with 15 to 20% of the tracer labelling colloidal material. The uptake appeared to be related to initial mass

proportions of colloids and colloidal aggregates, and subsequent changes in particle size spectrum. This uptake was proportional to any storage changes in the colloidal spectrum and hence the mass proportion of colloidal to colloidal aggregates in the original sample. Initial partition coefficients of the ^{65}Zn tracer between colloidal and truly dissolved fractions were 1.7 and 2.9 ($x10^3$) respectively for colloidal samples stored for 12 hours at room temperature or 2-4°C. Tracer uptake was preferential onto colloidal material that had not aggregated and therefore had a higher surface area to volume ratio. Colloidal particle transformations were apparent very rapidly. However, due to the dynamic equilibrium nature of the tracer/colloid association, changes in the tracer partitioning were somewhat ambiguous. To reduce this uncertainty when looking at colloidal labelling and aggregation transformation investigations, more particle reactive tracers could be used. Stordal et al. (1996) has been able to describe the kinetics of colloidal aggregation using ^{203}Hg to label colloids. This tracer is more particle reactive and there is little desorption effects once colloidal material is labelled.

The tracer/particle association was proved to be an exchangeable rather than a complexation interaction, as the colloid fraction of ^{65}Zn was affected by the addition of stable zinc. The overall partitioning of zinc did not change when more stable zinc was added, due re-equilibration of colloidal zinc (stable and radio) at a higher loading. Long-term storage experiments revealed significant coagulation of colloidal particles into loose organic polymer aggregates which had coatings of Mn hydroxides. The radiotracer had a high affinity for these aggregates which removed >95% of the tracer from the truly dissolved phase. Coprecipitation of Mn oxides with Fe and macroparticulate organic matter has been observed by Martin et al. (1995) in the highly productive Venice Lagoon. Aggregation of natural colloidal material by similar processes have been observed by Chin et al. (1998) and Stordal et al. (1996) both whom attribute aggregation in such circumstances to Brownian Motion processes. This stripping of trace metal tracer from the natural water column during the formation of highly hydrophobic aggregates has significant implications for trace metal removal in natural waters. Rapid polymer bridging aggregation in highly organic waters (as in the Beaulieu) and its effect on trace metal removal over colloid residence timescales and varying salinity conditions needs further investigation. The ambiguity of the tracer partitioning on colloidal aggregates and during larger aggregate formation does not necessarily imply a colloidal intermediate.

Detailed colloidal/trace metal size separation by field-flow fractionation indicated that the highest total concentration of "dissolved" (<0.4μm) metals (Fe, Mn and Zn) was in the truly dissolved <0.08μm and 0.08 to 0.134μm fractions. When data was normalised to surface area per fraction, the highest densities of trace metals (Fe, Mn and Zn) were found in the smallest colloidal fraction, indicating that this fraction is probably the best scavenger of trace metals. This has implications in estuarine systems where some metals (Cd, Ni, Cu, have been observed to shift their distribution from high to low molecular weight colloids as salinity increases (Powell et al., 1996). The FFF trace metal partitioning of Fe, Mn and Zn into the smallest colloids is concurrent with the compositional analysis of the aggregate strands which removed such a large percentage of the ^{65}Zn radiotracer.

The spatial and seasonal investigation of trace metal colloidal material in the Humber produced an extensive data set for colloidal trace metals and their behaviour in a highly turbid regime. The property salinity plots indicated the conservative/non-conservative behaviour of different trace metal species. They also indicated the limits of their applicability in this system where riverine inputs are seasonally variable and especially the complication of the Ouse inputs mid-transect. February data taken during a low salinity, high flow event clearly indicated the temporal and spatial variability of metal inputs and partitioning.

Generally iron was ~100% colloidal in the river end-member and was removed at low salinity regions by aggregation processes. The removal of inorganic Fe has been described as a two-stage process by Mayer (1982). The first stage is initial fast aggregation (includes organic colloids) and is temperature independent whereas the second stage, aggregation of smaller colloids with already formed aggregates, is slower and increases at higher temperatures. It would follow that more complete removal of colloidal iron would occur during the summer whilst removal of Fe associated with organic colloids would be less seasonal. Evidence for this proposed seasonally enhanced colloidal Fe removal is conflicting as the most rapid removal of Fe occurs in July and December. Factors such as particle population changes and tidal influence would alter this model in natural systems.

Other particle reactive or Fe associated metals (Pb and Mn) showed similarly high colloidal partitioning (80 and 80-90% respectively) and rapid removal in low salinity regions. Colloidal Mn consistently showed removal at lower salinities than colloidal Fe. This has been observed previously in the Humber by Coffey (1994) and by Sanudo-Wilhelmy et al. (1996) in San Francisco Bay. This delay in Fe coagulation removal may be linked to TMZ particle composition, shear characteristics or positioning in the estuary. It also indicates that Pb and Mn may be associated with particles other than Fe oxides which have different aggregation and removal kinetics.

Copper, zinc and nickel all showed lower colloidal partitioning (~20%). Zinc and nickel are mainly affected by dilution, as colloidal Ni and Zn showed conservative behaviour, as does the truly dissolved phase. Copper is also largely conservative, perhaps due to high affinity for dissolved organic material or colloids that will act more conservatively. The contrast in Cu, Zn and Ni behaviours from elements associated with inorganic oxides (i.e. lack of removal at low salinities) has led to the suggestion that such elements may be highly associated to a separate organic colloidal pool which is not as rapidly removed from the water column (Kraepiel et al., 1997).

Cadmium has very low colloidal partitioning (<20%) and displays a truly dissolved mid-estuarine maximum. This Cd particle desorption is due to chloro complex formation and also ionic exchanges with seawater major ions Ca^{2+} and Mg^{2+} (Elbaz-Poulichet et al., 1987; Williams and Millward, in press).

Any seasonal changes in trace metal behaviour and colloidal partitioning are difficult to observe due to variability in flow conditions, riverine inputs and tidal effects (spring/neap) that are not seasonally derived. Processing of metals by the TMZ is naturally very important in the Humber although difficult to predict. In the Humber and other estuaries the TMZ has been described as highly seasonal and tidally affected (Boyle et al., 1992; Morris, 1986; Uncles et al., in press). In the Humber, Williams and Millward (in press) have concluded that the behaviour of particulate trace metals in the low salinity region is a function of the mixing of spatially and temporally invariant trace metal concentrations of temporally suspended particulate material (TSPM) with seasonally variable trace metal concentrations of permanently suspended particulate material (PSPM) of which colloids will be an important component. They suggest that

processes within the TMZ will control the trace metal concentrations downstream rather than seasonality of riverine SPM. Colloidal data gathered here suggested that this may be the case. As a result, PSPM and colloids are clearly dominant in controlling sorption reactions within this TMZ and therefore more must be done to follow up understanding of their generation and transformations.

One of the major limitations to colloidal investigations at present is the lack of colloidal mass or composition data of comparable quality to trace metal partitioning data. Interpretation of trace metal phase changes is limited by the ambiguity of particle disaggregation/ desorption changes. This is also compounded by severe difficulties in temporal and spatial particle size spectrum and mass measurements using either conventional or light scattering techniques. If the artifacts associated with these measurements can be ignored, this data could be used for calculation of trace metal partitioning between colloidal or truly dissolved and larger particulate phases (Kd). The partition coefficients of different trace metals spatially and temporally in an estuarine system can add invaluable information as to the changing role and significance of colloidal material in the context of the complete particle spectrum. Without colloidal mass distributions (that can be dynamic in certain zones) colloidal mass must be assumed from very sparse data. A comparison of Kd values for colloidal/truly dissolved and particulate/total dissolved trace metals spatially and temporally from the Humber trace metal data was not possible due to the lack of colloidal mass and particulate trace metal data. It was also hoped to compare Kd values determined in the Humber with those published for smaller (molecular weight) colloids because several papers have recently indicated a change in trace metal partitioning inside the colloidal spectrum for a given estuary. For example: Powell et al. (1996) have illustrated that in the Ochlockonee Estuary, Ni, Cu and Cd reside preferentially in the high molecular weight fraction of the colloidal population but are converted to low molecular weight species as salinity increases. Similarly, Wells et al. (1998) have demonstrated that lead shows a preferential partitioning into the 8Kda to 0.2μm colloidal fraction whilst total dissolved Cu is found predominantly in the 1 to 8KDa phases in Narragansett Bay.

The investigation of colloidal Al in the Celtic Sea was designed as a follow up to reports (Hall pers. comm.) of high colloidal Al (90% of total dissolved) in contrast to

other measurements which indicated colloidal Al as only approximately 15% of total dissolved Al (Moran and Moore, 1989). Water profiles of reactive and dissolved (<0.4μm) aluminium were determined by the lumogallion method (Hydes and Liss, 1976). Profiles illustrated an Al surface maximum (~20-40metres), a Mediterranean Outflow Water (MOW) maximum at ~ 1000 to 1200m depth and an increase in reactive and total dissolved Al near bed. No reliable colloidal data were collected due to apparent contamination problems. Despite uncontaminated procedural and filtration blanks, an increased Al concentration in the truly dissolved fraction significantly above the original total dissolved Al measurements was repeatedly observed. It was suggested that break-up of small aggregates in the high shear conditions of the cross-flow system created new particle surfaces and therefore Al sites for lumogallion complexation. This is therefore a limitation of the CFF system and lumogallion method when dealing with colloidal material or aggregates.

Resuspension experiments with Celtic Sea sediment at ambient concentrations showed a release of truly dissolved Al which was most likely the result of authigenic mineral dissolution. High resolution investigation of Al partitioning in the Celtic Sea sediment confirmed that colloidal species were not a significant fraction. Although these experiments were similar to those carried out by Moran and Moore (1991), they clearly identified that the increase in total dissolved Al observed by these authors was not a colloidal species release and the net variations in particle/Al cycling could be observed over longer timescales. Sediment porewater measurements indicated that this was not a significant source of Al during resuspension. Using data from the resuspension experiments it was possible to assess the role of resuspension events in formation of the total dissolved Al (most likely truly dissolved) increase observed near bed in the majority of profiles. Using the net increase in dissolved Al it was possible to see that in the absence of significant scavenging of truly dissolved Al between resuspension events (nepheloid layers, benthic storms) the residual input of Al with ambient sediment resuspension concentrations could be sufficient to account for the 5-8nM increase in Al concentrations close to the bed.

The three main sections in this study were designed as discrete sections addressing specific areas of colloidal./trace metal interactions. However, aside from the filtration

artifact/protocol debate common to all the work, several links have emerged between the research topics. For example; when comparing river end-members metal groups have emerged depending on their propensity to form colloidal material. As has been previously documented iron is very highly colloidal. This is observed in the Humber work where Fe is generally >90% colloidal in the Trent River end-member and at higher salinities but also in the FFF work on the Beaulieu River samples where colloidal Fe comprised ~82% of the total dissolved (<0.4μm) iron. The lower colloidal percentage in the Beaulieu may be a result of lower molecular weight Fe colloids (humic associations) residing in the truly dissolved phase. Pb and Mn are also highly colloidal (60 to 80%) in the Trent, but manganese is less colloidal (~66%) in the Beaulieu River water. Partially colloidal metals in the Trent system include Ni, Zn and Cu (20%). This is in contrast to their higher colloidal partitioning in the Beaulieu (78% (this study) and 40% (Fang, 1995) respectively). Copper especially has been shown to have a strong complexation with organic ligands/DOM (Coale and Bruland, 1990). The higher partitioning of both these elements in the Beaulieu is probably linked to the much higher organic levels (~7-8mg/L DOC. Unusually, the colloidal partitioning of ^{65}Zn in the Beaulieu was nearer 10 to 20% (at equilibrium) but was entirely removed (>95%) onto aggregates of colloidal material. This phenomenon clear demonstrates the importance of conformational characteristics on trace metal scavenging. Cadmium shows low colloidal partitioning (<10%). Al in the Celtic Sea area proved also to have a small colloidal partition (<20%), probably as a result of rapid authigenic mineral dissolution and aggregation into sedimenting particles once in suspension.

The radiotracer work has highlighted the exchangeable nature of the association of trace metals (^{65}Zn) with colloidal material. From the closed system experiments and observations in the Trent/Humber system it is clear that the partitioning of a trace metals in natural systems determined a discrete time intervals cannot identify the overall function of colloidal/truly dissolved species interactions. Although net changes can be identified as conditions change (ionic strength/salinity down the estuary, total metal concentration) at present the techniques to differentiate between changes in a steady state or equilibrium conditions are not available. The coupling of colloidal material and metal species data with other control processes (for example within colloidal pumping) is still somewhat ambiguous.

Despite these problems, the research in this study has provided a new interpretation of trace metal speciation and processes in a variety of natural waters (Beaulieu River, Celtic Sea and Humber Estuary). Assessment of the role of colloidal and truly dissolved trace metals within the conventionally derived 'dissolved' fraction has enabled far better understanding of particle/trace metal interactions. This description of trace metal partitioning within these multicomponent systems has the potential to enhance their future modelling.

The variation in metal colloidal partitioning in different systems is likely to be a result of the inputs of metals into these systems, the affinity of a given trace metal for particle surfaces and also the nature (i.e. organic, inorganic) of the particulate and colloidal material in the system. Despite the implementation of improved sample handling techniques (CFF and FFF) for colloidal separation and also by using radiotracers to monitor trace metal/colloidal dynamics this work still leaves questions as to the role of colloidal material in the systems investigated. Improved understanding of the role of organic material and the behaviour and characterisation of colloidal populations (discrete or coupled) is required to further the findings of this study.

Future Colloidal Work:

The future work sections in conjunction with each chapter described the potential areas of future colloid research;

- improvement of the understanding of the nature and role of organic colloidal material,
- improvement in the knowledge of colloidal size spectrum distributions and composition variability in estuarine systems,
- application of universal CFF protocol and diverse separation techniques to overcome filtration artifact problems.

Colloidal photochemistry is still a potential area of colloidal/trace metal interaction that remains largely unaddressed.

Colloidal Photochemistry:

Several metal oxides and hydroxides (Mn, Fe) are known to under-go photoreductive dissolution in marine surface waters (Sunda et al., 1983; Waite and Morel, 1984; Zafiriou, 1984; Sunda and Huntsman, 1988). The large surface area to volume ratio and high organic association of colloidal material indicates that this particle population has greater potential to interact with incoming solar radiation than larger particles. Photochemical interactions within this size fraction are, as yet largely unaddressed, and investigations of this nature are planned as a future part of this study.

Manganese:

In seawater, manganese occurs in two dominant oxidation states; insoluble Mn IV oxides and as soluble Mn (II) ions. Some metastable Mn (III) also occurs which, like Mn (IV) is insoluble and may occurs with Mn (IV) in mixed oxidation state solids. In oceanic surface waters there is a pronounced dissolved Mn maximum and corresponding Mn (IV) minimum. Chemical oxidation of Mn (II) is very slow in seawater (Sung and Morgan, 1981) and there is substantial evidence that virtually all marine Mn (II) oxidation is bacterially mediated (Nealson and Tebo, 1980; Emerson et al., 1982; Sunda and Huntsman, 1987). Additionally, the formation of particulate Mn is

inhibited by sunlight due to the photoinhibition of Mn oxidising micro-organisms (Sunda and Huntsman, 1988). It has also been shown by Sunda et al. (1983), Waite et al. (1988) and Sunda and Huntsman (1994) that photochemically induced reduction of Mn (IV) does occur. It is possible that this photochemically induced reduction, associated with photoinhibition of microbial oxidation may act to maintain the characteristic oceanic Mn profile observed. Spokes and Liss (1995) have found that reduction of Mn (IV) to Mn (II) occurs through the mediation of humic acids.

Similarly, in estuarine waters, particulate Mn oxides may undergo photoassisted dissolution with organic matter and fulvic acids acting as chromophores (Waite et al. 1988). The presence of such chromophores can aid reduction of Mn IV to Mn II via a Mn IV complex and intramolecular electron transfer to Mn II (Zafiriou, 1984). It is suggested that light enhances this process due to photoionisation of organic molecules leading surface adsorption of fulvic acids (Waite et al., 1988). Mn II release is influenced by pH and the affinity of Mn^{2+} for particle surfaces.

Colloidal material with a potentially large photoexcitation surface area and close association with organic material (including fulvic acids) may prove a significant source of reduced Mn in these systems. Indeed, a colloidal source of truly dissolved Mn observed in the high salinity and low SPM reaches of the Humber in this study is initial evidence that such transformations may be important under certain circumstances.

Iron:

Present literature suggests that, in the absence of organic agents, solubilisation of colloidal Fe oxides occurs via photo-dissociation of ferric hydroxy groups at the colloid surface (Waite and Morel, 1984). However, the final concentration of Fe II, i.e. degree of dissolution, is dependent on pH, colloid surface area and chromophore concentration. At higher pH's Fe II can reoxidise. However at lower pH this photodissolution mechanism is most important as a source of Fe II as reoxidation is inhibited by H^+ ions (Miller et al., 1995). If Fe II is complexed by organic material it is not oxidised but naturally occurring organic materials significantly increase the initial rate of dissolution (Waite and Morel, 1984). Conditions such as these can exist in colloidal microenvironments or surfaces. The close association of organic material with colloids

as sites for excitation of Fe III reduction and complexation may explain the estuarine steady state concentrations of Fe II (Waite and Morel, 1984; Miller and Kester, 1994).

In both these photoreduction scenarios colloidal material, with characteristic large surface area and close association with organic chromophores could play a potentially significant role in the release of (Mn) or achievement of steady state concentration (Fe) of these trace metals. It would be worthwhile to investigate the role of colloidal material in the photochemical cycling of these metals using experimental (Xenon arc photolytic cell) and field (actinometer) approaches. There could be initially, an emphasis on freshwater systems depending on the high temporal resolution and sensitivity of trace metal analysis techniques available. The effects of variables such as; particle size, organic material levels, colloid composition (organic/ inorganic) and presence of other particle fractions on rate of photochemical dissolution should be investigated.

APPENDIX 1:

CONTENTS OF APPENDIX 1:

Cleaning of Minitan system and plates prior to blanks and survey (from Martin et al., 1995):

Starting with plates of unknown blanks:

Flush system with several litres of Milli-Q (MQ) water. Retentate tubing running to waste and good filtrate generation; approximately 50ml per minute at system pressure of 12psi.

Drain system.

Recirculate system with 0.1N NaOH solution for 10-15 minutes. Flow rate of 600mls per minute and 12Psi system pressure to ensure passage of cleaning solution through the filter plates.

Drain system.

Flushing of system with 6-10 litres of MQ water with emphasis on good filtrate generation to ensure good plate flushing..ie perhaps lower flow rate but similar system pressure (12psi). Monitor pH of both filtrate and retentate until reverts to original.

Drain system.

Recirculation of 0.1N HCl for 10-15 minutes. Again good flow (~50mls/minute) through filter plates.

Drain system.

Flushing of system with 6-10 litres of MQ or until pH of filtrate and retentates have returned to normal MQ values (~pH 7).

Drain system

Recirculation of 0.1N HNO_3 for 10-15 minutes. Good flow through filter plates.

Drain system.

Flushing of the system with 6-10 litres of fresh MQ until filtrate and retentate pH has returned to original values.

Recirculation of several more litres of MQ.
Check filtrate and retentate for good trace metal blanks.

System left undrained.

Tubing is dismantled and clean bagged. Tubing ends are sealed prior to bagging with parafilm as are all external metal components of the Minitan system. Acid cleaned caps are screwed onto the system inlets/outlets. System is kept short term (prior to use) in the fridge with plates in place full of remaining MQ.

(Re) Cleaning of new / older 0.4 μm filters

New filters (polycarbonate) are soaked for 24 to 48hrs in 10% v/v HNO_3 and then rinsed well with Milli-Q. Filters are stored in Milli-Q.

Clean filters left in the fridge for several months although trace metal clean my have incurred some sort of bacterial growth despite low temperatures. This may affect filtration pore size.

To remove bacterial cells the filters are soaked in 2M HCl whilst being sonicated to lyse any bacterial cells present. The high acidity will remove any associated trace metals released from the membrane matrix into solution.

The acid solution is discarded and the filters rinsed 3-5 times with MQ.
The filters are restored in the dark at 2 deg.C.

Prefiltration (0.4μm) protocol for Humber water samples;

All manipulations carried out in a laminar flow hood, with clean plastic ware and handling procedures i.e.; non-particle generating lab-coat, plastic gloves etc.

Prior to any sample filtration, filter and filtration apparatus blanks are completed to provide background trace metal levels for the procedure. The blanks are performed in the same way as described below but MQ is the sample that is filtered.

Each sample is left to settle for a short period.

A few mls of the samples are poured into a litre separating funnel. This is used to rinse the funnel and then is discarded. The separating funnel is connected to a polycarbonate filter holder that contains an acid rinsed 0.4um polycarbonate filter.

A few mls of sample is then filtered from the separating funnel through the filter into a clean litre bottle under vacuum. This small volume is used to precondition the filter and also rinse the litre bottle. It is discarded.

The remains of the entire sample can then be filtered. The filtrate sample was kept in the dark at 2-4 deg.C. until cross-flow filtered.

If it is noted that the filtration rate decreases the 0.4 filter is replaced and another small volume of sample is used to precondition the new filter before being discarded.

Minitan cross-flow filtration of 0.4μm prefiltered samples:

The system is assembled.

Several litres of MQ are flushed through the system.

System blanks are performed by filtration of MQ. Filtrate, retentate and original MQ(bottle blank) samples are collected.

The 0.4μm sample is well homogenised.

The system was firstly preconditioned with approximately 200mls of sample. This included passing as much of the preconditioning sample through the filter plate via recirculation or low flow and high pressure. Both can lead to problems of particle retention on the plates. The system was then drained.

The sample was the recirculated at a constant system pressure until the required volume of filtrate was generated. The first 10mls of filtrate were used to rinse the relevant sample bottle (the volume of this rinse is noted).

The system is drained and the retentate is collected in the original sample bottle.
A small volume for rinsing the sample bottle is removed and noted.
The required retentate volume is taken and the remaining retentate volume is noted.

The system is ready for the next sample

Flushing and filtration rates at a set system pressure were noted previous to and after filtration of the samples to check that no significant clogging of the filter plates perhaps by organics had occurred.
Flushing rates were approx. 600mls/min to kept the plates free of particles. Corresponding filtrate rates were between 35-50mls/min.

Cleaning of Minitan after use in Humber/seawater.

System is dismantled and plates removed.

If there is particle retention under or adjacent to the silicon separators this is washed off with jet of MQ or manually taking care not to damage the membrane.

The plate may also be soaked for 10-20 minutes in 3% hydrogen peroxide to remove any organic material. Ultrasonics may also be used to remove organics.

The plates are replaced in the system.

The system is filled with 0.1N NaOH and left for a maximum of 30 minutes. The system is drained and the system may be refilled with 0.1N NaOH.

The system is drained and flushed with 6-10 litres of MQ until pH of filtrate and retentate are same as originally.

HCl and HNO_3 soaks may also be done.

For long term storage the filter plates are removed and stored wet in MQ at 2-4 deg. C. The system is dried and stored separately in plastic bags.

APPENDIX 2:

CONTENTS OF APPENDIX 2:

Stable Zn concentrations for MQ and HCl leachates for laminar flow block and associated filters (0.4 and 0.01μm).

Example EDS trace for filamentous aggregates formed in radiotracer experiments.

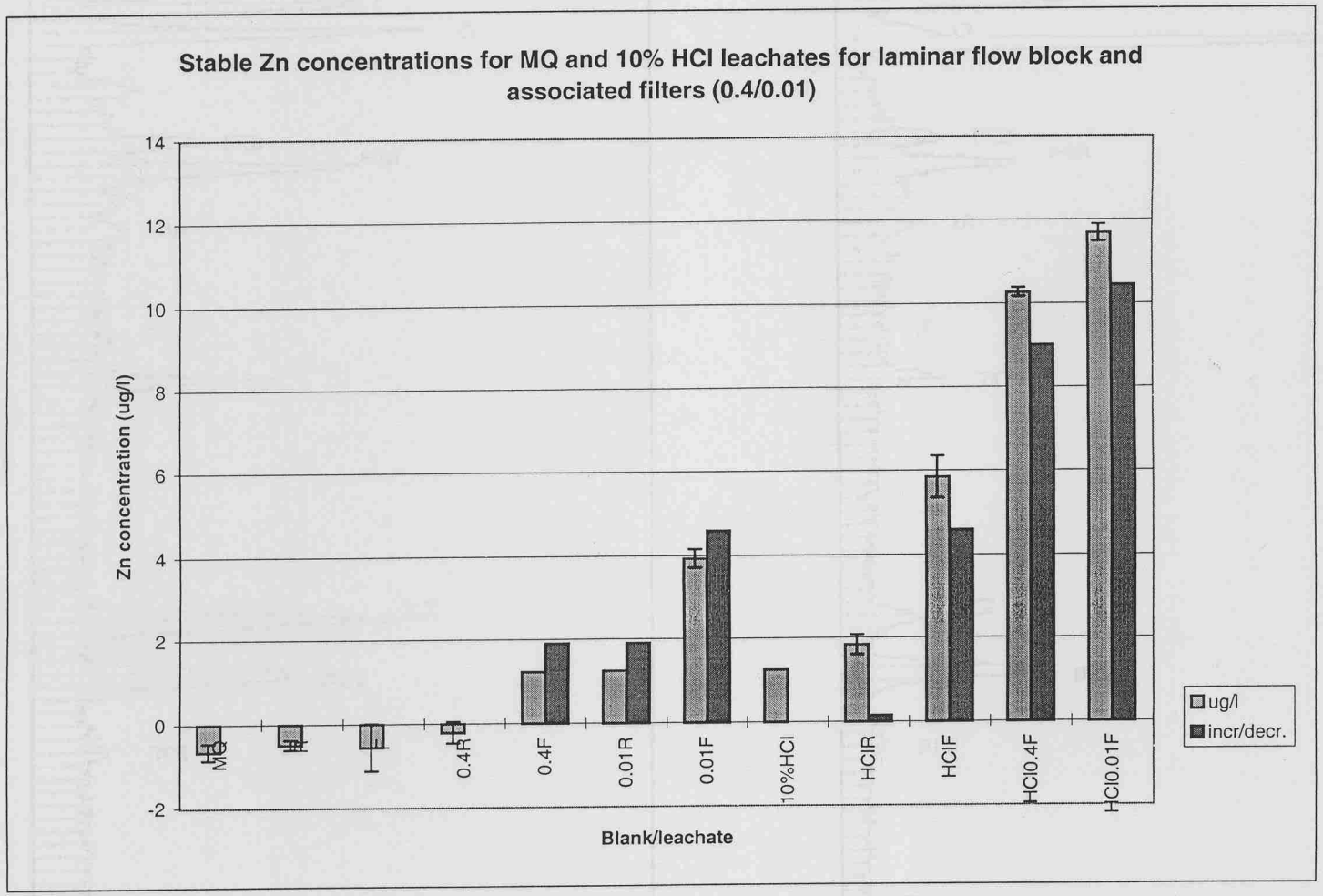
Stable Zn concentrations for MQ and 10% HCl leachates for laminar flow block and associated filters (0.4/0.01)
Zn concentration (ug/l)
14
12
10
8
6
4
2
0
-2
MQ
0.4R
0.4F
0.01R
0.01F
10%HCl
HClR
HClF
HCl0.4F
HCl0.01F
Blank/leachate
ug/l
incr/decr.

Example EDS traces for filamentous aggregates formed in radiotracer experiments.

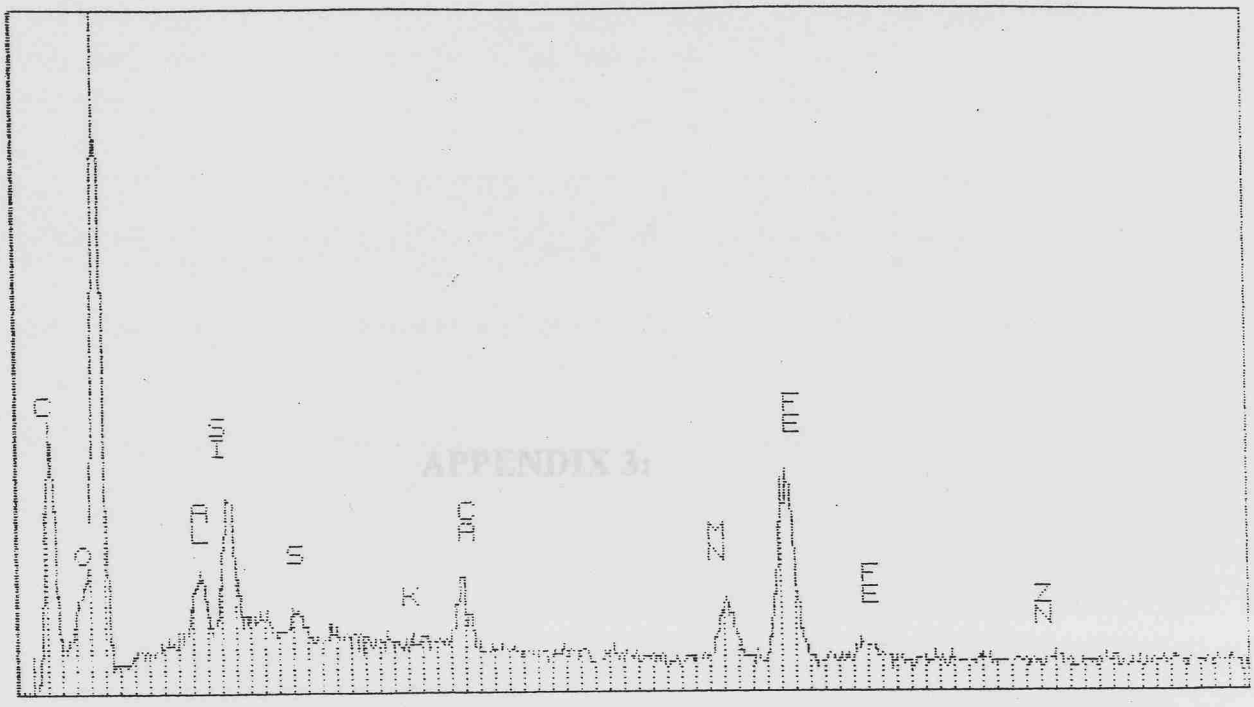

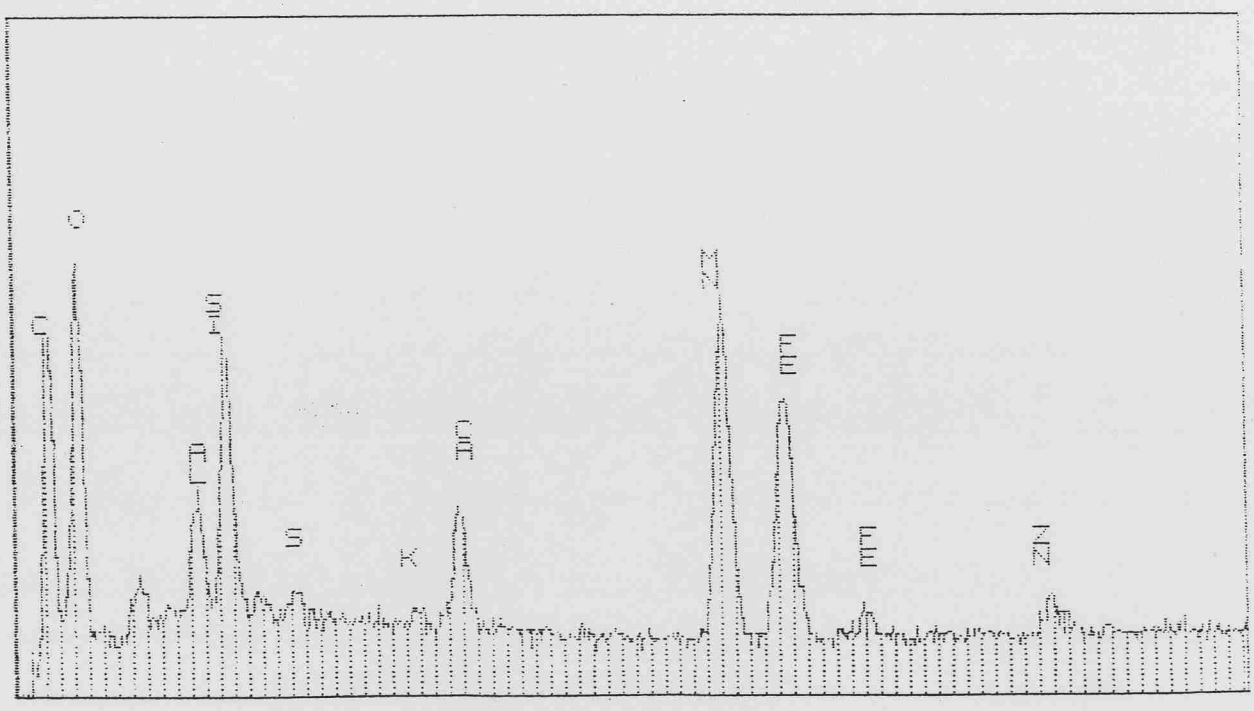

APPENDIX 3:

CONTENTS OF APPENDIX 3:

Mechanism of colloidal aggregation under low pH conditions.

Combined seasonal transects (percentage of total dissolved metal) in the Trent/Humber. (Iron, lead, manganese, zinc, copper, nickel, cadmium).

Mechanism of colloidal aggregation under low pH conditions

The size of the aggregates present in the acidified samples indicates there are significant processes that occur upon acidification that allow destabilisation of colloidal material and subsequent aggregation.

It has been previously determined that natural particles have organic coatings that will give a relatively homogenous adsorption surface (see Fiellia and Buffle, 1993) and that organically coated particles have like negative charges that will stabalise a colloidal sol (Neihof and Loeb, 1974; Hunter and Liss, 1979). Removal of particle organic coatings can increase the particle coagulation efficiency, α (fraction of collisions that result in aggregation) in natural waters (Gibbs, 1983) Changes in acidity, ionic strength and metal ion complexation can all affect stability of a colloidal dispersion and once destabilised (i.e. repulsion barrier has been attenuated) aggregation by Brownian motion of differential settling can occur where interparticle interactions are close enough for van der waal forces to predominate.

In natural waters (pH 7-8) but down to pH 3.5 (Buffle, 1990) organic coatings and macromolecules have like negative charges as a result of surface carboxylic acid functional groups that cause polymers and organic molecules to be expanded. Increased acidity leads to protonation of these forms and molecule compression. The neutral state caused during increasing protonation may result in destabilisation of organic molecules or coatings and colloidal aggregation. Exposed inorganic species are also likely to be affected by pH decrease upon sample acidification. Most surfaces of metal oxides or clay edges have Si-OH and Al-OH groups. Under progressively acidic conditions these groups will accept a proton and become positively charged. The point where the net charge is zero is the isoelectric point and will vary between species. eg;

SiO_2 = pH 2

Fe_2O_2 (haematite) = pH 6-7

(see Drever, 1982)

Hence as pH decreases upon acidification some inorganic species will become neutral and then positive at varying pHs and this will invariably lead to destabilisation of the suspension and therefore aggregation.

Parks (1967) predicted that the isoelectric points of aluminosilicates could be assessed by the number of SiOH and AlOH groups at the surface. An aluminosilicate surface with mostly SiOH groups will have a lower isoeletric point compared to a surface with mostly AlOH groups. Therefore aluminosilicate composition of the colloidal species determines stability/instability at a given pH. But only if organic coating that gives colloid surfaces their homogeneity is removed.

It is possible at low pHs if all the particles remain organically coated that there may be some restabilisation (repeptization) as all the particles become positively charged. The organic coating of a colloidal species may not necessarily be monolayer so despite low pH and changes in polymer structure or removal of the outer layer, the reaction of the coated particles and charge behaviour may still be relatively uniform. It is likely that the organic coatings are quite homogenous in nature between samples as this material (more refactory fulvic acid from terrestrial and marine sources) will be ubiquitous thoughout the riverine and estuarine system. Biogenic/phytoplankton humics are shorter lived. Whether the organic coating will be removed from colloidal particle upon acidification will depend on the bonding between the organic material and the inorganic species (covalent/charge/complexation etc.)
Work in this area to further these ideas was outside the scope of this study.

Seasonal iron fraction (percentage of total dissolved iron) transects in the Trent /Humber (1996)

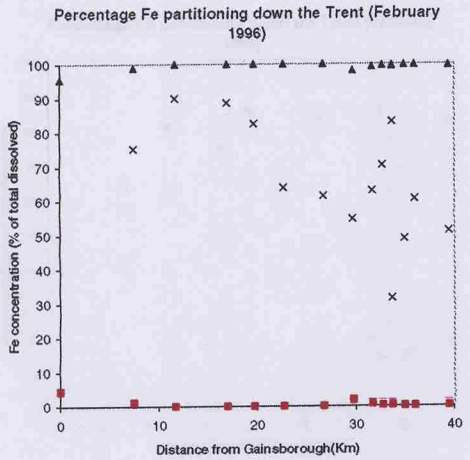

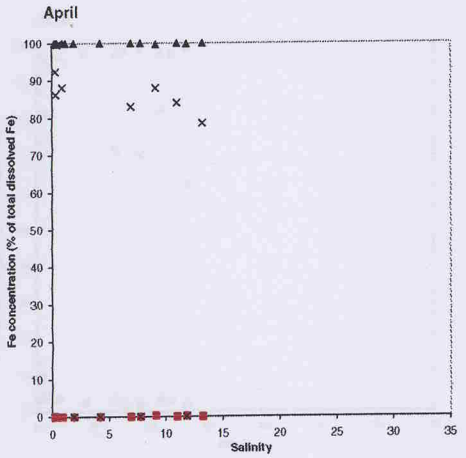

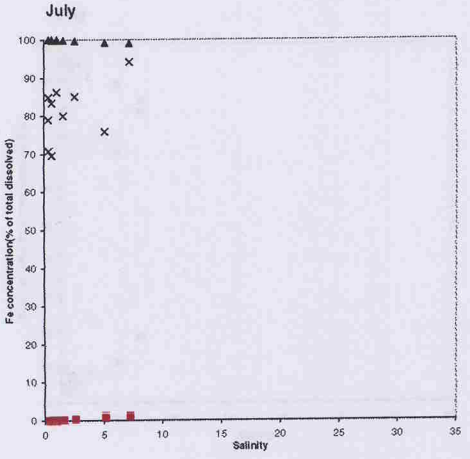

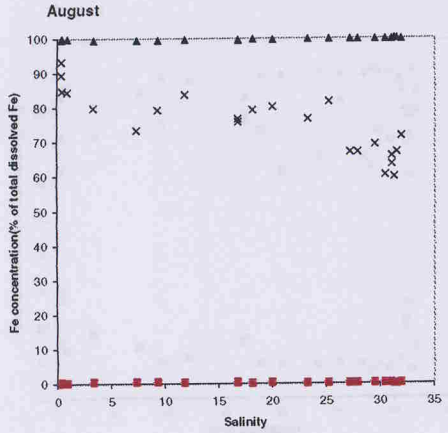

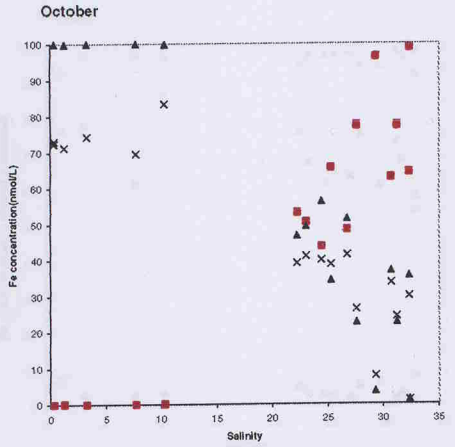

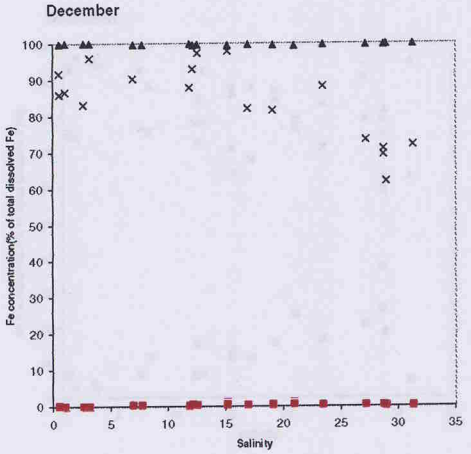

Seasonal lead fraction transects (percentage of total dissolved lead) in the Trent/Humber (1996)

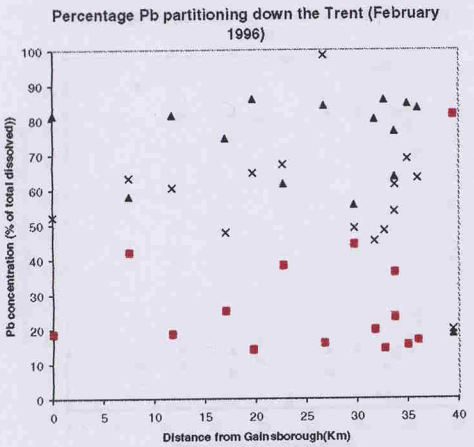

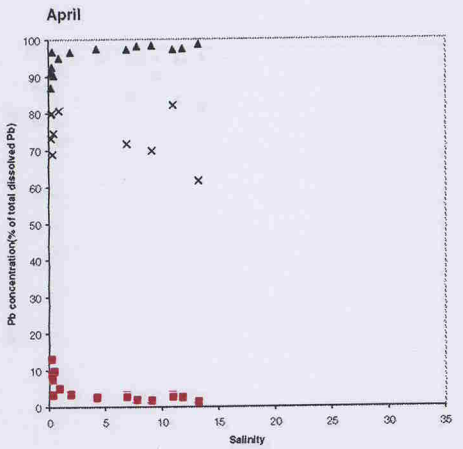

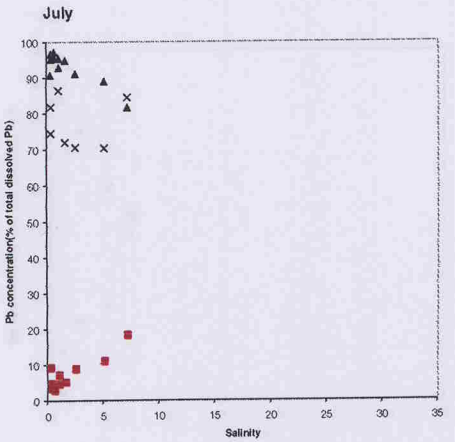

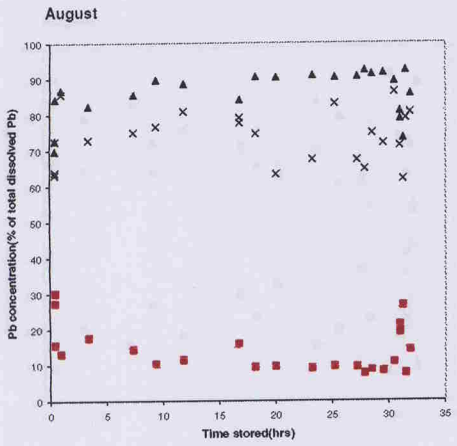

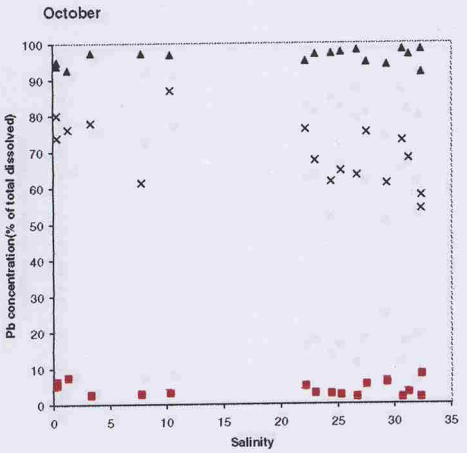

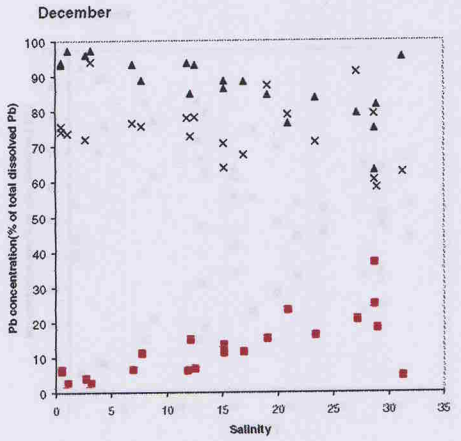

Seasonal manganese fraction transects (percentage of total dissolved manganese)

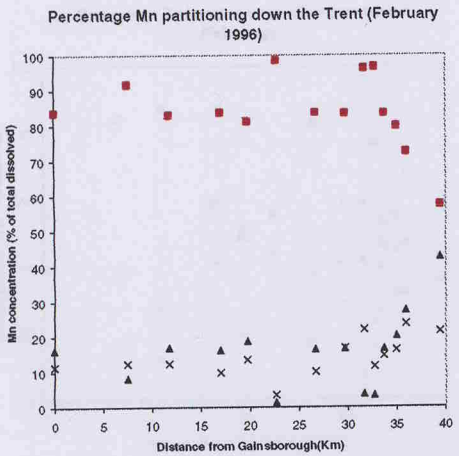

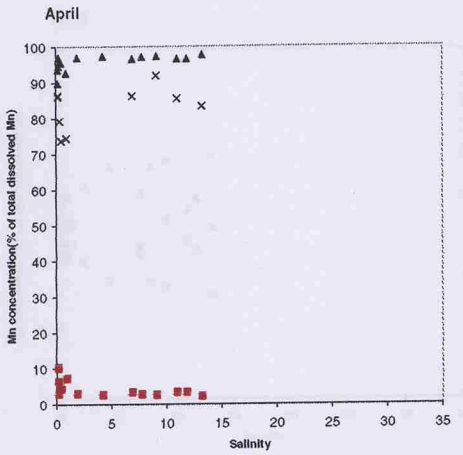

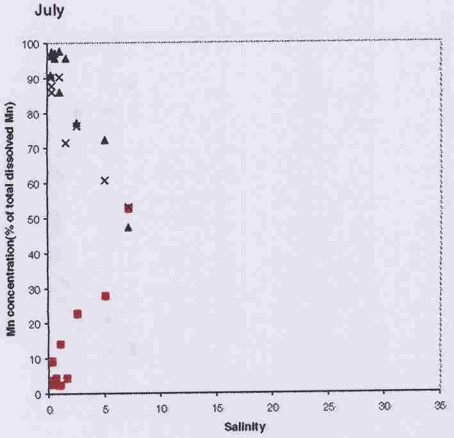

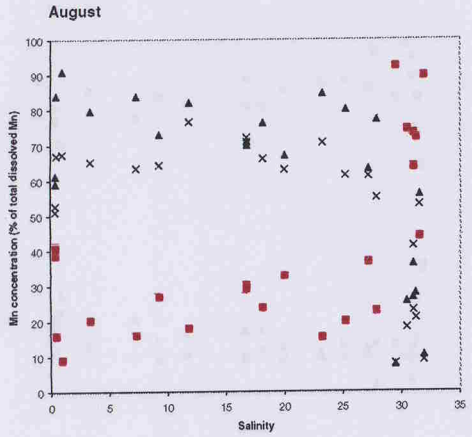

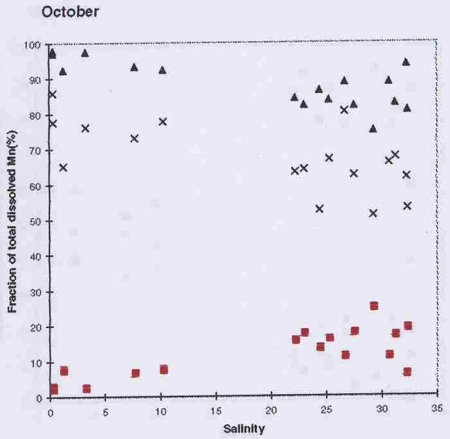

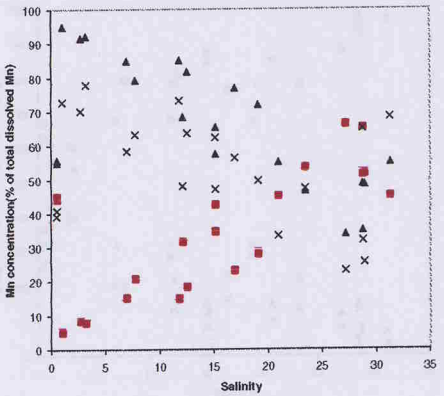

Seasonal zinc fraction transects (percentage of total dissolved zinc) in the Trent/Humber (1996)

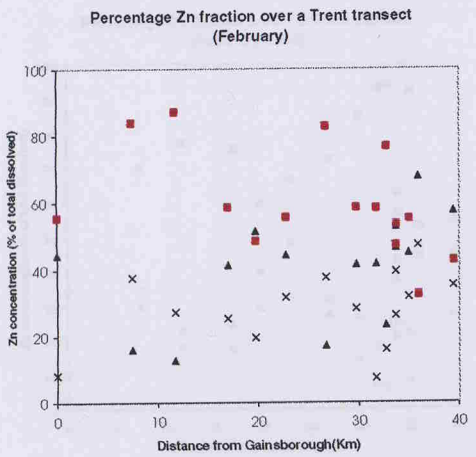

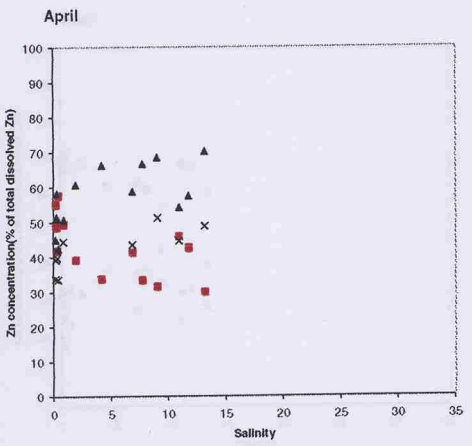

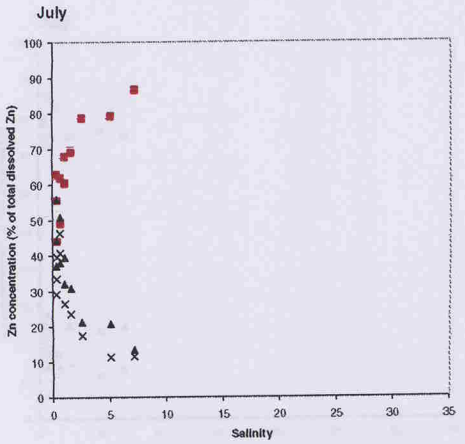

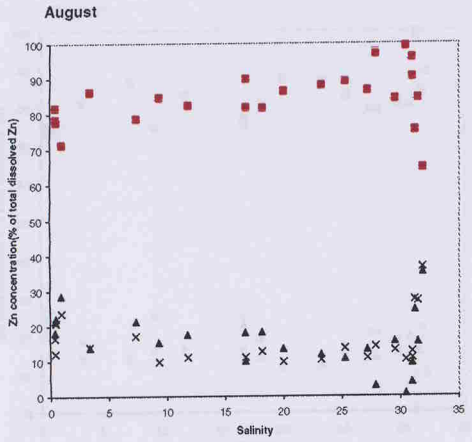

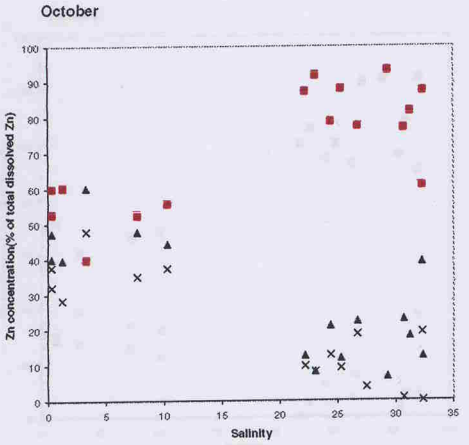

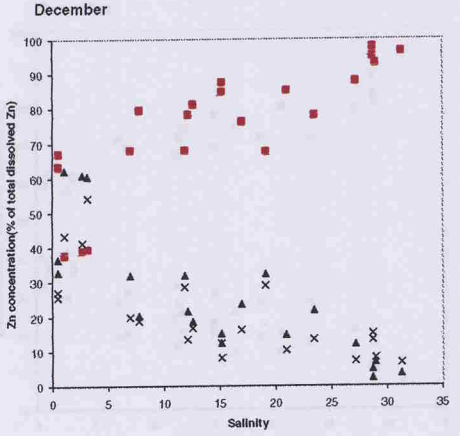

Seasonal copper fraction transect (percentage of total dissolved copper) in the Trent/Humber (1996)

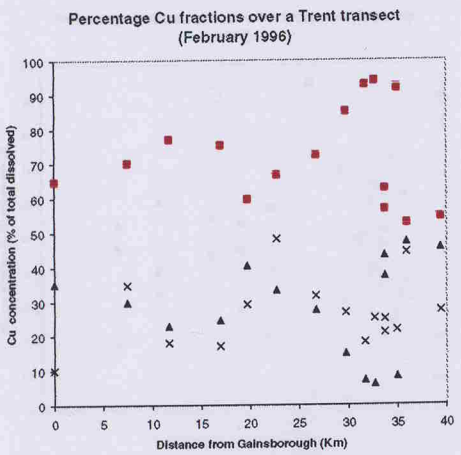

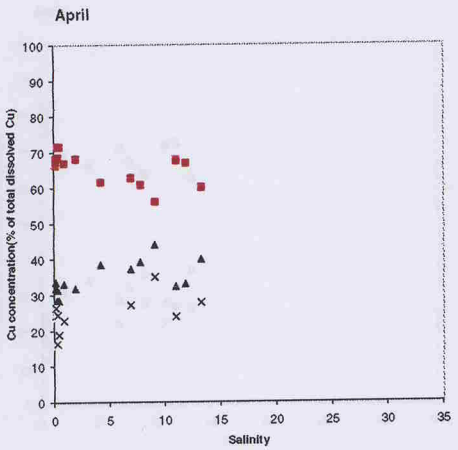

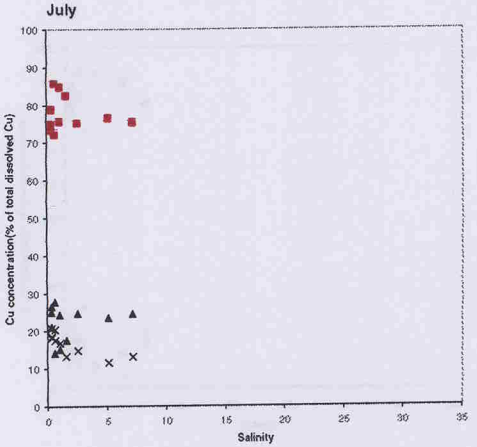

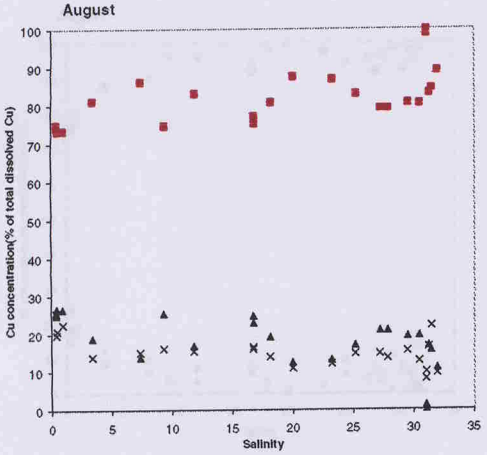

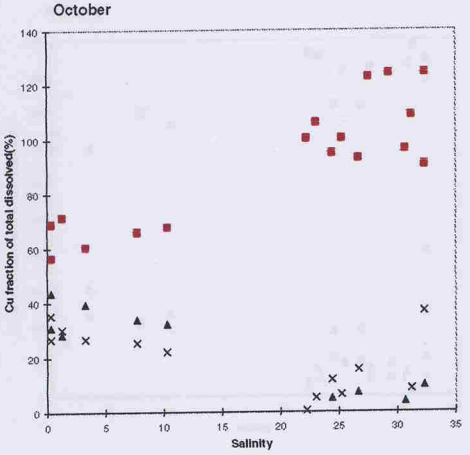

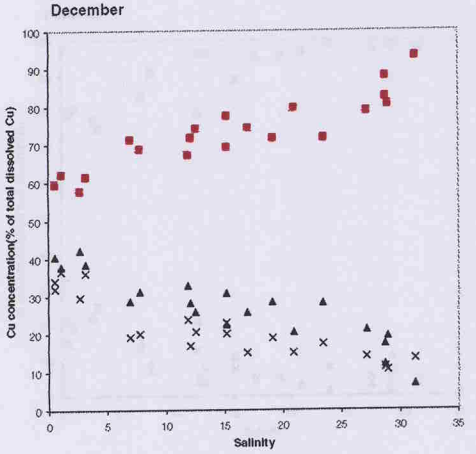

Seasonal nickel fraction transect (percentage of total dissolved nickel) in the Trent/Humber (1996)

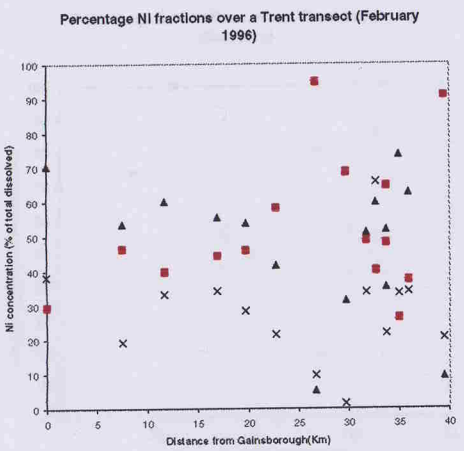

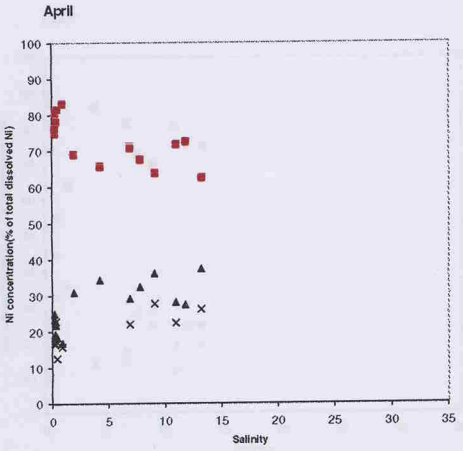

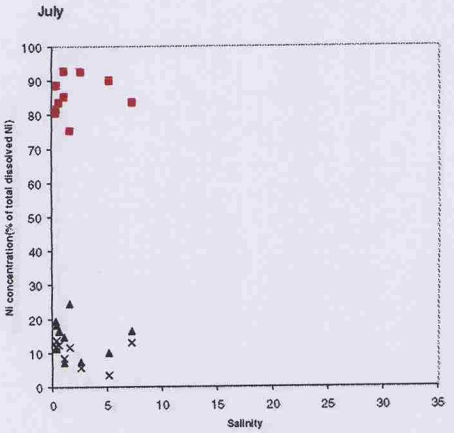

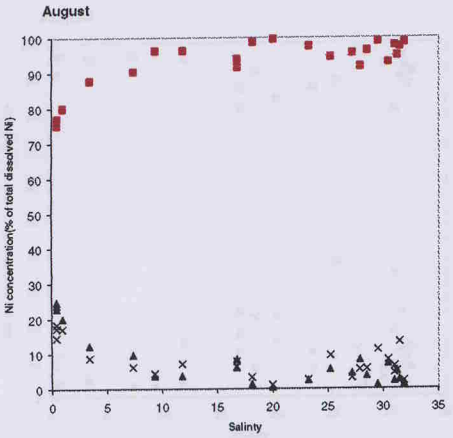

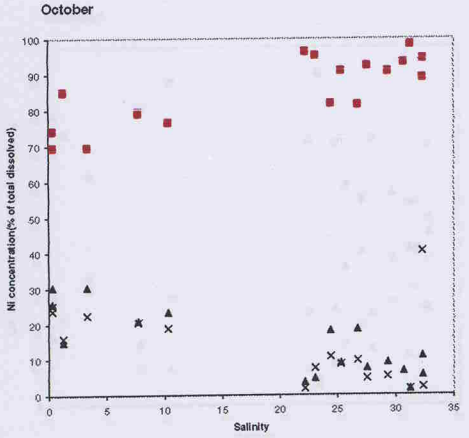

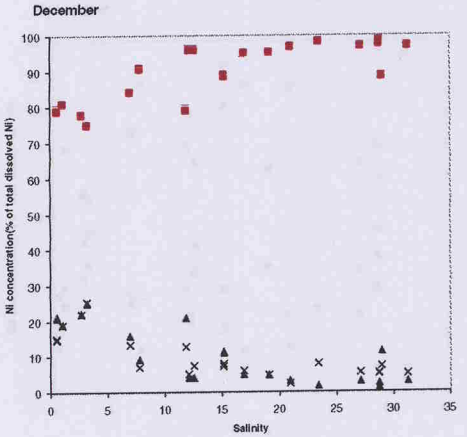

Seasonal cadmium fraction transect (percentage of total dissolved cadmium) in the Trent/Humber (1996)

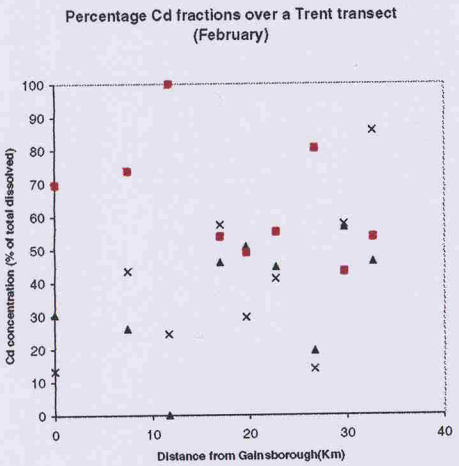

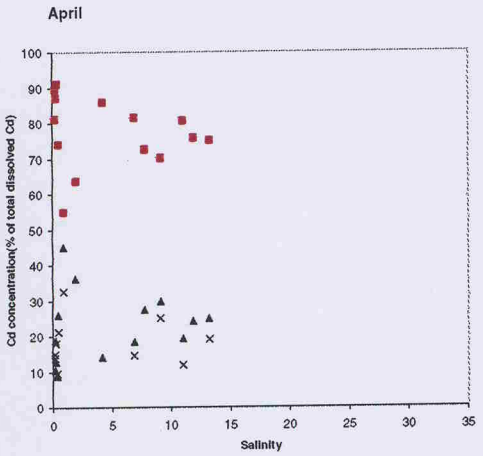

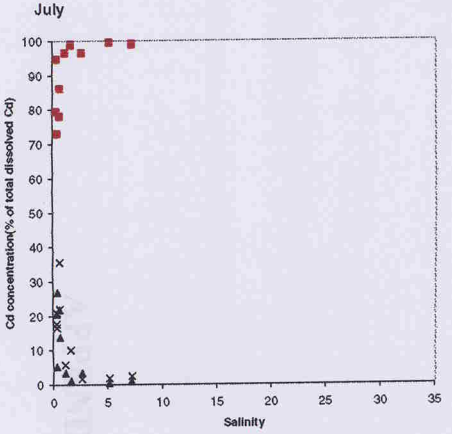

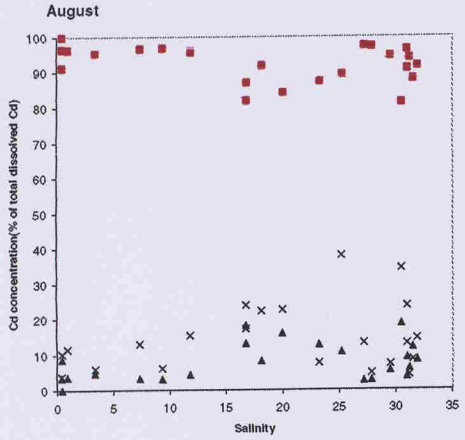

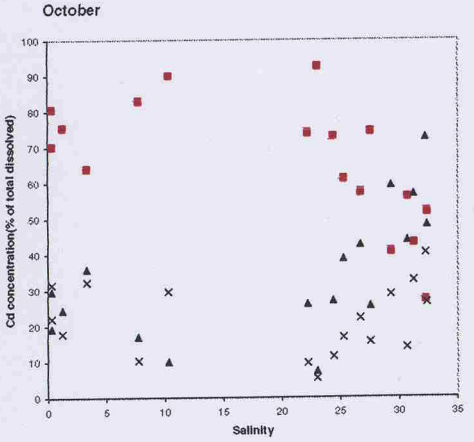

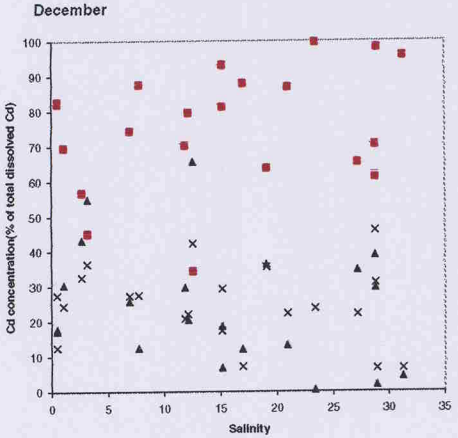

APPENDIX 4:

CONTENTS OF APPENDIX 4:

Lumogallion procedure (from Hydes and Liss 1976):

Aluminium buffer:

87g of sodium acetate trihydrate, or 78.3g of anhydrous sodium acetate is made up in 250ml of Milli-Q water. The solution is filtered through a 0.4μm filter. Acetic acid is added until 250μl of buffer in 20ml of seawater gives a pH of 5.

Lumogallion solution:

0.03g of lumogallion powder is mixed with 150ml of Milli-Q water. This gives a 0.02% lumogallion solution.

Aluminium standards:

For the primary standard;

1.758g of aluminium potassium sulphate is dissolved in 100ml of Milli-Q water in a 100ml volumetric flask.

For the secondary standard;

50μl of primary standard is added to 100ml of water (in a second volumetric flask). 40μl of this standard in 20ml of sample produces an Al spike of 1μg/l.

Mixed Reagent:

The mixed reagent comprises; ¼ buffer, ¼ lumogallion solution and ½ Milli-Q water.

Procedure:

20ml of sample is pipetted into 60ml preconditioned sample bottles. For each sample run reagent blanks and standard additions are incorporated with the samples to calibrate the technique.

For example:

Bottles 1-4: 20ml of Milli-Q water, 1ml mixed reagent.

Bottles 5-8: 20ml of Milli-Q water, 2ml mixed reagent.

Bottles 9-12: 20ml sample, 1ml mixed reagent.

Bottles 13-15: 20ml sample, 1ml mixed reagent, 40μl of Al secondary standard.

The technique is calibrated 5-6 times over the course of the samples to ensure good calibration in case of fluorimeter drift. The samples are mixed well and left overnight. The fluorescence of each sample is measured along with blanks, reagent blanks and standards by Perkin Elmer Fluorimeter LS-2.

Cleaning of new Nalgene bottles as reaction bottles for the lumogallion technique:

After several months of storage several lumogallion reaction bottles showed signs of growth on their interiors. To replace these bottles, new Nalgene bottles were aged with lumogallion solution.

All bottles were rinsed with Milli-Q.
Each bottle was filled with lumogallion solution as used in the detection procedure (20ml Milli-Q and 1ml mixed reagent(1:1:2; 0.02% lumogallion: sodium acetate buffer: Milli-Q).

The lumogallion reagent was left in the sample bottles for a week.
Lumogallion solution was discarded prior to sample analysis and bottle blanks were carried out to check bottles were clean before use.

Checks for sample bottle cleaning:

It has been suggested (D.Hydes pers comm.) that a Milli-Q rinse is sufficient cleaning procedure for sample bottles. Other authors use acid cleaning (10-50% HCl) but strong cleaning may cause sites in the plastic capable of Al adsorption.

To test this, 125ml sample bottles were cleaned in several ways, filled with seawater and left for differing lengths of time (one day to one week). Total reactive Al concentrations were determined using the lumogallion technique (Hydes and Liss, 1976) for each of the cleaning procedures used. These were;

Milli-Q rinse,
2% v/v Micro soak for one week, then Milli-Q rinse.
2% v/v Micro soak for one week, 10% HCl soak for one week, Milli-Q rinse.
2% v/v Micro soak for one week, 50% HCl soak for one week, Milli-Q rinse.

NB. for the resuspension experiments this pretreatment investigation was most relevant to the acid cleaned litre stirring bottles as the samples will only be in the 125ml bottles for a comparatively short period of time. Any adsorption of Al onto the bottle walls in the stirred experiments should be seen in the control.

Results showed (see Figure A5.1) that over 6 hours of storage there was significant decreases in total reactive Al in bottles pretreated with micro and both acid concentrations. There was no significant loss in the MQ rinsed bottles. After one week the total reactive Al loss (~1nM) was significant in all treated bottles.

Figure A5.1: Changes in total reactive Al with storage in pretreated bottles.

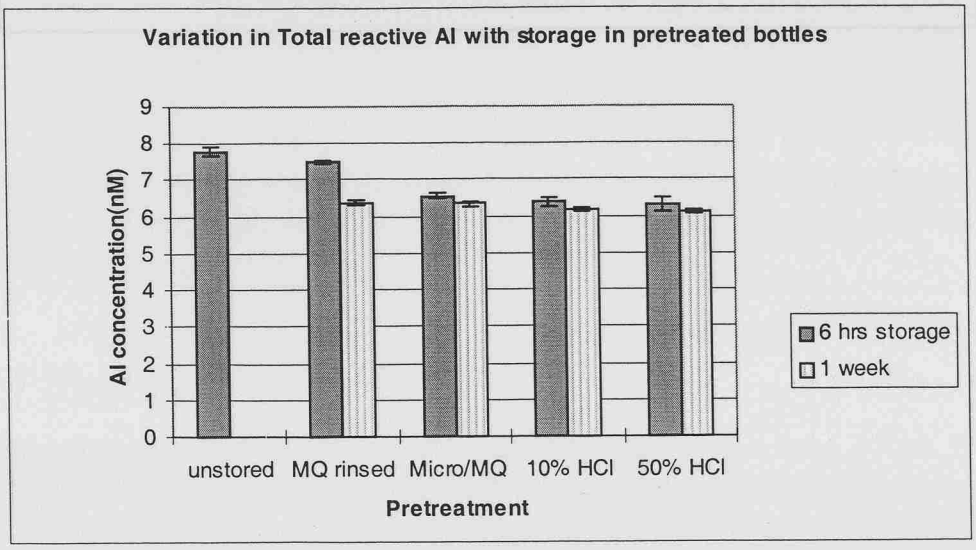

It was decided to preclean the bottles in 10% HCl for 24hrs after exposure to high Al concentrations but prerinse with Milli-Q prior to use. This milder cleaning should not allow any carry over of Al contamination and minimise adsorption of Al to bottle surfaces. This was confirmed by storage of seawater samples for 1.5 hours (maximum duration of storage in resuspension experiments until lumogallion analysis) without significant total reactive Al concentration alteration (see Figure A5.2 below). This cleaning technique was used in all the resuspension and subsequent experiments where Al was determined.

Figure A5.2: Total reactive Al concentration in seawater samples stored for 1.5 hours.

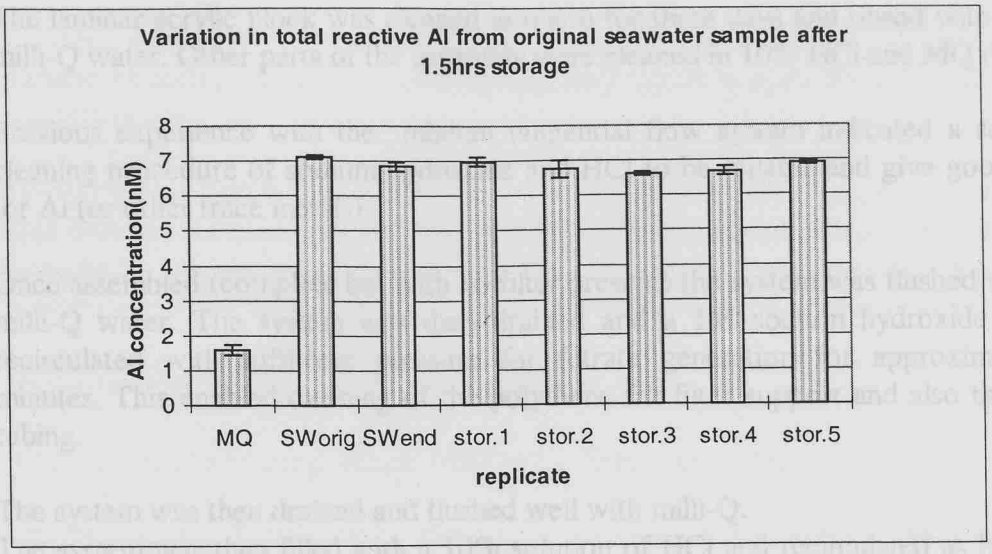

Laminar flow block cleaning (Discussed for Al but the same protocol was used for other trace metals):

The laminar acrylic block was cleaned in micro for three days and rinsed with RO and milli-Q water. Other parts of the assembly were cleaned in 10% HCl and MQ rinsed.

Previous experience with the minitan tangential flow system indicated a sequential cleaning procedure of sodium hydroxide and HCl to be reliable and give good blanks for Al (or other trace metals).

Once assembled (complete but with no filter present) the system was flushed well with milli-Q water. The system was then drained and a 1M sodium hydroxide solution recirculated with sufficient pressure for filtrate generation for approximately 30 minutes. This enabled cleaning of the polythene frit filter support and also the filtrate tubing.

The system was then drained and flushed well with milli-Q.
The system was then filled with a 10% solution of HCl and recirculated as before for 30 minutes.

After draining and flushing with Milli-Q the system was ready for use.
Tubing and frit blanks were determined seperately by flushing MQ through the system, firstly with no filtrate generation for a tubing blank and increased pressure to enable flushing of the polythene frit.

Due to the amphoteric nature of Al, total seawater blanks were also done for tubing and frit, sampling syringes amd complete filtrate blanks.

The 0.4μm and 0.01μm filters were cleaned separately by soaking in 10% HCl for 24-48 hours. The filters were rinsed with and stored in milli-Q after this leaching step.

Before use of the laminar flow blocks; blanks were done on for both 0.4 and 0.01μm filter set-ups. In each case this followed the same procedure as sample filtration.

Filtration blanks:

Milli-Q water is used as a sample.
A 0.4μm filter is inserted into the flow block.

With the retentate tube running to waste the system is flushed with the sample or milli-Q for a blank with pressure sufficient for filtrate generation. This serves to condition the system(in the case of a real sample) but also the first few mls of filtrate are used to precondition the filter and rinse the filtrate receptor bottle.

The milli-Q/sample is then recirculated until sufficient filtrate is generated for all subsequent analyses. The milli-Q filtrate is the blank for this filter fraction.

Sample 0.01μm filtration and blanks are carried out in the same way as for 0.4μm fractions except a 0.4μm filtrate constitutes the sample or milli-Q being reciculated through the system.

Previous work with aluminium has shown that due to its amphoteric nature or high particle concentrations Al contamination may occur despite Milli-Q blanks being uncontaminated.

To assess this problem in a cross-flow system, seawater blanks are also performed. This involves refiltration of a 0.4μm or 0.01μm filtrate sample. Due to the removal of particles by the previous filtration step any increase in Al concentration between the filtrate sample and the filtrate blank must have a source in the system or filters.

Stepwise sample filtration with laminar flow block:

Rinse syringe, tubing and sample bottle with 10ml of suspension.

Fill two 125ml bottles with sample by syringe. Draw sample from middle of homogenous suspension.

Pippette out 15mls for lumogallion analysis.

Insert 0.4μm filter into laminar flow block.

With R tube running to waste draw a small volume (~10ml) into the system to flush out old sample residues. Drain system.

With R tube in recirculation position run at normal speed (~2.0) to generate filtrate. First 10mls of filtrate is used to rinse filtrate bottle and discarded. Recirculate sample until dead volume (~40ml) is reached (top up sample bottle to enable maximum filtrate volume).

Remove 15mls of filtrate for lumogallion analysis.

Drain system.

Remove 0.4 filter and insert 0.01μm filter into laminar flow block.

Draw up rinse volume (~10ml) of 0.4 filtrate into system and then drain to waste.

Recirculate (~4.0 speed) 0.4 filtrate until ~15mls of 0.01 filtrate is generated (first 10mls of 0.01 filtrate is used to rinse filtrate receptor and then discarded).

Initial volume required for MQ blank and sample filtration is ~ 165ml
NB: 0.4μm filtrate can be topped up by filtering additional original sample once 0.4 analysis aliquot has been removed Same procedure is followed for seawater filtration blanks but larger volumes are required as 0.4 and 0.01 filtrates are refiltered to generate the 0.4μm and 0.01μm filtrate blanks.

REFERENCES:

Abdullah, M.I., El-Rayis, O.A. and Riley, J.P., 1976. Reassessment of chelating ion-exchange resin for trace metal analysis of seawater. *Analytica Chimica Acta* **84**, 363-368.

Ackroyd, D.R., Bale, A.J., Howland, R.J.M., Knox, S., Millward, G.E. and Morris, A.W. 1986. Distributions and behaviour of dissolved Cu, Zn and Mn in the Tamar Estuary. *Estuarine, Coastal and Shelf Science* **23**, 621-640.

Ali, W., O'Melia, C.R. and Edzwald, J.K., 1984. Colloidal stability of particles in lakes: measurement and significance. *Water Science and Technology* **17**, 701-712.

Allen, G.P., Saloman, J.C., Bassolet, P., du Penhoat, Y. and de Granpre, C., 1980. Effects of tides on mixing and suspended sediment transport in macrotidal estuaries. *Sedimentary Geology* **26**, 69-90.

Althaus, M. 1992. *Dissolved trace metals in the estuarine plumes of the Humber, Thames and Rhine Rivers.* PhD. Thesis, University of Southampton, UK.

Apte, S.C., Gardner, M.J., Gunn, A.M., Ravenscroft, J.E. and Vale, J. 1990 Trace metals in the Severn Estuary: a reappraisal. *Marine Pollution Bulletin* **21**, 393-396.

Baker, R.W. and Strathmann, H. 1970. Ultrafiltration of macromolecular solutions with high-flux membranes. *Journal of Applied Polymer Science* **14**, 1197-1214.

Bale, A.J., Morris, A.W. and Howland, R.J.M., 1985. Seasonal sediment movement in the Tamar Estuary, *Oceanologica Acta* **8**, 1-6.

Balls, P.W. 1985. Copper, lead and cadmium in coastal water of the western North Sea. *Marine Chemistry* **15**, 363-378.

Barnett, B., Forbes, S. and Ashcroft, C. 1989. Heavy metals on the south bank of the Humber Estuary. *Marine Pollution Bulletin* **20**, 17-21.

Barr, R., Watson, P.G., Ashcroft, C.R., Barnett, B.E. and Hilton, C. 1990. Humber Estuary-A case study. *Hydrobiologia* **195**, 127-143.

Baskaran, M. and Santschi, P.H., 1993. The role of particles and colloids in the transport of radionuclides in coastal environments of Texas. *Marine Chemistry* **43**, 95-114.

Baskaran, M., Santschi , P.H., Benoit, G. and Honeyman, B.D., 1992. Scavenging of thorium isotopes by colloids in seawater of the Gulf of Mexico. *Geochimica et Cosmochimica Acta.* **56**, 3375-3388.

Beckett, R. and Hart, B. 1993. Use of field-flow fractionation techniques to characterise aquatic particles, colloids and macromolecules. In: *Environmental Particles, Volume 2.* J. Buffle and H.P. Van Leeuwen (Eds.). Lewis. pp165-205.

Beckett, R., Jue, Z. and Giddings, J.C. 1987. Determination of molecular weight distributions of fulvic and humic acids using field-flow fractionation. *Environmental Science and Technology* **21**, 289-295.

Beckett, R., Nicholson, G., Hart, B.T., Hansen, M. and Giddings, J.C. 1988. Separation and size characterisation of colloidal particles in river water by sedimentation field-flow fractionation. *Water Research* **22**, 1535-1545.

Benjamin, M.M. and Leckie, J.O. 1981. Multiple site adsorption of cadmium, copper, zinc and lead on amorphous iron oxyhydroxide. *Journal of Colloid and Interface Science* **79**, 209-221.

Benoit, G., Oktay-Marshall, S.D., Cantu, A., Hood, E.M., Coleman, C.H., Corapcioglu M.O. and Santschi, P.H., 1994. Partitioning of Cu, Pb, Ag, Zn, Fe, Al, and Mn between filter retained particles, colloids , and solution in six Texas estuaries. *Marine Chemistry* **45**, 307-336.

Blatt, W.F., Dravid, A., Michaels, A.S. and Nelsen, L., 1970. Solute polarisation and cake formation in membrane ultrafiltration: Causes, consequences and control techniques. In: *Membrane science and technology*, J.E. Flinn (Ed). Plenum. pp47-97.

Bowen, W.R. and Jenner, F. 1995. Theoretical descriptions of membrane filtration of colloids and fine particles: an assessment and review. *Advances in Colloid and Interface Science* **56**, 141-200.

Boyle, E.A., Edmond, J.M. and Sholkovitz, E.R., 1977. The mechanism of iron removal in estuaries. *Geochimica et Cosmochimica Acta* **41**, 1313-1324.

Boyle, E.A., Huestead, S.S. and Grant, B. 1982. The chemical mass balance of the Amazon plume- II. Copper, nickel and cadmium. *Deep-Sea Research* **29**, 1355-1364.

Bruland, K.W. and Franks, R.P. 1983. Manganese, nickel, copper, zinc and cadmium in the western north Atlantic. In: *Trace metals in seawater*. C.S. Wong, E. Boyle, K. Bruland, J.D. Burton and E.D. Goldberg (Eds.). Plenum Press, New York. pp395-413.

Bruland, K.W., Coale, K.H. and Mart, L. 1985. Analysis of seawater for dissolved cadmium, copper and lead: An intercomparison of voltametric and atomic adsorption methods. *Marine Chemistry* **17**, 285-300.

Bruland, K.W., Franks, R.P., Knauer, G.A. and Martin, J.H. 1979. Sampling and analytical methods for the determination of Cu, Cd, Zn and Ni at the nanogram per litre level in seawater. *Analytica Chimica Acta* **105**, 233-245.

Buessler, K.O., Bauer, J.E., Chen, R.F., Eglinton, T.I., Gustafsson, O., Landing, W., Mopper, K., Moran, S.B., Santschi, P.H., VernonClark, R. and Wells, M.L., 1996. An intercomparison of cross-flow filtration techniques used for sampling marine colloids: Overview and organic carbon results. *Marine Chemistry* **55**, 1-31.

Buffle, J. 1990. *Complexation reactions in aquatic systems; an analytical approach.* Ellis Harwood series in analytical chemistry. Wiley, New York.

Buffle, J. and Leppard, G.G. 1995a. Characterisation of aquatic colloids and macromolecules.1. Structure and behaviour of colloidal material. *Environmental Science and Technology* **29**, 2169-2175.

Buffle, J. and Leppard, G.G. 1995b. Characterisation of aquatic colloids and macromolecules. 2. Key role of physical structures on analytical results. *Environmental Science and Technology* **29**, 2176-2184.

Buffle, J., Perret, D. and Newman, M. 1992. The use of filtration and ultrafiltration for size fractionation of aquatic particles, colloids and macromolecules. In: *Environmental Particles, volume 1* .J. Buffle and H.P. van Leeuwen .Eds. Lewis. pp171-230.

Burton, J.D., Althaus, M., Millward, G.E., Morris, A.W., Statham, P.J., Tappin, A.D. and Turner, A. 1993. Processes influencing the fate of trace metals in the North Sea. *Philosophical Transactions of the Royal Society London A* **343**, 557-568.

Cameron, A.J. and Liss, P.S. 1984. The stabilisation of 'dissolved' iron in freshwater. *Water Research* **18**, 179-185.

Campbell, J.A., Whitelaw, K., Riley, J.P., Head, P.C. and Jones, P.D. 1988. Contrasting behaviour of dissolved and particulate nickel and zinc in a polluted estuary. *The Science of the Total Environment* **71**, 141-155.

Caschetto, S. and Wollast, R. 1979. Vertical distribution of dissolved aluminium in the Mediterranean Sea. *Marine Chemistry* **7**, 141-155.

Chapman, D.L. 1913. A contribution to the theory of electrocapillarity. *Philosophical Magazine* **25**, 475-481.

Chen, Y-W., 1993. *Physicochemical characterisation of colloids in river waters and studies of experimental conditions*. Ph.D. Thesis. University of Geneva.

Chen, Y-W. and Buffle, J., 1996a. Physicochemical and microbial preservation of colloid characteristics of natural water samples. I: Experimental conditions. *Water Research* **30**, 2178-2184.

Chen, Y-W. and Buffle, J., 1996b. Physicochemical and microbial preservation of colloid characteristics of natural water samples. II: Physicochemical and microbial evolution. *Water Research* **30**, 2185-2192.

Chester, R. 1990. Marine Geochemistry. Unwin Hyman Ltd, London, U.K.

Chester, R., Nimmo, M. and Corcoran, P.A. 1997. Rain water-aerosol trace metal relationships at Cap Ferrat: A coastal site in the Western Mediterranean. *Marine Chemistry* **58**, 293-312.

Chiffoleau, J.F., Cossa, D., Auger, D. and Truquet, I. 1994. Trace metal distribution, partition and fluxes in the Seine Estuary (France) in low discharge regime. *Marine Chemistry* **47**, 145-158.

Chin, W-C., Orellana, M.V. and Verdugo, P., 1998. Spontaneous assembly of marine dissolved organic matter into polymer gels. *Nature* **391**, 568-572.

Chittleborough, D.J., Hotchin, D.M. and Beckett, R. 1992. Sedimentation field-flow fractionation: A new technique for the fractionation of soil colloids. *Soil Science* **153**, 341-348.

Chou, L. and Wollast, R. 1991. Interstitial water as a possible source of dissolved aluminium in the NW Mediterranean Sea. *CEC Water Pollution Report* **No. 28**, 349-367.

Coale, K.H. and Bruland, K.W. 1990. Spatial and temporal variability in copper complexation in the North Pacific. *Deep-Sea Research* **37**, 317-336.

Coffey, M., 1994. *The behaviour of trace metals in the Humber Estuary, U.K.* PhD. thesis. University of East Anglia, UK.

Comans, R.N. and van Dijk, C.P.J. 1988. Role of complexation processes in cadmium mobilisation during estuarine mixing. *Nature* **336**, 151-154.

Cooney, D.O. 1992. Adsorption of organic solutes on membrane filters during aqueous phase filtration. 1. Basic rate and equilibrium studies using toluidine blue. *Separation Science and Technology* **27**, 2001-2019.

Dai, M-H. and Martin, J-M., 1995. First data on trace metal level and behaviour in two major Arctic river-estuarine systems (Ob and Yenesey) and in the adjacent Kara Sea, Russia. *Earth and Planetary Science Letters* **131**, 127-141.

Dai, M-H., Martin, J.M. and Cauwet, G., 1995. The significant role of colloids in the transport and transformation of organic carbon and associated trace metals (Cd, Cu and Ni) in the Rhone delta (France). *Marine Chemistry* **51**, 159-175.

Danielsson, L-G., Magnusson, B. and Westerland, S., 1978. An improved metal extraction procedure for the determination of trace metals in seawater by atomic absorption spectrometry with electrothermal atomisation. *Analytica Chimica Acta* **98**, 45-57.

Danielsson, L-G., Magnusson, B., Westerland, S. and Zhang, K. 1982. Trace metal determinations in estuarine waters by electrothermal atomic absorption spectrometry after extraction of dithiocarbamate complexes into freon. *Analytica Chimica Acta* **144**, 183-188.

Danielsson, L-G., Magnusson, B., Westerland, S. and Zhang, K. 1983. Trace metals in the Gota River estuary. *Estuarine, Coastal and Shelf Science* **17**, 73-85.

Denman, N.E. 1979. Physical characters of the Humber. In: *The Humber Estuary.* NERC publication series c, No.20, pp5-8.

Deryagin, B.V. and Landau, L. 1941. *Acta Physica et Chimica URSS* **14**, 633.

Dolamore-Frank, J.A. 1983. *The analysis, occurrence and chemical speciation of zinc and chromium in natural waters.* PhD thesis, University of Southampton, UK.

Drever, J.I. 1982. *The geochemistry of natural waters.* Prentice Hall, New Jersey. pp 437.

Duinker, J.C. 1980. Suspended matter in estuaries: adsorption and desorption processes. In: *Chemistry and biogeochemistry of estuaries.* E. Olausson and I. Cato (Eds.). John Wiley, Chichester. pp121-151.

Duinker, J.C., Hillebrand, M.T.J., Nolting, R.F. and Wellershaus, S. 1982. The River Elbe: processes affecting the behaviour of metals and organochlorines during estuarine mixing. *Netherlands Journal of Sea Research* **15**, 141-169.

Eaton, A. 1979. Observations on the geochemistry of soluble copper, iron, nickel and zinc in the San Francisco Bay estuary. *Environmetal Science and Technology* **13**, 425-432.

Eckert, J.M. and Sholkovitz, E.R. 1976. The flocculation of iron, aluminium and humates from river water by electrolytes. *Geochimica et Cosmochimica Acta* **40**, 847-848.

Edmond, J.M., Spivack, A., Grant, B.C., Hu, M.H., Chen, Z., Chen, S. and Zeng, X. 1985. Chemical dynamics of the Changjiang estuary. *Continental Shelf Research* **4**, 17-36.

Edzwald, J.K. 1972. Coagulation in estuaries. *University of North Carolina , Sea grant publication.* 45pp.

Eisma, D. 1986. Flocculation and de-flocculation of suspended matter in estuaries. *Netherlands Journal of Sea Research* **20**, 183-199.

Eisma, D. 1991. Particle size of suspended matter in estuaries. *Geomarine Letters* **11**, 147-153.

Eisma, D. and Li, A. 1993. Changes in suspended matter flocc size during the tidal cycle in the Dollard estuary. *Netherlands Journal of Sea Research* **31 (2)**, 107-117.

Eisma, D., Bernard, P., Cadee, G.C., Ittekkot, V., Kalf, J., Laane, R., Martin, J-M., Mook,W.G., Avan, P. and Schumacher, T. 1991a . Suspended matter particle size in some Western European estuaries, Part 1 : particle-size distribution. *Netherlands Journal of Sea Research* **28**, 193-214.

Eisma, D., Bernard, P., Cadee, G.C., Ittekkot, V., Kalf, J., Laane, R., Martin, J-M., Mook,W.G., Avan, P. and Schumacher, T. 1991b . Suspended matter particle size in some Western European estuaries, Part 2 : a review on flocc formation and break-up. *Netherlands Journal of Sea Research* **28**, 215-220.

Elbaz-Poulichet, F., Hollinger, P., Huang, W.W. and Martin, J-M. 1984. Lead cycling in estuaries, illustrated by the Gironde Estuary, France. *Nature* **308**, 409-414.

Elbaz-Poulichet, F., Martin, J-M., Huang, W.W. and Zhu, J.X. 1987. Dissolved Cd behaviour in some selected French and Chinese estuaries. Consequences on Cd supply to the ocean. *Marine Chemistry* **22**, 125-136.

Elderfield, H., Hepworth, A., Edwards, P.N. and Holliday, L.M. 1979. Zinc in the Conwy River and Estuary. *Estuarine, Coastal and Shelf Science* **9**, 403-422.

Emerson, S., Kalhorn, S., Jacobs, L., Tebo, B.M., Nealson, K.H. and Rosson, R.A. 1982. Environmental oxidation rate of manganese (II): Bacterial catalysis. *Geochimica et Cosmochimica Acta* **46**, 1073-1079.

Fang, T-H., 1995. *Studies of the behaviour of trace metals during mixing in some estuaries of the Solent-region.* Ph.D. thesis. University of Southampton. U.K.

Figueres, G., Martin, J-M. and Meybeck, M., 1978. Iron behaviour in the Zaire. *Netherlands Journal of Sea Research* **12**, 329-337.

Filella, M. and Buffle, J. 1993. Factors affecting the stability of sub-micron colloids in natural waters. *Journal of Colloids and Surfaces A: Physicochemical and engineering aspects* **73**, 255-273.

Foley, G. 1994. Membrane fouling in cross-flow filtration: implications for measurement of the steady state specific cake resistance. *Biotechnology Techniques* **8**, 743-746.

Fox, L.E. 1988. The solubility of colloidal ferric hydroxide and its relevance to iron concentrations in river water. *Geochimica et Cosmochimica Acta* **52**, 771-777.

Fox, L.E. and Wofsy, S.C. 1983. Kinetics of removal of iron colloids from estuaries. *Geochimica et Cosmochimica Acta* **47**, 211-216.

Gameson, A.L.H. 1976. *Routine surveys of the tidal water of the Humber Basin. 1: physical parameters.* WRc Technical report TR25: 51.

Gameson, A.L.H. 1982. *The quality of the Humber Estuary, a review of the results of monitoring 1961-1981.* Yorkshire Water Authority, Leeds, UK.

Gibbs, R.J. 1983. Effect of natural organic coatings on the coagulation of particles. *Environmental Science and Technology* **17**, 237-240.

Gouy, M., 1910. *Journal de Chimie Physique* **9** , 457-460.

Grahame, D.C. 1947. The electrical double layer and the theory of electrocapillarity. *Chemical Reviews.* **41** , 441-501.

Grant, A. and Middleton, R. 1990. An assessment of metal contamination of sediments in the Humber Estuary, UK. *Estuarine, Coastal and Shelf Science* **31**, 71-85.

Grant, A. and Middleton, R. 1993. Trace metals in sediments from the Humber Estuary: A statistical analysis of spatial uniformity. *Netherlands Journal of Aquatic Ecology* **27**, 111-120.

Greenamoyer, J.M. and Moran, S.B., 1996. Evaluation of an Osmonics spiral-wound cross-flow filtration system for sub-μm sampling of Cd, Cu and Ni in seawater. *Marine Chemistry* **55**, 153-163.

Gregory, J., 1975. The effects of polymers on colloid stability. In*: Scientific basis of flocculation. NATO advanced studies series.* Ives K.J., (Ed). Sitjtoff and Noordhoff. pp101-130.

Guo, L.D., Coleman, C.H. and Santschi, P.H., 1994. The distribution of colloidal and dissolved organic carbon in the Gulf of Mexico. *Marine Chemistry* **45**, 105-119.

Gustafsson, O., Buessler, K.O. and Gschwend,P.M., 1996. On the integrity of cross-flow filtration for collecting marine organic colloids. *Marine Chemistry* **55**, 93-111.

Hall, G.E.M., Bonham-Carter, G.F., Horowitz, A.J., Lum, K., Lemieux, C., Quemerais, B. and Garbarino, J.R., 1996. The effect of using different 0.45μm filter membranes on 'dissolved' element concentrations in natural waters. *Applied Geochemistry* **11**, 243-249.

Hall, I.R. 1993. *Cycling of trace metals in coastal waters: Biogeochemical processes involving suspended particles.* PhD Thesis, University of Southampton, UK.

Healy, T.W. and Lamer, V.K., 1964. *Journal of colloid science* **19**, 323.

Heathershaw, A.D. and Codd, J.M. 1986. Depth controlled changes in grain size and carbonate content on a shelf edge sand bank. *Marine Geology* **72**, 211-224.

Holliday, L.M. and Liss, P.S. 1976. The behaviour of dissolved iron, manganese and zinc in the Beaulieu Estuary, S. England. *Estuarine, Coastal and Shelf Science* **4**, 349-353.

Honeyman, B.D. and Santschi, P.H., 1989. A Brownian-pumping model for oceanic trace metal scavenging: Evidence from Th isotopes. *Journal of Marine Research* **47**, 19-26.

Honeyman, B.D. and Santschi, P.H., 1992. The role of particles and colloids in the transport of radionuclides and trace metals in the oceans. In; *Environmental Particles, volume 1*. J. Buffle and H.P. van Leeuwen (Eds). Lewis. pp379-423.

Honeyman, B.D., Balistrieri, L.S. and Murray, J.W., 1988. Oceanic trace metal scavenging; the importance of particle concentration. *Deep Sea Research* **35**, 227-246.

Horowitz, A.J., Elrick, K.A. and Colberg, M.R., 1992. The effect of membrane filtration artifacts on dissolved trace element concentrations. *Water Research* **26**, 753-763.

Horowitz, A.J., Lum, K.R., Garbarino, J.R., Hall, G.E.M., Lemieux, C. and Demas, C.R., 1996a. Problems associated with using filtration to define dissolved trace element concentrations in natural water samples. *Environmental Science and Technology* **30**, 954-963.

Horowitz, A.J., Lum, K.R., Garbarino, J.R., Hall, G.E.M., Lemieux, C. and Demas, C.R., 1996b. The effect of membrane filtration on dissolved trace element concentrations. *Water, Air and Soil Pollution* **90**, 281-294.

Howard, A.G. and Statham, P.J. 1993. *Inorganic trace analysis; philosophy and practice.* Wiley.

Humber Estuary Committee. 1990. *The water quality of the Humber Estuary, 1989.* National Rivers Authority, UK.

Hunter, K.A. and Leonard, M.W. 1988. Colloidal stability and aggregation in estuaries 1. Aggregation kinetics of riverine dissolved iron after mixing with seawater. *Geochimica et Cosmochimica Acta.* **52**, 1123-1130.

Hunter, K.A. and Liss, P.S. 1982. Organic matter and the surface charge of suspended particles in estuarine waters. *Limnology and Oceanography* **27**, 322-335.

Hydes, D.J. 1979. Aluminium in Seawater: control by inorganic processes. *Science* **205**, 1260-1262.

Hydes, D.J. 1983. Distribution of Aluminium in waters of the North East Atlantic: 25°N to 35°N. *Geochimica et Cosmochimica Acta* **47**, 967-973.

Hydes, D.J. 1989. Seasonal variation in dissolved aluminium concentrations in coastal waters and biological limitation of the export of the riverine input of aluminium to the deep sea. *Continental Shelf Res*earch **9**, 919-929.

Hydes, D.J. and Kremling, K. 1993. Patchiness in dissolved metals (Al, Cd, Co, Cu, Mn, Ni) in North Sea surface waters: seasonal differences and influence of suspended sediment. *Continental shelf Research* **13**, 1083-1101.

Hydes, D.J. and Liss, P.S. 1976. Flourometric method for the determination of low concentrations of dissolved aluminium in natural waters. *Analyst* **101**, 922-931.

Hydes, D.J., de Lange, G.J. and de Baar, J.W. 1988. Dissolved Al in the Mediterranean. *Geochimica et Cosmochimica Acta* **52**, 2107-2114.

Iler, R.K. 1973. Effect of adsorbed alumina on the solubility of amorphous silica in water. *Journal of Colloid and Interface Science* **43**, 399-408.

Iler, R.K. 1979. *The chemistry of silica.* Wiley-interscience, New York.

Jaffe, D. and Walters, J.K. 1977. Intertidal trace metal concentrations in some sediments from the Humber Estuary. *The Science of the Total Environment* **7**, 1-15.

Jiao, D. and Sharma, M.M. 1994. Mechanism of cake build-up in cross-flow filtration of colloidal suspensions. *Journal of Colloid and Interface Science* **162**, 454-462.

Jickells,T. 1995. Atmospheric inputs of metals and nutrients to the oceans: their magnitude and effects. *Marine chemistry* **48**, 199-214.

Karaiskakis, G., Graff, K.A., Caldwell, K.D. and Giddings, J.C. 1982. Sedimentation field-flow fractionation of colloidal particles in river water. *International Journal of Environmental Analytical Chemistry* **12**, 1-15.

Kawakatsu, T., Nakao, S-I. and Kimura, S. 1993. Effects of the size and compressibility of suspended particles and surface pore size of membrane on flux in cross-flow filtration. *Journal of Membrane Science* **81**, 173-190.

Kilduff, J. and Weber, W.J. 1992. Transport and separation of organic macromolecules in ultrafiltration processes. *Environmental Science and Technology* **26**, 569-577.

Knox, S., Turner, D.R., Dickson, A.G., Liddicoat, M.I., Whitfield, M. and Butler, E.I. 1981. Statistical analysis of estuarine profiles: Application to manganese and ammonia in the Tamar Estuary. *Estuarine, Coastal and Shelf Science* **13**, 357-371.

Kraepiel, A.M.L., Chiffoleau, J-F., Martin, J-M. and Morel, F.M.M., 1997. Geochemistry of trace metals in the Gironde Estuary. *Geochimica et Cosmochimica Acta* **61**, 1421-1436.

Kramer, K.L.M., Vinhas, T. and Quevauviller, P. 1994. Estuarine reference material for trace elements: effect of flocculation upon homogeneity and stability. *Marine Chemistry* **46**, 77-87.

Kremling, K. 1985. The distribution of Cd, Cu, Ni, Mn and Al in the surface waters of the open Atlantic and European shelf area. *Deep Sea Research* **32**, 531-555.

Lamer, V.K. and Healy, T.W. 1963. Adsorption-flocculation reactions of macromolecules at the solid-liquid interface. *Reviews of Pure and Applied Chemistry* **13**, 112-133.

Laxen, D.P. 1985. Trace metal adsorption/coprecipitation on hydrous ferric oxide under realistic conditions. *Water Research* **19**, 1229-1236.

Laxen, D.P. and Chandler, I.M., 1982. Comparison of filtration techniques for size distribution in freshwaters. *Analytical Chemistry* **54**, 1350-1355.

Lead, J.R., Davison, W., Hamilton-Taylor, J. and Buffle, J., 1997. Characterising colloidal material in natural waters. *Aquatic Geochemistry* **3**, 213-232.

Lion, L.W., Altmann, R.S. and Leckie, J.O. 1982. Trace-metal adsorption characteristics of estuarine particulate matter: evaluation of contributions of Fe/Mn oxide and organic surface coatings. *Environmental Science and Technology* **16**, 660-666.

Liss, P.S., 1976. Conservative and non-conservative behaviour of dissolved constituents during estuarine mixing. In: *Estuarine Chemistry*, J.D. Burton and P.S. Liss (Eds). Academic press, London, UK. pp93-130.

Mackenzie, F.T., Stoffyn, M. and Wollast, R. 1978. Aluminium in seawater: control by biological activity. *Science* **199**, 680-682.

Mackey, D.J., O'Sullivan, J.E., Watson, R.J. and Pont, G.D. 1997. Interference effects in the extraction of trace metals from estuarine waters. *Marine Chemistry* **59**, 113-126.

Mackin, J.E. 1986. Control of dissolved Al distributions in marine sediments by clay reconstitution reactions: Experimental evidence leading to a unified theory. *Geochimica et Cosmochimica Acta* **50**, 207-214.

Mackin, J.E. and Aller, R.C. 1984a. Diagenesis of dissolved aluminium in organic-rich estuarine sediments. *Geochimica et Cosmochimica Acta* **48**, 299-313.

Mackin, J.E. and Aller, R.C. 1984b. Dissolved Al in sediments and waters of the East China Sea: implications for authigenic mineral formation. *Geochimica et Cosmochimica Acta* **48**, 218-297.

Mackin, J.E. and Aller, R.C. 1986. The effects of clay mineral reactions on dissolved Al distributions in sediments and waters of the Amazon continental shelf. *Continental Shelf Research* **8**, 89-106.

Mackin, J.E. and Aller, R.C. 1989. The nearshore marine and estuarine chemistry of dissolved aluminium and rapid authigenic mineral precipitation. *Reviews in Aquatic Sciences* **1**, 537-554.

Mackin, J.E. and Swider, K.T. 1987. Modelling the dissolution behaviour of standard clays in seawater. *Geochimica et Cosmochimica Acta* **51**, 2947-2964.

Maring, H.B. and Duce, R.A. 1987. The impact of atmospheric aerosols on trace metal chemistry in open ocean surface seawater. 1. Aluminium. *Earth and Planetary Science Letters* **84**, 381-392.

Martin, J.H. and Knauer, G.A. 1973. The elemental composition of plankton. *Geochimica et Cosmochimica Acta* **37**, 1639-1653.

Martin, J-M., Dai, M-H. and Cauwet, G. 1995. Significance of colloids in the biogeochemical cycling of organic carbon and trace metals in the Venice Lagoon (Italy). *Limnology and Oceanography* **40**, 119-131.

Martin, J-M., Mouchel, J.M. and Nirel, P., 1986. Some recent developments in the characterisation of estuarine particles. *Water Science and Technology* **18**, 83-92.

Mayer, L.M. 1982. Aggregation of colloidal iron during estuarine mixing: Kinetics, mechanism and seasonality. *Geochimica et Cosmochimica Acta* **46**, 2527-2535.

McCave, I.N. 1986. Local and global aspects of the bottom nepheloid layers in the world ocean. *Netherlands Journal of Sea Research* **20**, 167-181.

Measures, C.I. and Brown, E.T. 1998. Estimating dust input to the Atlantic Ocean using surface water aluminium concentrations. In: *The impact of desert dust across the Mediterranean*, S. Guerzoni and R.Chester (Eds.). Kluwer Academic publishers. pp301-311.

Measures, C.I., Edmond, J.M. and Jickells, T.D. 1986. Aluminium in the North-West Atlantic. *Geochimica et Cosmochimica Acta* **50**, 1423-1429.

Miller, W.L. and Kester, D. 1994. Photochemical iron reduction and iron bioavailability in seawater. *Journal of Marine Research* **52**, 325-343.

Miller, W.L., King, D.W., Lin, J. and Kester, D.R. 1995. Photochemical redox cycling of iron in coastal seawater. *Marine Chemistry* **50**, 63-77.

Millward, G.E., 1995. Processes affecting trace element speciation in estuaries; a review. *Analyst* **120**, 609-614.

Millward, G.E. and Glegg, G.A., 1997. Fluxes and retention of trace metals in the Humber Estuary. *Estuarine, Coastal and Shelf Science* **44 (Supp A)**, 97-105.

Millward, G.E. and Moore, R.M. 1982. The adsorption of Cu, Mn and Zn by iron oxyhydroxides in model estuarine systems. *Water Research* **16**, 981-985.

Millward, G.E. and Turner, A. 1995. Trace metals in estuaries. In: *Trace elements in natural waters*. B. Salbu and E. Steinnes (Eds). CRC Press, London. pp223-245.

Millward, G.E., Glegg, G.A. and Morris, A.W. 1992. Zn and Cu removal kinetics in estuarine waters. *Estuarine, Coastal and Shelf Science* **35**, 37-54.

Millward, G.E., Allen, J.I., Morris, A.W. and Turner, A. 1996. Distributions and fluxes of non-detrital particulate Fe, Mn, Cu, Zn in the Humber coastal zone. *Continental Shelf Research* **16**, 967-993.

Millward, G.E., Turner, A., Glasson, D.R. and Glegg, G.A. 1990. Intra and inter-estuarine variability of particle micro-structure. *Science of the Total Environment* **97/98**, 289-300.

Moir, D.N. 1981. Flocculation, dispersion and suspension stability. In: *Suspension Rheology; the flow properties and quality control of suspensions.* Seminar London. Warren Spring Laboratory pp1-13.

Moore, R.M. and Millward, G.E. 1984. Dissolved-particulate interactions of Al in ocean waters. *Geochimica et Cosmochimica Acta* **48**, 235-241.

Moore, R.M., Burton, J.D., Williams, P.J. and Young, M.L. 1979. The behaviour of dissolved organic material, iron and manganese in estuarine mixing. *Geochimica et Cosmochimica Acta* **43**, 919-926.

Moran, S.B., 1991. The application of cross-flow filtration to the collection of colloids and their associated metals in seawater. In: *Marine Particles; analysis and characterisation. Geophysical monograph,* **63**, 275-280

Moran, S.B. and Buessler, K.O., 1992. Short residence time of colloids in the upper ocean estimated from ^{238}U-^{243}Th disequlibria. *Nature* **359**, 221-223.

Moran, S.B. and Buessler, K.O., 1993. Size fractionated ^{234}Th in continental shelf waters off New England; implications for the role of colloids in oceanic trace metal scavenging. *Journal of Marine Research* **51**, 893-922.

Moran, S.B. and Moore, R.M., 1988a. Evidence from mesocosm studies for biological removal of dissolved aluminium from seawater . *Nature* **335**, 706-708.

Moran, S.B. and Moore, R.M., 1988b. Temporal variations in dissolved and particulate aluminium during a spring bloom. *Estuarine, coastal and shelf science* **27**, 205-215.

Moran, S.B. and Moore, R.M., 1989. The distribution of colloidal Aluminium and organic carbon in coastal and open ocean waters off Nova Scotia. *Geochimica et Cosmochimica Acta* **53**, 2519-2527.

Moran, S.B. and Moore, R.M. 1991. The potential source of dissolved aluminium from resuspended sediments to the North Atlantic deep water. *Geochimica et Cosmochimica Acta* **55**, 2745-2751.

Morley, N.H., Burton, J.D. and Statham, P.J. 1990. Observations on dissolved trace metals in the Gulf of Lions. *Water Pollution Research Report* **20**, 309-328.

Morris, A.W. 1986. Removal of trace metals in the very low salinity region of the Tamar Estuary, England. *Science of the Total Environment* **49**, 297-304.

Morris, A.W. 1988. The estuaries of the Humber and Thames. In*: Pollution of the North Sea: an assessment,* W. Salomons, B.L. Bayne, E.K. Duursma and U. Forstner (Eds.). Springer-Verlag, Berlin. 213-224.

Morris, A.W. and Bale, A.J. 1979. Effect of rapid precipitation of dissolved Mn in river water on estuarine Mn distributions. *Nature* **279**, 318-319.

Morris, A.W., Bale, A.J. and Howland, R.J.M. 1982. The dynamics of estuarine manganese cycling. *Estuarine, Coastal and Shelf Science* **14**, 175-192.

Morris, A.W., Howland, R.J.M. and Bale, A.J. 1978a. A filtration unit for use with continuous flow systems. *Estuarine, Coastal and Marine Science* **6**, 105-109.

Morris, A.W., Mantoura, R.F.C., Bale, A.J. and Howland, R.J.M. 1978b. Very low salinity regions of estuaries: important sites for chemical and biological reactions. *Nature* **274**, 678-680.

Muller, F.L.L. 1996. Interactions of Cu, Pb and Cd with the dissolved, colloidal and particulate components of estuarine and coastal waters. *Marine Chemistry* **52**, 245-268.

Muller, F.L.L., Tranter, M. and Balls, P.W. 1994a. Distributions and transport of chemical constituents in the Clyde Estuary. *Estuarine, Coastal and Shelf Science* **39**, 105-126.

Muller, F.L.L., Tappin, A.D., Statham, P.J., Burton, J.D. and Hydes, D.J. 1994b. Trace metal fronts in waters of the Celtic Sea. *Oceanologica Acta* **17**, 105-126.

Murphy, D.M. 1995. *Investigation of suspended particulate matter and associated contaminants in natural waters using sedimentation field-flow fractionation techniques.* PhD. Thesis, Monash University, Melbourne.

Nealson, K.H. and Tebo, B. 1980. Structural features of manganese precipitating bacteria. *Origins of Life* **10**, 117-126.

Neihof, R.A. and Loeb, G.I., 1972. The surface charge of particulate matter in seawater. *Limnology and Oceanography* **17**, 7-16.

Newton, P.P. and Liss, P.S. 1989. Surface charge characteristics of oceanic suspended particles. *Deep Sea Research* **36**, 759-767.

Ng, B., Turner, A., Tyler, A.O., Falconer, R.A. and Millward, G.E., 1996. Modelling contaminant geochemistry in estuaries. *Water Research* **30**, 63-74.

Niven, S.E.H. and Moore R.H., 1987. Effect of natural colloidal matter on the equilibrium adsorption of thorium in seawater. In *Radionuclides: A tool for oceanography*, J.Guary, P.Guegueniat and R.J. Pentreath (Eds). Elsevier Applied Science, New York. pp111-120.

Olafsson, J. 1983. Mercury concentrations in the North Atlantic in relation to cadmium aluminium and oceanic parameters. In: *Trace metals in seawater* . C.S.Wong, E.Boyle, K.W. Bruland, J.D. Burton and E.D.Goldberg. eds. NATO conference series. Plenum press. pp475-485.

Olsen, C.R., Cutshall, N.H. and Larsen, I.L., 1982. Pollutant-particle associations and dynamics in coastal marine environment: a review. *Marine Chemistry* **11**, 501-533 .

Orians, K.J. and Bruland, K.W. 1985. Dissolved aluminium in the central North Pacific. *Nature* **316**, 427-429.

Orians, K.J. and Bruland, K.W. 1986. The biogeochemistry of aluminium in the Pacific Ocean. *Earth and Planetary Science Letters* **78**, 397-410.

Ostapczuk, P. 1993. Present potential and limitations in the determination of trace elements by potentiometric stripping analysis. *Analytica Chimica Acta* **273**, 35-40.

Ottewill, R.H., 1977. Stability and instability in disperse systems. *Journal of Colloid and Interface Science* **58**, 357-373.

Paalman, M.A.A., Van-der-Weijden, C.H. and Loch, J.P.G. 1994. Sorption of cadmium on suspended matter under estuarine conditions; competition and complexation with major sea-water ions. *Water, Air and Soil Pollution* **73**, 49-60.

Pankow, J.F. and Morgan, J.J. 1981. Kinetics for the aquatic environment. *Environmental Science and Technology* **15**, 1155-1164.

Parks, G.A. 1967. Aqueous surface chemistry of oxides and complex oxide minerals. *Equilibrium concepts in natural water systems. American Chemical Society Advanced Chemistry Series* **67**, 121-160.

Powell, R., Landing, W.M. and Bauer, J.E., 1996. Colloidal trace metals, organic carbon and nitrogen in a southeastern US estuary. *Marine Chemistry* **55**, 165-176.

Quentel, F., Madec, C. and Courtot-Coupez, J. 1986. Influence of dissolved organic matter on the lead determination in seawater by anodic stripping voltametry. *Water Research* **20**, 325-333.

Salomons, W. 1980. Adsorption processes and hydrodynamic conditions in estuaries. *Environmental Technology Letters* **1**, 356-365.

Sanders, R.J., Jickells, T., Malcolm, S., Brown, J., Kirkwood, D., Reeve, A., Taylor, J., Horrobin, T. and Ashcroft, C. 1997. Nutrient fluxes through the Humber Estuary. *Journal of Sea Research* **37**, 3-23.

Sanudo-Wilhelmy, S.A., Rivera-Duarte, I. And Flegal, A.R., 1996. Distribution of colloidal trace metals in the San Francisco Bay estuary. *Geochimica et Cosmochimica Acta* **60**, 4933-4944.

Sharma, R.V., Edwards, R.T. and Beckett, R. 1993. Physical characterisation and quantification of bacteria by sedimentation field-flow fractionation. *Applied and Environmental Microbiology* **59**, 1864-1875.

Shaw, D.J., 1992. *Introduction to colloid and surface chemistry.* Butterworth and Heinemann, 306pp.

Shell UK., 1987. *The Humber Estuary, environmental background.* Shell UK Ltd.

Shiller, A.M. and Boyle, E.A. 1987. Variability of trace metals in the Mississippi River. *Geochimica et Cosmochimica Acta* **51**, 3273-3277.

Shiller, A.M. and Boyle, E.A. 1991. Trace elements in the Mississippi River Delta outflow region: behaviour at high discharge. *Geochimica et Cosmochimica Acta* **55**, 3241-3251.

Sholkovitz, E.R. 1976. Flocculation of dissolved organic and inorganic matter during the mixing of river water and seawater. *Geochimica et Cosmochimica Acta* **40**, 831-845.

Sholkovitz, E.R. 1978. The flocculation of dissolved Fe, Mn, Al, Ci, Ni, Co and Cd during estuarine mixing. *Earth and Planetary Science Letters* **41**, 77-86.

Sholkovitz, E.R. 1979. Chemical and physical processes controlling the chemical composition of suspended material in the River Tay Estuary. *Estuarine and Coastal Marine Science* **8**, 523-545.

Sholkovitz, E.R. and Copland, D. 1981. The coagulation, solubility and adsorption properties of Fe, Mn, Cu, Ni, Cd, Co and humic acids in river water. *Geochimica et Cosmochimica Acta* **45**, 181-189.

Sholkovitz, E.R., Boyle, E.A. and Price, N.B. 1978. The removal of dissolved humic acids and iron during estuarine mixing. *Earth and Planetary Science Letters* **41**, 77-86.

Smoluchowski, M. 1917. Versuch einer mathematischen theorie der koagulatiionskinetik kolloider losungen. *Zietschrift fuer Physikalische Chemie* **92**, 129-169.

Spokes, L.J. and Liss, P.S. 1995. Photochemically induced redox reactions in seawater, I. Cations. *Marine Chemistry* **49**, 201-213.

Statham, P.J. 1985. The determination of dissolved manganese and cadmium in seawater at low nmol l^{-1} concentrations by chelating and extraction followed by electrothermal atomic absorption spectrometry. *Analytica Chimica Acta* **169**, 149-159.

Stern, O. 1924, Zur theorie der electrolytishen doppelschicht. *Zeitschrift fuer Elektrochemie* **30** , 508-516.

Stoffyn, M. and MacKenzie, F.T. 1982. Fate of dissolved aluminium in the oceans. *Marine Chemistry* **11**, 105-127.

Stordal, M.C., Santschi, P.H. and Gill, G.A., 1996. Colloidal pumping: Evidence for the coagulation process using natural colloids tagged with ^{203}Hg. *Environmental Science and Technology* **30**, 3335-3340.

Strickland, J.D.H. and Parsons, T.R. 1972. *A practical handbook of seawater analysis.* Fisheries Research Board of Canada, Ottawa. pp17-19.

Sunda, W.G. and Huntsman, S.A. 1987. Microbial oxidation of manganese in a North Carolina estuary. *Limnology and Oceanography* **32**, 552-564.

Sunda, W.G. and Huntsman, S.A. 1988. Effect of sunlight on redox cycles of manganese in the southwestern Sargasso Sea. *Deep-Sea Research* **35**, 1297-1317.

Sunda, W.G. and Huntsman, S.A. 1994. Photoreduction of manganese oxides in seawater. *Marine chemistry* **46**, 133-152.

Sunda, W.G., Huntsman, S.A. and Harvey, G.R. 1983. Photoreduction of manganese oxides in seawater. *Nature* **301**, 234-236.

Sung, W. and Morgan, J.J. 1981. Oxidative removal of Mn (II) from solution by the FeOOH (lepidocrocite) surface. *Geochimica et Cosmochimica Acta* **45**, 2377-2383.

Tappin, A.D. 1988. *Studies of trace metals in shelf waters of the British Isles.* PhD. Thesis, University of Southampton, UK.

Taylor, H.E. and Shiller, A.M., 1995. Mississippi River methods comparison study: Implications for water quality monitoring of dissolved trace elements. *Environmental Science and Technology* **29**, 1313-1317.

Tessier, A., Campbell, P.G.C. and Bisson, M. 1979. Sequential extraction procedure for the speciation of particulate trace metals. *Analytical Chemistry* **51**, 844-851.

Turner, A., 1990. *Chemical dynamics in North Sea estuaries and plumes.* Ph.D. thesis, Polytechnic South West, Devon, U.K.

Turner, A. and Millward, G.E. 1994. Partitioning of trace metals in a macrotidal estuary: Implications for contaminant transport models. *Estuarine, Coastal and Shelf Science* **39**, 45-58.

Turner, A., Millward, G.E., Bale, A.J. and Morris, A.W., 1993. Application of the Kd concept to the study of trace metal removal and desorption during estuarine mixing. *Estuarine, Coastal and Shelf Science* **36**, 1-13.

Toy, D.F., 1973. Phosphorous. In *Comprehensive Inorganic Chemistry*, Vol. II. J.C. Bailar, H.J. Emeleus, R. Nyholm and A.F. Trotman-Dickenson (Eds). Pergamon Press, Oxford.

Uncles, R.J., Easton, A.E., Griffiths, M.L., Harris, C., Howland, R.J.M., King, R.S., Morris, A.W. and Plummer, D.H. Seasonality of the turbidity maximum in the Humber-Ouse Estuary. *Marine Pollution Bulletin* (In press).

Urquhart, C. 1979. Water quality investigations in the Humber Estuary. In: *The Humber Estuary*. NERC Publications Series C No.20, pp9-12.

Van Bennekom, A.J., Buma, A.G.J. and Nolting, R.F. 1991. Dissolved aluminium in the Weddell-Scotia confluence and effect of Al on the dissolution kinetics of biogenic silica. *Marine Chemistry* **35**, 423-434.

Van den Berg, C.M.G., Merks, A.G. and Duursma, E.G. 1987. Organic complexation and its control of the dissolved concentrations of copper and zinc in the Scheldt Estuary. *Estuarine, Coastal and Shelf Science* **24**, 785-797.

Verwey, E.J.W. and Overbeek, J.T,G. 1948. *Theory of the stability of lyphobic colloids.* Elsevier.

Waite, T.D. and Morel, F.M.M. 1984. Photoreductive dissolution of colloidal iron oxides in natural waters. *Environmental Science and Technology* **18**, 860-868.

Waite, T.D., Wrigley, I.C. and Szymczak, R. 1988. Photo-assisted dissolution of a colloidal manganese oxide in the presence of fulvic acid. *Environmental Science and Technology* **22**, 778-785.

Wells, M.L. and Goldberg, E.D., 1991. Occurrence of small colloids in seawater. *Nature* **353**, 342-344.

Wells, M.L. and Goldberg, E.D. 1994. The distribution of colloids in the North Atlantic and Southern oceans. *Limnology and Oceanography* **39**, 286-302.

Wells, M.L., Kozelka, P.B. and Bruland K.W., 1998. The complexation of 'dissolved' Cu, Zn, Cd and Pb by soluble and colloidal organic matter in Narragansett Bay, RI. *Marine Chemistry* **62**, 203-217.

Wen, L-S., Stordal, M.C., Tang, D. Gill, G.A. and Santschi, P.H., 1996. An ultraclean cross-flow ultrafiltration technique for the study of trace metal phase speciation in seawater. *Marine Chemistry* **55**, 129-152.

Westerland, S.F.G. and Ohman, P., 1991. Cadmium, copper, cobalt, nickel, lead and zinc in the water column of the Weddel Sea, Antarctica. *Geochimica et Cosmochimica Acta* **55**, 2127-2146.

Whitehouse, B.G., Petrick, G. and Ehrhardt, M., 1986. Cross-flow filtration of colloids from Baltic seawater. *Water Research* **20**, 1599-1601.

Whitehouse, B.G., Yeats, P.A. and Strain, P.M., 1990. Cross-flow filtration of colloids from aquatic environments. *Limnology and Oceanography* **35**, 1368-1375.

Williams, M.R. and Millward, G.E., Dynamics of particulate trace metals in the tidal reaches of the Ouse and Trent. *Marine Pollution Bulletin* (in press).

Windom, H., Smith, R., Rawlinson, C., Hungspreugs, M., Dharmuanji, S. and Wattayakorn, G. 1988. Trace metal transport in a tropical estuary. *Marine Chemistry* **24**, 293-305.

Windom, H., Wallace, G., Smith, R., Dudek, N., Maeda, M., Dulmage, R. and Storti, F. 1983. Behaviour of copper in southeastern United States estuaries. *Marine Chemistry* **12**, 183-193.

Yeats, P.A. and Strain, P.M. 1990. Oxidation of manganese in seawater: rate constants based on field data. *Estuarine, Coastal and Shelf Science* **31**, 11-24.

Zafiriou, O.C., Joussot-Dubien, J., Zepp, R.G. and Zika, R.G. 1984. Photochemistry of natural waters. *Environmental Science and Technology* **18(12)**, 358-371.

Data disc contents:

This table lists all the files included in the data disc. Some are referred to in the main text but others are included as complementary data.

File name/location	Description of file
Appendix 1:	
Carryover	Carryover of Zn, Mn and Fe with 6/9ml chloroform strips.
ExtnPb	Extractions of LMSW standards for lead (Initial).
Original Extn plots	Extractions of LMSW standards for Fe, Mn, Zn, Cu, Ni, Cd.
Stdtable	Concentrations of LMSW standards (by mass).
Appendix 2:	
CCstir	Coulter counter stirring data.
Collcompmodified	Coulter counter CFF/conventional filtration data.
Collgrav	Stored colloidal sample gravimetric data.
Eqmcorr2	Pilot radiochemistry Kd calculations.
Eqmnop	Pilot radiochemistry Kd calculations (no particles).
FFFtm	Field flow fractionation trace metals from Beaulieu colloidal sample.
Lamblnk	Laminar flow block zinc blanks.
Longznammended	Long term/stable zinc addition radiotracer data.
optvoltammnd	Optimal voltage for NaI detector.
Radmar2	Radiotracer experiment (March 2 1997).
Radmar4	Radiotracer experiment (March 4 1997).
TMFFFrecovand c	Trace metal extraction data for FFF samples.
Tmffftbl	Table of FFF trace metal data.
Zn65pild	Pilot experiment radiotracer data (geometric checks).
Zn65raw	Raw count data from pilot experiments.
Appendix 3:	
*month*background	Background data for February/April/July/August/October/ December.
Aprilfe	Iron data for April Trent/Humber survey.
AprJul*metal*	Trace metal data for April and July surveys.
Aug*metal*	Trace metal data for August survey.
Oct*metal*	Trace metal data for October survey.
Dec*metal*	Trace metal data for December survey.
Htrentfi	Trace metal data from February (Trent) survey.
Cfcalcs2	Concentration factor calculations for Oct, Jul/Aug, April survey samples.
Cfftabl	Concentration factor calculations for February and December survey samples.
Digabs	Sample digest effects on trace metal (Fe, Zn, Cu) concentrations (February).
Digcomp	Digestion of selected Humber samples on determined trace metal concentrations.

Appendix 3 cont..	
Digcompl	Further data e.g. recovery from Humber sample digestions.
Digrec	Recovery comparisons of digested samples (February).
Extand recovstds	Recovery data for extracted CRM's and LMSW standards (for all extraction batches).
extcomFe	Extraction comparisons of digested/non digested iron concentrations.
Febstorage and tra.	Trace metal data for February (blanks and storage).
Gfaasstd	Graphite furnace standard metal concentrations.
Refiltrate blanks TM	Minitan refiltrate blanks for trace metals (Humber survey).
Appendix 4:	
Alfff2	Field flow fractionation Al partitioning of Celtic Sea stock suspension (raw data).
Alreshigh	High resolution OMEX sediment resuspension data.
Alresdat	Raw Al resuspension data.
Blanks21	Initial Minitan MQ blanks on D216.
Botblank	Original Al blanks for lumogallion reaction bottles.
Bottle2	Lumogallion reaction and sample bottle checks for sediment resuspension experiments (storage effects, preconditioning).
collblnk	Original colloidal and truly dissolved Al data (D216). Also blanks tried after contamination. Some underway Al data.
Fffal	Worked up FFF Al data from Celtic Sea stock.
Leachat3	Sediment leachate/porewater data.
LFBblnkAl	Laminar flow blocks blanks for Al (MQ and sample refiltrate).
mastplot	Depth profile data for master variables.
Photoal	Photooxidation experiment (affects on lumogallion Al concentration).
Res30Oct	First resuspension experiment data.
Resnov1	Worked-up and combined Al resuspension data.
Ruth cor	Complete Al (total and dissolved) water column profile data (OMEX D216).
Storgrap	Alteration of Al concentration data for sample storage.
UnderAl	Underway (surface) Al concentration data.

SOUTHAMPTON UNIVERSITY LIBRARY

USER'S DECLARATION

AUTHOR: Parker ER TITLE: The role of colloidal material in the fate and cycling of trace metals in estuarine and coastal waters

DATE: 1999

I undertake not to reproduce this thesis, or any substantial portion of it, or to quote extensively from it without first obtaining the permission, in writing, of the Librarian of the University of Southampton.

To be signed by each user of this thesis

DATE	SIGNATURE	ADDRESS